

N 7 5 - 3 0 1 6 3 1

NASA CR-132559

VOLUME II
FINAL REPORT:
STUDY OF THE APPLICATION OF
HYDROGEN FUEL TO LONG-RANGE
SUBSONIC TRANSPORT AIRCRAFT

by G. D. Brewer & R. E. Morris
R. H. Lange & J. W. Moore

JANUARY 1975

CASE FILE
COPY

Prepared under Contract NAS 1-12972

for
LANGLEY RESEARCH CENTER
NATIONAL AERONAUTICS AND
SPACE ADMINISTRATION

by
LOCKHEED-CALIFORNIA COMPANY
AND
LOCKHEED-GEORGIA COMPANY



DIVISIONS OF LOCKHEED AIRCRAFT CORPORATION

1. REPORT NO. NASA CR-132559		2. GOVERNMENT ACCESSION NO.		3. RECIPIENT'S CATALOG NO.	
4. TITLE AND SUBTITLE Volume II Final Report: Study of the Application of Hydrogen Fuel to Long Range Subsonic Transport Aircraft				5. REPORT DATE January 1975	
				6. PERFORMING ORG CODE	
7. AUTHOR(S) Brewer, G.D. and Morris, R.E.; Lange, R.H. and Moore, J.W.				8. PERFORMING ORG REPORT NO. LR-26752-2	
9. PERFORMING ORGANIZATION NAME AND ADDRESS LOCKHEED-CALIFORNIA COMPANY Lockheed-Georgia Co. P.O BOX 551 and Marietta, Georgia BURBANK, CALIFORNIA 91520 30063				10. WORK UNIT NO.	
				11. CONTRACT OR GRANT NO. NAS 1-12972	
12. SPONSORING AGENCY NAME AND ADDRESS National Aeronautics and Space Administration Langley Research Center Hampton, Virginia 23665				13. TYPE OF REPORT AND PERIOD COVERED Contractor Final Report; Feb-Oct, 1974	
				14. SPONSORING AGENCY CODE	
15. SUPPLEMENTARY NOTES					
16. ABSTRACT This study was performed to investigate the feasibility, practicability, and potential advantages/disadvantages of using liquid hydrogen as fuel in long range, subsonic transport aircraft of advanced design. Both passenger and cargo-type aircraft were investigated. To provide a valid basis for comparison, conventional hydrocarbon (Jet A) fueled aircraft were designed to perform identical missions using the same advanced technology and meeting the same operational constraints. The liquid hydrogen and Jet A fueled aircraft were compared on the basis of weight, size, energy utilization, cost, noise, emissions, safety, and operational characteristics. A program of technology development was formulated.					
17. KEY WORDS (SUGGESTED BY AUTHOR(S)) Keywords: Hydrogen, subsonic transport aircraft, Jet A, cryogenic insulation, alternate fuel, exhaust emissions, noise, safety, energy utilization.				18. DISTRIBUTION STATEMENT	
19. SECURITY CLASSIF. (OF THIS REPORT) Unclassified		20. SECURITY CLASSIF. (OF THIS PAGE) Unclassified		21. NO. OF PAGES 351	
				22. PRICE*	

FOREWORD

This is the final report of a Study of the Application of Hydrogen Fuel to Long Range Subsonic Transport Aircraft performed under Contract NAS 1-12972 for NASA-Langley Research Center, Hampton, Virginia. The report presents documentation of the substance of work performed during the nine month period, February through October 1974. Volume I, NASA CR 132558, is a summary presentation of the work reported herein.

The work was divided in two vehicle categories: (1) passenger/cargo mission aircraft; and (2) all-cargo mission aircraft. Performance of the study was accomplished by the Advanced Design and Technology organizations of the Lockheed-California Company, Burbank (passenger/cargo missions), and the Lockheed-Georgia Company, Marietta (cargo-missions). Prime responsibility for contract execution rested with the California Company under the direction of G. Daniel Brewer as study manager. Robert E. Morris was project engineer for passenger aircraft. Deputy study manager for cargo mission aircraft analysis was R. H. Lange in Georgia. J. W. Moore served as project engineer for cargo aircraft. Other principal investigators were:

California Company

G. L. Dougherty

E. L. Bragdon

R. E. Skarshaug

K. E. Watson

R. L. Vaughn

R. Johnston

R. N. Jensen

R. D. Mijares

E. Himmel

D. E. Sherwood

Aerodynamics

Propulsion

Design

Cost

Weights

Stress

Vehicle Synthesis

Georgia Company

J. F. Honrath

F. R. Stone

E. P. Craven

S. G. Thompson

W. E. Warnock

J. F. Honrath

California Company

H. C. Moe

E. F. Versaw

D. M. Urie

G. F. Bollinger

G. T. Ellsworth
Kent Smith

N. Shapiro

J. Schulert

C. Slaughter

Thermodynamics

Fuel System

Flight Controls

Operations & Maintenance

Safety

Acoustics

Materials

Georgia Company

F. R. Stone

Mr. C. T. D'Aiutolo of the Aeronautical Systems Division of NASA-Langley Research Center, was the technical monitor for the contract.

All computations in this analysis were performed in U.S. Customary units and then converted to S.I. units.

SUMMARY

This study examined the feasibility of using liquid hydrogen as fuel in advanced designs of long range, subsonic transport aircraft, and assessed the potential advantages. Both passenger and cargo-type aircraft were investigated. Passenger aircraft were designed to perform all combinations of the following matrix of primary mission requirements:

PAYLOAD	36,300 kg (88,000 lb) = 400 Passengers + cargo)
RANGES	5,560 km (3000 n mi) and 10,190 km (5500 n mi)
CRUISE SPEEDS	Mach 0.80, 0.85 and 0.90

In addition, 600 and 800 passenger capacity aircraft were designed for Mach 0.85 cruise speed and for both ranges.

Cargo aircraft designs were studies to perform the following missions:

	<u>MISSION 1</u>	<u>MISSION 2</u>
PAYLOAD	56,700 kg (125,000 lb)	113,400 kg (250,000 lb)
RANGE	5560 km (3000 n mi)	10,190 kg (5500 n mi)
CRUISE SPEED	Mach 0.85	Mach 0.85

To serve as a basis for comparison, reference aircraft fueled with conventional hydrocarbon (Jet A) were designed to identical ground rules and for the same missions, except that the passenger airplane requirements were limited to only one speed, Mach 0.85.

Due to the low density, high energy content, and cryogenic temperature of liquid hydrogen (LH_2) it was anticipated that optimum designs of LH_2 fueled aircraft might require unusual design configurations to gain

maximum advantage from its use. This was found not to be the case. Although many unusual configurations were explored, the designs of LH_2 fueled aircraft selected as preferred configurations for both the passenger and cargo applications are conventional in appearance. Unusual design concepts which were investigated proved to be inferior.

In every case the hydrogen fueled aircraft, which were selected using minimum direct operating cost as the primary criterion, were found to be lighter, quieter, able to operate from shorter runways, require smaller engines, minimize pollution of the environment, and expend less energy in performing their design missions, relative to equivalent designs fueled with Jet A. In addition, the hydrogen aircraft are physically smaller in span, height, and wing area, but have larger fuselages.

The purchase price estimated for the LH_2 aircraft was somewhat higher than that of the reference designs. This was due to a high value accorded the hydrogen-peculiar items, for which there is insufficient data to establish a truly meaningful cost basis.

Direct operating costs of the hydrogen aircraft are significantly lower than that of their Jet A fueled counterparts if the fuels cost the same per unit of energy. The following table shows the additional cost which can be paid for LH_2 per unit of energy for the subject aircraft to have DOC's equal to their respective Jet A-fueled reference aircraft.

M 0.85 AIRCRAFT			ALLOWABLE ADDITIONAL COST FOR LH ₂ TO PRODUCE EQUAL DOC	
PAYLOAD		RANGE		
TYPE	WEIGHT			¢/GJ
400 PAX	36,300 kg (88,000 lb)	5560 km (3000 n. mi)	22.7	(21.5)
400 PAX	36,300 kg (88,000 lb)	10,190 km (5500 n. mi)	46.5	(44)
CARGO	56,700 kg (125,000 lb)	5560 km (3000 n. mi)	21.5	(20)
CARGO	113,400 kg (250,000 lb)	10,190 km (5500 n. mi)	52.8	(50)

An evaluation of operations, maintenance, and safety aspects of the hydrogen fueled aircraft revealed no significant features that would seriously affect airline-type turn-around schedules, compared to current practice with Jet A fuel. Equipment to perform operations like refueling will be different, but neither the number of personnel involved nor the elapsed time required should be adversely affected.

The examination of larger payloads (600 and 800 passengers) indicated an increasing flight efficiency for the larger aircraft. As payload increased, both direct operating cost and block fuel fraction (expressed as a percentage of gross weight) decreased.

TABLE OF CONTENTS

<u>Section</u>		<u>Page</u>
	FOREWORD	
	SUMMARY	
	LIST OF FIGURES	
	LIST OF TABLES	
	NOMENCLATURE	
1.	INTRODUCTION	1
2.	TECHNICAL APPROACH	7
3.	TECHNOLOGY DESCRIPTION	11
3.1	<u>HYDROGEN SYSTEMS</u>	11
3.1.1	LH ₂ Fuel System Description	14
3.1.2	LH ₂ Tank Structural Concepts	19
3.1.3	LH ₂ Tank Installation System	25
3.2	<u>PROPULSION</u>	30
3.2.1	Cycle Selection	34
3.2.2	Cycle Design Point	37
3.2.3	Nacelle Design	44
3.2.4	Installed Performance	47
3.3	<u>AERODYNAMICS</u>	49
3.3.1	Passenger Aircraft Aerodynamics	49
3.3.2	Cargo Aircraft Aerodynamics	67
3.4	<u>FLIGHT CONTROLS</u>	75
3.4.1	Empennage Size	77

TABLE OF CONTENTS (Continued)

<u>Section</u>	<u>Page</u>
3.5	82
<u>MATERIALS</u>	82
3.5.1	87
Airframe	89
3.5.2	91
Fuel Tank Structure	91
3.5.3	91
Insulation System, Fittings and Attach Members	91
3.6	91
<u>STRUCTURES</u>	91
3.6.1	92
Structural Design Criteria and Concepts	92
3.6.2	97
Structural Description	97
4.	97
PASSENGER AIRCRAFT	97
4.1	101
<u>REQUIREMENTS</u>	105
4.2	108
<u>CONFIGURATION SELECTION</u>	110
4.3	117
<u>PARAMETRIC ANALYSIS METHOD</u>	117
4.3.1	121
Weight Input Basis	129
4.3.2	138
Cost Methods and Factors	138
4.4	145
<u>INTERNAL TANK HYDROGEN AIRCRAFT</u>	145
4.4.1	145
Parametric Study Results	145
4.4.2	145
Configuration Description	145
4.4.3	145
Vehicle Data	145
4.5	145
<u>EXTERNAL TANK HYDROGEN AIRCRAFT</u>	145
4.5.1	145
Parametric Study Results	145
4.5.2	145
Configuration Description	145
4.5.3	145
Vehicle Data	145
4.6	145
<u>HYDROGEN PASSENGER AIRCRAFT CONFIGURATION SELECTION</u>	145
4.6.1	150
Operations and Maintenance Comparison	150

TABLE OF CONTENTS (Continued)

<u>Section</u>	<u>Page</u>
4.6.2 Safety Comparison	155
4.6.3 Characteristics Comparison	159
4.6.4 Summary and Selection	163
4.7 <u>REFERENCE (JET A) AIRCRAFT</u>	163
4.8 <u>BENEFITS EVALUATION: LH₂ VS. JET A PASSENGER AIRCRAFT</u>	164
4.8.1 Characteristics Comparison	164
4.8.2 Noise	177
4.8.3 Emissions	186
4.8.4 Safety	187
4.9 <u>LARGER PAYLOAD DESIGNS</u>	189
5. CARGO AIRCRAFT	265
5.1 <u>REQUIREMENTS</u>	205
5.2 <u>CONFIGURATION SELECTION</u>	206
5.3 <u>PARAMETRIC ANALYSIS</u>	210
5.3.1 Parametric Sizing Program	210
5.3.2 Parametric Constraints	211
5.3.3 Parametric Selection Process	212
5.3.4 Parametric Trends	212
5.4 <u>HYDROGEN NOSE LOADER CONFIGURATION</u>	219
5.4.1 Configuration Description	219

TABLE OF CONTENTS (Continued)

<u>Section</u>	<u>Page</u>
5.4.2	Weight Statement 238
5.4.3	Performance 239
5.4.4	Aircraft Price and Operating Cost 244
5.5	<u>HYDROGEN SWING TAIL CONFIGURATION</u> 244
5.5.1	Configuration Description 244
5.5.2	Weight Statement 253
5.5.3	Performance 256
5.5.4	Aircraft Price and Operating Cost 256
5.6	<u>HYDROGEN AIRCRAFT CONFIGURATION SELECTION</u> 259
5.6.1	Terminal Operations and Maintenance 259
5.6.2	Safety 260
5.6.3	Performance 260
5.6.4	Selection 260
5.7	<u>REFERENCE (JET A) CARGO AIRCRAFT</u> 263
5.7.1	Configuration Description 263
5.7.2	Weight Statement 271
5.7.3	Performance 271
5.7.4	Aircraft Price and Operating Cost 275
5.8	<u>BENEFITS EVALUATION</u> 275
5.8.1	Performance 275
5.8.2	Unit Price and Operational Cost 281
5.8.3	Energy Consumption 282
5.8.4	Noise Comparison 286
5.8.5	Emissions 290
5.8.6	Safety 290

TABLE OF CONTENTS (Continued)

<u>Section</u>	<u>Page</u>
6. RESEARCH AND TECHNOLOGY RECOMMENDATIONS	291
6.1 TECHNOLOGY DEVELOPMENT ITEMS	291
6.1.1 Studies	291
6.1.2 Experimental Development	298
6.1.3 Flight Operations	300
6.2 TECHNOLOGY DEVELOPMENT SCHEDULE	301
7. CONCLUSIONS	305
8. RECOMMENDATIONS	307
REFERENCES	R-1
APPENDIX A Properties of Hydrogen	A-1
APPENDIX B Example ASSET Autoplot Data Presentation	B-1
APPENDIX C External Loads Criteria and Loads	C-1
APPENDIX D Selected ASSET Computer Printout Pages	D-1
APPENDIX E Evaluation of Air Cushion Landing System as applied to Liquid Hydrogen - Fueled Cargo Transport	E-1

LIST OF FIGURES

<u>Figure</u>		<u>Page</u>
1	Energy Utilization in U.S. in 1970	3
2	Hydrogen Fuel System Elements	12
3	LH ₂ Fuel System Schematic	15
4	Integral Tank Concept	22
5	Non-Integral Tank Concept	23
6	Insulation Thickness vs. In-Flight Boiloff	27
7	Effect of Insulation Thickness on Vehicle Characteristics	28
8	Insulation Surface Temperature vs Insulation Thickness	29
9	Ground Boiloff Rates vs. Insulation Thickness	29
10	Economic Input of Insulation Thickness	31
11	Trend of Turbofan Turbine Inlet Temperatures vs. Qualification Date	33
12	Effect of Fan Pressure Ratio on Overall Efficiency vs. Mach Number - No Cowl Drag	35
13	Effect of Fan Pressure Ratio on Overall Efficiency vs. Mach Number - Cowl Drag Included	36
14	Effect of Cycle Pressure Ratio on Overall Efficiency vs. Mach Number - Cowl Drag Included	38
15	Cowl Drag Coefficient vs Mach Number	39
16	Effect of Turbine Inlet Temperature on Overall Efficiency vs. Mach Number - Cowl Drag Included	40
17	Effect of Bypass Ratio on Overall Efficiency - Cowl Drag Included	41
18	LH ₂ Engine/Nacelle Characteristics	45
19	Wing Pod Inlet Total Pressure Recovery - Variable Geometry Throat	48
20	Installed Thrust vs. Mach Number - Takeoff Rating - Jet A Fueled Engine	50
21	Installed Thrust vs. Mach Number - Takeoff Rating - LH ₂ Fueled Engine	51

LIST OF FIGURES (Continued)

<u>Figure</u>		<u>Page</u>
22	Comparative Engine Cruise Performance - Mach 0.85, 10,670 m (35,000 ft)	52
23	Installed Cruise SFC vs. Net Thrust - Jet A Fueled Engine	53
24	Installed Cruise SFC vs. Net Thrust - LH ₂ Fueled Engine	54
25	Characteristic "Design to" Wing Pressure Distributions	56
26	2-D Mach Divergence Characteristics	57
27	3-D Corrections to Mach Divergence	57
28	M Design and C _L Design Derivation	58
29	M Design and/M Divergence Relationship	59
30	Polar Shape Factor "Z"	61
31	Wing and Fuselage Pressure Drag	62
32	High-Lift (Flapped) Polar Synthesis for Advanced Design Parameters	63
33	High-Lift (Flapped) Polar Synthesis Variables	65
34	Wing Sweep Angle Selection	68
35	Wing Thickness Determination	70
36	Post Drag Rise Characteristics	71
37	Compressible Drag Rise Optimization	72
38	Effect of Approach Speed on Runway Acceptance Rates	74
39	Effect of Approach Speed on Gross Weight and DOC	76
40	Maximum Pitch Acceleration During Stall Recovery	78
41	Rudder Size for Directional Control With One Engine Inoperative	79
42	Aerodynamic Limits on Center of Gravity	80
43	Comparison of Aluminum Alloys at Room Temperature	83
44	Benefits of Advanced Materials on Aircraft Weight and Cost Parameters	88
45	Effect of Initial Cruise Altitude on Gross Weight and DOC	99
46	Matrix of Variables for Passenger Aircraft	100
47	Candidate Passenger Aircraft Configuration	103
48	ASSET Synthesis Cycle	106

LIST OF FIGURES (Continued)

<u>Figure</u>		<u>Page</u>
49	ASSET Program Schematic	106
50	Example - Parametric Data Autoplot	107
51	Aircraft Flyaway Cost Model	114
52	Sales Price vs. Operating Empty Weight	116
53	Effect of Thickness Ratio on Selection Parameters	118
54	Effect of Aspect Ratio on Selection Parameters	120
55	General Arrangement - LH ₂ Fuel, Internal Tank, M 0.85 Transport	123
56	Passenger Accomodations - 400 Pax	125
57	Geometry and Wing Characteristics	127
58	Tank Protection Concept (Ref. Figure 55) Section Through Forward End. (Lower) of Rear Tank - Looking Aft	131
59	Effect of Cruise Speed on Values of Selection Parameters (Internal Tanks)	135
60	Effect of Thickness Ratio on Selection Parameters	139
61	Effect of Aspect Ratio on Selection Parameters	140
62	General Arrangement - LH ₂ Fuel, External Tank, M 0.85 Transport	141
63	External LH ₂ Tanks - Geometry and Preliminary Structural Arrangement Concept	143
64	Effect of Cruise Speed on Value of Selection Parameters (External Tanks)	148
65	Candidate Hydrogen - Fueled Passenger Transport Aircraft	151
66	Schematic - LH ₂ Airport Fueling Facility	153
67	General Arrangement - Jet A Fuel, M 0.85 Transport	165
68	Size Comparison: LH ₂ vs Jet A Passenger Aircraft	174
69	Sensitivity of DOC to Fuel Price Short Range Passenger Aircraft	178
70	Sensitivity of DOC to Fuel Price Long Range Passenger Aircraft	179
71	Effect of Utilization on DOC	180
72	DOC Sensitivity to Maintenance Cost	181
73	90 EPNdB Contour Comparison - Passenger Aircraft	184
74	General Arrangement - LH ₂ Fuel, M 0.85, 800 Passenger Transport	191

LIST OF FIGURES (Continued)

<u>Figure</u>		<u>Page</u>
75	Passenger Cabin Arrangement - LH ₂ Fuel, 600 Passenger Transport	193
76	General Arrangement - LH ₂ Fuel, M.085, 800 Passenger Transport	195
77	Passenger Cabin Arrangement - 800 Passengers	197
78	Effect of Larger Payloads on Aircraft Characteristics (Short Range)	202
79	Effect of Larger Payloads on Aircraft Characteristics (Long Range)	203
80	Cargo Aircraft Configuration Concept	207
81	Generalized Aircraft Sizing Program (GASP)	210
82	Sample Parametric Data - Large Hydrogen Nose Loader	213
83	General Arrangement - LH ₂ Fuel, Cargo Transport, Small Nose Loader	221
84	General Arrangement - LH ₂ Fuel, Cargo Transport, Large Nose Loader	223
85	Candidate Hydrogen Tank Configurations	227
86	Payload - Range/Block Fuel	243
87	General Arrangement - LH ₂ Fuel, Cargo Transport, Small Swing Tail	247
88	General Arrangement - LH ₂ Fuel, Cargo Transport, Large Swing Tail	249
89	Payload - Range/Block Fuel	257
90	General Arrangement - Jet A Fuel, Small Cargo Transport	267
91	General Arrangement - Jet A Fuel, Large Cargo Transport	269
92	Payload - Range/Block Fuel	274
93	Sensitivity of DOC to Fuel Price (Small Cargo Aircraft)	283
94	Sensitivity of DOC to Fuel Price (Large Cargo Aircraft)	284
95	Direct Operating Cost - Utilization Sensitivity	285
96	Direct Operation Cost - Maintenance Cost Sensitivity	286
97	Takeoff Noise Footprint - Cargo Aircraft	287
98	Landing Noise Footprint - Cargo Aircraft	288
99	Technology Development Program	302

LIST OF TABLES

Table		Page
1	Basic Guidelines	8
2	Propulsion Technology Forecast for 1985 State-of-Art.	34
3	Engine Design Point Data, Sea Level Static - Standard Day	42
4	Baseline Propulsion System Weight	46
5	Compressor Bleed and Power Extraction	47
6	Composite Material Properties	84
7	Weight Factors as a Function of Percent Application of Advanced Materials	86
8	Plastic Foam Insulation Materials	89
9	Physical Properties of Films	90
10	Advanced Technology Weight Reduction Coefficients and Estimated Materials Distribution	110
11	Development Cost Factors	112
12	Engine Price and R&D Cost for Subsonic LH ₂ Aircraft	112
13	Investment Cost Factors	113
14	Selection Criteria Effects	119
15	Design Characteristics: Internal Tank LH ₂ Passenger Aircraft (Short Range)	133
16	Design Characteristics: Internal Tank LH ₂ Passenger Aircraft (Long Range)	134
17	Cost Summary: LH ₂ Internal Tank Aircraft, Mach 0.85	136
18	Direct Operating Costs: LH ₂ Internal Tank Aircraft, Mach 0.85	137
19	Design Characteristics: External Tank, LH ₂ Passenger Aircraft (Short Range)	146
20	Design Characteristics: External Tank, LH ₂ Passenger Aircraft (Long Range)	147
21	Cost Summary: LH ₂ External Tank Aircraft, Mach 0.85	149
22	Direct Operating Costs: LH ₂ External Tank Aircraft, Mach 0.85	150
23	Operations and Maintenance Comparison - LH ₂ Fueled Aircraft	156

LIST OF TABLES (Continued)

Table		Page
24	Safety Comparison: Internal vs. External LH ₂ Aircraft	160
25	Design Comparison: Internal vs. External LH ₂ Aircraft (Short Range)	161
26	Design Comparison: Internal vs. External LH ₂ Aircraft (Long Range)	162
27	Design Characteristics: Reference (Jet A) Passenger Aircraft	167
28	Cost Summary: Jet A Passenger Aircraft	168
29	Direct Operating Costs: Jet A Passenger Aircraft	169
30	Comparison of Final Design: LH ₂ vs. Jet A Passenger Aircraft (Short Range)	170
31	Comparison of Final Design: LH ₂ vs. Jet A Passenger Aircraft (Long Range)	171
32	Cost Comparison: LH ₂ vs Jet A Passenger Aircraft	175
33	Noise Comparison - Passenger Aircraft	183
34	Engine Emission Estimates (1)	187
35	Characteristics of 600 and 800 Passenger LH ₂ Aircraft (Short Range)	199
36	Characteristics of 600 and 800 Passenger LH ₂ Aircraft (Long Range)	200
37	Cost Data for 600 and 800 Passenger LH ₂ Aircraft	201
38	Cargo Mission Parameters	206
39	Cargo Aircraft Configuration Concept Comparison	208
40	Comparison - Double Row vs. Single Row Cargo Compartments	209
41	Aspect Ratio Selection - LH ₂ Swing Tail	215
42	Aspect Ratio Selection - LH ₂ Nose Loader	217
43	Hydrogen Tank Data - Design Options	232
44	Fuselage Data - Tank Options	234
45	Aircraft Data - Tank Options	235
46	Small Hydrogen Nose Loader Tank Data	238
47	Large Hydrogen Nose Loader Tank Data	239
48	Group Weight Statement - Small Hydrogen Nose Loader	240

LIST OF TABLES (Continued)

<u>Table</u>		<u>Page</u>
49	Group Weight Statement - Large Hydrogen Nose Loader	241
50	Price Summary - Hydrogen Nose Loader Aircraft	245
51	Small Hydrogen Swing Tail Tank Data	252
52	Small Hydrogen Swing Tail Tank Data	253
53	Group Weight Statement - Small Hydrogen Swing Tail	254
54	Group Weight Statement - Large Hydrogen Swing Tail	255
55	Price Summary - Hydrogen Swing Tail Aircraft	258
56	Small LH ₂ Cargo Aircraft Comparison	261
57	Large LH ₂ Cargo Aircraft Comparison	262
58	Aspect Ratio Selection - Jet A Cargo Aircraft	264
59	Group Weight Statement - Small Jet A Nose Loader	272
60	Group Weight Statement - Large Jet A Nose Loader	273
61	Price Summary - Jet A Aircraft	276
62	Comparison of Final Designs: LH ₂ vs Jet A Small Cargo Aircraft	277
63	Comparison of Final Designs: LH ₂ vs Jet A Large Cargo Aircraft	278
64	Aerodynamic Coefficient Comparison: LH ₂ vs Jet A Cargo Aircraft (Cruise Condition)	279
65	Unit Price and Operational Cost Summary: Cargo Aircraft	281
66	Noise Comparison - Cargo Aircraft	289

NOMENCLATURE

AR	= Aspect Ratio
ATA	= Air Transport Association
ATT	= Advanced Technology Transport
BPR	= Bypass Ratio
C_D	= Drag Coefficient
C_{Dc}	= Compressibility Drag Coefficient
$C_{D\alpha}$	= Friction Drag Coefficient
C_{Di}	= Induced Drag Coefficient
C_{DP}	= Profile Drag Coefficient
c	= Wing Chord
C_L	= Lift Coefficient
C_ℓ	= Section Lift Coefficient
CPR	= Cycle Pressure Ratio
DOC	= Direct Operating Cost
DTAM	= Deviation from std. ambient Temperature

NOMENCLATURE (Continued)

E_c	=	Young's Modules of Elasticity (compression)
E_t	=	Young's Modules of Elasticity (tension)
FAR	=	Federal Air Regulation
F_N	=	Net Thrust
FPR	=	Far Pressure Ratio
F_{t_u}	=	Ultimate fiber stress, tension
HP	=	High Pressure
H.P.EXT	=	Horsepower Extraction
IGV	=	Inlet Guide Vanes
IOC	=	Indirect Operating Cost or Initial Operational Capability
Jet A	=	Conventional Hydrocarbon fuel
KEAS	=	Knots Equivalent airspeed
L/D	=	Lift-to-Drag ratio
LH_2	=	Liquid Hydrogen
LHV	=	Fuel Lower Heating Value
LP	=	Low Pressure
M	=	Mach Number

NOMENCLATURE (Continued)

M_D	= Design Mach Number
OPR	= Overall Pressure Ratio
OEW	= Operating Empty Weight
P_{T_2}	= Average Fan Face Total Pressure
P_{T_0}	= Freestream Total Pressure
QEC	= Quick Engine Change Nacelle
SW	= Wing Reference Area
S_π	= Frontal area
SLS	= Sea Level Static
T/W	= Thrust to Weight Ratio
TIT	= Turbine Inlet Temperature
t_k	= wing thickness ratio
VjP	= Primary exhaust jet velocity
VjD	= Fan Duct exhaust jet velocity
V_o	= Flight velocity
V_r	= Takeoff rotate Velocity

NOMENCLATURE (Continued)

V_s = stall Velocity

$W_a \frac{\sqrt{\theta_{T_2}}}{\delta_{P_2}}$ = Engine corrected airflow

W_{pod} = Engine pod weight

W/S = Wing Loading (weight/wing area)

ZFW = Zero Fuel Weight

α = Angle of Attack

δ_{P_2} = Delta $P_2 = P_{T_2}$ PSIA/14.7

θ_{T_2} = Theta $T_2 = T_{T_2}$ °K/288.2

Δ = Increment

Λ = Wing Sweep Angle

SECTION 1

INTRODUCTION

Growing concern for the problem of providing adequate supplies of petroleum-derived fuels to meet U.S. demand, and recognition of the inevitable price that must be paid for our ever increasing dependence on foreign supplies, has led the NASA to a broad study effort to review energy trends and to evaluate the possibilities of alternate fuels for transport aircraft. The availability and cost of petroleum-derived fuel for commercial transport aircraft will continue to become less and less attractive in coming years. Ultimately, and it is simply a question of "how soon," rather than "if," an alternate fuel must be developed. The policy employed during the period of the Arab oil embargo, starting in October, 1973, which assigned commercial airlines a low priority in allocation of fuel stocks relative to household, industrial, and utility needs, will probably not be drastically revised. Accordingly, as shortages develop in the future, either because of international political or economic pressures, or as a result of depletion of natural resources, it may be assumed commercial air transport will suffer severe disruptions.

Serious consideration of changing to an alternate fuel for commercial transport aircraft must include assessment of the impact the choice would have not only on the aviation segment of American industry, i.e., the airlines, aircraft and engine manufacturers, fuel suppliers, and airport operators, but the debate must also include consideration of the energy and fuel needs of the entire spectrum of the U.S. economy. In addition, it is becoming more clearly recognized that the energy requirements and preferences of foreign governments must be considered and coordinated along with those of our own. In other words, selection of a "fuel of the future" for commercial aviation cannot be made logically without considering the requirements and opportunities of all other significant users of energy, both national and international.

Although the subject report is focused on consideration of just the commercial aviation aspects of the energy/fuel problem, the following is offered to help keep the problem in perspective.

The utilization of energy in the U.S. in 1970 is diagrammed in Figure 1, taken from Reference 1. Total consumption of energy in that year was 64.6 Q [quadrillion (10^{15}) Btu]. An additional quantity of fossil fuels, equivalent to 4.2 Q, was consumed in non-energy uses, primarily the manufacture of petro-chemicals, making the total 68.8 Q. Of this total, 23.7 percent (16.3 Q) was used in transportation, of which commercial aviation used only 7.5 percent (1.23 Q), a relatively insignificant amount. For instance, if somehow the total amount of fuel used by commercial aircraft in 1970 was made available for use by all the energy consuming sectors of the U.S. economy, it would provide energy for just 6-1/2 days at the 1970 rate of consumption.

By A.D. 2000, however, it is generally forecast U.S. energy consumption will amount to between 140 and 160 Q, and that the distribution of energy among the four basic end-uses (industry, transportation, household and commercial, and "other" plus losses) will remain substantially the same except that, according to projections made by the study of Reference 2, the share for transportation will increase to about 30 percent. Also, from the same source, it is predicted that within the transportation sector the share for commercial aviation will increase to about 32 percent by 2000. This would amount to between 13.4 and 15.3 Q/year for aircraft, a very considerable amount using either energy projection. It is equivalent to about 35 days supply of energy for the entire U.S. at the rate of consumption projected for A.D. 2000, or roughly 10 percent of the nation's total consumption that year. In more dramatic terms, the recoverable oil reserves in the Alaskan North Slope are currently estimated at 9.6 billion barrels. Since a maximum of only 17 percent of a barrel of crude oil can be refined to Jet A fuel specifications, the remainder going to other uses, the output of the entire North Slope oil field will supply U.S. commercial aviation for only about 8 months at the lower rate of consumption projected for A.D. 2000.

It is apparent that switching commercial aviation from a petroleum base product to an alternate fuel could have a significant impact on the nation's crude requirements within the time frame in which the change would be implemented.

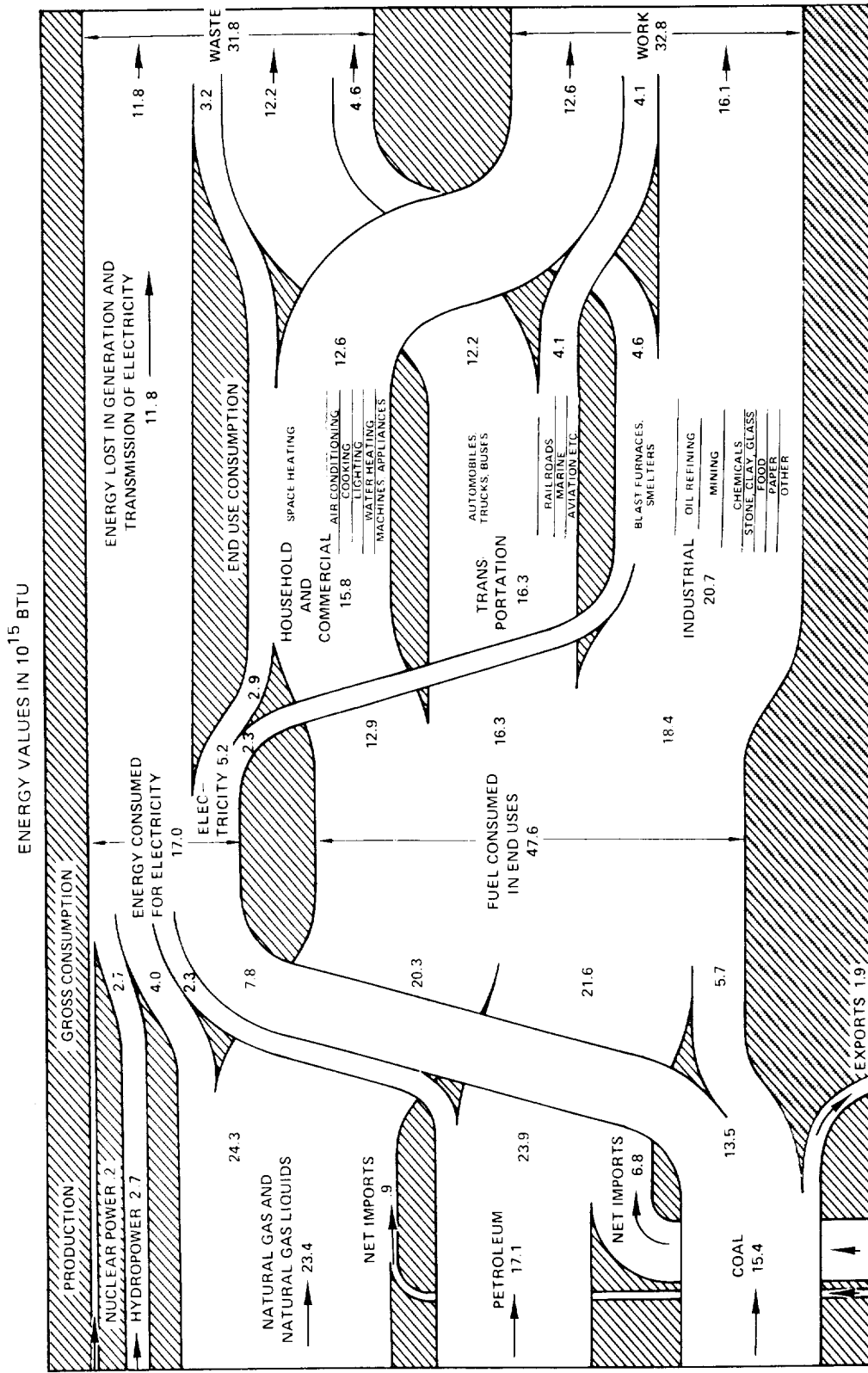


Figure 1. Energy Utilization in U.S. in 1970 (From September 1971 Scientific American)

These statistics are also a cogent answer to the frequently-heard plaint, "If the current fuel (Jet A) is going to be in short supply why shouldn't other users switch to an alternate, thereby prolonging the availability of Jet A for aviation?" At only 17 percent maximum conversion capability, the world does not possess enough petroleum to long supply the voracious appetite of commercial airliners if air travel service is to expand as predicted. Accordingly, there are a number of questions which need to be resolved:

- What is the preferred fuel for commercial aviation from the points of view of cost, emissions, energy, noise, practicability, and long range availability?
- How can the transition to the new fuel be implemented without serious disruption of commercial airline service or undue financial burden on the airlines?
- How much will it cost to provide facilities to store and handle the new fuel at airports, and how should it be capitalized?
- Since U.S. aircraft fly worldwide, the choice of a new fuel must be coordinated on an international basis. How should this be accomplished in order that other countries preferences for a new fuel might be properly considered along with that of our own?

This last question deserves emphasis because 1) up to now it has been virtually ignored in U.S. considerations, and 2) it has strong implications on answers to the other questions. Many nations, e.g., Japan and Italy, import nearly 100 percent of their petroleum requirements. None of the western European nations currently produces more than a small fraction of its petroleum needs although England with its North Sea potential may become self sufficient within a few years. In contrast, according to Reference 1, in 1970 the United States imported only 6.8 Q, less than 30 percent of our total petroleum requirements. It is apparent therefore, that many other countries will be more strongly motivated to find a satisfactory fuel and energy source which will relieve their dependence on imported crude oil than will the United States.

Within each country there may be circumstances or natural resources which offer unique potential solutions to their individual energy needs for industry, residential and commercial, and surface transportation. They may include a wide

variety of energy sources in addition to the conventional use of petroleum, natural gas, and coal, ranging from solar, nuclear, geothermal, hydro, and conversion of waste products, to photosynthesis for growing fuel in one form or another. For stationary power plants there are a large number of energy sources which can be used and there is no strong requirement that one locality employ the same solution as any other.

Commercial air transportation is a significant exception to this freedom of choice determination because air travel is international, and also because aircraft are necessarily designed to use a specific fuel, within fairly narrow limits. That is, for example, it is not practical to design an airplane to operate efficiently on both Jet A and hydrogen fuel interchangeably. Accordingly, if international air travel is to continue to flourish and expand as projected in the face of definite prospects that some countries may be unable to obtain adequate supplies of petroleum at all times, it becomes mandatory either that all nations agree to share their petroleum fuel supplies (this is recognized as, first, only a temporary solution, and second, as being impractical in event of an extended embargo), or that they will adopt an alternate fuel that can be commonly produced without hazard of control by a cartel.

Hydrogen offers many potential advantages for this application including the facts that 1) it can be manufactured from coal and water, or from water directly, using any of several processes and a wide variety of possible energy sources (Reference 3), and therefore can be considered to be free of the dangers of cartelization; and 2) used as a fuel for aircraft it has been shown to provide significant improvement in vehicle weight, performance, and cost, and to result in reduced pollution of the environment. Recognition of these advantages as a result of preliminary conceptual design studies has led to consideration of hydrogen as a leading candidate to replace Jet A as the fuel for commercial transport aircraft of the future.

The subject study was performed as one of the initial efforts in NASA's investigation of alternatives for the future. The objectives of this study were to:

- Assess the feasibility and potential advantages of using liquid hydrogen (LH_2) as fuel in long range, subsonic transport aircraft (both passenger and cargo types).

- Identify the problems and technology requirements peculiar to such aircraft.
- Outline a program for development of necessary technology on a timely basis.

The organization and methodology of the study is described in Section 2.

SECTION 2

TECHNICAL APPROACH

This investigation was intended to provide evidence to help answer some of the intriguing questions relative to use LH_2 in long-range, subsonic transport aircraft of the future; e.g., can efficient aircraft be designed to contain the large volume of low density fuel that will be required, can the structural and thermodynamic problems related to use of cryogenic liquid in commercial transport aircraft be satisfactorily resolved, can satisfactory operational and handling procedures be developed, how will the economics of transport aircraft be affected by the switch from hydrocarbon (Jet A) to LH_2 fuel, and how will air transport safety be affected? To provide that evidence, conceptual design studies were made of both passenger and cargo-type transport aircraft "...to the depth necessary to indicate both the technical and economic feasibility of liquid hydrogen-fueled transport aircraft" (Reference 4). To provide a basis for a valid comparison of physical, performance, and economic parameters, reference aircraft using Jet A fuel were sized to perform identical missions. Ground rules for the study are listed in Table 1.

The study was conducted in the sequence indicated schematically in the following diagram.

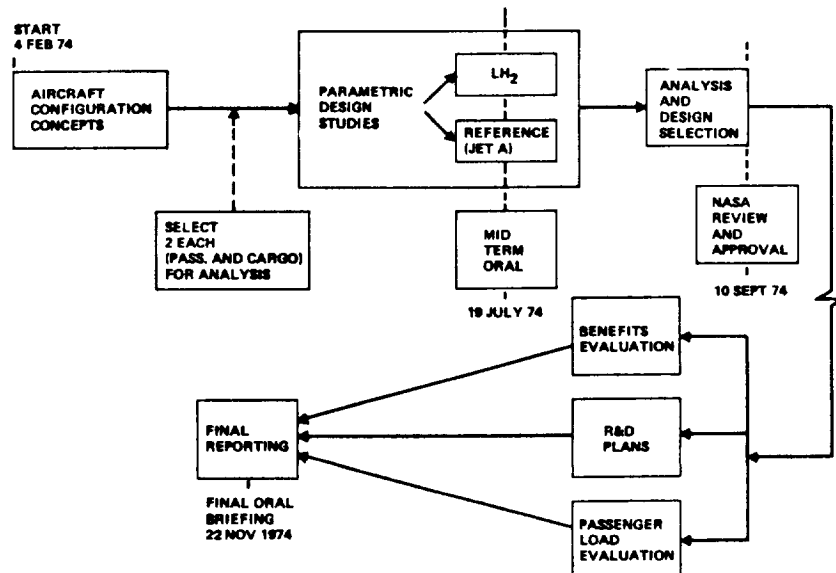


TABLE 1. BASIC GUIDELINES

Fuel: Liquid Hydrogen (assumed available at airport for this study)

Initial Operational Capability: 1990-95

Advanced Aircraft Technologies:

- Supercritical aerodynamics
- Composite materials
- Active controls
- Terminal area features

Advanced Engines: Contractor-derived performance for both LH₂ and Jet A fueled turbofans

Noise Goal: 5.18 km² (2 sq. mi.) area for 90 EPNdB contour (sum of takeoff + approach)

Emission Limit Goals:

- | | | |
|-----------------|-----------------|-----------------------|
| • Ground Idle | CO | 14 gm/kg. fuel burned |
| | HC | 2 gm/kg. fuel burned |
| • Takeoff Power | NO _x | 13 gm/kg. fuel burned |
| | Smoke | SAE 1179 Number 25 |

Landing and Takeoff: 2410 m (8000 ft.) runway, 32.2°C (90°F) day,
304.8 m (1000 ft.) alt.

Direct Operating Cost:

- 1967 ATA equations (international basis)
- 1973 dollars
- 350 aircraft production base
- Baseline fuel costs

LH ₂	=	\$3/1.054 GJ (\$3/10 ⁶ Btu = 15.48¢/lb.)
Jet A	=	\$2/1.054 GJ (\$2/10 ⁶ Btu = 24.8¢/gal. = 3.68¢/lb.)

All passenger aircraft were designed and evaluated at Lockheed-California Company and all cargo aircraft at Lockheed-Georgia Company. A large number of candidate aircraft configurations of both types were conceived and subjected to a critical qualitative evaluation. The two configurations given the highest ratings were selected for more detailed study and analysis.

Design studies were conducted to determine appropriate characteristics for the hydrogen-related systems required on board the aircraft. These studies included consideration of materials, structural, and thermodynamic requirements of the cryogenic fuel tanks, their structural support systems, thermal protection systems, and for the fuel system. Operations and maintenance procedures and requirements were considered in the design of these components and systems.

Engine decks were generated to parametrically represent the performance, size, and weight of advanced design, quiet turbofan engines using technology forecast to be available after 1985, consistent with initial aircraft operational capability in 1990-95. Decks were generated for engines designed for both fuels, liquid hydrogen (LH_2) and Jet A, the latter being the hydrocarbon fuel currently used in commercial transport aircraft.

Similarly, aerodynamic, weight and cost data were generated in parametric form to represent use of advanced technologies such as supercritical aerodynamics, advanced structural concepts and materials, active controls and advanced secondary systems.

With baseline component characteristics established and expressed in parametric form, parametric vehicle studies were then carried out using ASSET (Advanced System Synthesis and Evaluation Technique) at Lockheed-California Company and GASP (Generalized Aircraft Sizing Program) at Lockheed-Georgia Company. These computer programs were used to determine performance capability, weight, cost, and significant design tradeoffs for both LH_2 -fueled and Jet A-fueled aircraft representing the full range of variables specified for evaluation. The results were analyzed to determine the most satisfactory design of each candidate aircraft configuration for each design range and payload. The LH_2 fueled aircraft designs thus selected were then compared with each other for the purpose of choosing a preferred configuration which, following NASA review and approval, was then critically compared with the reference (Jet A) aircraft in "Benefits Evaluation." The design data and sensitivity tradeoffs derived parametrically provided the basis for comparing the performance and economic potential of LH_2 fueled long range transport aircraft with conventionally fueled aircraft of equivalent mission capability.

The characteristics of LH_2 fueled aircraft sized to carry larger passenger payloads were also determined. Aircraft designs capable of carrying 600 to 800 passengers were established based on the selected configuration to determine the influence of size on aircraft operating characteristics and economics.

Finally, a research and technology development program was formulated based on critical technology requirements identified during the study.

In following sections, the work performed during the study is discussed and the results and conclusions are presented. In Section 3, the technologies which provided the basis for the parametric study are described. Section 4 presents data relative to passenger aircraft and Section 5 is devoted to cargo aircraft. The research and technology development program is discussed in Section 6.

SECTION 3

TECHNOLOGY DESCRIPTION

In this section the technologies are defined which formed the basis for the aircraft parametric studies described in Sections 4 and 5.

3.1 HYDROGEN SYSTEMS

One of the purposes of this study was to explore the problems and possibilities related to the use of liquid hydrogen (LH_2) as the fuel for commercial transport aircraft. In an exploratory investigation such as this, it was necessary to examine the requirements of hydrogen-related structure and equipment in order to establish criteria for estimating hardware weights and costs, and to determine acceptable operational procedures which could be used as a basis for estimating costs. Some of the questions which are addressed in this brief discussion are:

- What is the condition of hydrogen as it would be used on-board the aircraft?
- How will the routine field operations of an airline be affected as a result of using LH_2 as the fuel?
- What are the principal components of the fuel system and what are their functions?
- How will the fuel be carried in the aircraft?

Some of these questions will be treated in more detail in subsequent sections.

For convenience, a tabulation of some of the general physical properties of hydrogen is presented in Appendix A, along with a brief description of chemical properties. Reference 5 is suggested as a convenient source for more specific data on the thermophysical properties of parahydrogen over a wide range of temperatures and pressures.

The aircraft designs of this study were predicated on the basis that hydrogen is stored on board in liquid form at a nominal absolute pressure of 145 kPa (21 psia),

which corresponds to an equilibrium temperature of -251.6°C (-421.3°F). To maintain the hydrogen at this cryogenic condition for extended periods without unacceptable loss due to boiloff, the tanks are carefully insulated. Fuel lines and valves which carry the LH_2 to the engines are also heavily insulated.

A conceptual diagram of the elements of an aircraft LH_2 fuel system is shown in Figure 2 (for a detailed description, see Paragraph 3.1.1). Nominal pressures and temperatures are shown on the diagram for each of the significant conditions which exist as the cryogenic fluid moves through the system from tank to engine combustion chamber. Tank-mounted, submerged pumps boost the pressure from the tank level to 241 kPa (35 psia) for delivery through the feed system as a sub-cooled liquid to high pressure pumps mounted in each engine nacelle. There the pressure is raised to approximately 5160 kPa (750 psi) where, as a gas, it passes through a heat exchanger and picks up heat from a secondary coolant, e.g., a mixture of sodium and potassium (NaK), which has been used to cool the engine high-pressure turbine stages. At this same point, another heat exchanger, also using an intermediate coolant, can be employed to cool the air bled from the compressor to

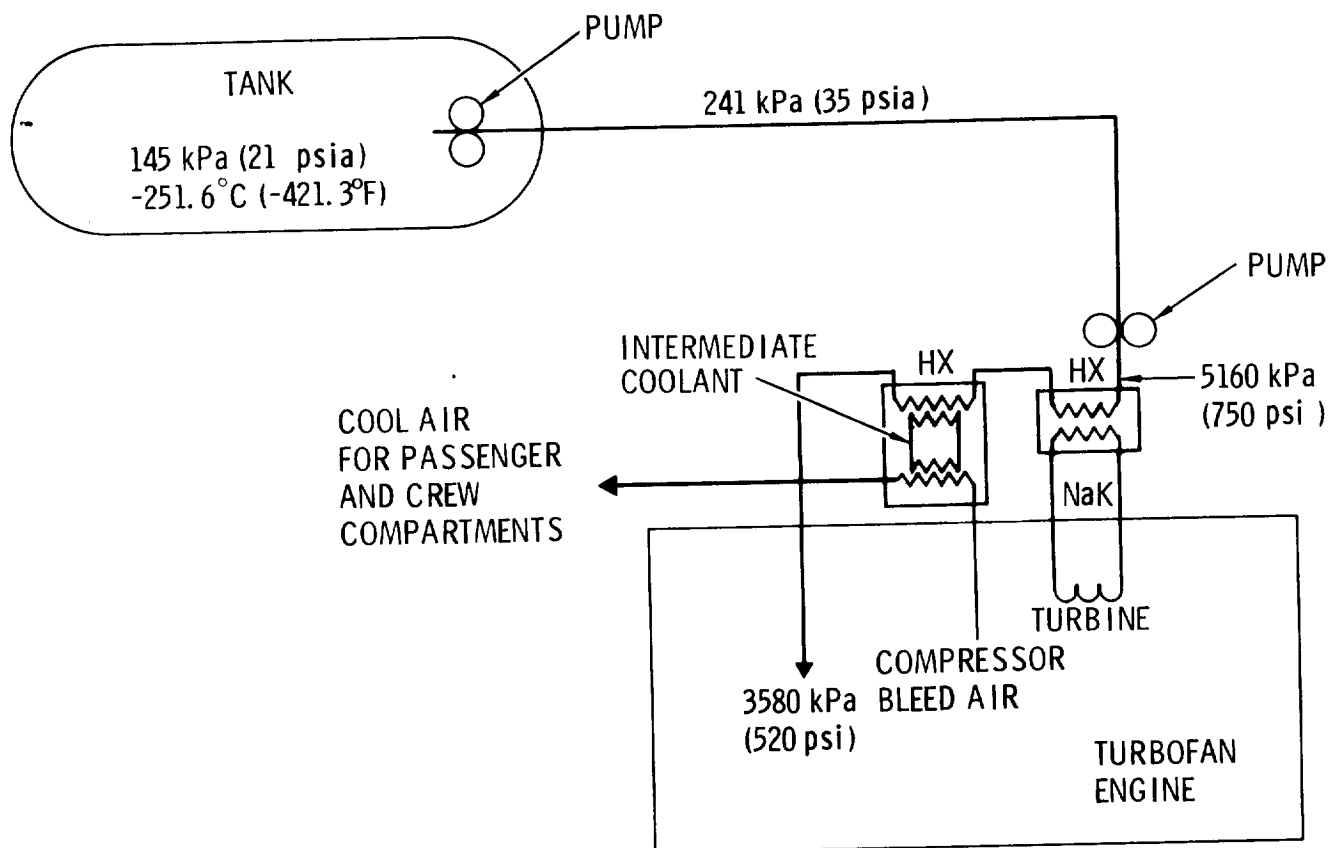


Figure 2. Hydrogen Fuel System Elements

pressurize the passenger and crew compartments, thus eliminating the need for conventional mechanical refrigeration equipment for an environmental control system (ECS). Accounting for the pressure drop through the heat exchangers, engine control valves, and fuel injection system, the fuel reacts in the engine combustion chamber at the nominal design pressure of 3580 kPa (520 psi).

As mentioned, the fuel tanks are carefully insulated to minimize loss of hydrogen by boiloff and to prevent frost buildup on the external surfaces. During service, some liquid hydrogen will be kept in the tanks at all times to maintain the system at cryogenic temperature, thus avoiding subjecting the tank structure and support system to extreme and repetitious temperature cycling, and eliminating the requirement for expensive and time-consuming chill-down and/or purge operations. Gaseous hydrogen, vented from the aircraft tanks to maintain design pressure during out-of-service periods, would generally be recovered and reliquefied, or could be used to fuel ground service power units.

For extended out-of-service periods, e.g., when some type of major maintenance not related to the tank or insulation system is required on the airplane, the tanks would be defueled and purged with nitrogen but maintained at a pressure slightly greater than ambient. This might be expected to occur not more than two or three times per year.

For inspection or repair of the tanks themselves, or their insulation system, after nitrogen purge the tanks would be vented to the atmosphere and could then be safely entered by maintenance personnel. During the early service life of the aircraft, it is expected that the regulating agencies will demand frequent tank and insulation inspections to assure continued flightworthiness and to gain service knowledge. In routine commercial airline service, after cryogenic tank design is well established, this kind of inspection would be considered to be in the same category as that required for aircraft primary structure, i.e., normally performed at intervals of 8,000 to 10,000 hours of operation, or roughly every two, or two and one-half years.

Operational procedures for LH_2 fueled aircraft are conceived as being not radically different from current practices. The equipment would be different of course, but the manpower and the elapsed time per function should be virtually the same. Because of existing safety regulations involving quantity/distance relationships, plus recognized psychological barriers, it is probable that, at least initially, hydrogen-fueled aircraft will be required to refuel at a distance of about

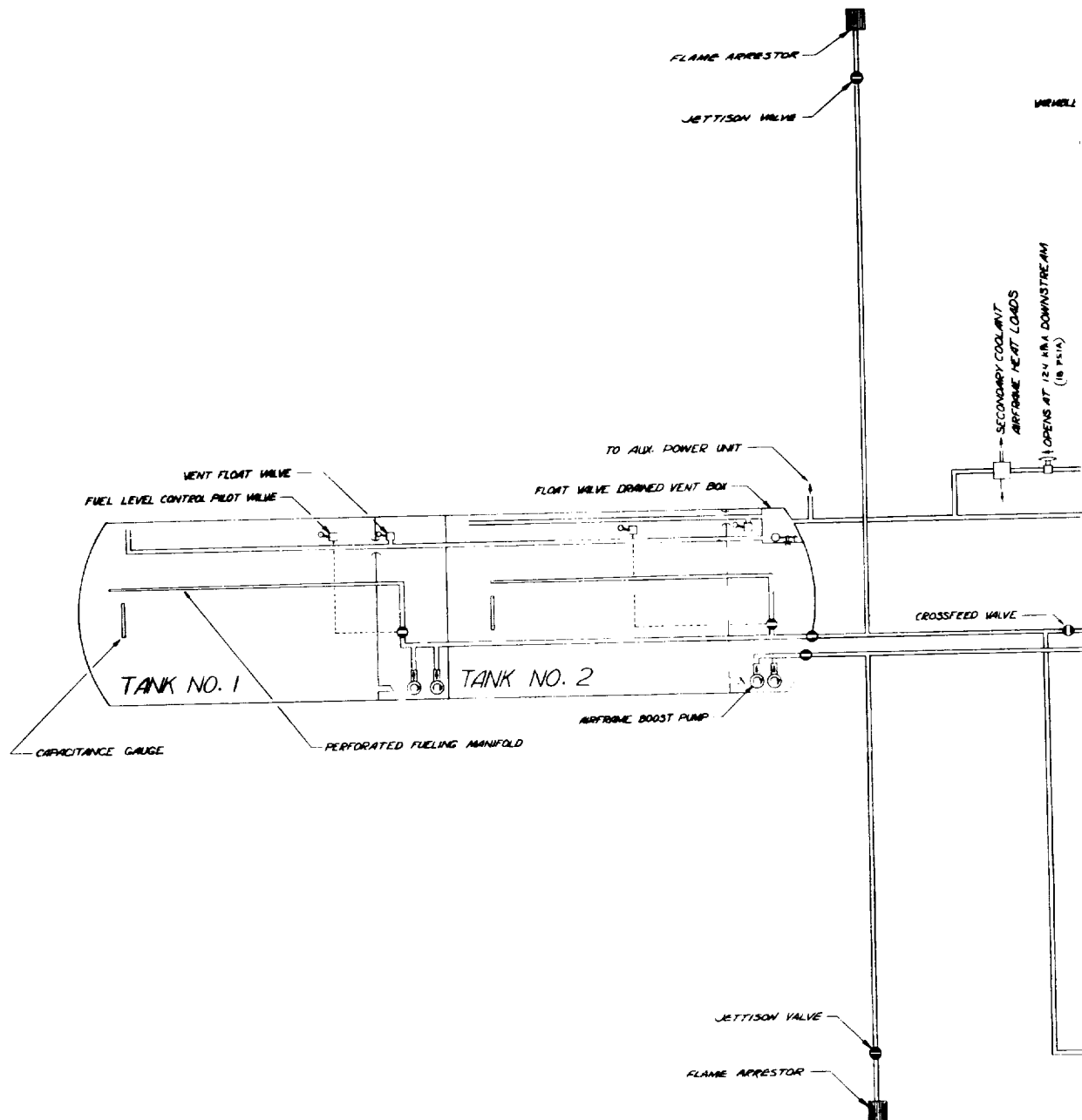
600 m (1800 ft) from passenger terminals. One concept of a feasible arrangement for an LH_2 fueling terminal at an airport is described in Section 4.7.1. Aircraft would be towed to the fueling area and a probe and drogue-type connection established between a service tower and the fueling point located in the tail of the airplane.

During a routine fueling process, estimated to require about 30 minutes for a normal turn-around, cabin attendants can perform housekeeping chores, cargo can be loaded, and food service stowed. Upon completion of these services the airplane would be towed to the passenger terminal, the people boarded, and the flight would then be ready for takeoff. In the event of an unscheduled ground hold of significant duration, a truck-mounted mobile unit could be employed to "top off" the fuel supply if required. With properly designed equipment and scheduling of operations there is no obvious reason a hydrogen-fueled airplane should require more time for turn-around than conventional Jet A-fueled aircraft.

3.1.1 LH_2 Fuel System Description

For the aircraft involved in this study, the LH_2 fuel system, illustrated in Figure 3, consists schematically of two pressurized and insulated tanks (each divided into two compartments), insulated feed lines to each of four turbofan engines and one auxiliary power unit, heat exchangers to transfer airframe and engine heat loads to the cryogenic fuel, fuel quantity gauging equipment, refueling, and defueling systems, and possibly a fuel jettison system.

Tank Vent and Pressurization - The fuel tanks are maintained at a pressure of 125 kPa (21 psia) by an absolute pressure regulator located between the common vent line for all fuel tanks and a lightning-protected vent with flame arrestor which permits overboard discharge of gaseous boiloff at the top of the vertical tail without the hazard of flame propagation back to the fuel tanks. This pressure was selected as a compromise between a number of considerations including the need to eliminate the possibility of air entering the system, unnecessarily penalizing tank weight, and minimizing flashing losses. If the tank pressure drops below 124 kPa (18 psia) because of exceptionally high engine fuel demand, a secondary absolute pressure regulator located in the No. 4 engine feed line opens, allowing a small amount of fuel at pump discharge pressure to be vaporized by heat from the airframe heat loads before it is conveyed to the tanks through the normal vent system.



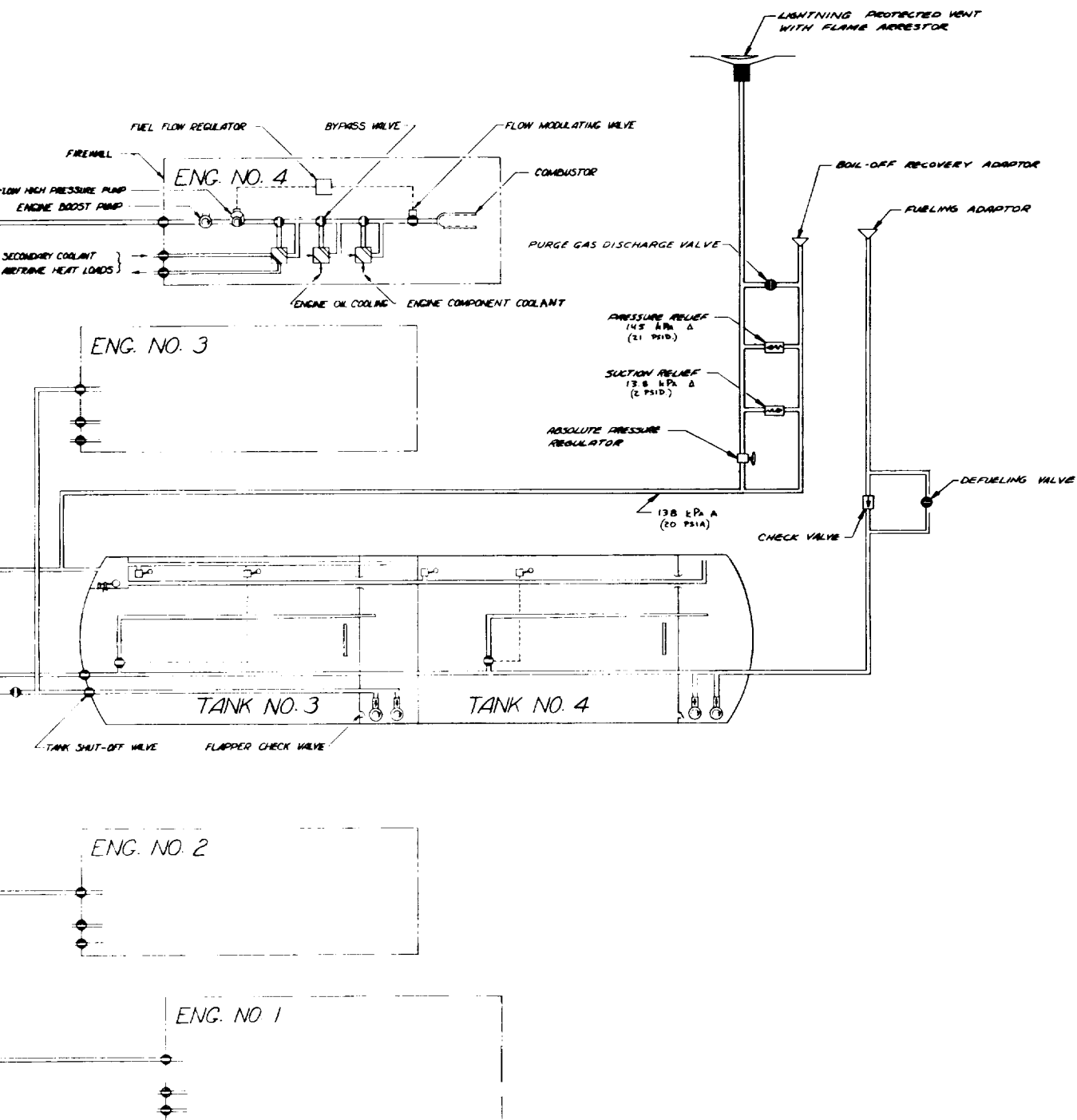


Figure 3. LH₂ Fuel System Schematic

In the event tank pressure exceeds 152 kPa (22 psi) above free stream ambient, a pressure relief valve opens to bleed off the excess pressure through the vent line flame arrestor. A tank rupture disc is also provided in the case of a dual failure of both the tank pressure regulator and the pressure relief valve. If, for any reason, the tank pressure falls below ambient outside pressure, suction relief is provided at 14 kPa (2 psi) below ambient to prevent collapse of the tanks. This condition could only exist if all of the fuel had been exhausted during a descent and if the normal vent closure did not occur, or as a result of an extended ground standby with empty fuel tanks, again if the vent valve was not actuated properly.

A boiloff recovery adaptor and valve are provided adjacent to the fueling adaptor to permit the operator to return gaseous boiloff to ground storage facilities for reliquefaction or use of the GH_2 in ground-based power units. This minimizes economic loss resulting from hydrogen boiloff during periods when the aircraft is out of service.

Vent openings are located in the forward and aft ends of each tank. Float-operated vent valves in the opening nearest the vent box prevent fuel from flowing by gravity into the vent box. Liquid fuel which collects in the vent box is drained into the adjacent fuel tank through a float-operated drain valve.

Propulsion Engine Feed System - Each fuel tank is normally connected to its identically numbered engine. However, a system of cross-feed valves permits any one tank to supply fuel to any engine if required or, by properly sequencing the operations of the cross-feed and refueling valves, permits transfer of fuel from one tank to another.

Two boost pumps are located in a surge box in each tank to ensure fuel availability and to prevent fuel starvation during aircraft maneuvering at low fuel levels. The boost pumps are designed to pump boiling hydrogen and to supply it to the main engine pumps in a subcooled state by means of vacuum-jacketed feed lines. All airframe and engine heat loads, with the exception of the tank pressurization heat loads, are added downstream of the high-pressure engine pumps.

APU Feed System - The auxiliary power unit is operated on gaseous hydrogen, thereby minimizing boiloff losses during the considerable periods of APU operation while on the ground. APU feed is available from the common tank vent line. If insufficient boiloff is released from the tanks, due to the presence of super-cooled hydrogen just subsequent to refueling, operation of the No. 4 tank-mounted

boost pump will maintain gas flow through the secondary coolant heat exchanger at 124 kPa (18 psia) to the APU.

Refueling and Defueling System - All tanks are refueled through a pair of pressure-fueling adaptors located at the bottom of the aft fuselage just aft of the tail bumper. Part of the refueling manifold is common with the No. 1 and No. 4 engine feed lines (see Figure 3). Inside each tank, a portion of the fueling manifold is perforated along its entire length to distribute the liquid hydrogen uniformly over the tank walls, thus minimizing the tank wall thermal stresses. A dual fuel-level control pilot valve in each tank stops the flow of fuel to that tank when it has reached its full level at approximately 96% of total volume. Integral with the float valve is a solenoid valve which permits manual or preset shut-off of the valve at any tank level and also prevents overfilling in the event of a float valve failure.

Boiloff occurring during the refueling process is returned to a ground hydrogen recovery system by means of a line connected to the boiloff recovery adaptor which is located immediately adjacent to the ground fueling adaptors. Thus, during the fueling operation, no hydrogen vapors are discharged overboard.

Prior to refueling tanks that have contained air, the fueling system must be purged through the fueling adaptor by an inert medium (e.g., gaseous nitrogen) to remove all oxygen, followed by gaseous hydrogen to remove all inerting gas. The purge system will utilize the purge gas discharge valve to discharge the purge gases around the pressure relief valve and overboard through the lightning protected vent.

Defueling may be accomplished through the defueling valve to the fueling adaptors by operating the boost pumps with open cross-feed valves. The tanks may be defueled individually or simultaneously.

Fuel Jettison System - It is not expected that a jettison system will be required; however, the requirement can be met by the system illustrated in Figure 3. It operates in a manner similar to the defueling system except that the hydrogen is routed through jettison valves and flame arrestors installed in dump masts located at the wing trailing edge outboard of the No. 1 and No. 4 engine nacelles. A specific decision regarding the need for a jettison system should await a more complete definition of the ground rules followed by a detail design study of the alternatives involved.

Fuel Quantity Indicating System - Capacitance gauges can be used to measure fuel volumes. The units would be calibrated to indicate fuel quantity in pounds at the fuel management panel and can be used in conjunction with the refuel pilot valve solenoids to load fuel to any predetermined level, or to shut down the refueling operation when the tanks are full as a back-up to the float pilot valve.

Fuel System Design Considerations - As a design objective, fuel system components such as pumps and valves will be designed for quick removal and field replacement in a manner commensurate with present commercial operation. System failure provisions should also provide for back-up of critical dispatch items as in current practice.

The broad aspects of flight safety require consideration and development of fuel system components and arrangement in terms of malfunction and leak detection, isolation, inerting and/or purging and fire containment. Safety criteria and acceptable design practices must be established based on current practice and philosophy, but with due consideration of the unique properties of hydrogen.

3.1.2 LH₂ Tank Structural Concepts

Design of tanks to contain liquid hydrogen efficiently in the subject aircraft is recognized as one of the crucial technical challenges. The task involves consideration of the following:

- Materials
- Structural concept
- Insulation arrangement
- Inspection and maintenance capability
- Purge requirements and capability

Materials used for tank construction must be resistant to hydrogen embrittlement, impermeable (or capable of being sealed) to gaseous hydrogen, and, depending on the insulation arrangement, retain satisfactory ductility and fracture resistance at cryogenic temperatures. In addition they must be amenable to repair and maintenance. Structural concept selection must in turn consider problems of

- differential thermal expansion,
- heat leaks to tank structure as a result of attachments, and
- materials compatibility

in addition to the fundamental problem of design for light weight while maintaining adequate structural integrity.

The influence of differential thermal expansion on aircraft structure is dependent on the insulation system employed for the fuel tanks. If cryogenic insulation is applied to the inside of the tanks, the tank walls remain at near-ambient temperature so differential thermal expansion, relative to the warm aircraft skin and primary structure, is minimized. Similarly, the problems of attachment and support for the tanks are simplified. On the other hand, if conditions require the cryogenic insulation to be applied to the exterior of the fuel tanks, the tank itself will significantly contract and expand as LH_2 at -252.8°C (-423°F) is introduced and used. Attachment problems are therefore severe, not only because of the dimensional changes which must be accounted for, but also because of the thermal "short" which may result.

The necessity of being able to inspect the tanks and to satisfactorily maintain them to airline standards is an aspect which cannot be overlooked. Finally, in those designs where the fuel tanks are within the aircraft framework and where it is therefore possible for leaking gaseous hydrogen to collect in a confined space, provision must be made for a purge system using either an inert gas or copious quantities of air.

Two basic types of tank designs were considered in the light of these requirements for the subject applications: integral, where the tank serves both as the container of the fuel and also carries the fuselage structural loads; and non-integral, in which case the tank merely contains the fuel and a separate structure is provided to resist fuselage axial, bending, and shear loads. It might immediately be concluded that if there was a reasonable chance of designing a structure to perform two separate functions, where the structural requirements of the two did not result in directly additive stresses, the choice between integral and nonintegral would be simple.

This is indeed the case, and in a previous study, the study of hydrogen-fueled supersonic transport aircraft documented in reference 6, it was found that the integral tank concept offered attractive advantages, both in weight and in volumetric efficiency. However, there are significant differences in the design conditions between a supersonic transport aircraft and a subsonic vehicle. For example, in the present study of long-range subsonic transport aircraft, the flight duration

is so long relative to that of the supersonic transport in the reference study, a comparison of 11.5 hours for a 10,200 km (5500 n.mi) mission vs. less than 3.5 hours for a 7,780 km (4200 n.mi) mission, it was felt the effect of heat leak through tank support structure, significantly greater for the integral concept, might overbalance some of the other considerations. Subsequent investigation found however, that although the heat loss attributable to the tank supports of the integral concept was larger than that through the pin joints of the nonintegral design, it was still a small fraction of the total and not of major significance. Another factor of major difference, the thermal environment at cruise condition, will be discussed later.

The integral tank concept is pictured in Figure 4. The sketch shows the basic tank is aluminum alloy skin (2219) with longitudinal stringers on the inside and with circular frames at 0.508 m (20 in) spacing. A bulkhead to dampen fuel slosh is located every 5.08 m (200 in) along the length of the tank. The tank is encased in a rigid, closed-cell plastic foam for cryogenic insulation which in turn is enclosed in a secondary vapor shield to prevent cryopumping in the event the foam insulation develops a crack. The tank is structurally connected to the aircraft fuselage by a truss-like interconnect structure consisting of a series of boron-reinforced fiberglass tubes of special design which were developed by Lockheed Missiles and Space Company in a separate study (Reference 7). This design of truss member was selected because it appears to offer maximum stiffness for minimum weight and minimum heat transfer.

A fiberglass sheath covers the entire tank, insulation, and support structure assembly to provide mechanical protection for the foam insulation and its vapor shield. In the event either the foam insulation or the aluminum tank requires repair, the fiberglass sheath would simply be cut away locally and then patched upon completion of the work. Inspection of the tank structure can be accomplished from inside the tank. A crawlhole can be provided in either end.

The nonintegral tank concept is illustrated in Figure 5. The difference in the two designs is apparent, particularly in the method of support. In the nonintegral concept the tank is simply a bladder which contains the fuel, resists internal pressure, and supports the weight of the fuel between four pin joints, two on either side. The pin joints are designed in the same manner as engine mounts to permit thermal expansion and contraction between the load points, yet offer firm

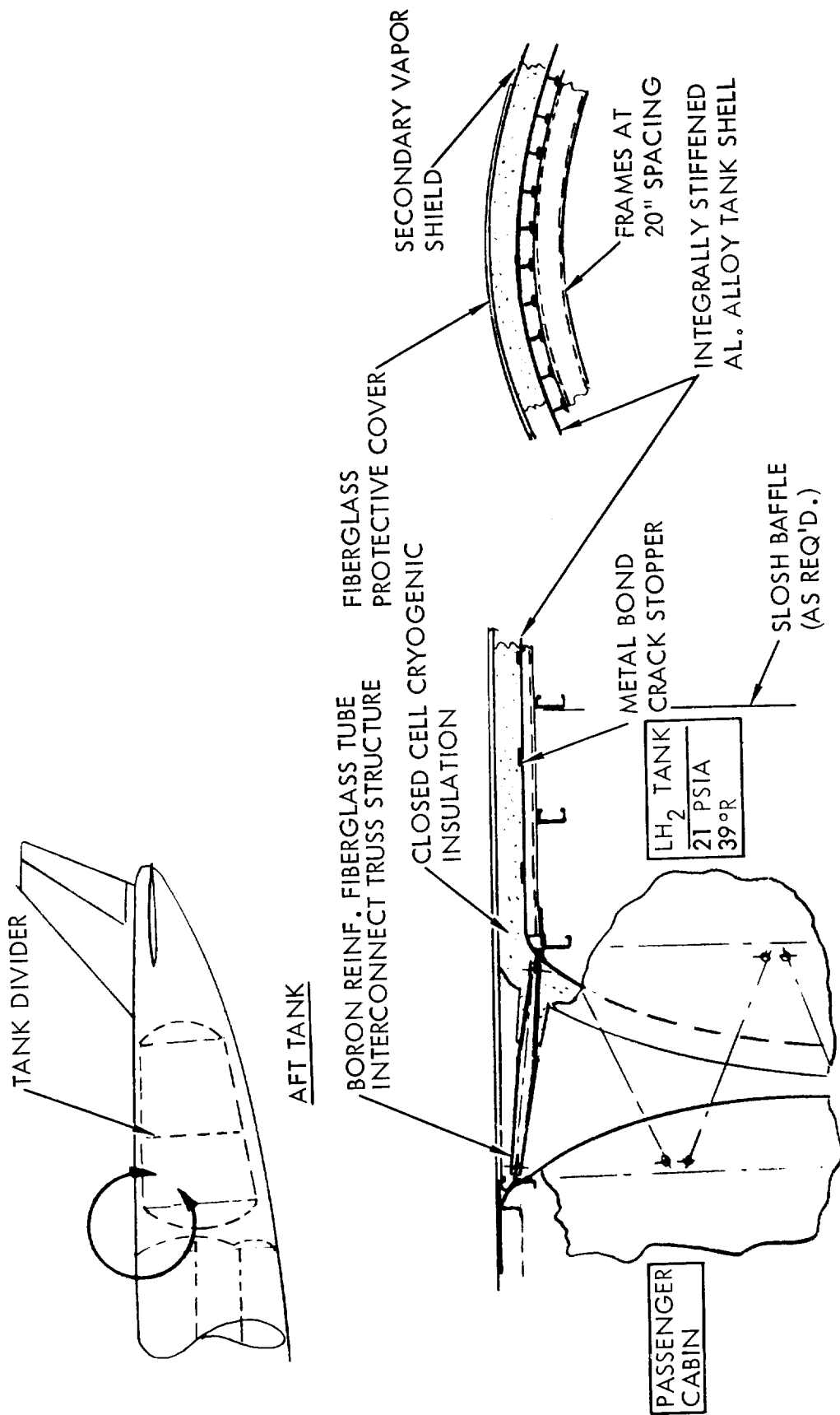


Figure 4. Integral Tank Concept

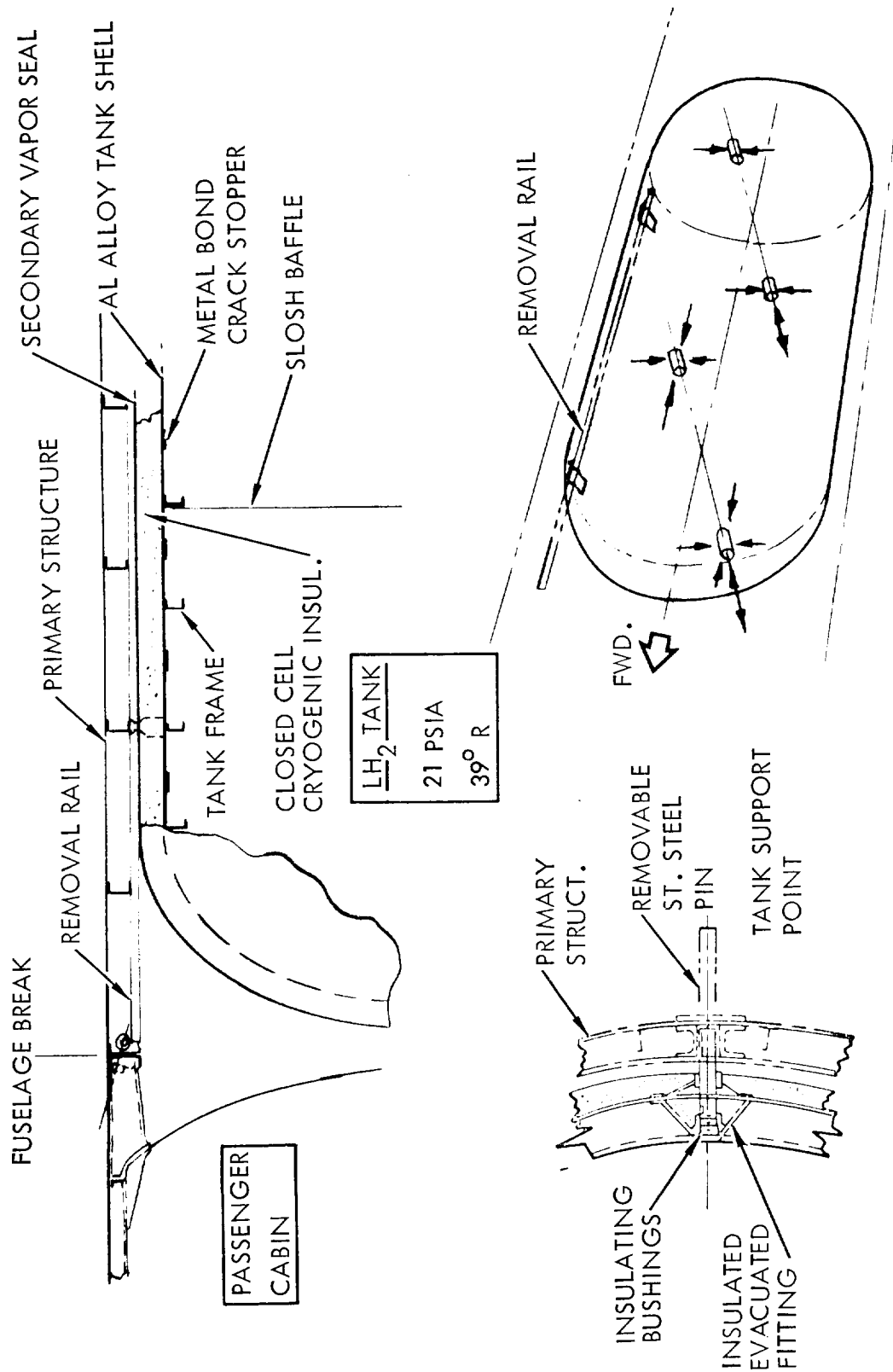


Figure 5. Non-Integral Tank Concept

mechanical support. The diagram in the lower right hand corner of the figure illustrates the degrees of freedom at each of the support points.

The bladder tank does not have longitudinal stringers; it depends on the rigid foam insulation, bonded to the welded aluminum tank, for resistnace to shear and compression buckling. A few circular frames are provided to maintain the tank shape and for baffles as required. Frames are also located at the pin support points.

Conventional fuselage skin/stringer/frame construction encloses the tank and provides its support. In order that inspection and maintenance can be performed on the tank and the insulation, it is necessary to provide a break point in the fuselage so it can be separated. The tank is then removed by sliding it out on a special rail built into the fuselage.

Comparing the two tank design concepts, the advantages of the integral are obvious. The tank structure and insulation are both easily inspected and maintained. It is not necessary to take the airplane apart to accomplish either. The volumetric efficiency advantage of the integral design is apparent when it is considered that an annular volume equal to the width of the fuselage frames in the nonintegral case, plus approximately an inch for clearance on the radius, multiplied by the length of the tank less its ends, is lost to the nonintegral concept. Numerically, comparisons of volumetric efficiency and that of tankage-weight fraction are illustrated by the following data from the report of Reference 6:

	Tank Concept	
	Nonintegral	Integral
Volumetric efficiency	0.855	0.927
Tankage-weight fraction	0.408	0.340

Volumetric efficiency is defined as the ratio of usable tank volume-to-volume occupied in the fuselage. Tankage-weight fraction is the ratio of the weight of the tank, insulation, and support structure to the weight of the hydrogen contained in the tank. It is recognized, of course, that the weight fractions for both tank concepts would be lower in a subsonic airplane application because of elimination of the requirement for the high temperature heat shield. Accordingly, the weight advantage for the integral tank design in subsonic transport aircraft would be a smaller percentage.

On the basis of this experience and these conclusions it was decided that the integral tank concept would be used wherever possible in the design studies of subsonic LH_2 transport aircraft. However, as reported in Section 5, it was found that there were overriding considerations in the case of the cargo aircraft which led to use of special designs of nonintegral tanks.

3.1.3 LH_2 Tank Insulation System

The fundamental requirements for the insulation applied to the LH_2 aircraft tanks are 1) to control hydrogen boiloff to acceptable levels, and 2) to eliminate or minimize frost buildup on the external surfaces. Criteria for selection of a candidate system for use in the present study were

- Weight
- Cost
- Maintainability
- Development status

As previously mentioned, an ideal cryogenic insulation could be applied either to the inside or the outside of the tank. There are advantages and disadvantages to both. In the case of internal insulation the advantage is in having a tank structure which is relatively conventional. The problem is that the insulation system, being constantly exposed to the hydrogen, must be impermeable so GH_2 cannot diffuse to the tank wall, thereby raising the thermal conductivity coefficient of the insulation to that of hydrogen and crippling its effectiveness. The external insulation approach presents the opposite set of problems, the insulation is exposed to the less rigorous requirement of preventing cryopumping which would occur if air diffused through the insulation and contacted the cold tank wall. However, attachment to and support of the tank structure becomes a problem, as does routine inspection of the tank.

Cryogenic insulation systems that have been developed for use in ground transportation and ground storage applications use Linde Superinsulation, which is a double wall, evacuated annulus containing multiple layers of highly reflective material. Unfortunately, it is too heavy for aircraft application and the probability of maintaining a satisfactory vacuum in the very large surface area of the annular jacket around a fuel tank for long periods with a lighter weight version of the existing design concept is not high. Moreover, Superinsulation also

represents a degree of thermal protection which is probably not necessary for aircraft use.

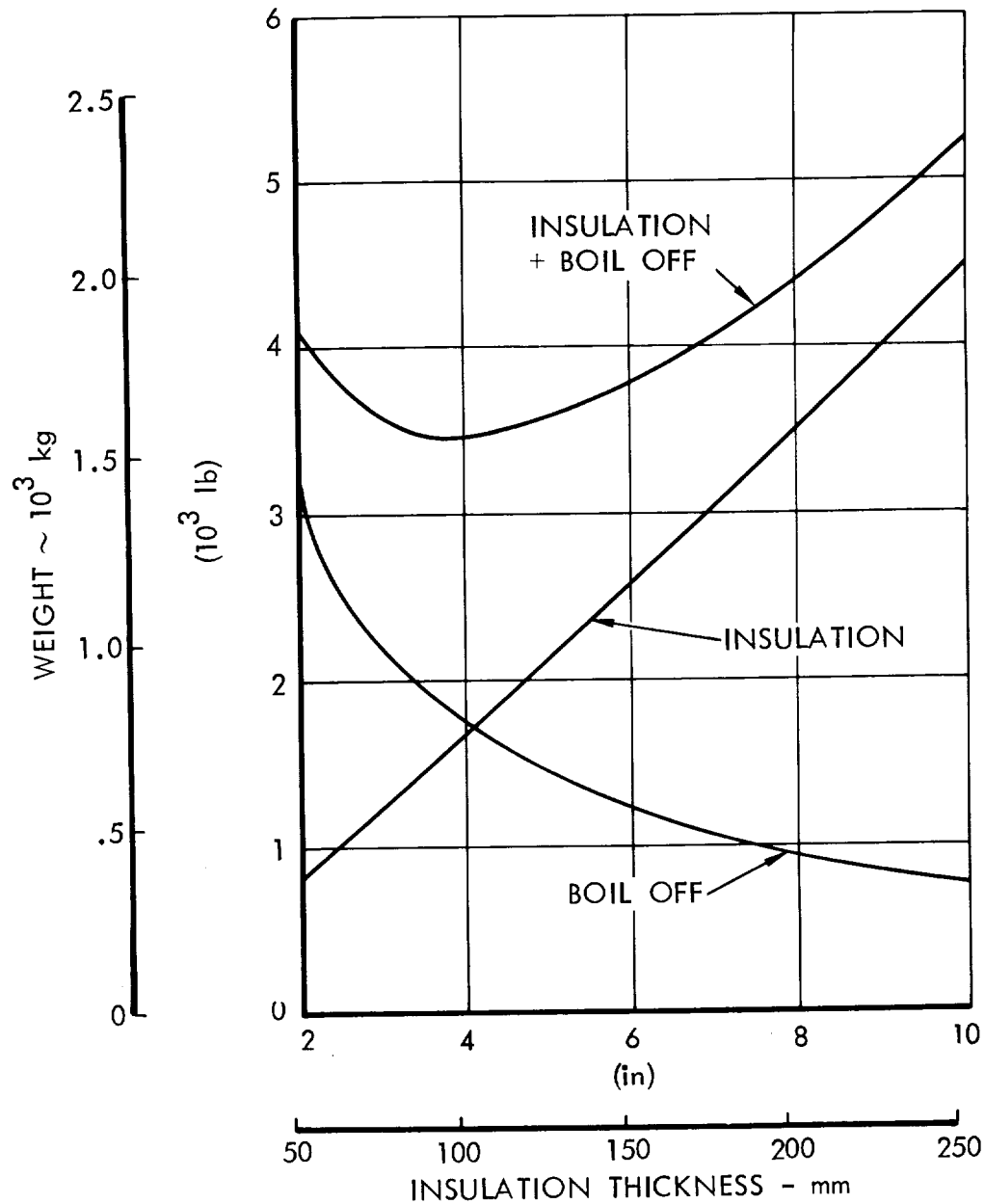
On the basis of work to date, the rigid foam insulants listed in Table 8, Section 3.5, seem to offer the most attractive potential for aircraft applications. The polyvinylchloride, reinforced polyurethane, and polymethacrylimide closed-cell foams are all promising candidates. These are none, however, which are impervious to GH_2 so consideration of the internal insulation system must await development of a suitable material. Accordingly, attention in this study was focused on the external insulation system. The characteristics of Rohacell 41S, the polymethacrylimide foam with fire retardant additives, were used to represent this general category of insulant in the parametric design study.

A design study was carried out to determine the thickness of insulation which should be applied to the outside of the hydrogen tanks of the subject aircraft to provide best thermal protection for least weight and cost. Preliminary sizing analysis provided characteristic data for a 10,190 km (5500 n.mi) range, M 0.85, 400 passenger airplane to use as a basis for the insulation thickness study.

The starting point was to derive the conventional tradeoff between insulation thickness and weight for both the insulation material and the boiloff hydrogen during flight. The result is shown in Figure 6. Minimum combined weight of insulation plus boiloff occurs at approximately 100 mm (4 in) of insulation.

Figure 7 translates insulation thickness into terms of airplane gross weight, block fuel required, and airplane production price. The data shown were calculated as an iteration of a preliminary sizing point vehicle, adjusting empty weights in accordance with the various insulation thicknesses, and accounting for the boiloff of hydrogen in flight. A very slight shift of the optimum point in the curves can be noted, showing a preferred thickness of insulation to be just in excess of 100 mm (4 in.).

The next step was to determine the limitations on insulation thickness which might be imposed by ground-hold conditions; specifically, the possibility of frost buildup on the external surface of the insulation, the the GH_2 boiloff rate while the aircraft is on the ground. These results of the analysis of the temperature of the external surface of the insulation are shown in Figure 8. The curve indicates there is no problem with frost buildup, the minimum temperature of the external surface of the insulation is about 23.4 C (45 F) with 100 mm (4 inches) of insulation.



DESIGN CONDITIONS:

INTEGRAL
INTERNAL TANK

RANGE = 10,190 km (5,500 n.mi.)

MACH = 0.85

FLIGHT TIME = 11.7 hrs.

FWD. TANK

VOL. = 246 m³ (8,700 ft³)

TANK PRESS. = 138 k Pa (20 psi)

Figure 6. Insulation Thickness vs. In-flight Boiloff

INTEGRAL
INTERNAL TANK

RANGE = 5500 NM

MACH = .85

FLIGHT TIME = 11.7 HRS

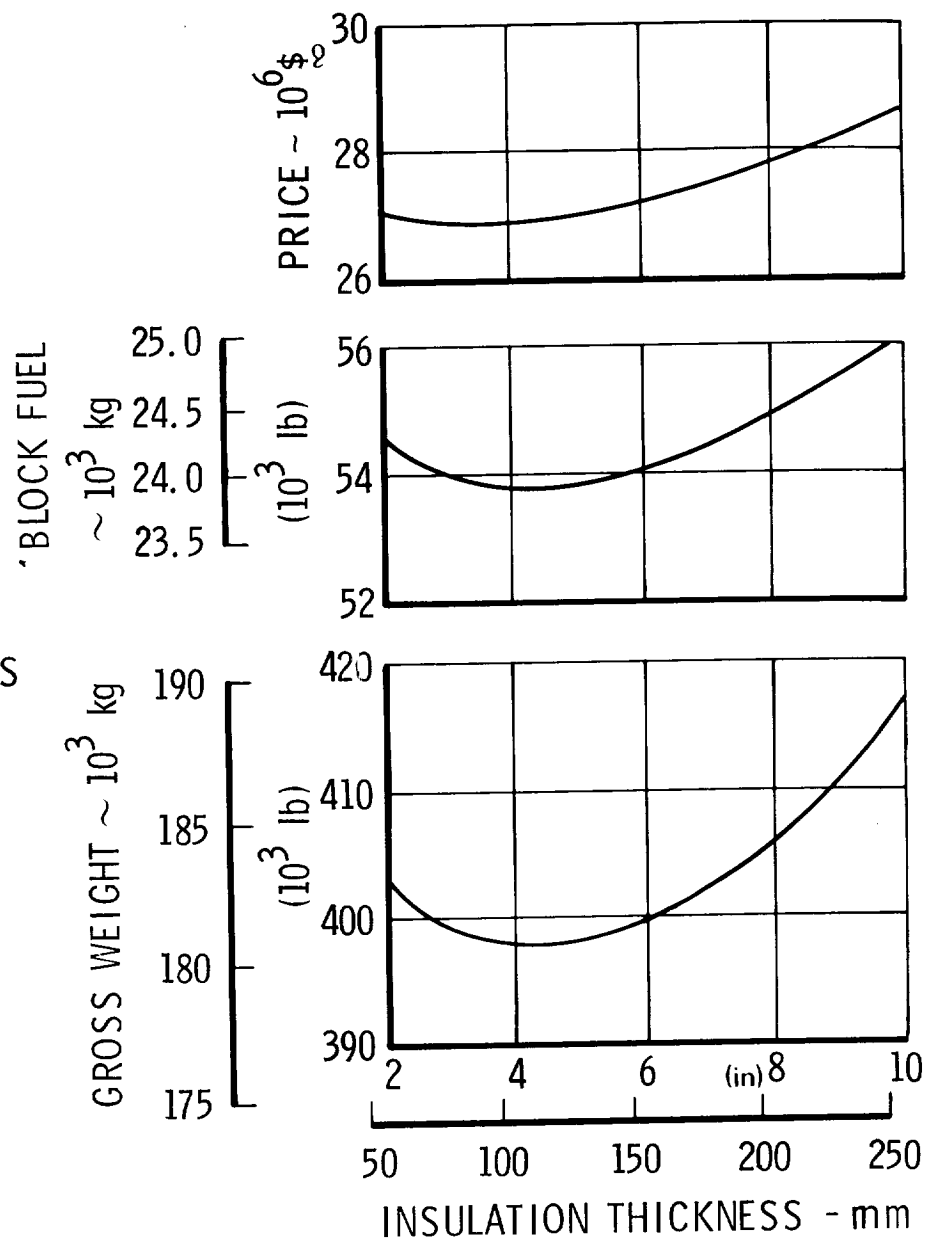


Figure 7. Effect of Insulation Thickness on Vehicle Characteristics

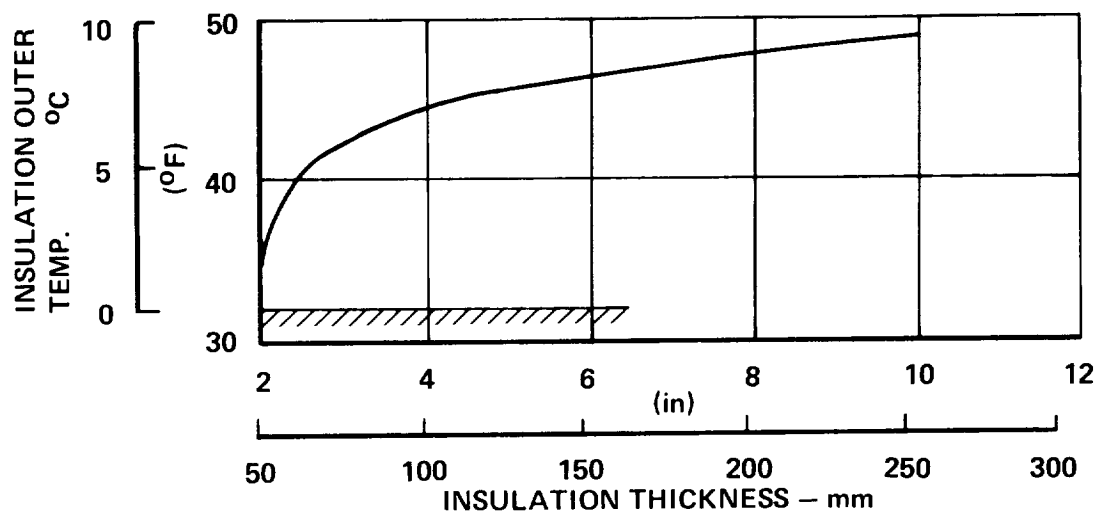


Figure 8. Insulation Surface Temperature vs. Insulation Thickness

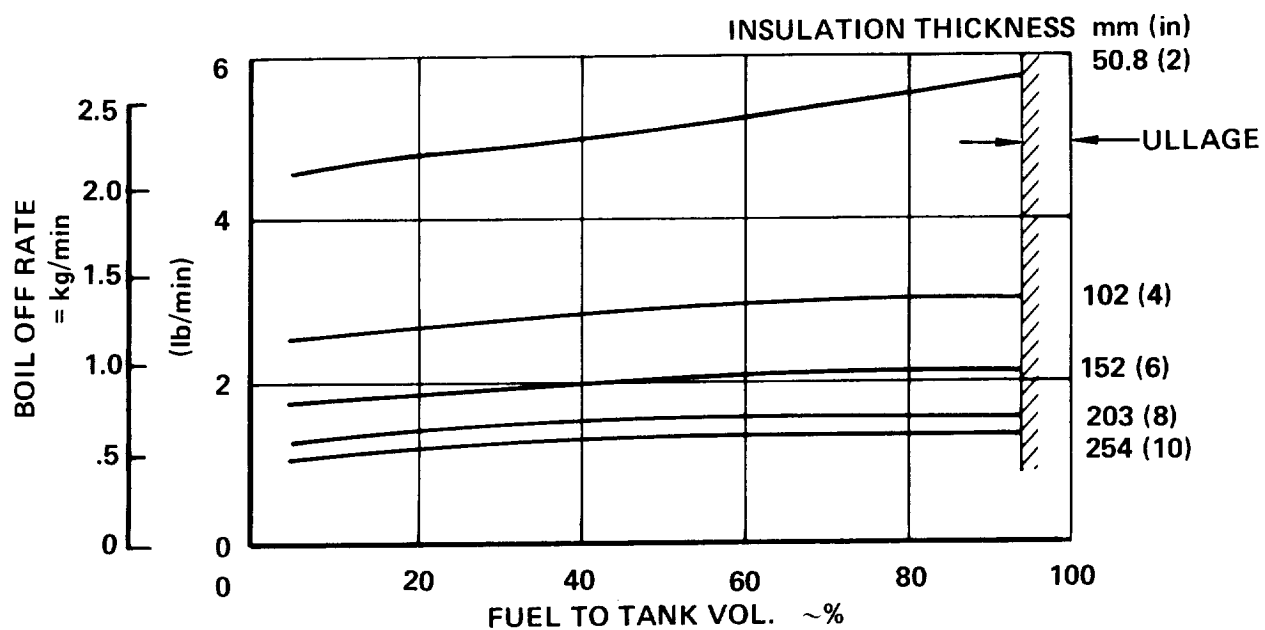


Figure 9. Ground Boiloff Rates vs. Insulation Thickness

Figure 9 shows the boiloff rate for various thicknesses of insulation as a function of quantity of fuel in the tank. Although the slopes are not great, the results indicate a small payoff for storing the aircraft during out-of-service periods with only small quantities of LH_2 in the tanks.

The final step in this analysis is shown in Figure 10, a plot which considers the economic aspects of the question. Airplane cost, amortized over 15 years and used an average of 3285 hours per year over that period, is plotted along with cost of block fuel and cost of hydrogen boiled off both during flight and on the ground, in terms of cost per flight hour as a function of insulation thickness. The minimum point in the top line, the cumulative effect of all factors, occurs at an insulation thickness of about 165 mm (6.5 in.). These results were obtained on the basis of no recovery of boiled-off hydrogen on the ground, e.g., as if vent gases were simply allowed to escape. In comparison, the minimum point in the second curve from the top, which includes in-flight boiloff but in effect assumes 100 percent recovery of ground boiloff, occurs at about 140 mm (5.5 in.) of insulation thickness. It also shows that recovery of ground boiloff hydrogen can make a difference of about \$68/flight hour based on a cost of LH_2 of \$3 per 1.054 GJ (10^6 Btu), the baseline cost selected for use in this study.

Based on these results a nominal thickness of 152 mm (6 in.) of foam insulation was selected to serve as a basis for performance and cost evaluations of the aircraft in this study.

3.2 PROPULSION

Engine cycles considered in this study were efficient, high bypass ratio turbofan engines of an advanced design which could be available for initial use in 1990.

Even though LH_2 and Jet A fueled subsonic transports require the same basic type of turbine engines, the engine designs are different. The temperature of the air conveniently available to cool the turbines of the Jet A fueled engines is essentially the temperature of the compressor discharge. Maximum metal temperature restrictions and the limited heat sink potential of the compressor discharge air thus restricts both the maximum compression ratio and the maximum turbine temperature available for Jet A fueled engine design.

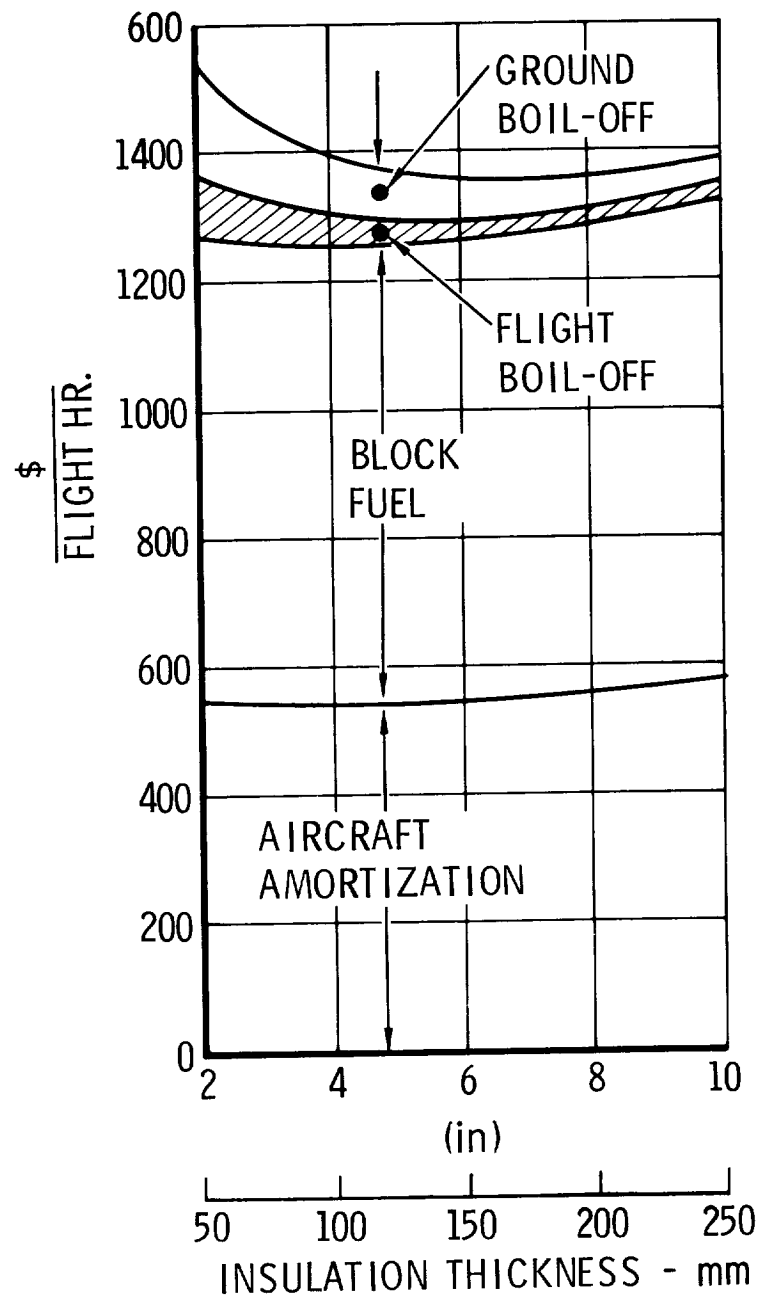


Figure 10. Economic Impact of Insulation Thickness

The cryogenic hydrogen of the LH_2 fueled aircraft provides a large heat sink which can be used for precooling the air or other medium used for turbine cooling. Therefore, unconstrained by other limits, the LH_2 fueled engine's compression ratio and turbine inlet temperature can be independently selected for the optimum overall propulsion performance. Practical limits of overall compression ratios and turbine inlet temperatures appear to be 40:1 and 2093°C (3800°F), respectively (see Figure 11) for engines which might be developed in the 1980's. However, selection of the best cycle parameters for subsonic transport aircraft depends upon a parametric evaluation related to mission requirements.

Although some advanced design Jet A fueled subsonic transport engine data were available from the Advanced Technology Transport (ATT) study, e.g., the P&WA STP433, these data were developed for a near Mach 1.0 transport and thus were biased for the higher speed aircraft design. Further, no comparable LH_2 fueled engine data were available. Therefore, in the interest of direct comparability and cycle optimization, Lockheed conducted its own cycle optimization study and generated the propulsion data for both the Jet A and LH_2 fueled engines used in the study using propulsion installation subroutines and the SYNTHA engine cycle program. In conjunction with the SYNTHA Corporation, Lockheed had previously established SYNTHA subroutines to properly represent the thermodynamic properties of combustion of either Jet A or hydrogen with air. Component efficiencies and technology forecasts for 1985 state-of-the-art are shown in Table 2. The forecasts are based on data and trends discussed below. Also shown are one engine supplier's projection made available for an earlier study.

While the eventual component performance levels achieved depend on the sustained levels of economic support for development, the Lockheed assumptions are believed reasonable. Small changes from these assumed levels will not materially affect the comparisons made between the performance of Jet A and LH_2 fueled aircraft.

Three basic methods were considered for cooling the turbines of the LH_2 fueled engine: (1) aircooling with compressor discharge air; (2) aircooling with compressor discharge air using a H_2 -to-air heat exchanger to chill the turbine cooling air; and (3) liquid metal cooling used in a closed loop with a H_2 -to-liquid metal heat exchanger. In the interest of simplification Lockheed assumed a liquid metal turbine cooling scheme for all LH_2 fueled engine flight performance. The lower high-pressure turbine efficiency used for the Jet A engine in Table 2 reflects the use of compressor discharge cooling air for that engine.

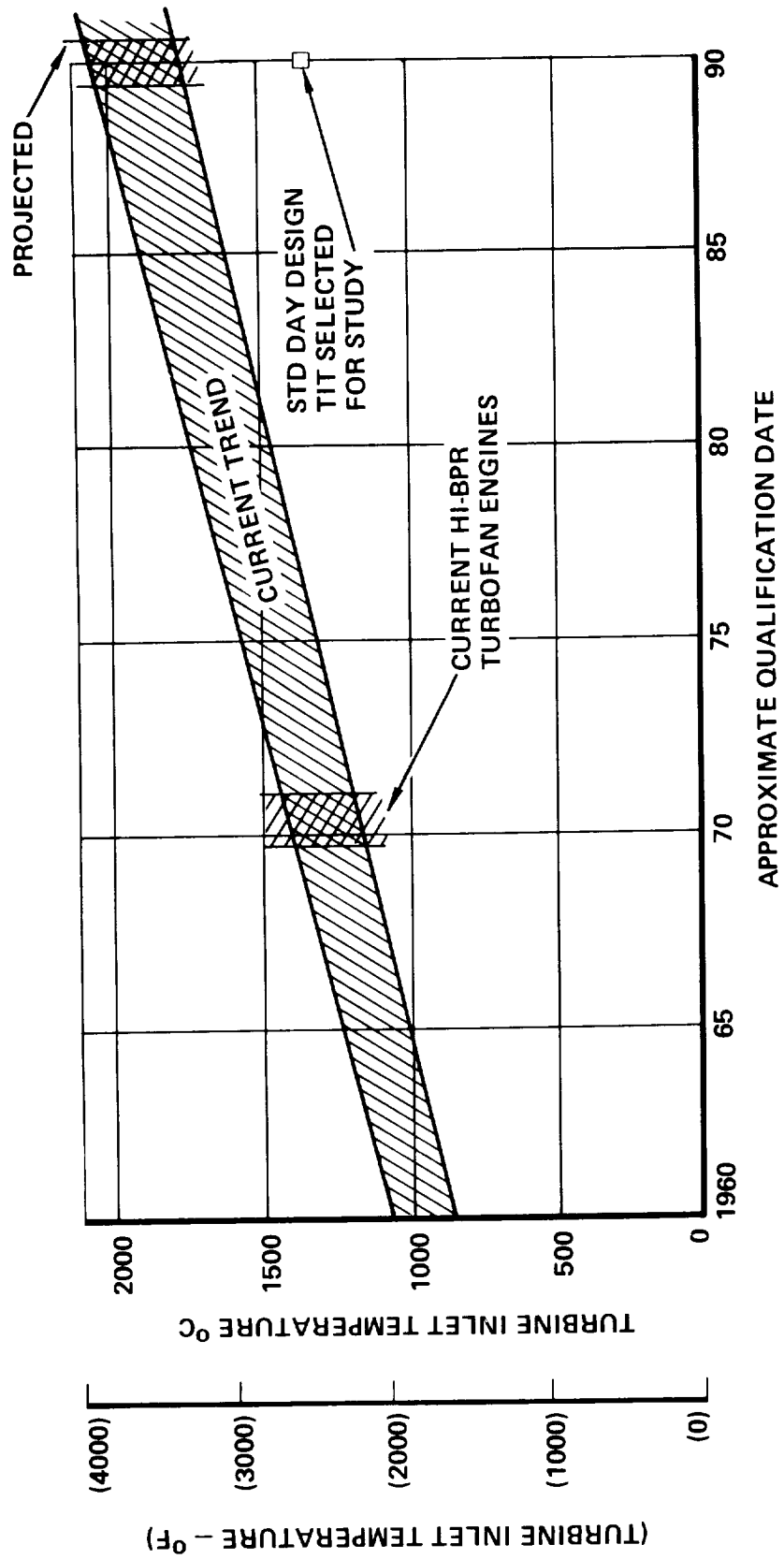


Figure 11. Trend of Turbofan Turbine Inlet Temperatures vs. Qualification Date

TABLE 2. PROPULSION TECHNOLOGY FORECAST
FOR 1985 STATE-OF-ART

	LOCKHEED FORECAST FOR PRESENT STUDY		ENGINE SUPPLIER FORECAST FOR 1980-1985 FROM PREVIOUS STUDY
	LH ₂	Jet A	
Fan Polytopic Efficiency (max)	91%	91%	85 - 91%
Compressor Polytopic Efficiency (max)	92%	92%	92.5%
Turbine Adiabatic Efficiency	HP 91% LP 91%	HP 90% LP 91%	90 - 92%
Combustion Efficiency	100%	100%	100%
Combustion Pressure Loss	4.5%	4.5%	6%

The Sens-Meyer paper (Reference 8) discusses current gas turbine design trends and speculates on the next generation of aircraft powerplants. The paper predicts gas turbine thrust/weight (T/W) values around 8 for the 1980-85 time period. Based on these and other data from studies such as Advanced Technology Transport (ATT) and the Quiet Clean STOL Experimental Engine (QCSEE) program, a thrust-to-weight ratio of approximately 7 was selected as a reasonable value for quieted, high bypass ratio engines which might be developed in the late 1980's.

3.2.1 Cycle Selection

A parametric study was made to select the best fan pressure ratio, overall pressure ratio, and turbine inlet temperature for the subject subsonic transport aircraft. The following figures present the results of this study. Figure 12 shows the parametric effects of fan pressure ratio at a constant turbine inlet temperature and a constant overall pressure ratio without cowl drag. These data show how overall efficiency increases with fan pressure ratio and Mach number when cowl drag is ignored. However, Figure 13 shows that when cowl drag is included in the parametric analysis, then fan pressure ratio optimizes as a function of Mach number and the overall efficiency reaches a maximum near the flight speed where

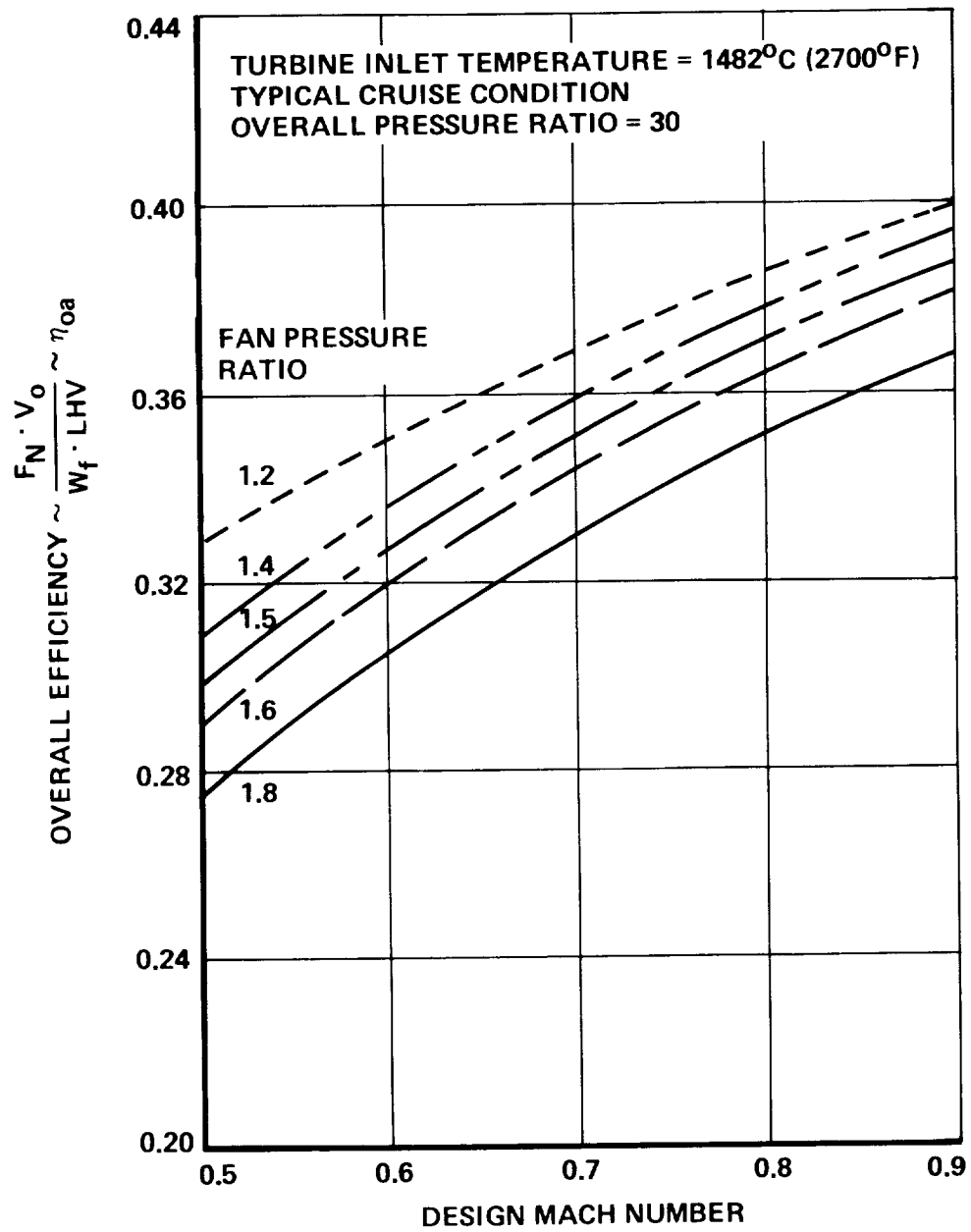


Figure 12. Effect of Fan Pressure Ratio on Overall Efficiency vs. Mach Number - No Cowl Drag

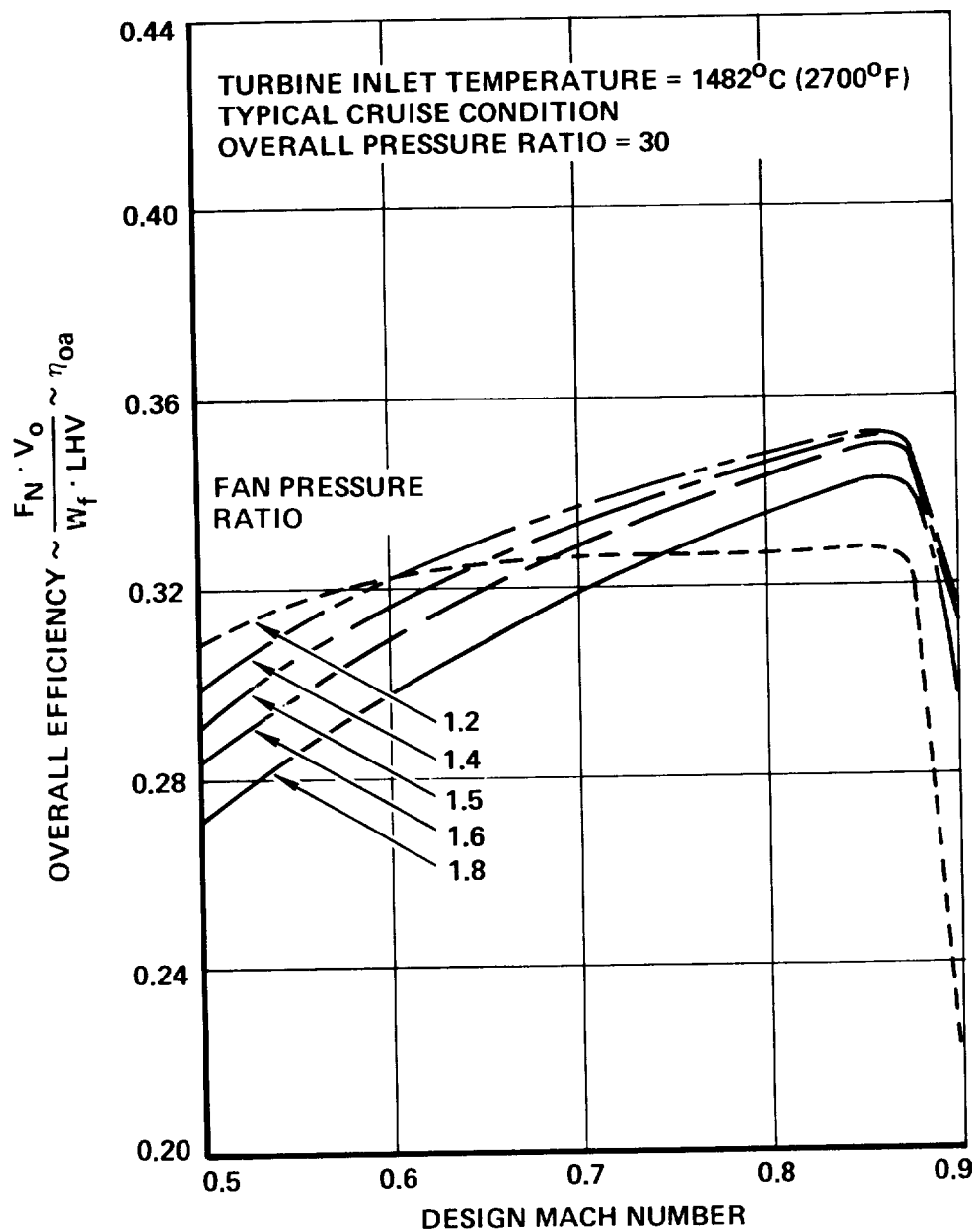


Figure 13. Effect of Fan Pressure Ratio on Overall Efficiency vs. Mach Number - Cowl Drag Included

the cowl drag rise occurs. Figure 14 shows that overall efficiency increases 2 percent to 3 percent as overall pressure ratio is increased from 30 to 35. The propulsion pod drag used in these studies is presented in Figure 15 and is based on Reference 9.

Figure 16 shows that at a constant fan pressure ratio and a constant overall pressure ratio, overall efficiency decreases slightly as turbine inlet temperature increases from 1371°C (2500°F) to 1593°C (2900°F). Based on these data, there is no incentive to increase the turbine temperatures of advanced high bypass turbofans above the turbine inlet temperatures of current high bypass turbofans (see Figure 11). Figure 17 shows the effect of the low pressure turbine energy split between the fan duct and the primary engine exhaust. High energy into the primary exhaust results in low bypass ratios and high energy in the fan results in high bypass ratios. It can be seen from the curve that overall efficiency optimizes near the condition where the fan jet and primary jet velocities are equal.

3.2.2 Cycle Design Point

The selected cycle design point for both the Jet A and LH₂ fueled engines was sea level static, standard day. The basic cycle assumptions are defined in Table 3. As noted, the cycle was set to provide a primary and fan stream exhaust velocity match at this condition. Table 3 also defines the engine component efficiencies selected from the cycle analysis study and used in the Jet A and LH₂ cycle performance development. Every effort was made to keep the hydrocarbon and hydrogen fueled engine cycle definitions as consistent as possible to prevent unrelated differences from biasing the study.

The engine base size was set at 155.7 kN (35,000 pounds) of installed net thrust. This performance level was achieved with a design turbine inlet temperature of 1416°C (2580°F) and an overall cycle pressure ratio (CPR) of 35.0. While higher CPR's would probably be available by 1985, it becomes more difficult to achieve high compressor efficiencies because of tolerance and sealing considerations in the relatively small gas generator. The fan stream and primary jet velocities matched at 254.5 m/s (835 ft/sec) and the resulting bypass ratio (BPR), at SLS, is approximately 13 for the LH₂ fueled engine and 11 for the JET A fueled engine. For the cruise condition the BPR values are 13.5 and 11.6, nearly at peak thermal efficiency as can be seen from Figure 17.

After a careful review of the available literature and accounting for weight, performance and acoustical criteria, a single stage fan was selected with a design

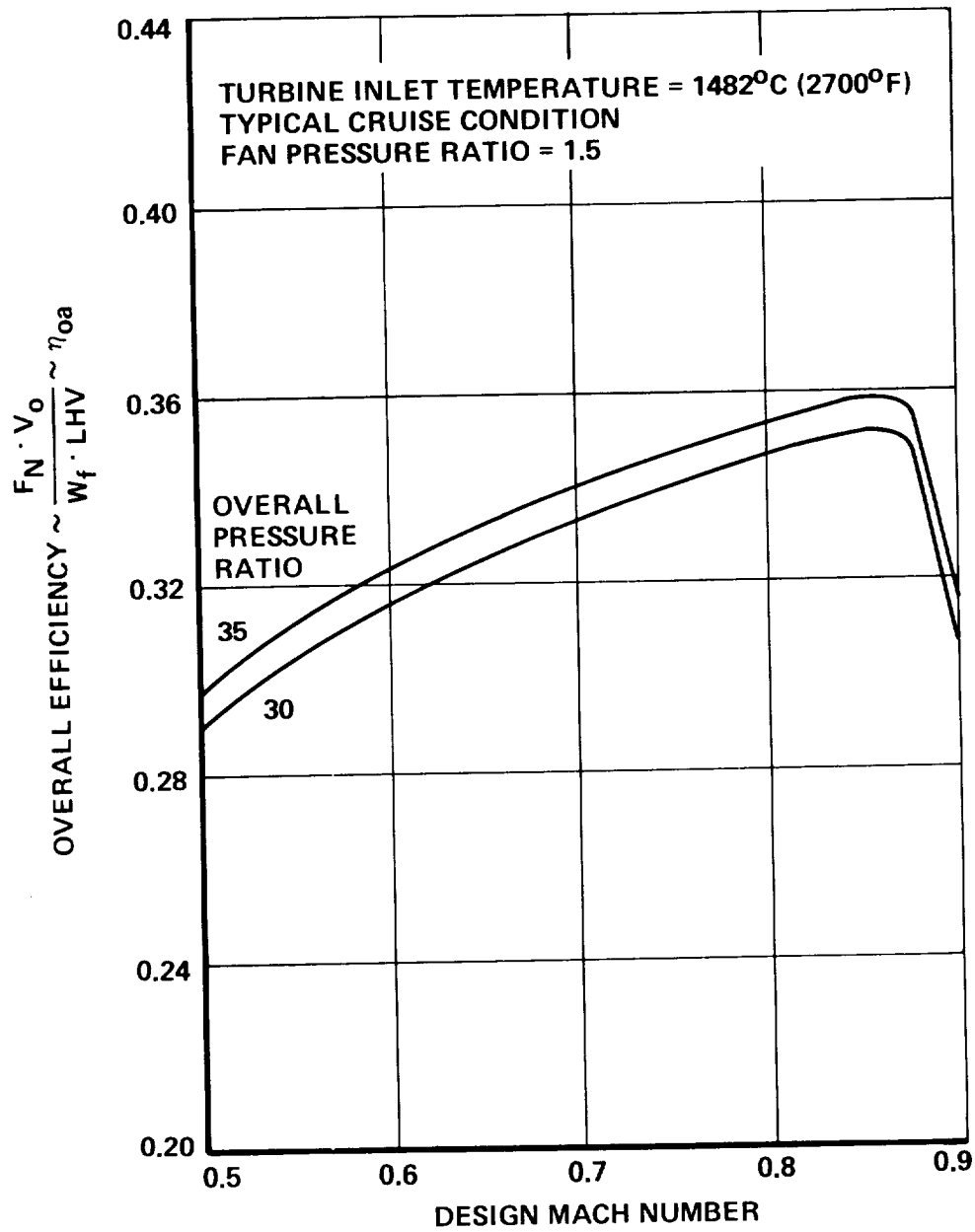


Figure 14. Effect of Cycle Pressure Ratio on Overall Efficiency vs. Mach Number - Cowl Drag Included

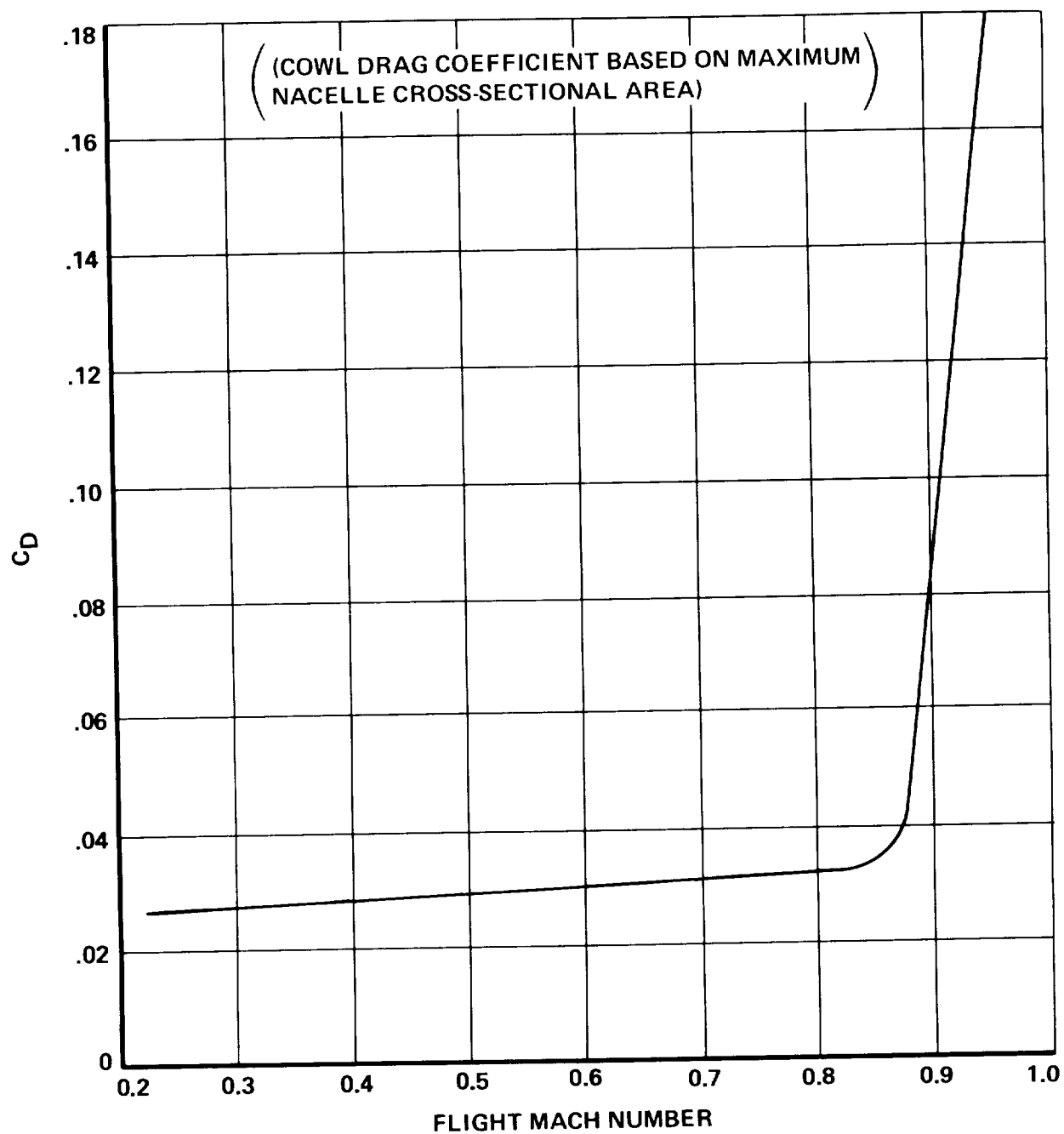


Figure 15. Cowl Drag Coefficient vs. Mach Number

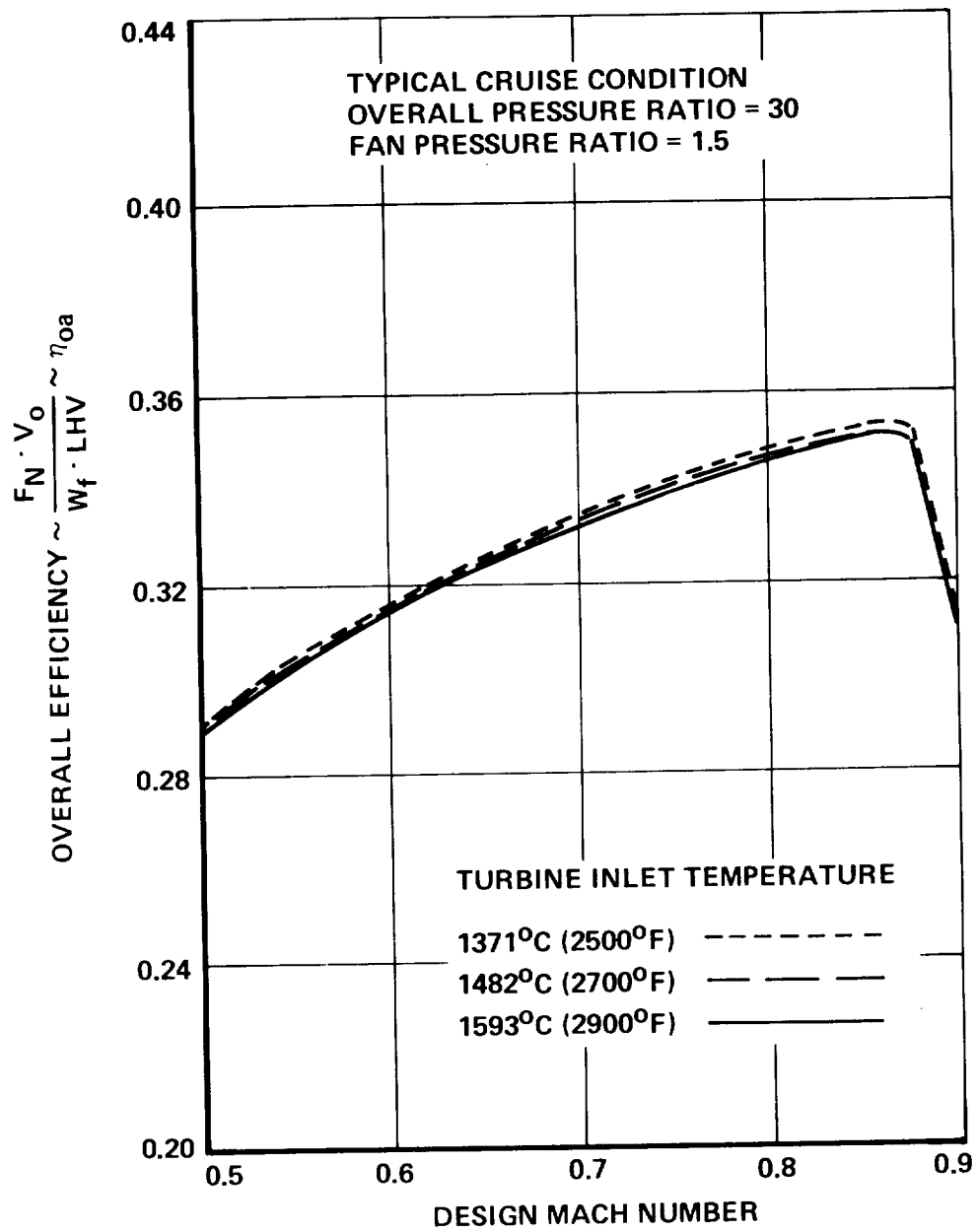


Figure 16. Effect of Turbine Inlet Temperature on Overall Efficiency vs. Mach Number - Cowl Drag Included

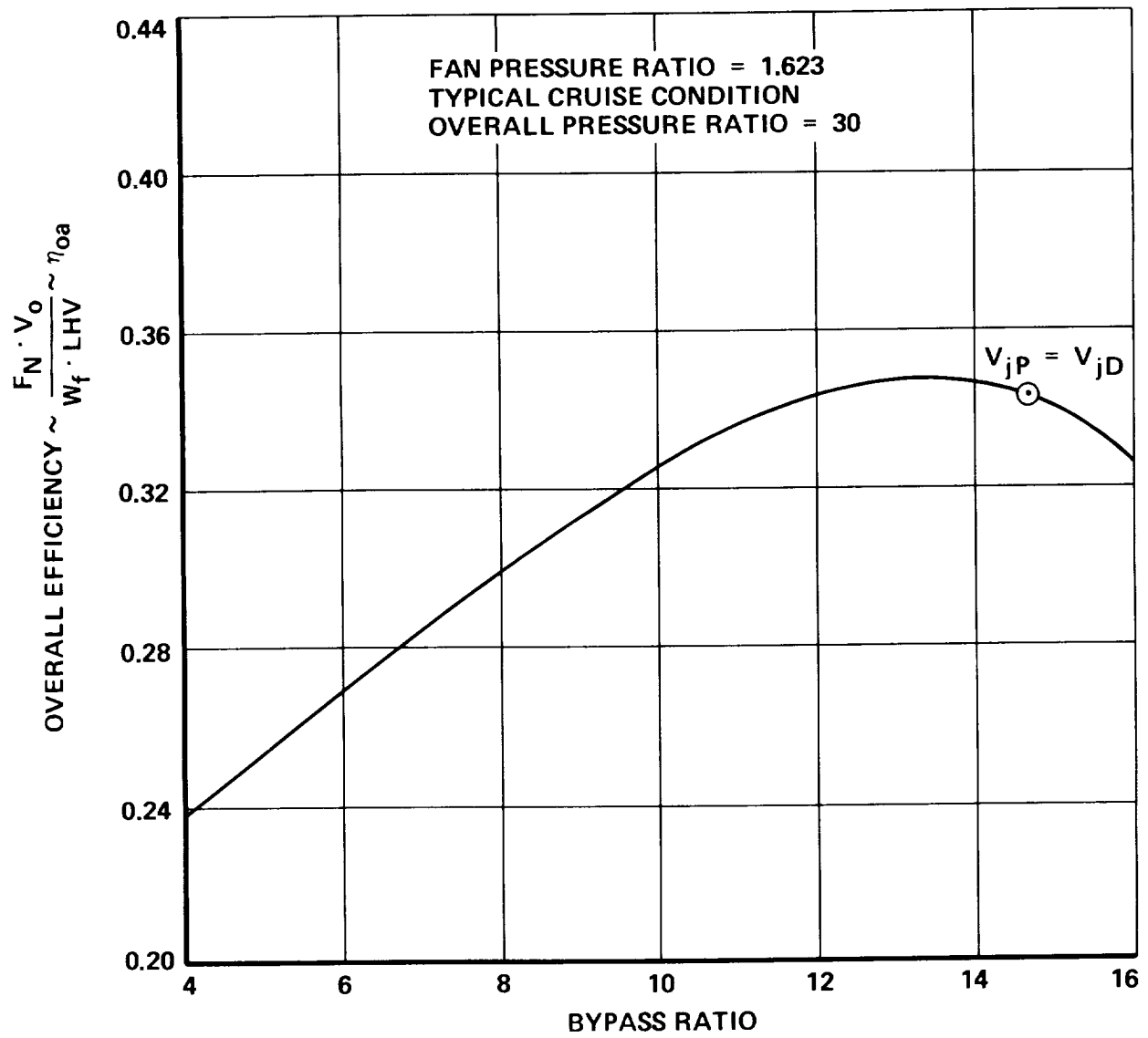


Figure 17. Effect of Bypass Ratio on Overall Efficiency - Cowl Drag Included

TABLE 3. ENGINE DESIGN POINT DATA, SEA LEVEL STATIC - STANDARD DAY

	HYDROGEN FUELED		HYDROCARBON FUELED	
I. BASE SIZE ENGINE				
INSTALLED NET THRUST	155.7 kN	(35000 lb)	155.7 kN	(35000 lb)
INSTALLED S.F.C.	0.092 kg/HR/daN	(0.094 lb/hr/lb)	0.275 kg/HR/daN	(0.281 lb/hr/lb)
TURBINE INLET TEMPERATURE	1416°C	(3040°R)	1416°C	(3040°R)
BYPASS RATIO		12.95		10.90
OVERALL PRESSURE RATIO		35.0		35.0
JET EXHAUST VELOCITY	254.5 m/sec	(835 ft/sec (Vj PRI & Vj DUCT MATCHED @ SLS)	254.5 m/s	(835 ft/sec)
II. FAN DESIGN				
STAGES		1		1
AIRFLOW - $W_a \sqrt{\theta_{T_2}/\delta_{T_2}}$	616.9 kg/sec	(1360 lb/sec)	615.1 kg/sec	(1356 ft/sec)
PRESSURE RATIO		1.51		1.51
POLYTROPIC EFFICIENCY		91%		91%
DIAMETER	2.144 m	(84.4 in.)	2.144 M	(84.4 in.)
TIP VELOCITY	423.7 m/sec	(1390 ft/sec)	423.7 m/sec	(1390 ft/sec)
FAN FACE MACH NO.		0.56		0.56
HUB/TIP RATIO		0.35		0.35
III. COMPRESSOR DESIGN				
COMPRESSOR PRESSURE RATIO		23.3		23.3
POLYTROPIC EFFICIENCY		92.0%		92.0%
AIRFLOW	43.5 kg/sec	(96 lb/sec)	51.3 kg/sec	(113 lb/sec)
IV. COMBUSTOR				
EFFICIENCY		100%		100%
TOTAL PRESSURE LOSS		4.5%		4.5%
V. HIGH PRESSURE TURBINE				
PRESSURE RATIO		3.9		4.6
STAGES		2		2
ADIABATIC EFFICIENCY		91%		90%
COOLING AIR		0		5%
VI. LOW PRESSURE TURBINE				
PRESSURE RATIO		7.4		6.2
STAGES		4		4
ADIABATIC EFFICIENCY		91%		91%
COOLING AIR		0		0
VII. NOZZLE DESIGN				
CONFIGURATION		COPLANER, FIXED CONVERGENT NOZZLE		SAME
PERFORMANCE - (VEL. COEF.)				
A. PRIMARY C_v		0.995		0.995
B. FAN C_v		0.995		0.995
VIII. ACOUSTIC TREATMENT				
A. INLET	{ VARIABLE GEOMETRY THROAT - THROAT MACH = 0.8 DURING TAKEOFF AND APPROACH, INLET WALL TREATMENT }			SAME
B. EXHAUST -				
1. FAN DUCT	{ ALL TREATMENT ON BOTH CORE ENGINE AND OUTER WALL, ONE TREATED DUCT RING }			SAME
2. PRIMARY	WALL TREATMENT			SAME
IX. NACELL GEOMETRY				
MAXIMUM DIAMETER	2.69 m	(106 in.)		
OVERALL LENGTH	7.19 m	(283 in.)		
INLET HIGHLIGHT DIAMETER	2.18 m	(86 in.)		SAME
INLET THROAT DIAMETER	1.98 m	(78 in.)		
CRUISE THROAT MACH NUMBER		0.73		

fan pressure ratio (FPR) of 1.5 and a tip speed of approximately 423.7 m/s (1390 ft/sec). The fan design point performance was based on a 91 percent polytropic efficiency which should be achievable by 1985. A fan face Mach number of 0.56 and a hub/tip ratio of 0.35 were chosen for the basic fan design. These values are consistent with current single stage fan designs. The resulting fan performance provides an air flow rate of approximately 617 kg/s (1360 lb/sec) at SLS and a maximum tip diameter of 2.14 m (84.4 in.). This diameter is near maximum from a practical standpoint since a QEC diameter of 2.44 m (96 inches) is the maximum allowable for highway transportation.

Having set both the overall compressor pressure ratio of 35.0 and the fan pressure ratio of 1.5, a compressor pressure ratio of 23.3 results. The compressor has a 92 percent polytropic efficiency and an air flow rate of approximately 45.4 kg/s (100 lb/sec). This compressor pressure ratio is achieved with a ten to twelve stage variable geometry stator design resulting in an average pressure rise of 1.37 to 1.30 per stage.

A combustor efficiency of 100 percent and a total pressure loss of 4.5 percent were used for both engine designs. The LH_2 high pressure turbine is designed to have a 3.9 pressure ratio at the design point and an overall adiabatic efficiency of 91 percent. The heat capacity of the liquid hydrogen is utilized, via an intermediate coolant, to cool the turbine blades and related nozzle guide vanes. The Jet A fueled engine has a slightly different high pressure turbine design having a pressure ratio of 4.6 and a 90 percent adiabatic efficiency (1 percent less than the LH_2 fueled turbine design). The Jet A fueled engine employs a more conventional design using 5 percent primary air flow to meet the turbine cooling requirements. The use of compressor discharge air to cool the turbine accounts for the difference in the turbine efficiency and design BPR, relative to the LH_2 fueled engine. This is because the Jet A fueled gas generator has to be slightly larger to compensate for the cycle energy lost in cooling the turbine.

The low pressure turbine consists of four stages, having an overall adiabatic efficiency of 91 percent and requires no cooling air flow. The LH_2 fueled engine has a design pressure ratio of 7.4 as a result of the higher BPR, compared to 6.2 for the Jet A fueled engine. Both the primary and fan stream nozzles have a 99.5 percent nozzle velocity coefficient.

The engine is controlled by scheduling the compressor rotor speed as a function of turbine inlet temperature (TIT) to provide a relatively constant corrected gas

flow to the low pressure turbine. The fan speed is allowed to balance out in the resulting cycle condition. The only limiter used is a maximum fan speed of 108 percent which affects a few high altitude, low Mach number flight conditions.

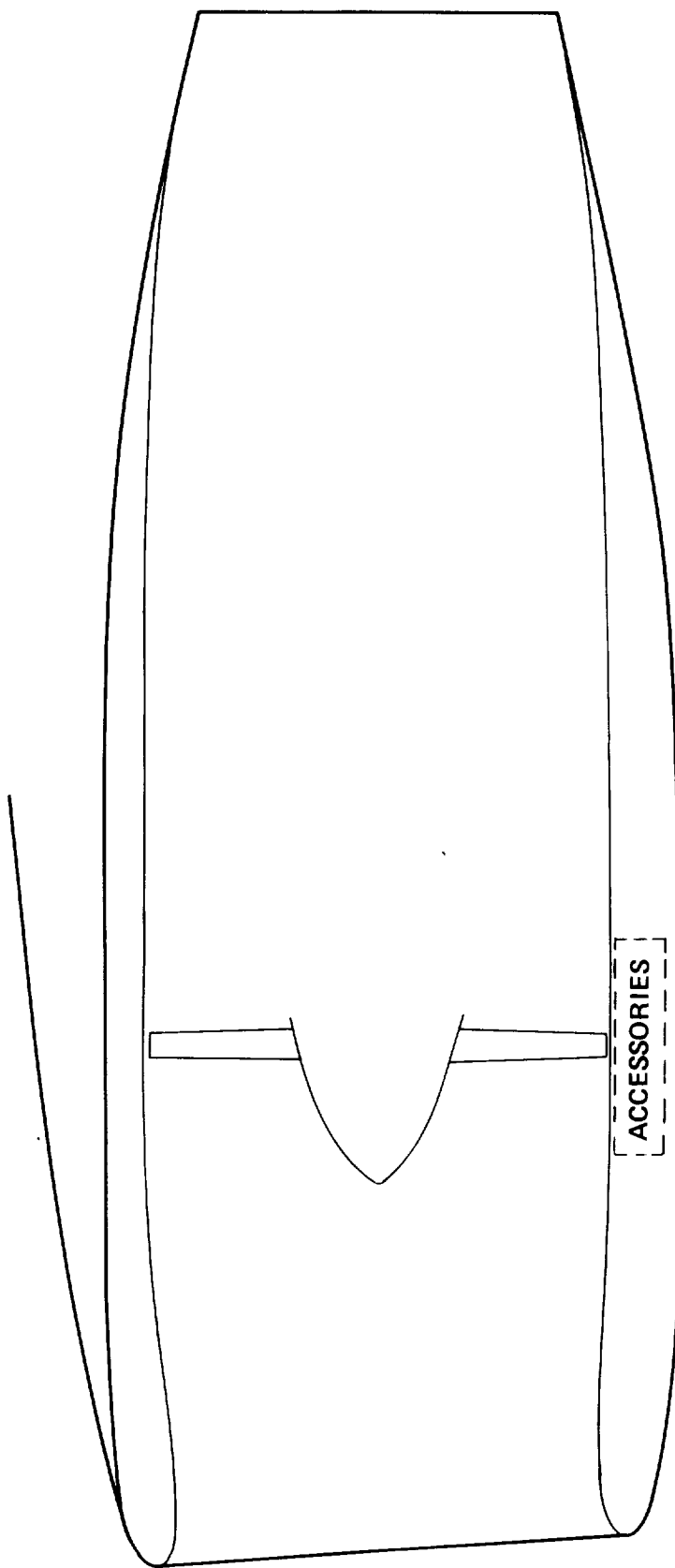
3.2.3 Nacelle Design

The overall nacelle design and engine installation arrangement is shown in Figure 18. In attempting to achieve the noise goals of FAR Part 36 minus 20 EPNdB and the 5.18 km^2 (2 mi^2 .) area of the 90 EPNdB contour, the nacelle was designed with a variable geometry inlet, and included inner and outer fan duct wall acoustic lining and one annular treated ring extending the full length of the duct. The inlet throat was sized to provide a throat Mach number of approximately 0.73 at the cruise flight condition. However, during takeoff and approach the inlet throat contracts to provide a 0.8 to 0.85 throat Mach number. The inlet lip configuration matches closely one used in the L-1011 design; however, the inlet length had to be increased significantly (approximately 60 percent relative to the L-1011) to allow for the mechanical aspects of the variable geometry design. The nacelle has co-planar exhaust nozzles and employs a clam shell type reverser. It was assumed that the fan design would have no inlet guide vanes (IGV) and a rotor-to-stator spacing of approximately three times the fan tip axial length. It was further assumed that no compressor noise would radiate forward because of the high inlet throat Mach number during takeoff and approach, and the turbine was designed with appropriate rotor/stator relationships and treatment so that turbine noise would not be a factor. For a description of the methods used in calculating noise levels, see Section 4.8.2.

The baseline propulsion system weight buildup is defined in Table 4 for a wing pod configuration. The engine weight was based on a predicted thrust-to-weight ratio of 7.06 daN/kg (7.2 lbf/lbm). This level should be achieved by 1985 since current high BPR engines have thrust-to-weight ratios of from 4.9 to 5.9 daN/kg (5 to 6 lbf/lbm). The total pod weight of 4291 kg (9460 pounds) provides a nacelle thrust-to-weight ratio of approximately 3.65 daN/kg (3.7 lbf/lbm). Since current installations have thrust-to-weight ratios of 2.94 to 3.43 daN/kg (3 to 3.5 lbf/lbm), it was assumed that a 3.63 daN/kg (3.7 lbf/lbm) engine T/W ratio would be achievable with the variable geometry inlet by 1985.

The baseline engine can be scaled over a thrust range from 11,100 to 20,000 daN (25,000 to 45,000 pounds) of installed SLS takeoff thrust without significant discrepancy. The physical nacelle/engine scaling factors used are also shown in

ENGINE DESIGN CONDITION: SLS, TIT = 1416°C (3040°R), FPR = 1.5, OAPR = 35
 BASE THRUST = 15,570 daN (35,000 LB) – INSTALLED



ENGINE/NACELLE DESIGN CHARACTERISTICS:

FAN HUB/TIP RATIO = 0.35	MAX NACELLE LENGTH = 7.19 M (283 IN.)
FAN DIAMETER = 2.14 M (84.4 IN.)	BARE ENGINE WEIGHT = 2440 KG (5380 LB)
INLET LENGTH = 2.36 M (93.0 IN.)	VARIABLE GEOMETRY INLET
NACELLE MAX DIAMETER = 2.69 M (106.0 IN.)	CLAM SHELL REVERSE

Figure 18. Baseline IH_2 Engine/Nacelle Characteristics

TABLE 4. BASELINE PROPULSION SYSTEM WEIGHT

Base Thrust = 15,570 daN (35,000 lb) (SLS, Installed)

TIT = 1416°C (3040°R) OAPR = 35.0

Fan Pressure Ratio = 1.51

<u>ITEM</u>	<u>kg</u>	<u>lb</u>
Bare Engine	2440.4	(5380)
Accessories and Gearbox	217.7	(480)
Inlet, Variable Geometry	455.9	(1005)
Mounting Brackets and Pylon Splitter Fairing	90.7	(200)
Nacelle	449.1	(990)
Gas Generator Cowl and Tail Pipe	231.3	(510)
Fan Duct Acoustic Ring	124.7	(275)
Thrust Reverser	281.2	(620)
Total Pod Weight/Engine	4,291.0	(9460)

NACELLE SCALING DATA

$$WT. \text{ POD} = WT_{\text{POD (REF)}} \left(\frac{F_{N_{\text{SLS}}}}{F_{N_{\text{SLS (REF)}}}} \right)^{1.07}$$

$$DIA. = DIA_{\text{(REF)}} \left(\frac{F_{N_{\text{SLS}}}}{F_{N_{\text{SLS (REF)}}}} \right)^{0.50}$$

$$LENGTH = LENGTH_{\text{(REF)}} \left(\frac{F_{N_{\text{SLS}}}}{F_{N_{\text{SLS (REF)}}}} \right)^{1.07}$$

Table 4 and are generally consistent with the current industry preliminary design performance data.

3.2.4 Installed Performance

The installed propulsion system performance was developed using the SYNTHA engine cycle program with the previously described design point data and off design characteristics of current high bypass ratio engines. The installed data are based on the inlet recovery shown in Figure 19. The inlet performance reflects Lockheed subsonic inlet experience and accounts for all normal internal losses, plus those associated with the variable geometry throat. A fan stream total pressure loss of 3 percent was used to account for the fan exhaust stream losses, including the acoustic ring and related blockage. The primary exhaust stream was debited for a 0.5 percent total pressure loss. The data are based on a lower heat value of 42,830 kJ/kg (18,400 BTU/lb) for Jet A fuel and 120,090 kJ/kg (51,590 BTU/lb) for LH₂ fuel. The compressor bleed and power extraction are shown in Table 5.

TABLE 5. COMPRESSOR BLEED AND POWER EXTRACTION

ALTITUDE METERS (FEET)	COMPRESSOR BLEED % CORE AIRFLOW	POWER EXTRACTION KILOWATTS
0 (0)	1.70	93.2 (125 HP)
1524 (5000)	2.04	93.2 (125 HP)
3048 (10000)	2.39	93.2 (125 HP)
4572 (15000)	2.73	93.2 (125 HP)
6096 (20000)	3.07	93.2 (125 HP)
7620 (25000)	3.42	93.2 (125 HP)
9144 (30000)	3.76	93.2 (125 HP)
10668 (35000)	4.09	93.2 (125 HP)
12192 (40000)	4.44	93.2 (125 HP)
13716 (45000)	4.77	93.2 (125 HP)

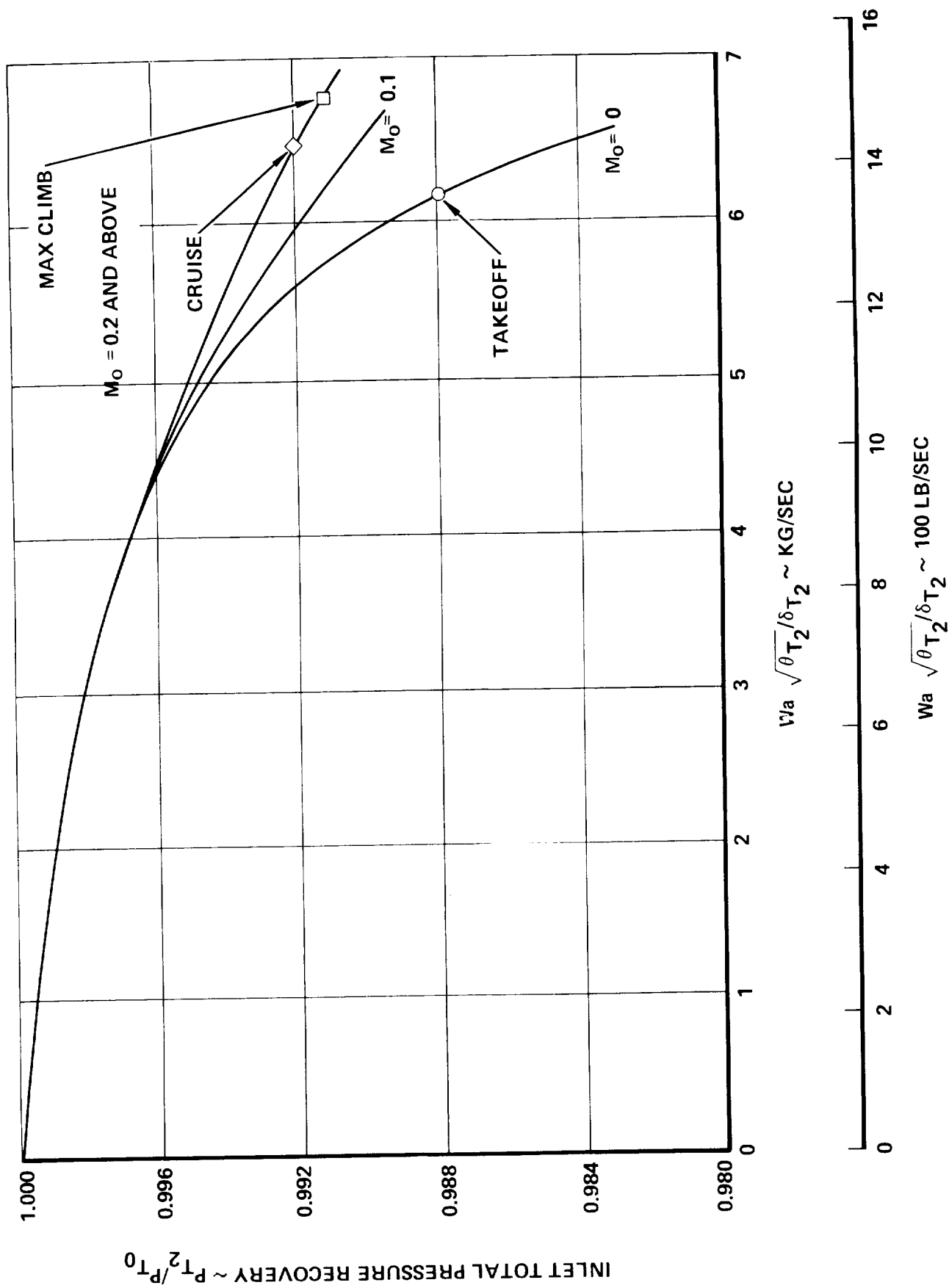


Figure 19. Wing Pod Inlet Total Pressure Recovery - Variable Geometry Throat

Because the aircraft takeoff design condition was 304.8M (1000 ft) altitude at 32.6° C (90° F) the engines were flat-rated to provide full thrust at this ambient temperature. Figures 20 and 21 present takeoff thrust vs Mach number for both engines. A cruise SFC comparison is shown in Figure 22 between the P&W JT9D and the Jet A and LH₂ fueled engines derived for this study. Note the Jet A fueled 1985 state-of-the-art engine has approximately 13 percent lower cruise SFC than the current engine. The SFC difference between the Jet A and LH₂ fueled engines is primarily due to the higher gravimetric heating value of the LH₂. Figures 23 and 23 present installed part power cruise SFC vs thrust for both the Jet A and LH₂ fueled engines at 10,670 m (35,000 ft).

3.3 AERODYNAMICS

The aerodynamic drag buildup procedures and mission analysis techniques employed for the passenger and the cargo aircraft in this study are very similar. The small differences which exist will not influence the conclusions of the study since a comparison of aircraft designed for the two types of missions was not intended. Such a comparison would not be realistic anyway, since cargo aircraft are generally designed to slightly different criteria than passenger aircraft in other technology areas also. Conclusions regarding configuration differences arising from the use of LH₂ in lieu of Jet A are valid for either type of aircraft and are relatively insensitive to any small differences in computational techniques or design criteria.

3.3.1 Passenger Aircraft Aerodynamics

The aerodynamics data for passenger aircraft developed for this study reflects "state-of-the-art" wide body Tristar flight test derived data, incremented by available unclassified "supercritical" data to project the potential of advanced technology design practices. These parametric data build-up procedures were applied to the cruise and off-cruise Mach number drag polar determination; take-off, approach, and landing polars; and $C_{l_{max}}$ for variations in all transport aircraft geometric and flight variables. Zero lift friction drag was estimated, using current practices, through the variables of flight Reynold's number, form factors, and roughness increments for each aircraft component.

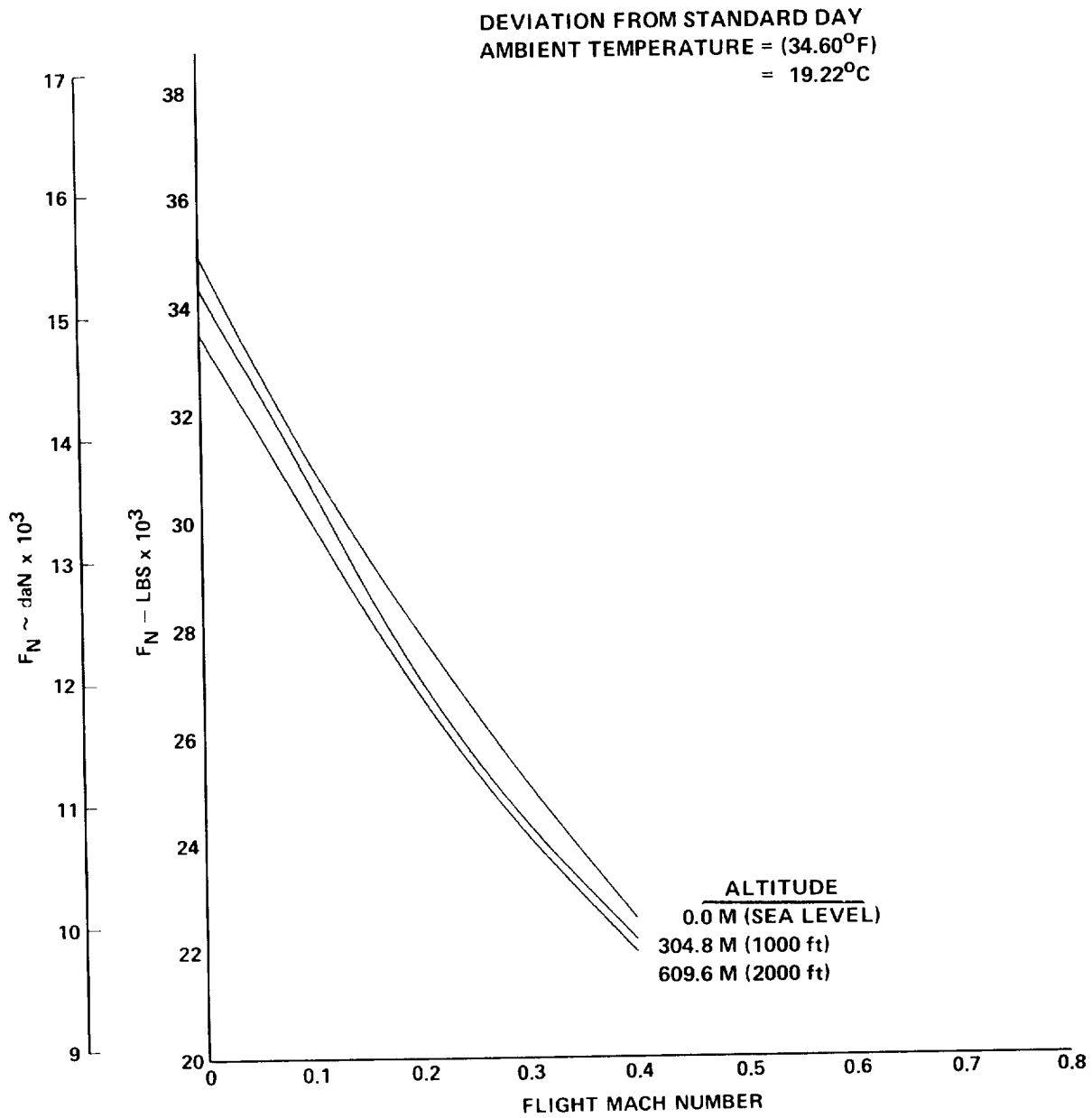


Figure 20. Installed Thrust vs. Mach Number - Takeoff Rating -
Jet A Fueled Engine

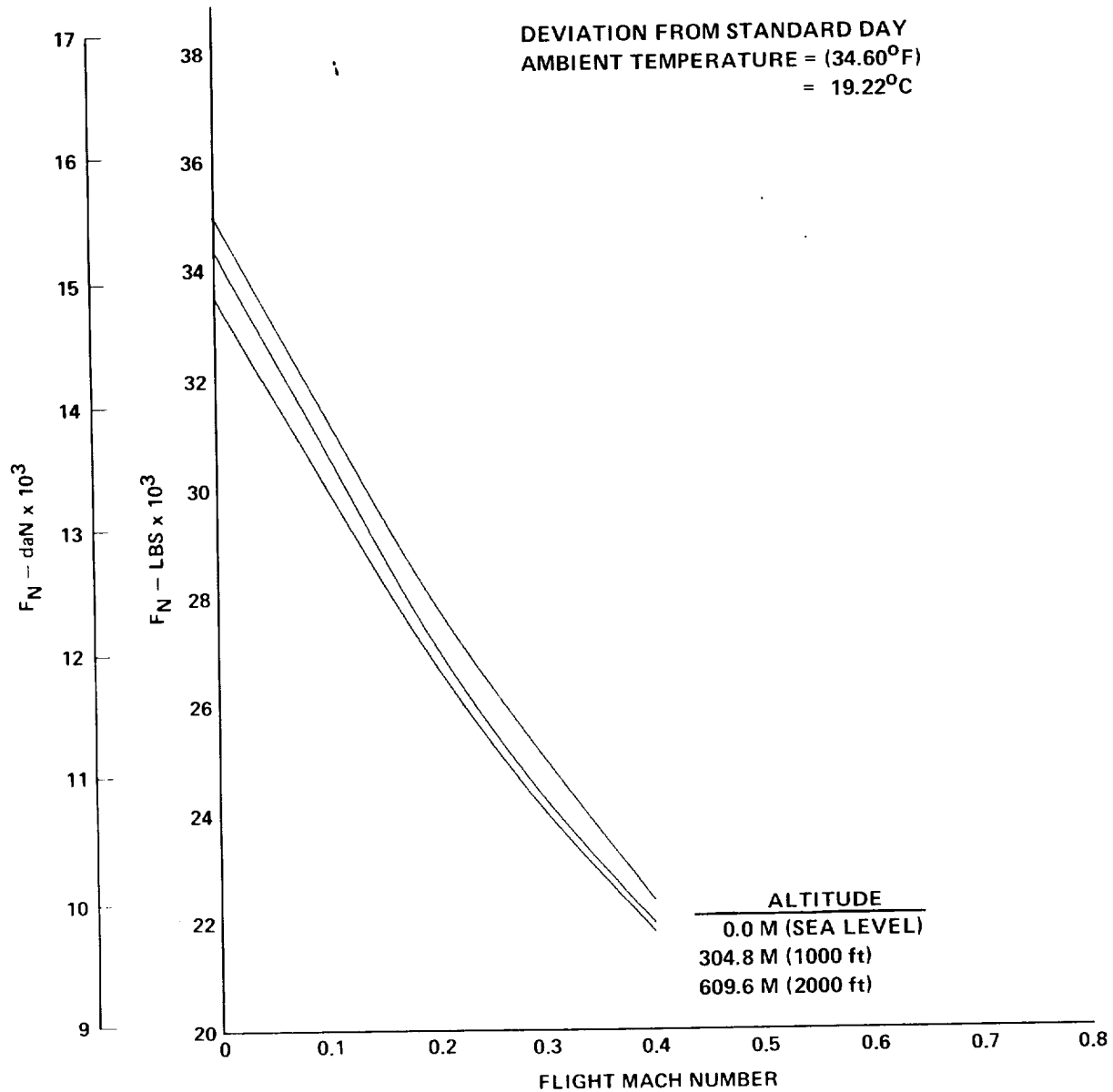


Figure 21. Installed Thrust vs. Mach Number - Takeoff Rating -
 LH₂ Fueled Engine

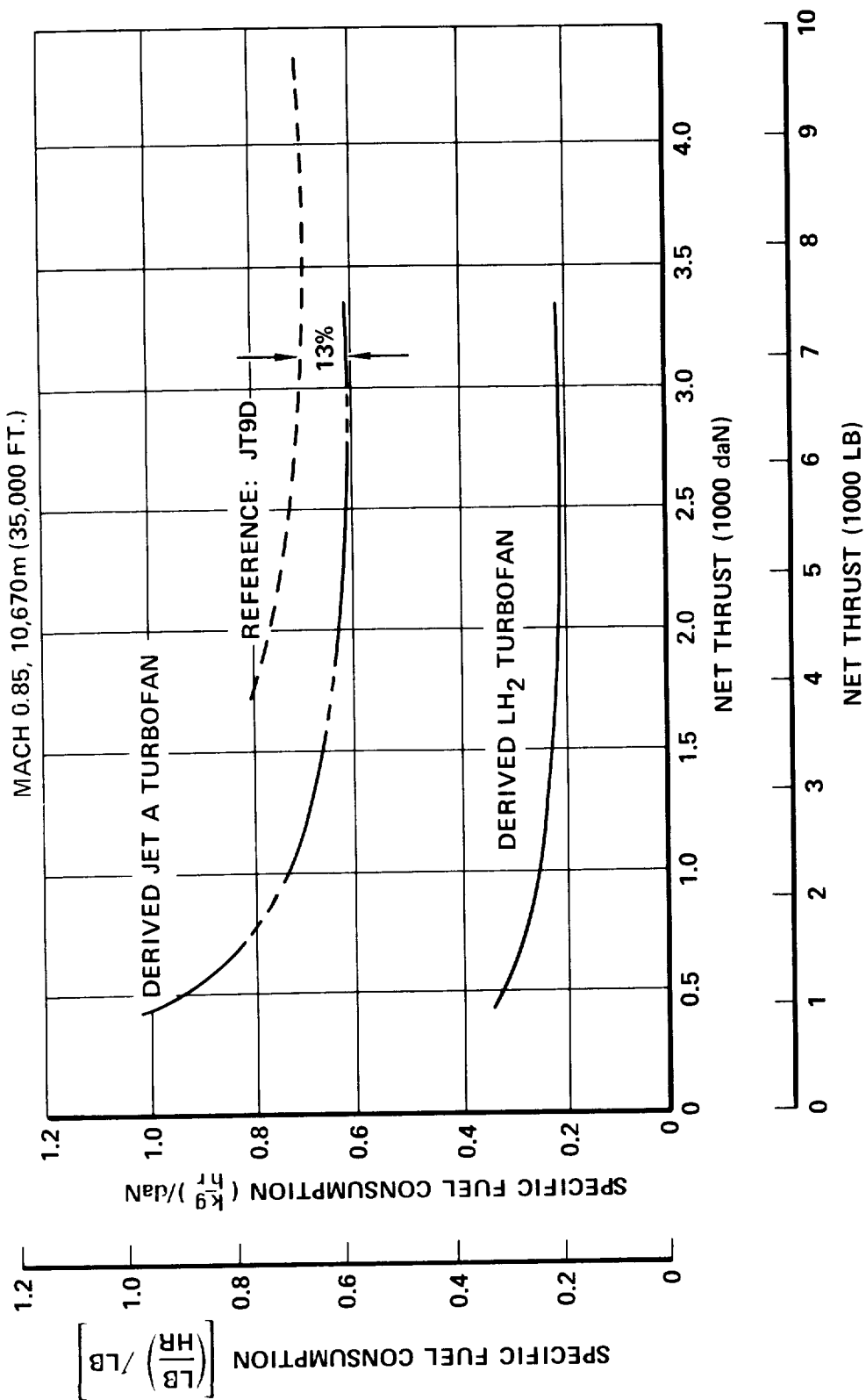


Figure 22. Comparative Engine Cruise Performance - Mach 0.85, 10, 670m (35,000 ft)

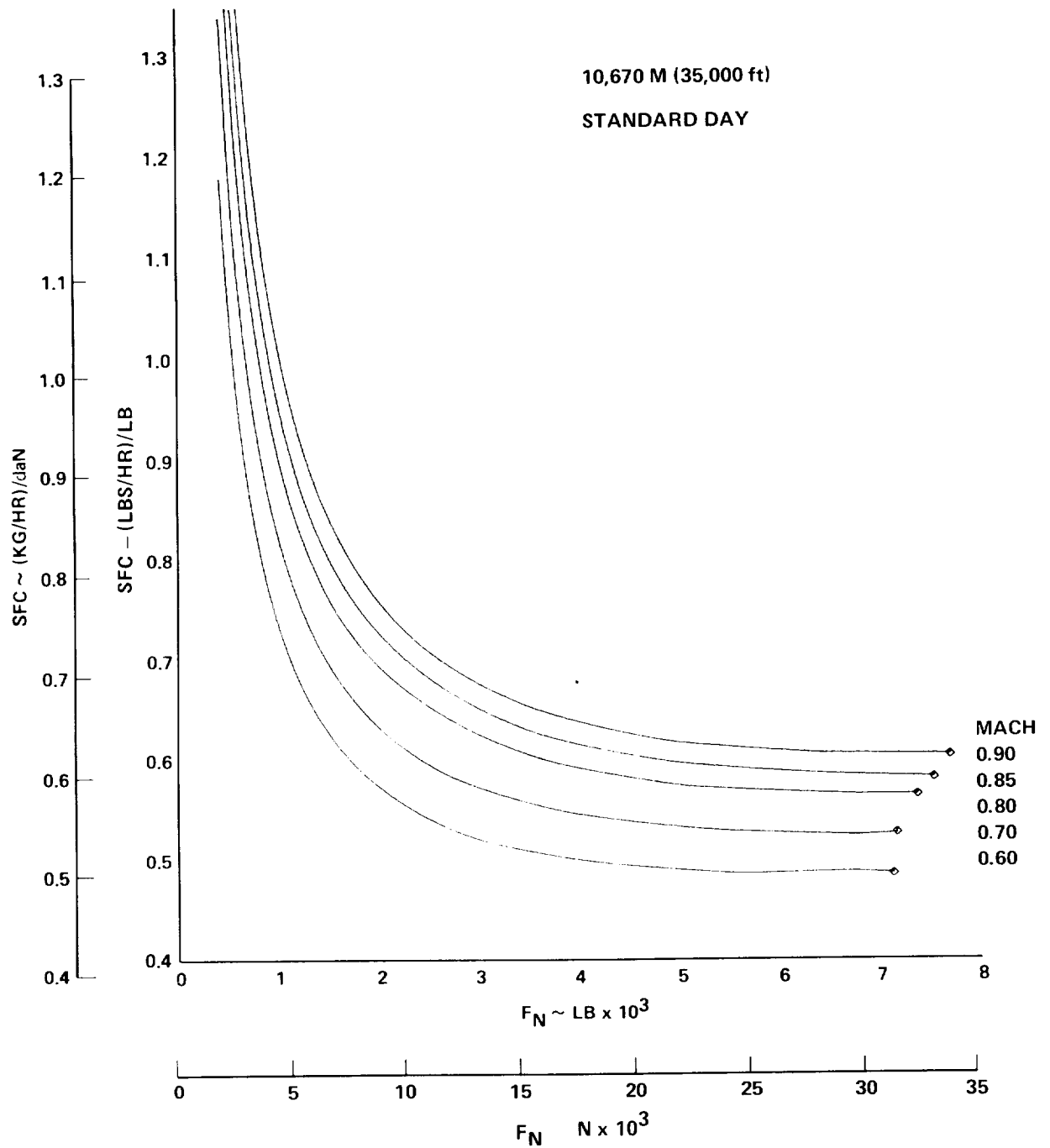


Figure 23. Installed Cruise SFC vs. Net Thrust - Jet A Fueled Engine

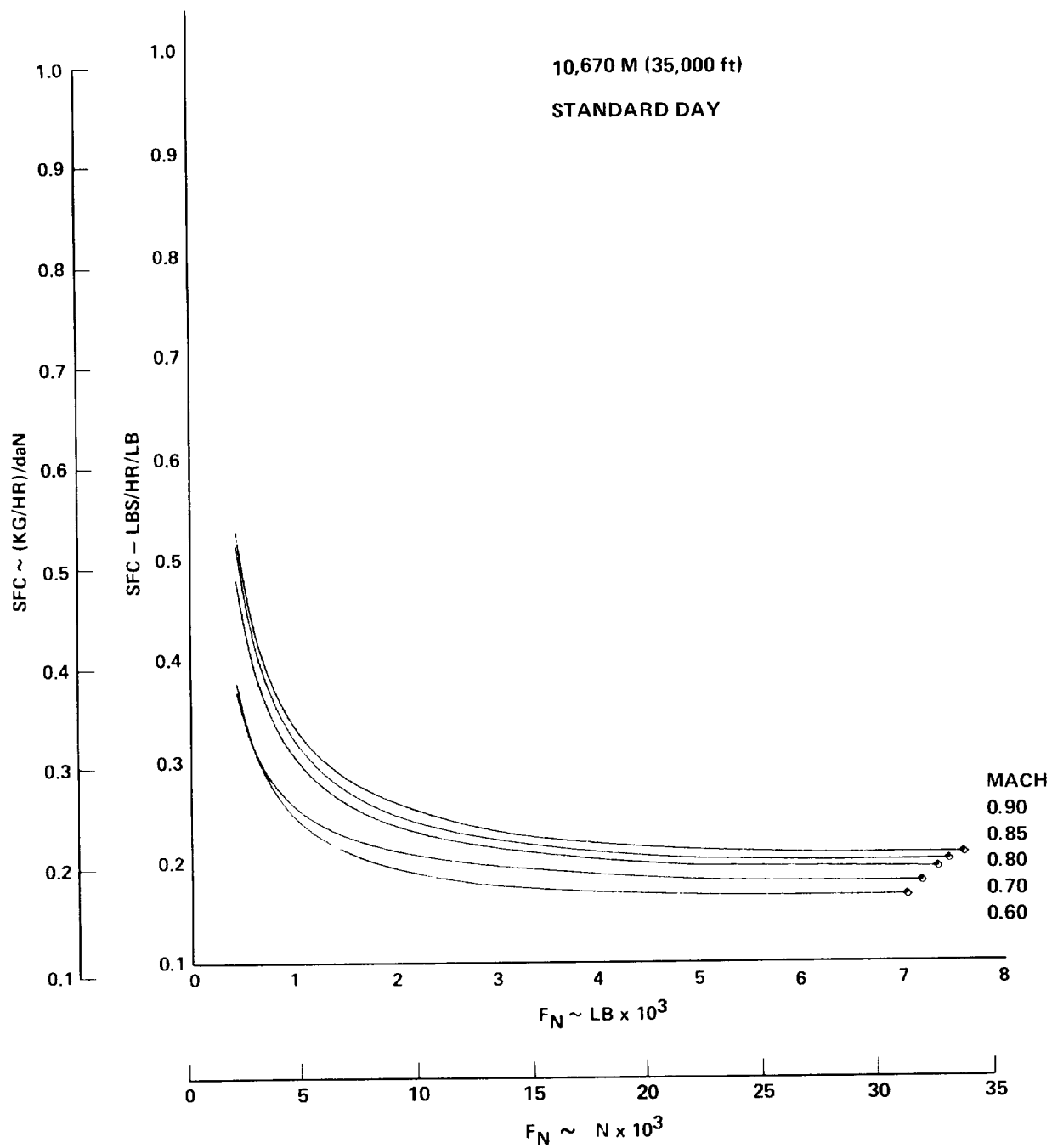


Figure 24. Installed Cruise SFC vs. Net Thrust - LH_2 Fueled Engine

3.3.1.1 Cruise and Off-Cruise Drag Polar Build-up Procedures - In arriving at a basis for predicting the predrag and postdrag rise characteristics of the parametric hydrogen fueled transports incorporating advanced technology "supercritical" wings, relationships were derived between "state-of-the-art" and "supercritical" technology using theory, 2-dimensional wind tunnel and available 3-dimensional wind tunnel, and flight test data.

Initial premises, see Figure 25, depicts the "design to" 2-D upper surface pressure distribution typical of L-1011, and advanced technology wing sections. Advanced technology implies that as the region of local supersonic flow develops on the upper surface and grows in extent the shock wave terminating such a region remains weak. This phenomenon is in contrast to a very strong upper surface shock and possible shock-induced separation associated with more conventional wing design practice. For either design philosophy, however, various combinations of drag divergent Mach number and lift coefficient can be attained by varying the thickness ratio while retaining the desired upper surface pressure distributions. It is further premised that for a given thickness ratio the advanced technology will attain a higher drag divergent Mach number, or conversely, for the same drag divergence a thicker wing can be tolerated with advanced technology. On Figure 26 the above discussed relationships are noted for available 2-D tests and theoretical prediction techniques. At a drag divergence level of 10 counts and lift coefficient of 0.50, advanced technology represents an increase in drag divergence Mach number of approximately 0.06 to 0.08 over conventional NASA 65 series airfoils design practice. "State-of-the-art" practices would produce lesser benefits.

To convert 2-dimensional divergence characteristics to 3-dimensional, the effects of sweep and aspect ratios must be known. From previous studies the relationships have been derived and are noted on Figure 27.

The divergence characteristics developed thus far relate 2-D to 3-D at 10 counts of drag rise. Figures 28 and 29 present the relationship between Mach design at a ΔC_{D_e} of ≈ 22 counts and Mach divergence at 10 counts at design lift coefficient. A 0.03 Mach number decrement is noted between $M_{DES} = M_{DIV.3-D}$ @ 22 counts and $M_{DIV.3-D}$ @ 10 counts.

In further developing the parametric drag build-up procedures for advanced technology application it has been premised that the L-1011 pre and post drag profile and compressibility drag characteristics from M_{Design} and $C_{LDesign}$ are

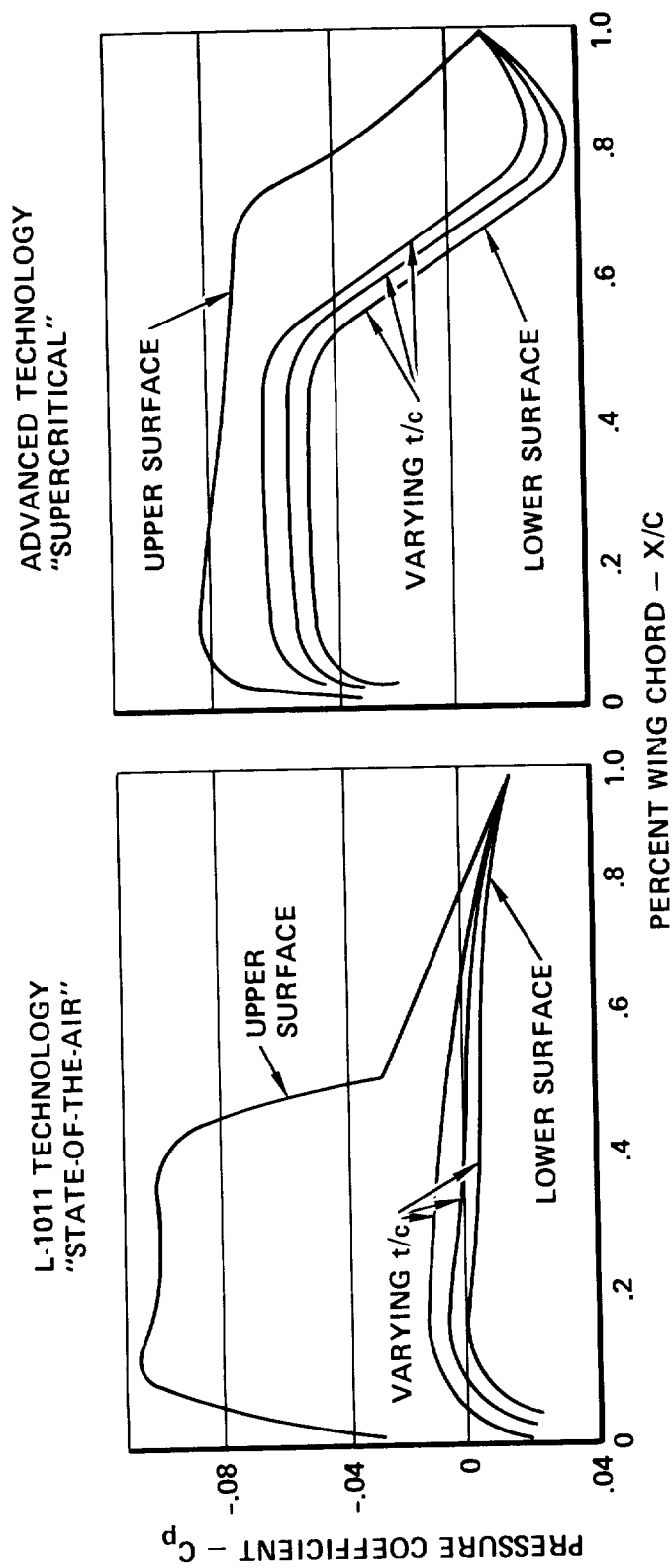


Figure 25. Characteristics "Design to" Wing Pressure Distributions

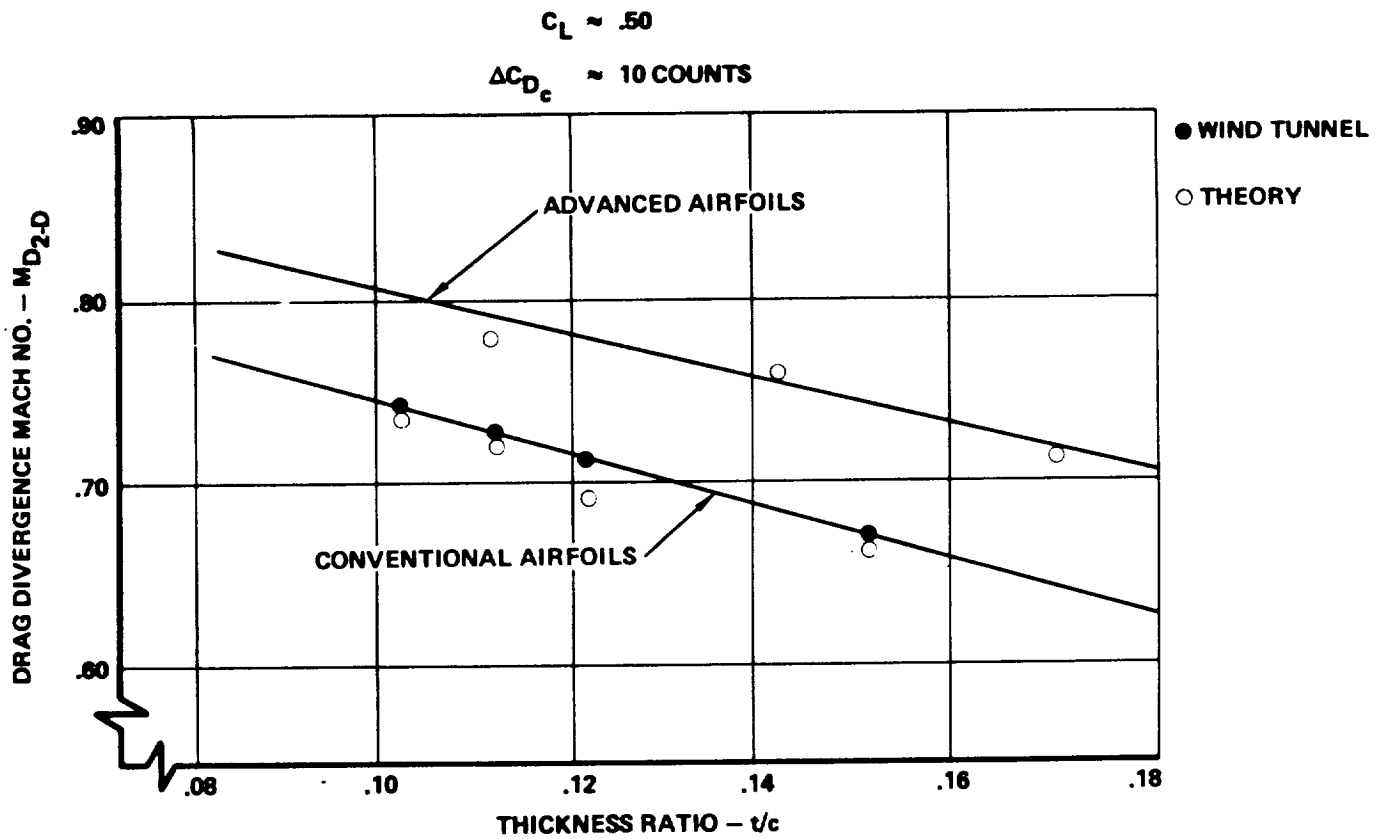


Figure 26. 2-D Mach Divergence Characteristics

$$M_{D \text{ 3-D}} = M_{\text{DIV. 2-D}} + \Delta M_{\Lambda} + \Delta M_{AR}$$

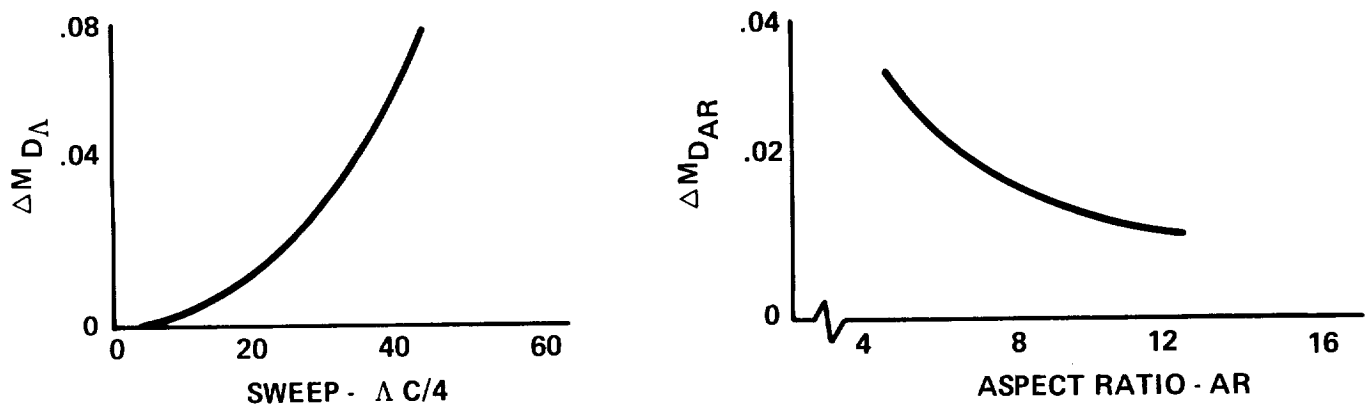


Figure 27. 3-D Corrections to Mach Divergence

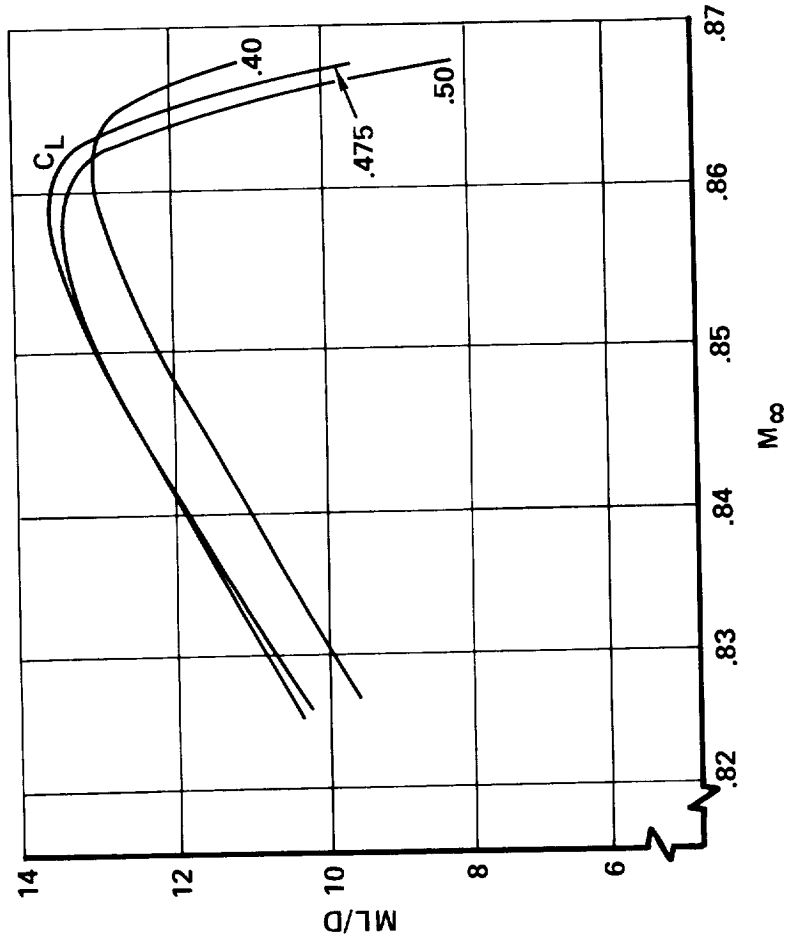
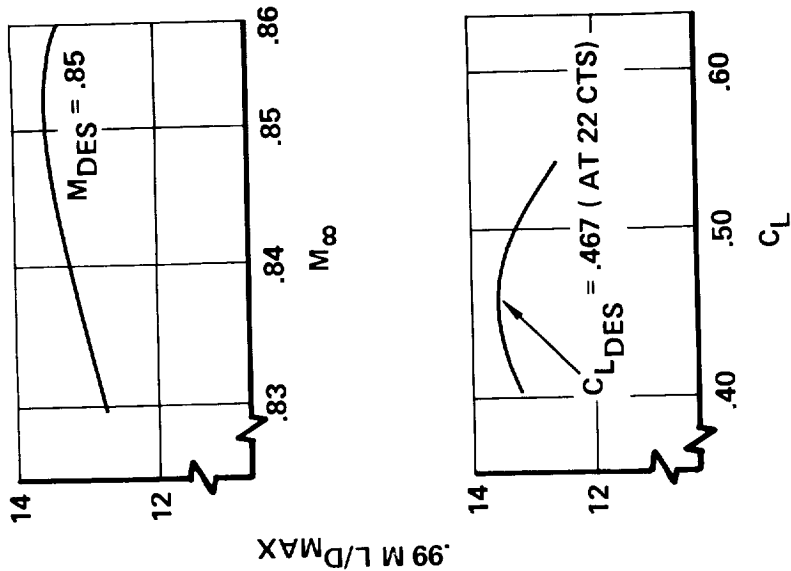
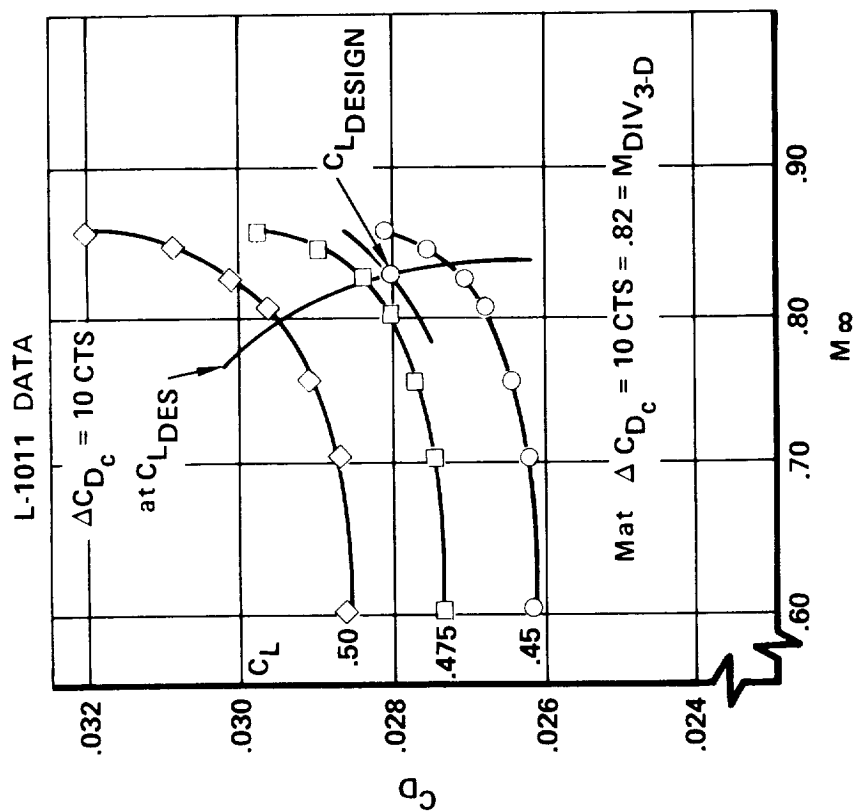


Figure 28. M_{DES} and $C_{L_{DES}}$ Derivation



$$M_{DES} - M_{DIV 3-D} = .85 - .82 = .03$$

OR

$$M_{DES} = M_{DIV 3-D} + .03 = M_{D 2-D} + \Delta M_{\Lambda} + \Delta M_{AR} + .03$$

Figure 29. M_{DES} Design M_{DIV} Divergence Relationship

representative of advanced technology wings. These characteristics are represented by the parameter "Z", see Figure 30 and $C_{D_{Pressure}}$ of Figure 31.

$$C_{D_{TOTAL}} = (C_{D_f}) 1.08 + \Delta C_{D_{P_{fuselage}}} + \Delta C_{D_{P_{wing}}} + C_L^2 / \pi AR "Z" + \Delta C_{D_{Trim}}$$

Where the 1.08 factor accounts for roughness.

To account for trim drag associated with the large negative pitching moments, a .04 C_L increment is assumed to be carried by the wing to develop the desired trimmed lift.

3.3.1.2 High Lift Drag Polar and $C_{L_{max}}$ Build-up Procedures - In building up the high lift polars for parametric transport aircraft it is first premised that the clean flaps-up polar has been defined at $M = 0.23$ by the procedures discussed in the previous section. The high lift flaps-down polars are then developed by adding to this polar, lift and profile drag increments as a function of wing and flap geometry (see Figure 32). As in the previous build-up methods, the B-1011 flight data has been used as the basis for developing these parametric procedures. Methods from the Royal Aeronautical Society (RAS) Data Sheets have been applied to these data to permit excursions in flap and wing geometric variables (Figure 33).

Maximum lift coefficients, using FAA certified B-1011 flight data as the base, have been modified for flap and wing geometry using the methods of the RAS data sheets.

In this study it was assumed that advanced design techniques applied to a high lift system would permit increases in $C_{L_{max}}$ of 10 percent greater than achievable by present state-of-the-art practice.

3.3.1.3 Wing Sweep Angle Selection - Selection of sweep angle for the cruise Mach number .85 hydrogen fueled passenger aircraft wing was based on the trade noted in Section 3.3.2.1.1. For those aircraft designed for cruise at $M = 0.80$ and $M = 0.90$, a decrement and increment respectively of 5 degrees was selected to retain pre and post-drag rise characteristics equivalent to the $M = 0.85$ design.

3.3.1.4 Approach Speed Considerations - Selection of passenger aircraft approach speeds was based on the considerations noted in Section 3.3.2.3.

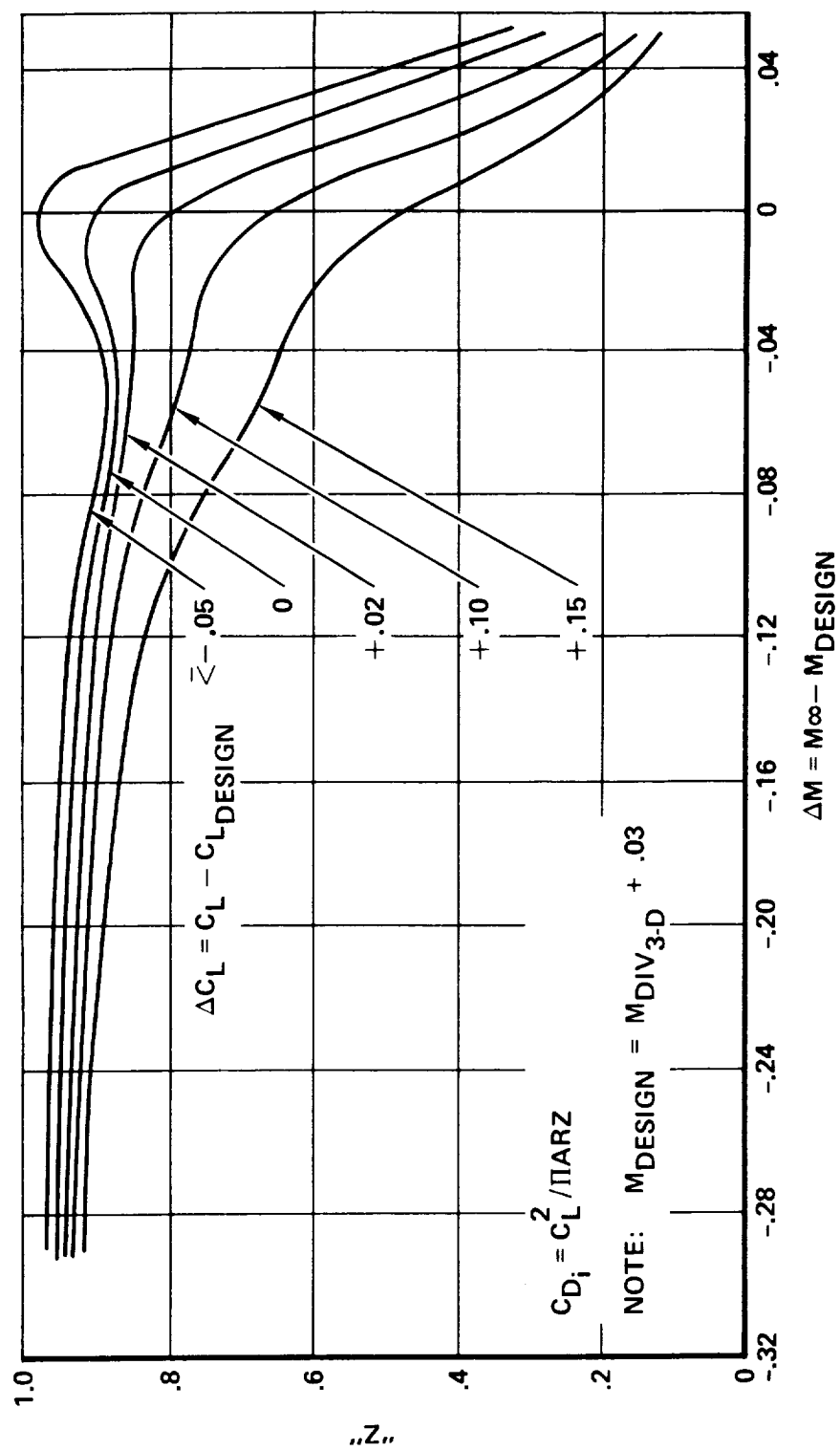


Figure 30. Polar Shape Factor "Z"

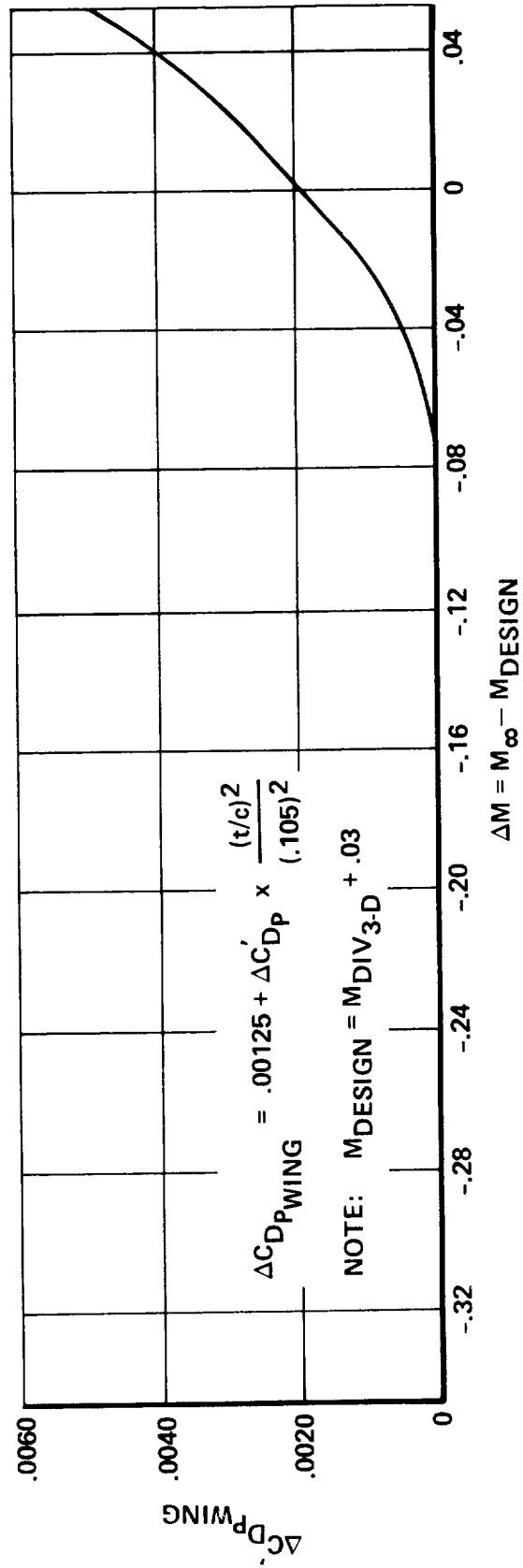
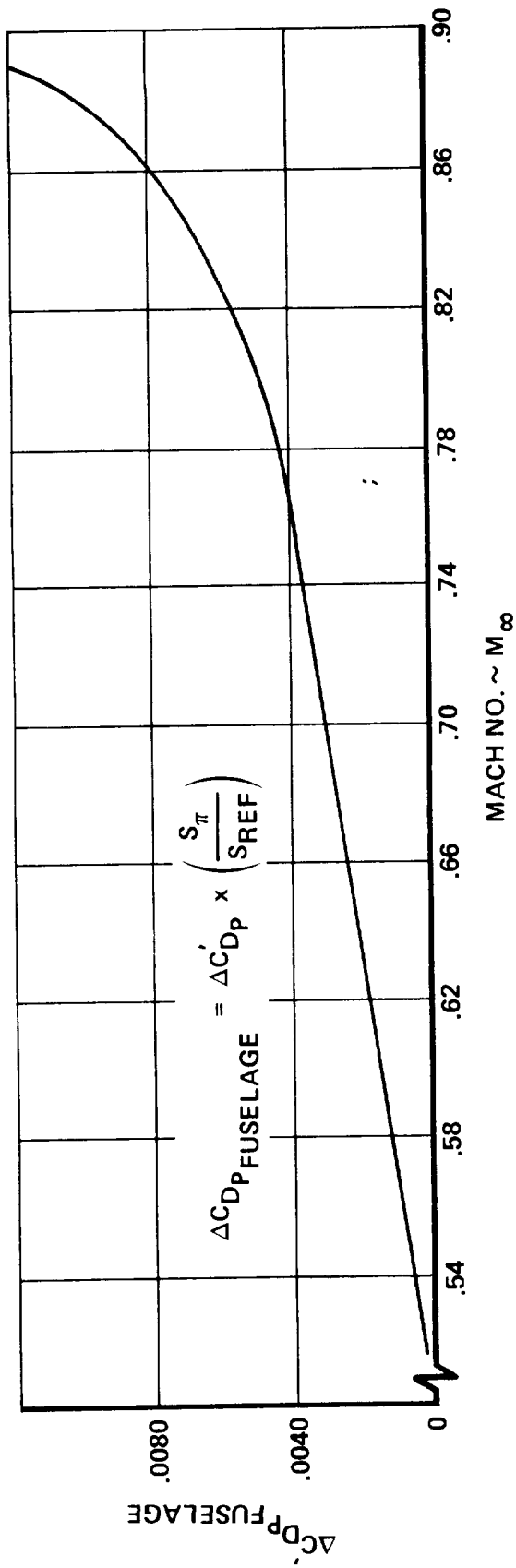
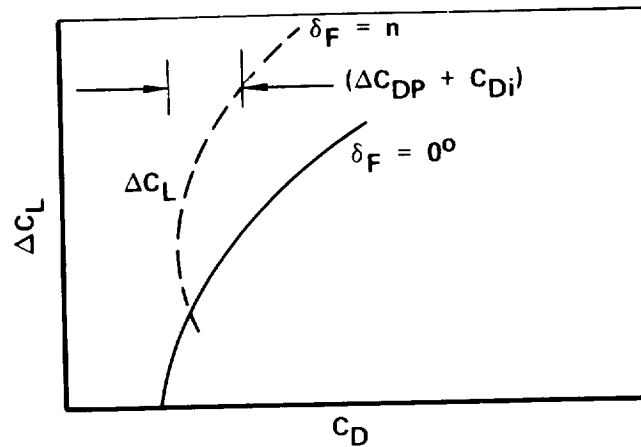


Figure 31. Wing and Fuselage Pressure Drag



BASIC BUILD-UP

$$C_{DF(\alpha=CONST)} = C_{DCLEAN} + \Delta C_{DP_{SLAT}} + \Delta C_{DP_{\delta F_n}} + \frac{(C_L + \Delta C_{L_{\delta F_n}})^2}{\pi AR} - \frac{C_L^2}{\pi AR}$$

C_{DCLEAN} : BASIC CLEAN POLAR BASED ON Z-METHOD OR EQUIVALENT ($M = 0.23$ AT SEA LEVEL)

$$\Delta C_{DP_{\delta F_n}} : \Delta C_{DP_{\delta F_n}} = \Delta C_{DP_{FLAP}} \times \mu_n \times \cos \Omega_{1/4}$$

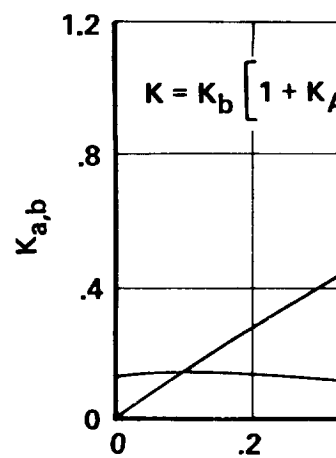
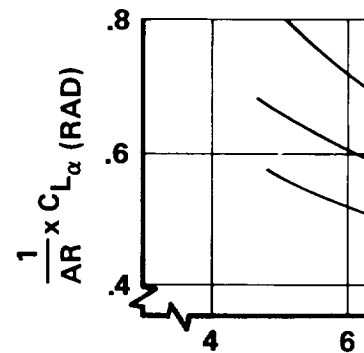
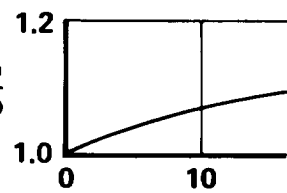
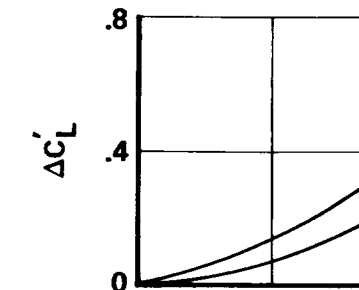
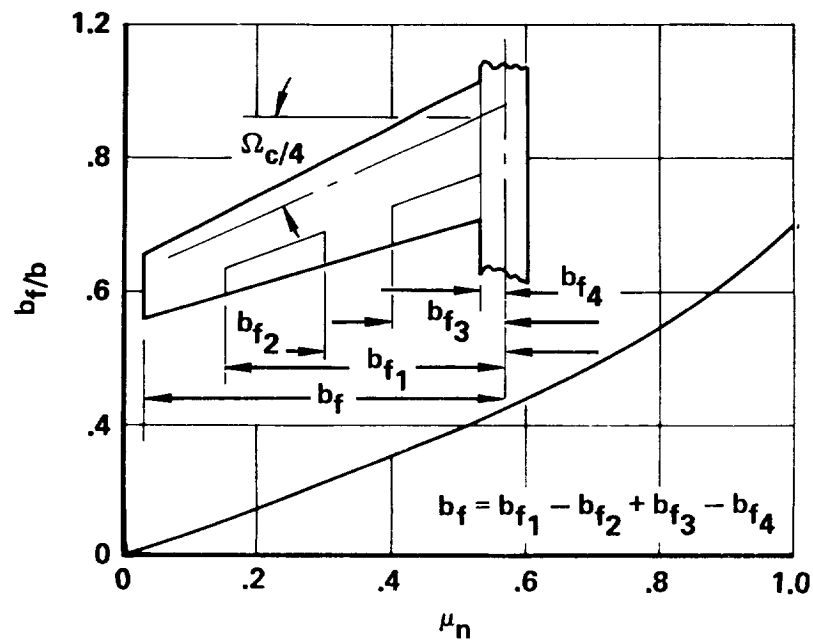
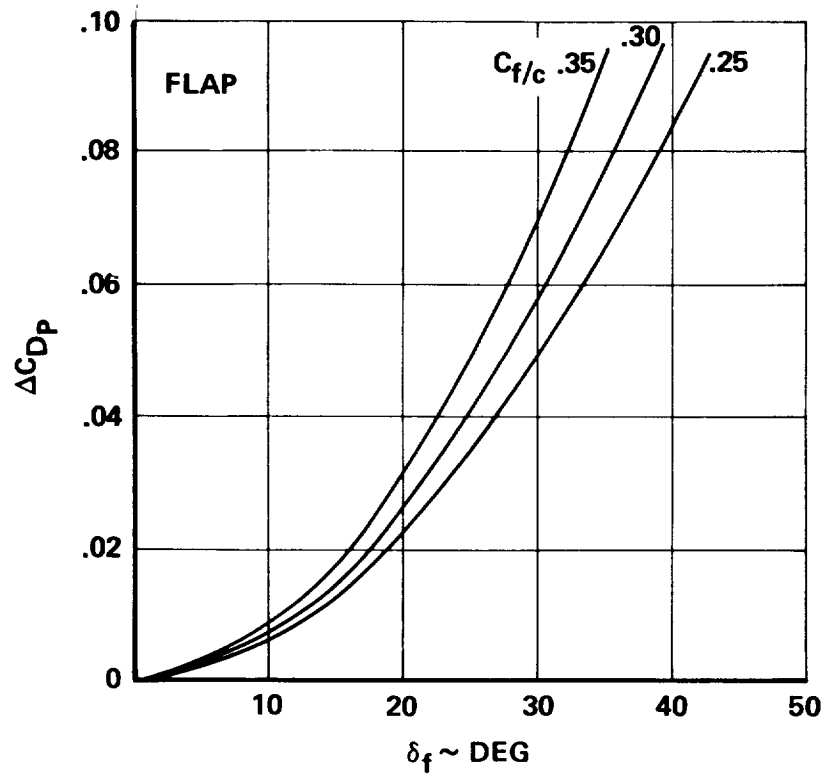
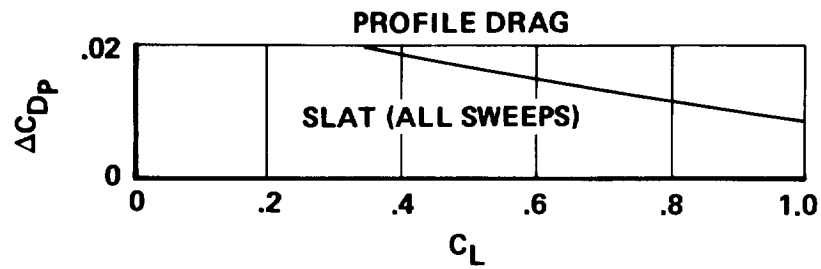
$$C_{LF} = C_{LCLEAN} + \Delta C_{L_{\delta F_n}}$$

$$\Delta C_{L_{\delta F_n}} : \Delta C_{L_{\delta F_n}} = \left[\Delta C'_L \left(\frac{c'}{c} \frac{C_{L\alpha}}{C_{L\alpha AR=6}} \right) + C_{LN} \left(\frac{c'}{c} - 1 \right) \right] K$$

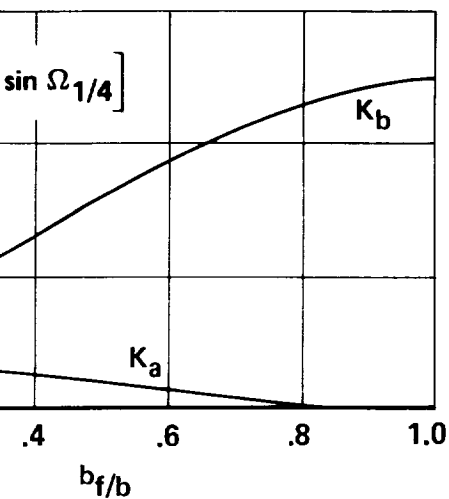
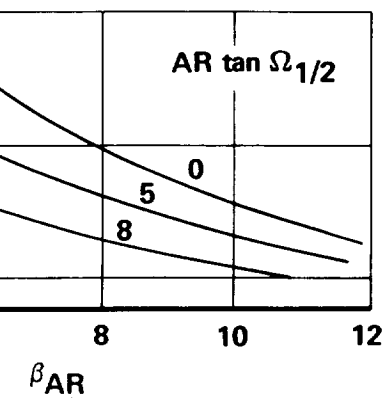
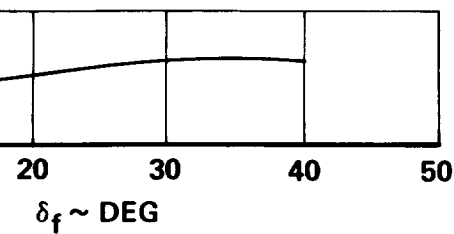
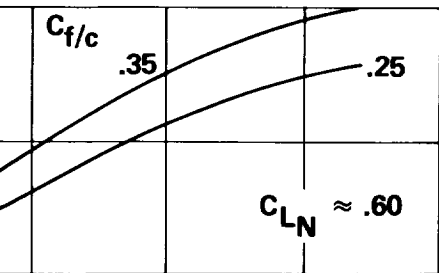
$$C_{LMAX_F} = C_{LMAX_{CLEAN}} + \Delta C_{LMAX_{\delta F_n}}$$

$$\Delta C_{LMAX_{\delta F_n}} : \Delta C_{LMAX_{\delta F_n}} = \Delta C_{\ell(c_f/c)} \times \frac{\Delta C_{L_{FLAP}}}{\Delta C_{\ell(b_f/b)}} \cos^2 \Omega_{1/4} + \Delta C_{L_{SLAT}}$$

Figure 32. High-Lift (Flapped) Polar Synthesis for Advanced Design Parametrics



LIFT INCREMENT



C_{LMAX}

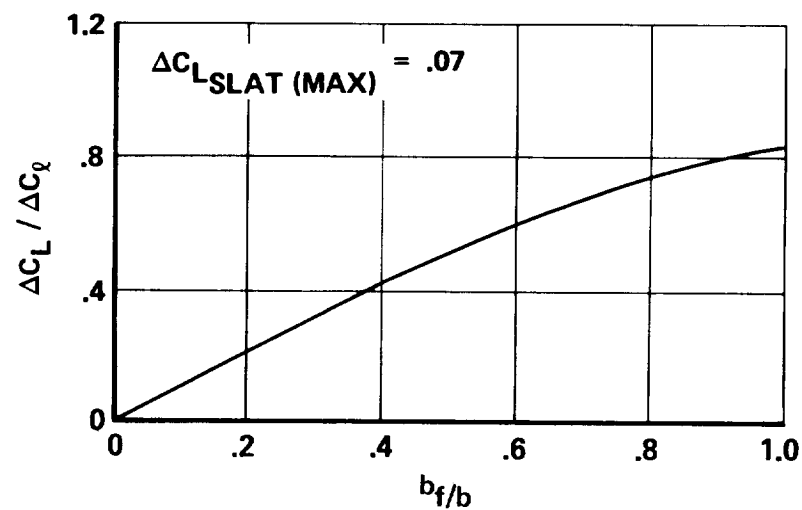
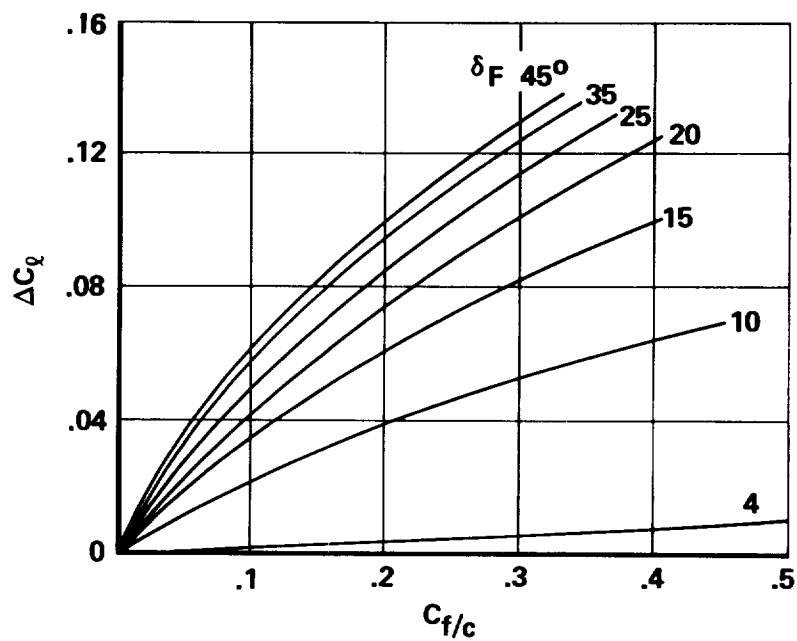
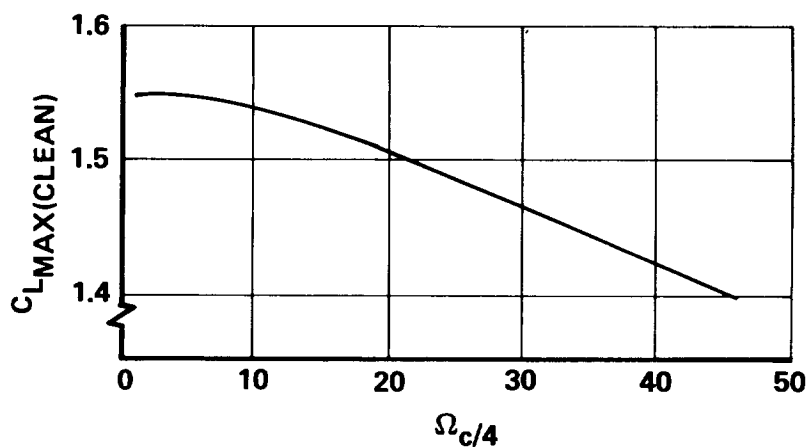


Figure 33. High-Lift (Flapped) Polar Synthesis Variables

3.3.2 Cargo Aircraft Aerodynamics

The aerodynamic characteristics of cargo aircraft involved in this study are based on the maximum use of supercritical aerodynamics as developed in conjunction with NASA-Langley during the ATT studies. The technology is defined in Section 3.2 of the Lockheed ATT report (Reference 10). Refinements in this data base have been made since the ATT studies and are included in the current study.

3.3.2.1 Cruise Characteristics - Since an optimum aerodynamic configuration does not necessarily result in an optimum configuration as defined by minimum weight or cost, the aircraft cruise configuration was defined early in this study by several parametric analyses. These parametric analyses were accomplished through use of a Generalized Aircraft Sizing Program (GASP) which utilizes predictions of structural weight, propulsion characteristics, and aerodynamic data to estimate the size and gross weight of aircraft constrained to meet given payload-range performance. Further description of this program is included in Section 5.3.1.

3.3.2.1.1 Wing Sweep Angle Selection - A parametric study for a preliminary version of the small hydrogen fueled aircraft at a wing loading of 562 kg/in^2 (115 lb/ft^2) and with a wing aspect ratio of 8 was conducted using wing sweep as the prime variable. The wing loading was chosen for this example because it permitted the 70 m/s (135 knot) approach speed selected for use in this study. The effects of wing sweep are essentially independent of aspect ratio. The results of this study are shown in Figure 34.

These data illustrate a decrease in gross weight of about 1.1 percent as sweep is decreased from 35 to 5 degrees. This slight weight decrease is considered to be offset by several qualitative factors, however, and a sweep angle of 30 degrees was selected. The adverse factors resulting from low sweep angle include increased gust sensitivity and increased potential for wing flutter. Both of these factors have the potential for requiring wing weight penalties not assessed in the parametric analysis. In addition, the low wing sweep angles would result in a configuration having an aerodynamically undesirable area distribution. The 30 degree wing sweep angle also provides wing section characteristics normal to the swept axis at 0.85 Mach number which are well substantiated by NASA-Langley data used in the ATT study.

EXAMPLE, LH₂ AIRCRAFT:

56,700 kg Payload, 5560 km Range, Mach = 0.85, AR 8.0, W/S 561.4 kg/m²
 (125,000 lb Payload, 3000 nm Range, Mach = 0.85, AR 8.0, W/S 115 lb/ft²)

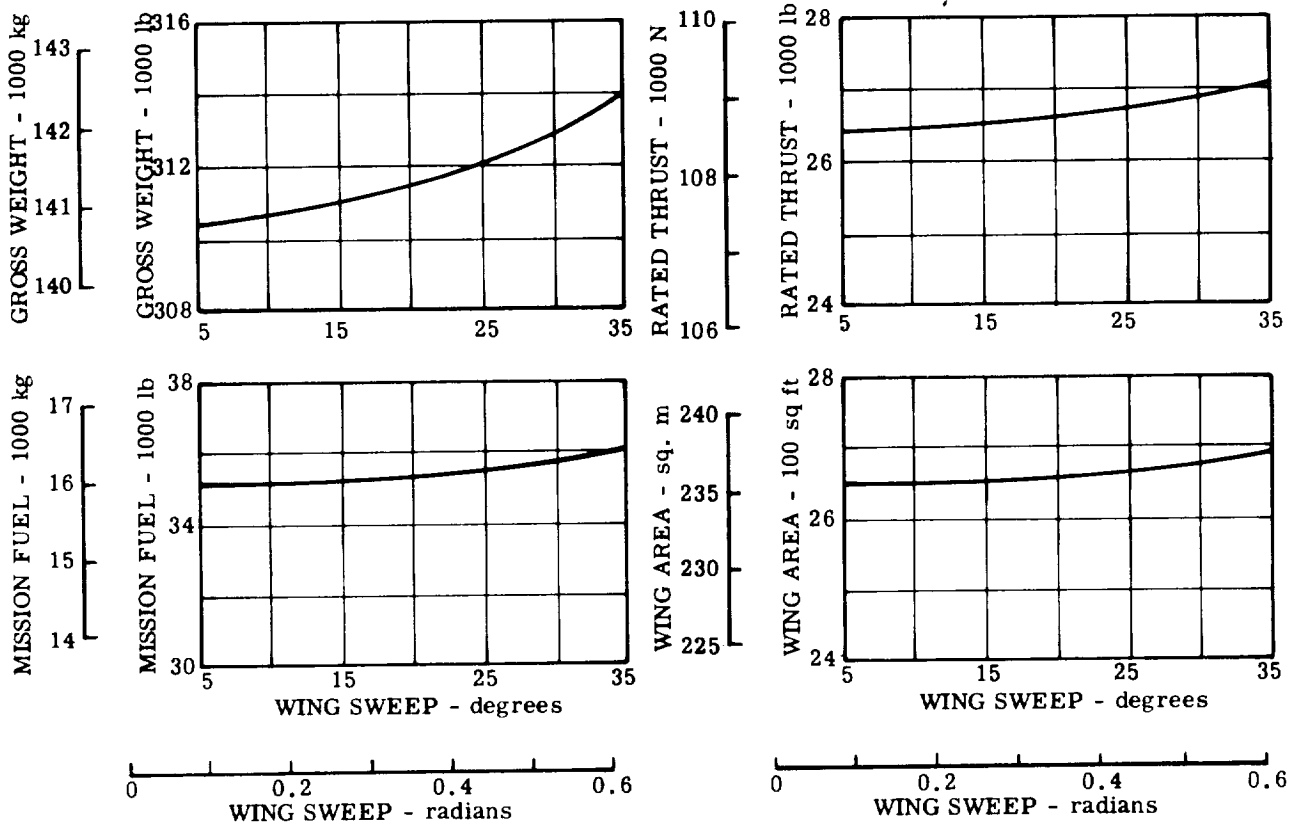


Figure 34. Wing Sweep Angle Selection

3.3.2.1.2 Wing Thickness - The wing thickness characteristics were defined by the empirical method described in the ATT report (Reference 10). This method defines the allowable wing thickness as a function of the basic drag rise Mach number, M_{DB} . The basic drag rise Mach number, in turn, is a function of the wing sweep and aspect ratio, the cruise Mach number and lift coefficient, and the wing technology level. Figure 35 shows wing thickness ratios as a function of the basic drag rise Mach number and lift coefficient and the supporting charts show the increment in drag rise Mach number which are functions of aspect ratio and wing sweep. An aerodynamic technology increment of 0.09 has been used for all cargo aircraft configurations. This technology factor, derived from NASA data, accounts for the differences in drag rise Mach number (for a given thickness ratio and cruise lift coefficient) between supercritical airfoil sections and NACA 6-series sections.

As shown on the figure, the basic drag rise Mach number is determined by subtracting the Mach number increments due to sweep angle, aspect ratio and technology level from the specified cruise Mach number.

The basic drag rise Mach number shown in Figure 35 assumes the aircraft is designed to fly 10 counts into the compressible drag rise. Figure 36 illustrates that, if the aircraft is designed to cruise further into the drag rise, then the basic drag rise Mach number will be decreased. Reference to Figure 35 shows that for a given cruise Mach number, a reduction in basic drag rise Mach number will allow a larger wing thickness.

The ATT configuration was designed for flight 22 counts into the drag rise. The optimum wing design must trade the reduction in wing structural weight against the increase in wing compressible drag which results from increases in wing thickness. This trade study was conducted and the results in Figure 37 show that the optimum DOC configuration is obtained when the aircraft is designed to fly 16 counts into the drag rise.

3.3.2.1.3 Drag Build-up - The cruise drag characteristics defined in this study are built up as follows:

- The zero lift drag of each component is estimated using the appropriate form factors and skin friction drag determined at the proper Reynolds number.
- A wing profile drag increment, as a function of variations in design Mach number and lift coefficient, is applied.

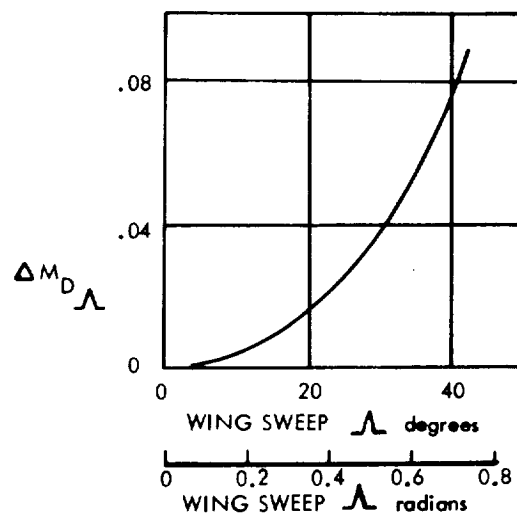
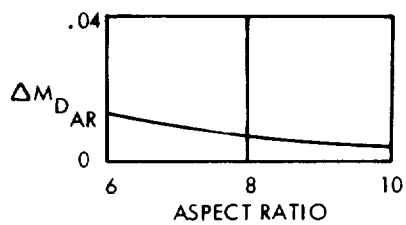
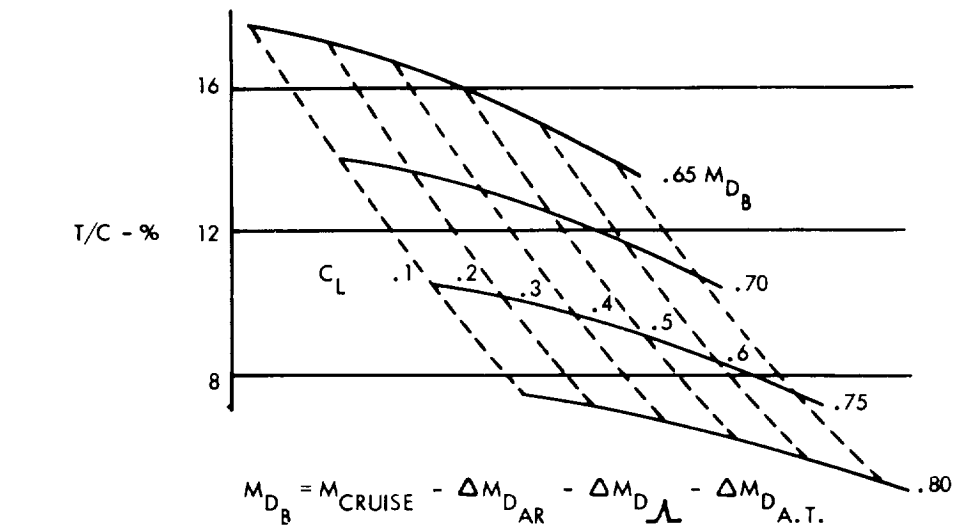


Figure 35. Wing Thickness Determination

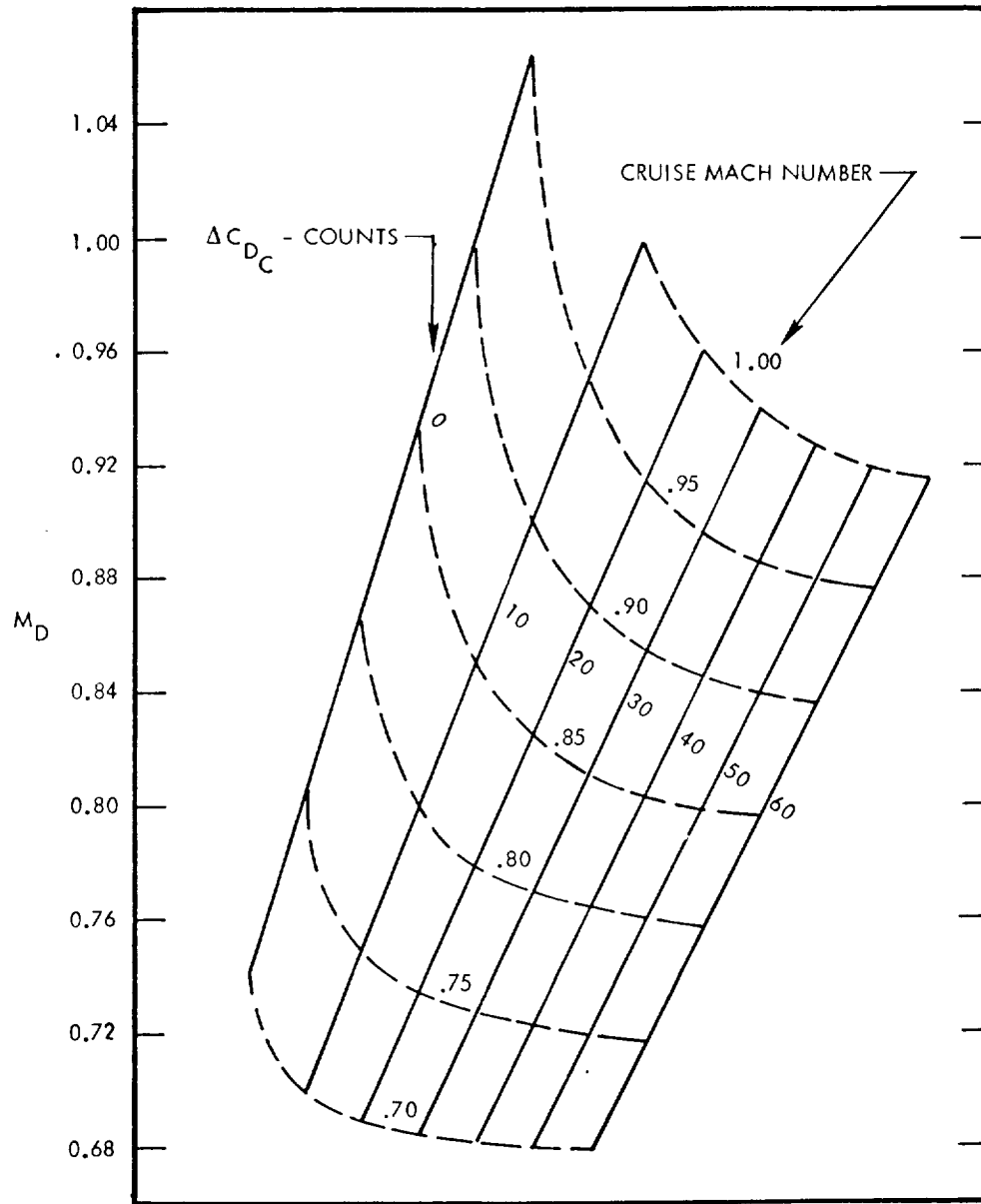
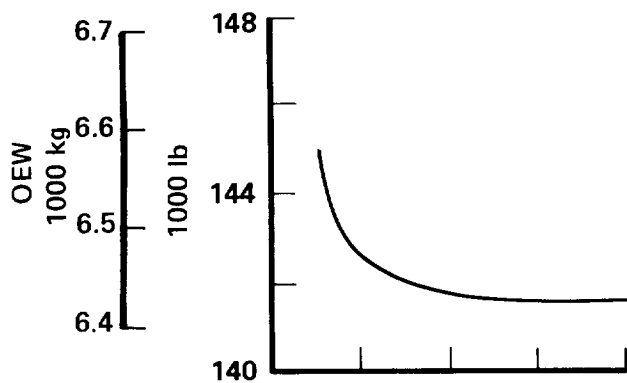


Figure 36. Post Drag Rise Characteristics



EXAMPLE:
 SMALL LH₂ FUELED NOSE LOADER
 CARGO AIRCRAFT:
 AR = 9
 $V_{AP} = 69.5 \text{ m/s (135 KEAS)}$
 $W/S = 560 \text{ kg/m}^2 \text{ 114.5 lb/ft}^2$
 (START OF CRUISE)

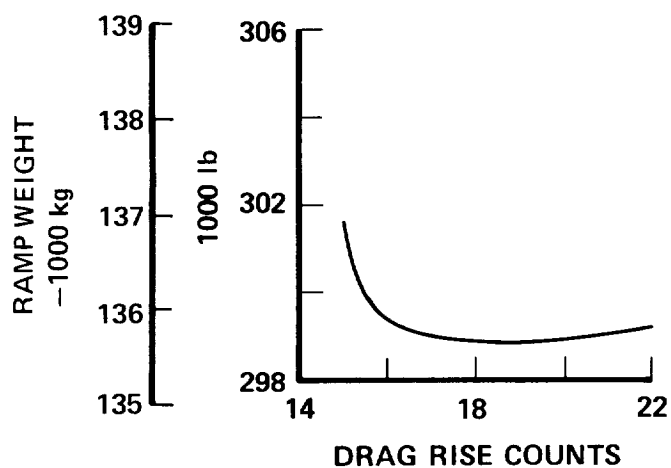
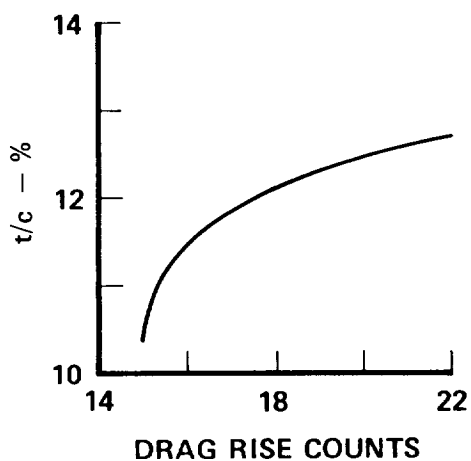
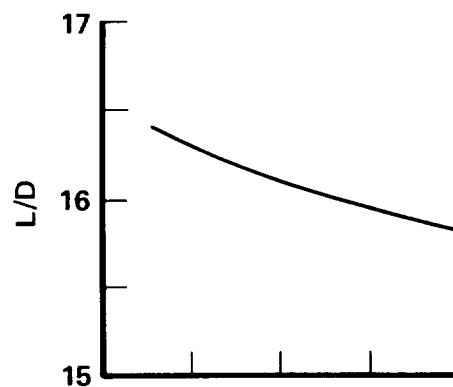
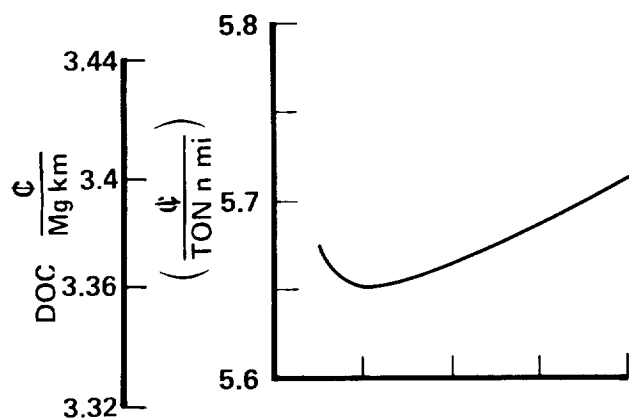


Figure 37. Compressible Drag Rise Optimization

- A compressible drag increment is applied. As previously described, a value of 16 counts results in a minimum DOC configuration and that value is used in this study.
- A 12 count trim drag increment (derived during the ATT study for most forward e.g., location) is applied. Roughness drag is computed as 8 percent of the parasite drag.
- Induced drag is determined based on use of an efficiency factor of 0.95.
- A miscellaneous drag increment is available to account for items such as wheel-well fairings or flap-track fairings as appropriate.

3.3.2.2 High Lift Characteristics - For supercritical airfoil sections, a $C_{l_{max}}$ value of 3.0 has been established for the landing and approach configurations for the aircraft presented. The wind tunnel data have been corrected for wing sweep, part span effects and flap chord length variations. In addition, reasonable corrections have been applied to correct the wind tunnel data to full scale Reynolds number and an adjustment has been made to account for the minimum speed effect as defined in FAR Part 25.103.

Aerodynamic characteristics compatible with this result are used in estimating the take-off and landing distances and the approach speed of the aircraft presented in this study.

3.3.2.3 Approach Speed Considerations - Preliminary information on results from a "runway operations analysis" supplied by NASA-Langley have been examined to review the effects of approach speed on runway acceptance rates. Portions of the data contained in that analysis are shown on Figure 38 for the maximum and minimum values of outer marker delivery accuracy. The figure shows that, if existing braking and reverse thrust capability is utilized [deceleration rate of 3.05 m/sec^2 (10 ft/sec^2)] acceptance rates increase with approach speeds for fixed separation distances between approaching aircraft. Acceptance rates remain essentially constant if approaching aircraft are not separated by fixed distances, but allowed to continue on final approach at any time unless the preceding airplane is still on the runway. At lower deceleration rates, acceptance rates are substantially reduced at higher approach speeds.

In summary, the results of the runway operations analysis showed that when currently existing deceleration capabilities are recognized, and when technology advances are incorporated in the total terminal area operation, runway acceptance

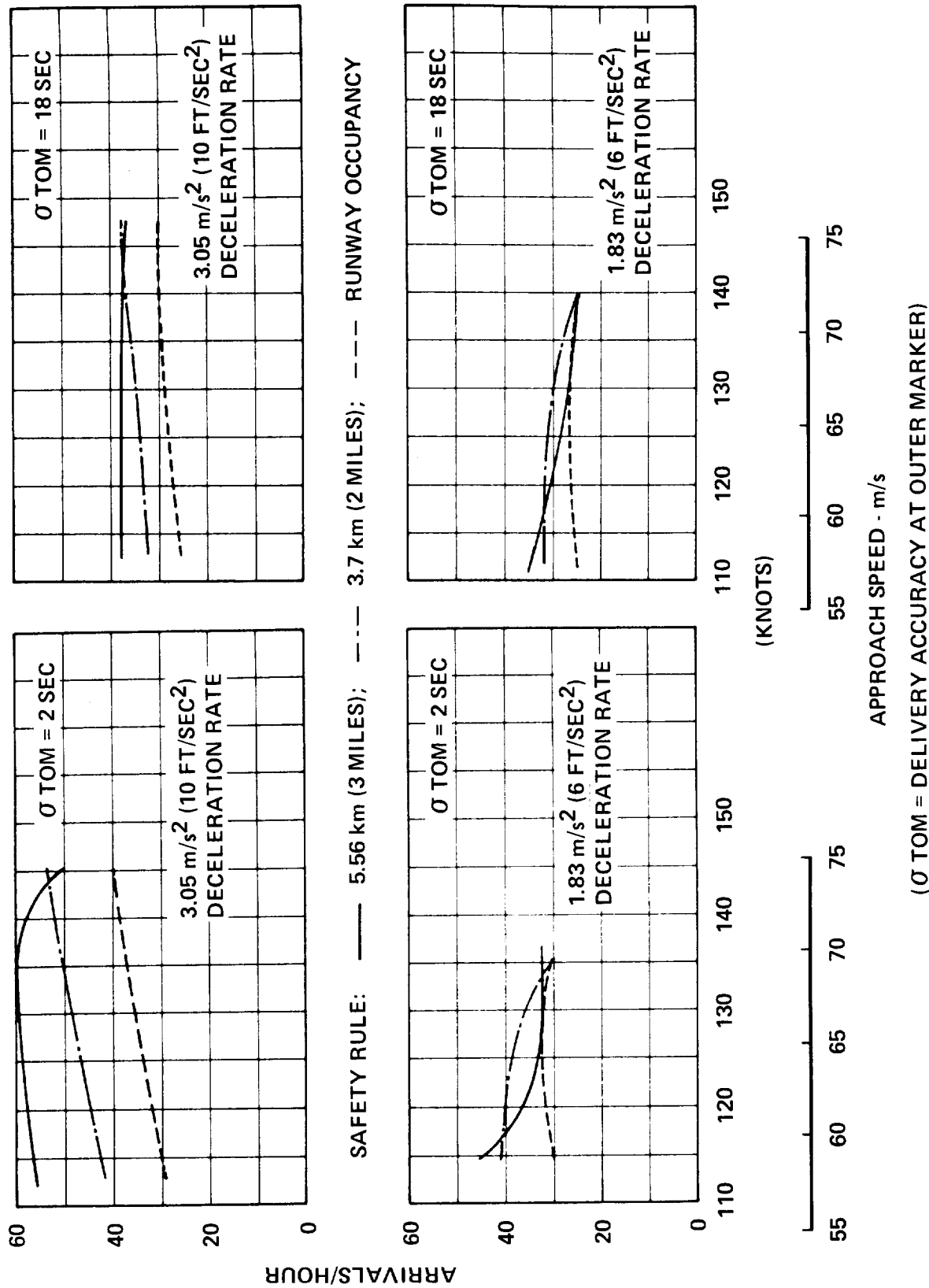


Figure 38. Effect of Approach Speed on Runway Acceptance Rates

rates either remain constant or improve as approach speeds are increased. On the other hand, as a limiting consideration, it is recognized that pilot work load increases if approach speed increases and some accident statistics show increasing accident rates as approach speeds increase. No quantitative analysis leading to conclusive tradeoffs of the various factors discussed here was attempted in the current program. However, the effect of lower approach speeds on gross weight and direct operating cost (DOC) for a typical aircraft in this study is shown in Figure 39. These data indicate an 18 percent increase in DOC if approach speed is lowered from 69.5 to 56.5 m/s (135 to 110 knots). An approach speed of 69.5 m/s (135 knots) was selected as a compromise value and was used to establish upper limits on wing loading in selecting airplane configuration characteristics.

3.4 FLIGHT CONTROLS

The philosophy of using active controls technology impacted the flight controls design in matching the empennage size and c.g. envelope for relaxed static stability. Examination of active controls applications for discrete load control and flutter suppression showed results of doubtful benefit for airplanes of this type. Considering the scope of the flight controls effort in this study it was deemed best to restrict active control usage to stability augmentation.

The restoration of static stability by active flight controls necessitates adoption of an aft c.g. tail sizing criterion replacing static margin. The tail size is established as a function of control power rather than as a passive contribution to inherent stability. The most demanding airplane nose down (AND) control power requirement for an airplane balanced in a statically unstable condition is that set by the need to restrict angle of attack at minimum speed. The criterion must assure sufficient AND pitch acceleration to avoid penetration beyond the maximum desired angle of attack. For an airplane with a distinct stall the limit need not exceed the stall angle.

Stall time histories from I-1011 flight tests were examined to obtain data on stall recovery. The maximum A N D pitch acceleration was measured during recovery from stalls in the landing configuration with forward and aft center of gravity positions at various weights. The total pitch acceleration resulted from the combined effects of inherent stick fixed pitch down tendency plus incremental A N D

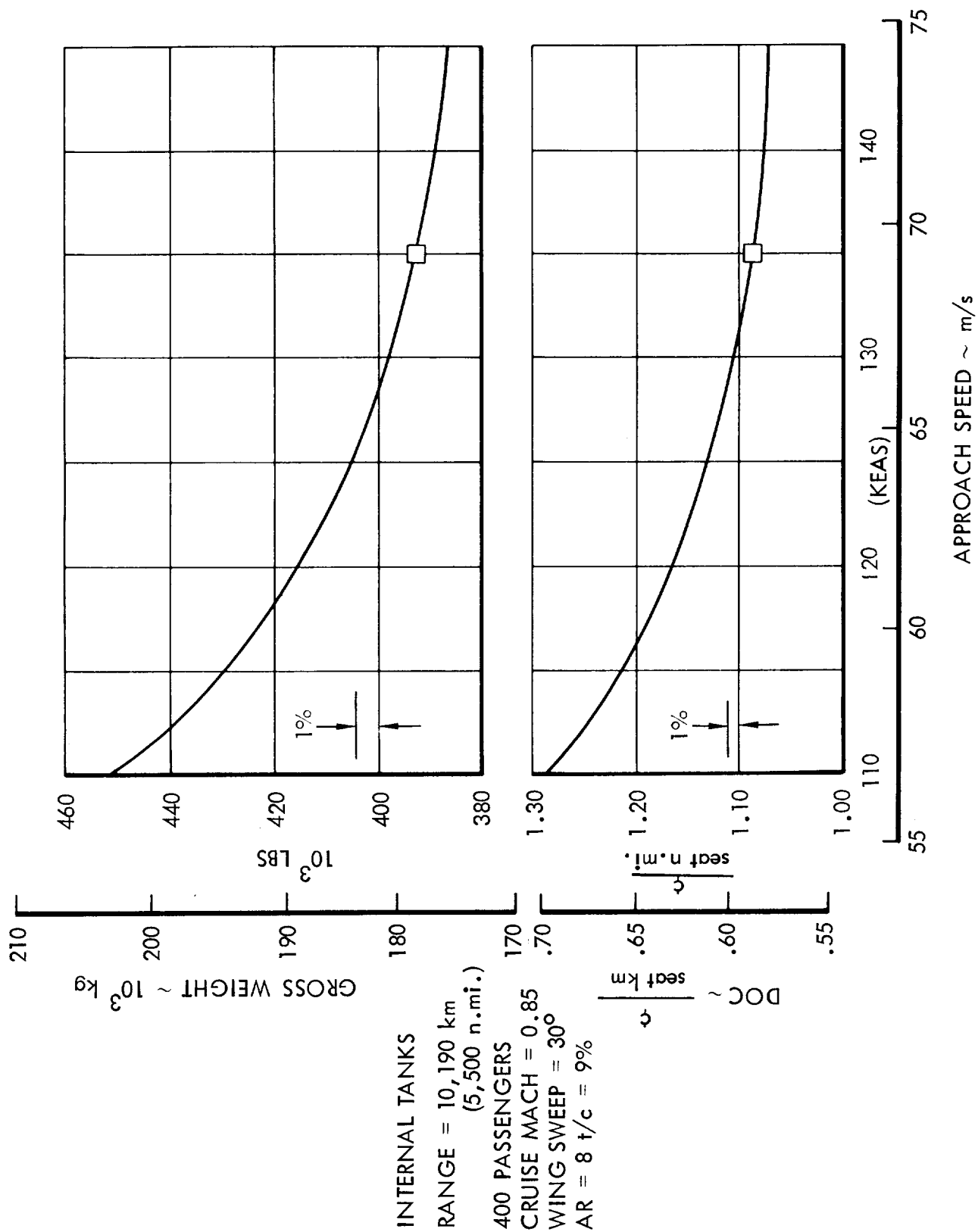


Figure 39. Effect of Approach Speed on Gross Weight and DOC

stabilizer input. The nose down acceleration from pitch down tendency is a function of static margin. Supplemental nose down control was commanded when the pilot was dissatisfied with the progress of recovery. In no instance was full A N D control capability employed. Apparently the resultant measured maximum pitch down accelerations were sufficient to satisfy the pilot that recovery from the stall was proceeding at an acceptable rate. A statistical distribution of the peak pitch accelerations is shown on Figure 40. The magnitude of the peak acceleration was equal to or less than $.08 \text{ radians/sec}^2$ in 87 percent of the cases. In the few recoveries with accelerations in excess of $-.1 \text{ rad/sec}^2$ the recovery was initiated well after the stall minimum speed was reached or else the peak acceleration occurred only for a brief interval. It can be concluded that $-.08 \text{ rad/sec}^2$ represents a useful upper boundary on the airplane nose down pitch acceleration needed to provide satisfactory recovery from a stall.

An airplane lacking inherent static stability and/or pitch down tendency at the stall must be provided with active envelope limiting as a component of the longitudinal stability augmentation system. The margin of control power required to perform the path over at the limit speed or angle of attack places an aft limit on the center of gravity position. The severity of the c.g. constraint depends on the size of the control power margin retained. It is proposed that for large subsonic transport airplanes essentially similar to the B-1011 the control power margin be sufficient to provide an A N D pitch acceleration of $-.08 \text{ rad/sec}^2$. Power effects at low weight and high thrust can erode this margin to about $-.05 \text{ rad/sec}^2$ at constant angles of attack. However, it should be assumed that the active control system will respond to power setting and flap position as well as angle of attack and that this will mitigate the effects of high thrust-to-weight ratio.

3.4.1 Fuselage Size

Flight controls sizing analysis was conducted in depth for the passenger transport configuration having liquid hydrogen fuel contained within the fuselage, Figure 41 (CL-1317-1). Empennage sizes for all other configurations included in the study were then based on those defined for the CL-1317-1 configuration. More detailed analysis of these other configurations would have negligible effect on the outcome of the study.

The aerodynamic limits on the CL-1317-1 center of gravity position are dependent upon the horizontal tail volume coefficient as shown on Figure 42. The forward limit is imposed by the requirement for airplane nose up stall in the landing configuration. Envelope limiting requirements, also in the landing configuration,

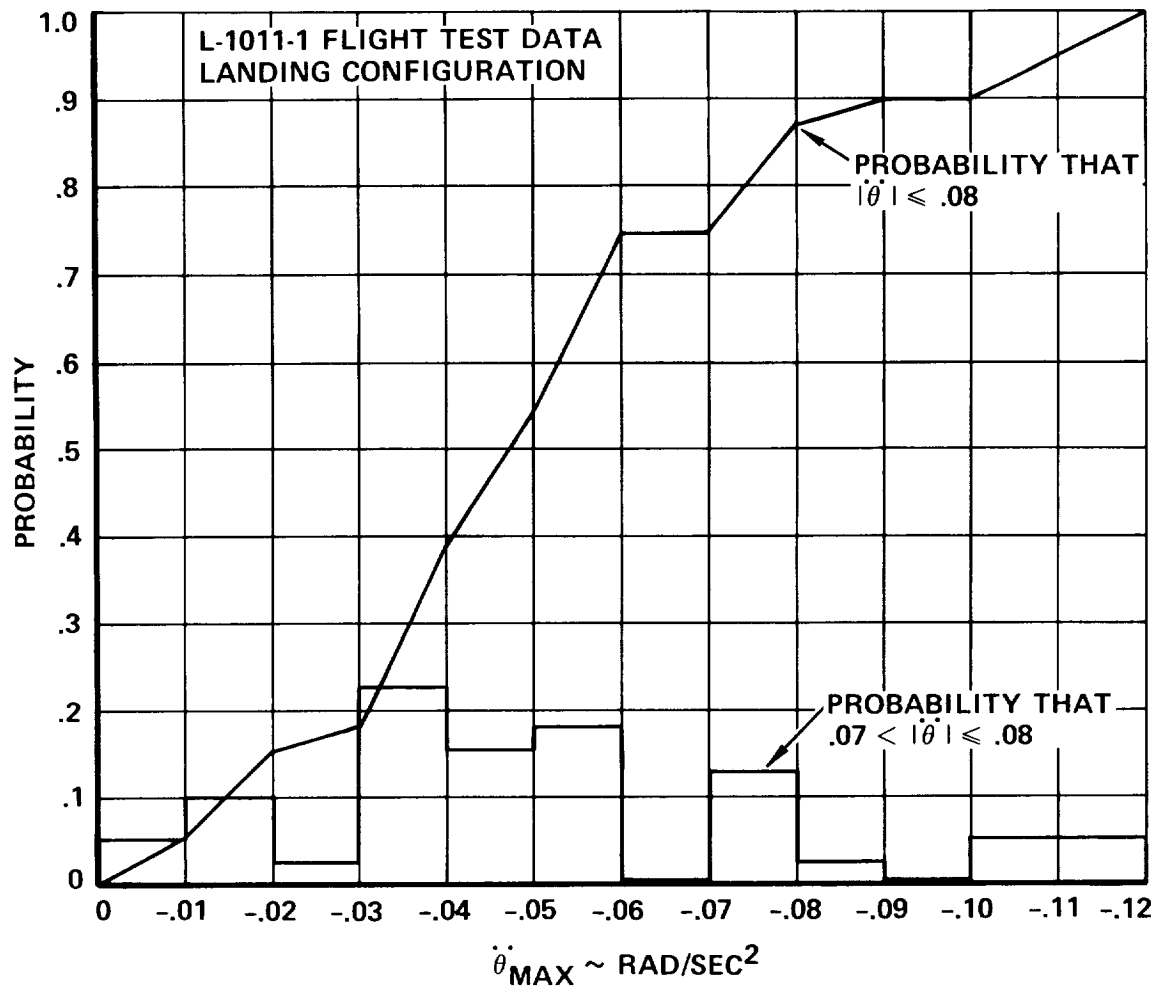


Figure 40. Maximum Pitch Acceleration During Stall Recovery

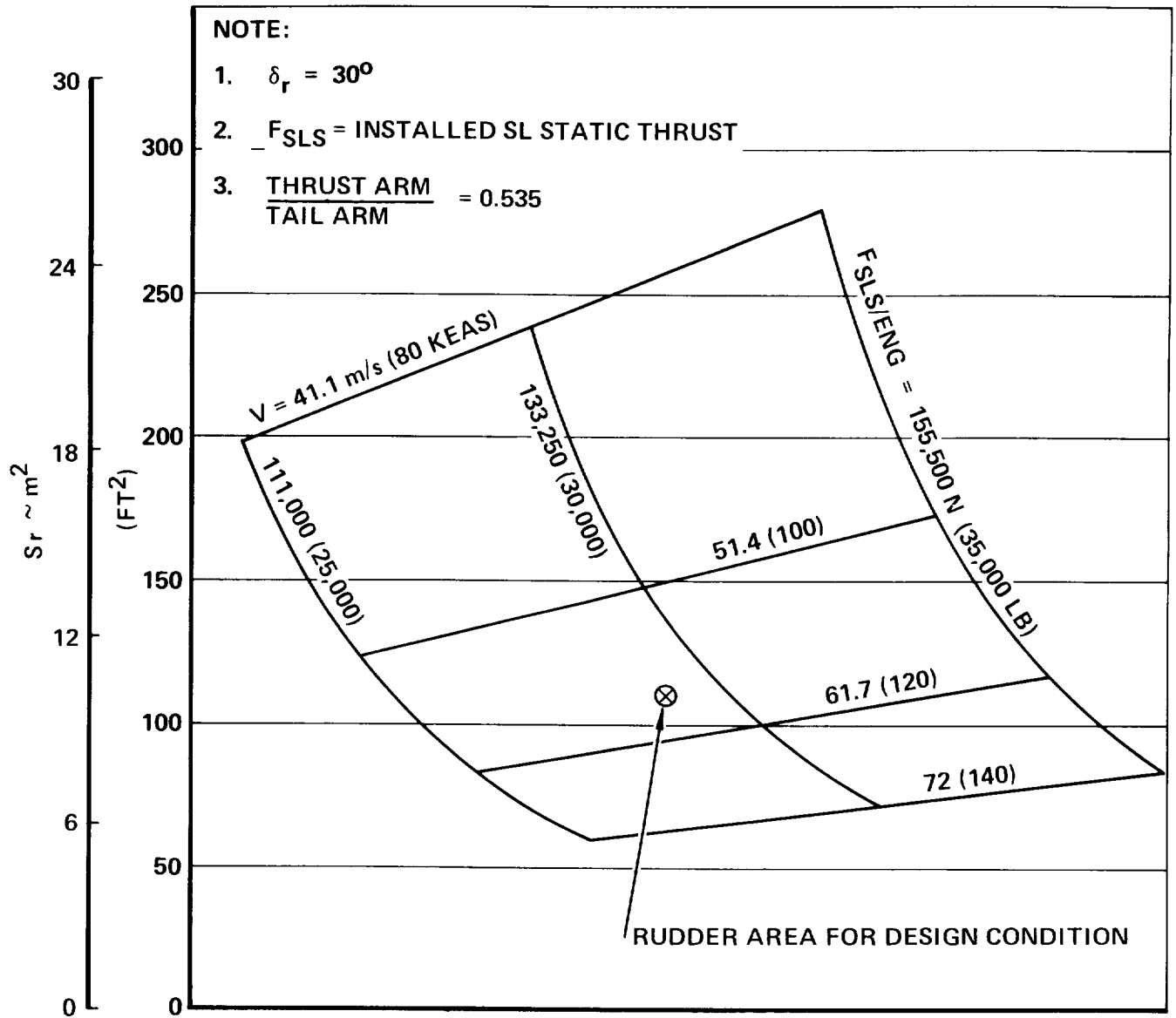


Figure 41. Rudder Size for Directional Control With One Engine Inoperative

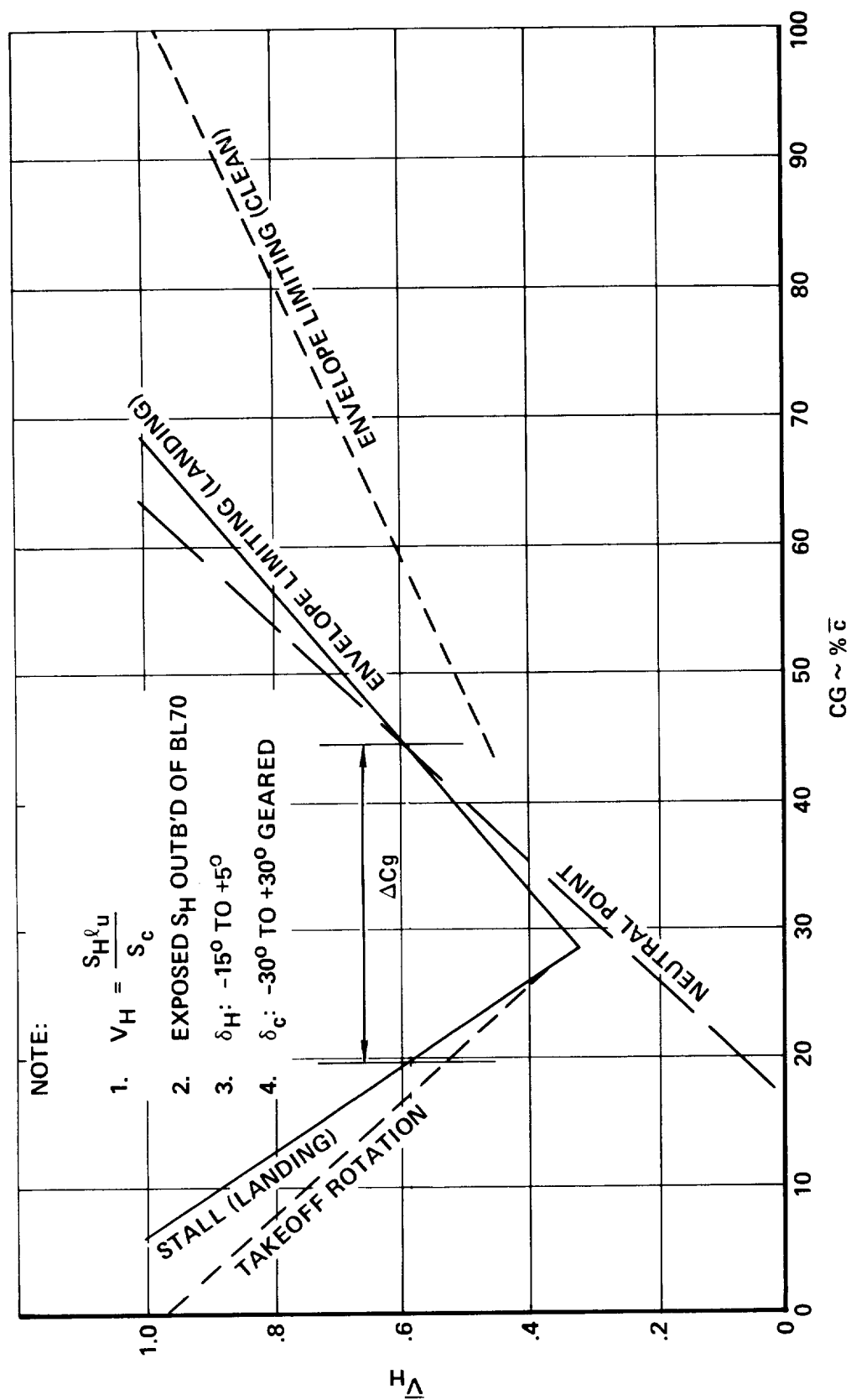


Figure 42. Aerodynamic Limits on Center of Gravity

place the aft limit. The neutral point is shown for reference, but was not a primary consideration in setting limits. Takeoff rotation and clean configuration envelope limiting, both potentially important conditions, were examined, but were found to be less critical. Their relationship to the c.g. envelope is shown. If it is assumed that the CL-1317-1 should have the same absolute c.g. travel as the L-1011-1, 1.7 m (67.5 in.) then a horizontal tail volume of .59 is required.

The vertical tail was sized to provide directional control sufficient to balance the load of an outboard engine at take-off thrust. The relationship between speed, nominal thrust and rudder area is shown on Figure 43. In order that air minimum control speed ($V_{MC_{AIR}}$) will not be restrictive at shorter field lengths a light take-off weight of 163,000 kg (360,000 pounds) and thrust-to-weight ratio (T/W) of .32 has been assumed. Stall speed (V_S) is 53 m/s (103 KEAS). For a normal take-off, L-1011 flight tests show that at this T/W, rotation speed (V_R) is related to stall speed by:

$$\frac{V_R}{V_S} = 1.15$$

The Federal Aviation Regulations require that V_R and $V_{MC_{AIR}}$ have the following relationship:

$$V_R \geq 1.05 V_{MC_{AIR}}$$

These two expressions establish a third:

$$V_{MC_{AIR}} = 1.1 V_S$$

$V_{MC_{AIR}}$ must then be 58 m/s (113 KEAS). Figure 44 shows that rudder area (S_P) is 10.7 m² (119 ft²) for this condition. The resulting vertical tail volume coefficient (V_v) is .071 if the rudder is 30 percent of the fin chord. With this tail the inherent directional stability is 80 percent of that for the L-1011. Active stabilization will restore directional stability to the level desired. Control power required for active stabilization is less than the amount made available by designing for engine-out control.

Because of the great body length and diameter relative to the tail size the exposed root chords of the recommended tails are positioned at a distance out from

the body of approximately 1/2 the fuselage boundary layer depth at the tail surface 1/4 MAC location. The areas and volume coefficients refer to the exposed dimensions.

3.5 MATERIALS

Definition of baseline materials for all configurations involved in this study is based on a materials technology which offers significant advantages in weight and integrity and is technically achievable for design commitment in the late 1980 time frame. Material and attendant processing costs are design parameters which were considered in selection of the various candidates. Selection of materials for the major structural components of the study configurations was based on the results reported in the NASA ATT study of Reference 10.

3.5.1 Airframe

Material usage in the wing, empennage, and portions of the fuselage which do not interface with LH_2 fuel is based on Reference 10, modified to fit the requirement of the subject aircraft. These materials must be corrosion resistant, fracture tough, fatigue resistant and stress corrosion resistant. Where hydrogen diffusion or a chance LH_2 exposure is a foreseeable happenstance, resistance to diffusion and embrittlement and/or low temperature ductility may be additional constraints. While not precluding the incidental application of other materials as the need arises, advanced materials (composites) and the high strength aluminum alloys emerge as the predominate airframe candidates. Figure 43 and Table 6 (taken from NASA CR114718, Reference 6) compare properties of some aluminum alloys and composite materials, respectively.

In selecting materials for application in the ATT studies, candidate materials were compared on the basis of weight and cost of specific applications to the airframe structure. Selections were made for three levels of application of advanced materials on the basis of cost per unit mass of weight saved. Technology factors, computed for the three levels of applications, were applied to the analytical weight equations used in the parametric airplane sizing program. The weight or technology factors were developed for a constant-size airplane by substituting different materials and structural concepts and computing the weights of structural elements for identical structural requirements. The full benefits of advanced materials were

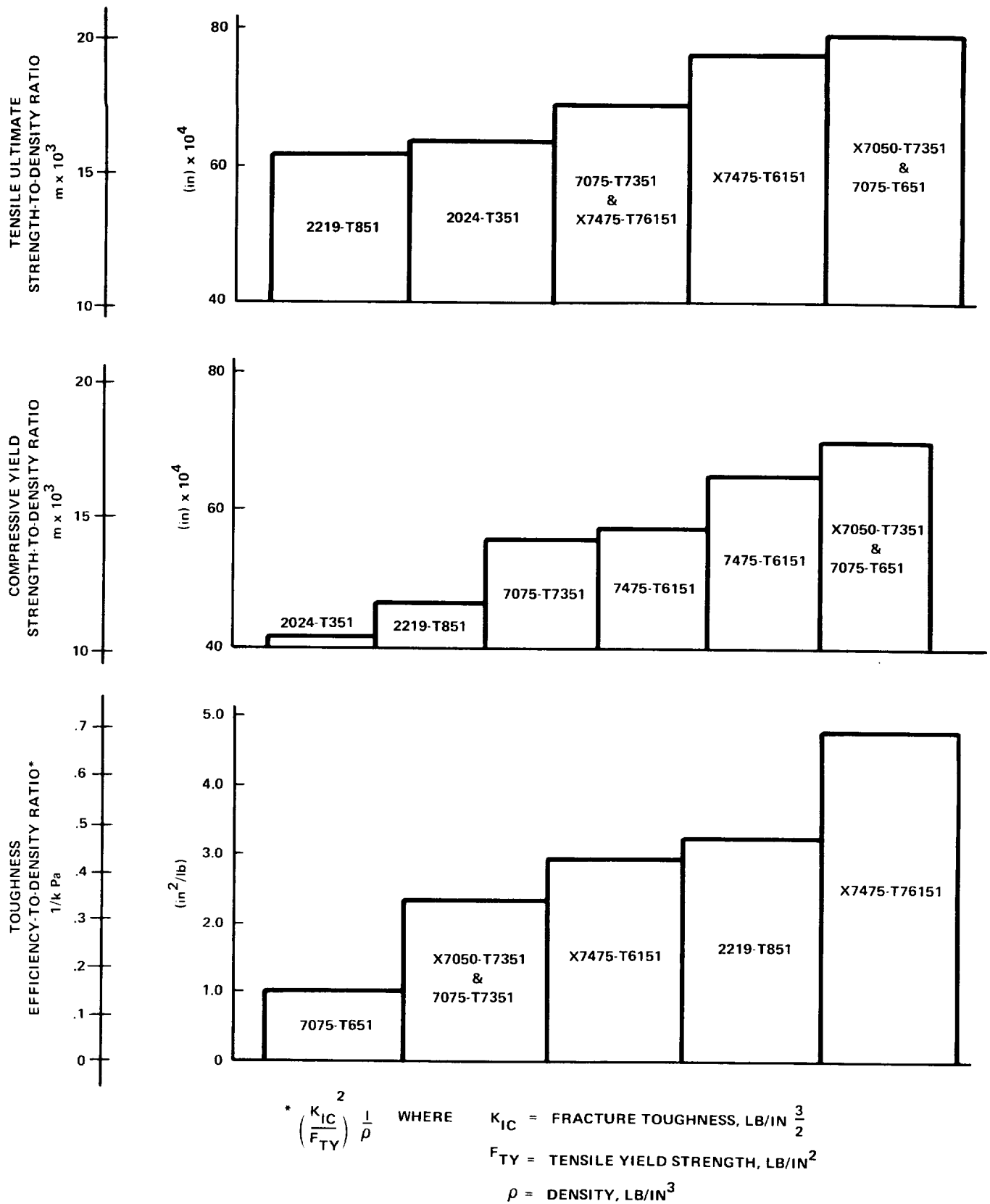


Figure 43. Comparison of Aluminum Alloys at Room Temperature

TABLE 6. COMPOSITE MATERIAL PROPERTIES - S.I. UNITS

MATERIAL	FIBER VOL.	DENSITY kg/m ³	TEST TEMP. °C	F _{tu} kPa	E _t MPa	F _{cu} kPa	E _c MPa	IZOD UN-NOTCH J	NOTCH J	DEPTH/RADIUS $\frac{\text{Notch}}{\text{Un-notch}}$ ratio
Boron/Epoxy Fiber B4 AVCO 5505/4 Matrix 2387 0° Fiber Flap Coupon	0.50	1.161	21	9,001	1,436	17,333	1,532	62.78	30.92	0.104 - 0.010
Fiberglass/ Epoxy S/901 Roving 0° Fiber E-787 Laminate Coupon	0.67	1.155	21	13,406	397	7,421			36.61	0.098 - 0.010
			-253	14,364	450	11,395				
Boron/Alum. Fiber 5.6 Mill Matrix - AL 6061-F 0° Fiber Flat Coupon	0.48	1.522	21	10,342	1,489	13,550	1,786		198.0	0.68
			-196	10,438	1,456	12,975	1,843		147.8	0.5
Boron/Polyimide Boron (4 mil filament tape) - Polyimide (P-13N) Fiber	0.50	1.153	21	8,618	1,532	8,379	1,436			
			-55	8,140	1,460	-	-			
			260	6,464	1,341	7,182	1,460			
Graphite/ Polyimide Modmar II (Graphite) - Skybond 703 Polyimide 0° Fiber	0.58 - 0.62	0.897	21	10,198	1,135	8,537	1,049			
			260	8,097	1,101	3,059	1,077			

*Unidirectional

TABLE 6. SUMMARY MATERIAL PROPERTIES - U.S. CUSTOMARY UNITS (Continued)

MATERIAL	THICK- NESS, IN.	TENSILE STRENGTH, KSI	E, KSI	E, KSI	E, KSI	E, KSI	E, KSI	70-90 UNIFORM ELONGATION, PERCENT	NOTCH FATIGUE STRENGTH	DEPTH/RADIUS
Boron/epoxy Fiber R4 AYCO 550570 Matrix 2387 0° Fiber Flat Coupon	0.50	0.0735	21	188.0	30.0	362.0	32.0	46.3	22.8	0.104 - 0.010
Fiberglass/ Epoxy S/901 Roving 0° Fiber E-727 Laminate Coupon	0.67	0.0731	21	250.0	3.3	155.0	31.0	39.5	27.0	0.098 - 0.010
Boron/Alum. Fiber 5.6 Mill Matrix - Al 6061-F 0° Fiber Flat Coupon	0.43	0.0950	21	216.0	31.1	283.0	37.3	146.0	0.68	
Boron/Polyimide Boron (4 mil filament tape)- Polyimide (P-13N) Fiber	0.50	0.0720	21	180.0	32.0	175.0	30.0	109.0	0.5	
Graphite/ Polyimide Kevlar 49 (Graphite) - Skybond 703 Polyimide 0° Fiber	0.53- 0.62	0.056	21	170.0	30.5	-	-	21.9		
			260	135.0	28.0	150.0	30.5			
			21	215.0	23.7	178.3	21.9			
			260	169.1	23.0	63.38	22.5			

*Unidirectional

realized by resizing the total airplane, including the power plant and other systems, to take advantage of the lower structural weights.

In computing the technology factors, candidate materials and structural concepts were examined for each element of the structure. A weight factor of 1.00 was assigned to the conventional aluminum structure. Each of the other concepts was sized to identical structural requirements. The ratio of the weight of the advanced material and concept to that of aluminum was defined as the weight factor.

The cost of each concept was compared to the cost of conventional aluminum structure, and the cost per unit of weight saved was tabulated. Selections were made for the three levels of technology. The maximum level utilized advanced materials where possible to obtain the minimum weight. An intermediate level of technology applied advanced materials to approximately 60 percent of the conventional structure by selecting materials and concepts with the lowest cost per unit of weight saved. A third level applied the concepts with the lowest cost per unit of weight saved to approximately 40 percent of the aluminum structure. The resulting weight factors are shown in Table 7.

TABLE 7. WEIGHT FACTORS AS A FUNCTION OF PERCENT APPLICATION OF ADVANCED MATERIALS

AIRFRAME COMPONENT	CONVENTIONAL STRUCTURE	PERCENT APPLICATION OF ADVANCED MATERIALS		
		30	60	40
Wing	1.00	0.515	0.635	0.715
Fuselage	1.00	0.605	0.664	0.782
Empennage	1.00	0.600	0.730	0.780
Nacelle and Power Plant	1.00	0.606	0.787	0.869
Landing Gear	1.00	0.814	0.848	0.860
Total Structure	1.00	0.604	0.691	0.774

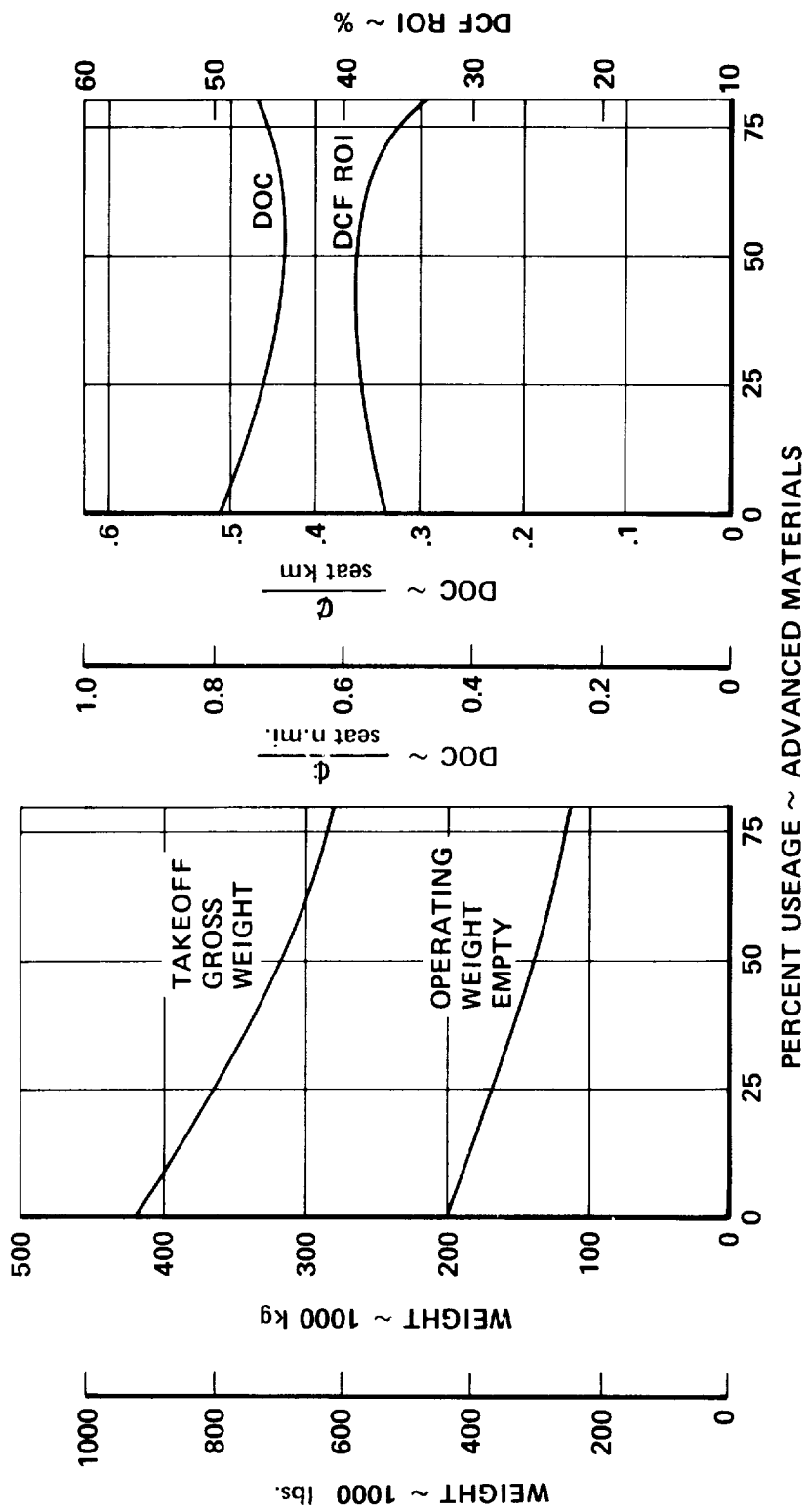
The weight factors of Table 7 were used in the parametric sizing program to size and price airplanes for each case. Direct operating costs were computed, and an economic analysis of each configuration was conducted to evaluate the return on investment. The results of these analyses for the APT study, shown in Figure 44, form the basis for selection of materials for the aircraft designs of the present study. As illustrated by Figure 44, DOC is minimized by the application of advanced materials to 50 percent of the airframe structure. Therefore, the structural materials and concepts and the weight factors corresponding to this selection were used in the development of all aircraft configurations presented herein.

3.5.3 Fuel Tank Structure

Use of LH_2 as a fuel requires that the tank materials be ductile at -253°C (-423°F), resistant to hydrogen diffusion and embrittlement, fracture tough, fatigue resistant, resistant to corrosion and stress corrosion, and also that they have a high strength-to-weight ratio. Further, they must be amenable to fabrication and repair processes so as to form a long-lived, leak-proof vessel. These characteristics are of particular importance to the structurally integral tank design concept.

On the basis of limited data, certain filamentary composites have exhibited compatibility with LH_2 . While insufficiently proven to qualify as tank structure for this study, they should be considered in the future. The NASA CR 114718 report, Reference 3, cited the compatibility of austenitic stainless steels with LH_2 but concluded they offer no advantage over high strength aluminum alloys for aircraft LH_2 fuel tank structure.

Room temperature property comparison of some high strength aluminum alloys is presented in Figure 45. The ductility of alloy 2219 at cryogenic temperatures, as well as its weldability, formability, stress corrosion resistance, high fracture toughness and resistance to flaw growth, are cited in the NASA CR 114718 report, Reference 3. Because of these characteristics, alloy 2219 was selected as the tank material for the supersonic transport study. The present study uses the 2219 alloy as the baseline material for tank structure based on identical rationale. Conservatively, no advantage was assumed for the tank material at cryogenic temperatures.



DATA FROM REFERENCE 9 FOR ATT INTERNATIONAL
CONFIGURATION MACH 0.95, PAYLOAD 38,500 kg (84,800 lbs.)

Figure 44. Benefits of Advanced Materials on Aircraft Weight and Cost Parameters

3.5.3 Insulation System, Fittings and Attach Members

The LH_2 tankage and delivery elements of the propulsion subsystem must be sheathed in materials through which the inner-to-outer thermal gradient ranges from -293°C (-423°F) to essentially ambient temperature, and the inward migration of substances from the environment (cryopumping) is negligible.

Attach fittings and members at the installation interface must not only sustain the mechanical loads but must also minimize heat transfer and cryopumping.

The materials must be capable of tolerating exposure to LH_2 or GH_2 in the event of a leak, weight must be minimized, and durability through repetitive flight and maintenance cycles must accommodate a realistic refurbishment schedule.

For purposes of this conceptual design study, a closed cell plastic foam, wrapped in a diffusion barrier material for insurance against cryopumping, and covered by an advanced composite material for protection against mechanical impact damage, was selected as a representative insulation system and external covering for the LH_2 tanks. Characteristics of various plastic foam insulation materials are presented in Table 8 and data for several candidate diffusion barrier materials are presented in Table 9, taken from Reference 6.

TABLE 8. PLASTIC FOAM INSULATION MATERIALS

MATERIAL	DENSITY kg/m^3	THERMAL CONDUCTIVITY $\text{W/m}^\circ\text{C}$	TENSILE STRENGTH kPa	COMPRESSION STRENGTH kPa
Polyethyleneimine Rigid, Closed Cell (Rohmco 14-31)	35	0.0313 (at 20°C)	981 (at 25°C)	59.1 (at 23°C)
Polyurethane Rigid, open Cell	32	0.0358 (at 12.8°C)	-	-
Polyurethane + 10% Chopped Glass Fibers Rigid, Closed Cell (A.D. Little Co.)	64	0.0208 (at -19.8°C)	-	-
Polyvinylchloride Rigid, Closed Cell (Kryoflex 8917)	50	0.015 (at -173°C)	1100 (at 27°C)	

TABLE 9. PHYSICAL PROPERTIES OF FILMS

BARRIER FILM	SPEC. GRAVITY	H ₂ PERMEABILITY cc/(100 in. ²) (24 hr) (atm/mil)	TEMP. LIMIT SERVICE LIFE	REMARKS
Polyester (Mylar)	1.39	600 (1 atm)	-73.3°C to 149°C (-100°F to 300°F)	Could possible be used at lower temp where no flex life required.
Polyvinyl fluoride (Tedlar)	1.57	950 (1 atm)	-73.3°C to 149°C (-100°F to 300°F)	Could possibly be used at lower temp where no flex life required.
Polyvinyl Chloride (Saran)	1.68	450	-54°C to 93.2°C (-65°F to 200°F)	Could possible be used at lower temp where no flex life required.
Teflon (FED)	2.15	2340 (1 atm)	-254°C to 204°C (-425°F to 400°F)	
Polyimide (Kapton)	1.42	250	-254°C to 243°C (-425°F to 470°F)	
Fluorohalocarbon (Aclar)	2.1	1500 (1 atm)	-73.3°C to 149°C (-100°F to 300°F)	Could possibly be used at lower temp where no flex life required.

It is important to point out that the materials technology essential to effective use of LH₂ in a commercial transport aircraft has yet to be developed. For example, the propensity of structural materials to become susceptible to hydrogen embrittlement as a result of years of exposure needs to be determined. The long term behavior of most candidate insulation, barrier and structural materials in the combined LH₂ and aircraft environment is unknown. Their compatibility with other aircraft materials, e.g., hydraulic fluid; repetitive cycling through the flight profile; and repetitive and prolonged exposures to acoustic vibration, are among the examples of development testing which must be performed. The ever tightening regulations covering fire, smoke and other hazards in commercial passenger transport aircraft must be

considered. Ultimately, the materials qualifying for the sheath, fitting and attach member components must do so under total subsystem static and fatigue tests simulative of the aircraft service environment.

3.6 STRUCTURES

3.6.1 Structural Design Criteria and Concepts

The structural design criteria, design concepts, and other structural data used in this study were derived primarily from the studies of References 10 and 6. The materials usage and design concepts are essentially the same as those developed by the Lockheed-Georgia Company in its studies of the application of advanced technologies to subsonic long-range transport aircraft. As discussed in Paragraph 3.5.1, these studies, reported in Reference 10, show that an advanced composites utilization of approximately 50 percent of the structure results in the lowest life-cycle cost and near minimum weight. This has been shown in Figure 44. Where the presence of LL_2 fuel tanks for aircraft of the present study require modifications to be made to the basic airframe structural concepts that were developed for the reference ATF aircraft, design concepts were utilized from the Lockheed-California Company studies of the hydrogen fueled advanced supersonic transport reported in Reference 6.

Preliminary analyses were conducted to establish the basic external loads for the LL_2 fueled passenger aircraft. These loads, which are presented in Appendix C, were used to assist in the estimation of the structural weight to account for the differences of the LL_2 airplane from its Jet A fueled counterpart. Included in these differences are the following: (1) smaller wing area; (2) lower wing loading; (3) lower ratio of takeoff weight to landing weight; and (4) no fuel in the wing. The first two of these differences tend to lower the wing weight of the LL_2 airplane; however, item (4) tends to increase the wing weight since the inertia load relief from fuel in the outer wing of the conventional Jet A fueled transport is not present in the LL_2 airplane. The lower gross weight of LL_2 fueled aircraft indicated by item (3), results in smaller, lighter landing gear and smaller engines.

The candidate design of LL_2 fueled aircraft carries its total fuel load in externally podded wing tanks. This concept represents a major deviation from the conventional aircraft configuration. The massive tanks on pylons above the wing

are located over the inboard engines and affect the aerodynamic performance, flutter characteristics, and wing loads. Co-location of the engine and the tanks permits the use of common structure to help minimize structural weight. The structural arrangements of the tank and pylon are shown in Figure 63 in Section 4.5. A preliminary stress analysis, utilizing the loads of Appendix C, was conducted to establish the feasibility of the design and to assist in the weight estimation of the tank installation and wing structure.

3.6.2 Structural Descriptions

Utilization of advanced composites for approximately 50 percent of the total structure to achieve minimum life-cycle cost results in a high percentage of graphite epoxy composites for the following primary structural components: wing box, ailerons, fuselage shell, empennage box structures, elevators, and rudder. The design concepts for these structural components, described in the following paragraphs, are conventional and are essentially the same for all the aircraft configurations, passenger and cargo. The exact materials distribution for each component are listed in Table 10.

3.6.2.1 Wing - The wing structure consists of a center wing box, inner wing box, outer wing box, leading and trailing edges, and flaps, ailerons and fairings.

Primary Box Structure - The primary box structure consists of the front and rear beams, ribs, and upper and lower surface panels. A typical surface panel is a bonded assembly of graphite-composite skins, graphite-composite tapered hat-section stringers, shear clips, titanium embeddings, and titanium spar caps. Portions of the lower-surface panel are removable to facilitate major inspection and repair work and would be manufactured as bonded assemblies of titanium sheet and stiffeners. The wing spars are constructed of graphite-composite honeycomb webs and titanium caps. A typical rib is a bonded assembly of graphite-composite honeycomb web, graphite-composite caps and rib-to-spar shear clips. Access holes are provided in the center of each rib web. Ribs which are subject to concentrated loads are provided with diffusion-bonded titanium fittings adhesively bonded to the composite rib structures. The spars are bonded assemblies of graphite-composite honeycomb webs, titanium caps, and diffusion-bonded titanium fittings. Ribs and surface panels are of aluminum honeycomb construction.

The trailing-edge structure located aft of the rear spar on the outer wing is constructed of aluminum-honeycomb surface panels and ribs, with titanium hinge and actuator support fittings. The leading-edge structure is constructed of aluminum-honeycomb skins and aluminum intercostals and is supported by titanium ribs, which also serve to support the slat-drive mechanism.

Leading Edge Slats - The leading edge slats are of aluminum sheet and stiffener construction.

Trailing Edge Flaps - The trailing edge flaps are of aluminum sheet and stiffener construction.

Ailerons - The ailerons are constructed of graphite/epoxy honeycomb surfaces.

Fairings - The fairings are constructed of aluminum sheet and formers.

3.6.2.2 Fuselage - The fuselage structure includes structural shells, chine longerons, floor and floor beams, main frames, bulkheads, pressure bulkhead, nose-landing-gear beams, keel beams, and the empennage mounting platform. A typical shell structure is a bonded assembly of graphite-epoxy composite skins, stringers, shear clips, and ring frames. The chine longerons are titanium extrusions and serve to splice the upper and lower sections and provide edge members for the floor. The floor panels are bonded assemblies of graphite-epoxy composite skins, stringers, shear clips, and titanium rails. The main frames, which provide the primary attachment points for the wing and empennage, are manufactured of compound composite-reinforced aluminum forgings. All bulkheads are of graphite-epoxy composite honeycomb construction. The pressure bulkhead is constructed as a stiffened graphite composite dome. The nose landing gear beams are of graphite honeycomb construction. The rear portion of these beams supports the nose landing gear trunion and drag brace and are manufactured from diffusion-bonded titanium. The keel beams are constructed in a similar manner. A structural panel is attached to the lower edge of each keel beam; these panels are bonded assemblies of graphite composite skins, longerons and intercostals and serve to carry a portion of the fuselage bending load across the landing gear area. The empennage mounting platform is a bonded assembly of graphite composite honeycomb web and diffusion-bonded titanium longerons.

The secondary structure is constructed of 50 percent aluminum and 50 percent graphite/epoxy skin-stringer construction.

3.6.2.3 Empennage - The structural arrangement described in this section is for the tee tail condifuration of the cargo airplanes. The passenger airplanes have a more conventional empennage configuration and, therefore, differ somewhat in details; however, the basic structural concepts and the materials usage are very much the same.

The empennage structure is an all-flying horizontal stabilizer pivoted at the top of the vertical stabilizer. The vertical stabilizer structure consists of the structural box, hinge-support beams, actuator-support fittings, leading edge, fixed trailing edge, and the upper fairing structure. The structural box is a bonded assembly of surface panels, spars and ribs. The surface panels are bonded assemblies of graphite-composite skins, hat-section stringers, shear clips and titanium reinforcements. The spars are constructed of graphite-composite honeycomb webs and titanium spar caps. The ribs are bonded assemblies of graphite-composite honeycomb webs, graphite-composite caps, and shear clips. The two hinge-support beams located above the box structure are manufactured from diffusion-bonded titanium and are attached to the box structure with mechanical fasteners. Replaceable titanium hinge fittings are bolted to the aft end of the beams. The two beams are joined by web and intercostal members which are of graphite-composite honeycomb construction. The horizontal stabilizer actuator fittings are diffusion-bonded titanium and are bolted to the structural box. The vertical stabilizer secondary structure is of aluminum honeycomb construction with titanium fittings.

The structure of the horizontal stabilizer is similar in construction to the vertical stabilizer except that the stabilizer structure is fabricated in three parts, the left and right stabilizer boxes and a center box.

3.6.2.4 Nacelle - The nacelle design is described in Paragraph 3.2.3. Recent Lockheed-California Company studies, performed under NASA contract (Reference 28), have shown the weight and cost saving potential of design concepts that integrate acoustic suppression treatment into advanced composite structural arrangements. Therefore, graphite-epoxy and graphite-polyimide advanced composites are utilized extensively in the inlet and the fan duct walls. Where it is advantageous, and where operating temperatures do not exceed the composite capabilities, the acoustic treatment is integrated into the honeycomb sandwich structure.

Titanium is used in those areas that are too hot for the use of the graphite-polyimide composites.

3.6.2.5 Pylon - The primary structure consists of an upper main graphite-composite box complex with a lower titanium box that attaches to the engine fore and aft mounts. Waffle-shaped composite inboard and outboard main box skins are formed with titanium beam caps and pylon-support fittings formed into the skins. The skins are formed into the upper box by adding composite webs and stiffeners to the main beams.

The lower box is made of conventional titanium sheet and stiffener construction. The dividing step face between the upper and lower box is also titanium to complete the firewall along with the lower box.

The pylon leading-edge fairings are aluminum sheet and aluminum honeycomb, which forms an electrical connection from the honeycomb nacelle nose cowl to the wing leading edge. The fairings just under the wing are composites. The fairing aft of the pylon main box is composite honeycomb.

3.6.2.6 Landing Gear - The landing gear structural members are titanium and epoxy-graphite materials. High-strength alloy steels are used where dictated by environmental conditions.

Wheels are designed to be fabricated by diffusion bonding titanium, permitting the attainment of the allowable stress levels of titanium by using multiple laminations. This results in a more efficient utilization of material than is possible in mechanical forgings.

SECTION 4

PASSENGER AIRCRAFT

The passenger aircraft analyzed during the study are described in this section. The parametric analysis method which was employed is described, along with the basis for estimating weights and costs for the aircraft. The two LH₂ fueled aircraft design concepts which were studied in some detail are then defined, along with a Jet A fueled configuration which served as a baseline, or point of reference, for comparison with the preferred LH₂ design. The results of the comparison provide an evaluation of the benefits to be derived from using hydrogen as the fuel for advanced design passenger aircraft.

4.1 REQUIREMENTS

The passenger aircraft missions require that a nominal payload of 400 passengers be carried 1560 km (8000 n.mi) and 10,190 km (5500 n.mi) at Mach numbers of 0.80, 0.85 and 0.90. The basic guidelines established for the study are listed in Table 1, Section 2.

To further define the vehicle requirements the following ground rules were adopted:

Payload Definition: The design payload is defined as:

$$\text{PAYLOAD} = \text{NO. PASSENGERS} \times 200 \frac{\text{LBS.}}{\text{PASS.}} \times 1.10$$

In other words, an allowance of 91 kg (200 lbs.) was made for each passenger plus baggage, and an additional 10% was allowed for revenue cargo. For 400 passengers this then amounts to a total payload of 39,900 kg (88,000 lbs.).

Cargo Volume: The cargo volume, which is commensurate with today's wide-bodies, assumes a baggage allowance of 0.141 m³ (5 ft.³) per passenger and a cargo density of 160 kg/m³ (10 lbs/ft³). The total cargo volume for 400 passengers amounts to

about 134 m^3 (4743 ft.³) with 127 m^3 (4143 ft.³) in containers and an allowance of 17 m^3 (600 ft.³) for loose cargo.

Passenger Accommodations: A mix of 10 percent first class to 90 percent coach passengers with a seat spacing of 0.965 m (38 in.) for first class and 0.86 m (34 in.) for coach was used.

Fuel Volume: The fuel volume was defined as that required to hold the block plus reserve fuel at the design range. No allowance was made for off-loading of payload for fuel.

Performance Constraints: In addition to the field length specified in the basic guidelines of the study (Table 1), two other critical performance constraints were imposed so that an equitable basis would exist for selection of preferred aircraft designs among the hundreds that would be parametrically generated.

- An initial minimum cruise altitude of 10,350 m (34,000 ft.) was established as compatible with current passenger aircraft and ATC practice. The effect of different altitudes on gross weight and DOC for a typical aircraft in this study is shown in Figure 45.
- A landing approach speed of 69.4 m/s (135 KEAS) was selected for reasons discussed in Paragraph 3.3.2.3.

Matrix of Variables: The matrix of variables evaluated during this study; mission, configuration, geometry and performance, are grouped in Figure 46. The actual number of discrete parametric, airplane designs generated amounts to 3580 to allow selection of optimum aircraft depending on the criteria chosen.

Selection Criteria: The selection criteria used in choosing aircraft from the array of parametric results, in order of decreasing importance, are:

- Direct Operating Cost. (DOC)
- Block fuel weight.
- Airplane price.
- Gross weight.

As discussed in Section 4.4.1, the ordering of these selection criteria is important because different aircraft would be selected depending on the criteria applied.

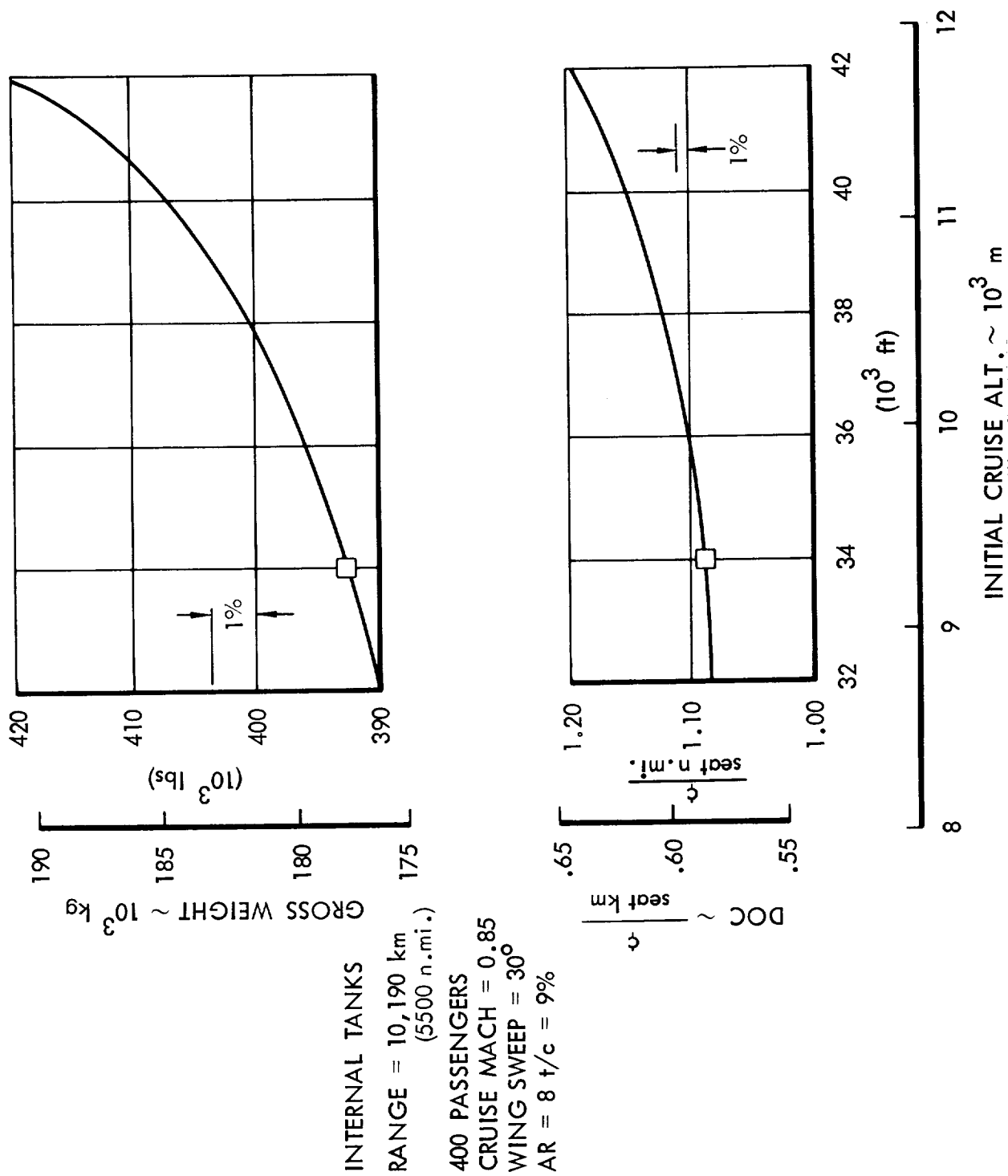


Figure 45. Effect of Initial Cruise Attitude on Gross Weight and DOC


	LH ₂ AIRCRAFT	JET A AIRCRAFT
MACH NO.	0.8, 0.85, 0.90	0.85
RANGE km (n.mi.)	10,190, 5560 (5500, 3000)	10,190, 5560 (5500, 3000)
PAYLOAD kg (lb)	39,800 (88,000)	39,800 88,000
CONFIGURATION	Internal tank, External tank	Conventional
WING SWEEP DEGREES	25, 30, 37	30
ASPECT RATIO	6, 8, 10, 12 (each Mach)	6, 8, 10, 12
WING THICKNESS RATIO %	6 through 15 (4 values each Mach)	7, 9, 11, 13
WING LOADING LB/FT ² kg/m ² (lb/ft ²)	39, 48.8, 58.5, 68.3 (for each Mach) (80, 100, 120, 140)	48.8, 56.1, 63.3, 70.7 (100, 115, 130, 145)
THRUST/WEIGHT (T.O.)	.25, .30, .35, .40 (each Mach)	.26, .30, .34, .38

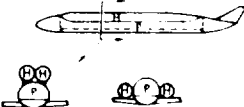
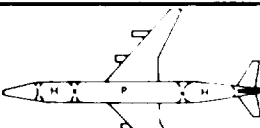

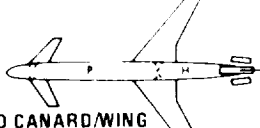
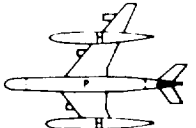
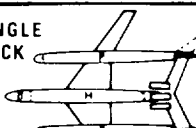
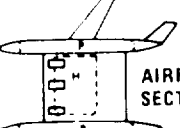

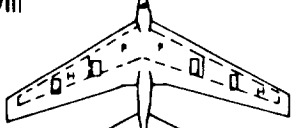
Figure 46. Matrix of Variables for Passenger Aircraft

9.	<u>OTHER</u>	<u>COMMENTS</u>	
	—	<u>REJECT</u> BECAUSE OF PASSENGER PROXIMITY TO FUEL	
	—	—	
	—	<u>REJECT</u> EXCESSIVE TRIM DRAG DUE TO FWD C.G. & TAIL DWN. LOAD	
	—	<u>REJECT</u> - - TECHNICAL RISK HIGH FOR SLIGHT ADVANTAGE IN PASSENGER SAFETY COMPARED TO NO. 11 C. G. TRAVEL (LOADABILITY) LIMITED BY CANARD SIZE.	
	TANKS COULD BE REMOVED EASILY	—	
	PASSENGERS SUBJECTED TO TRANSITORY "G" LOADS IN TURNS	<u>REJECT</u> - NO APPARENT ADVANTAGE OVER ABOVE CONFIGURATION	
	—	<u>REJECT</u> - POOR L/D, LARGE WETTED AREA, HIGH STRUCT. WT.	
	<ul style="list-style-type: none"> • MACH NO. LIMITED TO ~ .75 FOR REASONABLE T/C & SWEEP • WING SHIELDING GOOD FOR NOISE REDUCTION 	<u>REJECT</u> - WILL NOT MEET M.9 CRUISE WITH REASONABLE T/C &/OR SWEEP	

THESE TWO CONFIGURATIONS
SELECTED FOR PARAMETRIC
EVALUATION AND DESIGN
STUDY

Figure 47. Candidate Passenger Aircraft Configurations

1. AERODYNAMIC EASIBILITY PERFORMANCE HEIGHT CONTROL	4. FUEL CONTAINMENT EFFICIENCY • THICK/DIA • SWET/VOL.	5. GROWTH POTENTIAL 8000 PASS 5500 NM	6. WEIGHT TRENDS (ESTIMATES)	7. TERMINAL COMPATIBILITY	8. TECHNICAL RISK
(NOT CALCULATED) STABILITY NORMAL	• HIGH S_{wet}/VOL • HIGH t/DIA	OK	—	OK	AVERAGE
17.5 to 17.8 STABILITY NORMAL	• GOOD VOL. EFFICIENCY • LOW t/DIA	OK	W TO = 381,000	OK	AVERAGE
4 TO 16.8 TAIL DOWNLOAD C.G. DEGRADES L/D	• GOOD VOL. EFFICIENCY • LOW t/DIA	• MAX. WT. PAYLOAD LIMITED BY TAIL SIZE MAX. P.L. PL  C.G. FWD.	W TO = 414,000	OK	CG TRAVEL
LEVEL 115% MAC TO 16.5 D LOADED D. CG IN "UP" TION	• SAME AS ABOVE	• SAME AS ABOVE	W TO = 398,000	OK	CANARD PROBLEMS
4.6 BILITY NORMAL ER PROBLEM?	• LESS EFFICIENT THAN FUS. FUEL • MEDIUM t/DIA	OK • TANKS CAN BE SIZED INDEPENDENTLY OF FUSELAGE	W TO = 406,000	OK	TORSION LOAD ON WING
14.5) TER?	• GOOD VOL. EFFICIENCY • LOW t/DIA	OK	W TO = 420,000	• DUPLICATE PASS. LOADING FACILITIES • WIDE TRACK	STRUCT. COUPLING
13 WETTED AREA. 'AR)	• POOR EFF. • LARGE $S_{wet}/VOL.$	• OK BUT REQUIRES MORE WING SPAN	W TO = 436,000	• WIDE TRACK • DUPLICATE LOADING FACILITIES	AVERAGE
= 19.5 EDS GUST LEVATION	• SAME AS ABOVE	• OK BUT REQUIRES MORE WING SPAN	W TO = 504,000	• EXCESSIVE SPAN ($\approx 300'$)	LOW W/S (30) REQUIRES GUST ALLEVIATION TO REDUCE LOAD FACTOR & GIVE REASONABLE RIDE QUALITIES

<div> <div>CRITERIA</div> <div>CONFIGURATION CONCEPTS</div> </div>		1. <u>PASSENGER SAFETY</u> • CRASH • EMER. EXIT • LOADING	2. <u>STRUCTURE/TANKAGE</u> <u>FEASIBILITY</u>	3. <u>AE</u> <u>F</u> • PE • FL
FUEL IN FUSELAGE	I  FUEL PARALLEL & ADJACENT TO PASSENGERS	<ul style="list-style-type: none"> • MAX. PASS. EXPOSURE TO FUEL IN EVENT OF LEAKAGE OR CRASH • EMERGENCY EXITS IN ZONE OF PROBABLE SPILL &/OR FIRE 	<ul style="list-style-type: none"> • LIMITED TO NON-INTEGRAL TANKAGE • TANKS MUST BE REMOVED FOR REPAIR 	<ul style="list-style-type: none"> • L/D • LAT • C.G. • NOR
	II  FUEL FORE & AFT	<ul style="list-style-type: none"> • EXPOSED TO FUEL ON ENDS ONLY 	<ul style="list-style-type: none"> • TANKS CAN BE INTEGRAL OR NON-INTEGRAL 	<ul style="list-style-type: none"> • L/D • CG/S
	III  ALL FUEL AFT	<ul style="list-style-type: none"> • EXPOSED ON AFT SIDE ONLY • FUEL SPILL BEHIND ON SURVIVABLE CRASH 	<ul style="list-style-type: none"> • TANKS CAN BE INTEGRAL OR NON-INTEGRAL 	<ul style="list-style-type: none"> • L/D = 1 • LARGE @ FWD • CG TRA
	IV  FWD CANARD/WING ALL FUEL & PROP. AFT	<ul style="list-style-type: none"> • SAME AS ABOVE 	<ul style="list-style-type: none"> • SAME AS ABOVE 	<ul style="list-style-type: none"> • $\frac{L}{D} = 10$ • CANAR BY FW • DIREC
FUEL IN PODS	V  TWIN PODDED	<ul style="list-style-type: none"> • MAX. SEPARATION • BEST FROM SAFETY & PROXIMITY 	<ul style="list-style-type: none"> • TANKS INTEG. OR NON-INTEG. • STRUCT. PENALTY FOR WING 	<ul style="list-style-type: none"> • L/D = 1 • CG/STA • FLUTT
	VI SINGLE DECK  CENTRAL PODDED	<ul style="list-style-type: none"> • SAME AS ABOVE 	<ul style="list-style-type: none"> • TANKS INTEG. OR NON-INTEG. 	<ul style="list-style-type: none"> • L/D • FLU
FUEL IN WING	VII  INBOARD FUEL AIRFOIL SECT	<ul style="list-style-type: none"> • PASS. ADJACENT TO FUEL IN MID-FUSELAGE 	<ul style="list-style-type: none"> • DIFFICULT TANK INTEGRATION. REQUIRES BI-FURCULATED APPROACH 	<ul style="list-style-type: none"> • L/D • (HIG LOW
	VIII  FLYING WING	<ul style="list-style-type: none"> • PASS. ADJACENT TO FUEL AT ENDS ONLY 	<ul style="list-style-type: none"> • SAME AS ABOVE 	<ul style="list-style-type: none"> • L/ • N • A

4.3 PARAMETRIC ANALYSIS METHOD

The focal point for the technology data generated as described in Section 3 is the ASSET (Advanced System Synthesis and Evaluation Technique) synthesis model. This model is designed to size, weigh, perform, and cost large numbers of aircraft design options parametrically. The synthesis cycle required to size the vehicle for given payload/mission requirements is accomplished within ASSET by integrating data describing vehicle geometry, aerodynamics, propulsion, structures/materials/weights, and cost. A schematic presentation of the inputs and outputs involved in the synthesis cycle is shown on Figure 48. The key elements and the flow of information through ASSET are depicted on Figure 49.

The three major subprograms in ASSET are sizing, performance, and costing. The Sizing subprogram sizes each parametric aircraft to the design mission. The design characteristics and component weights of the sized aircraft are then transferred to (1) the Costing subprogram, which computes aircraft cost on the basis of component weights and materials, engine cycle and size, avionics packages, production and operational schedules, and input cost factors, and (2) the Performance subprogram which computes acceleration, maximum speed, ceiling, landing and takeoff distances, and other performance parameters. The ASSET program output consists of a group weight statement; vehicle geometry description; mission profile summary; a summary of the vehicle's performance evaluation; RDT&E, production, and operational cost breakdowns for each candidate vehicle; and summaries of these data for the matrices of candidate aircraft. Plots of these weight, cost, size and performance parametric data can be automatically plotted on 35 mm microfilm from which hard copies are made.

The final data from the ASSET runs is presented in both tabulated and auto-plotted carpet format. Figure 50 is an example of an automatically plotted carpet plot, complete with three sample constraint lines. From a series of working level autoplot presentations the final vehicle characteristics desired such as gross weight, cost, range, etc. can be selected. Appendix B includes a sample of the actual output.

Included in the schematic of Figure 49 is an optional capability to calculate jet noise, incorporated in the ASSET program. The calculation method is based on Aerospace Information Report No. 876. When parametric variations are made to thrust, wing loading and any other performance and/or aircraft characteristics, different

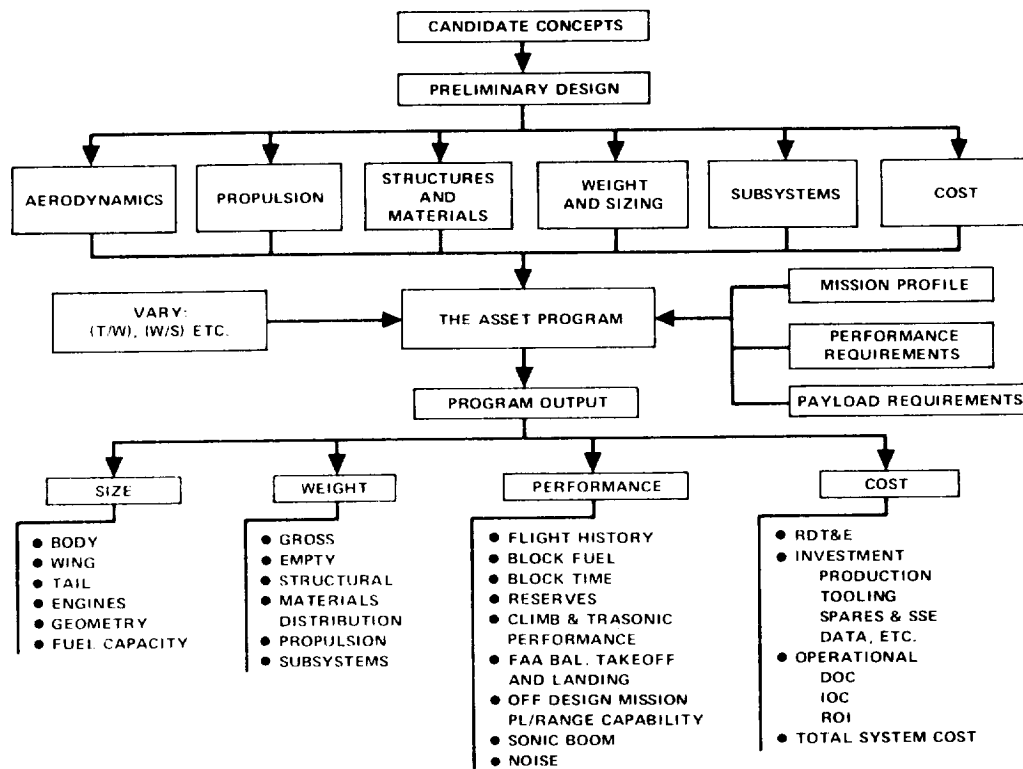


Figure 48. Asset Synthesis Cycle

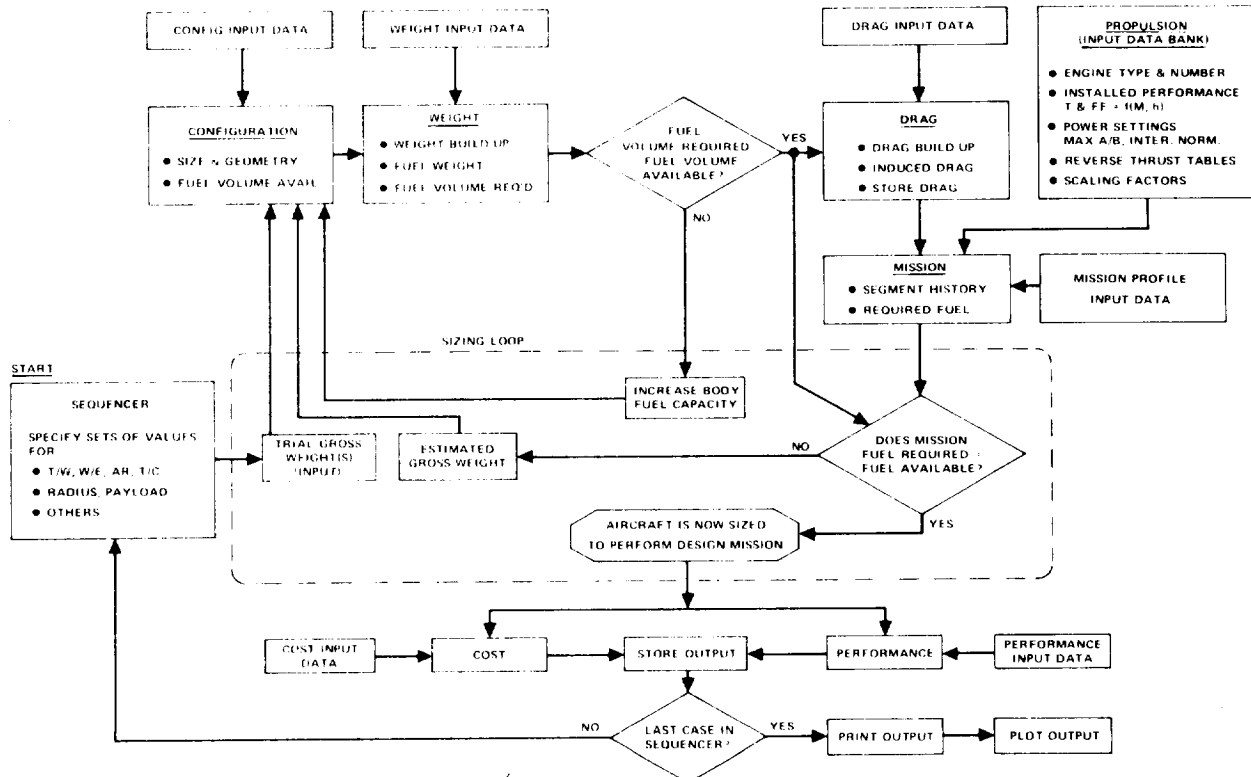


Figure 49. Asset Program Schematic

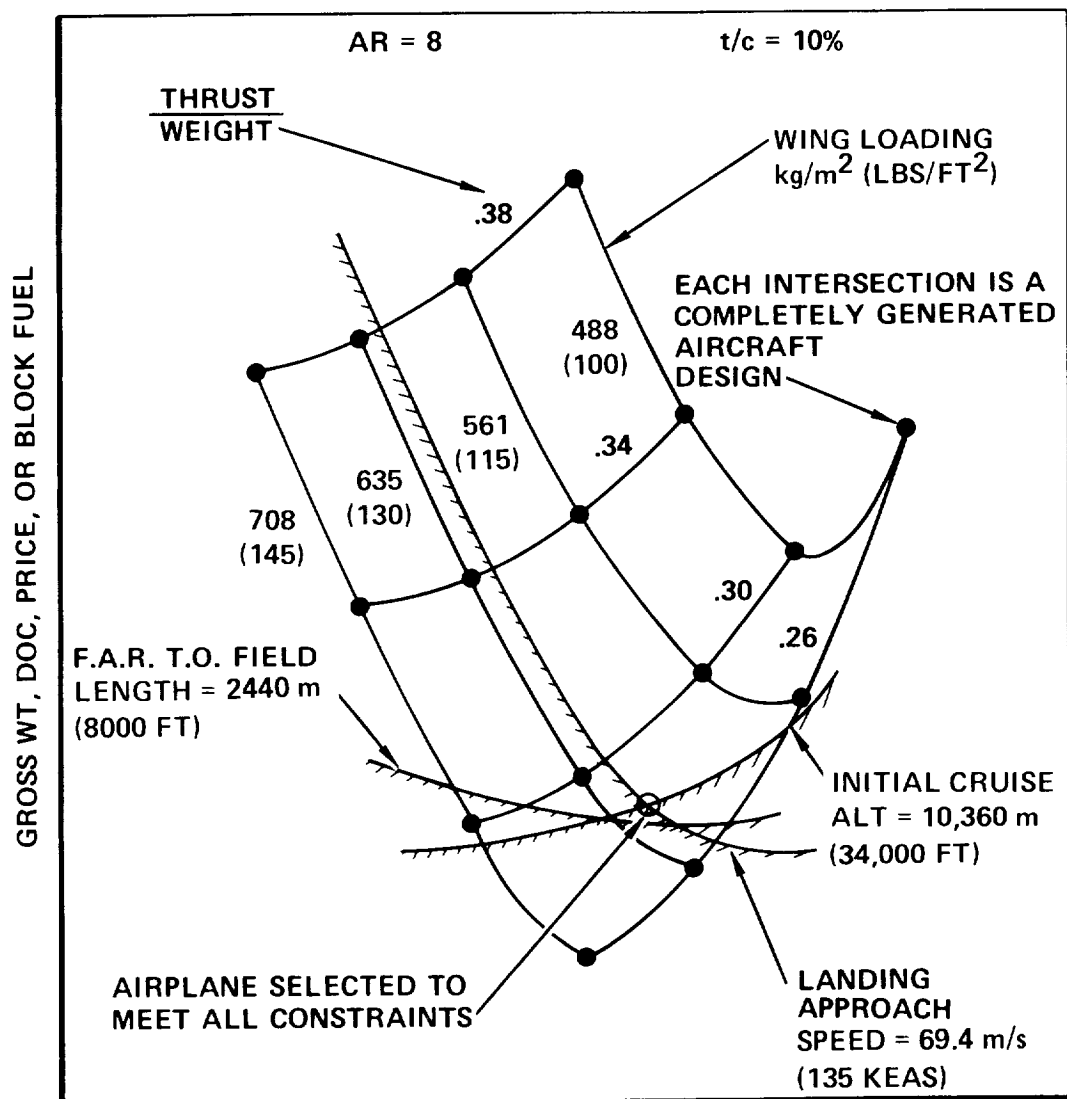


Figure 50. Example - Parametric Data Autoplot

takeoff flight profiles are effected which results in a change in the noise footprint. The inputs required are:

- Engine exhaust characteristics such as; velocity, density and area for each exhaust stream, i.e., core engine or fan duct.
- The engine exhaust noise directivity profile.
- The number of microphones and their location relative to the point of brake release.
- Exhaust noise suppressor effectiveness.
- Aircraft characteristics.

During takeoff both the flyover 6.48 km ((3.5 n.mi.) from brake release) and peak sideline 0.648 km ((0.35 n.mi.) from runway centerline) noise levels are computed, the greater of which is the critical noise level. At each microphone location noise calculations are made at half second intervals to build up a noise history for use in computing the duration correction factor. This correction factor is added to the tone corrected perceived noise level and results in the effective perceived noise level (EPNL) which is the noise evaluation quantity. This method of predicting noise generated, is applicable to both conventional turbojet and turbofan engines. The noise calculation described does not include fan, compressor, machinery, combustion or aerodynamic noise which are treated in a separate analysis described in 4.8.3.

4.3.1 Weight Input Basis

Conventionally fueled (Jet A), subsonic passenger transport weight estimating equations were modified to account for features required by LH₂ fuel. These features are described as follows:

Wing - Locating the LH₂ tanks on over-the-wing pylons causes a 10 percent increase in wing weight due to the high loads experienced when landing with nearly full tanks.

Body - Modified to account for the large volume, low density LH₂ when carried inside the fuselage and a 6 percent increase in body weight for the double-deck floor.

Tanks and Fuel System - The LH₂ tankage and fuel system installation is based on the design concept described in Section 3.1. For external wing-mounted tanks, the tank and pylon weight is 26.93 percent of the contained LH₂ weight while

insulation is 11.63 percent of the LH_2 weight. Unusable and boil-off LH_2 weight is 2.56 percent of the maximum LH_2 weight for all tank arrangements. Fuel system weight is approximately 80 percent greater than for a comparably-sized Jet A fueled airplane. This provides for larger line sizes and insulation. For the internal tank configurations, the weight increment for tanks, thermal protection and installation is approximately 29 percent of the contained fuel weight for both integral and non-integral tanks.

Propulsion - The LH_2 fueled turbofan engine weight is scaled from a baseline engine with 156 k N (35,000 pounds) of SLS thrust which weighs 2430 kg (5,380 pounds) bare and 3100 kg (6,845 pounds) installed including:

- Accessories and Gearbox
- Mounting and Splitter Pairing
- Gas Generator Cowl and Tail Pipe
- Fan Duct Acoustic Ring

Installed engine weight per aircraft is expressed in pounds as:

$$\text{WENG} = (0.19557) \text{ NENG (TSLS/35,000)}^{1.07} (35,000)$$

where

NENG = Total number of engines

TSLS = Installed Sea Level Static Thrust/Eng.

Nozzle and pylon weight per aircraft, before incorporating advanced composites, is equal to an additional 37.87 percent of the installed engine weight. On the same basis, the air inlets are 14.68 percent of engine weight. The remaining propulsion items, including thrust reversers, engine controls, starting system and oil system weigh approximately 11.5 percent of the installed engine weight. Total propulsion weight, excluding LH_2 tanks and fuel system, is therefore expressed as:

$$\text{WPTOT} = 1.6405 \text{ WENG}$$

4.3.4.3 Advanced Composites - Weight reduction coefficients were applied to the resulting equations to account for the advanced reinforced composites expected in the 1990-1995 IOC time period. These weight reduction coefficients were taken from

the Gelac Advanced Technology Transport Study (Reference 10) and are based on the recommended intermediate technology as discussed in Section 3.5.1. Table 10 lists the weight reduction coefficients along with the estimated materials distribution for each structural group and surface controls.

4.3.2 Cost Methods and Factors

The costs for the liquid hydrogen subsonic airplanes and the Jet A reference airplanes were produced through a series of subroutines in the ASSET Program. The subroutines provide estimates for the Development, Production and Operations costs.

The development cost estimates were based on 1973 dollars but considered a 1985 technology base for the development of the airframe, engines and subsystems. Applied research on liquid hydrogen application to aircraft design and operations was considered accomplished prior to the start of development of the LH₂ aircraft.

The production cost model estimates the production cost for the airframe, engines, avionics, and spares. The production cost estimate for the airframe is produced through the assignment of labor hours and material dollars for the various components of the airframe. The values for the labor hours and material dollars are dependent upon the material type, the type of component, and the complexity of shape and assembly.

TABLE 10. ADVANCED TECHNOLOGY WEIGHT REDUCTION COEFFICIENTS
AND ESTIMATED MATERIALS DISTRIBUTION

STRUCT. GROUP	WT. COEF.	MATERIALS DISTRIBUTION (% OF TOTAL WT.)				
		ALUM.	TI.	STEEL	COMPOS.	OTHER
Wing	0.635	44	4	2	48	2
Tail	0.730	49	15	2	32	2
Body	0.664	38	4	2	50	6
Landing Gear	0.848	8	15	20	20	37
Nacelles, pylon	0.787	5	30	30	35	0
Air Ind.	0.787	45	5	4	41	5
Surface Controls	0.950	20	5	20	5	50

The operations cost is the Direct Operating Cost (DOC) as calculated by the ATA method, see Basic Guidelines, Table 1.

4.3.2.1 Development - The development cost subroutine consists of a series of cost estimating relationships for the following items:

- Design Engineering
- Development Tooling
- Development Test Articles
- Flight Test
- Special Support Equipment
- Technical Data
- Engine Development
- Avionics Development

The development cost estimates for the LH₂ subsonic airplane and the Jet A reference airplane used the L-1011 experience as the basis for extrapolation. The development cost model was calibrated to L-1011 experience for the Jet A reference airplane and then adjusted for the added development required for the liquid hydrogen system. The primary structural arrangement of the LH₂ airplane is similar to the L-1011 and adjustments are only required for the addition of the tankage, pumps, plumbing, and controls for the LH₂ system. Adjustments were also made to the development items to account for the added design, testing, and flight test fuel costs. The adjustments that were made to the development categories are shown in Table 11.

The total development cost was amortized over the entire production run of 350 aircraft and was added to the aircraft production cost, including profit, to arrive at the total aircraft price.

Engine development is included in the total price of the engine along with profit and engine warranty. The breakout of the engine R&D from the total price of the engine is shown in Table 12. Engine price and engine R&D are shown for a range of engine thrust levels.

TABLE 11. DEVELOPMENT COST FACTORS

	<u>JET A REFERENCE AIRPLANE</u>	<u>LH₂ AIRPLANE</u>
Maximum Design Mach Number	0.85	0.80, 0.85, 0.90
Number of Aircraft in Flight Test	6.0	6.0
Complexity Factor for Engineering	1.0	1.15
Complexity Factor for Tooling	1.0	1.10
Complexity Factor for Flight Test	1.0	1.05
Production Rate for Development (No./Mo.)	1.0	1.0

TABLE 12. ENGINE PRICE AND R&D COST
FOR SUBSONIC LH₂ AIRCRAFT

Thrust, lbf					
N	89,000	110,500	133,500	155,500	178,000
(lb)	(20,000)	(25,000)	(30,000)	(35,000)	(40,000)
Engine R&D (\$ Millions)	350.57	411.86	470.00	525.11	578.26
Engine Price (\$) (Including Profit)	626,143	764,180	898,964	1,031,360	1,161,468
Engine R&D (\$) Amortization*	175,286	205,928	235,000	262,555	289,129
Total Price/Engine (\$)	801,429	970,108	1,133,964	1,293,915	1,450,597

*Based on 2000 engines.

4.3.2.1 Investment - The investment cost for the subsonic LH₂ airplane includes the production cost for the airframe, engine, avionics, aircraft spares, production tooling, sustaining engineering, quality assurance, and technical data. Operator and maintenance trainers are not included. The number of trainers required is normally determined through a complete analysis of airline requirements and policy as to training concepts. However, such an analysis was beyond the scope of this study and their costs are not included. The cost factors associated with the production cost for the aircraft and spares are shown in Table 13.

The production cost model is illustrated in Figure 51. The cost model obtains the weights for the various components of the airplane from the ASSET Program. The weight for each component is subdivided into weights by material types. The proper labor hours and material cost factors are applied to each component for each material type, and aggregated to determine the airframe cost. Sizing and learning curve factors are applied to the total airframe cost to determine the proper cost at the production quantity stipulated. The cost for sustaining engineering, production tooling, etc., are determined and added to the airframe cost. The costs for engine and avionics are also added to the airframe cost to produce the total manufacturing

TABLE 13. INVESTMENT COST FACTORS

	<u>JET A REFERENCE AIRPLANE</u>	<u>LH₂ AIRPLANE</u>
Production quantity		
Airframe	350	350
Engine (incl. spares)	1,960	1,960
Learning Curve Slopes (%)		
Airframe		
Labor	80	80
Material	96	96
Engine	92	92
Avionics	100	100
Avionics Cost (\$ per unit)	500,000	500,000
Engine Production Complexity	1.0	1.2

cost for the airplane. Warranty, insurance, taxes and profit are included to determine the flyaway price without the prorata share of the development cost.

The relative sale price between representative liquid hydrogen and Jet A-fueled airplanes derived in this study and that of current jet transports is illustrated in Figure 52. The plot is in terms of sales price versus operating empty weight (OEW) with the dollars per unit of empty weight also noted. The sales price for current transports appears to fall between \$143/kg (\$65/lb) and \$183/kg (\$83/lb) OEW whereas the estimate for the advanced design LH₂ airplane is \$242/kg (\$110/lb). The advanced design Jet A airplane is estimated to cost \$238/kg (\$108/lb). The sales prices for the current jet aircraft now in production are in 1973 prices in order to be consistent with the 1973 dollar price for the liquid hydrogen airplane. The cost for the LH₂ airplane shown is for the 5560 km (3000 n.mi) Mach 0.85 version, although the 10,100 km (5500 n.mi) Mach 0.85 airplane is very close to the same price in terms of dollars per unit of empty weight, e.g., \$245/kg (\$111/lb).

4.4.2.2 Operations Cost - The 1967 AFA equations were used for determining the direct operating cost. The basic input factors used for calculation of the DOC are shown here.

Pilot Crew

International Crew Constant

\$180/hour

Fuel and Oil

Jet A = \$27/1,000 gal (\$2/10⁶ Btu = 3.63¢/lb)

LH₂ = \$34/1,000 gal (\$3/10⁶ Btu = 16.48¢/lb)

A 5% hold-off cost of block fuel is included in the fuel cost for the LH₂ airplane.

Insurance

Premium rate of 2.0 percent of the airplane price

Depreciation

Write-off period

15 years

Residual value

0

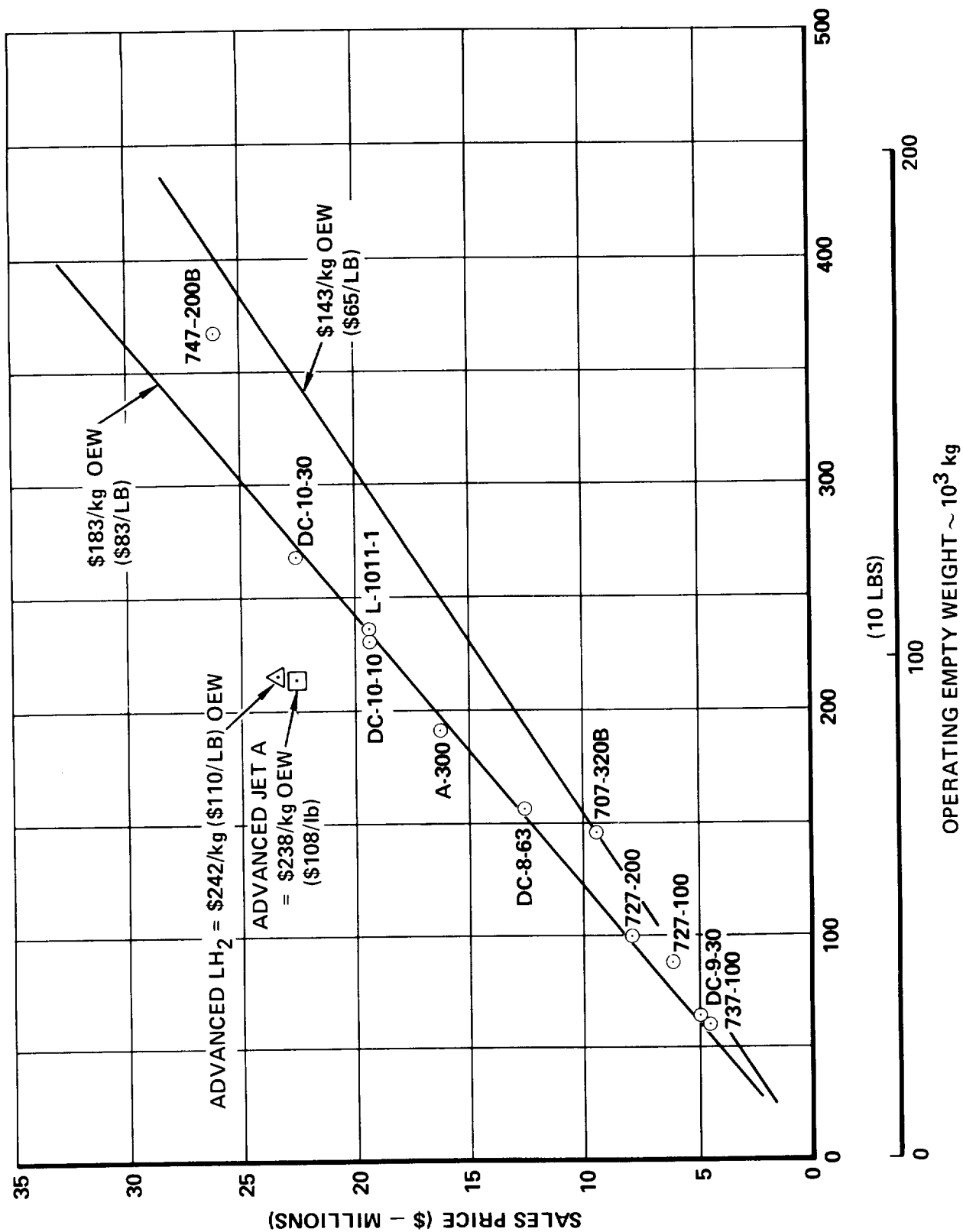


Figure 52. Sales Price Vs. Operating Empty Weight

Spares Ratio

Airframe	10 percent
Engine	40 percent
Avionics	10 percent

Utilization*

5560 km (3000 n.mi) range	3600 hours per year
10,190 km (5500 n.mi) range	4000 hours per year

Maintenance

Maintenance labor rate	\$5.00 per hour
Maintenance burden factor	1.8

Maintenance Factor

	<u>Jet A</u>	<u>LL₂</u>
Engine Labor	1.0	0.67
Engine Material	1.0	0.67

The engine labor and material maintenance cost for the LL₂ airplane was reduced by one-third because of the elimination of coking and other deposits in the combustion and turbine section, and the uniform distribution of heat in the burners. Because of these same beneficial effects, engine life with LL₂ fuel is expected to be prolonged, perhaps also by 33 percent; however, for conservatism, no credit was assumed for reduced engine spares because of increased engine life.

4.3 INTERNAL "PARE HYDROGEN AIRCRAFT"

4.3.1 Parametric Study Results

Section 4.1 described the method by which a point design aircraft meeting all constraints is selected from an array of parametric designs. From these selected designs the effect of a chosen design variable can be examined for a particular configuration and range. For example, Figure 53 shows the effect of wing thickness

*During the initial parametric design evaluation, a utilization of 3285 hours/year was used for aircraft of both ranges.

WING GEOMETRY STUDY

INTERNAL TANKS

RANGE = 10,190 km (5500 n.mi.)

400 PASSENGERS

CRUISE MACH = .85

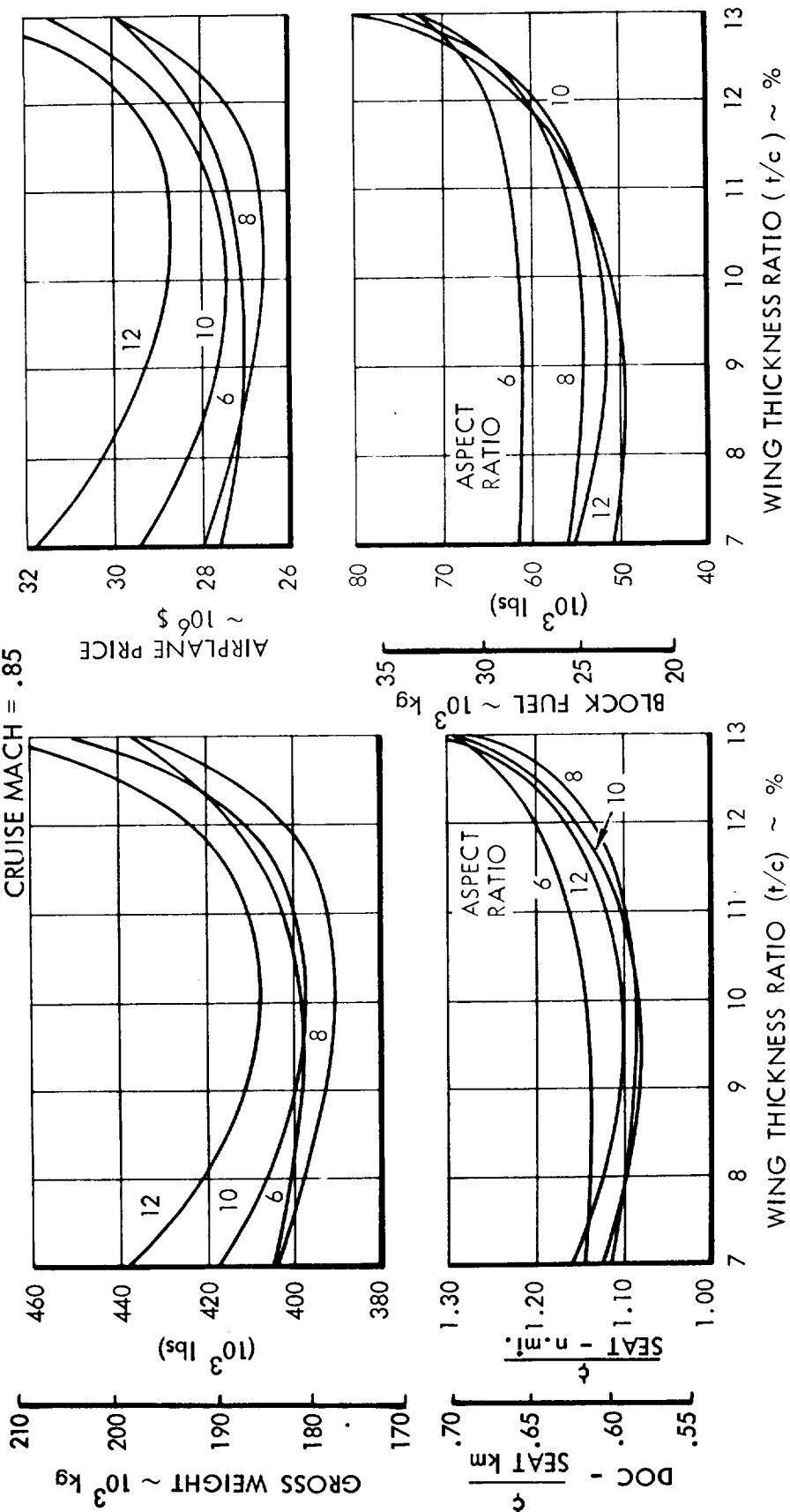


Figure 53. Effect of Thickness Ratio on Selection Parameters

ratio (t/c) on DOC, gross weight, block fuel and airplane price for the Mach 0.85, 10,190 km (5500 n.mi.) internal tank configuration. From this information it is seen that minimum DOC occurs in the 9 - 10 percent region for all aspect ratios. A thickness of 10 percent was selected to favor the physical space necessary for containment of gear, flaptracks, etc. With the wing thickness thus established, the effect of aspect ratio was isolated and the results are presented in Figure 54. Inspection of the curves shows that minimum price, weight, DOC and fuel do not occur at the same aspect ratio. This is summarized in Table 14 where each vehicle has been selected by a different criteria. The aspect ratios which produced preferred values for each of the selection criteria are shown for reference. In all cases where a conflict existed, the vehicle desired was chosen on the basis of minimum DOC.

This method of selecting final vehicle design characteristics was followed for each of the airplane designs involved in this study.

TABLE 14. SELECTION CRITERIA EFFECTS

<ul style="list-style-type: none"> • LB₂ Passenger Aircraft • Internal Tanks • 10,190 km (5500 n.mi.) • Mach 0.85 • t/c = 10% 					
CRITERIA	DOC ($\$/Cost km$) ($\$/Seat n.mi$)	WEIGHT kg. (lb.)	BLOCK FUEL - kg. (lb.)	PRICE ~ $\$10^6$	ASPECT RATIO (Ref.)
Minimum DOC	0.585 (1.08)	178,000 (392,000)	24,000 (53,000)	26.90	9.0
Minimum Weight and Price	0.592 (1.095)	177,000 (390,500)	25,100 (55,600)	(25.56)	7.5
Minimum Fuel	0.596 (1.106)	185,000 (408,000)	25,000 (50,800)	28.80	12.0

*Fuel cost = $\$3/1.054 GJ$ = $\$3/\text{Million BTU's.}$
= 15.63 $\$/lb$

WING GEOMETRY STUDY

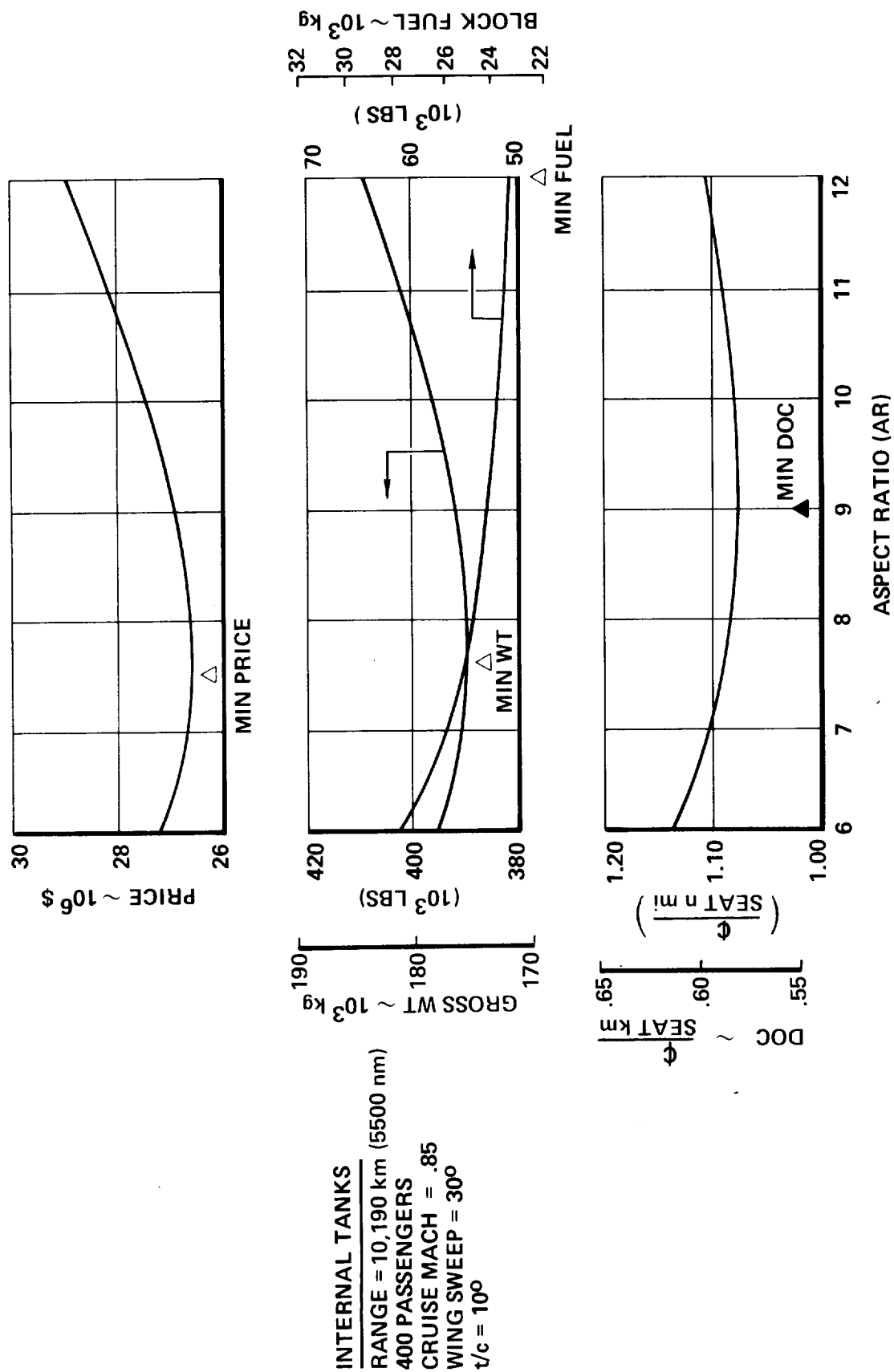


Figure 54. Effect of Aspect Ratio on Selection Parameters

4.4.2 Configuration Description

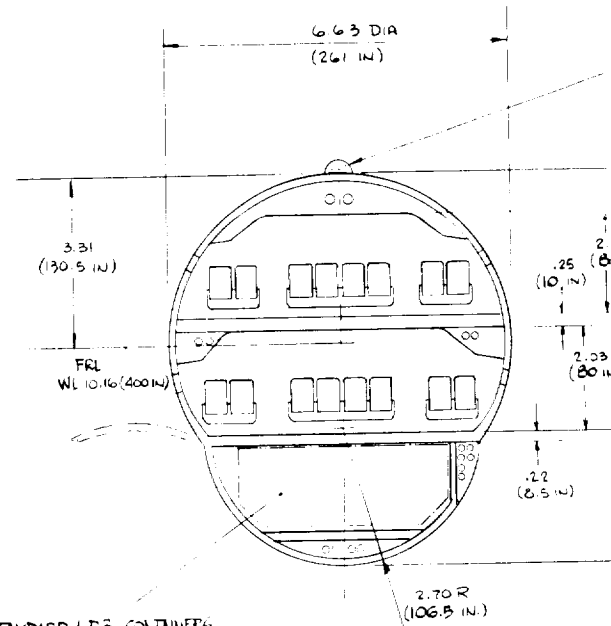
A general arrangement drawing of the internal tank, M 0.85, 10,190 km (5500 n.mi) 400 passenger aircraft is shown in Figure 55. Externally, the aircraft is entirely conventional in appearance. Internally, it is quite different. The passenger compartment is located in the central section of the fuselage in a double deck arrangement. Liquid hydrogen fuel tanks are located fore and aft of the passenger compartment. They occupy the full available cross section of the fuselage, except for provision for protective, crushable structure around the bottom areas. No provision was made for a passageway through or around the forward tank to permit movement between flight station and passengers, although such access could reasonably be afforded. Consultation with several airline representatives on the subject failed to reveal any strong requirement for such access; however, it is felt this subject requires further study to determine whether flight safety and/or passenger welfare demands the physical presence of a member of the aircraft flight crew in the passenger compartment. In the absence of such evidence the design was shown without such provision, and accordingly, the flight station was provided with special lavatory and galley facilities.

Passenger accommodations are shown in Figure 56 which shows the 10/90 percent class mix and seat spacing of 0.965 m (38 in.) and 0.86 m (34 in.) respectively, for first class and coach. In keeping with the requirements of FAR 25 and current wide-body standards, the arrangement includes adequate doors, lavatory and galley facilities. Stairwells at each end of the cabin allow access to either deck in flight.

All cargo is contained in the pressurized fuselage, below the lower deck which has space for thirteen cargo containers plus an additional 17 m^3 (600 ft^3) for loose cargo. Further details of the design are discussed below.

Wing: The wing configuration is shown in Figure 57 for a Mach 0.85 wing with a sweep angle of 35° . (Subsequent studies reduced this to 30°). The high lift devices include 15 percent leading edge slats and 35 percent double-slotted flaps where shown. Spoilers are used in flight, for direct lift control, and for landing ground run deceleration. Conventional ailerons are fitted outboard of the flaps.

Landing Gear: The main gear consists of two 4-wheel bogies mounted aft of the rear spar. They retract inward into the fuselage. The space between the retracted gear contains the hydraulic service center.

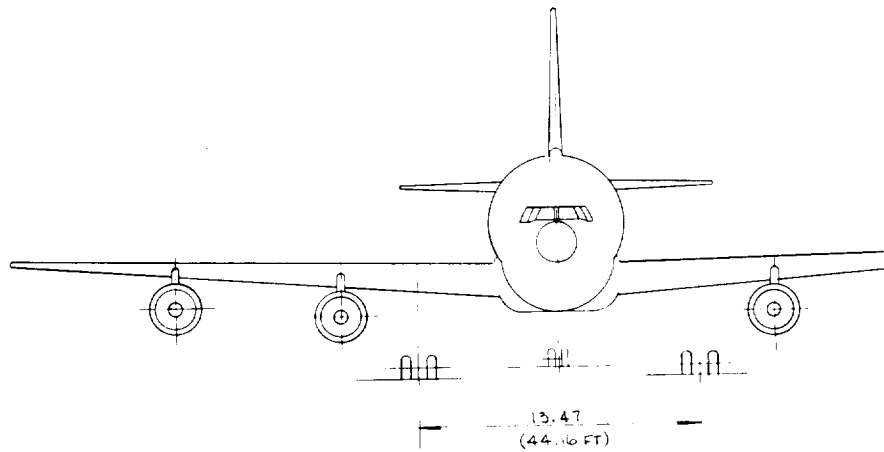


13 STANDARD LPS CONTAINERS

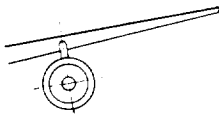
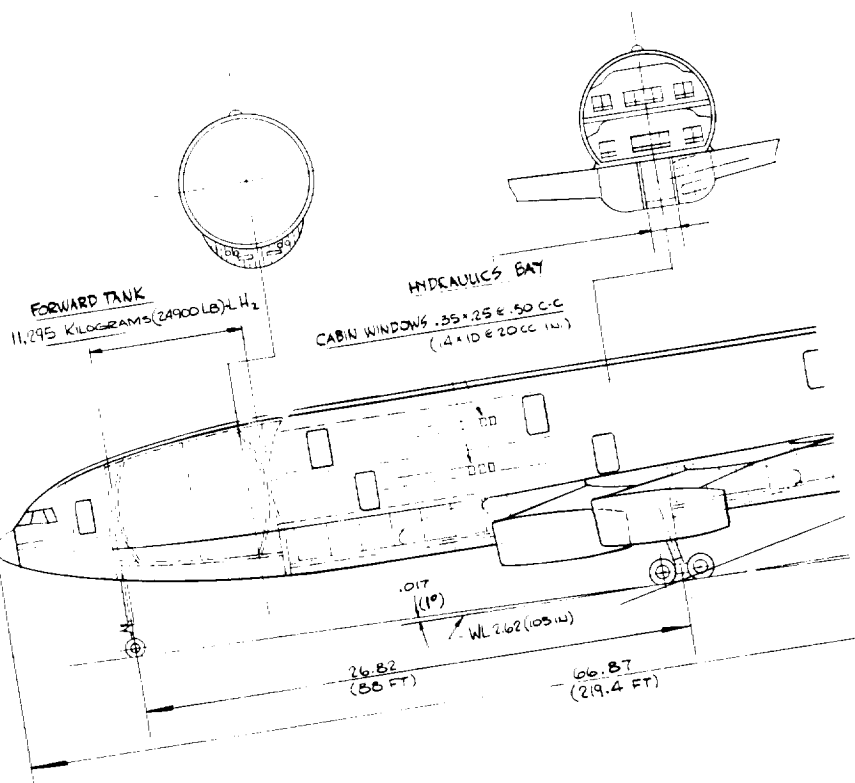
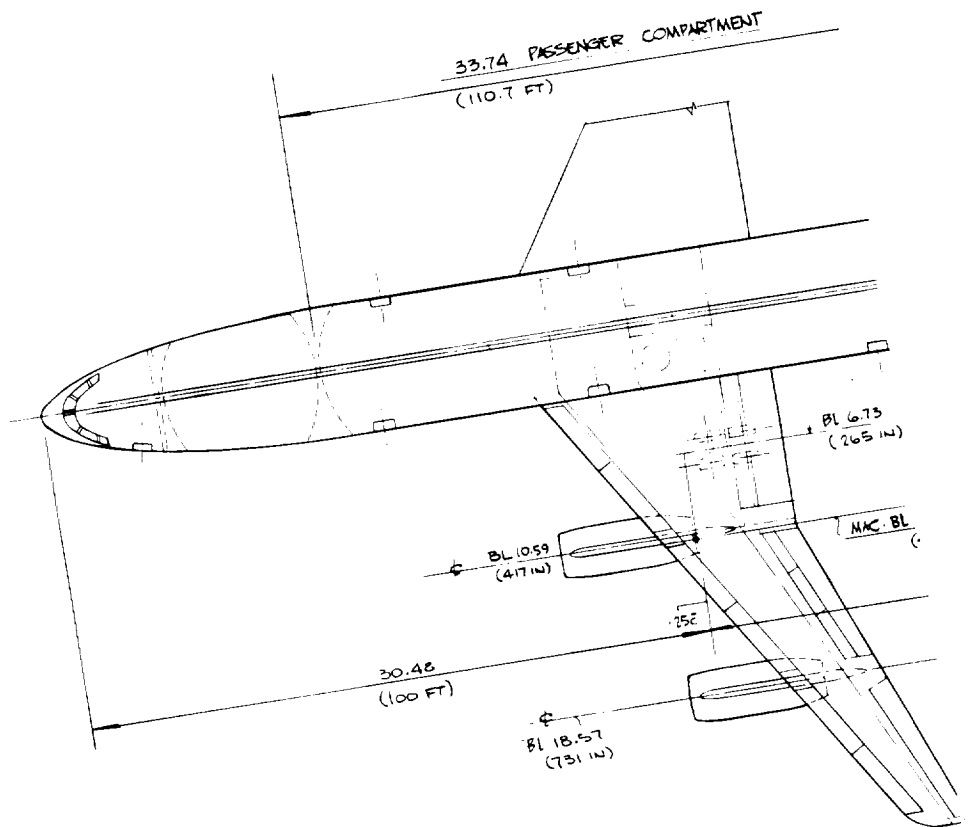
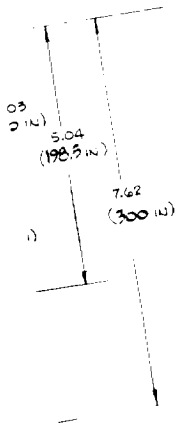
@ 9.10 CU. METERS (321 CU. FT) EACH
= 117.2 CU. METERS (4143 CU. FT.) TOTAL

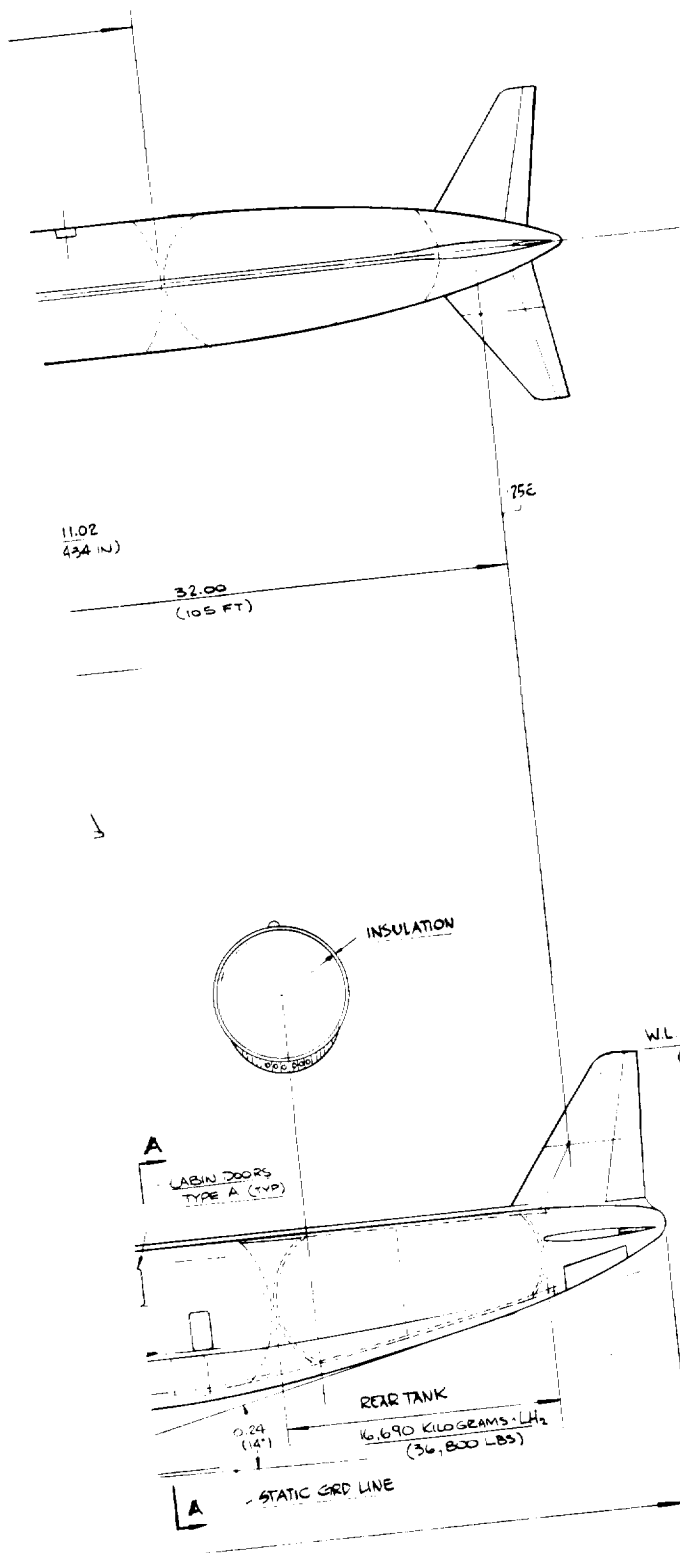
SEC A A

SCALE 1/400



GH₂ VENT LINE
MECH CONTROLS
AND ELECTRICAL ROUTING





CHARACTERISTICS

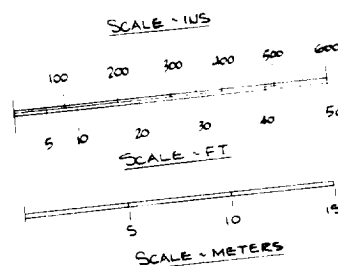
	WING	H TAIL	V TAIL
AREA - SQ. METER	312.4 (3363 SQ FT)	56.67 (610 SQ FT)	30.84 (332 SQ FT)
ASPECT RATIO	9.0	4.0	1.60
TAPER RATIO	30	30	30
SPAN	53.04 (174 FT)	15.09 (49.5 FT)	7.02 (23.04 FT)
ROOT CHORD	9.06 (29.74 FT)	5.76 (18.9 FT)	6.76 (22.17 FT)
TIP CHORD	2.72 (8.92 FT)	1.73 (5.67 FT)	2.03 (6.65 FT)
MAC	6.46 (21.20 FT)	4.10 (13.44 FT)	4.83 (15.84 FT)
SWEEEP @ 75C	.052 (30")	.052 (30")	.052 (30")

GROSS WEIGHT ~ 177,675 KILOGRAMS (391,700 LBS)

PASSENGERS ~ 400

TOTAL FUEL CAPACITY ~ 27,940 KILOGRAMS (61,600 LB) ~ INTEGRAL TANKS

POWER PLANT: 4 TURBOFANS ~ 127,660 NEWTONS (28,700 LB) ~ S.L.S.T.



2. LINEAR DIMENSIONS IN METERS (FT OR IN.)
 ANGLES IN RADIAN (DEGREES)
 1. DIMENSIONS IN SI (ENGL-SH) UNITS.
 NOTE.

Figure 55. General Arrangement - LH_2 Fuel, Internal Tank, M 0.85 Transport

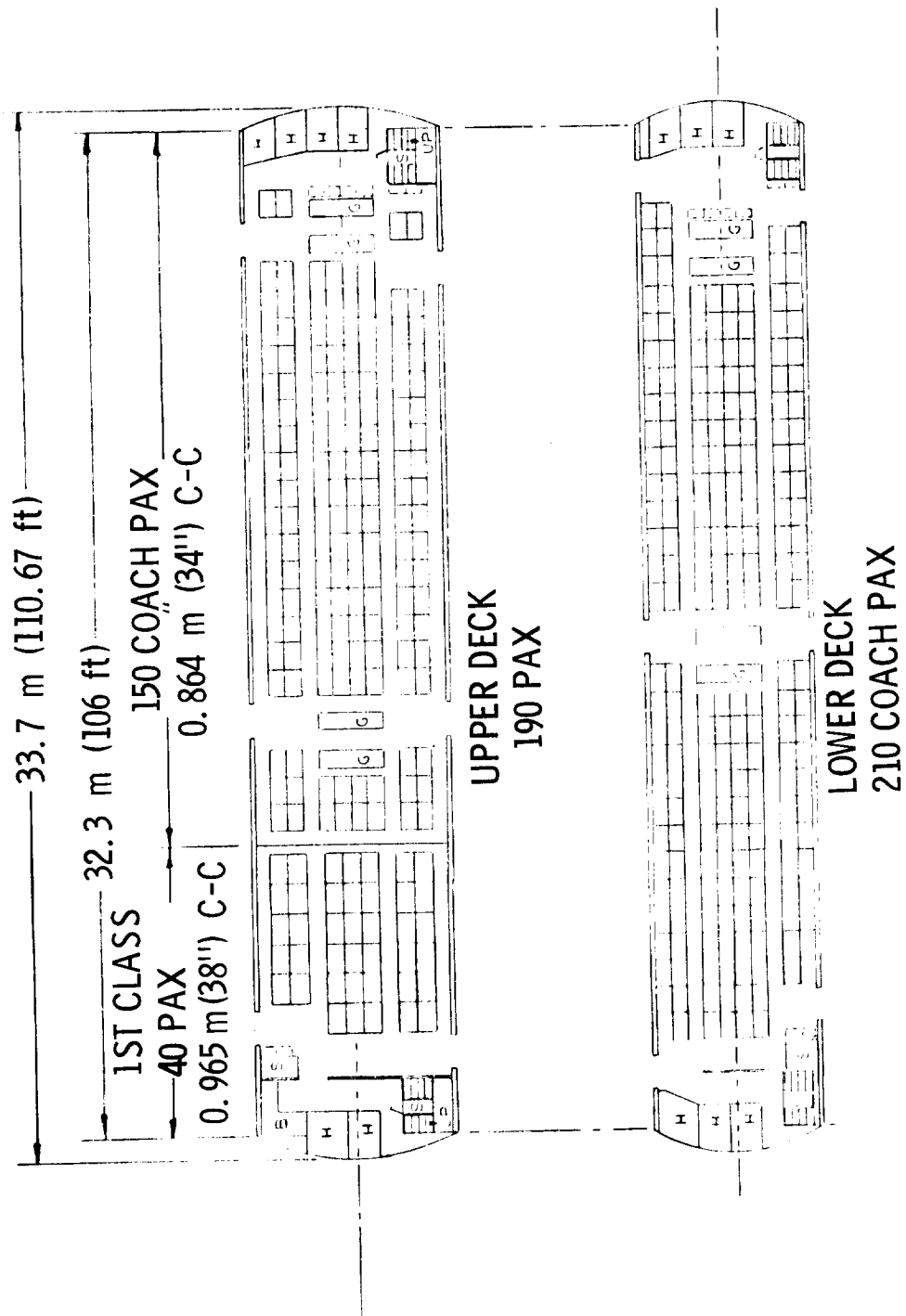
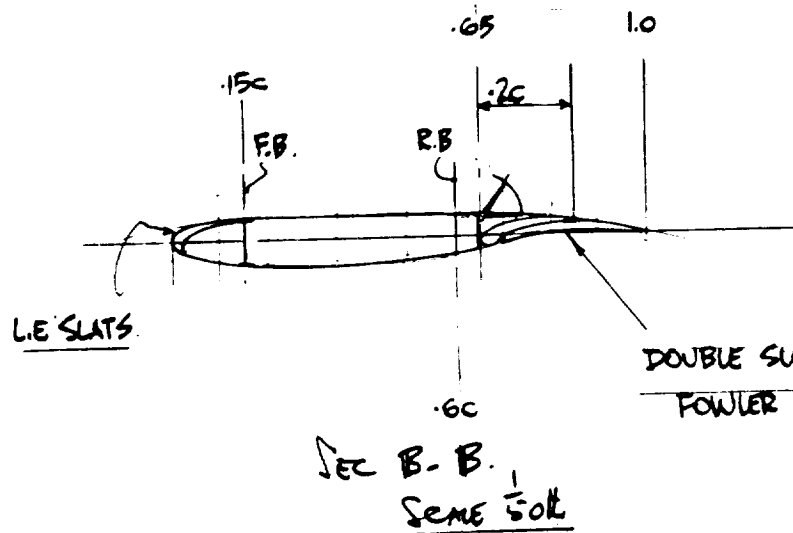
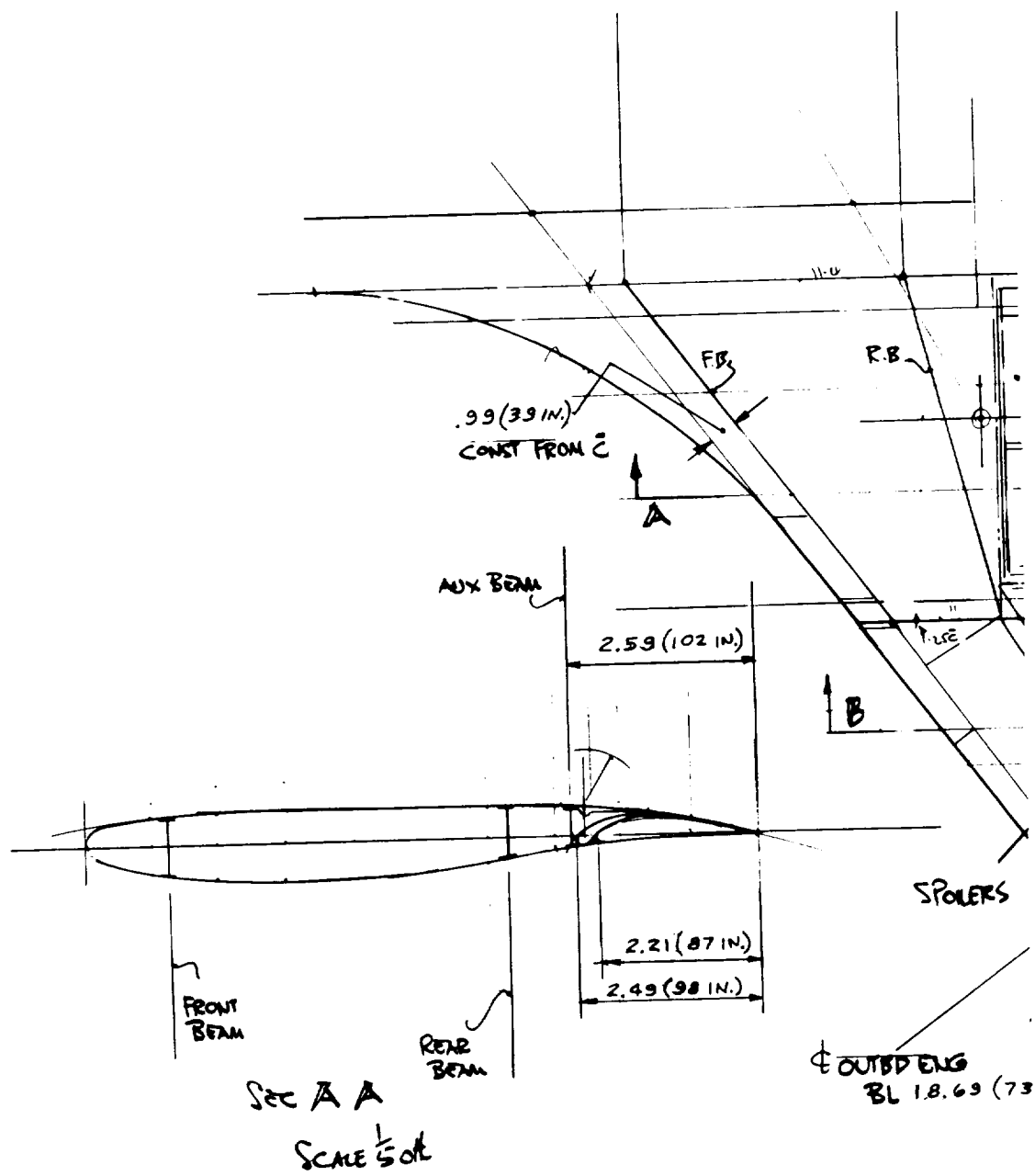
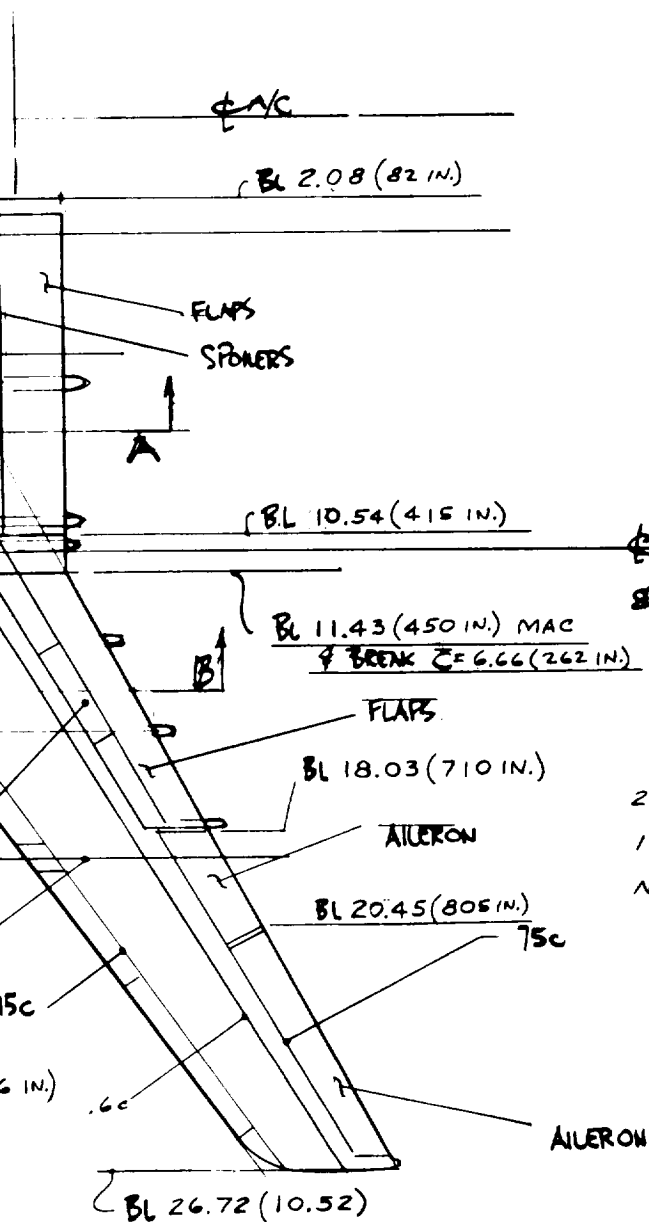


Figure 56. Passenger Accommodations - 400 Pax





2. LINEAR DIMENSIONS IN METERS (FT. OR IN.)
 1. DIMENSIONS IN SI (ENGLISH) UNITS
 NOTE:

REF.

$$\begin{aligned}
 S_w &= 335.4 (3610 \text{ SQ. FT.}) \\
 AR &= 8.5 \\
 \lambda &= .40 \\
 b &= 53.40 (175.2 \text{ FT.}) \\
 C_R &= 8.96 (29.4 \text{ FT.}) \\
 C_T &= 3.58 (11.76 \text{ FT.}) \\
 \Lambda_{.25c} &= .61 \text{ RAD. } (35^\circ) \\
 \bar{c} &= 6.66 (262 \text{ IN.})
 \end{aligned}$$

$$\begin{aligned}
 M_C &= .85 \\
 \text{SWEEP} &= 35^\circ \\
 &4/10/74
 \end{aligned}$$

TTED
LAPS

Figure 57. Geometry and Wing Characteristics

Hydrogen Tank and Systems: The hydrogen tank structural concept selected for purposes of this study is the integral type described in Section 3.1.2. All aircraft structural loads in addition to the fuel dynamic and pressure loads are taken by the tank shell. Loads are transferred from the vehicle structure to the tank ends by low heat-leak boron reinforced fiberglass tubes arranged in an interconnect truss structure. As described in Section 3.1.3, six inches of closed-cell plastic foam insulation, e.g., Rohacell 41S (see Table 8) covers the tank. This is then wrapped by a vapor shield (Kapton) which is to prevent cryopumping in event a crack develops in the foam insulation. A fiberglass or composite layer covers the entire tank section to provide protection from physical damage.

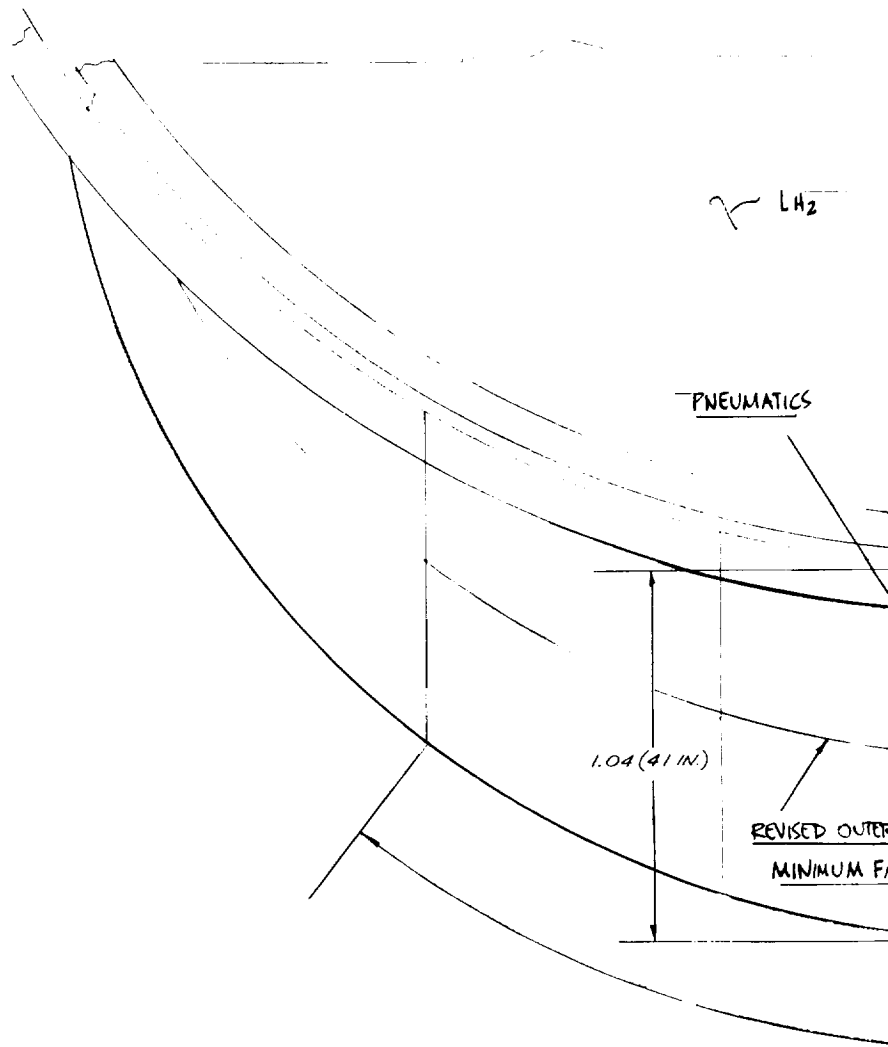
The tank is thus generally protected from mechanical damage by the foam insulation and its fiberglass cover. Further special protection from both foreign object damage and damage from maneuvers such as overrotation or tail scrape is provided on the bottom of the tank as shown in Figure 58. An energy absorbing, aluminum honeycomb structure is supported from the tank bottom. In this manner protection is also provided for plumbing or other aircraft systems routed adjacent to the tank.

The tank and mounting is designed for both inflight structural and fatigue loads (fail safe considerations) and to withstand the emergency crash load requirements of FAR 25 with a full fuel load.

4.4.3 Vehicle Data

Pertinent vehicle data for the 5560 km (3000 n.mi.) internal tank aircraft is shown in Table 15 for the cruise Mach numbers of 0.80, 0.85 and 0.90. Similar data for the 10,190 km (5500 n.mi.) version is shown in Table 16. Significant trends of selection criteria with Mach number are shown in Figure 59 for both ranges. DOC, block fuel, price and gross weight all increase with higher cruise speeds with an attendant reduction in block time of 1.2 hours for the 10,190 km (5500 n.mi.) range, and 0.7 hours for the 5560 km (3000 n.mi.) range.

4.4.3.1 Aircraft Cost Summaries - Table 17 presents cost summaries for the Mach 0.85 IH_2 internal tank airplanes. The engine R&D is shown separately in this summary table although it is included in the price of the engine in the aircraft sizing program (ASSET). The Avionics is considered as off-the-shelf and R&D and price reduction with quantity is not considered. The "Airframe Manufacturing Cost" includes the fabrication and assembly of the aircraft structure and subsystems including the installation of the systems, avionics and engines. The "other Airframe Cost" incl



SE
OF
(Re

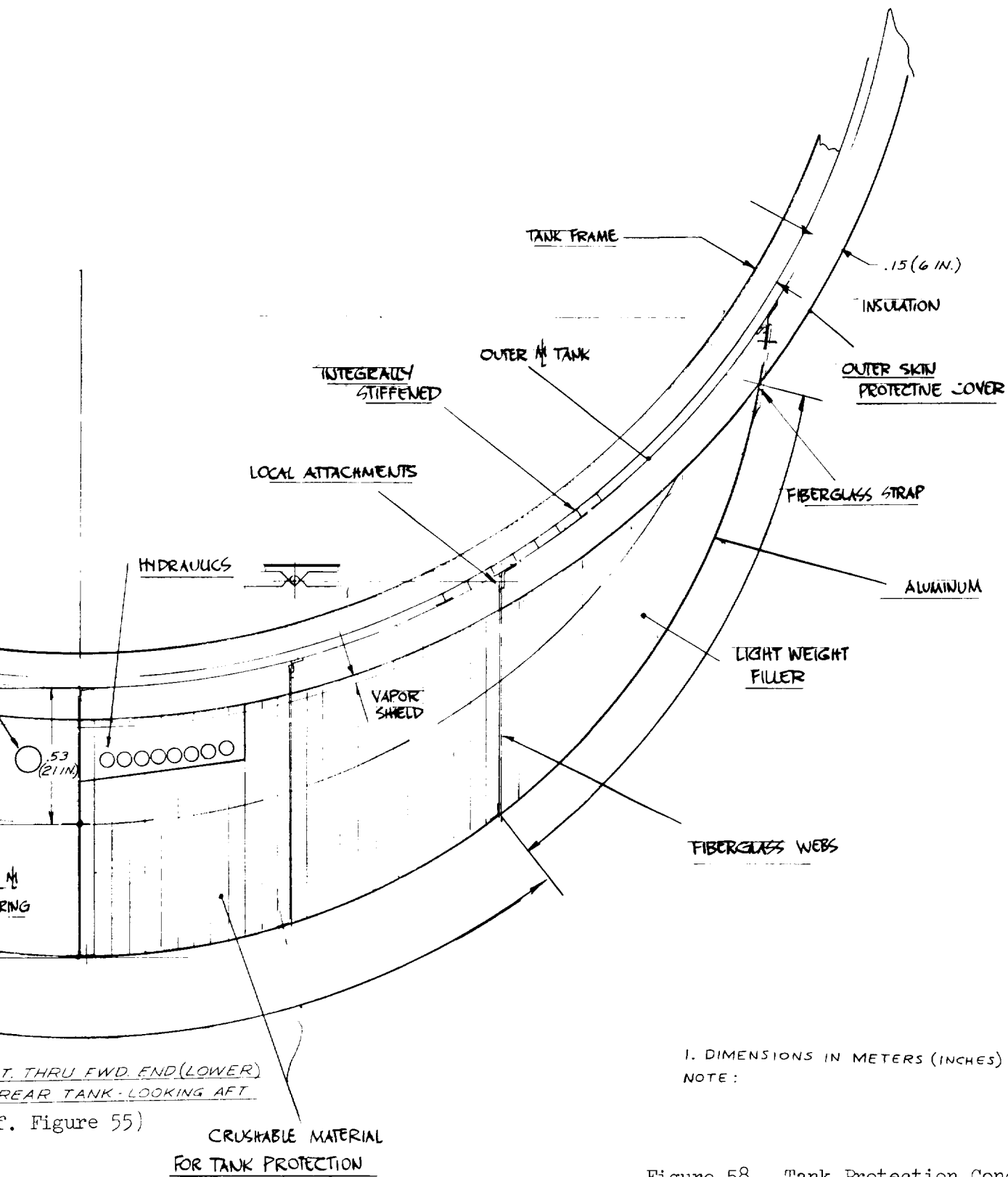
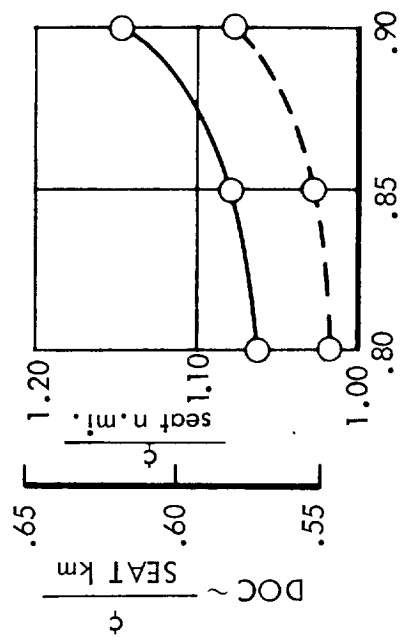
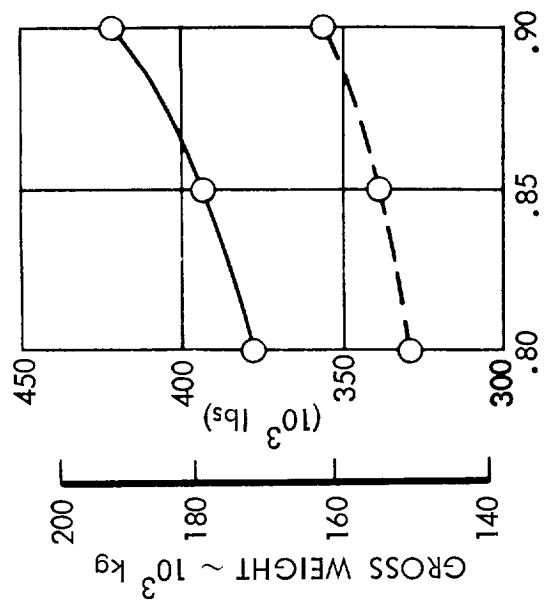


TABLE 16. DESIGN CHARACTERISTICS: INTERNAL TANK, LH₂ PASSENGER AIRCRAFT (LONG RANGE)
400 PAX; Payload = 39,900 kg (88,000 lb); Range = 10,190 km (5500 n mi)

CRUISE MACH NUMBER	SI	CUSTOMARY	0.80		0.85		0.90	
			SI	CUSTOMARY	SI	CUSTOMARY	SI	CUSTOMARY
Gross Weight	kg	lb	171,000	377,100	177,000	391,700	190,500	420,100
Total Fuel Weight	kg	lb	26,500	58,500	27,900	61,600	31,400	69,300
Operating Empty Weight	kg	lb	704,600	230,600	109,200	242,100	119,200	262,800
Wing Area	m ²	ft ²	294	3,160	312	3,360	348	3,750
Sweep	deg	deg	25	25	30	30	37	37
Span	m	ft	55.3	173	53	174	52.8	173
Fuselage Length	m	ft	56.2	217	67.8	219	68.6	225
L/D (Cruise)	-	-	16.6	16.6	16.1	16.1	15.0	15.0
SFC (Cruise)	$\frac{\text{kg}}{\text{hr}}/\text{daN}$	$\frac{\text{lb}}{\text{hr}}/\text{lb}$	0.197	0.193	0.203	0.199	0.210	0.206
Thrust per Engine	N	lb	112,400	25,260	127,800	28,690	150,800	33,820
FAR T.O. Field Length	m	ft	2,100	6890	1,900	6240	1,710	5,610
FAR Landing Field Length	m	ft	1,770	5,810	1,770	5,810	1,760	5,770
Energy Utilization	$\frac{\text{kJ}}{\text{seat km}}$	$\frac{\text{Btu}}{\text{seat n mi}}$	675	1185	705	1239	789	1387
Airplane Price	$\frac{\$10^6}{\text{seat km}}$	$\frac{\$10^6}{\text{seat n mi}}$	25.4	25.4	26.9	26.9	29.5	29.5
DOC*	$\frac{\$}{\text{seat km}}$	$\frac{\$}{\text{seat n mi}}$	0.563	1.061	0.581	1.079	0.618	1.145

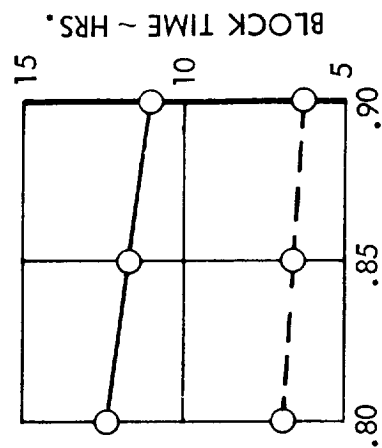
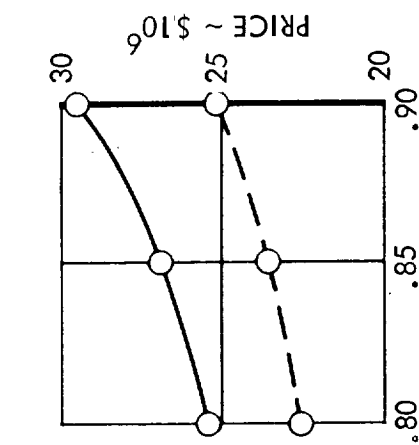
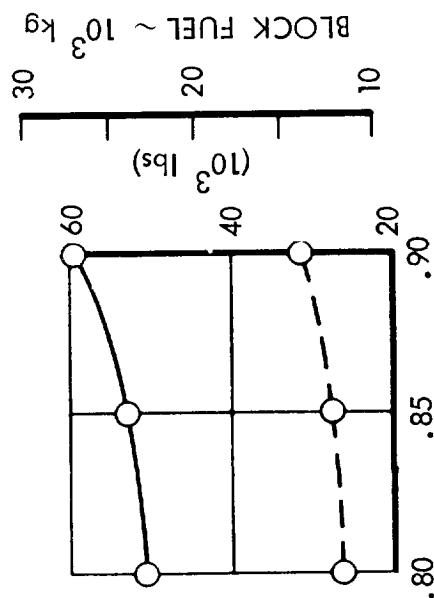
*Based on LH₂ Fuel Cost = \$3/1.054 GJ (\$3/10⁶ Btu = 15.48 ¢/lb)



INTERNAL TANK
LH₂ PASSENGER AIRCRAFT

— 10,190 km (5,500 n.mi.)
--- 5,560 km (3,000 n.mi.)

CRUISE MACH NO.



CRUISE MACH NO.

Figure 59. Effect of Cruise Speed on Values of Selection Parameters (Internal Tanks)

TABLE 17. COST SUMMARY: LH₂ INTERNAL TANK AIRCRAFT, MACH 0.85

		COSTS IN \$10 ⁶	
	RANGE	5560 km	10,190 km
<u>Development</u>			
Airframe		\$ 590.54	\$ 669.47
Engine		412.00	454.95
Avionics		-	-
Total		\$1,002.54	\$1,124.42
<u>Production</u>			
Airframe Manufacturing Cost		\$ 11.31	\$ 12.98
Other Airframe Cost			
Sustaining Engineering		.78	.90
Tool Maintenance		1.03	1.19
Quality Assurance		1.07	1.24
Miscellaneous		.29	.33
Profit		2.28	2.62
Warranty		.72	.83
Engine		3.10	3.50
Avionics		.50	.50
Subtotal		\$ 21.08	\$ 24.09
R&D per Aircraft*		2.51	2.82
Total Aircraft Price		\$ 23.59	\$ 26.91
*Based on 350 aircraft and 2000 engines			

those costs which are in support of the manufacturing process and warranty and profit. The purchase cost for the engine and avionics includes warranty and profit. The R&D per aircraft includes the airframe R&D amortized over 350 aircraft and the engine R&D amortized over 2000 engines. All costs are in 1973 dollars.

The higher cost for the longer range airplane is due only to the additional structure and higher thrust engines to accommodate the additional fuel. As stated in Paragraph 4.3.2.1, the cost per unit weight of operating weight empty is virtually the same for vehicles of both ranges, i.e., \$242.5/kg (\$10/lb).

4.3.3.2 Direct Operating Cost (DOC) - Table 18 shows the breakdown of DOC for the Mach 0.85 LH₂ internal tank airplanes for both the 5560 km (3000 n.mi.) and the

TABLE 18. DIRECT OPERATING COSTS: LH₂ INTERNAL TANK AIRCRAFT, MACH 0.85

RANGE	5,560 km		10,190 km	
UNITS	\$/km	\$/n mi	\$/km	\$/n mi
Crew	0.233	0.432	0.230	0.426
Maintenance				
Airframe Labor (Including Burden)	0.143	0.265	0.136	0.253
Engine Labor (Including Burden)	0.063	0.117	0.063	0.117
Airframe Material	0.069	0.128	0.069	0.128
Engine Material	0.074	0.136	0.077	0.142
Fuel* and Oil	0.812	1.504	0.844	1.563
Insurance	0.179	0.315	0.189	0.350
Depreciation	<u>0.651</u>	<u>1.206</u>	<u>0.723</u>	<u>1.339</u>
Total DOC	2.015	4.103	2.331	4.318
Total Unit DOC	<u>¢</u>	<u>¢</u>	<u>¢</u>	<u>¢</u>
	seat km	seat n mi	seat km	seat n mi
	0.554	1.026	0.583	1.080
*Based on LH ₂ fuel cost = \$3/1.054 GJ (\$3/10 ⁶ Btu)				

10,190 km (5500 n.mi.) range aircraft. The DOC's presented for each of the candidate airplanes used in the parametric analysis are based on an annual utilization of 3285 hours regardless of range. The final evaluation of the selected airplanes is based on a utilization of 3600 hours for the 5560 km (3000 n.mi.) airplane and 4000 hours for the 10,190 km (5500 n.mi.) airplane. These two utilizations predicate different structural lives for a constant depreciation period (15 years). Since the longer range airplane has fewer takeoff and landings it is reasonable to assume that its structural life could be extended over that for the shorter range airplane. The DOC's based on the utilizations of 3600 and 4000 hours for the 5560 km (3000 n.mi.) and 10,190 km (5500 n.mi.) ranges, respectively, are shown in the final comparison in Section 4.8.

4.5 EXTERNAL TANK HYDROGEN AIRCRAFT

4.5.1 Parametric Study Results

The rationale of design selection described in Section 4.4.1 for the internal tank aircraft was also used for the external tank version. Figure 60 shows the effect of wing thickness ratio on the selection criteria for the longer range mission. A 10% thickness was chosen. The effect of aspect ratio is examined in Figure 61. As with the internal tank aircraft, the choice of selection criteria (price, block fuel, gross weight, or DOC) results in different aircraft. The final selection was on the basis of minimum DOC and resulted in an aspect ratio of 8. Similar data was generated and vehicles selected for the other Mach numbers of 0.80 and 0.90, as well as for each Mach number of the 5560 km (3000 n.mi.) aircraft. Based on these data, preferred designs of external tank LH_2 -fueled aircraft were derived. The results are presented in Paragraph 4.5.3.

4.5.2 Configuration Description

The most striking feature of the external tank aircraft design shown in Figure 62 is of course the large wing-mounted tanks. Their physical size prevents mounting below the wing. To minimize drag the tank is supported on a pylon with a height of approximately 1/3 the tank diameter. The tank is of integral construction covered with 6" of closed-cell plastic foam insulation protected by an external fiberglass reinforced composite cover. Figure 63 is a preliminary design layout showing a feasible structural arrangement concept of the tank and supporting pylon.

EXTERNAL TANKS

RANGE = 10,190 km (5,500 n mi)

400 PASSENGERS

MACH = 0.85

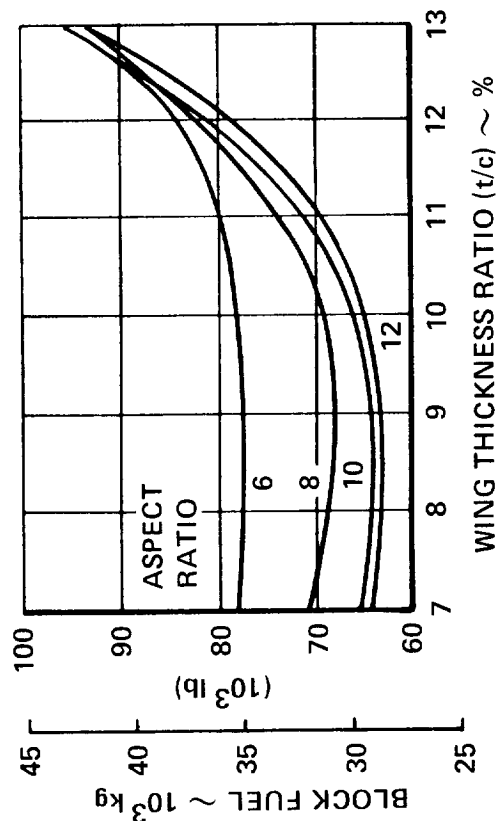
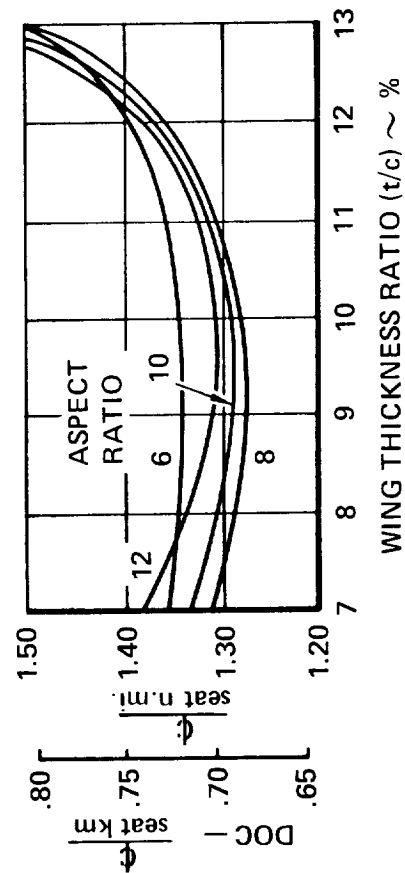
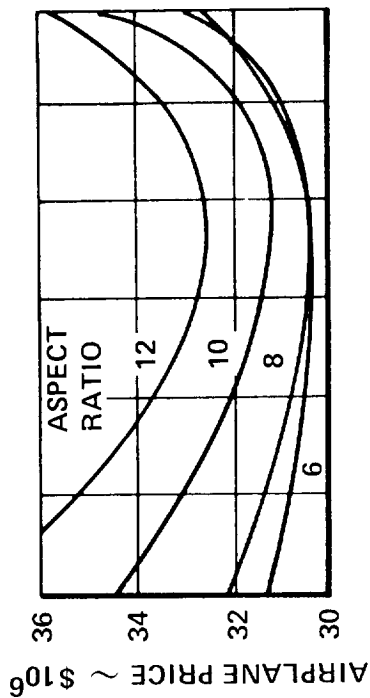
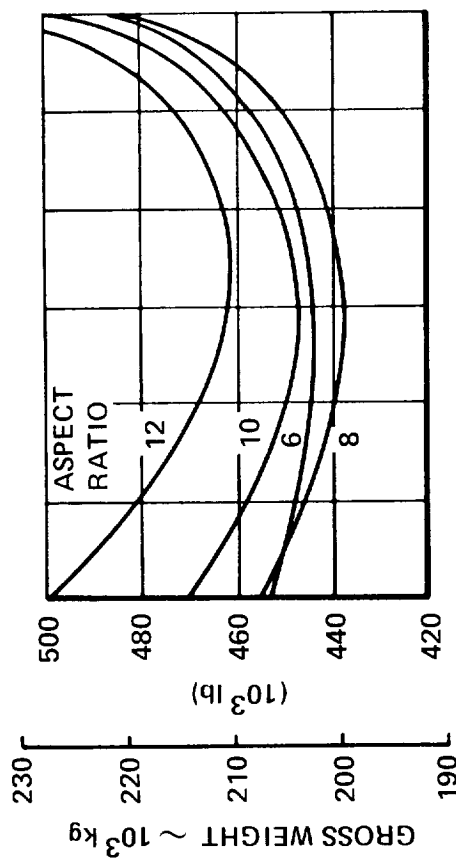


Figure 60. Effect of thickness Ratio on Selection Parameters

WING GEOMETRY STUDY

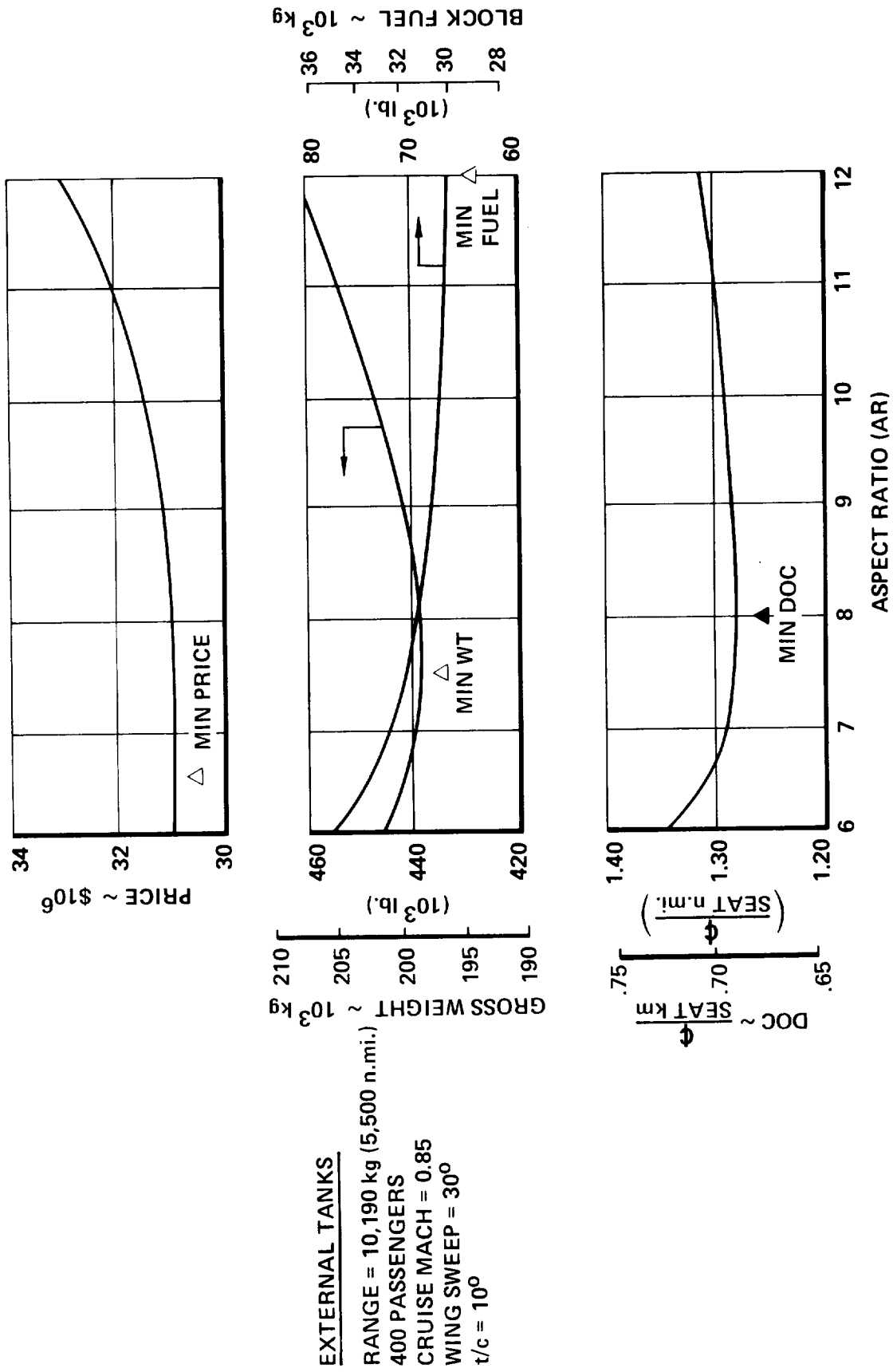
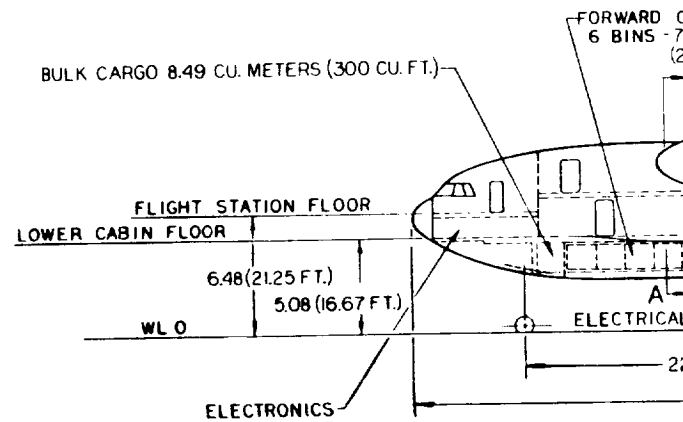
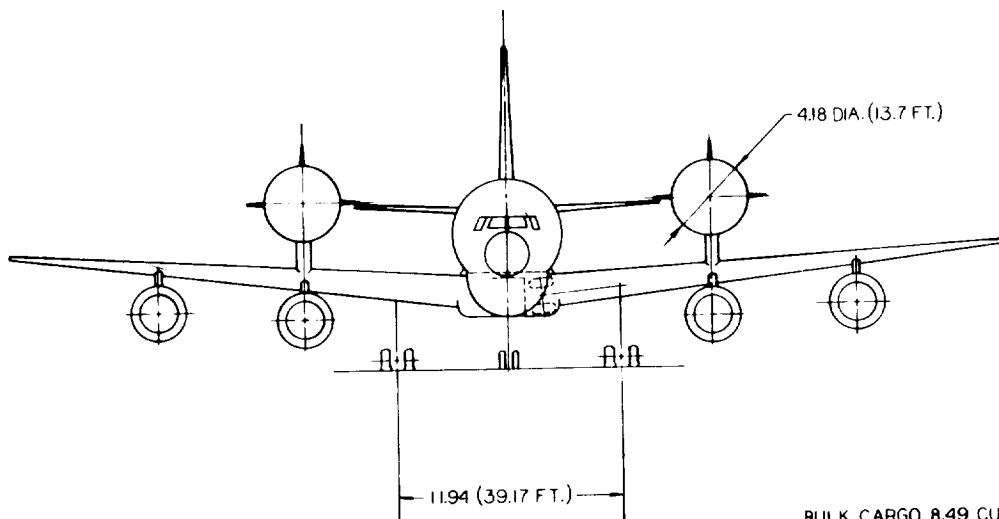
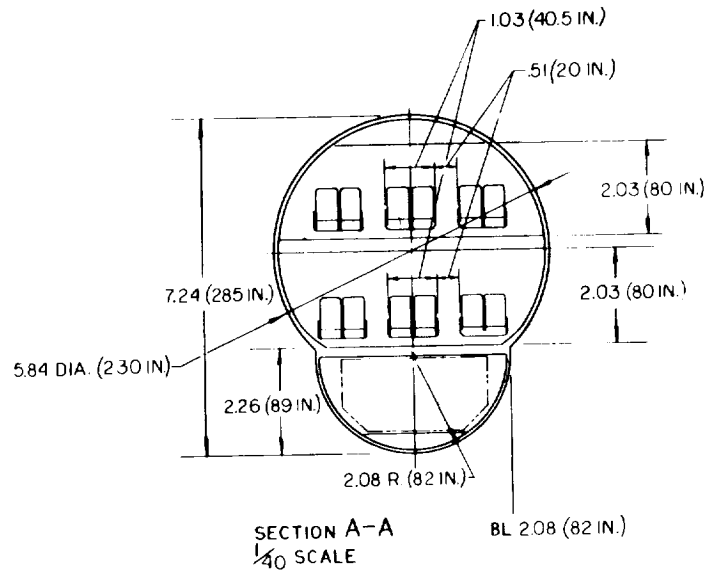
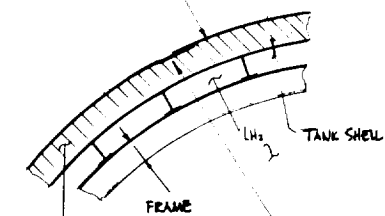


Figure 61. Effect of Aspect Ratio on Selection Parameters

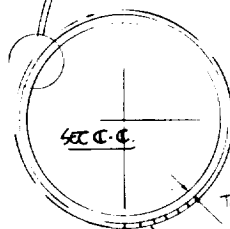


OUTER PROTECTIVE SKIN



RADIAL AND LONGITUDINAL
EXPANSION JOINTS

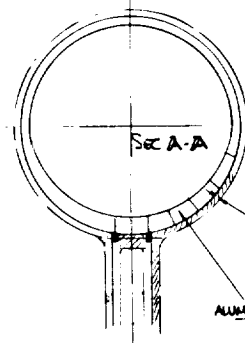
INSULATION



SEC C-C

TANK
FRAME

INTEGRALLY
STIFFENED SKIN
OVER CYLINDRICAL
SECTION



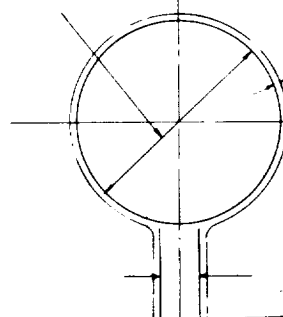
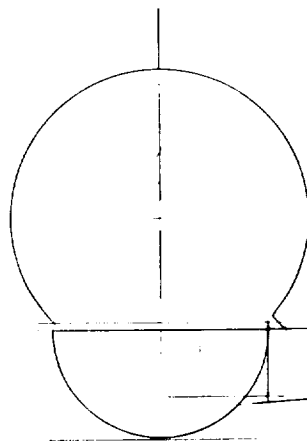
SEC A-A

INSULATION

ALUMINUM FORGINGS

TANK
INSIDE DIA 4.27 (14 FT)

SL 10.90 (478 IN)



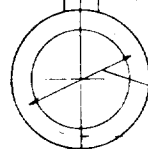
INSULATION
.152 (6 IN)

STRUCTURE
.76 (30 IN.)

PROTECTIVE
NOSE STRUCTURE

.66 (26 IN.)

9.14 (30 FT)



HIGH LIGHT
DIA

TSP
O

STATIC QRD

The fuselage of this aircraft has been reduced in size compared to the internal tank version. Six abreast seating in a double deck arrangement is provided in a 10/90 percent class mix for the 400 passengers. Cargo volume, lavatory and galley facilities are equivalent to those on the internal tank aircraft.

The tank arrangement of this aircraft simplifies the fuel system arrangement since only one engine crossfeed line and refuel line are carried across the aircraft fuselage in the wing box.

4.5.3 Vehicle Data

Design and performance data for the selected configuration of the 5560 km (3000 n.mi.) range external tank aircraft are shown in Table 19 for the cruise Mach numbers of 0.80, 0.85 and 0.90. Similar data for the 10,190 km (5500 n.mi.) version are shown in Table 20. Copies of pertinent pages of the ASSET computer printouts of these two aircraft are included in Appendix D. Significant trends of selection criteria with Mach number are shown in Figure 64 for both ranges. DOC, block fuel, price and gross weight all increase with higher cruise speeds with an attendant reduction of 1.2 hours in block time for the longer range mission and 0.7 of an hour for the 5560 km range. Comparisons of the external tank aircraft designs with corresponding internal tank configurations are presented in Section 4.7.

4.5.4.1 Cost Summary - Table 21 presents the development and production costs for the Mach 0.85 H_2 airplanes with external tanks. The higher cost for the external tank configuration over the internal tank configuration is due to the added structure and linkage weight necessary for the external installation. The cost per kilogram of operating empty weight for the external configuration (\$246.9/kg) is slightly higher than for the internal tank configuration but the primary reason for the increase in cost of the airplane is the increase in structural weight.

4.5.4.2 Direct Operating Cost (DOC) - Table 22 shows the DOC breakdown for the Mach 0.85 external tank H_2 airplanes for both ranges.

4.6 HYDROGEN PASSENGER AIRCRAFT CONFIGURATION SELECTION

In this section the two H_2 fueled passenger transport aircraft configurations which have been described are compared. The candidate designs are depicted in

TABLE 19. DESIGN CHARACTERISTICS: MATERIAL TANK, LH₂ PASSENGER AIRCRAFT (SHORT RANGE)
4,000 PAX; Payload = 33,900 kg (75,000 lb); Range = 5560 km (3600 n mi)

CRUISE MACH NUMBER	SI	CUSTOMARY	0.80		0.85		0.90	
			SI	CUSTOMARY	SI	CUSTOMARY	SI	CUSTOMARY
Gross Weight	kg	lb	154,200	340,900	160,000	352,300	167,200	369,300
Fuel Weight	kg	lb	17,100	37,800	18,400	40,700	20,300	44,700
Operating Empty Weight	kg	lb	37,400	215,100	101,700	223,600	107,000	236,600
Wing Area	m ²	sq ft	27.8	2,990	296	3,170	318	3,420
Sweep	deg	deg	25	25	30	30	37	37
Span	m	ft	50	164	48.7	160	47.2	155
Fuselage Length	m	ft	60	197	60	197	60	197
L/D (Cruise)	-	-	14	14	13.1	13.1	12.2	12.2
SFC (Cruise)	$\frac{\text{kg}}{\text{hr}}/\text{daN}$	$\frac{\text{lb}}{\text{hr}}/\text{lb}$	0.196	0.192	0.203	0.200	0.210	0.206
Thrust per Engine	N	lb	123,200	27,700	135,000	30,390	156,000	35,090
FAR T.O. Field Length	m	ft	1,638	5,370	1,537	5,040	1,423	4,670
FAR Landing Field Length	m	ft	1,773	5,820	1,760	5,780	1,770	5,800
Energy Utilization	$\frac{\text{kJ}}{\text{seat km}}$	$\frac{\text{Btu}}{\text{seat n mi}}$	754	1326	814	1430	895	1572
Airplane Price	$\frac{\$10^6}{\text{seat km}}$	$\frac{\$10^6}{\text{seat n mi}}$	23.9	23.9	25.0	25.0	26.7	26.7
DOC*	$\frac{\$}{\text{seat km}}$	$\frac{\$}{\text{seat n mi}}$	0.600	1.110	0.615	1.134	0.642	1.187

*Based on LH₂ Fuel Cost = \$3/1.054 GJ(\$3/10⁶ Btu = 15.48 ¢/lb)

TABLE 1. DESIGN DATA SUMMARY: AIRCRAFT DATA, AND AIRCRAFT AIR DATA (100 RANGE)

100 FAR; Fuel cost = \$3/10⁶ Btu; SFC = 0.196 lb/hr/lb; L/D = 14; Range = 1,170 km (727 mi)

AIRCRAFT DATA	UNIT	100 FAR	1,170		1,170		CUSTOMARY	SI	CUSTOMARY
			WT	THrust	WT	THrust			
Aircraft Weight	kg	lb	145,000	145,000	145,000	145,000	436,800	212,200	468,800
Fuel Weight	kg	lb	80,000	80,000	80,000	80,000	31,000	41,300	91,100
Operating Empty Weight	kg	lb	65,000	65,000	65,000	65,000	267,800	131,000	289,700
Wing Area	m ²	ft ²	325	3,120	325	3,120	3,680	375	4,040
Span	m	ft	30	30	30	30	30	37	37
Span	m	ft	71.3	175	71.3	175	171	51.3	168
Fuselage Length	m	ft	31	127	31	127	197	60	197
L/D (Cruise)	-	-	14	14	14	14	13.4	12.5	12.5
SFC (Cruise)	kg/hr/lb	lb/hr/lb	0.196	0.192	0.203	0.199	0.199	0.210	0.206
Thrust per Engine	N	lb	153,000	34,410	172,000	38,760	38,760	200,800	45,120
FAR T.O. Field Length	m	ft	1,735	5,700	1,610	5,290	5,290	1,500	4,930
FAR Landing Field Length	m	ft	1,772	5,830	1,770	5,810	5,810	1,760	5,790
Energy Utilization	kJ/seat km	Btu/seat n mi	869	1575	931	1634	1634	1040	1827
Airplane Price	\$10 ⁶ /seat	\$10 ⁶ /seat	23.5	23.5	30.2	30.2	30.2	33.0	33.0
100*	\$/seat km	\$/seat n mi	0.002	1.444	0.690	1.277	1.277	0.732	1.357

*Based on LH₂ Fuel Cost = \$3/10⁶ Btu = 15.48 ¢/lb

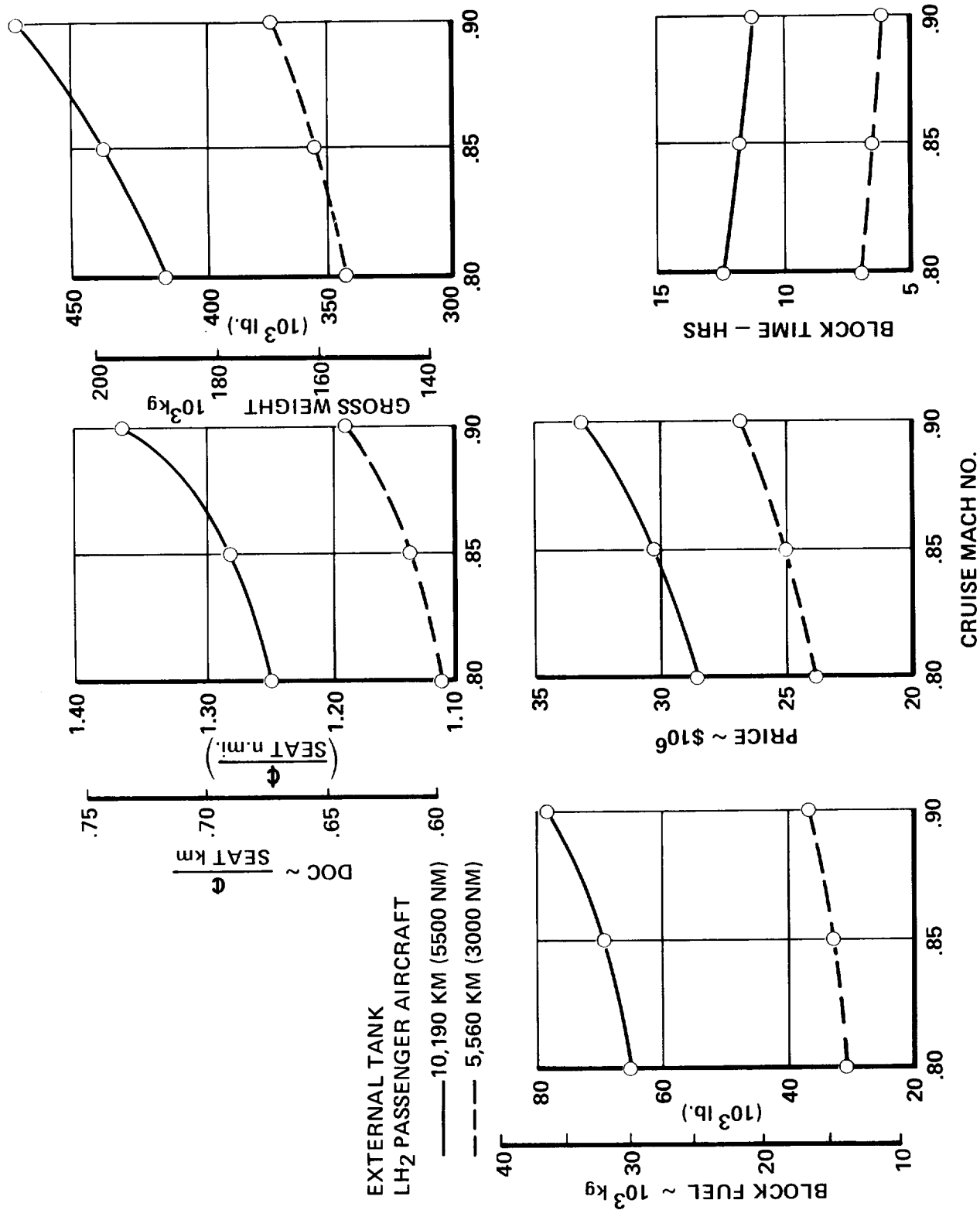


Figure 64. Effect of Cruise Speed on Values of Selection Parameters (External Tanks)

TABLE 21. COST SUMMARY: LH₂ EXTERNAL TANK AIRCRAFT, MACH 0.85

		COSTS IN \$10 ⁶	
	RANGE	5560 km	10,190 km
<u>Development</u>			
Airframe		\$ 659.00	\$ 805.82
Engine		473.64	564.62
Avionics		-	-
Total		\$1,132.64	\$1,370.44
<u>Production</u>			
Airframe Manufacturing Cost		\$ 11.60	\$ 14.00
Other Airframe Cost			
Sustaining Engineering		.80	.98
Fuel Maintenance		1.06	1.29
Quality Assurance		1.11	1.35
Miscellaneous		.29	.36
Profit		2.34	2.83
Warranty		.74	.90
Engine		3.69	4.59
Avionics		.50	.50
Subtotal		\$ 22.13	\$ 26.80
R&D per Aircraft*		2.83	3.43
Total Aircraft Price		\$ 24.96	\$ 30.23

*Based on 350 aircraft and 2000 engines

TABLE 22. DIRECT OPERATING COSTS: LH₂ EXTERNAL TANK
AIRCRAFT, MACH 0.85

RANGE	5,560 km		10,190 km	
UNITS	\$/km	\$/n mi	\$/km	\$/n mi
Crew	0.233	0.432	0.232	0.430
Maintenance				
Airframe Labor*	0.142	0.263	0.137	0.254
Engine Labor*	0.071	0.131	0.076	0.141
Airframe Material	0.071	0.131	0.075	0.138
Engine Material	0.087	0.161	0.099	0.184
Fuel and Oil	0.973	1.803	1.112	2.060
Insurance	0.179	0.333	0.212	0.392
Depreciation	<u>0.692</u>	<u>1.282</u>	<u>0.816</u>	<u>1.512</u>
Total DOC	2.448	4.536	2.759	5.111
Total Unit DOC	$\frac{\phi}{\text{seat km}}$	$\frac{\phi}{\text{seat n mi}}$	$\frac{\phi}{\text{seat km}}$	$\frac{\phi}{\text{seat n mi}}$
	0.612	1.134	0.690	1.278
*Including burden				

Figure 65. One is selected for further analysis and later comparison with the reference Jet A designs. The characteristics which are compared as bases for the selection include operational and maintenance features and safety potential, as well as the customary qualities of weight, size, energy consumption, and cost.

4.6.1 Operations and Maintenance Comparison

In order to properly assess the relative merits of the candidate LH₂-fueled aircraft designs, it was necessary to first consider how such aircraft might be handled in typical routine operational situations. For example, how would refueling be accomplished, what type of service equipment and procedures might be used, and what unique servicing requirements might exist which would influence the choice between the candidate aircraft configurations.

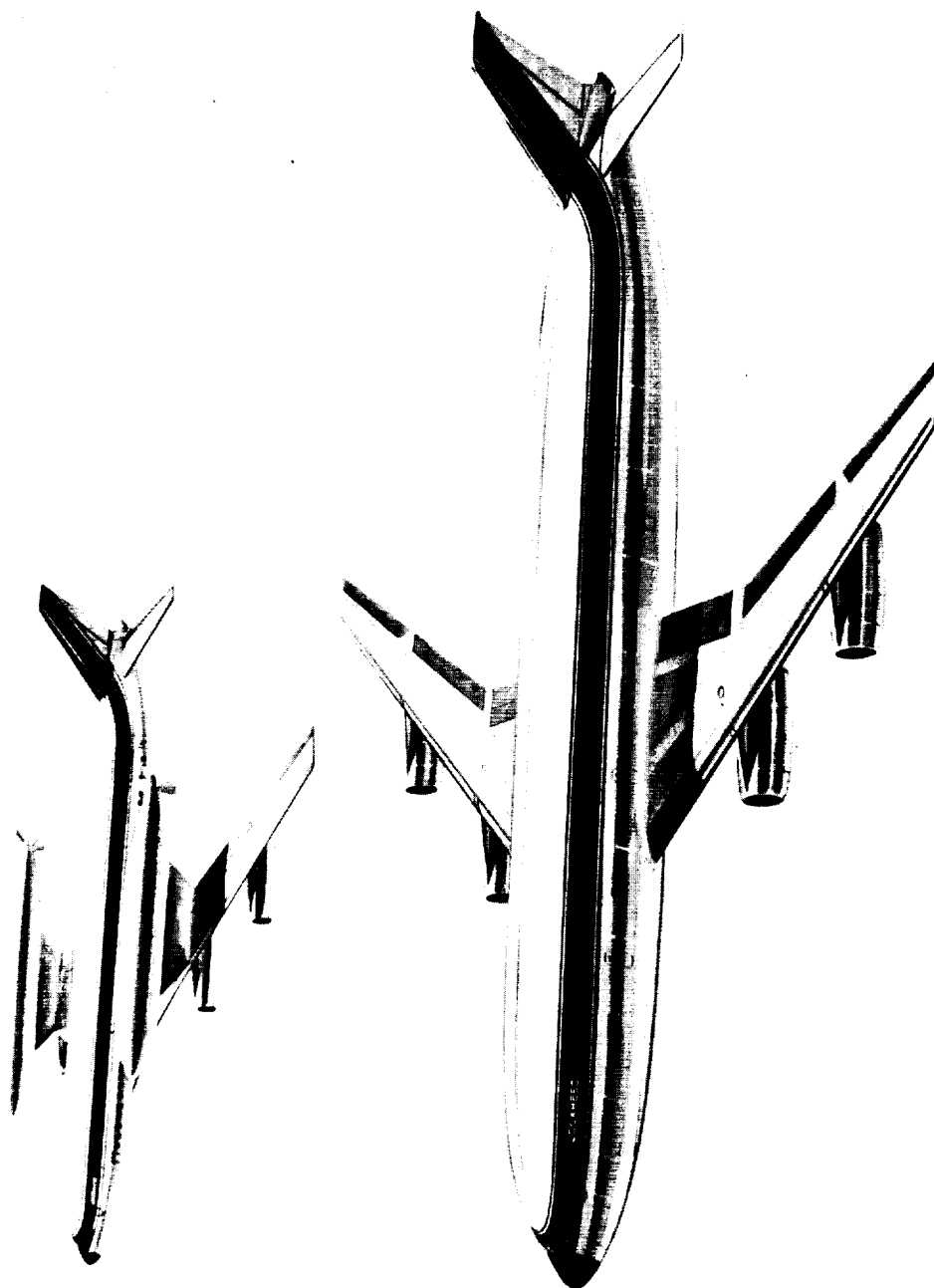


Figure 65. Candidate Hydrogen - Fueled Passenger Transport Aircraft

First, considering the refueling operation, a conceptually feasible arrangement for an airport fueling facility is shown in Figure 66. As mentioned in Section 3.1, it is assumed that initially, because of existing quantity/distance relationships, such a facility might be located perhaps 548 m (1800 ft) from the passenger terminal. The sequence of operations involved in readying an aircraft for flight is also described briefly in Section 3.1. Equipment to perform the various refueling functions is conceptually described in following paragraphs.

As illustrated in Figure 66, an airport fueling facility would include a liquefaction plant, cryogenically insulated storage tanks to contain the LH_2 fuel and the liquid nitrogen for cooling and purging, and associated equipment. Power requirements for this equipment could be supplied at least in part by boil-off hydrogen gas. The fueling pipe loop allows continual circulation of LH_2 . The loop need not be circular of course, it can be of any configuration to suit the airport geometry. During the aircraft tank warm-up or cool-down periods, as well as during refueling, vent gases can be captured and recirculated to the liquefaction plant or to use in ground power stations. Other utilities, gaseous hydrogen, nitrogen, electricity, and water, parallel the above-ground LH_2 lines. A defueling area would permit rapid defueling of LH_2 aircraft if required. The fueling towers are unique and are discussed in paragraphs that follow.

It seems apparent that the safest and most logical fueling point locations for the LH_2 aircraft would be high and away from the passenger and flight stations. For example, for the Internal Tank aircraft the fueling connection could be high on the tail cone or in the vertical stabilizer tip, thereby negating leak and spill hazards by allowing escaped gases to float well above the aircraft and ground personnel. The possibility of accidental ignition of the gas at this height (approximately 60 feet above ground level) would be minimal and if it did occur, would pose no serious hazard to personnel or damage to the aircraft. Further, fueling at this point would allow normal activity in and around the aircraft during the fueling operation. The height does require that special equipment be used, which leads to the fueling tower concept.

The fueling tower concept provides many desirable features for LH_2 aircraft fueling. Fuel would be passed into the aircraft by a guided boom similar to those used in air-to-air fueling. The boom would incorporate the following features:

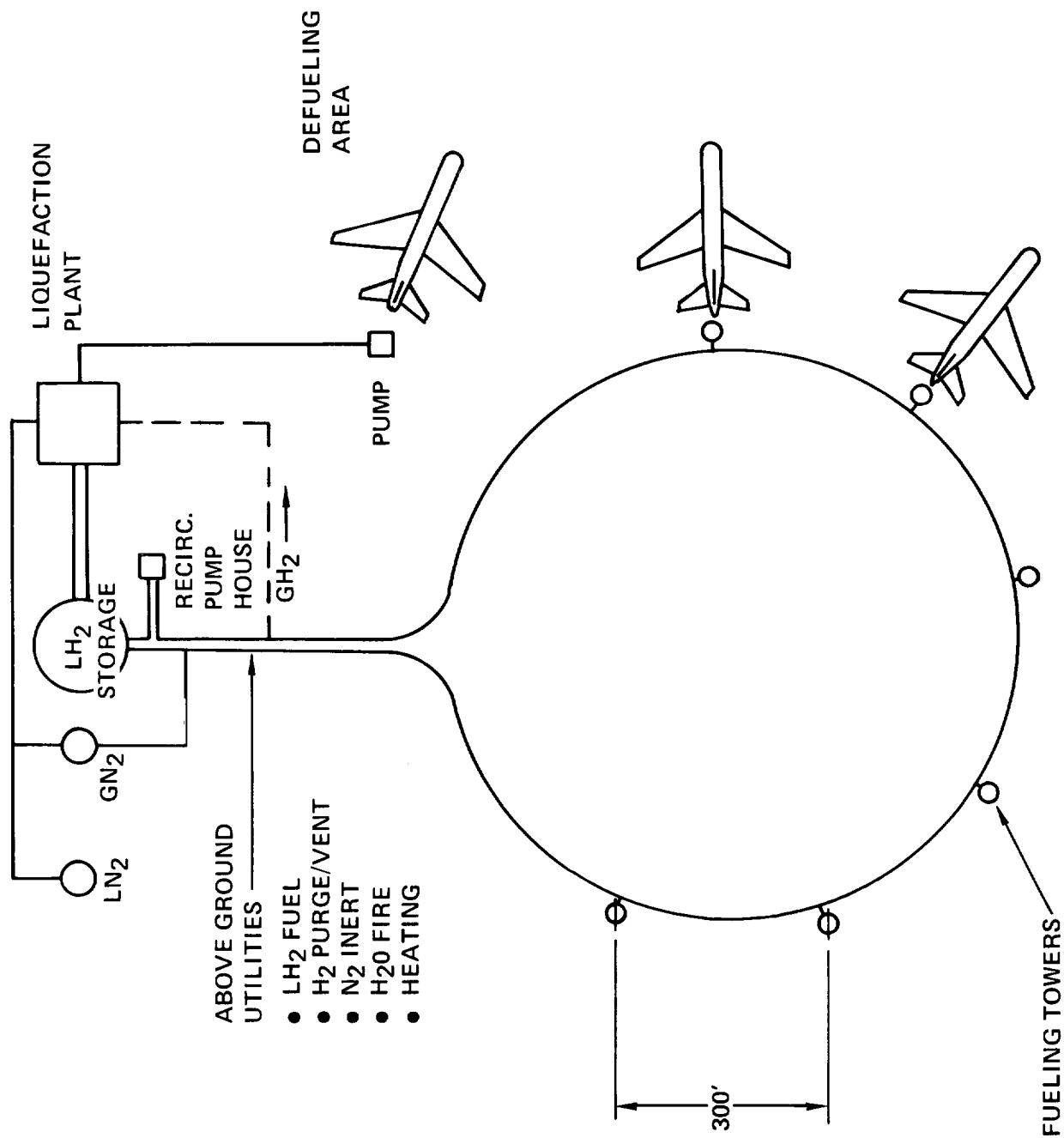


Figure 66. Schematic - LH₂ Airport Fueling Facility

- Sequenced operations
- Positive aircraft grounding
- Fire and leak detection systems
- Self-checking and redundant controls
- Self-purging
- Dual flow capability - LH_2 in and GH_2 out
- Automatic flow shutdown and deluge immediately upon leak or flame detection
- Directable water nozzles

These capabilities, plus locating the refueling connection high on the airplane and at one of the extremities, should eliminate many concerns over LH_2 fueling, so far as procedural, safety design, operation and work area deficiencies which accounted for the majority of the mishaps reported in a NASA review of accidents and incidents which have occurred with hydrogen in the space program (Reference 11).

The aircraft would be backed in to the fueling station where the guided boom would be connected to the aircraft by personnel located in the tower. The fueling boom would allow the LH_2 to enter the aircraft and hydrogen boil-off gas from the aircraft to be returned to the ground supply system. Redundant and automatic safety features built in the tower would allow all other activities around the aircraft to proceed normally.

After the aircraft is fueled, the boil-off gas would then be used to fuel on-board auxiliary power units. During out-of-service periods, the APU's may continue to provide services, or the boil-off gas may again be captured and returned to the liquefaction plant, or otherwise consumed. If the hangaring of a fueled aircraft is required, the vent capture lines would be attached to the aircraft immediately upon its entering the hangar.

For extended out-of-service periods, the aircraft would be defueled, and the tanks filled with an inert gas. This would allow hangaring and mechanical servicing without further precautions. Modern aircraft are rarely out-of-service longer than 48 hours so defueling operations of LH_2 aircraft would be expected to occur very infrequently.

With these general operational and equipment concepts in mind, the candidate Internal Tank and External Tank LH_2 aircraft designs were compared and evaluated. The following subjects were considered:

- Tank accessibility
- Fuel component accessibility
- Fuel line routing
- Fueling/defueling points
- Insulation repair methods
- Fueling practices/safety
- Maintenance practices/safety (isolating, purging, and inerting)
- Vents
- Leak and fire detection systems
- Redundancy/safety requirements

The results of the evaluation are summarized in Table 23.

It was concluded that from an operations point of view, the Internal Tank design was preferred. Considering maintenance aspects, the External Tank configuration offered definite advantages. Other considerations such as safety, vehicle performance, cost, energy utilization, etc., are compared in following sections leading to an ultimate choice between the two aircraft configurations.

4.6.2 Safety Comparison

The good safety record and procedures associated with the production, storage, handling, and use of liquid hydrogen as a fuel in the U.S. space program and in various industrial applications provides a solid basis for development of safety criteria for LH_2 fueled aircraft. Most of the same problem areas affecting the safe operation of conventional Jet A aircraft must be dealt with in LH_2 fueled airplanes, with special solutions required in many cases to safely utilize the physical characteristics of LH_2 . The two candidate configurations of external and internal LH_2 fuel tanks were analyzed to determine if either had a clear advantage over the other in the following areas of safety concern:

TABLE 23. OPERATIONS AND MAINTENANCE COMPARISON -
LH₂ FUELED AIRCRAFT

CONDITION	REMARKS	ADVANTAGE
<u>OPERATIONS:</u> <ul style="list-style-type: none"> ● Refueling ● Vent Gas Control During Out-Of-Service Periods ● Passenger Loading and Associated Servicing 	<p>Single point refueling possible with either system</p> <p>Internal tanks have single vent line located at highest point on the aircraft</p> <p>External tanks inhibit access to fuselage</p>	<p>Neither</p> <p>Internal</p> <p>Internal</p>
<u>MAINTENANCE:</u> <ul style="list-style-type: none"> ● Fuel System ● Tanks Inspection and Repair ● Tank Replacement 	<p>Engine supply and refuel systems with external tanks provide simpler plumbing arrangement</p> <p>Accessibility is better with external tanks</p> <p>Aircraft would be out-of-service for extended period with internal tanks</p>	<p>External</p> <p>External</p> <p>External</p>

- Vulnerability to Engine Burst

Designing for protection against engine turbine and fan wheel burst is a fundamental requirement. The fuel tanks, fuel lines, hydraulic systems, flight controls, electrical systems, passenger and crew accommodations, insofar as possible must be located to minimize the effects of an engine burst. The application of protective armor to the engines, or to the external LH₂ fuel tanks and other vulnerable fuselage areas in the dispersion angles of an engine burst, can be one solution to the problem. However, lightweight protective armor capable of such protection has not been developed. Such development is required to support an external tank configuration. The internal tank arrangement should be less vulnerable to an engine burst but will require engine burst strike zone study when detail engine configuration dimensions become available.

- Crashworthiness

Prevention of fuel tank rupture and/or fire, and the safe evacuation of the passengers are primary concerns in present day and future aircraft involved in survivable accidents. Studies have shown that the incorporation of controlled "break-away" patterns for structural members such as landing gear supports can be used to prevent the rupture of wing fuel tanks. This "breakaway" concept could be applied to the external tank configuration permitting a safe separation during a survivable accident. The internal tank arrangement does not lend itself to such a concept and requires safeguards in the form of energy absorbing materials to attain a similar level of safety. This protection is provided in the designs of the Internal Tank configurations presented herein.

- Passenger Evacuation During an Emergency

Emergency evacuation from the LH_2 fueled airplane should be conventional assuming the airplane is relatively intact with no fuel tank ruptures. The external fuel tank version offers little advantage over the internal arrangement or vice versa in the event of tank rupture and/or fire. The airplane will have multiple doors for passengers to evacuate from. Selection of forward or aft doors, right hand or left hand, should provide the passengers and crew a safe location to exit from. If the fire is widely spread, blocking all exits, the rapid burning and low heat radiation characteristics of hydrogen compared to conventional fuels can be used to an advantage. Rather than hurrying evacuation while the exits are blocked with fire, it may be possible to delay long enough to allow the exits to clear but before secondary fires intensity. A disadvantage is the normally colorless nature of a hydrogen/air flame. People could walk or run into a hydrogen-air flame before they realize it is there. The formation of water vapor as a clue to the presence of hydrogen is generally not reliable during hydrogen burning because of the rapid dissipation of the vapor from the heat of combustion. Smoke is present as a clue only when other material is being consumed. Studies are needed to determine the feasibility of using an additive or other means to give leaking and/or burning hydrogen a distinctive color or identifying characteristic.

- Collision Vulnerability; Mid-Air and Ground

Accident records support the selection of the internal tank arrangement as less vulnerable to collision. The external tank version would be subject to more collision with ground service equipment, terminal facilities, other airplanes, and even

bird strikes. The more vulnerable areas of the external tanks would require protection to preclude tank rupture from minor mishaps. Additional study is indicated to determine the effects of collision damage, both mid-air and ground, on continued safe flight, ground safety, fuel tank impact resistance and protection.

- Separation of Fuel from Passenger Areas

The external tank configuration offers safer fuel line routing possibilities in that lines to the engines will be short with a minimum of joints. Fuselage penetration will be the minimum required to provide crossfeed capability between the two proposed external tanks. Fuel pumps and associated wiring and valves, and the vent system, can be located in the wing area for maximum separation from the passenger compartment. However, a disadvantage is the need for the external tanks to parallel the passenger compartment. Major accidents involving an external tank might involve the fuselage as well. The internal tank arrangement will require crossfeed fuel lines running almost the length of the fuselage, with valves, fuel pumps, and the tank vent system all within the fuselage shell. An assessment of the safety aspects of this design configuration including evaluation of effects of insulation failure, isolation of these components from the passenger area, leak detection, and passenger protection in survivable accidents will require the development of additional design details from follow-on studies.

- Wheels-Up Landings, Overrotation on Take-Off and Tail-Down Flare on Landing

The choice of the external tank configuration over the internal arrangement is clear in cases of inadvertent (pilot error) fuselage contact with the runway. Wheels up landing, although rare, must also be considered as possible and again the external tank arrangement is inherently safer.

Achievement of a level of safety for the internal tank design comparable to the external version requires fuselage energy absorbing material or special skid/bumper devices capable of isolating the fuselage fuel tanks from the runway and preventing tank rupture. As noted previously, the internal tank aircraft designs shown in this study all incorporate this protection and include appropriate weight penalties.

- Lightning Strike

The external tank configuration will be more vulnerable to lightning strikes. Development of adequate protection to solve this problem will require a full review and study of the effects of lightning on the LH_2 fueled airplane especially in the area of the vent system.

● Conclusions

A summary of the safety consideration is presented in Table 24. Either fuel tank arrangement, external or internal, could be selected. Design solutions to satisfy the areas of concern could bring both candidates to an equal level of safety. However, the magnitude of the task of solving the protection requirement against engine burst for the external tank configuration makes the internal tank approach more feasible and therefore more attractive. The major safety concerns for the internal tanks, from a safety comparison, are in the areas of crashworthiness and fuel system complexity within the fuselage shell. Such complexity and proximity of fuel tanks make it difficult to assure on a conceptual level, that the passengers will be adequately protected against the effects of leaking fuel and subsequent fire danger. Design studies and experimental testing of representative structures are needed.

4.6.3 Characteristics Comparison

The design and performance characteristics of the Internal Tank and External Tank LH_2 fueled passenger aircraft are presented in detail in Sections 4.4 and 4.5, respectively. For convenience in comparing the two design concepts, significant data for the Mach 0.85 cruise speed designs of each are repeated in Table 25 for the 5560 km (3000 n.mi.) versions, and in Table 26 for the 10,190 km (5500 n.mi.) versions. Each table includes a column which shows a factor for comparing the values of each parameter listed. The comparison presents values of the External Tank design relative to those for the Internal Tank. For example, in Table 25 the gross weight of the External Tank airplane is 4 percent greater than that of the Internal Tank design.

In only three of the 15 parameters listed is the Internal Tank design found to have a rating not as favorable as the External Tank configuration. These are span, fuselage length, and FAR T.O. Field Length. The increase in span is so small as to be of no significance. It results from the difference in aspect ratio selected for the two designs. The increase in fuselage length stems directly from the fact the internal tank design is made long enough to contain the hydrogen tanks plus the passengers. The greater field length requirement may at first glance appear significant; however, it must be realized the allowable field length is 2440 m (8000 ft.) and both LH_2 designs are comfortably within the limit. The fact the External Tank concept can takeoff in such a short distance results from its poor L/D in cruise, which requires larger engines, and which in turn provides a higher thrust-to-weight ratio for takeoff.

TABLE 24. SAFETY COMPARISON:
INTERNAL VS EXTERNAL TANK LH₂ AIRCRAFT

CONDITION	REMARKS	ADVANTAGE
1. Vulnerability to engine burst	External Tanks require armor protection to be acceptable	Internal
2. Crashworthiness	External Tanks can be designed to "breakaway"	External
3. Passenger evacuation during emergency		
• No fire	External arrangement requires evacuation toward fuel tanks	Internal
• Fire in fuel area	Passengers should remain in sealed cabin	Neither-based on present information
4. Mid-air and ground collision vulnerability	External Tanks are more vulnerable to minor collisions	Internal
5. Separation of fuel from passenger areas	Average separation distance greater for Internal Tank arrangement	Internal
6. Fuel line length to engines and line entry into fuselage	Safe practice dictates minimal entry of fuel lines into fuselage. Short runs with a minimum of breaks from tank to engines make for a safer system	External
7. Wheels-up landings, over-rotation on take-off and tail-down flare on landing	The fuselage tanks require energy absorbing material or devices between the tanks and fuselage skin	External
8. Lightning strike	External Tanks vulnerable - require protection	Internal
9. GH ₂ leak	Ends of Internal Tanks require forced venting or purge	External

TABLE 25. DESIGN COMPARISON: INTERNAL VS. INTERNAL TANK, LH₂ AIRCRAFT (SHORT RANGE)
(MACH = 0.85, 400 PAX, 5500 km)

	SI	CUSTOMARY	EXTERNAL TANKS			INTERNAL TANKS			FACTOR (EXT./INT.)
			SI	CUSTOMARY	SI	CUSTOMARY	SI	CUSTOMARY	
Gross Weight	kg	lb	159,800	352,300	153,500	338,500			1.04
Fuel Weight	kg	lb	18,500	40,700	16,300	36,000			1.13
Operating Empty Weight	kg	lb	101,400	223,600	97,300	214,500			1.04
Wing Area	m ²	ft ²	294	3170	286	3077			1.03
Span	m	ft	48.7	160	50.6	166			0.96
Fuselage Length	m	ft	60	197	64	210			0.94
FAR T.O. Field Length	m	ft	1536	5040	1788	5860			0.86
L/D (Cruise)	-	-	13.1	13.1	15.2	15.2			0.86
SFC (Cruise)	kg/daN hr	lb/hr	0.203	0.200	0.203	0.200			-
Thrust per Engine	N	lb	135,000	30,390	111,000	24,960			1.22
FAR T.O. Field Length	m	ft	1536	5040	1788	5860			0.86
FAR Landing Field Length	m	ft	1760	5780	1770	5810			0.99
Energy Utilization	$\frac{\text{kJ}}{\text{seat km}}$	$\frac{\text{Btu}}{\text{seat n mi}}$	814	1430	680	1193			1.20
Airplane Price	$\frac{\$10^6}{\text{seat km}}$	$\frac{\$10^6}{\text{seat n mi}}$	25.0	25.0	23.6	23.6			1.06
DOC*	$\frac{\phi}{\text{seat km}}$	$\frac{\phi}{\text{seat n mi}}$	0.612	1.134	0.554	1.026			1.11

*Based on LH₂ Fuel Cost = \$3/1.054 GJ(\$3/10⁶ Btu = 15.48 ¢/lb)

TABLE 6. DESIGN CONDITIONS: (a) 1980; (b) 1985; (c) 1990

	ST		CUSTOMARY	EXTERNAL TASKS		INTERNAL TASKS		FACTOR (EXT./INT.)
	SI	CU		SI	CUSTOMARY	SI	CUSTOMARY	
Gross Weight	kg	lb		198,100	436,800	177,700	391,700	1.12
Fuel Weight	kg	lb		36,700	81,000	27,900	61,600	1.31
Operating Empty Weight	kg	lb		121,300	267,800	109,900	242,100	1.11
Wing Area	m ²	ft ²		333	3640	312	3360	1.08
Span	m	ft		52.1	171	53	174	0.98
Fuselage Length	m	ft		60	197	66.8	219	0.90
L/D (Cruise)	-	-		13.4	13.4	16.1	16.1	0.83
SFC (Cruise)	kg/dan hr	lb/hr/lb		0.202	0.199	0.202	0.199	-
Thrust per Engine	N	lb		172,100	38,760	127,500	28,690	1.35
FAR T.O. Field Length	m	ft		1610	5290	1900	6240	0.85
FAR Landing Field Length	m	ft		1770	5810	1700	5810	-
Energy Utilization	kJ seat km	Btu seat n mi		931	1634	705	1239	1.32
Airplane Price	\$10 ⁶	\$10 ⁶		30.2	30.2	26.9	26.9	1.12
DOC*	\$ seat km	\$ seat n mi		0.688	1.277	0.576	1.079	1.18

*Based on LH₂ Fuel Cost = \$3/1.05¢; GJ(\$3/10⁶ Btu = 15.48 ¢/lb)

The last three items in the table are the most significant. In each of these, energy utilization, airplane price, and direct operating cost, the Internal Tank configuration is the obvious choice by a large margin.

It is of interest to note that the advantage of the Internal Tank design decreases with range. It is possible that at shorter ranges the External Tank configuration may offer some advantages.

4.6.4 Summary and Selection

The following is a summary of the conclusions reached regarding the two design concepts in each of the areas of consideration:

<u>Characteristic</u>	<u>Preferred Tank Arrangement</u>
Operations	Internal
Maintenance	External
Safety	Internal
Weight	Internal
Size	External
Energy utilization	Internal
Price	Internal
Direct Operating Cost	Internal

It was recommended to NASA that the Internal Tank design concept for H_2 -fueled passenger aircraft be selected for further analysis and subsequent comparison with the reference Jet A aircraft. The recommendation was accepted.

4.7 REFERENCE (JET A) AIRCRAFT

Following the rationale and method already described for the selection of the hydrogen-fueled aircraft, characteristics of the reference (Jet A-fueled) aircraft were chosen for ranges of 5560 km and 10,190 km. The sensitivity studies resulted in selection of wing thickness of 10 percent and an aspect ratio of 9 for both ranges. As stated in the study ground rules, the only cruise Mach number investigated for the Jet A-fueled aircraft was 0.85.

The general arrangement of the Jet A reference aircraft is shown in Figure 67, using the long range version for illustration. The fuselage arrangement is the same as that of the external tank hydrogen aircraft described in Section 4.5.2. All fuel is contained in the wing box structure resulting in some load relief for this wing compared to the hydrogen design.

A tabulation of vehicle data for both the 5560 km (3000 n.mi.) and 10,190 km (5500 n.mi.), Mach 0.85 aircraft is shown in Table 27. Table 28 presents a summary of development and production costs for the Jet A airplanes. A breakdown of Direct Operating Costs is presented in Table 29. As noted, the fuel price basis shown in the table is the baseline cost specified for purposes of this study.

A comparison of these reference Jet A aircraft with corresponding designs of the preferred configuration of LH_2 fueled vehicles is presented in the following section.

4.8 BENEFITS EVALUATION: LH_2 VS JET A PASSENGER AIRCRAFT

One of the objectives of this study was to assess the potential advantages of using liquid hydrogen as fuel in long range, subsonic transport aircraft, compared with using conventional hydrocarbon fuel (Jet A) in equivalent advanced design aircraft. The results of this comparison are presented in this section.

4.8.1 Characteristics Comparison

The characteristics of the reference Jet A passenger aircraft are presented in Section 4.7. A description of the LH_2 fueled Internal Tank aircraft concept, the configuration selected in Section 4.6 for comparison with the reference Jet A aircraft, is presented in Section 4.4. Note, however, that the design characteristics and performance of the aircraft presented in the present section differ somewhat from those given in preceding sections. Values presented herein represent a final iteration of the designs and are referred to as "Final Design."

For convenience, Tables 30 and 31 present a summary of significant design and performance data for final designs of the aircraft using each fuel. Table 30 lists data for the 5560 km (3000 n.mi.), Mach 0.85 aircraft and Table 31 shows similar information for the 10,190 km (5500 n.mi.) Mach 0.85 designs. Each table also shows a factor which compares the value of each parameter listed for the Jet A design

CHARACTERISTICS	WING	HORIZ.	VERT.
AREA (SQ. M.)	388.8	78.4	47.7
ASPECT RATIO	9	4	1.6
SPAN (M.)	59.13	17.71	8.74
ROOT CHORD (M.)	9.39	6.32	7.80
TIP CHORD (M.)	3.75	2.53	3.12
TAPER RATIO	.4	.4	.4
MAC (M.)	7.01	4.72	5.82
SWEEP (RAD.)	.52	.61	.61
T/C ROOT (°)	11.8	9	9
T/C TIP (°)	8.5	9	9

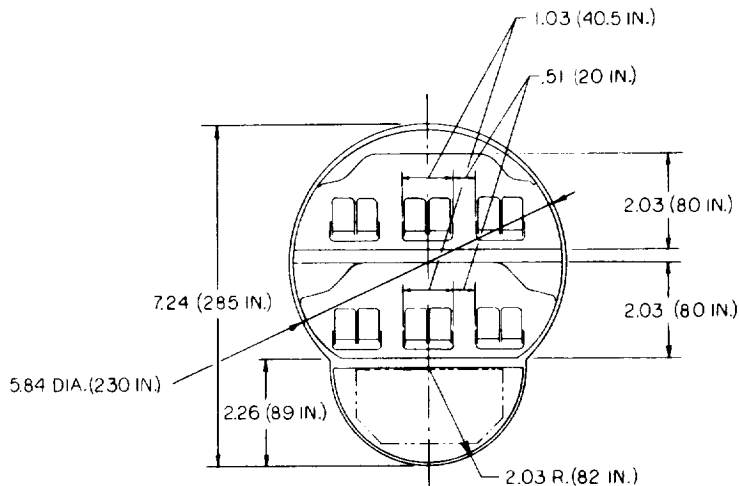
ENGINE THRUST - 145,418 NEWTONS
GROSS WEIGHT - 237,275 KG.
RANGE - 10,192 KM.

CARGO VOLUME - TOTAL 117.3 CU. METERS

CHARACTERISTICS	WING	HORIZ	VERT
AREA (SQ. FT)	4184.7	844.2	513.5
ASPECT RATIO	9	4	1.6
SPAN (FT)	194	58.11	28.66
ROOT CHORD (IN)	369.8	249	307.1
TIP CHORD (IN)	147.8	99.6	122.8
TAPER RATIO	.4	.4	.4
MAC (IN)	276	186	229
SWEEP - $\frac{1}{4}$ (DEG)	30	35	35
T/C ROOT (°)	11.8	9	9
T/C TIP (°)	8.5	9	9

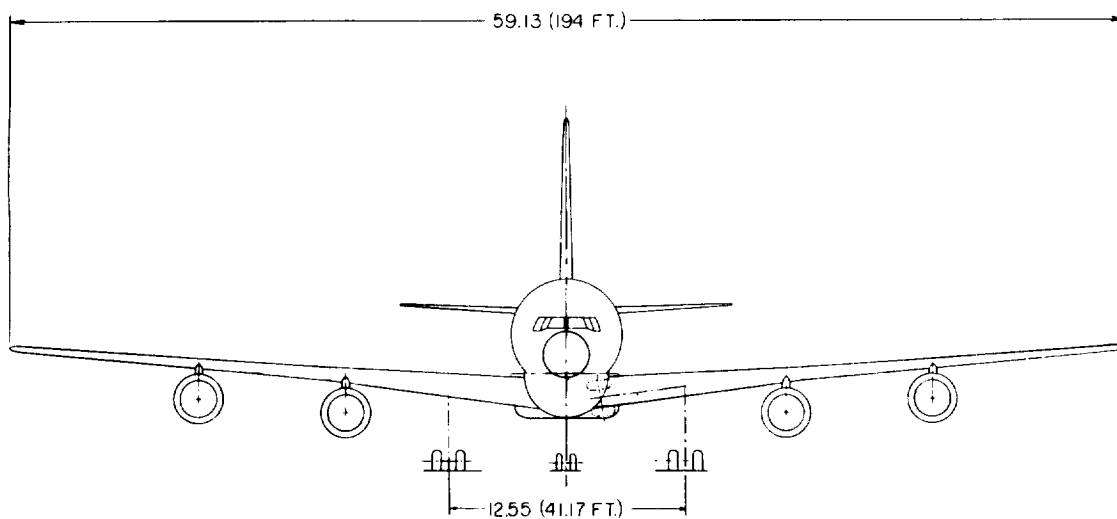
ENGINE THRUST - 32 693 LBS
GROSS WEIGHT - 523 094 LBS
RANGE 5500 N.M.

PASSENGERS - TOTAL - 400 - 10% - 90% MIX
CARGO VOLUME - TOTAL 4143 CU-FT



SECTION A-A

SCALE 1/40



BULK CARGO
8.49 CU. METERS
(300 CU. FT.)

LOWER CABIN FLOOR

5.08 (16.67 FT.)

W.L.O.

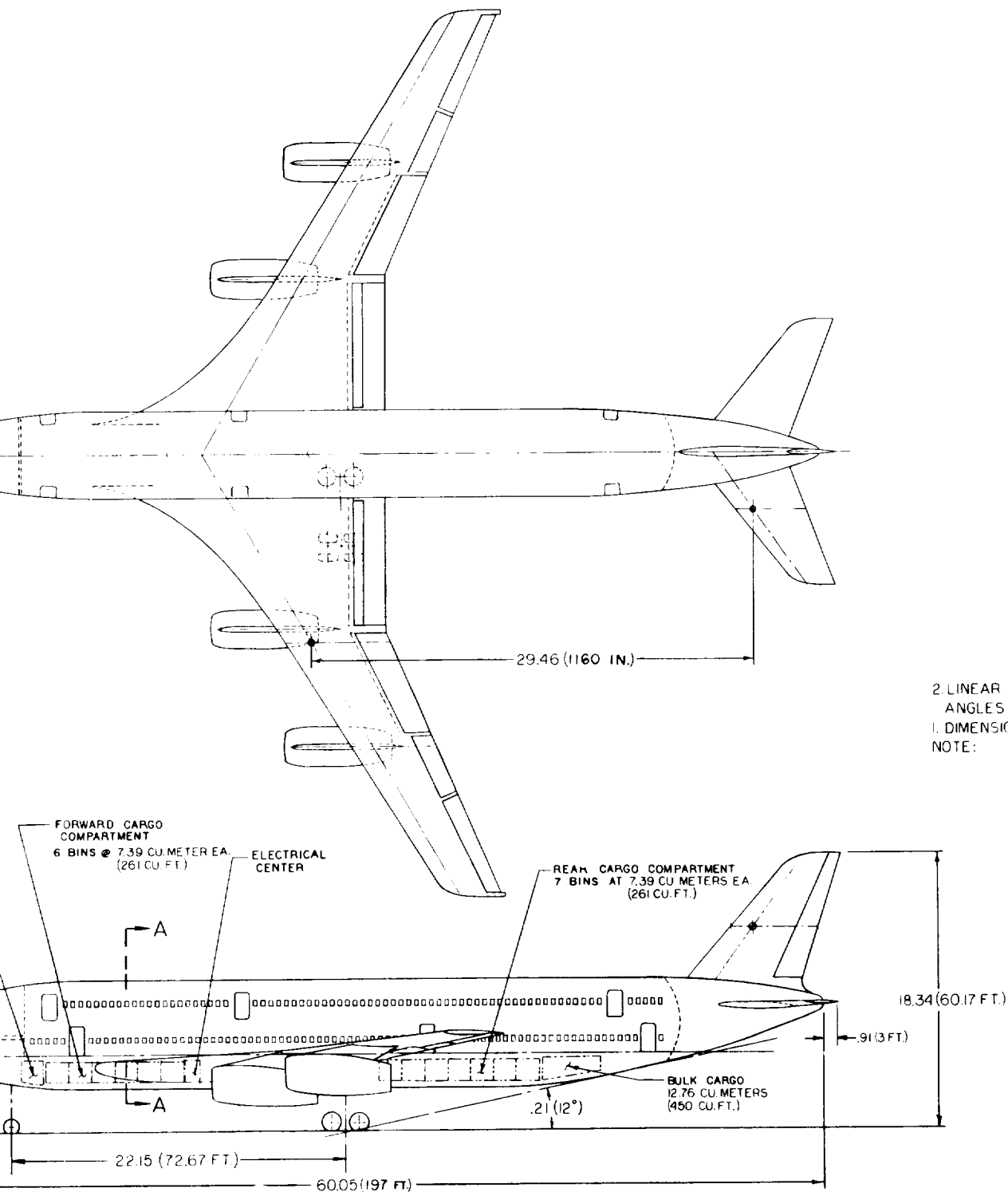


Figure 67. General Arrangement - Jet A Fuel, M 0.85 Transport

TABLE 17. DESIGN CHARACTERISTICS: REFERENCE (JET A) PASSENGER AIRCRAFT
 MAX 3.75; 400 PAX; Payload = 39,900 kg (88,000 lb)

	SI	CUSTOMARY	SI	CUSTOMARY	SI	CUSTOMARY
RANGE	km	n mi	5560	3000	10,190	5500
Gross Weight	kg	lb	153,200	404,300	237,000	523,100
Fuel Weight	kg	lb	47,800	105,700	86,400	190,700
Operating Empty Weight	kg	lb	95,500	210,600	110,700	244,400
Wing Area	m ²	ft ²	300	3,230	390	4,190
Span	m	ft	52.1	171	59.1	194
Fuselage Length	m	ft	60	197	60	197
L/D (Cruise)	-	-	16.7	16.7	17.9	17.9
SFC (Cruise)	$\frac{\text{kg}}{\text{hr}}/\text{daN}$	$\frac{\text{lb}}{\text{hr}}/\text{lb}$	0.592	0.582	0.592	0.582
Thrust per Engine	N	lb	114,500	25,770	145,500	32,690
FAR T.O. Field Length	m	ft	2,437	7,980	2,440	7,990
FAR Landing Field Length	m	ft	1,760	5,760	1,590	5,210
Energy Utilization	$\frac{\text{kJ}}{\text{seat km}}$	$\frac{\text{Btu}}{\text{seat n mi}}$	718	1,260	788	1,384
Airplane Price	$\$10^6$	$\$10^6$	22.6	22.6	26.5	26.5
DOC*	$\frac{\$}{\text{seat km}}$	$\frac{\$}{\text{seat n mi}}$	0.496	0.92	0.545	1.01

*Based on Jet A Fuel Cost = \$2/1.054 GJ(\$2/10⁶ Btu = 3.68¢/lb = 24.8¢/gal)

TABLE 28. COST SUMMARY: JET A PASSENGER AIRCRAFT

		COSTS IN \$10 ⁶	
	RANGE	5560 km	10,190 km
<u>Development</u>			
Airframe		\$ 565.99	\$ 692.51
Engine		350.85	416.57
Avionics		-	-
Total		\$ 916.84	\$1,109.08
<u>Production</u>			
Airframe Manufacturing Cost		\$ 11.11	\$ 12.87
Other Airframe Cost			
Sustaining Engineering		.76	.88
Tool Maintenance		1.00	1.16
Quality Assurance		1.04	1.21
Miscellaneous		.28	.32
Profit		2.24	2.59
Warranty		.71	.82
Engine		2.66	3.29
Avionics		.50	.50
Subtotal		\$ 20.30	\$ 23.64
R&D per Aircraft*		2.32	2.81
Total Aircraft Price		\$ 22.62	\$ 26.45

*Based on 350 aircraft and 2000 engines

TABLE 29. DIRECT OPERATING COSTS: JET A PASSENGER AIRCRAFT

RANGE	5,560 km		10,190 km	
UNITS	\$/km	\$/n mi	\$/km	\$/n mi
Crew	0.238	0.440	0.238	0.440
Maintenance				
Airframe Labor (Including Burden)	0.149	0.276	0.148	0.274
Engine Labor (Including Burden)	0.097	0.180	0.103	0.190
Airframe Material	0.068	0.126	0.068	0.127
Engine Material	0.095	0.176	0.108	0.199
Fuel* and Oil	0.556	1.031	0.610	1.131
Insurance	0.163	0.303	0.186	0.344
Depreciation	<u>0.623</u>	<u>1.155</u>	<u>0.709</u>	<u>1.314</u>
Total DOC	1.989	3.687	2.170	4.019
Total Unit DOC	$\frac{\phi}{\text{seat km}}$	$\frac{\phi}{\text{seat n mi}}$	$\frac{\phi}{\text{seat km}}$	$\frac{\phi}{\text{seat n mi}}$
	0.497	0.922	0.543	1.005

*Based on Jet A fuel cost = \$2/1.054 GJ (\$2/10⁶ Btu = 24.8¢/gal.)

with that of the LH₂ fueled airplane. Thus, in Table 30 the gross weight of the 5560 km range reference airplane is 21 percent greater than that of the LH₂ airplane designed to perform an identical mission using the same technology base. Copies of pertinent sheets of the ASSET computer printouts for each of these final design aircraft are presented in Appendix D.

Generally, comparing the values listed in the columns of both tables, it is seen that the LH₂ aircraft offer significant advantage in almost every category of comparison at both ranges. The penalties occasioned by the density and cryogenic temperature of liquid hydrogen, reflected in the values shown for Lift/Drag, are

TABLE 30. COMPARISON OF FLIGHT DATA: LH₂ VS JET A PASSENGER AIRCRAFT (SHORT RANGE)
 [M = 1.85; 400 PAY; 5500 km (3000 n.m.)]

	SI	US/NA	LH ₂		JET A		FACTOR (JET A/LH ₂)
			SI	CUSTOMARY	SI	CUSTOMARY	
Takeoff Gross Weight	kg	lb	152,000	335,200	183,200	404,300	1.21
Operating Empty Weight	kg	lb	96,500	212,900	95,500	210,600	0.99
Block Fuel Weight	kg	lb	12,700	28,000	37,400	82,400	2.95
Total Fuel Weight	kg	lb	15,600	34,300	47,800	105,700	3.08
Wing Area	m ²	ft ²	283	3,047	301	3,235	1.06
Wing Loading, Takeoff	kg/m ²	lb/ft ²	537	110	610	125	1.14
Landing	kg/m ²	lb/ft ²	488	100	488	100	1.0
Span	m	ft	50.5	165.6	52	170.6	1.03
Fuselage Length	m	ft	64	210	60	197	0.94
Lift/Drag (Cruise)			14.86	14.86	16.66	16.66	1.12
Specific Fuel Consumption (Cruise)	kg/hr	(lb/hr)/lb	0.203	0.200	0.592	0.582	2.91
Thrust per Engine (SLS)	N	lb	110,000	24,720	114,500	25,770	1.04
Thrust/Weight (SLS)	N/kg	-	2.90	0.295	2.51	0.255	0.87
FAR T.O. Distance	m	ft	1,790	5,860	2,437	7,980	1.36
FAR Landing Distance	m	ft	1,770	5,804	1,760	5,760	0.99
Approach Speed (EAS)	m/s	knots	69.5	135	69	134	0.99
Weight Fractions	percent	percent					
Fuel			10.2	10.2	26.2	26.2	2.57
Payload			26.3	26.3	21.8	21.8	0.83
Structure			31.7	31.4	27.8	27.8	0.89
Propulsion			10.7	10.7	6.7	6.4	0.60
Equipment and Operating Items			21.7	21.4	17.8	17.8	0.83
Energy Utilization	kJ seat km	Btu seat n.m.	1,510	1,204	1,580	1,260	1.05

TABLE 31. COMPARISON OF FINAL DESIGNS: LH₂ VS JET A PASSENGER AIRCRAFT (LONG RANGE)
 [M = 0.85; 400 PAY; 10,190 km (5500 n mi)]

	U1	CUSTOMARY	LH ₂		JET A		FACTOR (JET A/LH ₂)
			SI	CUSTOMARY	SI	CUSTOMARY	
Takeoff Gross Weight	kg	lb	177,500	391,700	237,200	523,200	1.34
Operating Empty Weight	kg	lb	110,000	242,100	110,800	244,400	1.01
Block Fuel Weight	kg	lb	24,000	52,900	75,000	165,500	3.13
Total Fuel Weight	kg	lb	27,900	61,600	86,500	190,800	3.10
Wing Area	m ²	ft ²	313	3,363	389	4,186	1.24
Wing Loading, Takeoff	kg/m ²	lb/ft ²	569	116.5	610	125	1.07
Landing	kg/m ²	lb/ft ²	493	101	513	106	1.05
Span	m	ft	53	174	59.2	194.1	1.12
Fuselage Length	m	ft	66.7	219	60	197	0.90
Lift/Drag (Cruise)			16.07	16.07	17.91	17.91	1.12
Specific Fuel Consumption (Cruise)	kg/hr	(lb/hr)/($\frac{lb}{hr}$)	0.203	0.199	0.590	0.581	2.92
Thrust per Engine (SLS)	N	lb	127,700	26,700	145,400	32,700	1.14
Thrust/Weight (SLS)	N/kg	-	2.88	0.293	2.45	0.25	0.85
FAR T.O. Distance	m	ft	1,900	6,240	2,435	7,990	1.28
FAR Landing Distance	m	ft	1,770	5,810	1,590	5,210	0.90
Approach Speed (EAS)	m/s	knots	69.5	135	63.7	124	0.92
Weight Fractions	percent	percent					
Fuel			15.7	15.7	36.5	36.5	2.23
Payload			22.5	22.5	16.9	16.8	0.75
Structure			30.7	30.7	26.0	26.0	0.85
Propulsion			12.3	12.3	6.4	6.4	0.52
Equipment and Operating Items			18.8	18.8	14.3	14.3	0.76
Energy Utilization	kJ/seat km	Btu/seat n.m.	1,550	1,239	1,735	1,384	1.12

more than overcome by the tremendous advantage of the heating value of the fuel, cf., values listed for specific fuel consumption. Basically the LH_2 aircraft are lighter, require smaller wings but larger fuselages, use smaller engines, can takeoff in shorter distances, and use less energy per seat mile in performing their missions. It is also noted that at the shorter range, a comparatively smaller advantage is realized. This latter is a trend which could be anticipated. Since the basis for the superiority of the LH_2 -fueled aircraft lies in the high heating value of the fuel, a design mission which requires a large amount of fuel will automatically offer the maximum payoff for using LH_2 .

The heating values of the fuels used in this study are 42,800 kJ/kg (18,400 Btu/lb) for Jet A, and 120,000 kJ/kg (51,590 Btu/lb) for hydrogen. This is a ratio of 2.8 in favor of hydrogen which accounts for the principle portion of the difference in specific fuel consumptions (SFC) listed in the tables. The ratio of cruise SFC's, Jet A-to- LH_2 , listed in Table 31 is 2.92. The extra advantage given the hydrogen system over the factor of 2.8 expected from comparison of the heating values, is due to the requirement to cool the high pressure turbine stages of the Jet A engine with air bled from its compressor.

It should be noted that a corollary advantage which could have been claimed for the LH_2 engine, viz., accounting for the heat added to the fuel as a result of using it to cool the air for the passenger cabin and flight station, was not included in the assessment of its performance. It is estimated this probably accounts for two to three percent conservatism in the performance potential of LH_2 fueled engines for this type of aircraft application.

The ratio of block fuel consumed by aircraft using each type of fuel is in the ratio of 3.13, using the data in Table 31 for the long range aircraft for purposes of an example. It might normally be expected that the fuel used to perform a mission would be in approximately the same ratio as the SFC's realized in cruise. Actually, there is a leverage factor which works to the advantage of the aircraft with the more efficient engine or fuel system. Because that aircraft uses less fuel, it has a lower gross weight to accelerate and to lift to cruise conditions. This reduced work requirement, compensated somewhat by the lower L/D of the hydrogen fueled aircraft, produces an iterative fuel saving which compounds to produce the final block fuel weight relationship listed.

The lower gross weight for the LH_2 aircraft provides additional advantages in costing which are not necessarily immediately obvious. Aircraft with lower gross weights generally tend toward

- Lower operating costs — because items such as wheels, tires, and brakes, all significant maintenance cost items, are sized on that basis.
- Smaller engines — which serve to minimize procurement costs and also lower maintenance costs.

In addition, of course, lighter aircraft are easier to handle on the ground and tend to minimize size and cost of equipment required, although this is not a factor of great significance unless the ground handling equipment is purchased specifically for the subject aircraft.

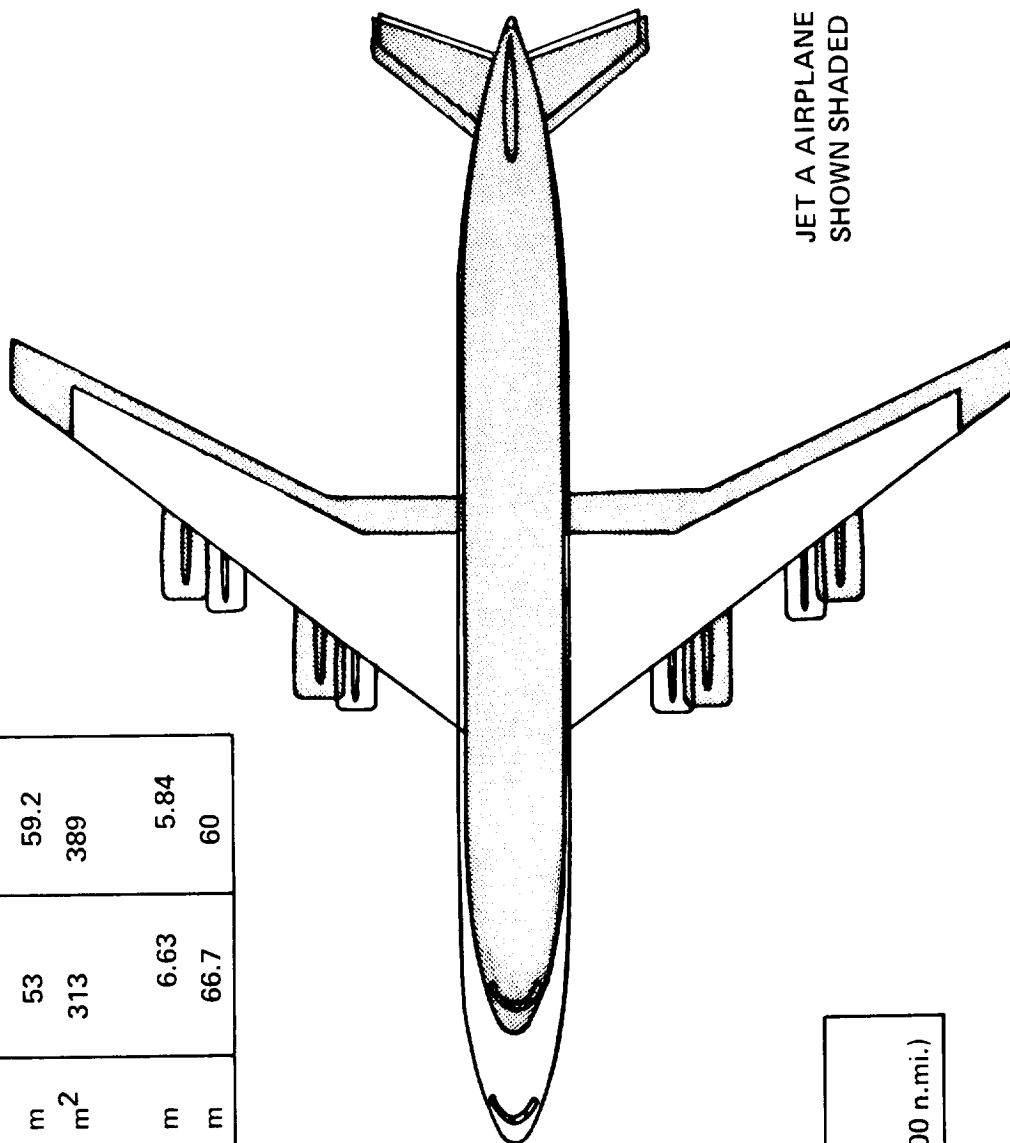
The very low density of LH_2 , plus the requirement for a thick insulation system around the tanks to contain the fuel at cryogenic temperature, poses design problems which ultimately are reflected in weight and drag penalties for the aircraft. Thus, even though LH_2 airplanes require only about one-third the weight of fuel, the operating empty weights of the LH_2 and Jet A designs are virtually the same. The hydrogen design is nearly two percent greater in the case of the shorter range mission, and not quite one percent less for the longer range mission. The lift/drag ratios in cruise reflect a penalty for the LH_2 aircraft amounting to approximately 10 percent for both missions.

In spite of these penalties occasioned by the density and temperature of liquid hydrogen, as previously observed the tremendous advantage of the large heating value of the fuel more than compensates. Figure 68 illustrates the major physical size differences using the long range aircraft for comparison. The span of the LH_2 airplane is 6.2 m (20.1 ft.) less, the wing area is almost 20 percent smaller; however, the fuselage is 6.7 m (22 ft.) longer and 0.79 m (2.6 ft.) larger in diameter in order to provide room for the fuel tanks in the fuselage.

A factor of particular interest is the comparison of energy utilization. This is the amount of energy expended in performing the mission, expressed in terms of available seats x distance traveled. The LH_2 aircraft uses 12 percent less energy in transporting 400 passengers a distance of 10,200 km (5500 n.mi.) at M 0.85 than does a comparable design aircraft which uses Jet A fuel. For the 5570 km (3000 n.mi.) range mission the LH_2 aircraft uses 5 percent less energy than the Jet A fueled design.

Table 32 is a summary of costs calculated for the subject aircraft. The basis for these cost estimates is presented in Section 4.4 for the Internal Tank LH_2 aircraft, and in Section 4.7 for the Jet A aircraft. One notable difference is in the

		LH2	JET A
WING			
SPAN	m	53	59.2
AREA	m ²	313	389
FUSELAGE			
DIA	m	6.63	5.84
LENGTH	m	66.7	60



M = 0.85
 400 PAX
 10,190 km (5500 n.mi.)

Figure 68. Size Comparison: LH₂ Vs. Jet A Passenger Aircraft

TABLE 32. COST COMPARISON:
 LH_2 VS JET A PASSENGER AIRCRAFT
 (Refer to Tables 30 and 31 for Vehicle Data)

		COSTS IN \$10 ⁶				
		RANGE	5,570 km		10,200 km	
		FUEL	LH ₂	JET A	LH ₂	JET A
<u>Development</u>						
Airframe			594.2	566.0	669.5	692.5
Engine			408.0	350.9	455.0	416.6
TOTAL			1002.2	916.9	1124.0	1109.1
<u>Production</u>						
Airframe			17.33	17.14	20.10	19.86
Engine			3.07	2.66	3.50	3.29
Avionics			0.50	0.50	0.50	0.50
R&D Amortization*			2.51	2.32	2.82	2.81
TOTAL			23.41	22.62	26.92	26.46
<u>Direct Operating Cost</u> - $\frac{\phi}{\text{Seat km}}$			0.532	0.480	0.541	0.502
$(\frac{\phi}{\text{Seat n mi}})$			(0.986)	(0.890)	(1.004)	(0.931)
① <u>Fuel Cost:</u>						
Jet A = \$2/1.054 GJ (\$2/10 ⁶ Btu = 24.8¢/gal = 3.68¢/lb)						
LH ₂ = \$3/1.054 GJ (\$3/10 ⁶ Btu = 15.48¢/lb)						

*Based on 350 aircraft and 2000 engines

Direct Operating Cost. In the preceding sections, a nominal utilization of 3285 hours per year was used. For the final design versions shown herein, utilizations of 3285 hours per year was used. For the final design versions shown herein, utilization of 3600 hrs/yr and 4000 hrs/yr, were used in calculating DOC's for the 5560 km and the 10,190 km range aircraft, respectively. In the comparison shown in Table 32 the LH_2 aircraft are seen to cost more, both to develop and to produce, than their Jet A counterparts. The production cost of the shorter range LH_2 aircraft is 4 percent greater than its reference airplane and the longer range LH_2 vehicle costs 1.6 percent more than the corresponding Jet A fueled aircraft.

In considering the development costs, it should be noted that the cost of basic hydrogen technology development was assumed to be funded separate and apart from the traditional aircraft development costs represented in the table. As discussed later in this report, Section 6.0, a six year program is suggested during which such technology development would occur before a decision need be made to proceed with development of a commercial transport airplane. The cost of this basic technology development is not included in the costs shown in Table 32.

Direct operating cost (DOC) is very sensitive to fuel cost. As noted in Table 32, the fuel prices which were specified for use in this study to establish baseline DOC's were \$2 per 1.054 GJ ($\$2/10^6$ Btu) for Jet A, equivalent to 24.8¢/gal. or 3.68¢/lb., and \$3 per 1.054 GJ (\$3 per million Btu's) for LH_2 , which is equal to 15.48¢/lb. The sensitivity of DOC to fuel cost is shown in Figure 69 for the shorter range aircraft and in Figure 70 for the longer range vehicles. The price of Jet A fuel expressed in the more familiar terminology of cents per gallon is shown for reference across the top of the grid in both figures.

To provide perspective for these comparisons, Figure 70 shows recent prices paid by U.S. airlines for Jet A fuel, and some recent estimates of prices forecast for LH_2 . In September, 1974, according to Reference 12, domestic trunk airlines in the United States reported paying 24¢/gal. for Jet A fuel. In the same month the U.S. International carriers reported paying an average of 38¢/gal. Recent estimates of the potential cost of manufacturing gaseous hydrogen from coal (or lignite) plus water, pipelining it to a vicinity near an airport, and there liquefying and storing it ready for use in aircraft are also indicated on the figure. The \$2.50 per 1.054 kJ (10^6 Btu) estimate of Reference 13 was based on use of \$4.41/Mg (\$4/ton) coal, a 2760 Mg/day (2500 ton/day) processing plant, and pipelining the gaseous hydrogen 1853 km (1000 n. mi) to the airport. The \$3.05/1.054 kJ (10^6 Btu) estimate

of Reference 14* was based on use of \$2.76/Mg (\$2.50/ton) lignite, a 1101 Mg/day (1000 ton/day) processing plant, and pipelining 556 km (300 n. mi) to the airport.

The dotted line on Figures 69 and 70, drawn horizontally to represent constant DOC on both figures, shows that from the estimated production cost of \$2.50 per 1.054 GJ (10^6 Btu) for LH_2 , airlines could afford to pay 21.5¢ more per 1.054 GJ for LH_3 for the shorter range mission and a 44¢ differential for LH_3 for flying the longer range mission. Expressed from another point of view, if LH_2 is available at this price, for routes of 5560 km (3000 n. mi), when Jet A fuel exceeds a price of about 20¢/gal. the airlines could demonstrate lower DOC's if they were able to operate aircraft fueled with LH_3 . The corresponding breakeven point for the price of Jet A on the 10,190 km route is about 26¢/gal.

For all of the cost calculations presented in this section the basis in utilization has been 3600 hours per year for the 5560 km range aircraft and 4000 hr./yr. for the 10,190 km range vehicles. Figure 71 illustrates the effect variation in utilization would have on DOC for aircraft using both fuels and for both ranges. The DOC's were calculated using the nominal fuel prices specified in the guidelines for the study. The squares indicate baseline conditions. There is no significant difference in the sensitivity of aircraft using either fuel to utilization rate.

Figure 72 shows the sensitivity of DOC of the subject aircraft to maintenance costs. Again, the DOC calculations were based on the nominal prices specified for the fuels. Varying the cost of maintenance by plus and minus 10 percent has no effect on the relative rating of the aircraft on a DOC basis. DOC is relatively insensitive to changes in maintenance costs.

4.4. Noise

Federal noise standards for commercial transport aircraft were introduced in 1969 by the Federal Aviation Administration through FAR Part 36 (Reference 15), and all new airplane programs since then have included in their design requirements the meeting or bettering of the noise limits of the Regulation. These noise limits, which vary with the takeoff gross weight of the airplane, are specified in effective perceived noise level (EPNL) in units of EPNdB. This subjective noise measure weighs

*Reference 14 presents cost data adding to \$2.30/1.054 GJ (10^6 Btu) through liquefaction. An additional cost of 25¢/1.054 GJ was added (based on data from Reference 13) for storage.

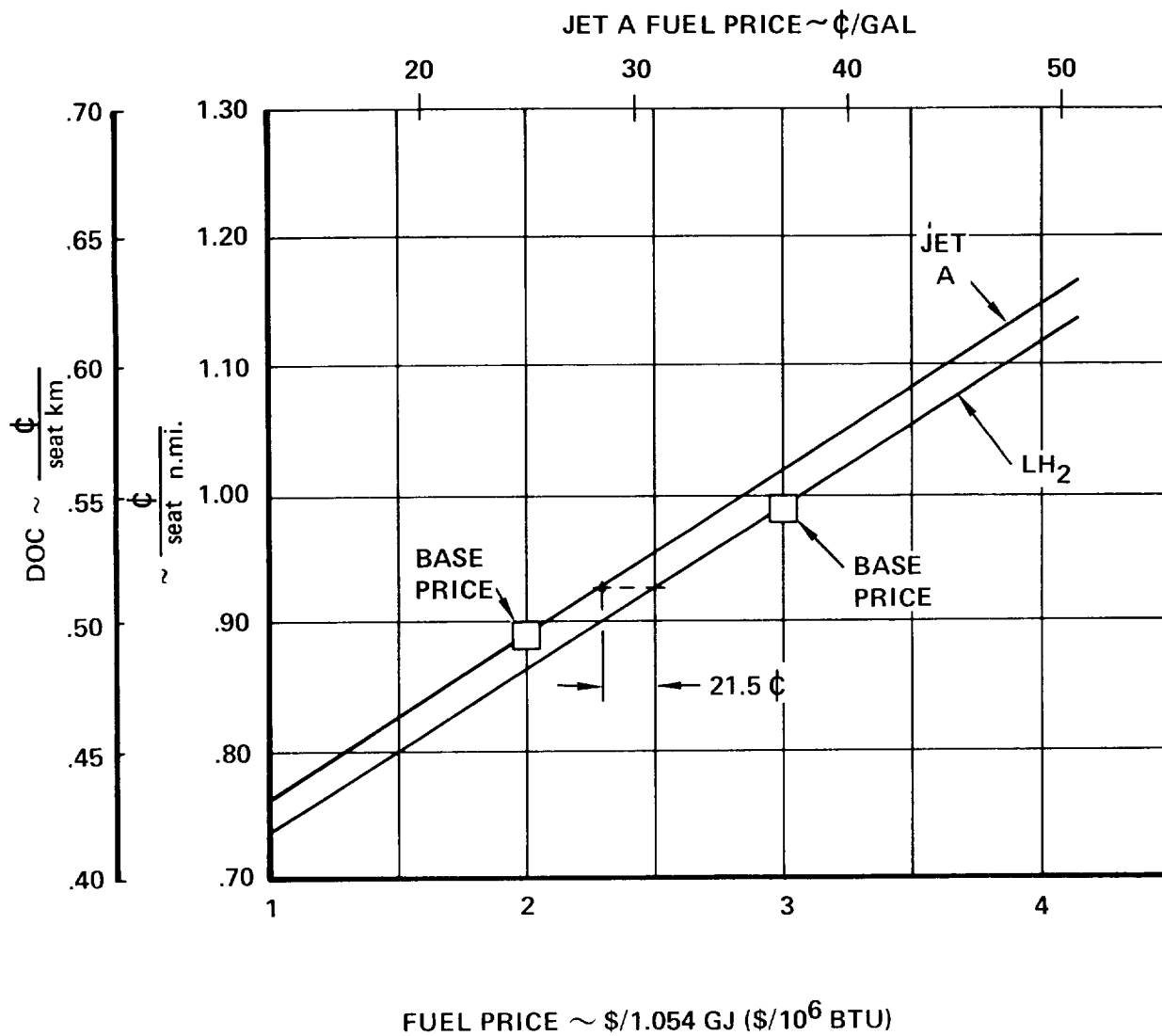


Figure 69. Sensitivity of DOC to Fuel Price (Short Range Passenger Aircraft)

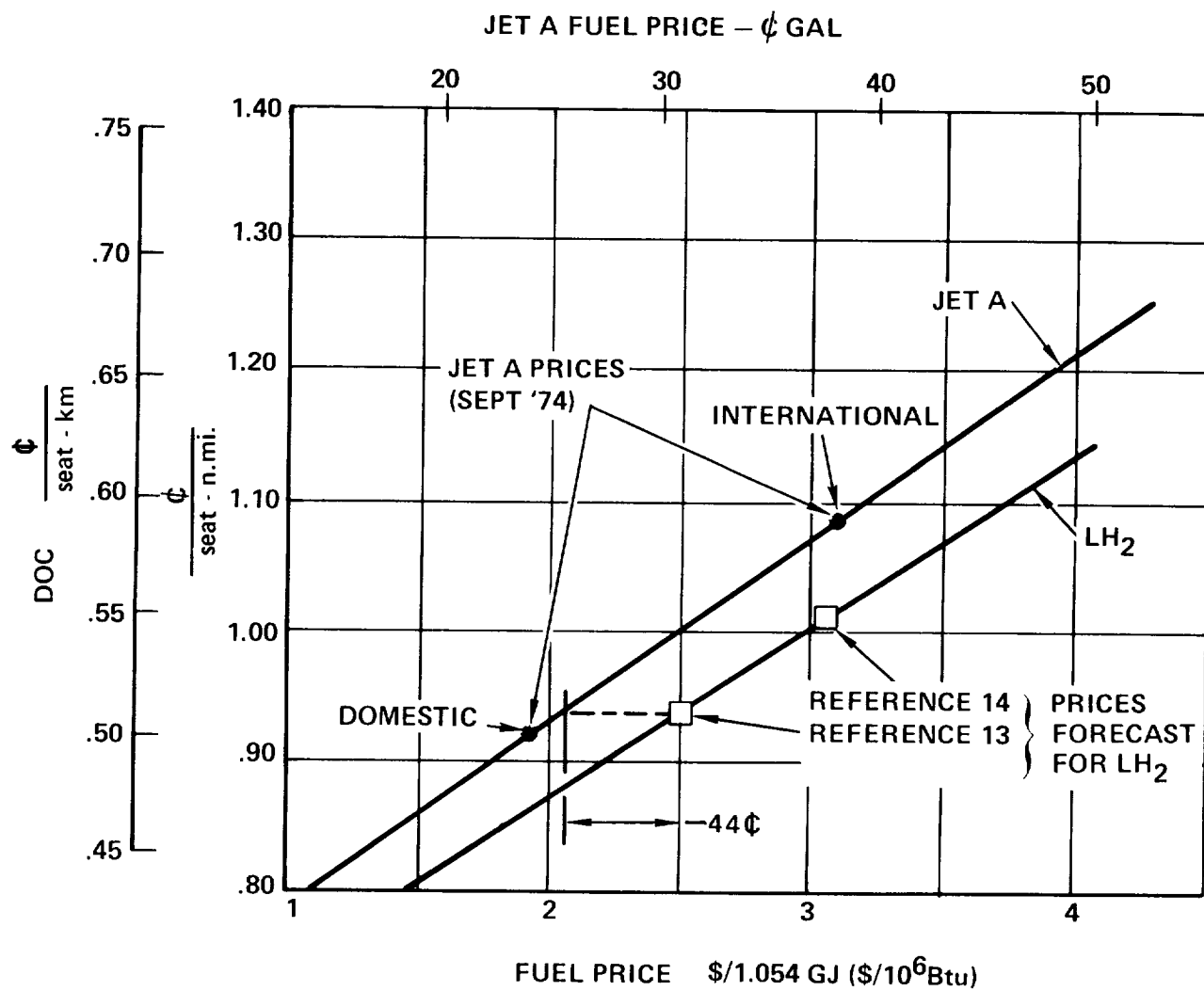


Figure 70. Sensitivity of DOC to Fuel Price (Long Range Passenger Aircraft)

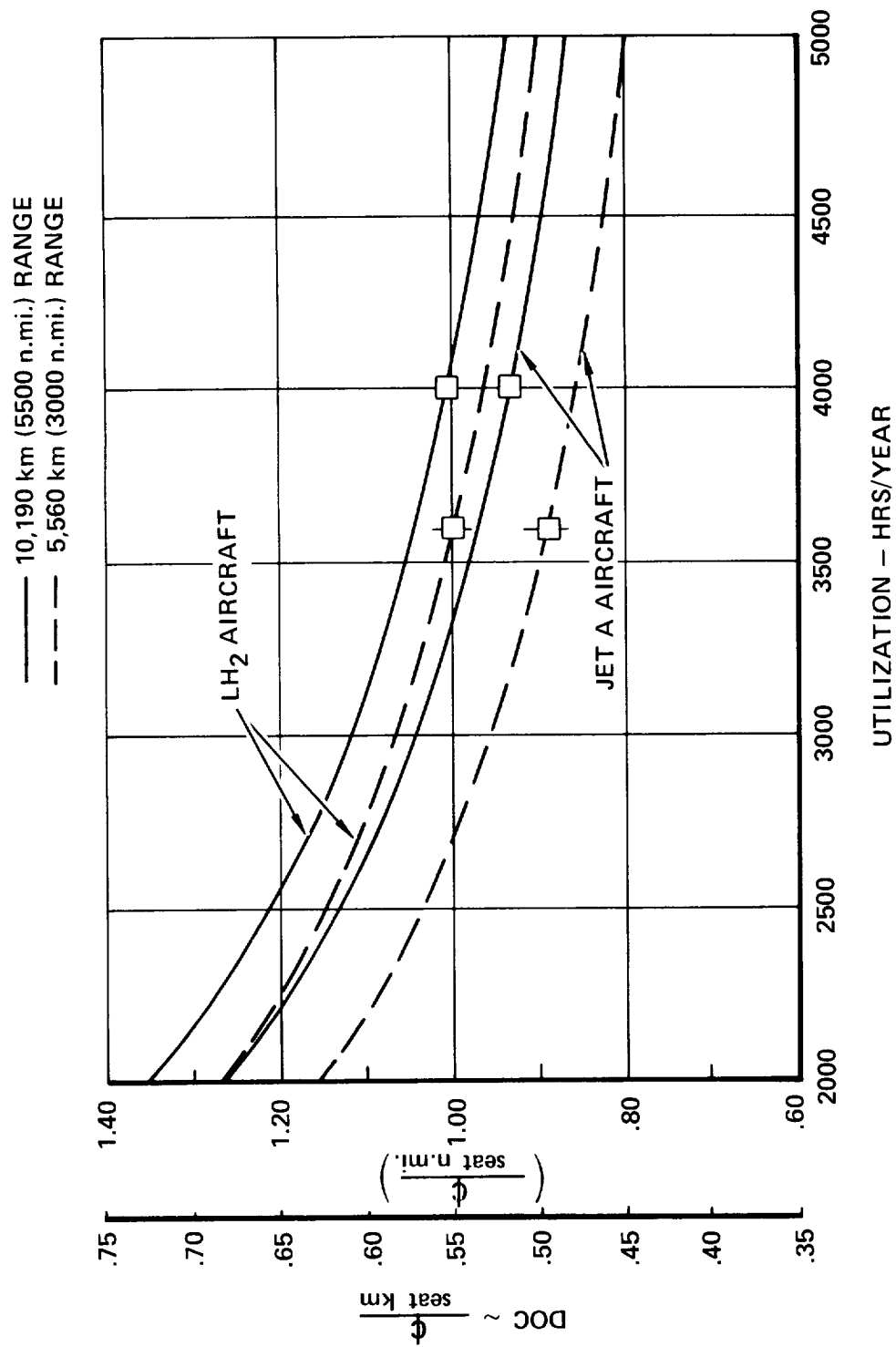


Figure 71. Effect of Utilization on DOC

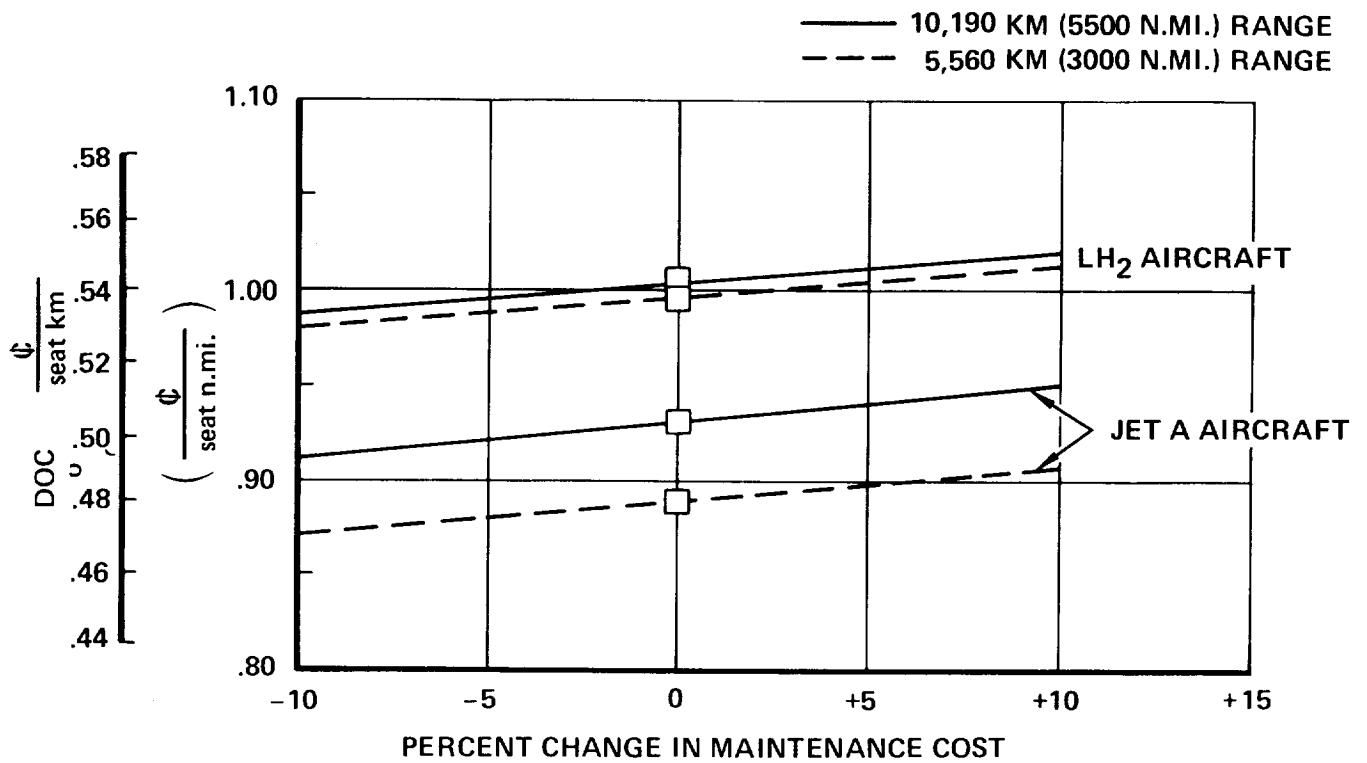


Figure 72. DOC Sensitivity to Maintenance Cost

the one-third octave-band frequency spectra of flyover noise according to an empirical human noisiness response and includes a pure tone penalty and duration correction. Noise limits must be met at takeoff, sideline, and approach points.

For more complete evaluation of the noise impact of aircraft operation on the community than is provided by the three-point system of FAR Part 36, maximum noise contours, often referred to as "footprints," are utilized. The evaluation may be in terms of areas enclosed by contours at specified noise levels, or contour plots drawn to proper scale may be superimposed on the map of any particular airport community to indicate noise exposure patterns.

The noise analysis of the passenger transport aircraft considered four vehicles; the selected LH₂-fueled designs and reference Jet A-fueled aircraft of equivalent mission capability, one each for 5560 and 10,190 km (3000 and 5500 n mi) range carrying a payload of 39,900 kg (88,000 lb). Two noise goals — to meet limits of FAR Part 36 minus 20 EPNdB, and to achieve an enclosed area of 5.180 km² (2 square miles) for the approach-plus-takeoff 90 EPNdB contour — guided the study.

The acoustical design of the power plants for the LH₂ study aircraft included a variable geometry inlet, which would control forward radiated noise effectively. Also, provision was made for sufficient multidegree of freedom acoustical lining in the primary nozzle to reduce core engine and turbine noise so that they would not be major contributors to total flyover noise. Jet noise, calculated by the SAE method of Reference 16, was found to be negligible. Aft radiated fan noise then remained as the controlling acoustical factor, and a full length treated fan discharge duct with one treated ring splitter was incorporated in the nacelle design to obtain at least 20 dB suppression, to match what could reasonably be expected for the inlet and the core engine.

The calculation of engine noise generation and liner performance were based on the largely empirical noise prediction methods of Reference 17. Airframe noise, produced by the motion of the airplane through the air, was determined by a Lockheed-California Company developed procedure (Reference 18) and was found to contribute significantly to approach noise. The basic airplane noise characteristics along with airplane performance information were inputs to the Lockheed-California Company "Noise Definition" procedure (Reference 19), which was used to establish FAR Part 36 noise levels and the 90 EPNdB maximum noise contours for the four airplanes. The results are given in Table 33. The 90 EPNdB contours are shown on Figure 73.

TABLE 33. NOISE COMPARISON - PASSENGER AIRCRAFT

FUEL	RANGE km (n.mi.)	TOGW kg (lb)	FAR PART 36 EPNL (EPNdB)						AREA WITHIN 90 EPNdB CONTOUR km ² (mi. ²)		
			TAKEOFF		SIDELINE		APPROACH		TAKEOFF	APPROACH	TOTAL
			LIMIT	AIRPLANE	LIMIT	AIRPLANE	LIMIT	AIRPLANE			
Jet A	5,560 (3,000)	183,420 (404,370)	105.1	92.68	106.9	86.40	106.9	96.63	8.8 (3.4)	1.8 (0.7)	10.6 (4.1)
LH ₂	5,560 (3,000)	153,525 (338,463)	103.8	88.11	106.3	86.38	106.3	97.86	6.7 (2.6)	3.1 (1.2)	9.8 (3.8)
Jet A	10,190 (5,500)	237,320 (523,193)	107.0	94.23	107.6	87.80	107.6	96.70	10.4 (4.0)	1.8 (0.7)	12.2 (4.7)
LH ₂	10,190 (5,500)	177,590 (391,740)	104.9	89.20	106.8	87.16	106.8	98.44	7.3 (2.8)	3.8 (1.5)	11.1 (4.3)
Jet A	6,280 (3,390)	195,050 (430,000)	105.6	96.02	107.0	94.95	107.0	102.79	9.45 (3.65)	7.72 (2.98)	17.17 (6.63)

For reference, the average of noise levels measured during FAR certification tests of the L-1011, recognized to be the quietest U.S.-built airliner in operation, and the areas of its 90 EPNdB contour are as follows:

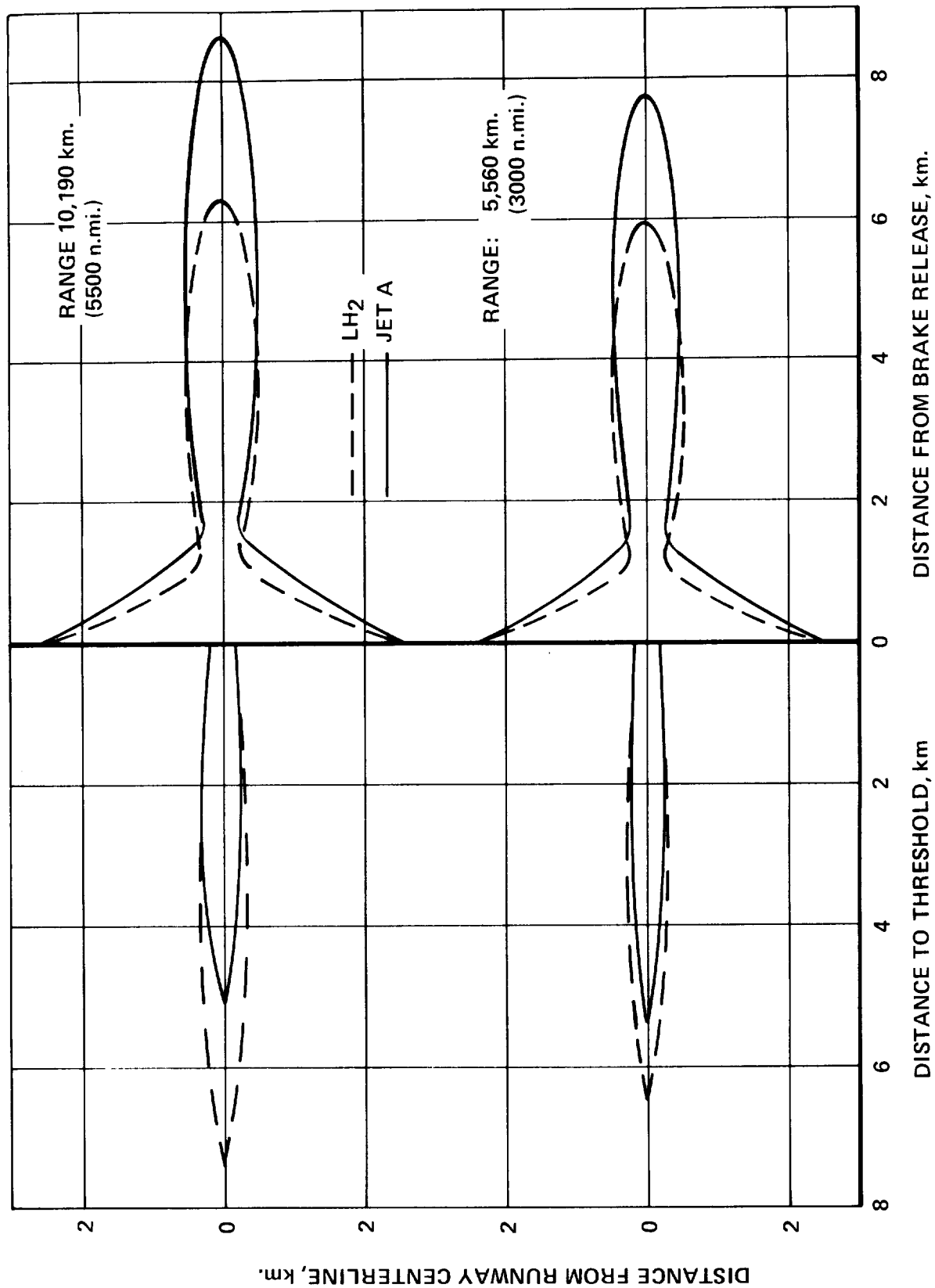


Figure 73. 90 EPNdB Contour Comparison - Passenger Aircraft

Examining the FAR Part 36 noise values for the study airplanes, it is seen that the LH₂ aircraft are 5 EPNdB quieter on takeoff than Jet A aircraft. This is due primarily to the lighter takeoff weight of the LH₂ aircraft. The sideline differences are negligible and are due to the design requirement that all engines be 20 dB quieter than FAR 36 limits. On approach however, the LH₂ aircraft are noisier. This stems from the fact the LH₂ aircraft have smaller engines, they have lower L/D, and are about the same weight as the Jet A fueled aircraft after flying a full range mission. Consequently, the LH₂ aircraft must operate their smaller engines at a more advanced throttle setting to maintain a 3 degree glide slope in approach, and are therefore noisier.

It is also seen that the goal of 20 dB lower than current limits is achieved only at the sideline. Levels about 15 dB below current limits are achieved for takeoff, but only about 10 dB for approach. Takeoff levels possibly could be reduced further by additional nacelle treatment and by improved airplane performance. Further reduction of approach noise, however, is limited by the airframe noise floor, which is approximately equal to the treated engine noise of this study. Consequently, even if the engines were not operating at all during landing approach, the noise would only be about 3 dB less than shown.

With regard to the 90 EPNdB contours, the same comments apply as were made in the preceding paragraph for the FAR Part 36 values. The total areas achieved are apparently about twice as great as the goal of 5.180 square kilometers (2 square st. mi). However, there is an artificiality in the results because of the duration correction of the EPNL procedure. Since at start of takeoff roll, the airplane's forward velocity is zero, the duration correction approaches infinity. A small velocity of 16 knots was assumed for the passenger aircraft to avoid this problem, but still gave an unrealistically wide footprint. If the EPNL were considered only after the airplane had achieved approximately lift-off speed, the 90 EPNdB areas would be decreased by about 2.5 km² (1 sq. mi). Any improvement in takeoff noise aimed at meeting FAR 36 minus 20 dB would decrease takeoff contour area further; the enclosed area is very sensitive to basic noise changes. However, the original goal may not be realistic since the approach contour area, which is normally the smaller of the two, is about one-half of the goal area. As discussed above, the approach noise, because of the airframe noise floor, is not amenable to additional substantial reductions.

4.8.3 Emissions

Table 34 compares the estimated exhaust emissions of the hydrocarbon and hydrogen fueled engines derived for this study with the goals specified by NASA as target values (Reference 4). The estimated levels are based on data obtained from References 20, 21, 22, and 23. As can be seen the estimates of carbon monoxide (CO) and unburned hydrocarbons for the hydrocarbon fueled engines at idle power are double the NASA goals. However, these engines will not produce visible smoke during takeoff. The hydrogen fueled engines produce no CO, unburned HC or smoke because there are no carbon atoms in the fuel.

The goals for engine emissions are specified in terms of 1000 weight units of fuel burned. It is not meaningful to compare emissions from hydrocarbon fueled engines with hydrogen fueled engines on this basis because of the large difference in heating values of the fuels. Accordingly, NO_x emissions were adjusted to a basis of heat release equal to one weight unit of hydrocarbon fuel by dividing the LH_2 value by 2.81. These adjusted estimates show that hydrocarbon and hydrogen fueled engines would have about the same rate of oxides of nitrogen (NO_x) formation and that the NO_x emissions from both fuels will meet the specified goals. However, theoretical chemical kinetics predicts that much lower NO_x emissions are possible with hydrogen by lowering primary combustion zone fuel/air ratios and dwell time. That is, considerably more potential exists for minimizing nitrogen oxide emissions with hydrogen than with kerosene because of the ease with which hydrogen can be introduced into the combustor as a gaseous fuel, its high diffusivity, its wide flammability range, and its higher burning velocity. However additional combustor research will be required to determine practicable achievable lower limits. Reference 24 indicates that NO_x emissions at cruise altitude will be approximately seventeen percent of the emissions per 1000 weight units of fuel at takeoff.

The principle exhaust product resulting from combustion of hydrogen with air is water vapor. Some concern has been expressed that large numbers of LH_2 fueled aircraft might wreak havoc with atmospheric conditions because of the water vapor deposited at cruise altitude. Calculations show that such fears are groundless. The 10,190 km range 400 passenger LH_2 fueled airplane whose characteristics are shown in Table 31 produces 20.2 kg of water/km (82.4 lb/n mi) during cruise. The corresponding Jet A fueled aircraft makes 10.3 kg of water/km (41.9 lb/n mi). Although the LH_2 fueled airplane produces nearly twice as much water vapor, the total is still so small compared with the amount that is already in the atmosphere

TABLE 34. ENGINE EMISSION ESTIMATES (1)

EMISSION TYPE	ENGINE CONDITION	GOALS	ESTIMATED EMISSION LEVEL	
			HYDROCARBON	HYDROGEN
CO	Idle	14	30	0
Unburned HC	Idle	2	4	0
Smoke (2)	Takeoff	25	15	0
NO _x	Takeoff	13	12	≤12 (3)
<p>(1) Emissions expressed as weight unit of emissions per 1000 weight units of fuel, g/kg, (except see note 3).</p> <p>(2) SAE 1179 smoke number.</p> <p>(3) Because of the much greater heating value of hydrogen this estimate has been converted, by dividing by 2.81, the ratio of fuel heating values, to equivalent energy weight units of hydrocarbon fuel.</p>				

the comparison is meaningless. For example, the water vapor emitted by the subject LH₂ airplane during cruise would be a layer approximately 1.2 μm (0.00008 in.) thick across the width of the engine exhaust nozzles.

4.8.4 Safety

This section compares safety aspects of using LH₂ and Jet A fuels in aircraft and suggests areas where experimental data and technological advances are needed to develop an LH₂ fueled aircraft. Some of the safety aspects are:

1. The ullage space in the tank of a Jet A fueled aircraft is flammable or detonable over a broad range of pressures and temperatures; that is, from about 100°F to 160°F at sea level and from about 40°F to 90°F at 50,000 foot altitude because a mixture of air and fuel vapor exists in the tank. On the other hand, the vapor space in a LH₂ tank is not flammable because air is excluded from the tank.
2. Assuming the energy release from a Jet A and a hydrogen fire is the same, one could expect significantly less damage to the surroundings from the hydrogen fire because of its relatively rapid burning rate and low emissivity (radiant heat transfer).

3. Since much less radiant heat transfer, smoke, and noxious products of combustion are produced from H_2 fires compared to Jet A fires, in a survivable crash where a fuel fire ensues, passenger safety should be greatly enhanced if the fuel is LH_2 .
4. Assuming deflagration does not occur, large leakage of H_2 within the aircraft is likely to be more hazardous than leakage of Jet A because of the hazard of detonation in a confined space.
5. LH_2 is non-toxic, however it presents a unique health hazard to personnel because contact with the eyes or skin can cause freezing of the tissue. Jet A fuel is a minor skin irritant but its vapors are toxic at levels of 500 ppm.
6. Rapid diffusion and evaporation of spilled LH_2 limits the time when a flammable mixture might be present. A spill of a quantity of Jet A having equal energy content would present a hazard for a much longer time span and over a much larger area.
7. Flammable mixtures of both H_2 and Jet A can be ignited by a hot surface or electrical spark. The relative hazard of the two fuels can be judged by considering the following facts: The hot surface ignition temperature of H_2 and Jet A is about $593^{\circ}C$ ($1100^{\circ}F$) and $216^{\circ}C$ ($420^{\circ}F$), respectively. The minimum energy required to ignite the fuels is about 0.02 and 0.2 millijoules for H_2 and Jet A respectively. Thus, it is concluded that H_2 is safer from the point of view of hot surface ignition but less safe from ignition by sparks from electrical discharges.

Technological Advances Required — Some of the areas where experimental data and technological advances are needed to develop safe LH_2 fueled aircraft are illustrated by the following. For many years, the FAA has considered $1092^{\circ}C$ ($2000^{\circ}F$) as the typical flame temperature of a powerplant fire. Accordingly, Technical Service Orders (TSO), an FAA document, specify fire resistant properties of equipment which must function during powerplant fire conditions. Fire detection devices and hoses carrying flammable fluids within designated fire zones are examples of equipment subject to TSO regulation. To show TSO compliance, this equipment must withstand fire from a standard burner which has a flame temperature of $1092^{\circ}C$ ($2000^{\circ}F$). Since the typical flame temperature in a LH_2 fueled powerplant fire is not known, research should be undertaken to determine it. The FAA's National Aviation Facility

Experimental Center at Atlantic City, New Jersey, has done full scale testing using hydrocarbon fuels. Similar work is needed using LH_2 .

The following is a list of required technological advances.

1. The characteristics (flame temperature, heat flux) of a typical LH_2 fuel system or powerplant fire should be determined.
2. Optimum means of fire detection and extinguishment should be developed for all areas of the aircraft.
3. The extreme volatility of LH_2 and its wide flammability range, plus the likelihood that fuel tanks or plumbing will be located in confined spaces, indicates that some type of leak detection system must be developed to warn the crew of a flammable atmosphere wherever it might exist within critical areas of the aircraft.
4. The minimum energy required to ignite flammable mixtures of H_2 and air is about 0.02 millijoules which is an order of magnitude less than that required to ignite hydrocarbon/air mixtures. Therefore, new standards of shielding or rendering vapor-tight must be developed for equipment which may be exposed to a H_2 /air atmosphere.
5. At certain times during both ground and flight operation, gaseous hydrogen will be vented from the fuel tanks. Research leading to an effective vent exit design (flame arrestors, etc.) which would prevent damage to the aircraft if vent gas is ignited should be undertaken. The possibility of always maintaining an inert atmosphere within the tank during maintenance or servicing cannot be guaranteed; therefore, every effort must be made to prevent flashing at the vent exit from entering the tank.

In summary it is believed that the hazards associated with the use of LH_2 are less than those associated with Jet A, but because of their differing physical and combustion properties, new designs and operational procedures will be required to make certain that today's level of fire protection is met and even exceeded.

4.9 LARGER PAYLOAD DESIGNS

The effect of larger payload requirements on LH_2 aircraft design and operational characteristics was investigated by establishing designs to carry 600 and 800

passengers over the specified ranges at M 0.85 cruise speed. All aircraft were designed to the same guidelines used throughout the study for the 400 passenger vehicles.

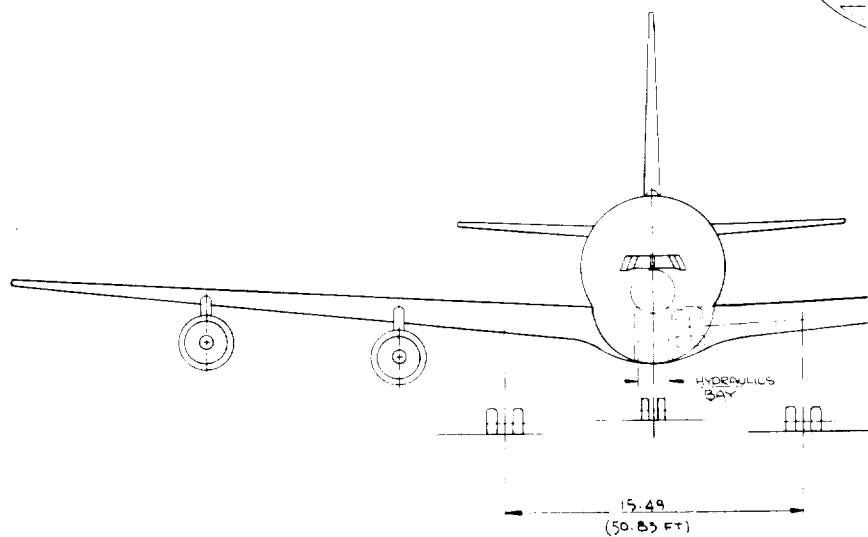
Figures 74 and 75, 76 and 77 illustrate the general arrangements and the passenger cabin arrangements evolved for the 600 and 800 passenger versions, respectively. The Internal Tank design concept selected for the 400 passenger aircraft was used. Both aircraft retain the double deck passenger arrangement, with fuel tanks both forward and aft. In order to enlarge the passenger compartment to carry the required complement, yet not exceed a realistic fuselage length, the fuselage diameter as well as its length was increased. The 600 passenger airplane has a body diameter of 7.52 m (24.7 ft) and carries 10 seats per deck per row in a 3-4-3 arrangement for a total of 20 per seat row. The 800 passenger vehicle has corresponding dimensions of 8.0 m (26.3 ft) and carries 11 seats/deck/row in a 3-5-3 arrangement for a total of 22/seat row. These dimensions retain approximately the same fuselage fineness ratio as the 400 PAX design and permit appropriate rotation angles.

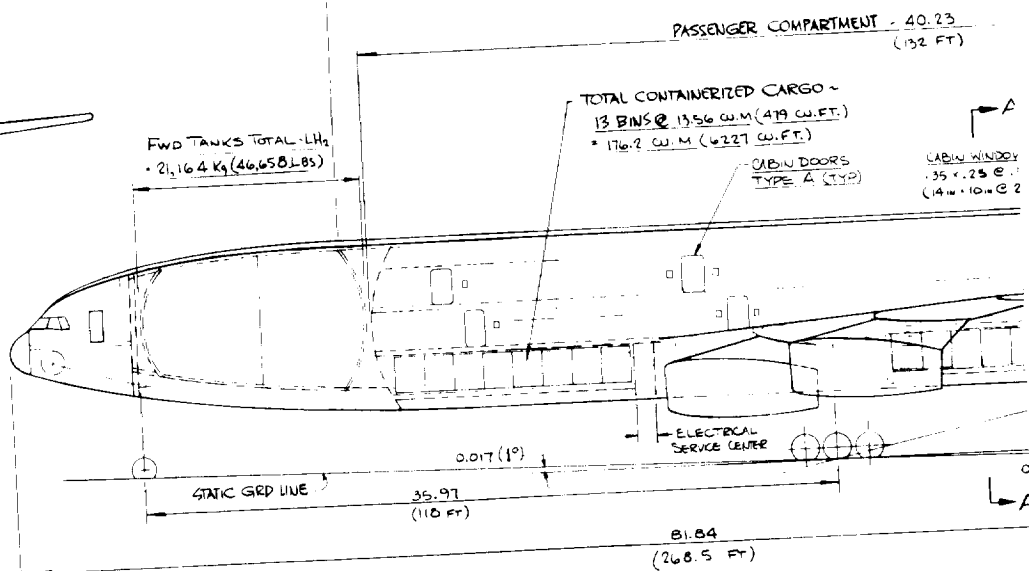
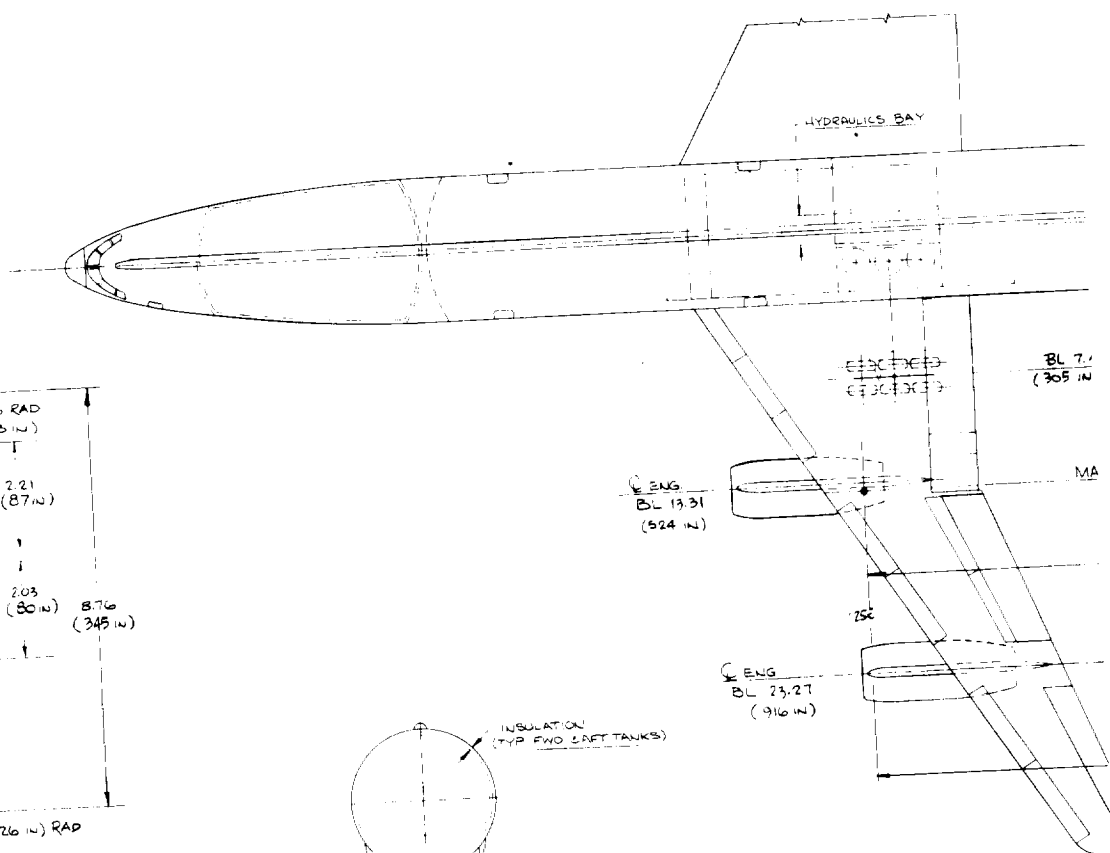
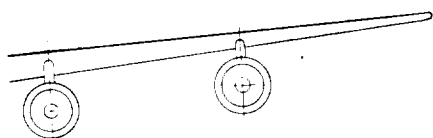
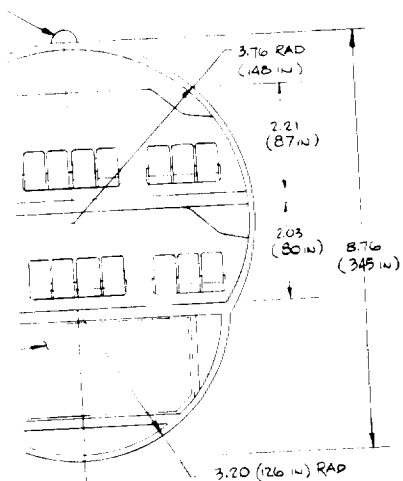
Parametric relationships were explored using the ASSET computer program to find the most satisfactory combination of airplane design variables which meet all the guideline constraints. The results are listed in Table 35 for the 5560 km (3000 n mi) range airplanes and in Table 36 for the 10,190 km (5500 n mi) range vehicles. The payload weight requirement was calculated on the same basis as for the 400 PAX design described previously, i.e., in addition to an allowance of 90.7 kg (200 lb) per passenger, an additional 10 percent was included for revenue cargo. Summary cost data for the aircraft are presented in Table 37.

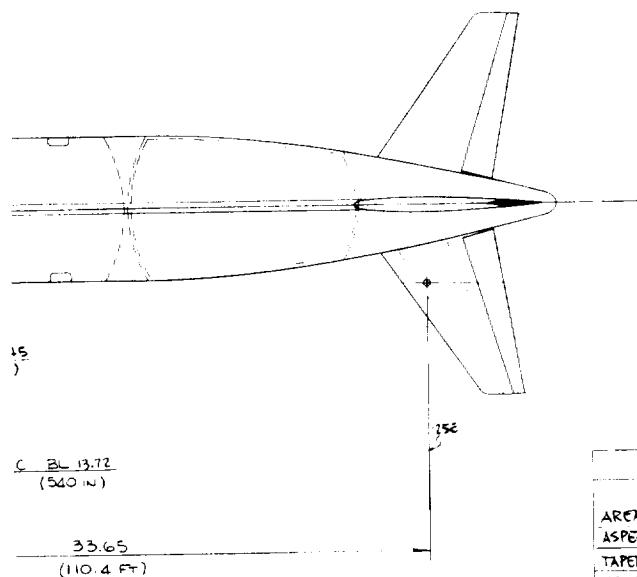
Trends of some of the significant parameters which are functions of aircraft size are plotted in Figures 78 and 79 for the 5560 km range and the 10,190 km range aircraft, respectively. Aircraft gross weight, block fuel fraction, price and direct operating cost are all plotted to show their variation with passenger capacities ranging from 400 to 800. The increasing flight efficiency (higher L/D) of larger aircraft is apparent in the decrease of the percentage of block fuel consumed. This is also reflected in a lower DOC as aircraft size increases.

MECH. CONTROLS
= ELECTRICAL ROUTING

CARGO BIN (SINGLE)
13.56 CU. METERS
(479 W. FT)







CHARACTERISTICS

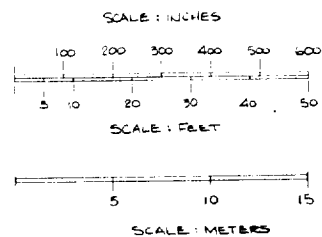
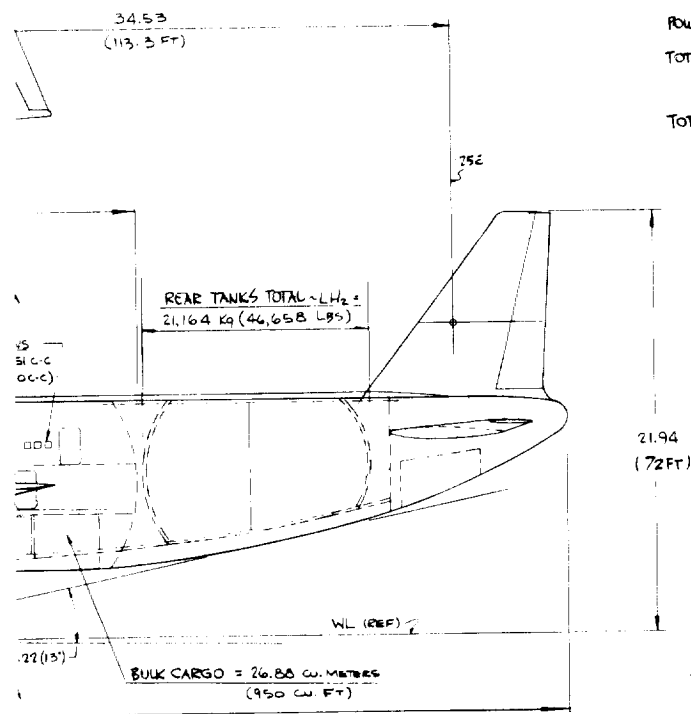
	WING	HORIZ TAIL	VERT TAIL (REF)
AREA - SQ METERS	490 (6297 SQ FT)	97 (1046 SQ FT)	58 (626 SQ FT)
ASPECT RATIO	9	4	1.6
TAPER RATIO	.30	.30	.30
SPAN	66.55 (218.4 FT)	19.76 (64.84 FT)	9.64 (31.63 FT)
ROOT CHORD	11.38 (37.32 FT)	7.56 (24.81 FT)	9.28 (30.46 FT)
TIP CHORD	3.41 (11.20 FT)	2.27 (7.44 FT)	2.78 (9.14 FT)
MAC	8.11 (26.61 FT)	5.41 (17.74 FT)	6.63 (21.76 FT)
SWEEP 25°	0.52 (30°)	0.52 (30°)	0.52 (30°)

DESIGN TAKE-OFF GROSS WT = 278,715 Kg (614,450 LBS)

POWER PLANTS 4 TURBOFANS 2 184,950 NEWTONS (41,475 LBS) S.L.S.T.

TOTAL LH₂ FUEL = 42,328 Kg (93,315 LBS)

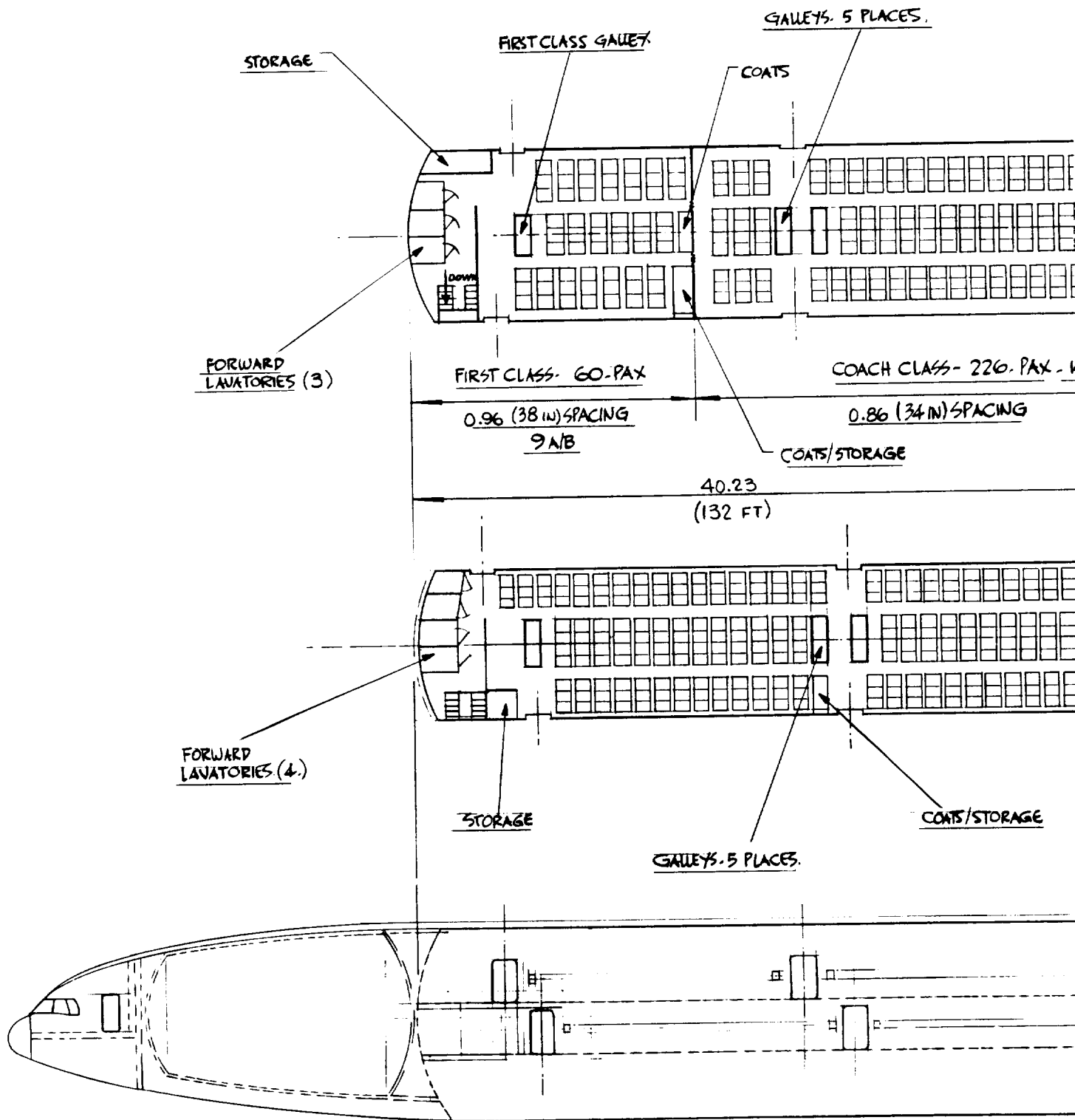
TOTAL PASSENGERS = 600 10%-90% MAX

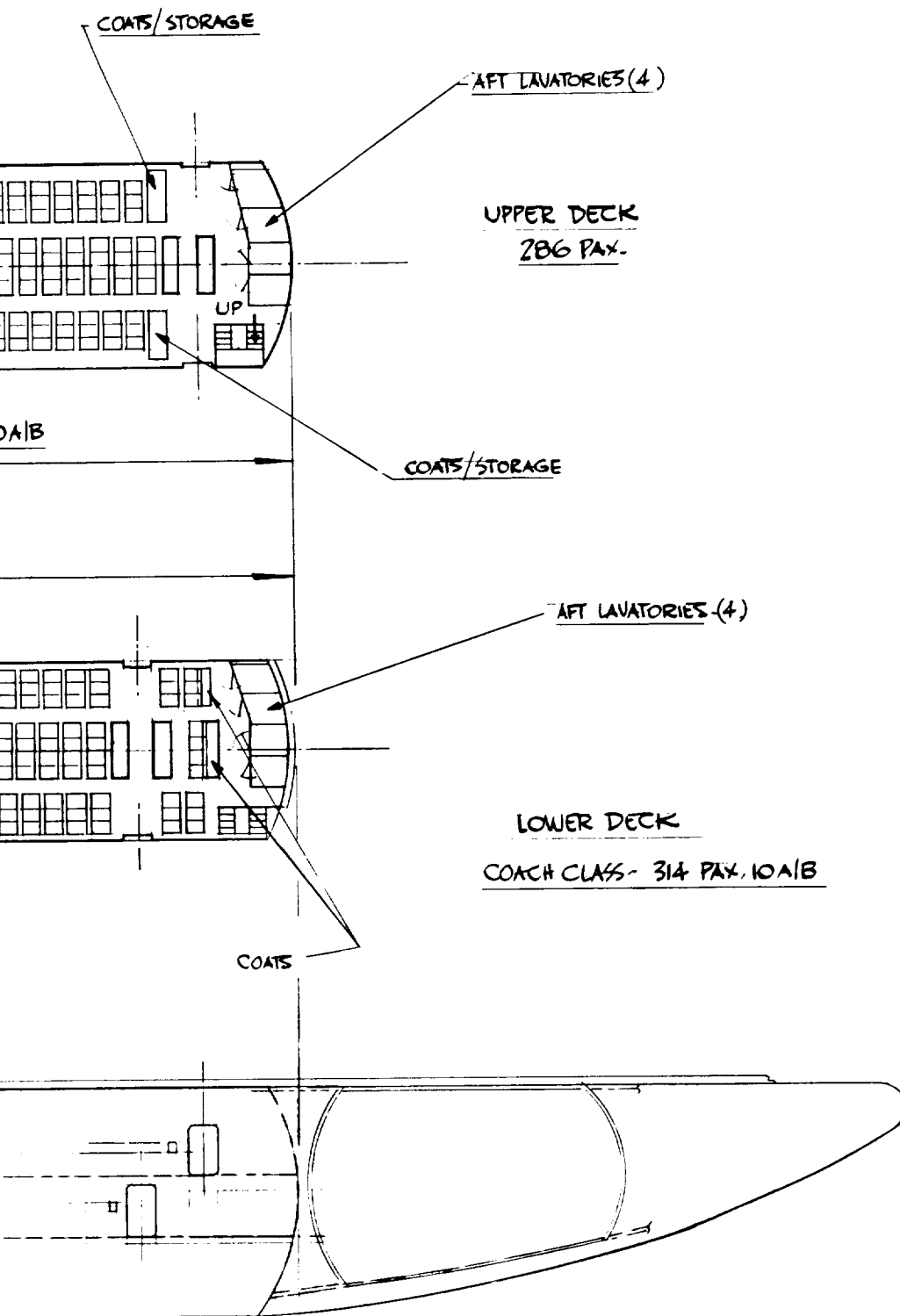


2. LINEAR DIMENSIONS IN METERS (FT = IN)
 ANGLES IN RADIAN (DEGREES)
 1. DIMENSIONS IN SI (ENGLISH) UNITS.

NOTE:

Figure 7¹⁴. General Arrangement - LH₂ Fuel,
 M 0.85, 600 Passenger Transport





SEATING ARRANGEMENT

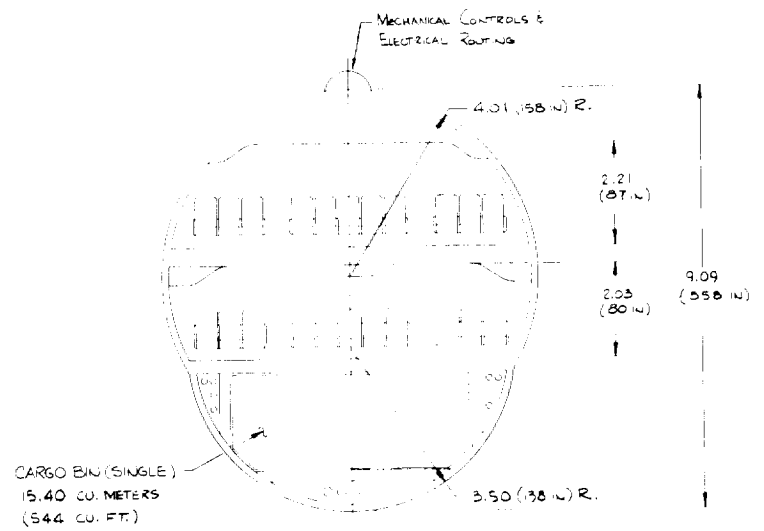
TOTAL PASSENGERS = 600

10% - 90% MIX

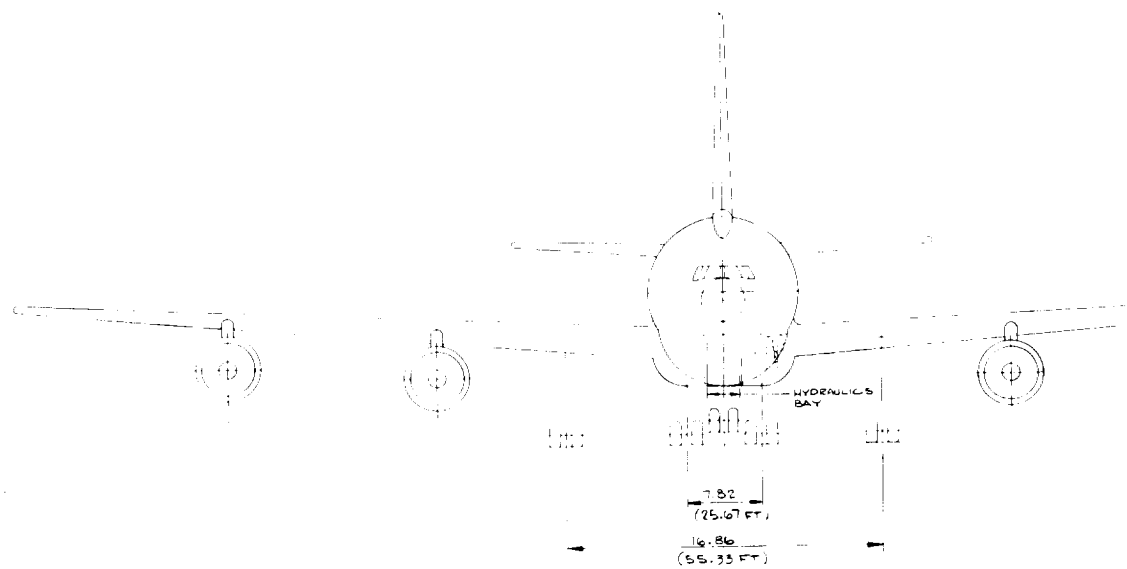
LINEAR DIMENSIONS IN METERS (FT OR IN)

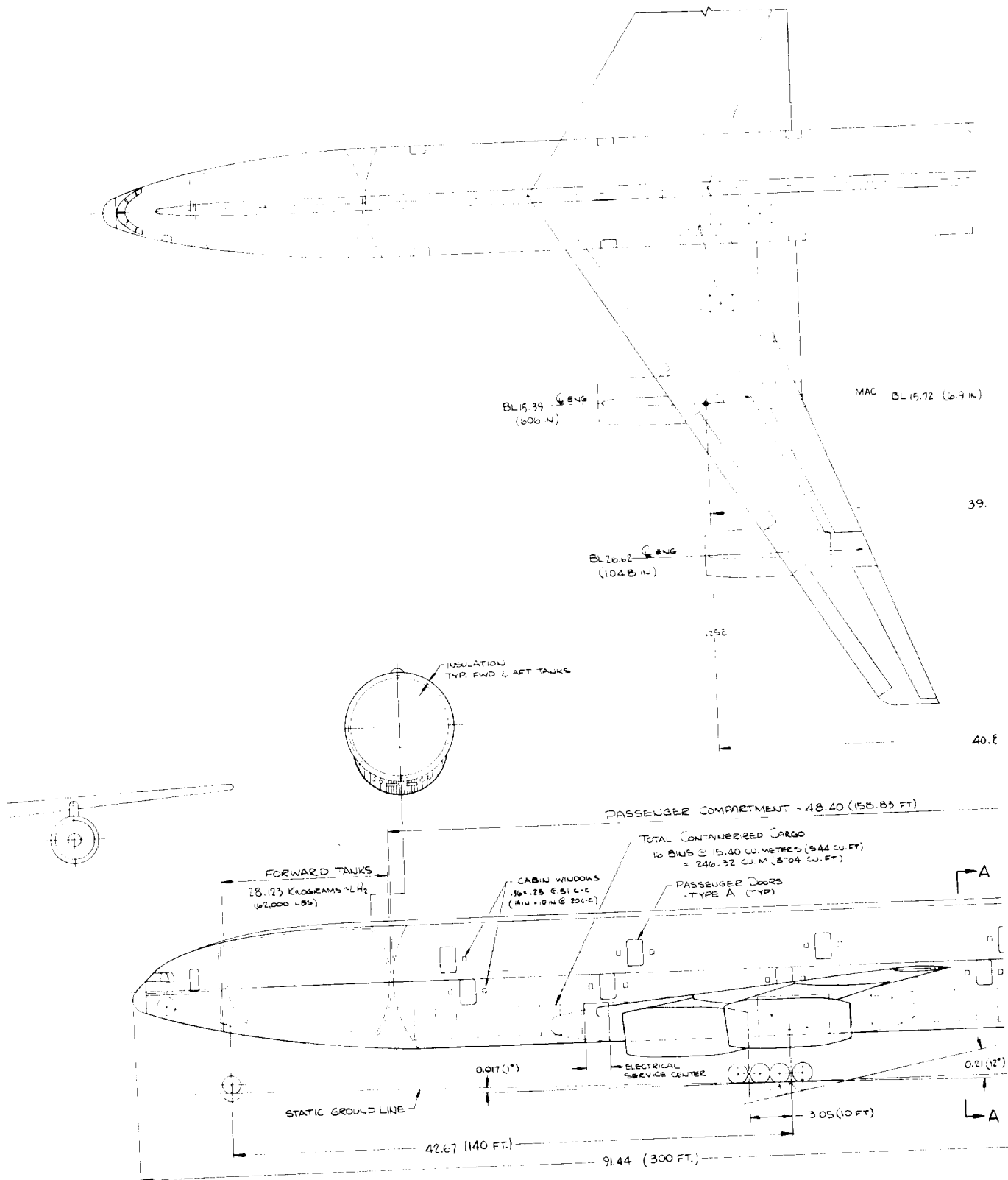
NOTE:

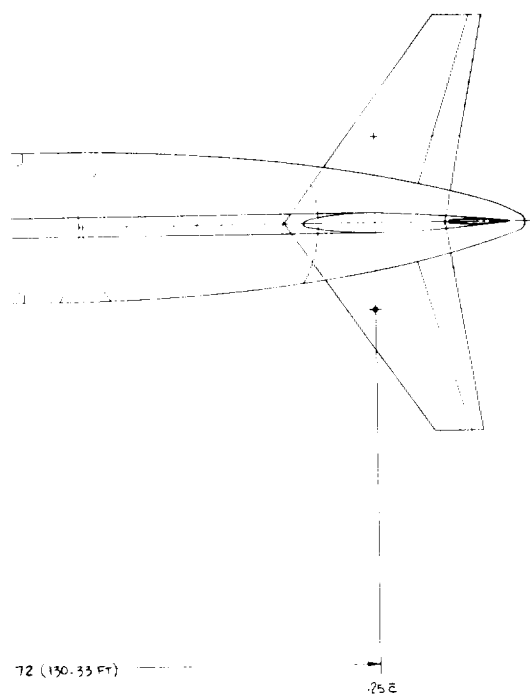
Figure 75. Passenger Cabin Arrangement -
LH₂ Fuel, 600 Passenger Transport



SECTION A-A
SCALE: 1/40







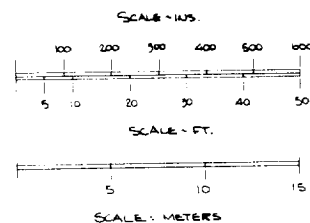
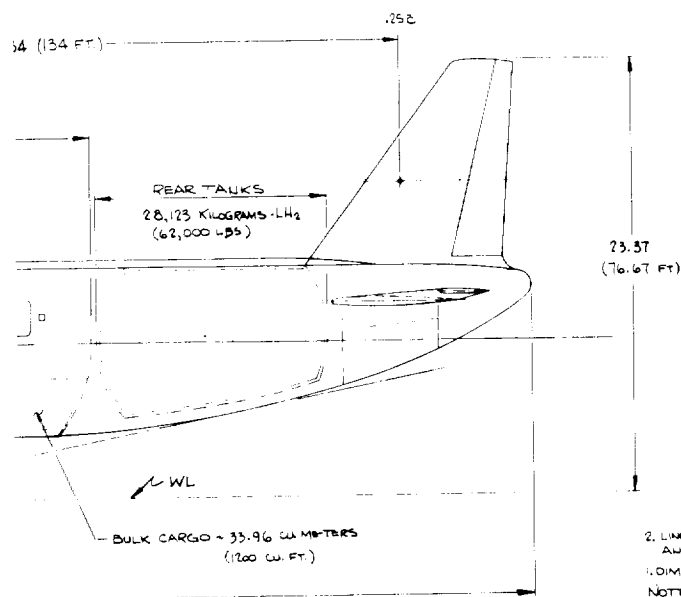
CHARACTERISTICS	WING	H/TAIL	V/TAIL
AREA - SQ METERS	654 (7039 SQ FT)	126.84 (1365.55 SQ FT)	75.02 (807.55 SQ FT)
ASPECT RATIO	9.0	4.0	1.60
TAPER RATIO	.30	.30	.30
SPAN	76.41 (250.7 FT)	6.86 (22.50 FT)	3.54 (11.61 FT)
ROOT CHORD	4.00 (13.12 FT)	2.64 (8.66 FT)	3.21 (10.53 FT)
TIP CHORD	1.20 (3.94 FT)	0.79 (2.59 FT)	0.96 (3.15 FT)
MAC	2.85 (9.35 FT)	1.83 (5.97 FT)	2.29 (7.50 FT)
SWEEP @ .25C	0.52 (30°)	0.52 (30°)	0.52 (30°)

GROSS WEIGHT ~ 368,775 KILOGRAMS (813,000 LBS)

PASSENGERS ~ 800

TOTAL FUEL CAPACITY ~ 56,425 KILOGRAMS (124,000 LBS) ~ INTEGRAL TANKS

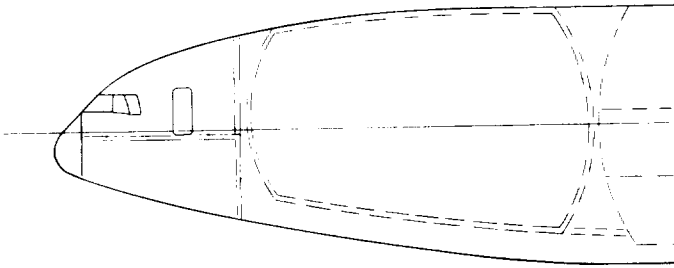
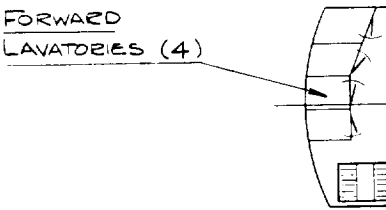
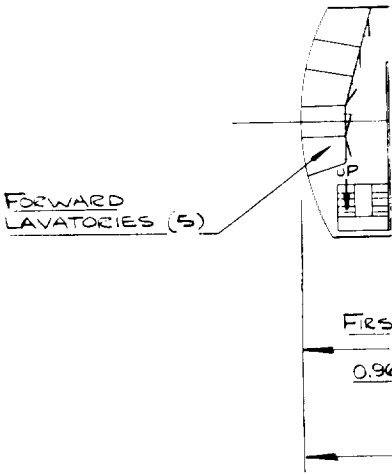
POWER PLANT ~ 4 TURBOFANS @ 264,875 NEWTONS (59,350 LB) S.L.S.T.



2. LINEAR DIMENSIONS IN METERS (FT OR IN)
 ANGLES IN RADIAN (DEGREES)
 1. DIMENSIONS IN SI (ENGLISH) UNITS.
 NOTE:

Figure 76. General Arrangement - LH₂ Fuel,
 M 0.85, 800 Passenger Transport

FIRST CLASS



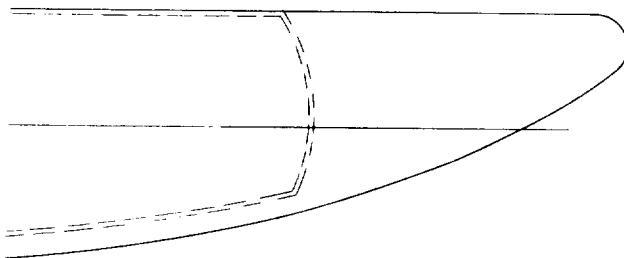
AFT LAVATORIES (5)

UPPER DECK
400 PAX

AFT LAVATORIES (4)

LOWER DECK ~ 11 A/B
COACH CLASS ~ 400 PAX

SEATING ARRANGEMENT
TOTAL PASSENGERS ~ 800
10% - 90% MIX



2. LINEAR DIMENSIONS IN METERS (FT OR IN)

1. DIMENSIONS IN SI (ENGLISH) UNITS

NOTE:

Figure 77. Passenger Cabin Arrangement -
800 Passengers

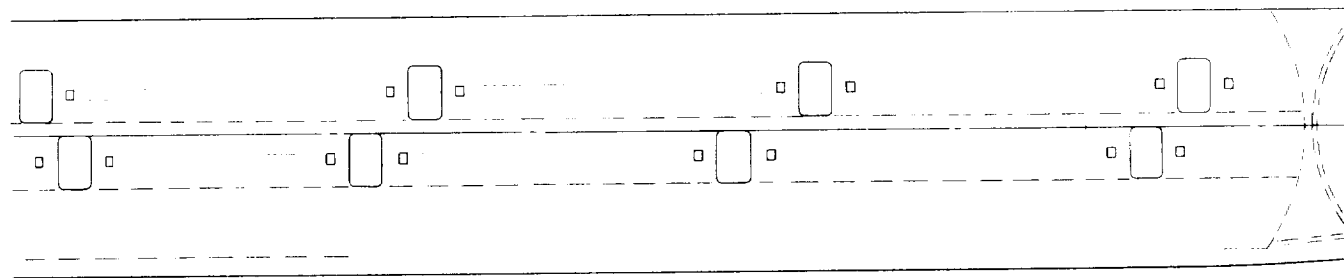
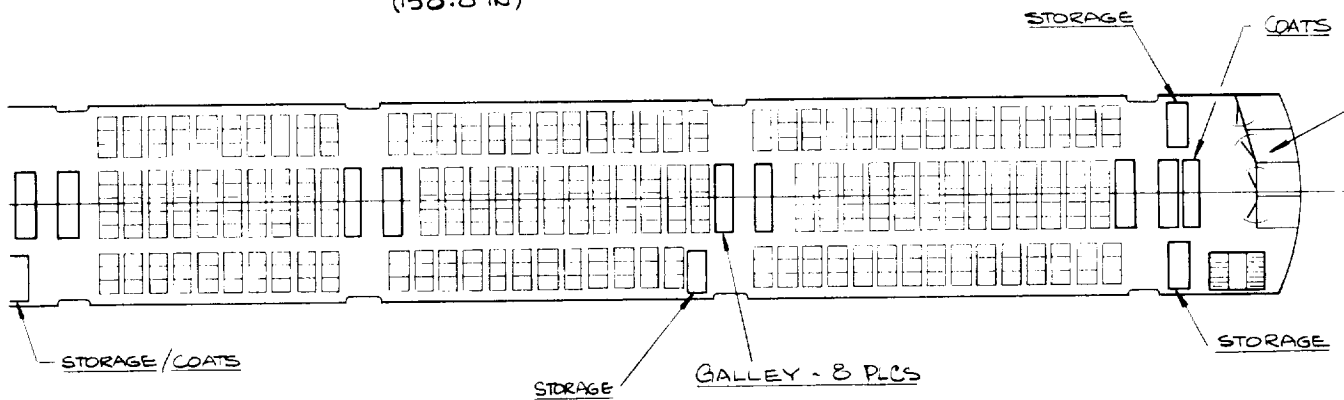
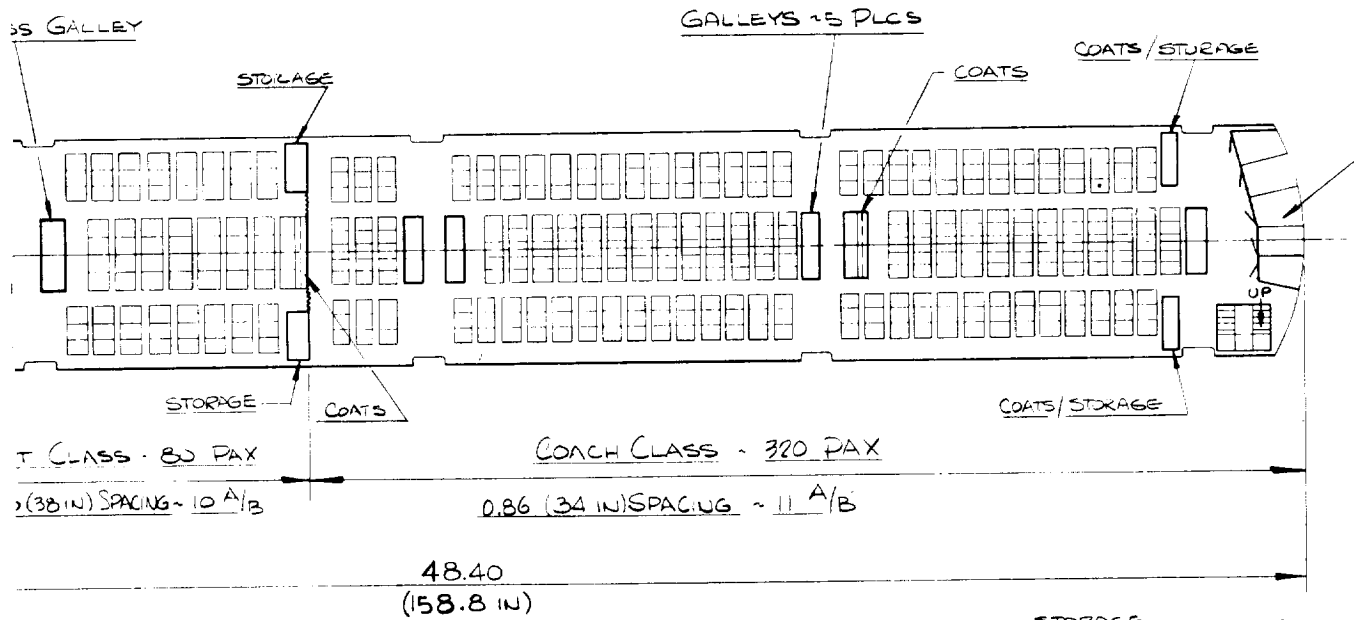


TABLE 35. CHARACTERISTICS OF 600 AND 800 PASSENGER
LH₂ AIRCRAFT (SHORT RANGE)

	SI	CUSTOMARY	600 PASSENGERS		800 PASSENGERS	
			SI	CUSTOMARY	SI	CUSTOMARY
Payload	kg	lb	59,900	132,000	79,900	176,000
Range	km	nmi	5,560	3,000	5,560	3,000
Cruise Speed	Mach	Mach	0.85	0.85	0.85	0.85
Takeoff Gross Weight	kg	lb	231,000	509,760	316,000	697,450
Operating Empty Weight	kg	lb	148,700	328,630	207,200	457,750
Block Fuel Weight	kg	lb	18,100	40,000	23,500	51,750
Total Fuel Weight	kg	lb	22,300	49,130	28,900	63,700
Wing Area	m ²	ft ²	433	4,655	594	6,399
Wing Loading, Takeoff	kg/m ²	lbs/ft ²	535	109.5	532	109
Span	m	ft	62.4	204.7	73.2	204
Fuselage Length	m	ft	68.9	236.0	81.3	266.7
Lift/Drag (Cruise)	-	-	15.9	15.9	16.85	16.85
Specific Fuel Consumption (cruise)	$\frac{\text{kg}}{\text{hr}}/\text{daN}$	$\frac{\text{lb}}{\text{hr}}/\text{lb}$	0.204	0.200	0.204	0.200
Thrust per Engine (SLS)	N	lb	156,000	35,050	203,600	46,200
Thrust/Weight (SLS)	N/kg	-	2.70	0.275	2.60	0.265
FAR T.O. Distance	m	ft	1,883	6,188	1,920	6,345
FAR Landing Distance	m	ft	1,775	5,823	1,778	5,833
Approach Speed (EAS)	m/s	knots	69.5	135	69.9	135
Weight Fractions	Percent	Percent				
Fuel			9.6	9.6	9.1	9.1
Payload			25.9	25.9	25.2	25.2
Structure			34.4	34.4	37.0	37.0
Propulsion			10.1	10.1	9.7	9.7
Equipment and Operating Items			20.0	20.0	19.0	19.0
Energy Utilization	$\frac{\text{kJ}}{\text{Seat km}}$	$\frac{\text{Btu}}{\text{Seat nmi}}$	652	1,146	633	1,112

TABLE 36. CHARACTERISTICS OF 600 AND 800 PASSENGER LH₂ AIRCRAFT (LONG RANGE)

	SI	CUSTOMARY	600 PASSENGERS		800 PASSENGERS	
			SI	CUSTOMARY	SI	CUSTOMARY
Payload	kg	lb	59,900	132,000	79,900	176,000
Range	km	nmi	10,190	5,500	10,190	5,500
Cruise Speed	Mach	Mach	0.85	0.85	0.85	0.85
Takeoff Gross Weight	kg	lb	278,700	614,450	380,200	839,990
Operating Empty Weight	kg	lb	176,500	389,130	244,800	541,550
Block Fuel Weight	kg	lb	36,300	80,000	47,500	104,580
Total Fuel Weight	kg	lb	42,300	93,320	55,500	122,440
Wing Area	m ²	ft ²	491	5,297	679	7,304
Wing Loading, Takeoff	kg/m ²	lb/ft ²	566	116	561	115
Span	m	ft	66.6	218.3	78.2	256.4
Pinchout Length	m	ft	82	268.9	91.6	300.2
Wt/Wing (Gross)	-	-	16.65	16.65	17.45	17.45
Specific Fuel Consumption (Gross)	kg/whr	lb/hr/lb	0.203	0.199	0.204	0.200
Thrust per Engine (Gross)	N	lb	185,200	41,480	258,000	58,550
Thrust/Weight (Gross)	N/kg	-	2.65	0.270	2.51	0.255
FAK Takeoff Distance	m	ft	2,040	6,686	2,150	7,000
FAK Landing Distance	m	ft	1,777	5,831	1,777	5,830
Approach Speed (FAK)	m/s	knots	69.5	135	69.5	135
Weight Fractions	Percent	Percent				
Fuel			15.1	15.1	14.6	14.6
Payload			21.5	21.5	21.0	21.0
Structure			34.5	34.5	37.1	37.1
Propulsion			11.8	11.8	11.2	11.2
Equipment and Operating Items			17.1	17.1	16.1	16.1
Energy Utilization	kJ/Gent. km	Btu/Gent. nmi	712	1,251	697	1,206

TABLE 37. COST DATA FOR 600 AND 800 PASSENGER LH₂ AIRCRAFT

RANGE	5,560 km		10,190 km	
PASSENGER CAPACITY	600	800	600	800
<u>Development Cost</u> $\$10^6$				
Airframe	830.3	1073.5	973.9	1247.3
Engine	525.1	641.0	593.0	713.0
Total	1355.4	1714.5	1566.9	1960.3
<u>Production Cost</u> $\$10^6$				
Airframe	25.88	34.83	31.55	42.43
Engine	4.19	5.36	4.87	6.11
Avionics	0.50	0.50	0.50	0.50
R&D Amortization*	3.42	4.35	3.97	4.99
Total	33.99	45.04	40.89	54.03
<u>Direct Operating Cost</u> $\frac{\phi}{\text{seat km}}$	0.493	0.475	0.523	0.506
$\frac{\phi}{(\text{seat n mi})}$	(0.913)	(0.881)	(0.969)	(0.938)
<p>@ fuel cost:</p> <p>Jet A = $\\$2/1.054 \text{ GJ}$ ($\\$2/10^6 \text{ Btu} = 24.8\phi/\text{gal} = 3.68\phi/\text{lb}$)</p> <p>LH₂ = $\\$3/1.054 \text{ GJ}$ ($\\$3/10^6 \text{ Btu} = 15.48\phi/\text{gal}$)</p>				

*Based on 350 aircraft and 2000 engines

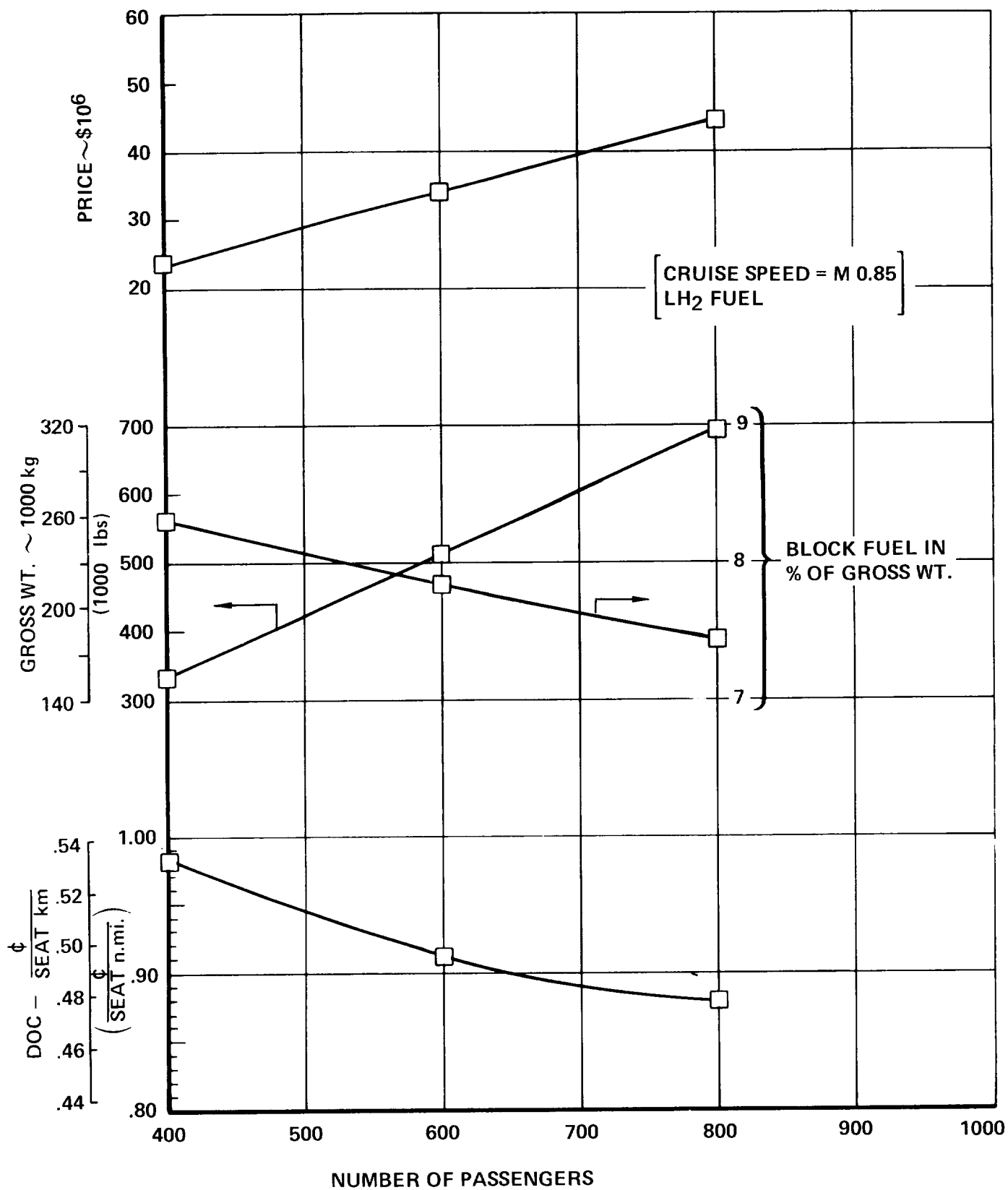


Figure 78. Effect of Larger Payloads on Aircraft Characteristics (Short Range)

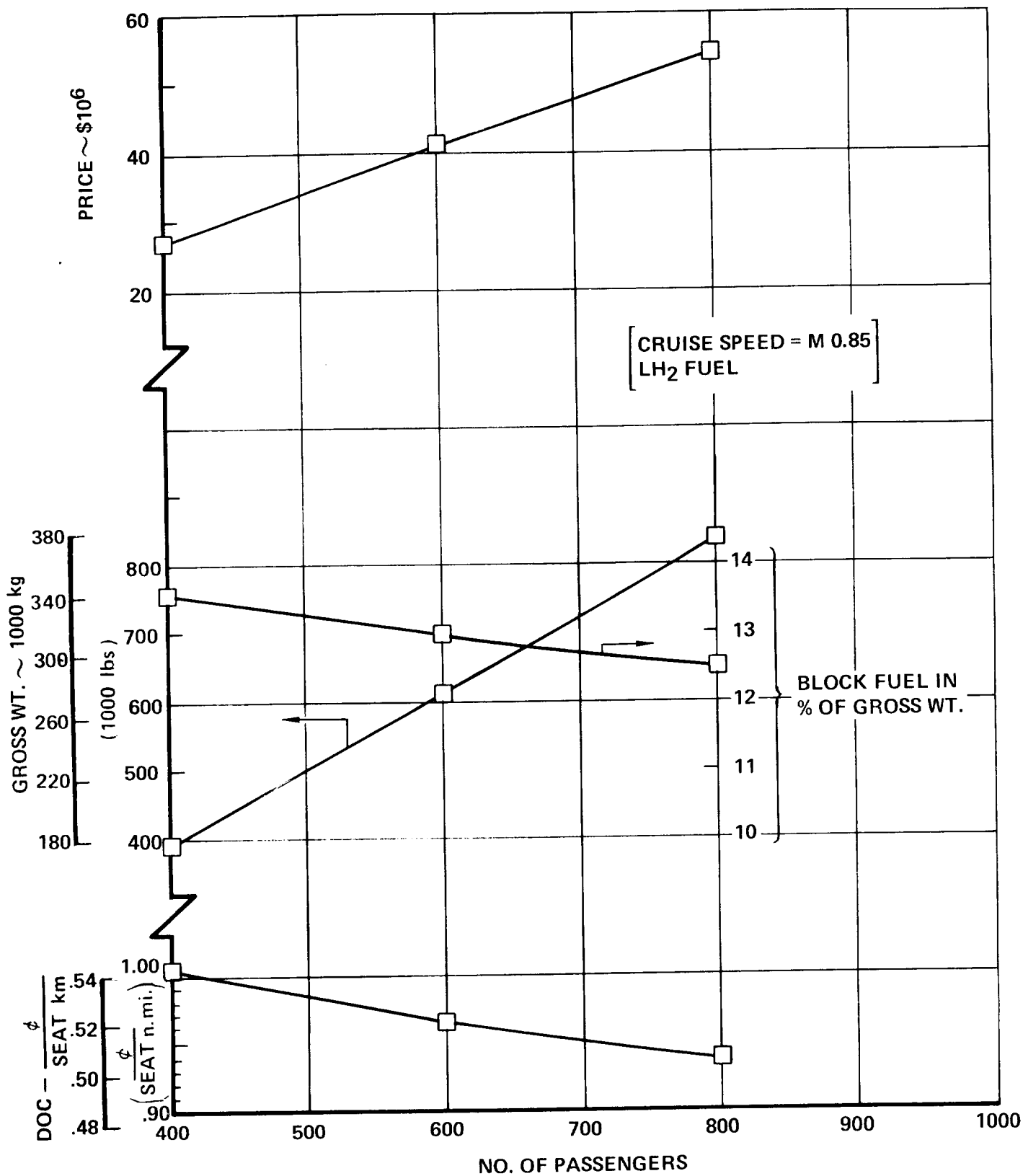


Figure 79. Effect of Larger Payloads on Aircraft Characteristics (Long Range)

SECTION 5

CARGO AIRCRAFT

The cargo aircraft analyzed during the study are described in this section. The parametric procedures used to evaluate candidate designs and to define preferred configurations of cargo aircraft are described. Two preferred designs of LH_2 fueled cargo aircraft are described for each mission, in addition to the Jet A fueled configurations which, as in the case of the passenger aircraft, serve as a point of reference for evaluating the benefits of using hydrogen as a fuel for advanced technology cargo aircraft.

5.1 REQUIREMENTS

Cargo aircraft were designed to perform two missions. One was to transport 56,700 kilograms (125,000 pounds) for a distance of 5,560 kilometers (3000 nautical miles). The second was to transport 113,400 kilograms (250,000 pounds) for a distance of 10,190 kilometers (5,500 nautical miles). Subsequent paragraphs refer to the aircraft configured to satisfy these missions as the small and large aircraft, respectively.

A cruise speed of Mach 0.85 was selected for both missions. This decision was based on qualitative judgment rather than on a quantitative analysis. It was felt that cargo aircraft designed for initial operation during the 1990-1995 time frame will require a cruise speed compatible with the speed of commercial passenger aircraft. This compatibility will decrease the number of potential traffic delays occurring within the controlled airspace environment. Cruise speeds faster than Mach 0.85 were not felt to be justified as commercial cargo transport is more sensitive to time of day delivery than to speed of delivery.

The above and other pertinent mission parameters are summarized in Table 38. Landing distance and approach speed for the small aircraft are based upon a landing weight which includes full payload and fifty percent mission fuel. The large aircraft landing weight conditions are full payload and mission reserve fuel only.

TABLE 38. CARGO MISSION PARAMETERS

	SMALL AIRCRAFT	LARGE AIRCRAFT
Payload - kg (lb)	56,700 (125,000)	113,400 (250,000)
Range - km (n mi)	5,556 (3,000)	10,186 (5,500)
Speed - Mach	0.85	0.85
Initial Cruise Altitude - m (ft)	10,972 (36,000)	10,972 (36,000)
Maximum Runway Length - m (ft)	2438.4 (8,000)	2438.4 (8,000)
Maximum Approach Speed - m/s (keas)	69.44 (135)	69.44 (135)

3.3.1 CONFIGURATION SELECTION

The density of liquid hydrogen fuel compared to current Jet A fuel, approximately a four-to-one volume ratio for equal energy content, plus the requirement for a thick layer of insulation around the tank to minimize boiloff, presents a unique configuration problem. The location and design of the hydrogen fuel tankage was a significant element in the task of selecting preferred configuration concepts for the hydrogen aircraft. The initial task was, therefore, to evaluate various candidate concepts of airframe and hydrogen tank integration.

Schematic representations of the configuration concepts considered for the small aircraft are shown on Figure 30. Evaluation data and configuration selection are given on Table 39. The nose loader and swing tail concepts were selected for more detailed study and evaluation. The swing tail concepts requires the minimum gross weight and provides acceptable operational characteristics. Although the gross weights of the center and pod tank concepts were less than the gross weight of the nose loader concept, these designs were rejected due to poor cargo compartment design and low hydrogen tank efficiency, i.e., high surface-to-volume ratio, respectively.

The cargo compartment for the above parametric aircraft was sized to contain a single row of 2.59 m (8.5 ft) wide by 2.90 m (9.5 ft) high containers. The single row will store four containers, three 12.19 m (40 ft) in length and one

Single row cargo compartment illustrated

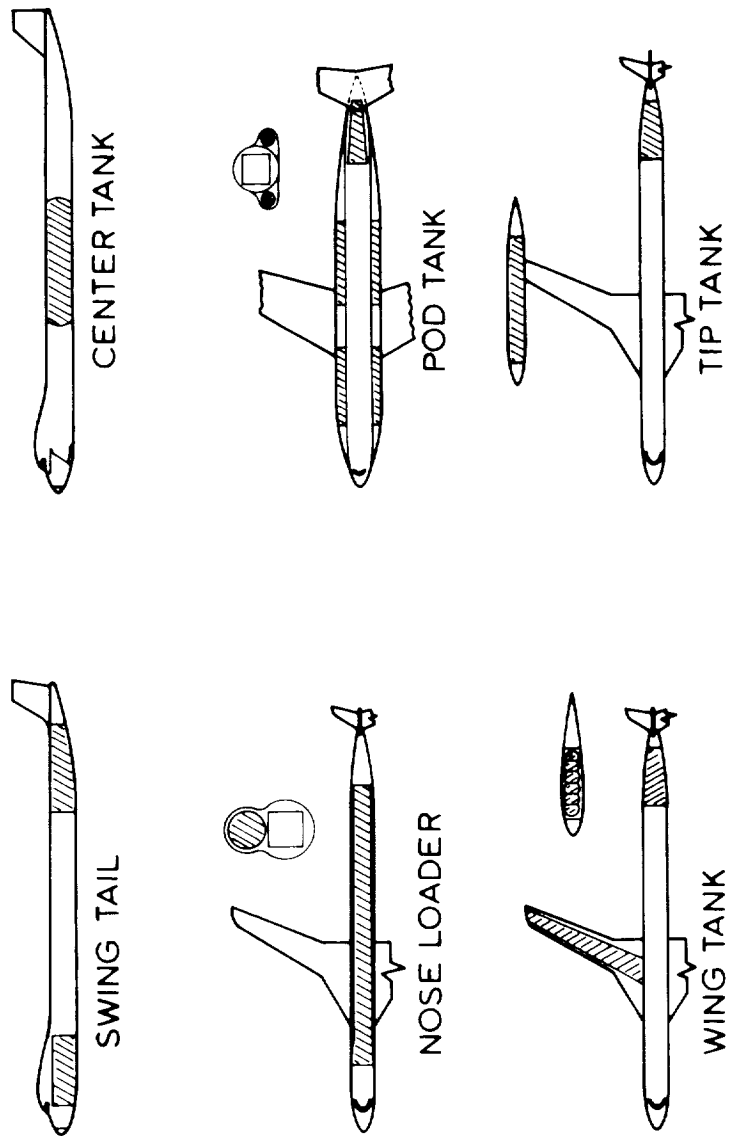


Figure 80. Cargo Aircraft Configuration Concept

TABLE 30. CARGO AIRCRAFT CONFIGURATION CONCEPT COMPARISON

CONCEPT IDENTIFICATION	CARGO LOADING ACCESS	CARGO TERMINAL COMPATIBILITY	AERODYNAMIC FEASIBILITY	WEIGHT TRENDS GROSS WEIGHT	TANK ACCESS & STRUCTURAL SIMPLICITY	OTHER	SELECTED CONCEPT
SWING TAIL	Aft opening	Poor	$L/D \approx 15.7$ Low wetted area	137,438 kg (303,000 lb)	Fair	Swing tail complicates control; plumbing and structure at hinge joint.	Selected
CENTER TANK	Fwd and Aft opening	Poor	$L/D \approx 15.6$	141,067 kg (311,000 lb)	Fair	Fore & aft cargo distribution required to maintain C.G.	Reject - Unacceptable because of required fwd and aft cargo compartments
NOSELOADER	Fwd opening	Excellent	$L/D \approx 15.6$	145,603 kg (321,000 lb)	Good		Selected
POD TANK	Fwd opening	Fair	$L/D \approx 15.6$	144,242 kg (318,000 lb)	Poor	Poor tank efficiency	Reject - High number small tank results in poor efficiency
WING TANK	Fwd opening	Fair	$L/D \approx 13.6$ Low AR High r/c & sweep	153,767 kg (339,000 lb)	Poor	Poor tank efficiency	Reject - Low L/D due to required wing geometry
TIP TANK	Fwd opening	Excellent	$L/D \approx 15.4$ Maximum wetted area	164,654 kg (363,000 lb)	Good	Flutter problem Wing weight penalty	Reject - High wetted area results in excess weight

6.10 m (20 ft) in length. The compartment dimensions are 2.74 m (9.0 ft) wide by 3.05 m (10 ft) high by 43.89 m (144 ft) in length for an average cargo cube density of 153.78 kg/m³ (9.6 lb/ft³).

Subsequent to the selection of the swing tail and nose loader concepts, a study was performed to compare the single row cargo compartment with a double row type. The double row compartment is 5.33 m (17.5 ft) wide, 3.05 m (10 ft) high and 22.56 m (74 ft) in length. Each row will store 3 containers of various lengths, one 12.19 m (40 ft), one 6.10 m (20 ft), and one 3.05 m (10 ft). Average cargo cube density is also 153.78 kg/m³.

Aircraft configured for the double row compartment are compared to the single row aircraft on Table 40. The lower fuselage surface area of the double row configuration results in lower fuselage weight and skin friction drag, therefore, less gross weight required to perform the mission. Based upon this comparison, all subsequent study aircraft are configured for the double row compartment.

TABLE 40. COMPARISON — DOUBLE ROW VS SINGLE ROW
CARGO COMPARTMENTS

	DOUBLE ROW		SINGLE ROW	
	SWING TAIL	NOSE LOADER	SWING TAIL	NOSE LOADER
Compartment Width - m	5.334	5.334	2.74	2.74
ft	17.5	17.5	9.0	9.0
Compartment Length - m	22.56	22.56	43.89	43.89
ft	74	74	144	144
Fuselage Surface Area - m ²	845.42	1012.64	1068.38	1161.29
ft ²	9,100	10,900	11,500	12,500
Mission Fuel - kg	15,966	17,191	16,783	18,824
lb	35,200	37,900	37,000	41,500
Operating Weight - kg	56,382	62,868	63,594	70,851
lb	124,300	138,600	140,200	156,200
Gross Weight - kg	128,730	136,077	137,484	145,693
lb	283,800	300,000	303,100	321,200

A concept selection parametric evaluation was also performed for the large aircraft with the resulting concept selections being identical to those of the small aircraft; the swing tail and nose loader.

5.2 PARAMETRIC ANALYSIS

5.2.1 Parametric Sizing Program

The parametric analysis method used is a modification of that described in Section 3.2.3 of the ATP report (Reference 10). The noise iteration was not used since a fixed engine cycle was employed. The method was changed to enable definition of the approach speed characteristic. Since the fuel tanks for the cargo aircraft are contained in the fuselage, iterations on fuselage size were necessary if the estimated fuel volume had to be modified to meet fuel requirements. A schematic of the program is given in Figure 81.

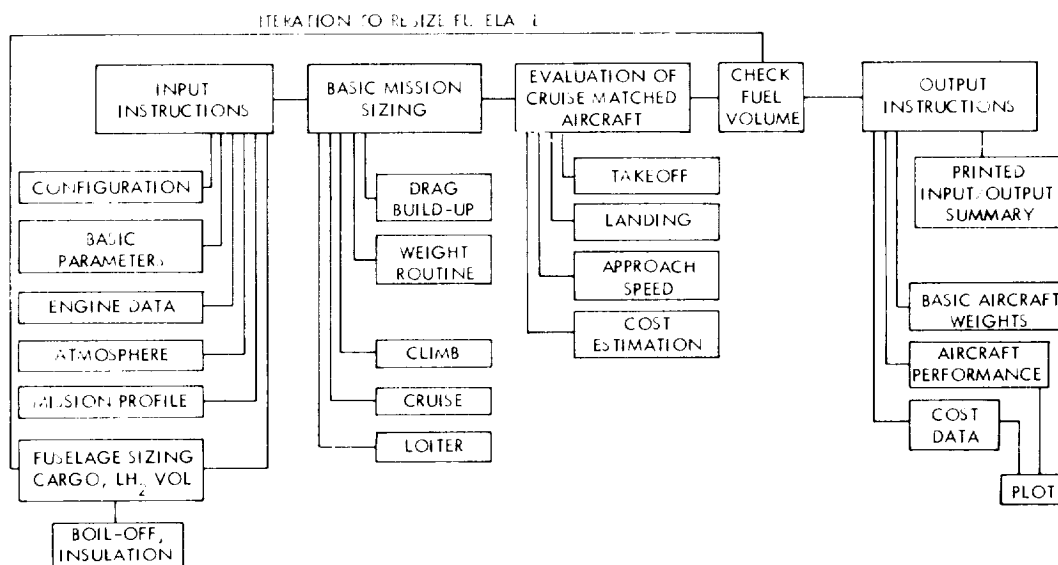


Figure 81. Generalized Aircraft Sizing Program (GASP)

The schematic illustrates a computer program which, when provided basic data such as fuselage size, engine data, mission requirements, and atmospheric data,

- Estimates the drag and weight characteristics of a given configuration
- Evaluates the capability of this configuration to meet the mission requirements.

This process is arranged in a loop in order that the aircraft size, primarily wing and empennage areas and engine size, can be iterated until the aircraft is sized to exactly meet the mission payload-range requirements. After a configuration is properly sized, the routine determines the takeoff and landing field lengths, the approach speed, unit price and the operating costs of the aircraft.

This routine is arranged so that configuration changes resulting from primary variables such as wing aspect ratio, wing sweep angle, cruise altitude, and cruise wing loading or lift coefficient can be automatically evaluated during one execution of the program. A complete description of the sized aircraft, including weights, aerodynamic, geometric, costs, and airport performance characteristics can be selected for output from the computer.

The mission consists of takeoff, climb, and cruise segments. No range credit is allowed for descent. The cruise segment is computed using a constant altitude, constant speed technique. Fuel reserves were provided for international flight and allow for 10 percent extra cruise time, plus 30 minutes hold, plus fuel for an additional cruise of 370.4 km (200 n.mi.) to an alternate airport.

5.3.2 Parametric Constraints

In addition to the characteristics defined previously, several other factors were held constant. For example:

- The minimum initial cruise altitude for cargo aircraft was established as 10,970 m (36,000 ft).
- The maximum cruise lift coefficient was not to exceed a 2-dimensional value of 0.7.
- Tail sizing was held constant with the parametric values established in Section 3.4 of this report.

- All configurations have T tails. The empennage surfaces have 8.5 percent thick airfoil sections and are swept 0.61 radians.
- All configurations have four engines mounted under the wing.

5.3.3 Parametric Selection Process

A sample of the output and usage of the parametric data is given in Figure 82, which shows the variations in aircraft weight, operating costs, approach speed and airport performance which result from parametric variations in aspect ratio and cruise wing loading for cruise matched engines. Since the aircraft are optimized on the basis of minimum DOC, the various constraints are superimposed on the DOC plot. In this case, the diagram shows that the aircraft is sized by the 69.5 m/s (135 knot) approach speed limitation and that a considerable margin is available before the 7,040 m (8000 ft) runway length constraint becomes critical.

5.3.4 Parametric Trends

The results of the parametric studies of the small and large hydrogen nose loader and wing tail configurations are given in Tables 41 and 42, respectively. These data show that the aspect ratio 9 aircraft have the minimum direct operating costs and were, accordingly, the selected configurations. It should be noted, however, that the aspect ratio 8 aircraft are lighter and have the minimum aircraft price. Also, because of their relatively poorer cruise efficiency, they have larger engines which results in better takeoff performance and higher fuel usage. On the other hand, higher aspect ratio configurations have better cruise efficiency and smaller thrust requirements resulting in less fuel usage than the lower aspect ratio configurations and poorer takeoff field lengths.

As shown, the small aircraft, with their landing weights including 50 percent of the initial fuel are nominally designed for a 561 kg/m^2 (115 lb/ft^2) initial cruise wing loading. The large configurations were designed to land with only the specified fuel reserve and are nominally sized for an initial cruise wing loading of 610 kg/m^2 (125 lb/ft^2). Because of the lower cruise lift coefficient associated with the lower design wing loading, the small aircraft can tolerate a somewhat larger wing thickness ratio than the large aircraft with their relatively higher cruise lift coefficient.

TABLE 41. ASPECT RATIO SELECTION - IH₂ SWING TAIL

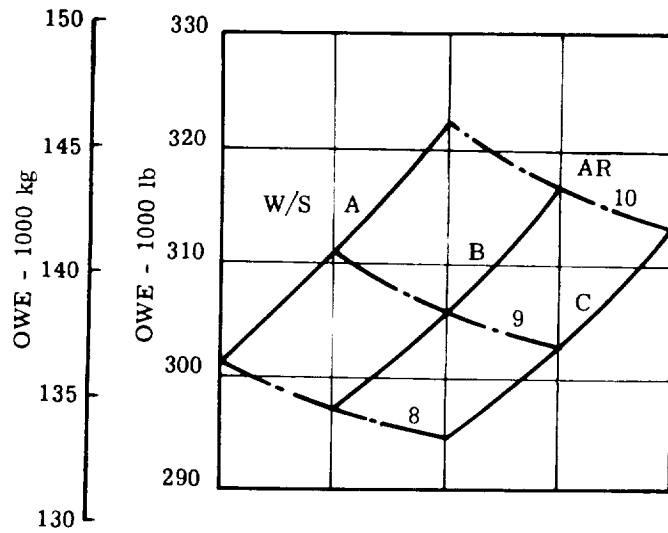
SI UNITS

ASPECT RATIO	$\frac{56,700 \text{ kg} - 5560 \text{ km}}{\text{UTILIZATION} = 3600 \text{ Hr/Yr}}$				$\frac{113,400 \text{ kg} - 10,190 \text{ km}}{\text{UTILIZATION} = 4000 \text{ Hr/Yr}}$			
	8	9	10	11	8	9	10	11
W/S - kg/m ²	559.77	558.84	558.06	557.48	617.08	613.52	610.59	608.05
t/c - %	11.62	11.49	11.39	11.33	11.18	11.07	11.00	10.95
Cruise L/D	15.65	16.2	16.67	17.09	17.26	18.04	18.72	19.32
S _W - m ²	240.9	242.9	245.6	249.0	493.3	501.0	510.8	522.4
Oper. Wt. - kg	64,707	65,988	67,564	69,384	143,591	147,933	153,274	159,482
Total Fuel - kg	15,087	14,760	14,552	14,433	51,039	49,744	48,984	48,622
Block Fuel - kg	12,380	12,110	11,938	11,840	43,964	42,818	42,141	41,812
Gross Wt. - kg	136,493	137,446	138,815	140,516	308,028	311,075	315,656	321,502
Engine Thrust - N	111,200	108,200	106,100	104,800	227,600	219,900	215,400	212,200
T.O. Dist. - m	1712.9	1758.4	1798.0	1832.8	2112.9	2175.7	2231.7	2282.3
Land. Dist. - m	2247	2232.1	2222.0	2214.7	2389.6	2377.4	2367.7	2359.2
Price - \$ X 10 ⁶	19.357	19.584	19.900	20.288	40.918	41.771	42.898	44.256
DOC - φ/Mg km	3.44	3.42	3.42	3.45	3.04	3.03	3.04	3.08
SFC - $\frac{\text{kg}}{\text{hr}}$	0.22	0.22	0.22	0.22	0.223	0.223	0.223	0.223

TABLE 41. ASPECT RATIO SELECTION - W/S SWING TAIL (Continued)

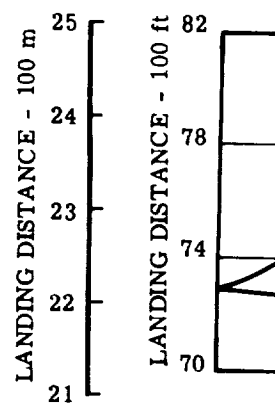
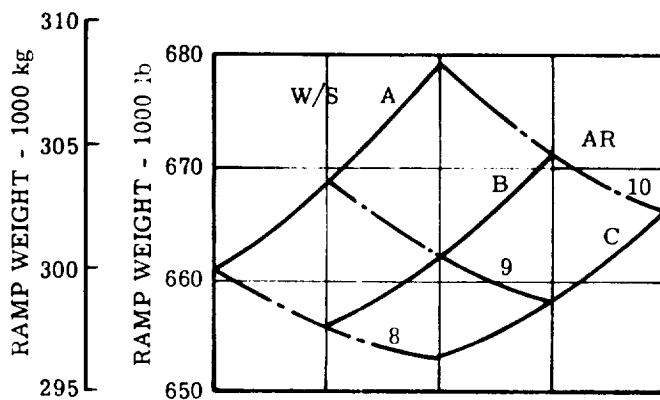
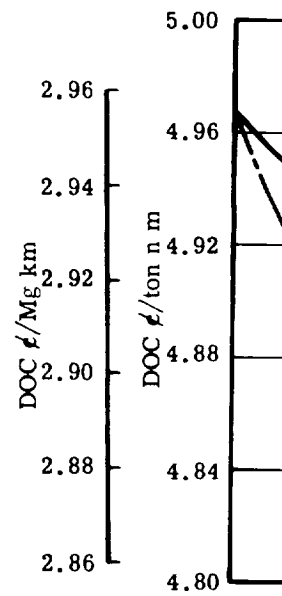
CUSTOMARY UNITS

ASPECT RATIO	$\frac{125,000 \text{ lb} - 3000 \text{ n m}}{\text{UTILIZATION} = 3600 \text{ Hr/Yr}}$					$\frac{250,000 \text{ lb} - 5500 \text{ n m}}{\text{UTILIZATION} = 3600 \text{ Hr/Yr}}$				
	8	9	10	11	12	8	9	10	11	12
$W/S - \text{lb/ft}^2$	114.66	111.47	111.31	111.19		126.40	125.67	125.07		124.55
$t/c - \%$	11.62	11.49	11.39	11.33		11.18	11.07	11.00		10.95
Cruise L/D	15.65	16.2	16.67	17.09		17.26	18.04	18.72		19.32
$S_w - \text{ft}^2$	2593	2615	2644	2680		5310	5393	5498		5623
Oper. Wt. - lb	142,654	145,478	148,953	152,966		316,565	326,137	337,912		351,599
Total Fuel - lb	33,263	32,540	32,082	31,819		112,522	109,667	107,993		107,193
Block Fuel - lb	27,294	26,697	26,319	26,103		96,925	94,398	92,906		92,179
Gross Wt. - lb	300,916	303,018	306,035	309,785		679,087	685,804	695,904		708,791
Engine Thrust - lb	25,004	24,318	23,858	23,565		51,167	49,439	48,341		47,700
T.O. Dist. - ft	5620	5769	5899	6013		6932	7138	7322		7488
Land. Dist. - ft	7373	7323	7290	7266		7840	7800	7768		7740
Price - \$ X 10^6	19.357	19.584	19.900	20.280		40.918	41.771	42.898		44.256
DOC - ϕ /ATM	5.78	5.75	5.76	5.79		5.11	5.09	5.11		5.17
SFC - lb/hr/lb	0.216	0.216	0.216	0.216		0.219	0.219	0.219		0.219



W/S	kg/m ²	lb/ft ²
A	561.4	115
B	610.3	125
C	659.1	135

$\alpha = 0.52$ radians
(30 degrees)



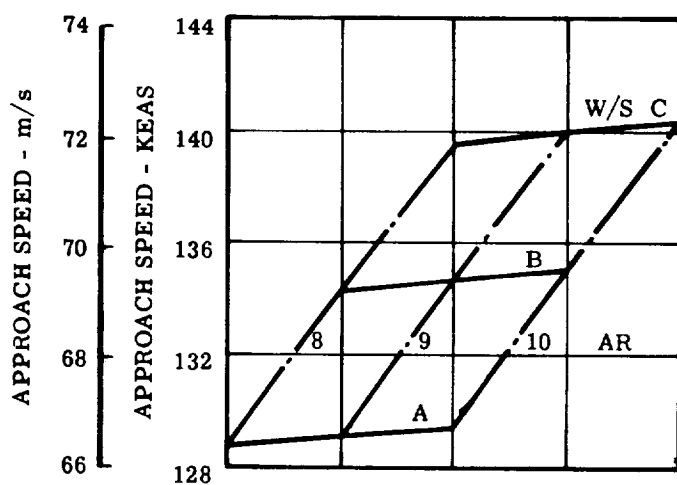
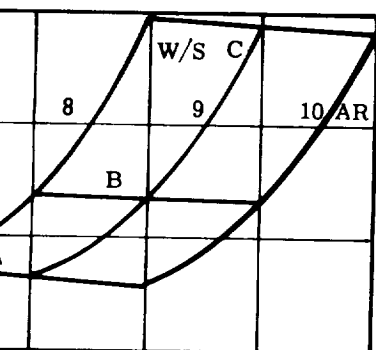
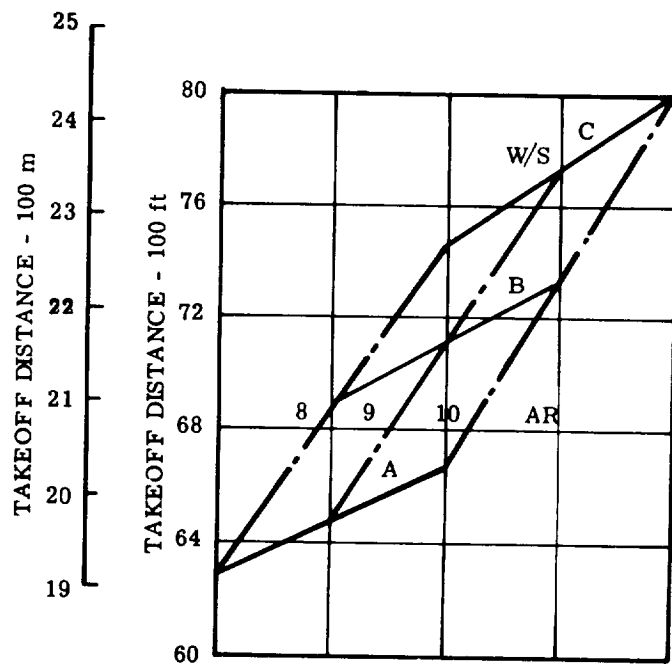
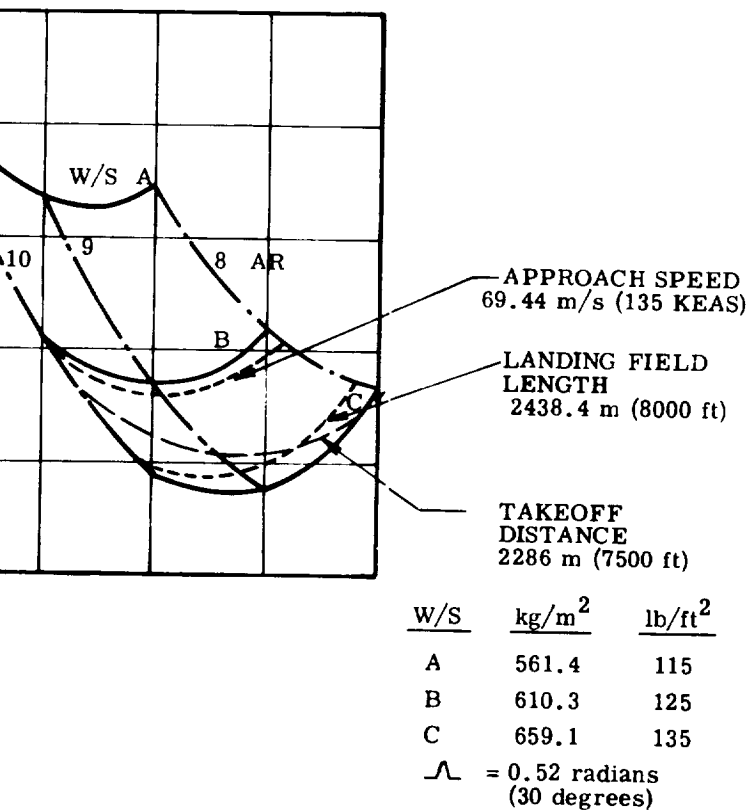


Figure 82. Sample Parametric Data - Large Hydrogen Nose Loader

TABLE 42. ASPECT RATIO SELECTION - LH₂ NOSE LOADER

SI UNITS

ASPECT RATIO	56,700 kg - 5560 km UTILIZATION = 3600 Hr/Yr					113,400 kg - 10,190 km UTILIZATION = 4000 Hr/Yr				
	8	9	10	11		8	9	10	11	
W/S - kg/m ²	559.57	558.60	557.82	557.13		617.23	613.42	610.45	608.0	
t/c - %	11.62	11.49	11.39	11.33		11.18	11.07	11.00	10.95	
Cruise L/D	15.73	16.29	16.77	17.18		17.28	18.06	18.74	19.34	
S _w - m ²	238.0	240.1	242.8	245.5		474.9	482.4	491.6	502.5	
Oper. Wt. - kg	63,373	64,626	66,167	67,949		134,101	138,212	143,268	149,136	
Total Fuel - kg	14,772	14,449	14,243	14,125		49,099	47,842	47,099	46,733	
Block Fuel - kg	12,121	11,854	11,685	11,588		42,293	41,181	40,519	40,188	
Gross Wt. - kg	134,844	135,773	137,110	138,773		296,598	299,453	303,764	309,267	
Engine Thrust - N	109,300	106,300	104,200	102,900		218,900	211,500	206,700	203,900	
T.O. Dist. - m	1724.3	1770.0	1809.6	1844.3		2159.2	2227.8	2289.0	2344.2	
Land. Dist. - m	2247.6	2232.4	2222.0	2214.7		2389.3	2376.8	2366.8	2358.8	
Price - \$ X 10 ⁶	18.951	19.173	19.482	19.861		38.188	38.992	40.056	41.337	
DOC - ¢/Mg km	3.38	3.36	3.37	3.38		2.90	2.89	2.90	2.93	
SFC - $\frac{\text{kg}}{\text{daN hr}}$	0.219	0.219	0.219	0.219		0.223	0.223	0.223	0.223	

TABLE 42. ASPECT RATIO SELECTION - LH₂ NOSE LOADER (Continued)

ASPECT RATIO	125,000 lb - 3000 n m UTILIZATION = 3600 Hr/Yr					250,000 lb - 5500 n m UTILIZATION = 4000 Hr/Yr				
	8	9	10	11	11	8	9	10	11	11
W/S - lb/ft ²	114.62	114.42	114.26	114.12	114.12	126.43	125.65	125.04	124.54	
t/c - %	11.62	11.49	11.39	11.33	11.33	11.18	11.07	11.00	10.95	
Cruise L/D	15.73	16.29	16.77	17.18	17.18	17.28	18.06	18.74	19.34	
S _w - ft ²	2562	2584	2613	2648	2648	5112	5192	5292	5409	
Oper. Wt. - lb	139,715	142,416	145,875	149,803	149,803	295,642	304,707	315,851	328,789	
Total Fuel - lb	32,566	31,354	31,401	31,141	31,141	108,244	105,474	103,835	103,029	
Block Fuel - lb	26,724	26,135	25,762	25,548	25,548	93,241	90,790	89,330	88,599	
Gross Wt. - lb	297,281	299,330	302,277	305,944	305,944	653,887	660,181	669,686	681,818	
Engine Thrust - lb	24,568	23,890	23,436	23,145	23,145	49,220	47,546	46,477	45,844	
T.O. Dist. - ft	5657	5807	5937	6051	6051	7084	7309	7510	7691	
Land. Dist. - ft	7374	7324	7290	7266	7266	7839	7798	7765	7739	
Price - \$ X 10 ⁶	18.951	19.173	19.482	19.861	19.861	38.188	38.992	40.056	41.337	
DOC - ¢/Ton n mi	5.68	5.65	5.66	5.68	5.68	4.87	4.85	4.87	4.92	
SFC - $\frac{\text{lb}}{\text{hr}}/\text{lb}$	0.215	0.215	0.215	0.215	0.215	0.219	0.219	0.219	0.219	

5.4 HYDROGEN NOSE LOADER CONFIGURATION

5.4.1 Configuration Description

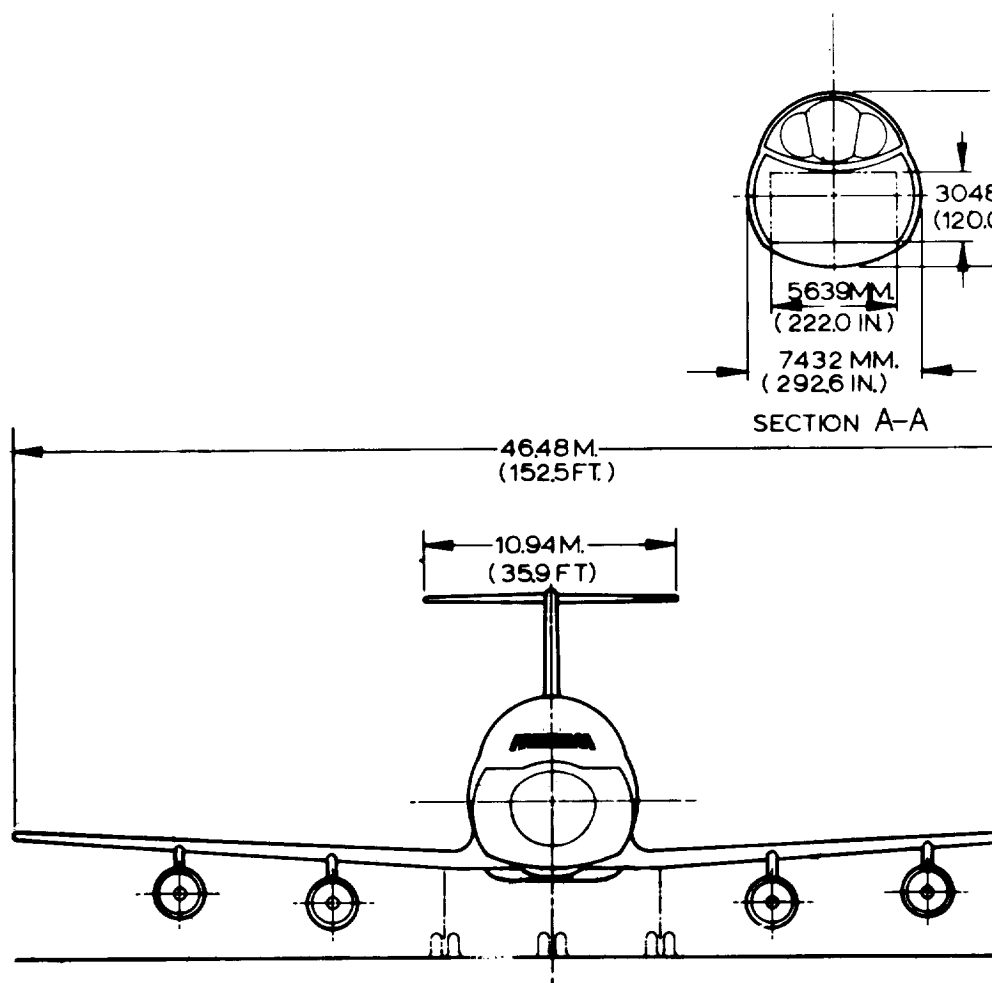
The nose loader aircraft shown in Figures 83 and 84 are configured and sized to perform the specified missions. Configuration characteristics common to both aircraft include supercritical wing design, a T-tail empennage, four pylon wing-mounted engines, and landing gear flotation acceptable to commercial fixed base operations. Mounting the wing in the low position on the small aircraft enables the wing structure to be used also for the landing gear attach structure and allow for sufficient engine nacelle ground clearance with a cargo floor height above ground level of 4.72 m (15.5 ft). The mid-wing position is required on the large aircraft to obtain proper engine nacelle ground clearance and to provide proper cargo floor height above ground level.

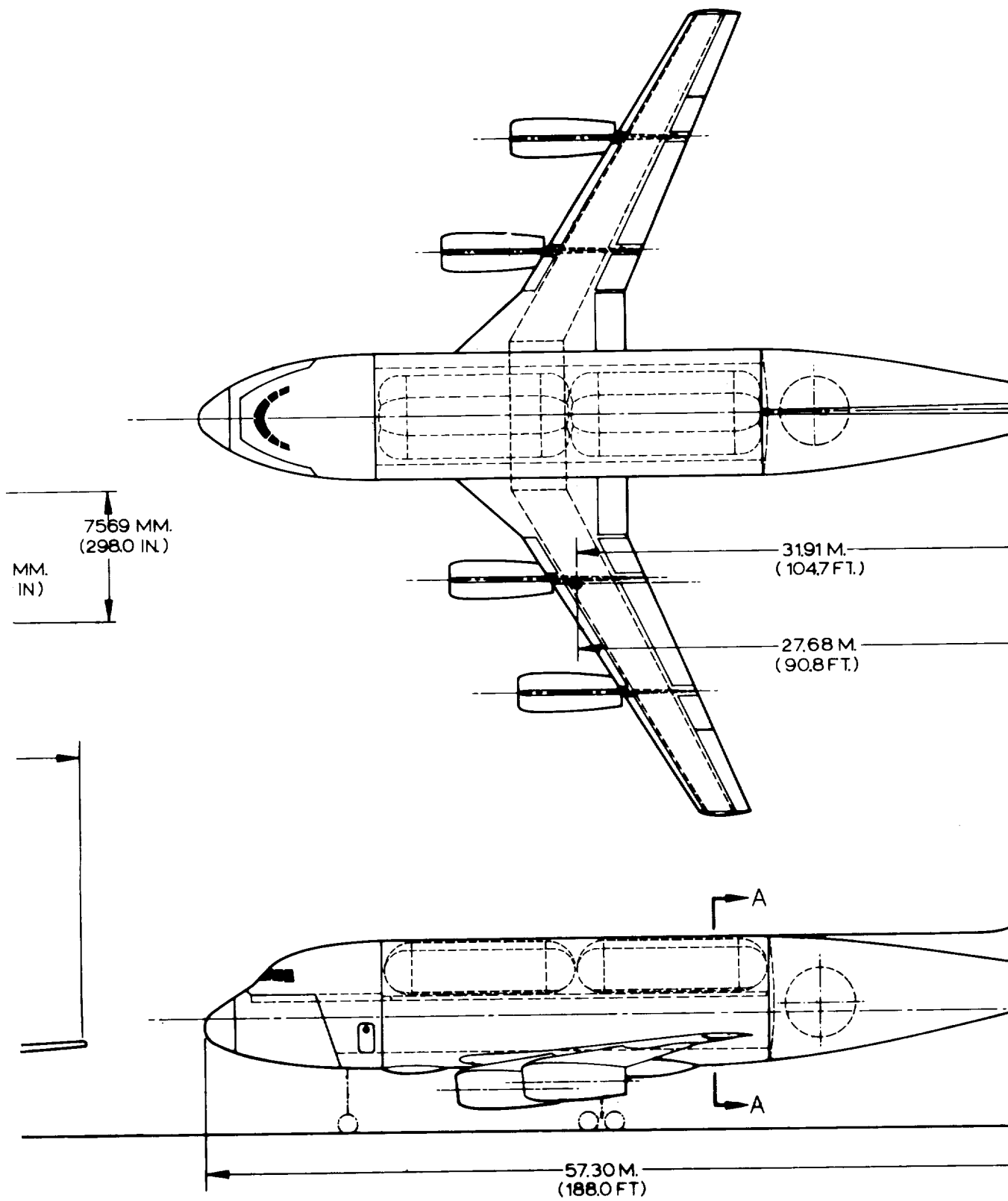
High lift devices on the wing leading and trailing edges are required to give adequate low-speed characteristics and handling qualities. These consist of a retractable leading-edge slat, and a double-slotted Fowler-type flap. Flight controls consist of a system of spoilers and ailerons for lateral control, an all-flying horizontal stabilizer having a geared elevator for longitudinal control, and a rudder system for directional control. The flight control systems are powered hydraulically by four independent systems to insure the necessary reliability. Electronic signaling, fly-by-wire, is used to activate the systems.

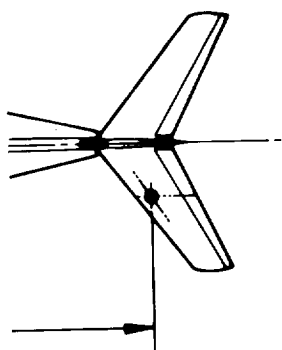
The flight station is arranged to accommodate a crew of three including a flight engineer. Inflight access from the flight station to the cargo compartment is provided.

The cargo compartment width and height are 5.60 and 3.05 m (18.5 and 10 ft) with lengths of 22.56 m (74 ft) and 43.9 m (144 ft) for the small and large aircraft, respectively. Cargo loading access to the compartment is provided by a full compartment cross-section nose visor door. The compartment dimensions are compatible with the loading of a double row of containers of sizes specified in Section 5.2. Compartment length allows the use of various container lengths, 12.20, 6.10, or 3.05 m (40, 20, or 10 ft). Full compartment length inflight cargo scanning aisles are provided along the outboard side of each row of containers.

Airconditioning and pressurization systems are provided for the flight station, cargo compartment, and the upper fuselage lobe liquid hydrogen tank compartment.







SURFACE CHARACTERISTICS

	<u>WING</u>	<u>HORIZ</u>	<u>VERT</u>
AREA-SQ.M.(SQ.FT.)	240.1(2584)	25.46(274)	34.47(371)
SWEEP-RAD.(DEG.)	0.52(30)	0.61(35)	0.61(35)
ASPECT RATIO	9.00	4.70	1.24
TAPER RATIO	0.40	0.40	0.80
t/c-%	11.49	8.5	8.5

VOLUME DATA

<u>ITEM</u>	<u>CU. M.</u>	<u>CU. FT.</u>
FWD TANK	97.5	3444
MID TANK	97.5	3444
AFT TANK	26.9	950
TOTAL	221.9	7838

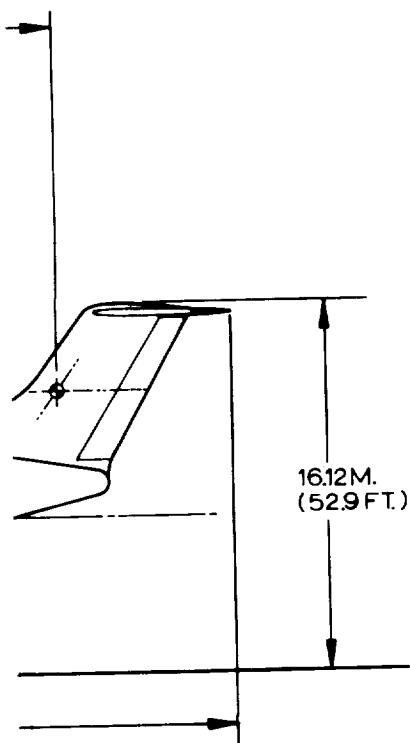
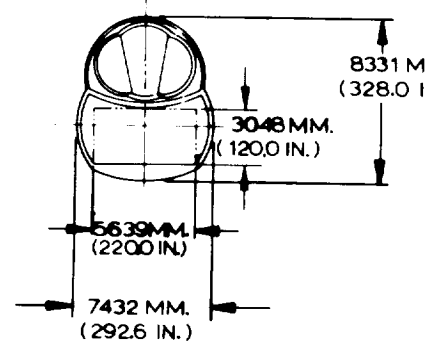
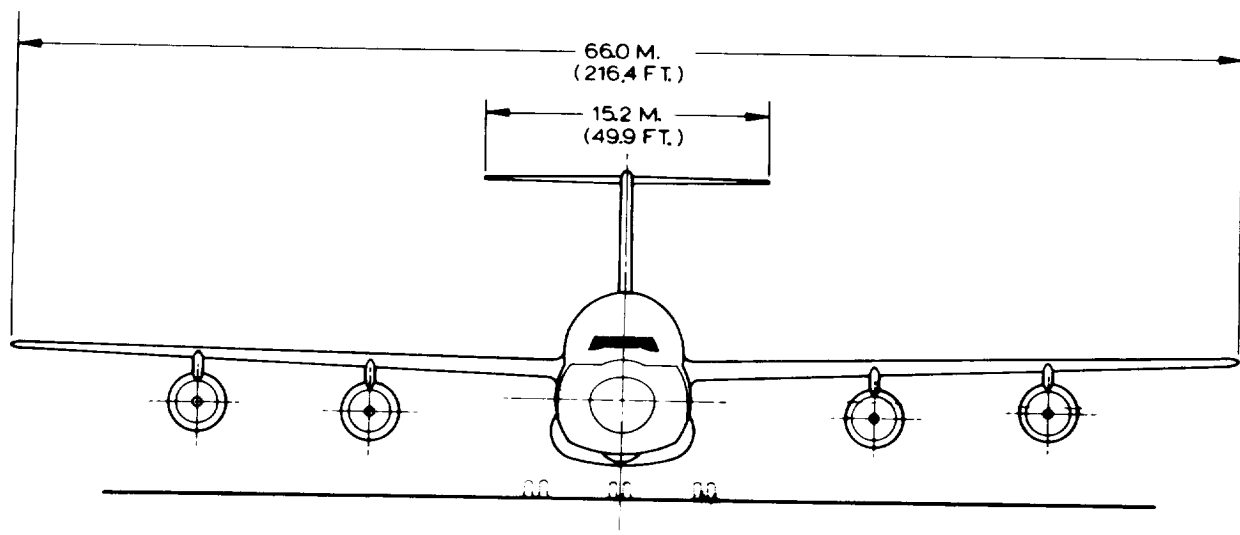


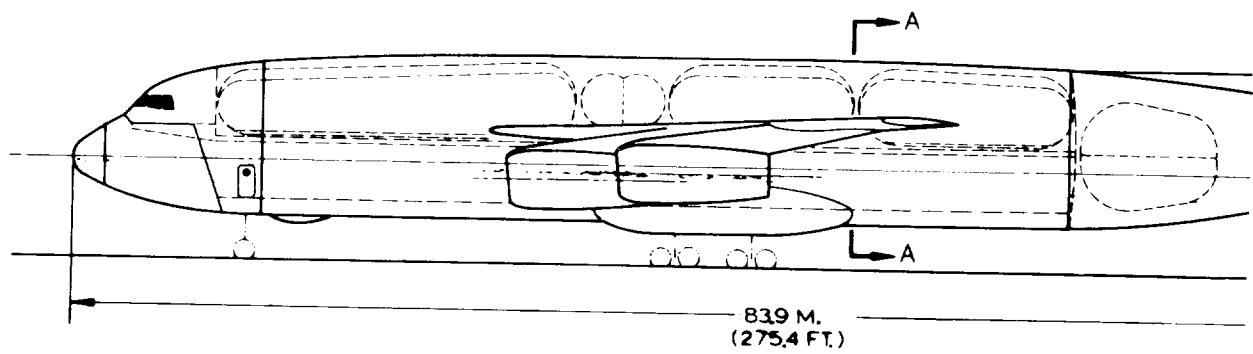
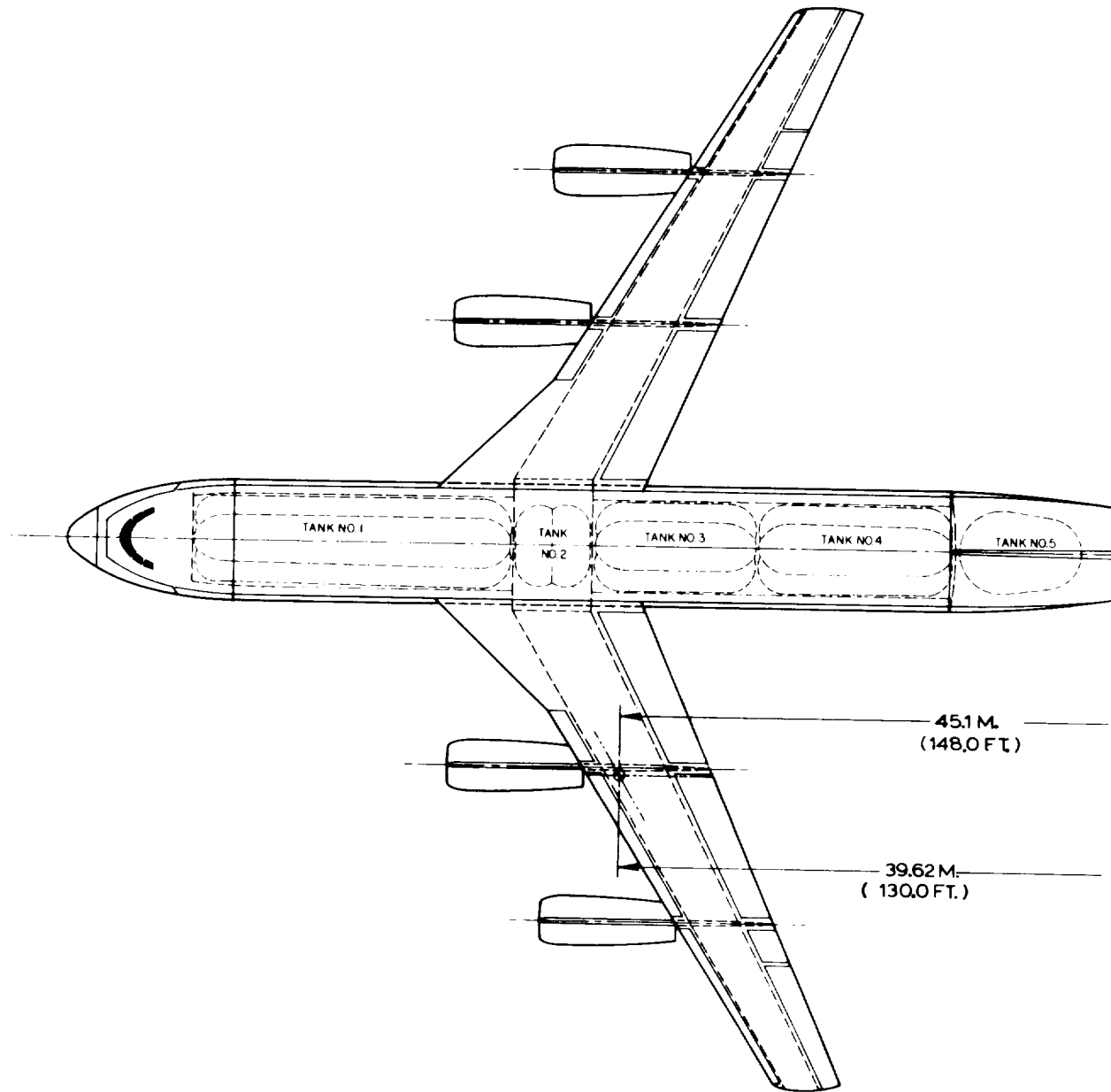
Figure 83. General Arrangement - LH₂ Fuel,
Cargo Transport, Small Nose Loader

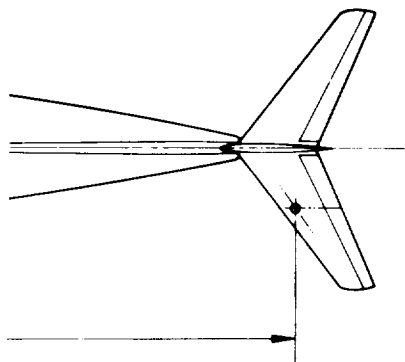


SECTION A-A

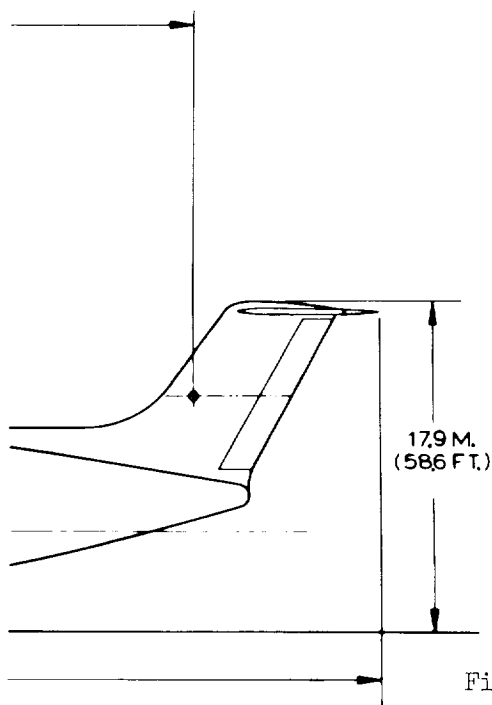


M.
N.)





	SURFACE CHARACTERISTICS		
	WING	HORIZ	VERT
ARE A - SQ. M. (SQ. FT.)	483.4 (5203)	49.2 (529)	65.2 (702)
SWEEP - RAD (DEG)	0.52 (30)	0.61 (35)	0.61 (35)
ASPECT RATIO	9.0	4.7	1.24
TAPER RATIO	0.4	0.4	0.8
t/c - %	11.07	8.5	8.5



ITEM	VOLUME DATA	
	CUM.	CU. FT.
TANK NO. 1	257.7	9,100
TANK NO. 2	51.7	1,825
TANK NO. 3	135.9	4,800
TANK NO. 4	152.9	5,400
TANK NO. 5	123.2	4,350
TOTAL	721.4	25,475

Figure 84. General Arrangement - LH₂ Fuel, Cargo Transport, Large Nose Loader

The tank compartment is pressurized by engine bleed air cooled to approximately the ambient stagnation temperature by a ram-air heat exchanger. The pressurized air enters the forward end of the tank compartment and exits at the aft end to provide continuous purging air flow. The tank compartment is separated from the cargo compartment by a horizontal bulkhead and is maintained at a pressure approximately 10.3 kPa (1.5 psi) below the cargo compartment such that any leakage is always from the cargo compartment to the tank compartment. Blow-out panels are provided in the separation bulkhead to prevent structural damage should decompression occur in either compartment. A single spherical tank is located in the unpressurized aft-fuselage section. The volume of this tank is minimized to maintain proper aircraft balance.

5.4.1.1 Liquid Hydrogen Tank Configuration Selection - The three-lobe hydrogen tank was selected for the nose loader aircraft based on evaluation of six aircraft configurations derived from three candidate hydrogen tank shapes and two tank isolation concepts. Each of the six aircraft were configured to perform the 56,700 kg (125,000 lb) payload 5,560 km (3,000 n.mi.) mission. Three hydrogen tanks were incorporated in each aircraft with a total volume of 232 m³ (8,200 ft³). Two tanks of various candidate shapes were located above the cargo compartment and a spherical shape tank was located in the aft fuselage of all aircraft. The various candidate tank shapes and the required fuselage configuration for each are shown in Figure 85. All tanks were designed to the following criteria:

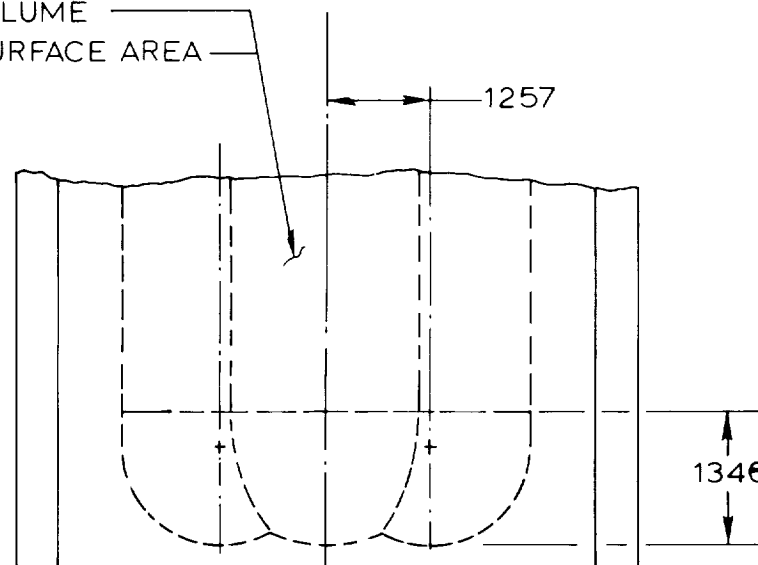
- Material - 2019 aluminum
- Minimum skin gage - 0.10 cm (0.04 in.)
- Construction - skin and stringer
- Pressure - 137.9 kPa (20 psia)
- Insulation - 15.24 cm (6 inch) thick closed-cell plastic foam
- Tank structure is non-integral with airframe structure

The two tank isolation concepts are defined as follows:

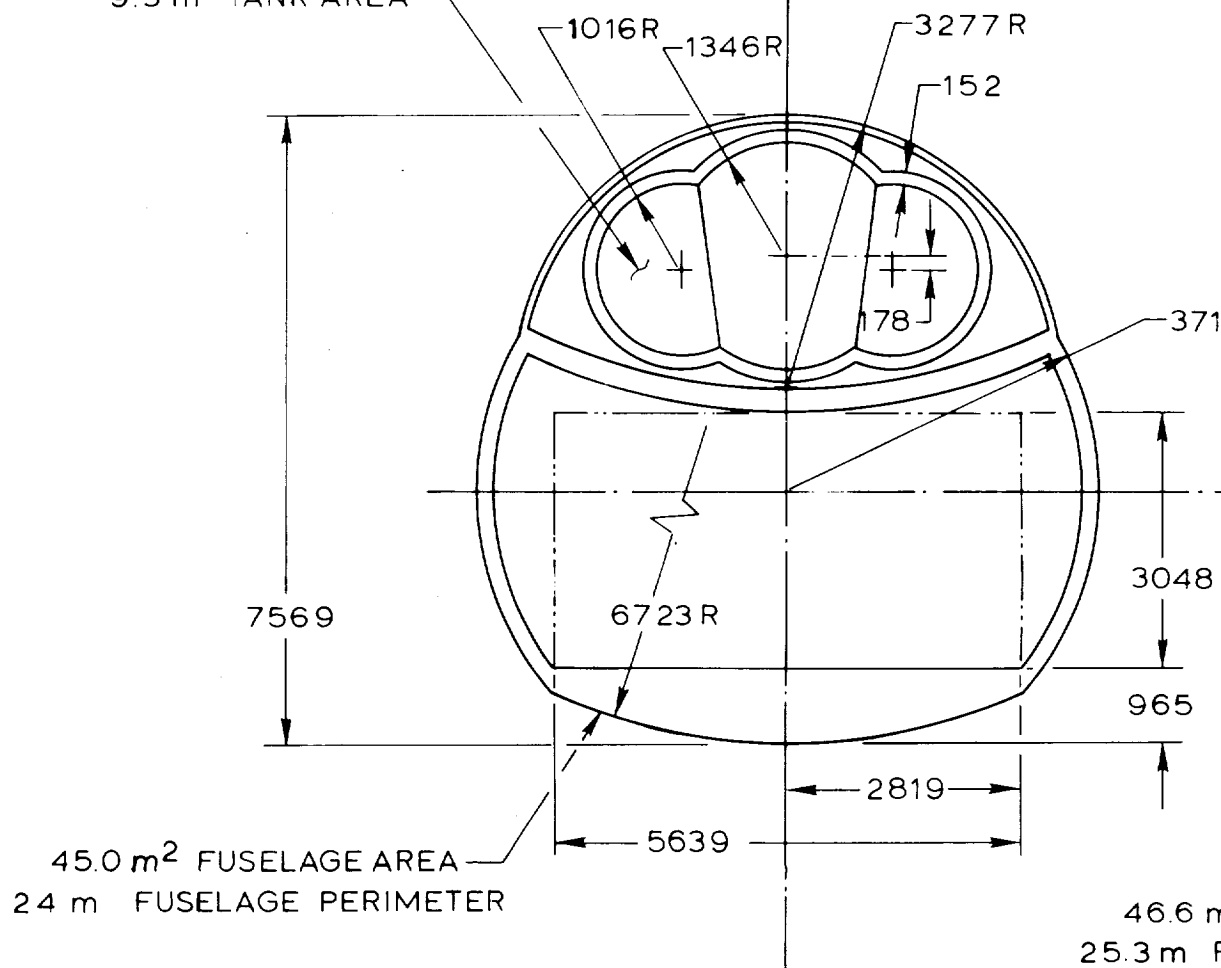
Concept 1 (Unpressurized)

As shown on Figure 85 each fuselage configuration is divided into two compartments, the cargo compartment and the hydrogen tank compartment. The upper or tank compartment is unpressurized,

97.5 m³ TANK VOLUME
129.4 m² TANK SURFACE AREA



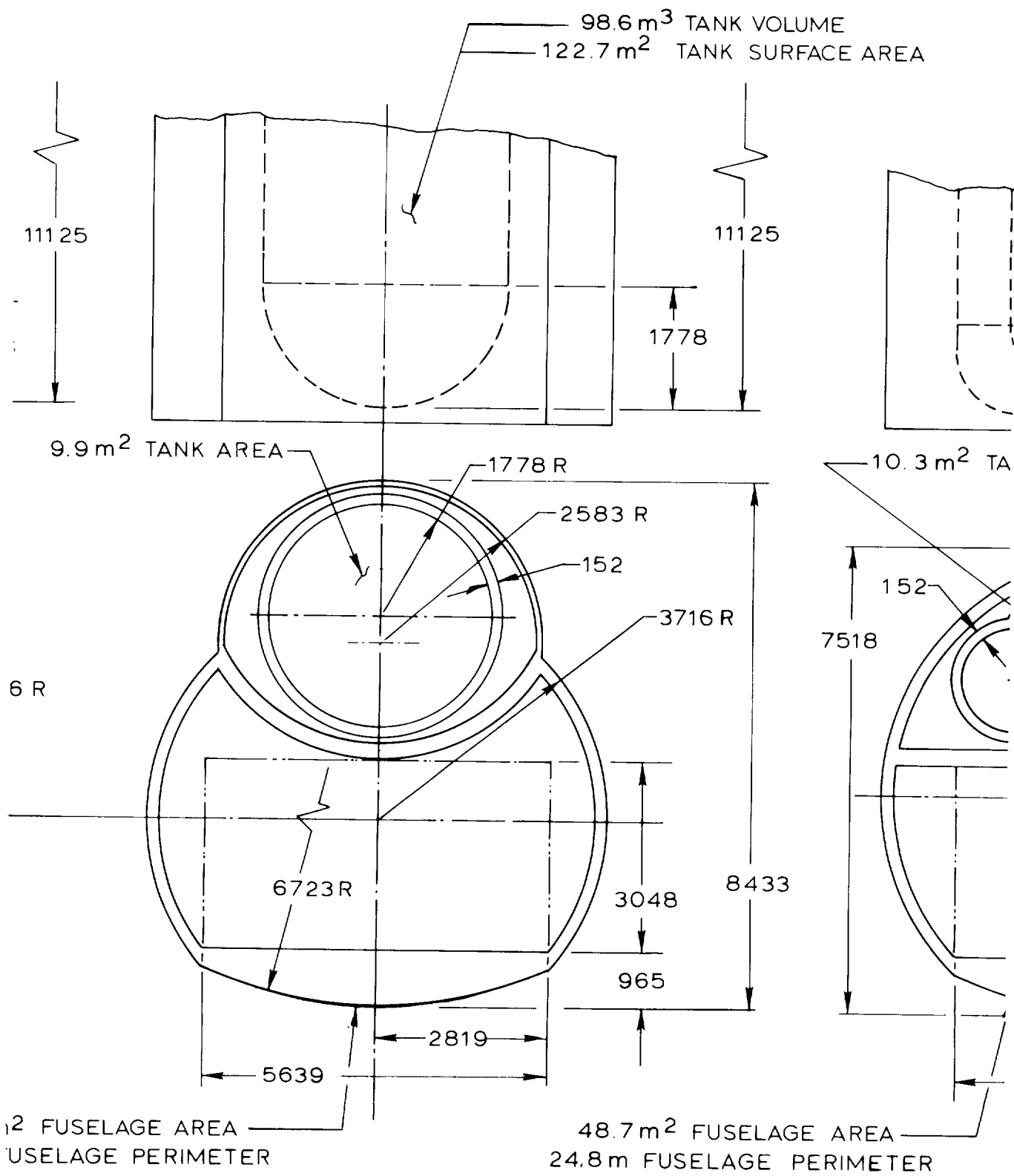
9.3 m² TANK AREA



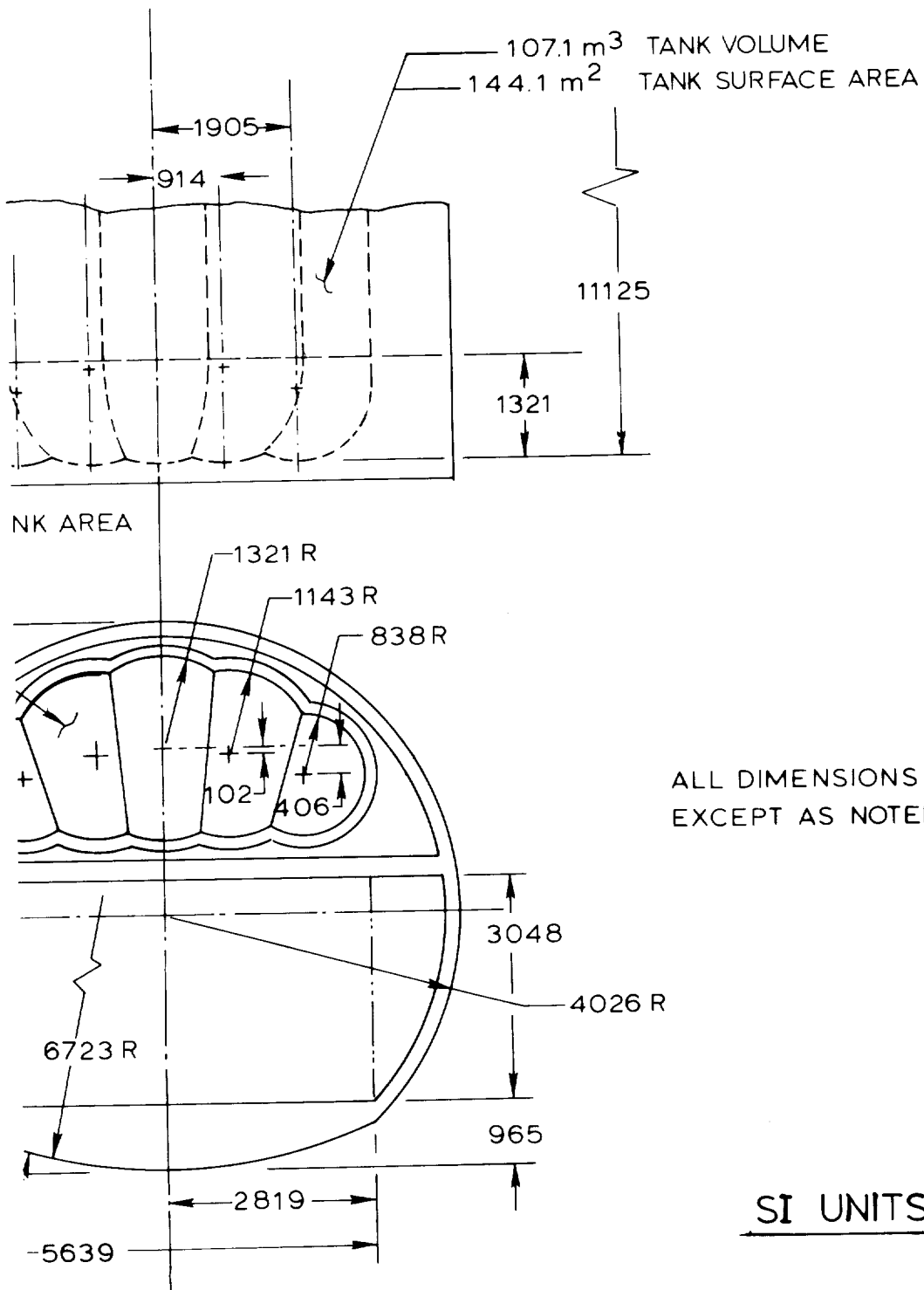
45.0 m² FUSELAGE AREA
24 m FUSELAGE PERIMETER

BASELINE

46.6 m
25.3 m F



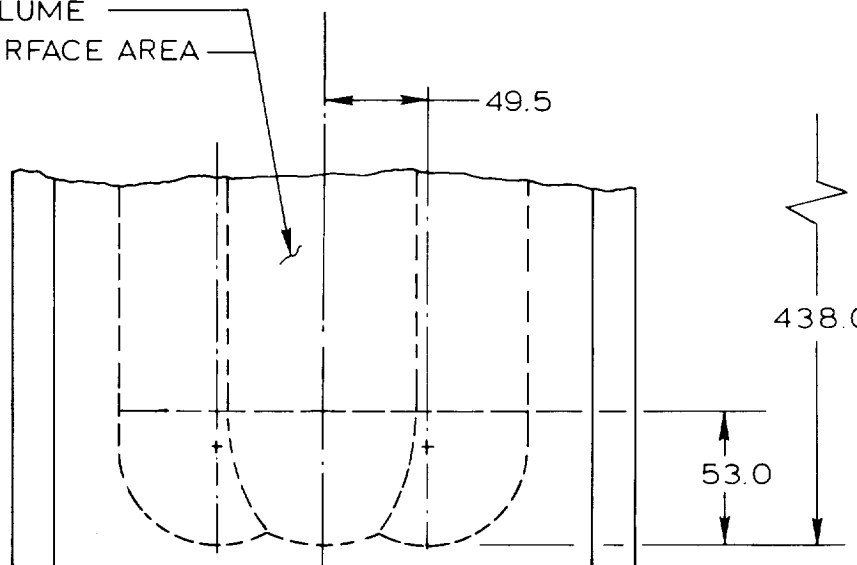
OPTION-1



OPTION -2

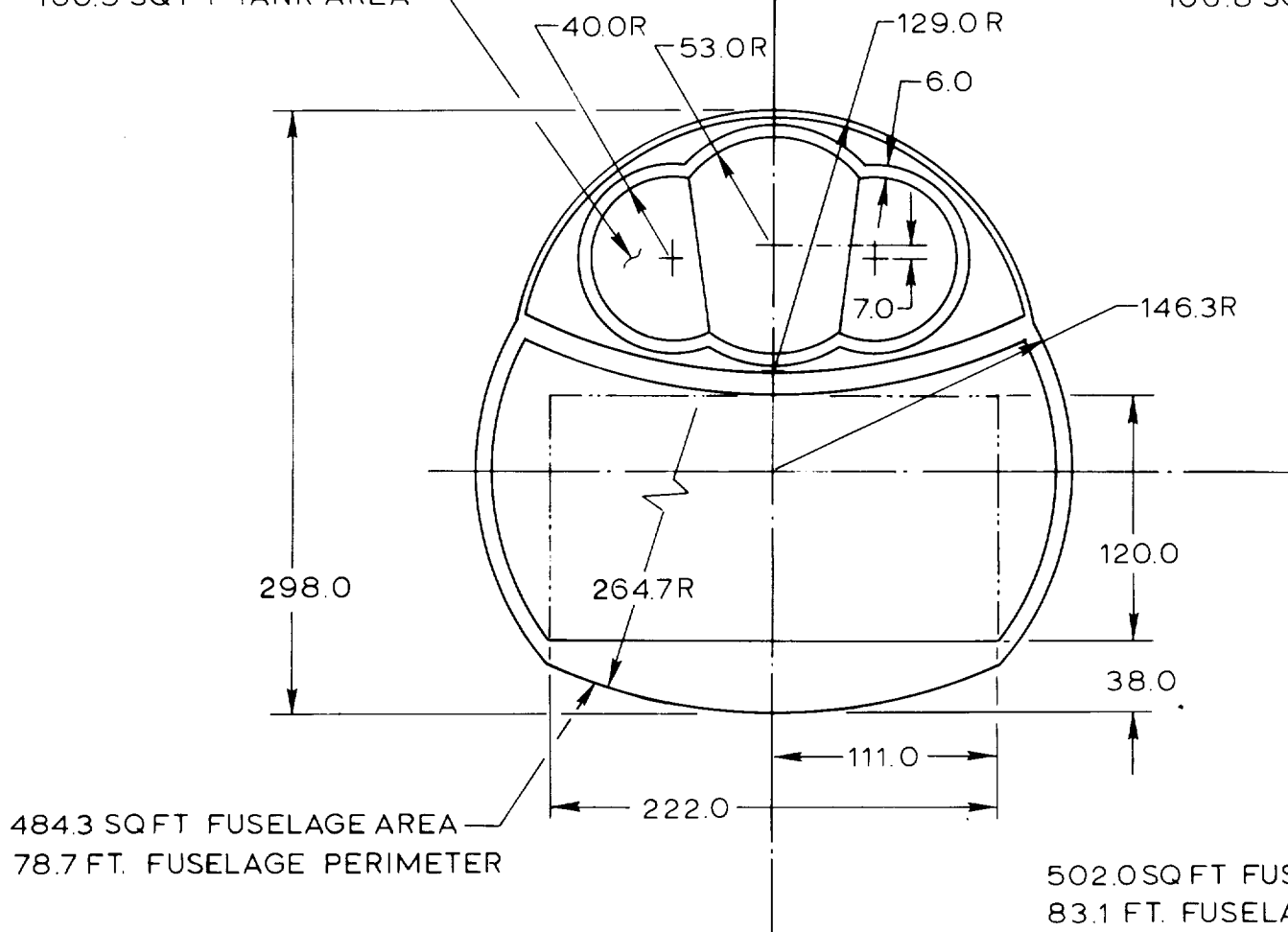
Figure 85. Candidate Hydrogen Tank Configurations (Sheet 1 of 2)

3444.0 CU FT. TANK VOLUME
1393.0 SQ FT TANK SURFACE AREA



100.5 SQ FT TANK AREA

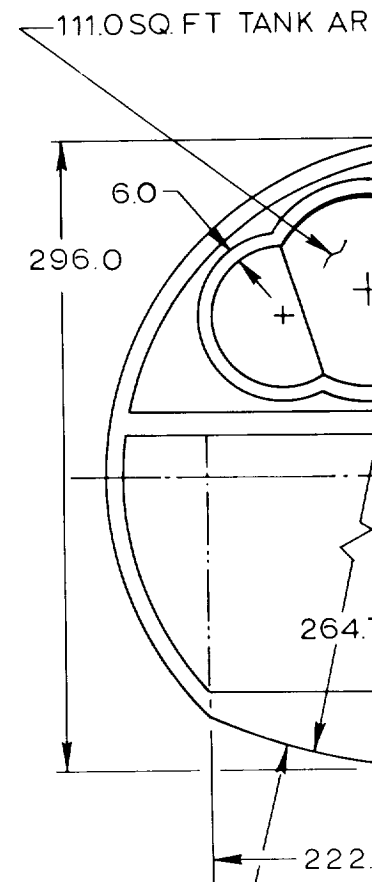
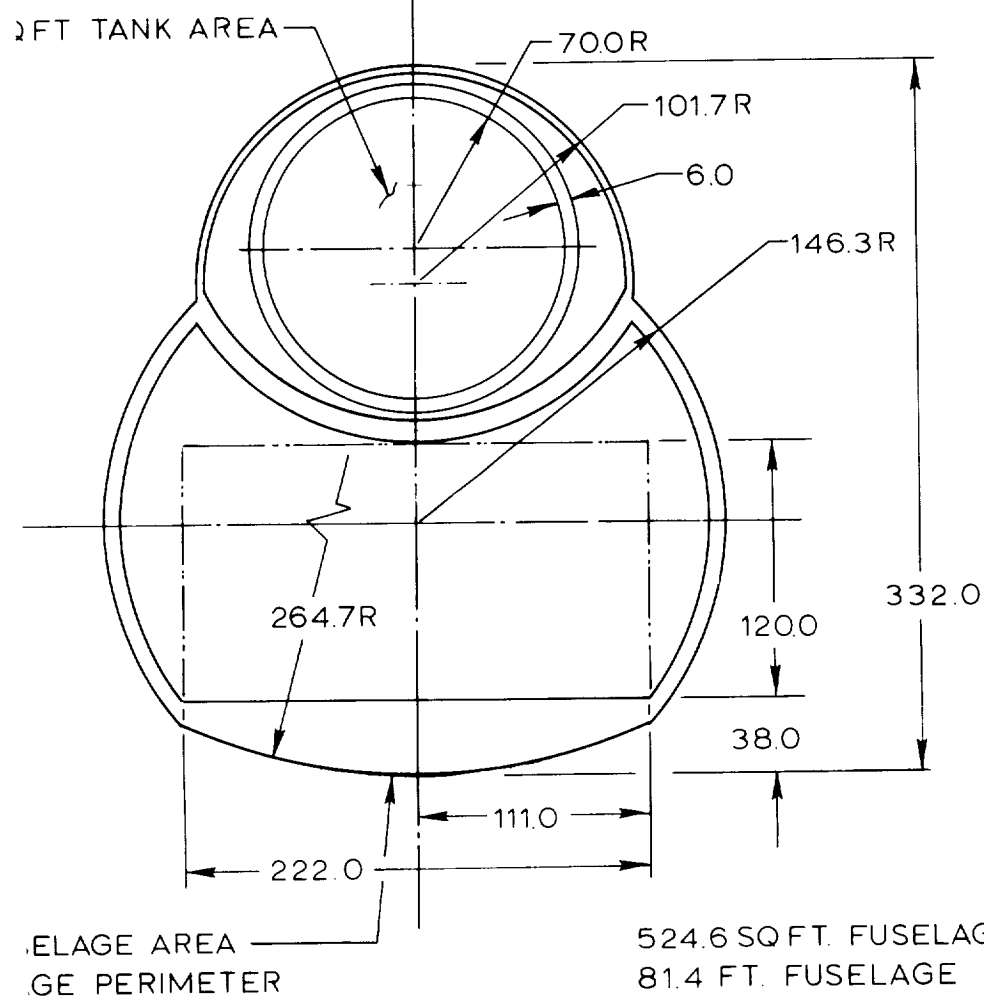
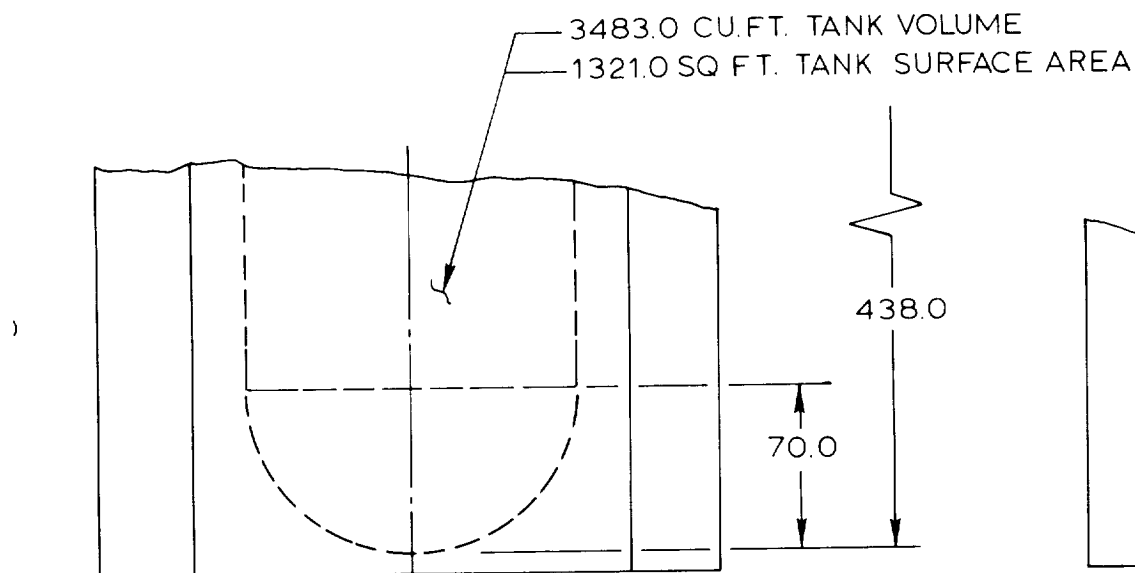
106.8 SQ



484.3 SQ FT FUSELAGE AREA
78.7 FT. FUSELAGE PERIMETER

502.0 SQ FT FUS
83.1 FT. FUSELA

BASELINE



OPTION -1

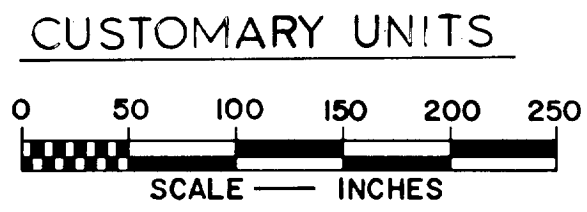
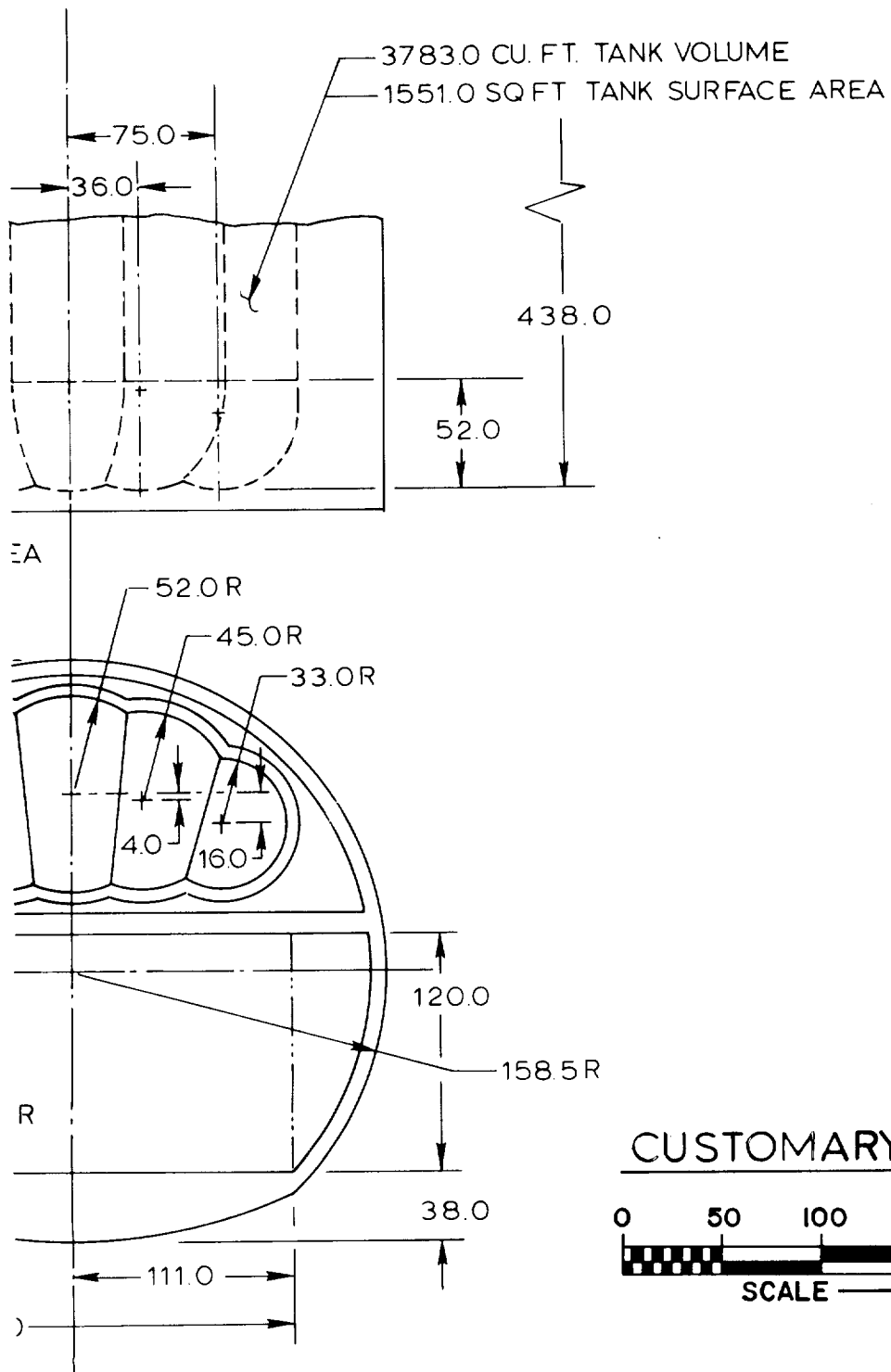


Figure 85. Candidate Hydrogen Tank Configurations (Sheet 2 of 2)

PTION - 2

therefore, the pressure bulkhead separating the cargo from the tank compartment provides the necessary means of isolating the hydrogen tanks. Tank shapes utilizing this concept are identified as baseline, Option 1, and Option 2 in subsequent tables.

Concept 2 (Pressurized)

For this concept both the tank and cargo compartments are pressurized. A pressure differential of approximately 10.3 kPa (1.5 psi) is maintained across the bulkhead separating the two compartments by maintaining a lower pressure in the tank compartment than is maintained in the cargo compartment. Leakage is always, therefore, from the cargo compartment to the tank compartment. Pressurization air flow provides a continuous purging of the tank compartment of any possible hydrogen gas accumulation. Blow-out panels are provided in the separation bulkhead for purposes of safety in the event of a compartment decompression failure. Tank shapes utilizing this isolation concept are identified in subsequent charts as Baseline-A, Options-1A, and Option-2A.

Hydrogen tank and fuselage characteristics data common to both tank isolation concepts, except as noted, are summarized on Tables 43 and 44.

Evaluation data for the six study aircraft are shown on Table 45. The data are in the form of differentials compared to Baseline and Baseline-A for Option 1, 1A, 2, and 2A. It can be readily seen from these data that common trends are established for both tank isolation concepts. The pressurized tank compartment, tank isolation concept 2, requires the minimum fuel and gross weight to perform the stated mission, therefore, only the evaluation data for this concept will be discussed in detail. Tank weight and boiloff fuel requirements for the baseline shape are greater than those of the cylindrical option 1A tank. This advantage is more than offset, however, by the lower weight of the baseline fuselage configurations as indicated by the summation of the boiloff fuel, tank, and fuselage weights. This sum is 1270 kg (2801 lb) greater for the cylindrical tank when compared to the baseline tank. The five-lobe option 2A tank exceeds the baseline tank in values for all comparison parameters and is thus eliminated.

TABLE 43. HYDROGEN TANK DATA — DESIGN OPTIONS

SI UNITS

	3-LOBE	CYLINDER	5-LOBE
<u>Fwd Tank</u>			
Section Area - m^2	9.3	9.9	10.3
Perimeter - m	11.89	10.97	13.2
Length - m	11.13	11.13	11.13
Surface Area - m^2	129.4	122.7	144.1
Volume - m^3	97.5	98.6	107.1
Weight - kg^*	1370.8	1346.3	1515
<u>Mid Tank</u>			
(Same as Fwd Tank)			
<u>Aft Tank</u>			
Diameter - m	4.14	3.99	3.25
Surface Area - m^2	53.8	50.0	33.2
Weight - kg^*	626	591	380.1
<u>Aircraft Total</u>			
Surface Area - m^2	312.6	295.4	321.4
Volume - m^3	232.2	232.2	232.2
Efficiency - m^3/m^2	2.44	2.58	2.37
Weight - kg^*	3367.5	3283.6	3410.1
*Includes 0.152 m insulation and tank mounting provisions			

TABLE 43. HYDROGEN TANK DATA — DESIGN OPTIONS (Continued)

CUSTOMARY UNITS

	3-LOBE	CYLINDER	5-LOBE
<u>Fwd Tank</u>			
Section Area - sq ft	100.5	106.8	111.0
Perimeter - ft	39.0	36.0	43.3
Length - ft	36.5	36.5	36.5
Surface Area - sq ft	1393	1321	1551
Volume - cu ft	3444	3483	3783
Weight - lb*	3022	2968	3340
<u>Mid Tank</u>			
(Same as Fwd Tank)			
<u>Aft Tank</u>			
Diameter - ft	13.58	13.09	10.66
Surface Area - sq ft	579	538	357
Weight - lb*	1380	1303	838
<u>Aircraft Total</u>			
Surface Area - sq ft	3365	3180	3459
Volume - cu ft	8200	8200	8200
Efficiency - cu ft/sq ft	2.44	2.58	2.37
Weight - lb*	7424	7239	7518
*Includes 6-inch insulation and tank mounting provisions			

TABLE 44. FUSELAGE DATA — TANK OPTIONS

CUSTOMARY UNITS			
	3-LOBE	CYLINDER	5-LOBE
Height - ft	24.83	27.67	24.67
Width - ft	24.38	24.38	26.42
Length - ft	170.7	172.4	174.6
Maximum Section Area - sq ft	484	502	525
Equivalent Diameter - ft	24.84	25.29	25.85
Maximum Perimeter - ft	78.7	83.1	81.4
Pressurized Volume - cu ft	29,623	34,098	34,539
Pressurized Volume - cu ft*	41,671	47,305	49,917
Surface Area - sq ft	11,877	12,657	12,546
SI UNITS			
	3-LOBE	CYLINDER	5-LOBE
Height - m	7.57	8.43	7.52
Width - m	7.43	7.43	8.05
Length - m	52.03	52.55	53.22
Maximum Section Area - m ²	44.97	46.64	48.77
Equivalent Diameter - m	7.57	7.71	7.88
Maximum Perimeter - m	23.99	25.33	24.81
Pressurized Volume - m ³	838.83	965.55	978.04
Pressurized Volume - m ³ *	1,179.99	1,339.53	1,413.49
Surface Area - m ²	1,103.41	1,175.87	1,165.56
*Pressurized configuration identified as Baseline-A, Opt 1A, and Opt 2A			

TABLE 1.5. AIRCRAFT DATA - TANK OPTIONS

SI UNITS

	UNPRESSURIZED*			PRESSURIZED*		
	BL	OPT-1	OPT-2	BL-A	OPT-1A	OPT-2A
Mission Fuel - kg	16,769	+449	+1036	16,180	+499	+480
% Boil Off	4.84	-0.26	+0.14	6.61	-0.67	+0.19
Boil Off Fuel - kg	812	-23	+75	1070	-79	+64
Tank Weight - kg	3367	-84	+43	3367	-84	+43
Fuselage Weight - kg	28,418	+553	+6081	21,080	+1433	+1342
B.O. + Tank + Fuselage - kg	32,597	+446	+6199	25,517	+1271	+1448
Operating Weight - kg	78,545	+1346	+8961	68,694	+2535	+2435
Gross Weight - kg	152,014	+1796	+9997	141,573	+3034	+2903
Required Volume - m ³	241.6	+6.5	+15	233.1	+7.2	+6.9
Available Volume - m ³	232.2	-	-	232.2	-	-
Volume Deficiency - m ³	9.4	+6.5	+15	0.9	+7.2	+6.9

*Upper Fuselage Compartment

TABLE 15. AIRCRAFT DATA - 1000 FEET (Continued)

CUSTOMARY UNITS

	UNPRESSURIZED*			PRESSURIZED*		
	BL	OPT-1	OPT-2	BL-A	OPT-1A	OPT-2A
Mission Fuel - lb	36,970	+990	+2285	35,670	+1101	+1059
% Boil Off	4.84	-0.26	+0.14	6.61	-0.67	+0.19
Boil Off Fuel - lb	1789	-51	+166	2358	-174	+140
Tank Weight - lb	7424	-185	+94	7424	-185	+94
Fuselage Weight - lb	62,651	+1220	+13,406	46,474	+3160	+2958
B.O. + Tank + Fuselage - lb	71,864	+984	+13,666	56,256	+2801	+3192
Operating Weight - lb	273,163	+2969	+19,755	151,444	+5588	+5368
Gross Weight - lb	335,133	+3959	+22,039	312,114	+6689	+6400
Required Volume - cu ft	8531	+229	+528	8231	+255	+245
Available Volume - cu ft	8200	-	-	8200	-	-
Volume Deficiency - cu ft	331	+229	+528	31	+255	+245

*Upper Fuselage Compartment

The three-lobe Baseline-A configuration requires both the minimum mission fuel and gross weight to perform the stated mission and is the selected configuration. The selected configuration and the remaining five study aircraft are all deficient in required fuel tank volume as shown on Table 45. The selected configuration requires an additional 0.88 m^3 (31 ft^3) with the other aircraft requiring from a minimum of 7.82 m^3 (276 ft^3) to a maximum of 24.32 m^3 (859 ft^3). Adjustments in these volumes were not made as the benefits of the selected configuration would only be further magnified from the resulting resizing effect of increased tank weight.

Caution should be used in the application of the above results to other studies. It is felt that an insufficient number of fuselage and tank shapes were studied to conclude that the multi-lobe tank would provide the optimum results under all conditions of mission definition, cargo compartment size, basic fuselage radius, and others.

5.4.1.2 Propulsion System - The propulsion system consists of four pylon wing-mounted by-pass ratio 12.95 engines of the type described in Section 3.2. The sizes selected for these applications have sea level static thrust ratings of 106,270 N ($23,800 \text{ lb}$) for the small aircraft and 212,180 N ($47,700 \text{ lb}$) for the large aircraft. Ground operable thrust reversers are incorporated into each installation.

At the design cruise altitude of 10,970 m ($36,000 \text{ ft}$) and cruise Mach number of 0.85, the specific fuel consumption for both aircraft is $0.213 \frac{\text{kg}}{\text{hr}}/\text{daN}$ ($0.209 \frac{\text{lb}}{\text{hr}}/\text{lb}$). Including inflight boiloff of the liquid hydrogen, these specifics become $0.219 \frac{\text{kg}}{\text{hr}}/\text{daN}$ ($0.215 \frac{\text{lb}}{\text{hr}}/\text{lb}$) and $0.213 \frac{\text{kg}}{\text{hr}}/\text{daN}$ ($0.219 \frac{\text{lb}}{\text{hr}}/\text{lb}$) for the small and the large cargo aircraft, respectively.

5.4.1.3 Hydrogen System - Hydrogen system technology is described in Section 3.1. The tank designs used for the nose loader cargo aircraft are of the non-integral type. They differ in concept from that employed in the passenger aircraft (Section 4) because of the irregular shape of the space available above the cargo compartment, and because the aft tank did not occupy the full cross section of the fuselage.

Tank size characteristics and fuel boiloff data are given in Tables 46 and 47 for the small and large nose loader aircraft, respectively. Tank volumes shown are greater than required to contain the stated fuel weight. The additional volume is that required for fluid expansion, tank contraction, structure and equipment allowance, and ullage. Inflight boiloff data are based upon a mission block time of 6.54 hours and an average fuel flow rate of 1,754 kg/hr (3867 lb/hr) for the small

TABLE 46. SMALL HYDROGEN NOSE LOADER TANK DATA

CUSTOMARY UNITS					
TANK DESCRIPTION	GROSS VOLUME cu ft	USABLE FUEL lb	SURFACE AREA sq ft	INFLIGHT BOILOFF lb	GROUND BOILOFF lb/hr
Fwd	3444	14276	1393	410	97
Mid	3444	14276	1393	410	97
Aft	950	3939	467	19	32
Total	7838	32491	3253	839	226
SI UNITS					
TANK DESCRIPTION	GROSS VOLUME m ³	USABLE FUEL kg	SURFACE AREA m ²	INFLIGHT BOILOFF kg	GROUND BOILOFF kg/hr
Fwd	97.5	6475	129.4	186	44
Mid	97.5	6475	129.4	186	44
Aft	26.9	1787	43.4	8.6	15
Total	221.9	14738	302.2	381	103

aircraft. Corresponding values for the large aircraft are 11.67 hours and 3364 kg/hr (7416 lb/hr). Closed-cell plastic foam 5.08 cm (six inches) thick is used for cryogenic insulation on all tank exterior surfaces.

5.4.3 Weight Statement

Weight prediction is accomplished through the utilization of weight parametric sizing subroutines included in the performance program described in Section 5.3. Weight methods are provided for estimating each aircraft component or structure and subsystem consistent with Mil-Std-1794 ASG (Group Weight Statement) (Reference 25) and the results are presented for each item in the specific format. The useful load items, or operating equipment items are included, along with the payload weight. The mission fuel is input from the performance subroutines. Group

TABLE 47. LARGE HYDROGEN NOSE LOADER TANK DATA

CUSTOMARY UNITS					
TANK DESCRIPTION*	GROSS VOLUME cu ft	USABLE FUEL lb	SURFACE AREA sq ft	INFLIGHT BOILOFF lb	GROUND BOILOFF lb/hr
1	9100	38561	2740	1420	192
2	1825	7733	615	95	43
3	4800	20340	1370	840	96
4	5400	22883	1640	995	115
5	4350	18433	1250	220	87
Total	25475	107950	7615	3530	533
SI UNITS					
TANK DESCRIPTION*	GROSS VOLUME m ³	USABLE FUEL kg	SURFACE AREA m ²	INFLIGHT BOILOFF kg	GROUND BOILOFF kg/hr
1	257.7	17490	254.6	644	87
2	51.7	3508	57.1	43	19.5
3	135.9	9276	127.3	381	34
4	152.9	10380	152.4	433	52
5	123.7	8361	116.1	100	39
Total	721.4	48965	707.5	1601	242

* See Figure 84

Weight Statements for the small and large nose loader aircraft are given on Tables 48 and 49.

5.4.3 Performance

The performance characteristics of the final design of LH₂ fueled nose loader aircraft are summarized herein. These data are provided for the final aircraft; minor differences from the characteristics of the parametric series of aircraft defined in Table 42 resulted from final iteration and refinements of the selected aircraft.

TABLE 48. GROUP WEIGHT STATEMENT: SMALL HYDROGEN NOSE LOADER

56,700 kg Payload, 5560 km Range, Mach 0.85 Speed
 (125,000 lb Payload, 3000 n m Range, Mach 0.85 Speed)

ITEM	KILOGRAM	POUND
Structure	40,660	89,639
Wing	11,273	24,853
Empennage	1,537	3,389
Horizontal Tail	724	1,597
Vertical Tail	813	1,792
Fuselage	18,927	41,726
Landing Gear	6,611	14,575
Nose	860	1,895
Main	5,752	12,680
Nacelle and Pylon	2,312	5,096
Nacelle	883	1,946
Pylon	1,429	3,150
Propulsion System	13,940	30,732
Engines	7,756	17,099
Fuel System	933	2,057
Thrust Reversers	703	1,549
Inlet	896	1,975
Oil Tanks	3,470	7,650
Miscellaneous	182	402
Systems and Equipment	8,334	18,373
Auxiliary Power System	234	516
Surface Controls	1,597	3,522
Instruments	337	742
Hydraulics and Pneumatics	745	1,642
Electrical	1,200	2,646
Avionics	987	2,175
Furnishings	1,807	3,983
Airconditioning and AI	1,377	3,036
Auxiliary Gear - Equipment	50	111
Weight Empty	62,934	138,744
Operating Equipment	1,691	3,732
Operating Weight	64,625	142,476
Cargo Payload	56,700	125,000
Zero Fuel Weight	121,325	267,476
Fuel	14,449	31,854
Gross Weight	135,774	299,330

TABLE 49. GROUP WEIGHT STATEMENT: LARGE HYDROGEN NOSE LOADER

113,400 kg Payload, 10,190 km Range, Mach 0.85 Speed
 (250,000 lb Payload, 5500 n mi Range, Mach 0.85 Speed)

ITEM	KILOGRAM	POUND
Structure	92,848	204,701
Wing	32,390	71,409
Empennage	2,943	6,490
Horizontal Tail	1,456	3,211
Vertical Tail	1,487	3,279
Fuselage	38,473	84,819
Landing Gear	14,197	31,301
Nose	1,845	4,069
Main	12,352	27,232
Nacelle and Pylon	4,845	10,682
Nacelle	1,850	4,079
Pylon	2,995	6,603
Propulsion System	31,066	68,489
Engines	16,257	35,841
Fuel System	1,544	3,403
Thrust Reversers	1,473	3,247
Inlet	1,878	4,140
Oil Tanks	9,538	21,028
Miscellaneous	377	830
Systems and Equipment	11,535	25,428
Auxiliary Power System	366	806
Surface Controls	2,853	6,289
Instruments	406	894
Hydraulics and Pneumatics	1,329	2,931
Electrical	1,519	3,349
Avionics	987	2,175
Furnishings	2,345	4,950
Airconditioning and AI	1,719	3,789
Auxiliary Gear - Equipment	111	245
Weight Empty	135,349	298,618
Operating Equipment	3,214	7,087
Operating Weight	138,663	305,705
Cargo Payload	113,400	250,000
Zero Fuel Weight	252,063	555,705
Fuel	48,005	105,832
Gross Weight	300,068	661,537

Both the large and the small aircraft are constrained by the 69.5 m/s (135 knot) approach speed consideration. The small aircraft has a relatively high thrust-to-weight ratio which results from cruise matching at a relatively high altitude coupled with its poorer L/D ratio. As a result, the takeoff distance is much shorter than the specified requirement and it has been compromised by selection of a low flap setting of 0.21 radians (12 degrees) which will result in good climb out characteristics and relatively good noise characteristics. The thrust of the large aircraft is more nearly matched to meet both cruise and takeoff requirements and a much larger takeoff distance results. A higher flap deflection of 0.35 radians (20 degrees) has been selected for this aircraft. The takeoff distances were determined using commercial rules at a field elevation of 305 m (1000 ft) and an ambient temperature of 305⁰K (90⁰F) and are 1768 and 2185 m (5800 and 7170 ft) for the small and large aircraft, respectively. The landing distances at the same ambient conditions and with commercial rules, are 2231 and 2304 m (7320 and 7560 ft), respectively, for the small and large aircraft. The landing flap deflection is 0.3 radians (10 degrees). As previously discussed, a larger fuel percentage is included in the landing weight of the small aircraft than for the large aircraft.

A payload-range diagram, including block fuel characteristics, for the hydrogen none loader aircraft is given in Figure 86. These data have been defined for the design mission, a ferry mission, and a short range point carrying full payload; because of the limited data generated in the parametric analysis, the exact curvature of the payload range curves has not been defined and the diagram is schematically presented.

The diagram defines the maximum payload allowed for the structural weight provided. Since fuel volume requirements are critical in a hydrogen fueled aircraft, the fuel capacity has been defined by the design mission; all missions at or beyond the design point range utilize the total fuel capacity of the aircraft.

A summary of the aerodynamic characteristics of these aircraft is given in the following table.

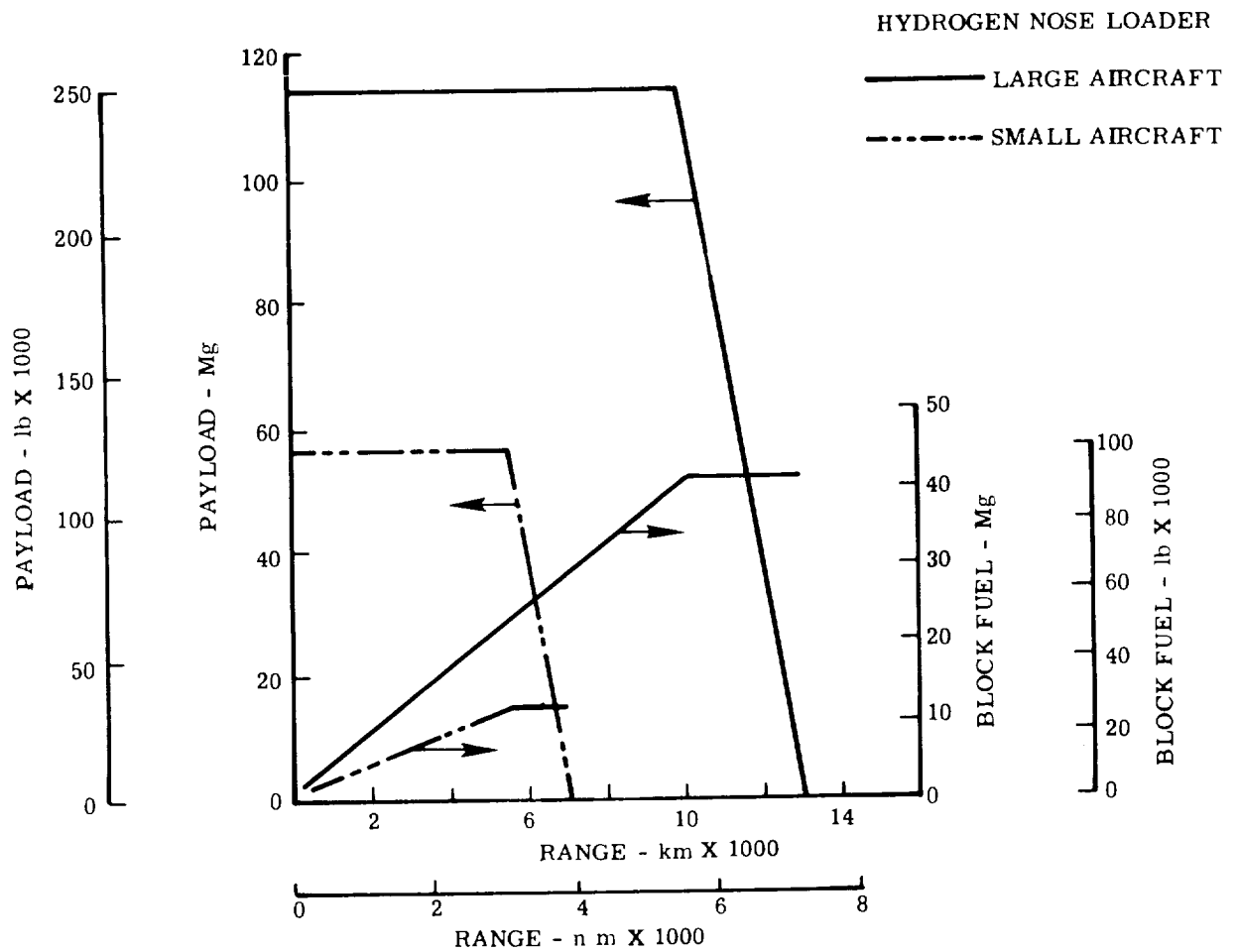


Figure 86. Payload - Range/Block Fuel: Nose Loader Aircraft

AERODYNAMIC CHARACTERISTICS: HYDROGEN-NOSELOADER

	SMALL	LARGE
Wing Area - m^2 (ft^2)	240.06 (2584)	483.38 (5203)
Wing t/c - Percent	11.49	11.07
Wing Aspect Ratio	9	9
Initial Cruise Wing Loading - kg/m^2	558.60	613.42
Initial Cruise Wing Loading - lb/ft^2	114.42	125.65
Initial Cruise C_L	.475	.522
Initial Cruise L/D Ratio	16.29	18.03

5.4.4 Aircraft Price and Operating Cost

Unit price for the small aircraft is 19.2 million dollars and for the large aircraft 39.1 million dollars. Elements of these unit prices are given in Table 50. Direct operating cost for the small and large aircraft are respectively, 3.36 and 7.89 $\$/Mgkm$ (5.65 and 4.86 C/Ton n.mi.), based upon a yearly utilization of 3600 and 4000 hours and stage lengths of 5,560 and 10,190 kilometers (3000 and 5500 nautical miles), and the cost of HH_2 specified in the study guidelines.

5.5 HYDROGEN SWING TAIL CONFIGURATION

5.5.1 Configuration Description

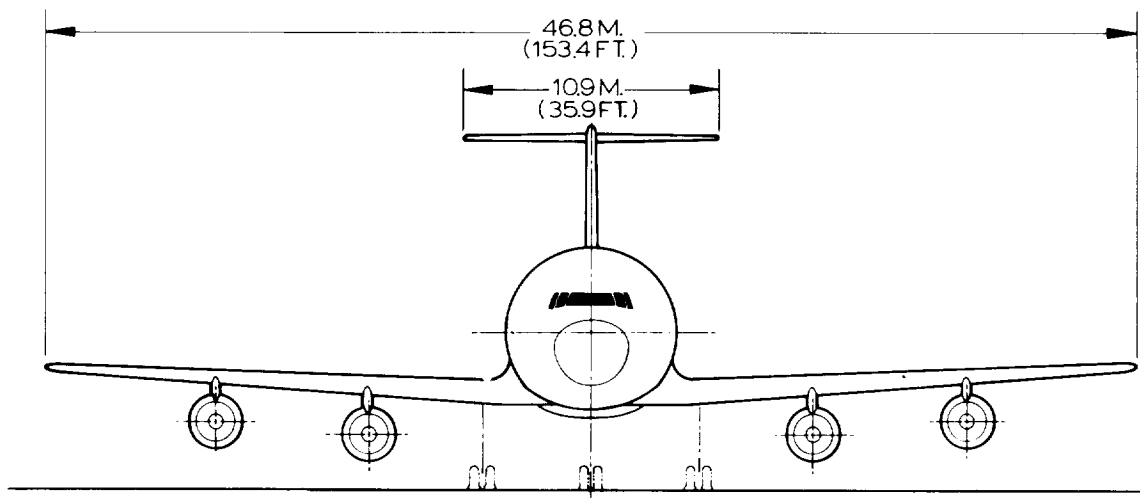
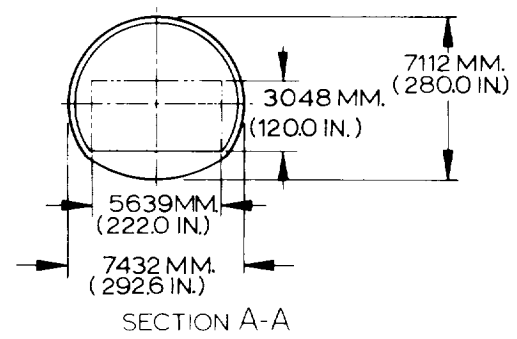
The swing tail aircraft shown in Figures 87 and 88 are configured to satisfy the same mission profiles as the nose loader aircraft just described. Again, both aircraft have a cruise speed capability of Mach 0.85. The configuration descriptions are identical to comparable hydrogen nose loader aircraft described in Paragraph 5.4.1 with the following exceptions:

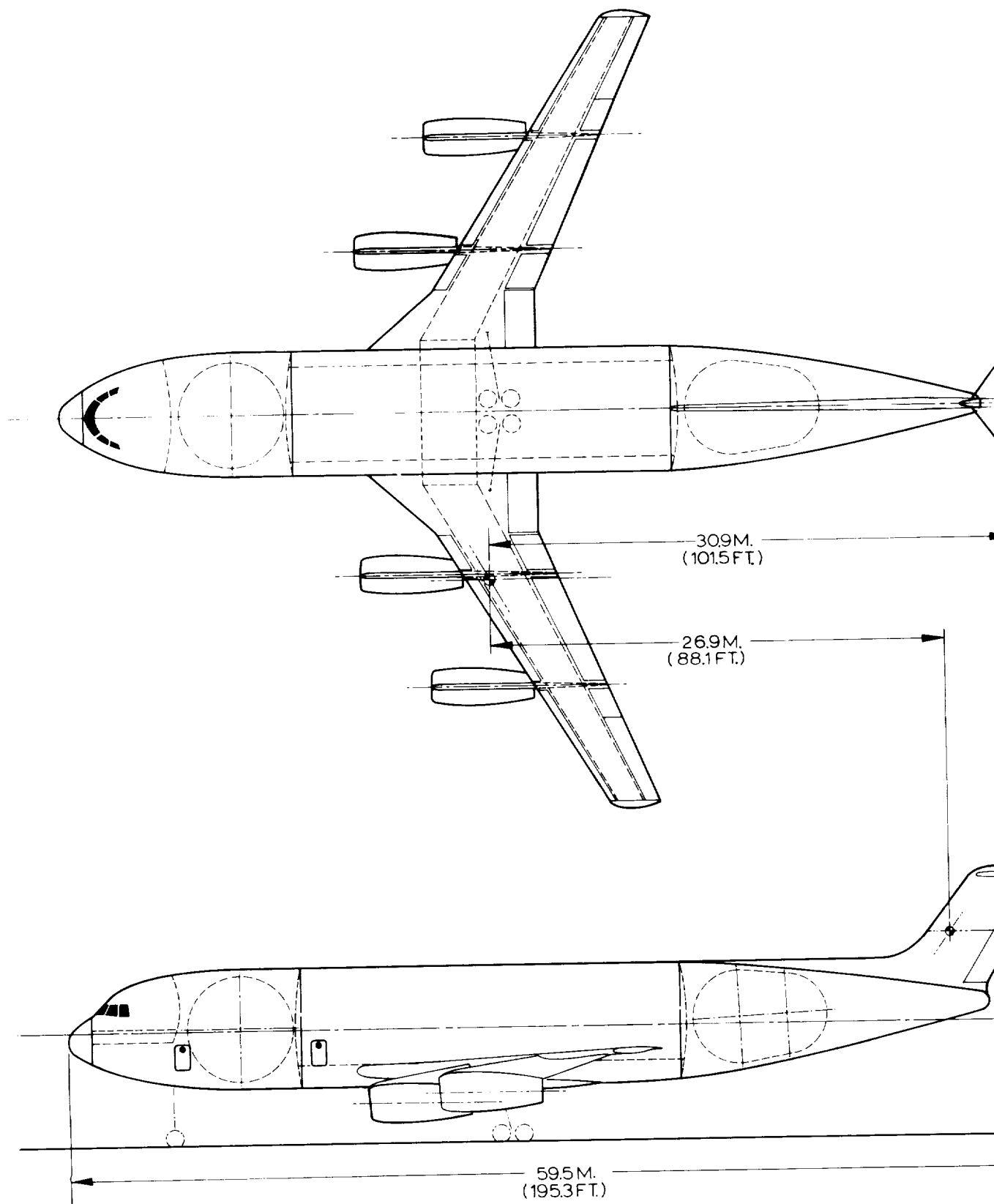
- Tank configuration and location
- High wing position for large aircraft

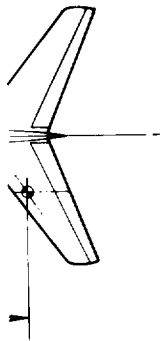
TABLE 50. PRICE SUMMARY — HYDROGEN NOSE LOADER AIRCRAFT

		COST IN \$10 ⁶	
	RANGE	SMALL	LARGE
<u>Development</u>			
Airframe		\$540.6	\$1,033.7
Engine		390.0	578.3
Avionics		-	-
Total		\$930.6	\$1,612.0
<u>Production</u>			
Airframe Manufacturing Cost		\$ 8.6	\$ 18.4
Other Airframe Cost		4.8	10.4
Sustaining Engineering		0.6	1.3
Tool Maintenance		0.8	1.8
Quality Assurance		0.9	1.8
Miscellaneous		0.2	0.5
Profit		1.7	3.8
Warranty		0.6	1.2
Engine		3.0	5.6
Avionics		0.5	0.5
Subtotal		\$ 16.9	\$ 34.9
R&D per Aircraft*		2.3	4.2
Total Aircraft Price		\$ 19.2	\$ 39.1

*Based on 350 aircraft and 2000 engines







SURFACE CHARACTERISTICS

<u>ITEM</u>	<u>WING</u>	<u>HORIZ.</u>	<u>VERT.</u>
AREA - SQ. M. (SQ. FT.)	242.94 (2615)	25.46 (2740)	34.26 (368.8)
SWEEP - RAD(DEG.)	0.52 (30)	0.61 (35)	0.61 (35)
ASPECT RATIO	9.00	4.70	1.24
TAPER RATIO	0.4	0.4	0.8
t/c - %	11.49	8.5	8.5

VOLUME DATA

<u>ITEM</u>	<u>CU. M.</u>	<u>CU. FT.</u>
FWD TANK	113.27	4000
AFT TANK	113.27	4000
TOTAL	226.54	8000

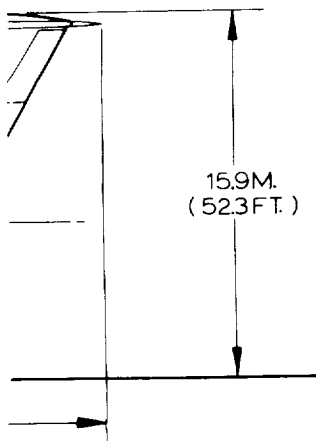
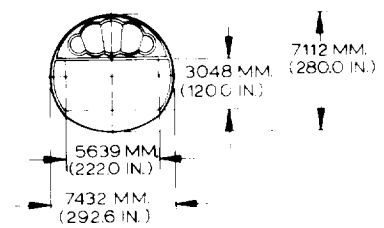
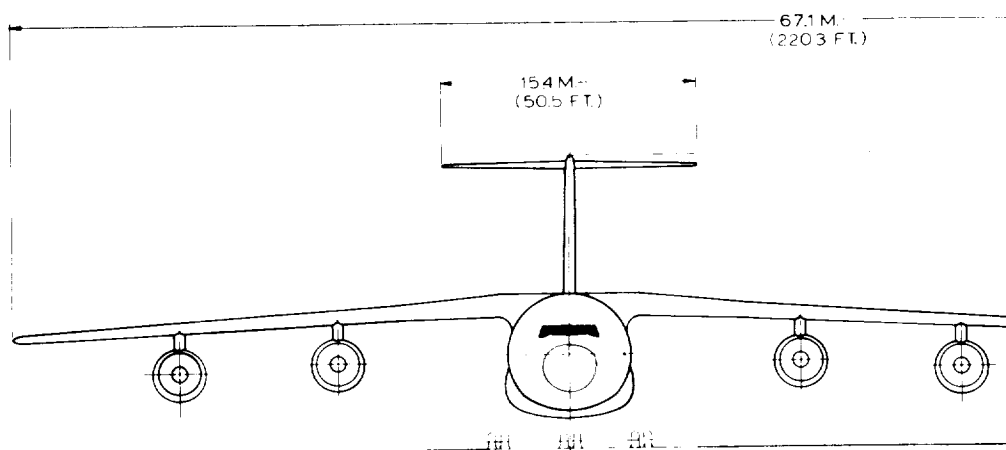
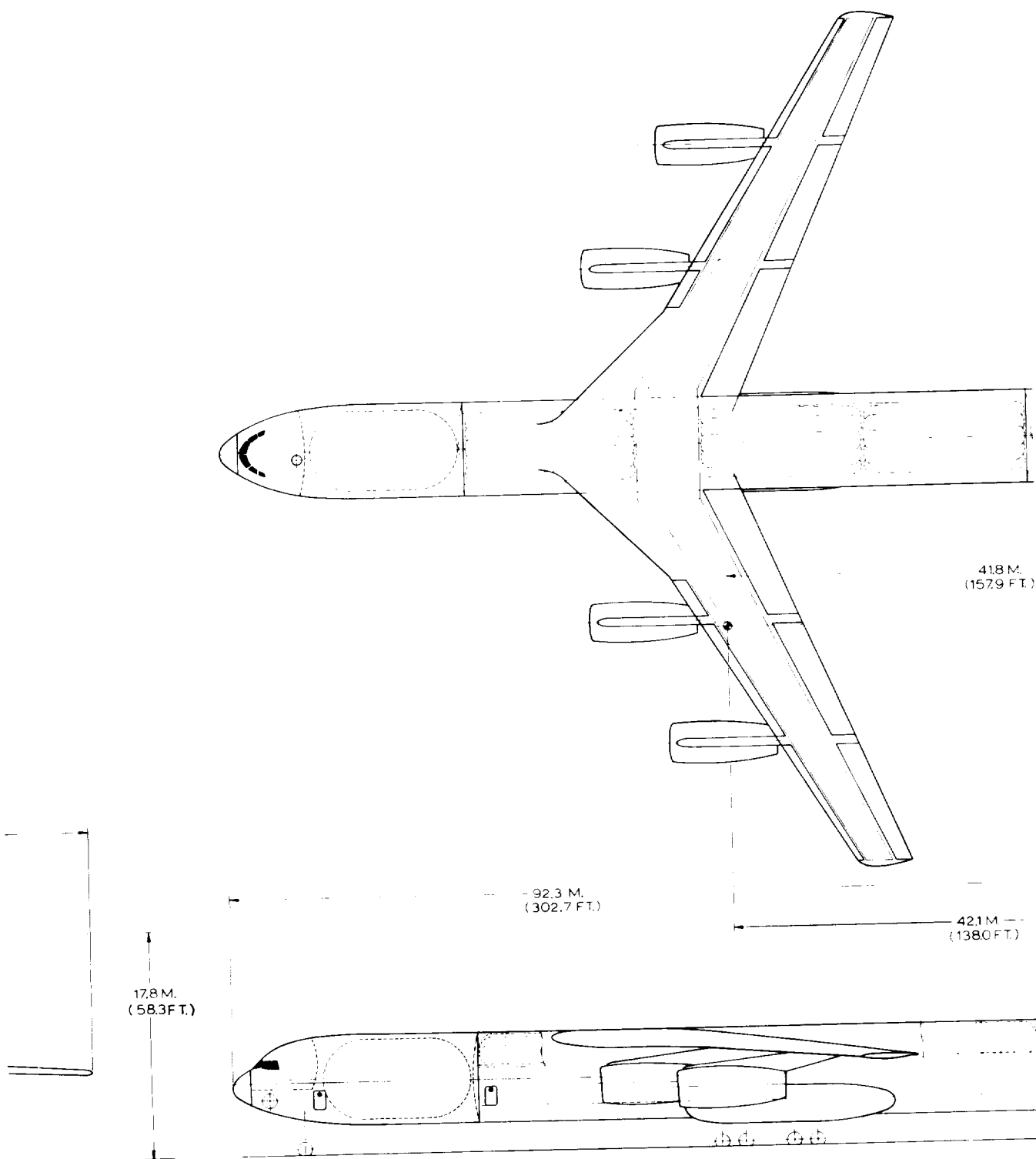


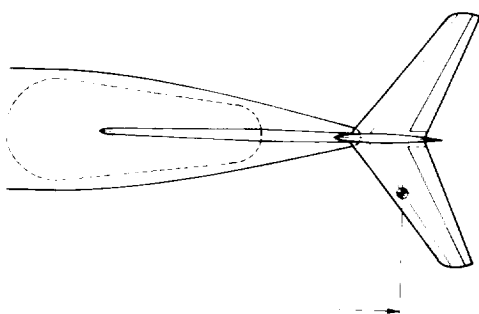
Figure 87. General Arrangement - LH₂ Fuel,
Cargo Transport, Small Swing Tail



SECTION A-A







SURFACE CHARACTERISTICS

	<u>WING</u>	<u>HORIZ.</u>	<u>VERT.</u>
AREA - SQ M (SQ FT)	498.6 (5367)	48.3 (520)	639 (688)
SWEEP RAD. (DEG.)	0.52 (30)	0.61 (35)	0.61 (35)
ASPECT RATIO	90	47	124
TAPER RATIO	04	04	08
t/c %	11.07	85	85

VOLUME DATA

<u>ITEM</u>	<u>CU. M.</u>	<u>CU. FT.</u>
FWD SECTION TANK	263.0	9287
CENTER SECTION-		
FWD TANK	868	3066
MID TANK	81.0	2861
AFT TANK	81.0	2861
AFT SECTION TANK	235.7	8325
TOTAL	747.5	26400

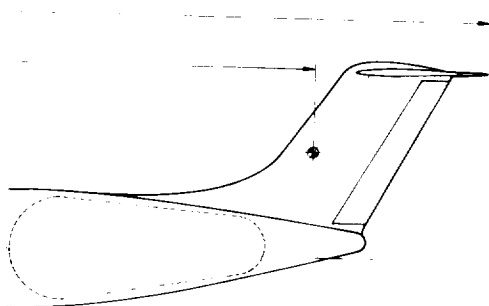


Figure 88. General Arrangement - LH₂ Fuel,
Cargo Transport, Large Swing Tail

- Access to cargo compartment
- Areas of pressurization

The small aircraft has two equal volume tanks located in unpressurized areas immediately forward and aft of the cargo compartment. The forward tank is spherical in shape while the aft conforms closely to the aft fuselage taper and consists of spherical end domes of slightly different diameters connected by a tapering section. The large aircraft also has two tanks located in unpressurized areas fore and aft of the cargo compartment and, in addition, has three multilobe tanks located above the cargo compartment. The fuel is essentially balanced around the cg of the aircraft for both cargo transport versions.

The high wing position for the large aircraft was dictated by the requirement for proper engine nacelle ground clearance while not exceeding a 4.72 meter maximum cargo floor height above the ground.

Cargo access to the aircraft is provided by swinging the tail horizontally 1.57 radians (90 degrees). The service to the tail section is continuous and is not disconnected at any time. This includes control cables, electrical service, hydraulic, fuel and vent lines.

The center fuselage, which contains the cargo compartment, is pressurized and has a dome on either extreme. The flight station is also pressurized but is separated from the cargo compartment by an unpressurized area containing the forward LH₂ tank. This prevents inflight access to the cargo compartment.

Five-lobe tanks were selected for use in the large swing tail aircraft due to the restricted area above the cargo compartment. A tradeoff of added boiloff due to the increased surface-to-volume ratio of the tanks versus the increased fuselage length required to contain the required fuel in more efficient three-lobe tanks indicated that complete utilization of the area above the cargo compartment was the more cost effective solution.

5.5.1.1 Propulsion System - The propulsion system consists of four pylon wing-mounted by-pass ratio 12.95 engines (refer to Section 3.2) with sea level static thrust of 108,181 N (24,320 lb) for the small aircraft and 218,541 N (49,130 lb) for the large aircraft. Ground operable thrust reversers are incorporated into each engine installation.

At the design cruise altitude of 10,973 m (36,000 ft) and cruise Mach number of 0.85 the specific fuel consumption for both aircraft is $0.213 \frac{\text{kg}}{\text{hr}}/\text{daN}$ ($0.209 \frac{\text{lb}}{\text{hr}}/\text{lb}$). Including inflight boiloff of the liquid hydrogen, these specifics become 0.219 and $0.223 \frac{\text{kg}}{\text{hr}}/\text{daN}$ for the small and large aircraft, respectively.

5.5.1.2 Hydrogen System - Tank size characteristics and fuel boiloff data are given in Tables 51 and 52 for the small and large swing tail aircraft, respectively. Inflight boiloff data are based upon a mission block time of 6.54 hours and a fuel average flow rate of 1784 kg/hr for the small aircraft. These values for the large aircraft are 11.67 hours and 3464 kg/hr. Closed-cell plastic foam insulation 15.24 cm (six inches) thick is used on all tank exterior surfaces.

TABLE 51. SMALL HYDROGEN SWING TAIL TANK DATA

CUSTOMARY UNITS					
TANK DESCRIPTION	GROSS VOLUME cu ft	USABLE FUEL lb	SURFACE AREA sq ft	INFLIGHT BOILOFF lb	GROUND BOILOFF lb/hr
Fwd	4000	16596	1219	316	83
Aft	4000	16596	1263	425	89
Total	8000	33192	2482	741	172
SI UNITS					
TANK DESCRIPTION	GROSS VOLUME m ³	USABLE FUEL kg	SURFACE AREA m ²	INFLIGHT BOILOFF kg	GROUND BOILOFF kg/hr
Fwd	113.3	7528	113.3	143	38
Aft	113.3	7528	117.3	193	40
Total	226.6	15056	230.6	336	78

TABLE 52. LARGE HYDROGEN SWING TAIL TANK DATA

CUSTOMARY UNITS					
TANK DESCRIPTION*	GROSS VOLUME cu ft	USABLE FUEL lb	SURFACE AREA sq ft	INFLIGHT BOILOFF lb	GROUND BOILOFF lb/hr
1	9287	39068	2280	1090	160
2	3066	12898	1913	1072	135
3	2861	12035	1441	1017	102
4	2861	12035	1441	1017	102
5	8325	35022	2562	1195	180
Total	26400	111058	9637	5391	679
SI UNITS					
TANK DESCRIPTION*	GROSS VOLUME m ³	USABLE FUEL kg	SURFACE AREA m ²	INFLIGHT BOILOFF kg	GROUND BOILOFF kg/hr
1	263.0	17721	211.8	494	73
2	86.8	5850	177.7	486	61
3	81.0	5459	133.9	461	46.2
4	81.0	5459	133.9	461	46.2
5	235.7	15886	238.0	542	82
Total	747.6	50375	895.3	2445	308

* See Figure 88

5.5.2 Weight Statement

Weight prediction methods are described in Section 5.3 and discussion of weight statements in Paragraph 5.4.2. Group weight statements for the swing tail aircraft are presented on Tables 53 and 54.

TABLE 53. GROUP WEIGHT STATEMENT: SMALL HYDROGEN SWING TAIL

56,700 kg Payload, 5560 km Range, Mach 0.85 Speed
 (125,000 lb Payload, 3000 n m Range, Mach 0.85 Speed)

ITEM	KILOGRAM	POUND
Structure	42,251	93,148
Wing	11,484	25,317
Empennage	1,538	3,391
Horizontal Tail	727	1,603
Vertical Tail	811	1,788
Fuselage	20,184	44,599
Landing Gear	6,689	14,747
Roe	869	1,917
Main	5,820	12,830
Nacelle and Pylon	2,356	5,194
Nacelle	900	1,983
Pylon	1,456	3,211
Propulsion System	13,713	30,232
Engines	7,904	17,426
Fuel System	957	2,110
Thrust Reversers	716	1,579
Inlet	913	2,013
Oil Tanks	3,036	6,694
Miscellaneous	187	410
Systems and Equipment	8,324	18,352
Auxiliary Power System	234	519
Surface Controls	1,611	3,551
Instruments	342	754
Hydraulics and Pneumatics	751	1,655
Electrical	1,232	2,693
Avionics	986	2,175
Furnishings	1,835	4,045
Airconditioning and Al	1,292	2,848
Auxiliary Gear - Equipment	51	112
Weight Empty	64,288	141,732
Operating Equipment	1,699	3,746
Operating Weight	65,987	145,478
Cargo Payload	56,700	125,000
Zero Fuel Weight	122,687	270,478
Fuel	14,760	32,540
Gross Weight	137,447	303,018

TABLE 54. GROUP WEIGHT STATEMENT LARGE HYDROGEN SWING TAIL

113,400 kg Payload, 10,190 km Range, Mach 0.85 Speed
 (250,000 lb Payload, 5500 n m Range, Mach 0.85 Speed)

ITEM	KILOGRAM	POUND
Structure	98,986	218,227
Wing	33,728	74,357
Empennage	2,928	6,457
Horizontal Tail	1,452	3,201
Vertical Tail	1,476	3,256
Fuselage	42,679	94,091
Landing Gear	14,652	32,301
Nose	1,905	4,199
Main	12,747	28,102
Nacelle and Pylon	4,999	11,021
Nacelle	1,909	4,208
Pylon	3,090	6,813
Propulsion System	32,914	72,564
Engines	16,774	36,981
Fuel System	1,618	3,567
Thrust Reversers	1,520	3,351
Inlet	1,937	4,271
H ₂ Tanks	10,677	23,537
Miscellaneous	388	857
Systems and Equipment	11,630	25,641
Auxiliary Power System	373	823
Surface Controls	2,917	6,432
Instruments	418	922
Hydraulics and Pneumatics	1,359	2,997
Electrical	1,578	3,479
Avionics	987	2,175
Furnishings	2,290	5,048
Airconditioning and Al	1,593	3,512
Auxiliary Gear - Equipment	115	253
Weight Empty	143,530	316,432
Operating Equipment	3,242	7,150
Operating Weight	146,772	323,582
Cargo Payload	113,400	250,000
Zero Fuel Weight	260,172	573,582
Fuel	49,432	108,978
Gross Weight	309,604	682,560

5.5.3 Performance

The performance characteristics of the selected hydrogen swing tail aircraft are very similar to those defined for the hydrogen nose loader aircraft; they are also constrained by the 69.5 m/s approach speed condition.

The takeoff distances are 1759 and 2188 m for the small and large aircraft, respectively. The landing distances for the small and large aircraft are 2031 and 2304 m, respectively.

The payload-range and block fuel data are given in Figure 89.

A summary of the aerodynamic characteristics of these swing tail aircraft is given in the following table.

AERODYNAMIC CHARACTERISTICS HYDROGEN SWING TAIL

	SMALL	LARGE
Wing Area - m^2 (ft^2)	242.9 (2615)	498.6 (5367)
Wing L/c - Percent	11.49	11.07
Wing Aspect Ratio	9	9
Initial Cruise Wing Loading - kg/m^2	558.84	613.52
Initial Cruise Wing Loading - lb/ft^2	114.47	125.67
Initial Cruise C_L	.475	.502
Initial Cruise L/D Ratio	16.20	15.07

5.5.4 Aircraft Price and Operating Cost

Unit price for the small aircraft is 19.6 million dollars and for the large aircraft is 41.4 million dollars. Elements of these unit prices are given in Table 55. Direct operating cost for the small and large aircraft are, respectively, 3.42 and 3.01 ϕ /Mtkm (5.75 and 5.00 ϕ /Ton n.mi.) based upon a yearly utilization of 3600 and 4000 hours and stage lengths of 5560 and 10,190 kilometers.

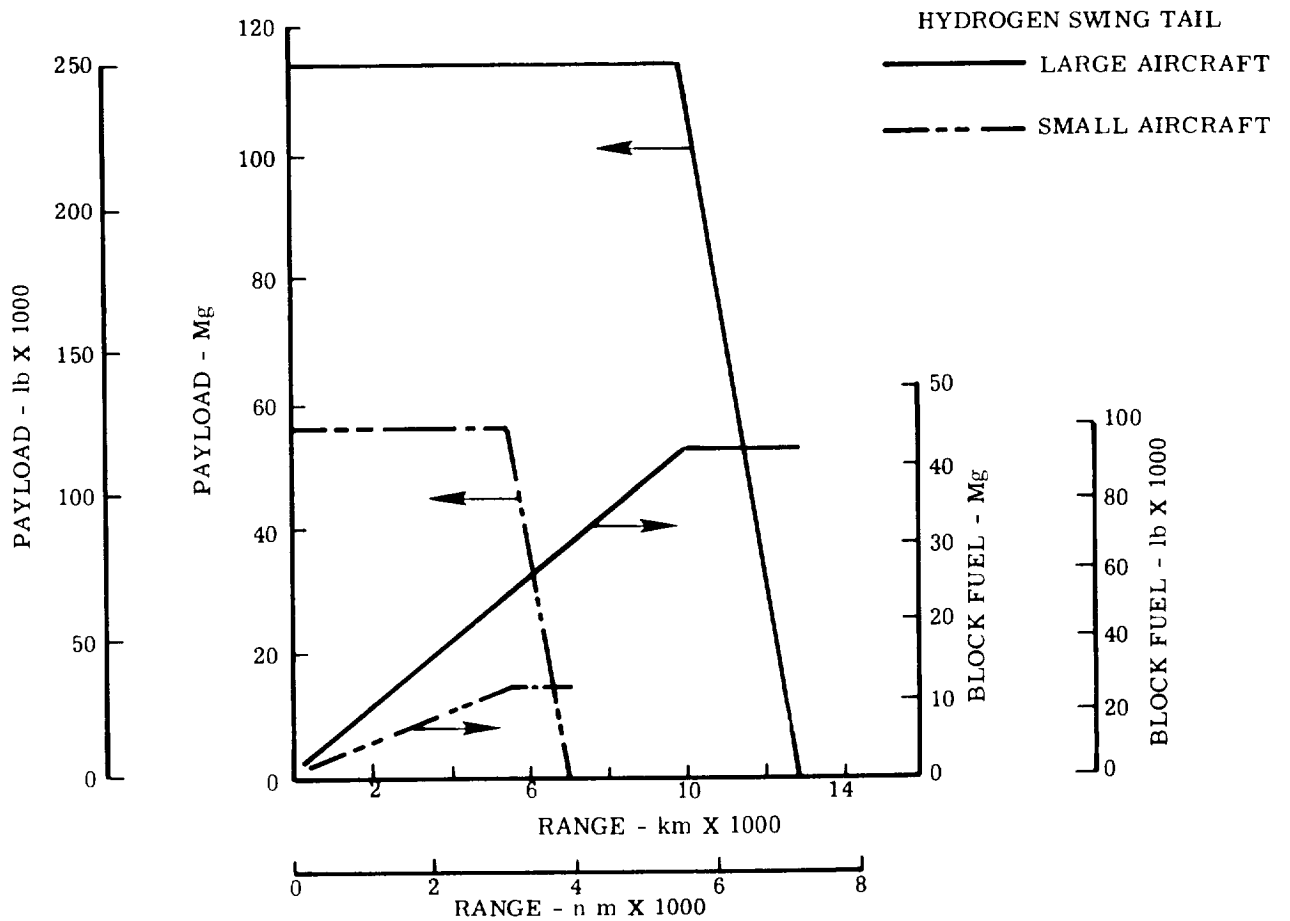


Figure 89. Payload - Range/Block Fuel: Swing Tail Aircraft

TABLE 55. PRICE SUMMARY — HYDROGEN SWING TAIL AIRCRAFT

		COST IN \$10 ⁶	
	RANGE	SMALL	LARGE
<u>Development</u>			
Airframe		\$548.9	\$1,067.8
Engine		400.0	578.3
Avionics		—	—
Total		\$948.9	\$1,646.1
<u>Production</u>			
Airframe Manufacturing Cost		\$ 8.8	\$ 19.7
Other Airframe Cost		4.9	11.1
Sustaining Engineering		0.6	1.4
Tool Maintenance		0.8	1.9
Quality Assurance		0.9	2.0
Miscellaneous		0.2	0.5
Profit		1.8	4.0
Warranty		0.6	1.3
Engine		3.0	5.9
Avionics		0.5	0.5
Subtotal		\$ 17.2	\$ 37.2
R&D per Aircraft*		2.4	4.2
Total Aircraft Price		\$ 19.6	\$ 41.4
*Based on 350 aircraft and 2000 engines			

5.6 HYDROGEN AIRCRAFT CONFIGURATION SELECTION

In this section the two liquid hydrogen fueled cargo aircraft, the nose loader and swing tail configurations, are compared on the basis of terminal operational environment compatibility, maintenance, safety, and performance. One configuration is selected for subsequent comparison with reference designs of Jet A fueled aircraft to illustrate the potential benefits of using hydrogen fuel.

5.6.1 Terminal Operations and Maintenance

The cargo terminal operational environment envisioned for the 1990 to 1995 cargo aircraft is one of maximum automation. Aircraft will be positioned at gate areas adjacent to fixed base cargo terminals. Loading "fingers" will extend from the terminal such that when the cargo compartment floor is aligned with this "finger" it in effect becomes an extension of the terminal floor. Automated loading systems will be used to move loaded containers from the terminal, over the finger and into the cargo compartment in a minimum elapsed time. The nose loader configuration is more compatible to the fixed base terminal than the swing tail configuration. With the nose visor door open the aircraft can be taxied into position to mate with the terminal "finger." However, the swing tail aircraft would require a terminal finger that is extended to mate with the swing tail aircraft after it is parked and the aft fuselage is rotated to provide access to the cargo compartment. A larger gate area is also required by the swing tail aircraft to provide clearance for the aft fuselage rotation.

Aircraft maintenance as it pertains to hydrogen tank removal is complex to perform on the swing tail aircraft when compared to performing the same function on the nose loader. Tank removal on the swing tail requires a station plane joint be provided in the fuselage structure. Separation of the fuselage sections at this joint allows the tank to be removed. This separation of the fuselage and remating upon completion of tank maintenance will require complex ground support equipment. Access to the nose loader fuselage upper lobe tanks is provided by removable structural panels. These panels would be located along the crown of the upper lobe. Upon removal of the panels the tanks could then be hoisted vertically for removal. The aft fuselage tank would be removed through fuselage lower surface doors.

The control and fuel systems which must span the hinge joint of the aft fuselage on the swing tail aircraft will add complexity to the routine maintenance task.

5.6.2 Safety

Specific areas of concern regarding safety of hydrogen fueled aircraft are discussed in Section 4.6.2. Although the safety aspects of the two configurations of cargo aircraft are considered to be approximately equivalent, there are some indications the nose loader is the safer aircraft. The major portion of the hydrogen fuel is contained in tanks above the cargo compartment which offers some degree of protection to the tanks should the aircraft be involved in an accident during the takeoff or landing mode. A potential source of hydrogen gas leaks and therefore a source of a potential safety hazard is the hinge joint of the swing tail aft fuselage. Hydrogen fuel lines must span this joint and are subjected to abuse each time the aft fuselage is rotated.

5.6.3 Performance

Performance and characteristics comparisons of the nose loader and swing tail configurations are given in Tables 56 and 57. The factor (ST/NL) column on these tables given a direct comparison of each parameter using the nose loader as the base. Inspection of these data shows that performance is maximized by the nose loader configuration. It is of interest to note on the small aircraft, that although the swing tail tank wetted area is significantly less than the nose loader tank wetted area, the fuselage wetted area of the swing tail aircraft is slightly greater than that of the nose loader aircraft. This indicates for this payload and range requirement, fuselage efficiency is of more importance than tank efficiency.

On the large swing tail aircraft, the need to minimize fuselage length to accommodate the required takeoff rotation angle dictated the placement of hydrogen tanks above the cargo compartment. The use of these 5-lobe tanks resulted in both tank and fuselage wetted area of the swing tail aircraft being greater than corresponding areas of the nose loader configuration.

5.6.4 Selection

Concluding from the above, the nose loader configuration offers advantages in the terminal operational environment, maintenance, safety and performance compared to the swing tail configuration. With NASA concurrence, the nose loader was

TABLE 56. DESIGN COMPARISON: NOSE LOADER VS SWING TAIL LH₂ SMALL CARGO AIRCRAFT

56,700 kg (125,000 lb); 5560 km (3000 n mi); M = 0.85

	SI	CUSTOMARY	SWING TAIL		NOSE LOADER		FACTOR (ST/NL)
			SI	CUSTOMARY	SI	CUSTOMARY	
Gross Wt.	kg	lb	137,441	303,000	135,763	299,300	1.012
Fuel Wt.	kg	lb	14,742	32,500	14,470	31,900	1.090
Operating Empty Wt.	kg	lb	65,999	145,500	64,638	142,500	1.021
Wing Area	m ²	ft ²	242.9	2615	240.1	2584	1.012
Span	m	ft	46.76	153.4	46.48	152.5	1.006
Fuselage Length	m	ft	54.77	179.7	52.03	170.7	1.053
L/D (Cruise)			16.2	16.2	16.3	16.3	0.940
SFC (Cruise)	$\frac{\text{kg}}{\text{hr}}/\text{daN}$	$\frac{\text{lb}}{\text{hr}}/\text{lb}$	0.22	0.216	0.219	0.215	1.00
Thrust per Engine	N	lb	108,086	24,300	106,307	23,900	1.017
FAR T.O. Field Length	m	ft	1758.7	5770	1767.8	5800	0.950
FAR Landing Field Length	m	ft	2231.1	7320	2231.1	7320	1.00
Energy Utilization	$\frac{\text{kJ}}{\text{Mg km}}$	$\frac{\text{Btu}}{\text{ton n.mi.}}$	4606	7346	4502	7181	1.023
Price	$\$10^6$	$\$10^6$	19.6	19.6	19.2	19.2	1.020
DOC*	$\frac{\$}{\text{Mg km}}$	$\frac{\$}{\text{ton n.mi.}}$	3.42	5.75	3.36	5.65	1.018

* LH₂ Fuel Cost = $\$3/1.054 \text{ GJ} = \$3/10^6 \text{ Btu} = 15.48\phi/\text{lb}$

TABLE 57. DESIGN COMPARISON: NOSE LOADER VS SWING TAIL LH₂ LARGE CARGO AIRCRAFT

113,400 kg (250,000 lb); 10,190 km (5500 n mi); M = 0.85

	SI	CUSTOMARY	SWING TAIL		NOSE LOADER		FACTOR (ST/NL)
			SI	CUSTOMARY	SI	CUSTOMARY	
Gross Wt.	kg	lb	308,627	682,600	300,056	661,500	1.032
Fuel Wt.	kg	lb	59,442	109,000	47,991	105,800	1.030
Operating Empty Wt.	kg	lb	146,785	323,600	138,666	305,700	1.059
Wing Area	m ²	ft ²	598.6	5,367	483.3	5,203	1.032
Span	m	ft	66.66.9	219.8	65.9	215.4	1.016
Fuselage Length	m	ft	85.0	279.0	77.0	252.7	1.104
L/D (Cruise)			18.07	18.07	18.03	18.03	1.00
SFC (Cruise)	kg/dan	lb/hr	0.223	0.219	0.223	0.219	1.00
Thrust Per Engine	N	lb	218,396	49,100	212,170	47,700	1.029
FAR T.O. Field Length	m	ft	2188	7,180	2185	7,170	1.00
FAR Landing Field Length	m	ft	2304	7,560	2304	7,560	1.00
Energy Utilization	kJ Mg km	Btu ton n.mi.	4413	7,039	4286	6,835	1.030
Price	\$10 ⁶ Mg km	\$10 ⁶	41,441	44,441	39,121	39,121	1.059
DOC*	\$ Mg km	\$ ton n.mi.	3.01	5.06	2.89	4.86	1.041

* LH₂ Fuel Cost = \$3/1.054 GJ = \$3/10⁶ Btu = 15.48¢/lb

selected as the LH_2 configuration to be compared to the reference Jet A fueled cargo aircraft.

5.7 REFERENCE (JET A) CARGO AIRCRAFT

A parametric analysis identical to that described in Section 5.3 for the hydrogen fueled cargo aircraft was performed to determine preferred design characteristics for the reference (Jet A-fueled) aircraft. Table 58 shows the results of this analysis. Since the fuel required by these vehicles is about three times greater, by weight, than is required by the hydrogen fueled aircraft designed for the same mission, the characteristics of these aircraft vary from those described for the hydrogen configurations. For example, the large aircraft is constrained by the 2,440 meter takeoff distance requirement rather than by approach speed. Since it is defined by takeoff requirements which are sensitive to available thrust, there is a much larger wing loading variation with aspect ratio than is associated with the approach constraint which is not dependent on available thrust.

The small Jet A aircraft is sized by the landing approach speed constraint; however, the takeoff distance is about 396 m (1,300 ft.) greater than for the small hydrogen fueled aircraft because of the greater takeoff weight which results from the much larger fuel weight of the Jet A aircraft. As shown in the tabulation, the small Jet A aircraft has a minimum DOL at an aspect ratio of 10, although the variation due to aspect ratio for this configuration is very small.

5.7.1 Configuration Description

The Jet A cargo aircraft shown in Figures 90 and 91 are configured to perform the specified missions at a cruise speed of Mach 0.85. Both the small and large Jet A aircraft have essentially the same configuration description as stated for the hydrogen nose loader aircraft in Section 5.4.1 of this report, with the following exceptions:

- Fuel storage is relocated from fuselage tanks to wing tanks.
- The upper fuselage hydrogen tank storage lobe is removed, although the basic fuselage diameter is the same.

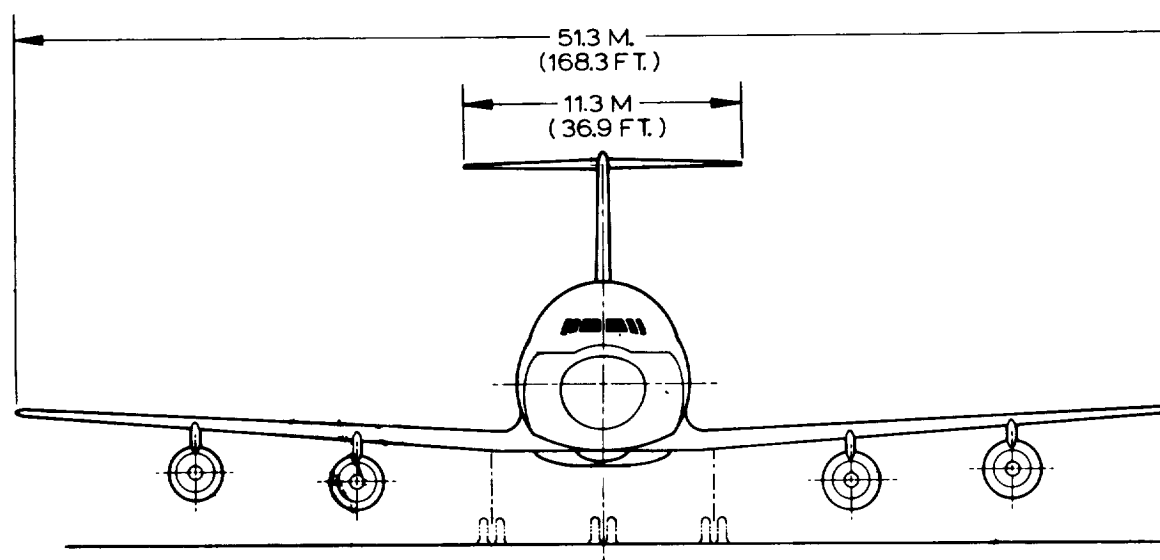
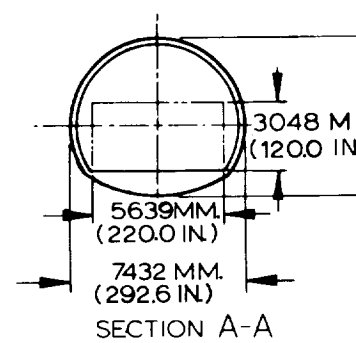
TABLE 58. ASPECT RATIO SELECTION - JET A CARGO AIRCRAFT

SI UNITS

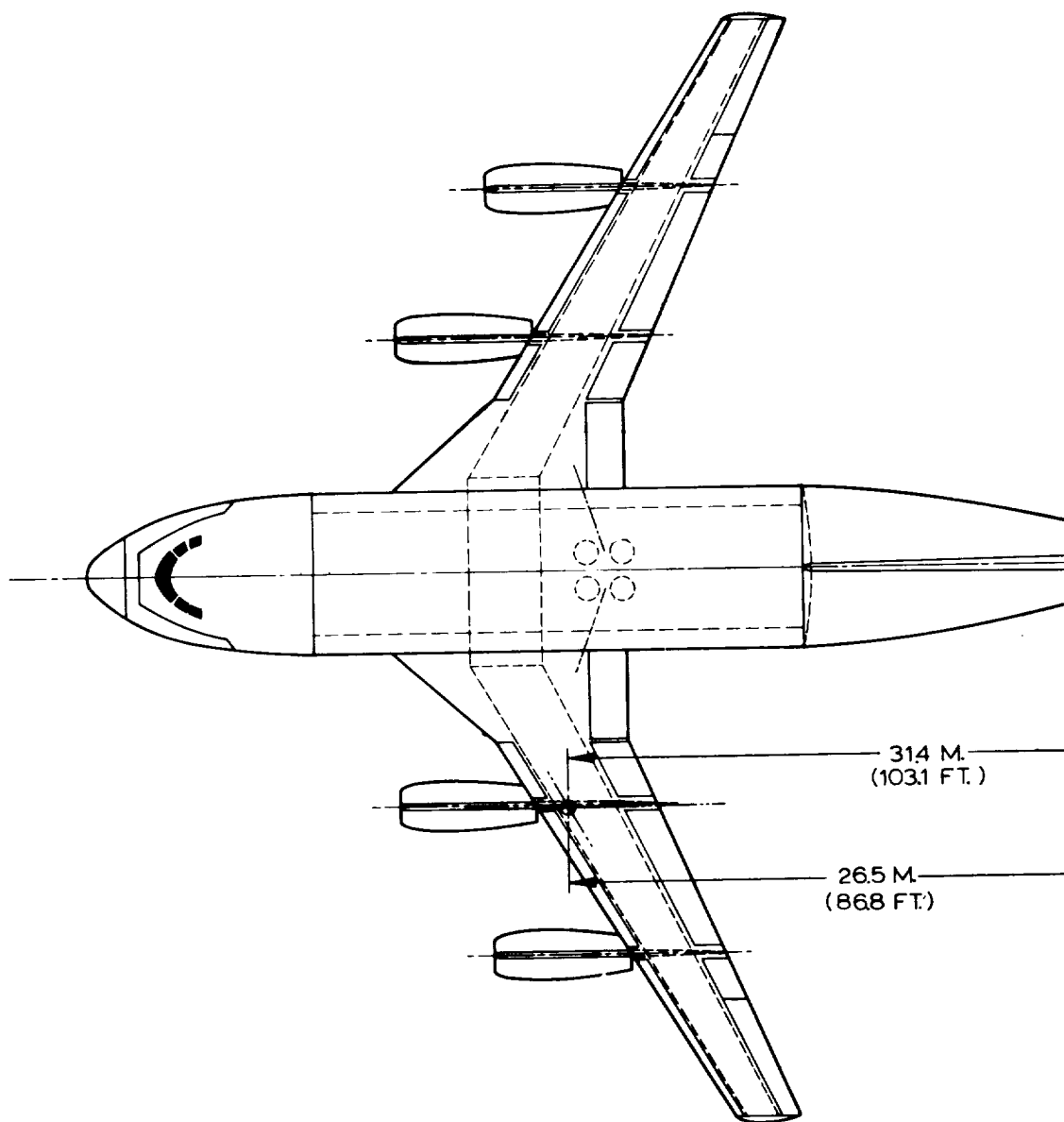
ASPECT RATIO	56,700 kg - 5560 km UTILIZATION = 3600 Hr/Yr					113,400 kg - 10,190 km UTILIZATION = 4000 Hr/Yr				
	8	9	10	11		8	9	10	11	
W/S - kg/m ²	601.0	598.5	596.4	594.6		610.5	592.6	579.0	568.3	
t/c - %	11.31	11.19	11.11	11.05		11.23	11.24	11.24	11.25	
Cruise L/D	16.74	17.38	17.93	18.39		18.67	19.50	20.16	20.7	
S _w - m ²	261.6	261.9	263.2	265.4		638.8	658.3	679.9	703.5	
Oper. Wt. - kg	61,821	62,578	63,709	65,131		135,270	138,823	143,799	149,920	
Total Fuel - kg	43,077	41,873	41,082	40,590		151,707	148,562	147,466	147,814	
Block Fuel - kg	35,632	34,589	33,900	33,464		132,301	129,236	128,035	128,140	
Gross Wt. - kg	161,597	161,150	161,491	162,420		400,375	400,781	404,662	411,132	
Engine Thrust - N	121,200	116,400	113,000	110,700		269,600	258,300	252,000	249,200	
T.O. Dist - m	2103.7	2159.5	2207.4	2248.5		2438.4	2438.4	2438.4	2438.4	
Land. Dist - m	2228.4	2220.5	2214.7	2210.1		2358.5	2317.7	2284.5	2257.4	
Price - \$ X 10 ⁶	18.022	18.147	18.382	18.702		37.196	37.978	39.144	40.614	
DOC - ¢/Mg km	3.03	3.00	3.00	3.00		2.67	2.66	2.68	2.73	
SFC - $\frac{\text{kg}}{\text{daN hr}}$	0.620	0.620	0.620	0.620		0.620	0.620	0.620	0.620	

TABLE 58. ASPECT RATIO SELECTION - JET A CARGO AIRCRAFT (Continued)

ASPECT RATIO	125,000 lb - 3000 n m UTILIZATION = 3600 Hr/Yr					250,000 lb - 5500 n m UTILIZATION = 4000 Hr/Yr				
	8	9	10	11		8	9	10	11	
W/S - lb/ft ²	123.11	122.59	122.16	121.79		125.05	121.38	118.60	116.4	
t/c - %	11.31	11.19	11.11	11.05		11.23	11.24	11.24	11.25	
Cruise L/D	16.74	17.38	17.93	18.39		18.67	19.50	20.16	20.7	
S _w - ft ²	2816	2819	2833	2857		6876	7086	7318	7572	
Oper. Wt. - lb	136,292	137,961	140,455	143,590		298,219	306,048	317,022	330,518	
Total Fuel - lb	94,969	92,315	90,572	89,486		334,456	327,524	325,106	325,874	
Block Fuel - lb	78,556	76,256	74,736	73,776		291,673	284,917	282,269	282,500	
Gross Wt. - lb	356,261	355,276	356,027	358,076		882,675	883,571	892,128	906,392	
Engine Thrust - lb	27256	26166	25413	24897		60604	58063	56663	56031	
T.O. Dist. - ft	6902	7085	7242	7377		8000	8000	8000	8000	
Land. Dist. - ft	7311	7285	7266	7251		7738	7604	7495	7406	
Price - \$ X 10 ⁶	18.022	18.147	18.382	18.702		37.196	37.978	39.144	40.614	
DOC - ¢/ton n mi	5.09	5.05	5.04	5.05		4.48	4.47	4.51	4.59	
SFC - $\frac{\text{lb}}{\text{hr}}/\text{lb}$	0.608	0.608	0.608	0.608		0.608	0.608	0.608	0.608	

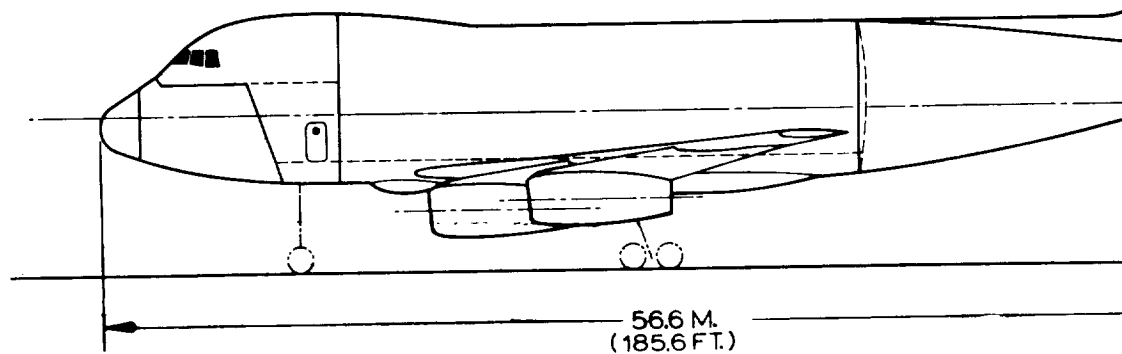


6756 MM.
(2660 IN.)

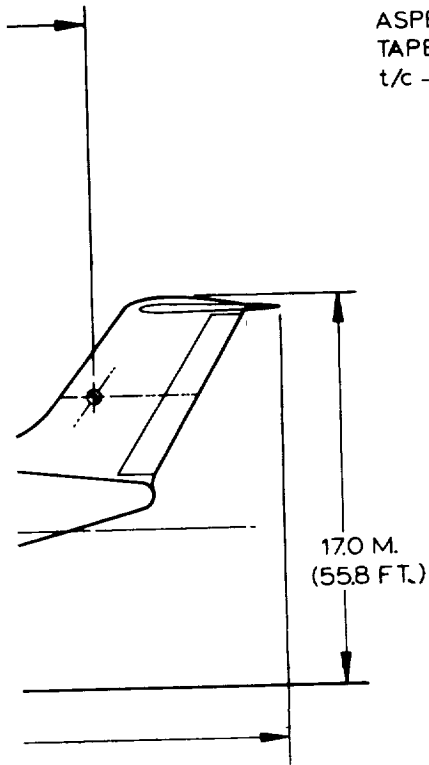
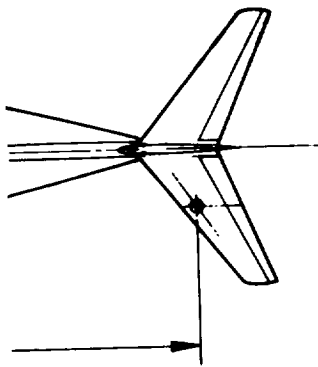


314 M.
(1031 FT.)

26.5 M.
(868 FT.)



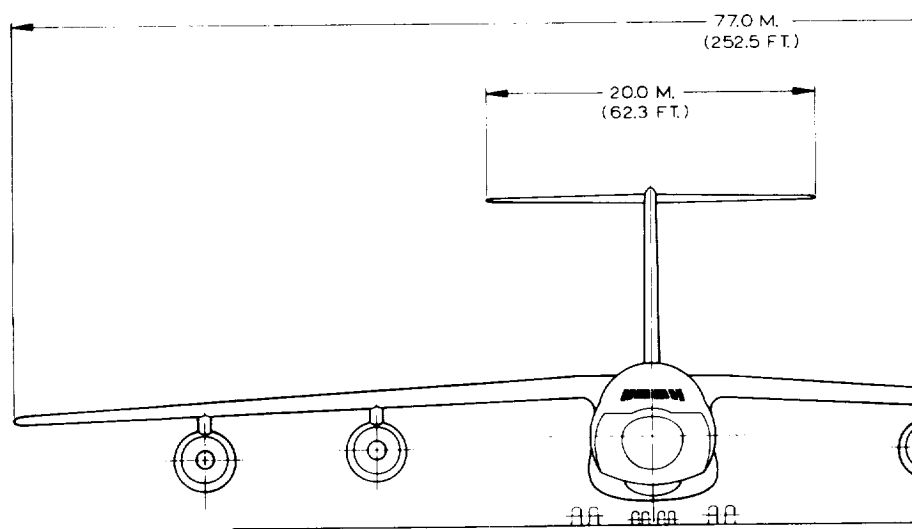
56.6 M.
(185.6 FT.)



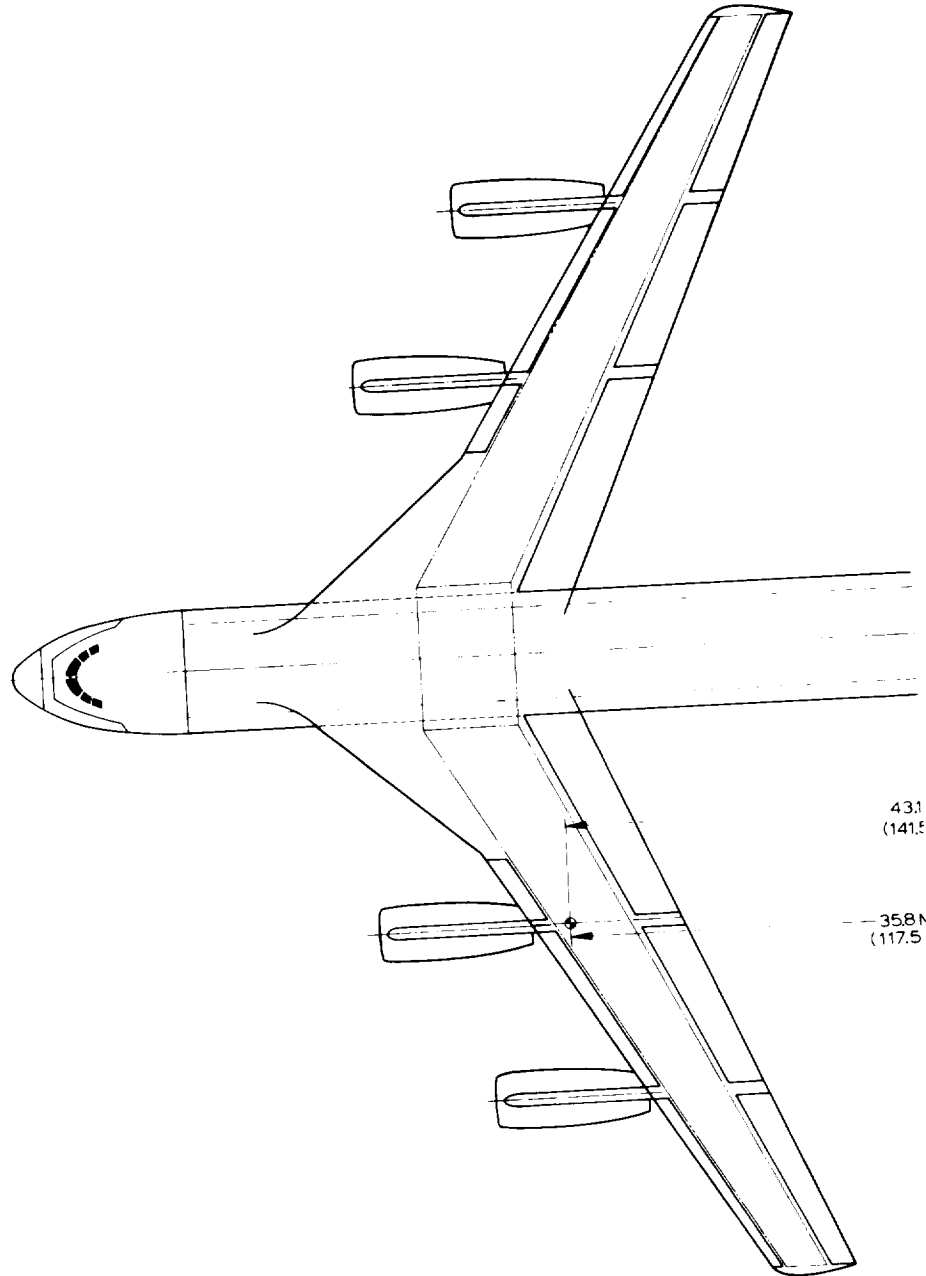
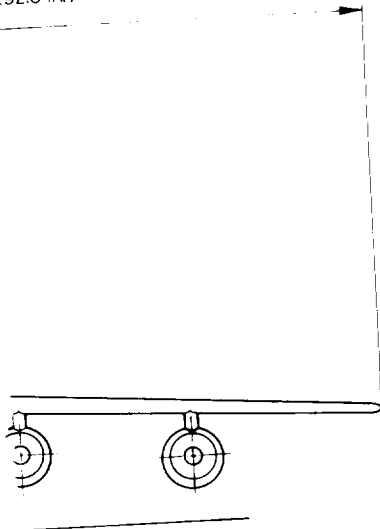
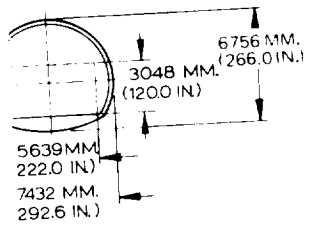
SURFACE CHARACTERISTICS

	<u>WING</u>	<u>HORIZ.</u>	<u>VERT.</u>
AREA-SQ. M. (SQ. FT.)	2632 (2833)	269(289.6)	42.3 (455.0)
SWEEP-RAD (DEG)	0.52 (30)	0.61(35)	0.61(35)
ASPECT RATIO	10.00	4.70	1.24
TAPER RATIO	0.40	0.40	0.80
t/c -%	11.11	8.5	8.5

Figure 90. General Arrangement - Jet A Fuel,
Small Cargo Transport

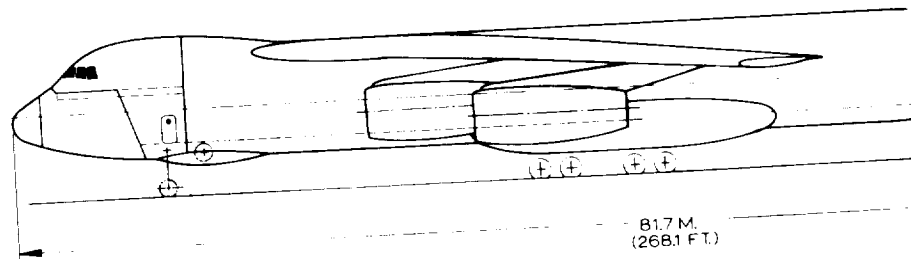


SECTION AA

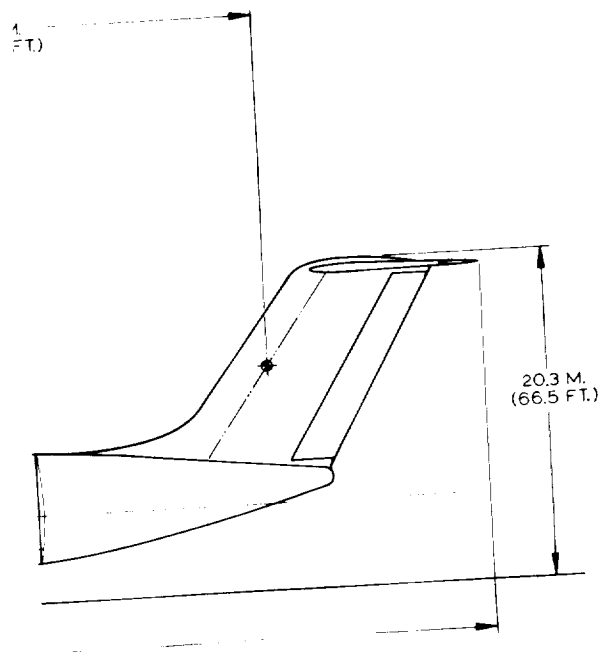
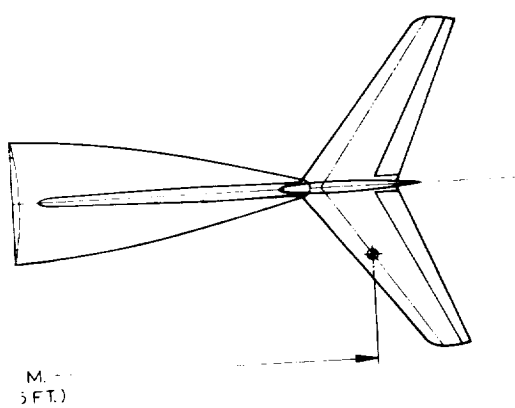


43.1
(141.5)

35.8
(117.5)



81.7 M.
(268.1 FT.)



SURFACE CHARACTERISTICS

	WING	HORIZ.	VERT.
AREA - SQ. M. (SQ. FT.)	6581 (7084)	81.7 (879)	1146 (1234)
SWEEP-RAD (DEG)	0.52 (30)	0.61 (35)	0.61 (35)
ASPECT RATIO	9.0	4.7	1.24
TAPER RATIO	0.4	0.4	0.8
t/c %	1123	85	85

Figure 91. General Arrangement - Jet A Fuel,
Large Cargo Transport

- The large aircraft uses a high-wing position rather than the mid-wing position of the large hydrogen aircraft to maintain nacelle ground clearance while not exceeding a floor height dimension of 4.72 meters (15.5 feet). The double-lobe type fuselage shape of the hydrogen aircraft with its structural tie at the intersection of the two lobes is compatible with the mid-wing position. However, the single upper contour fuselage shape of the Jet A aircraft with its unbroken upper fuselage structural rings is not readily adaptable to the mid-wing position.

5.7.1.1 Propulsion System - The propulsion system consists of four pylon wing-mounted by-pass ratio 10.9 engines (see Section 3.2) with sea level static thrust of 113,029 N (25,140 lb) for the small aircraft and 258,397 N (58,090 lb) for the large aircraft. Ground operable thrust reversers are incorporated into each engine.

At the design cruise altitude of 10,973 m (36,000 ft) and cruise Mach number of 0.85 the specific fuel consumption for both aircraft is $0.620 \frac{\text{kg}}{\text{hr}}/\text{daN}$ ($0.608 \frac{\text{lb}}{\text{hr}}/\text{lb}$).

5.7.2 Weight Statement

Weight prediction methods are described in Section 5.3 and discussion of weight statements in Paragraph 5.4.2. Group weight statements for the reference (Jet A) aircraft are presented on Tables 59 and 60.

5.7.3 Performance

The performance characteristics of the Jet A aircraft differ from those of the hydrogen fueled aircraft in several ways. First, the large Jet A aircraft is constrained by the 2440 m (8000 ft) takeoff field length requirement while all the other aircraft are sized by the approach speed condition. Second, the payload-range diagrams have the more customary shape which results when the aircraft have more fuel capacity than is required for the design mission.

The takeoff distance of the small aircraft is given for a 0.21 radian (12 degree) flap deflection and is 2207 m (7240 ft); the takeoff distance of the large aircraft is given for 0.35 radian (20 degrees) flap deflection and is 2440 m (8000 ft). Landing distances are 2216 and 2143 m (7270 and 7030 ft) for the small and large aircraft, respectively. The payload-range and block fuel characteristics for these aircraft are given in Figure 92.

TABLE 59. GROUP WEIGHT STATEMENT: SMALL JET A NOSE LOADER

56,700 kg Payload, 5560 km Range, Mach 0.85 Speed
 (125,000 lb Payload, 3000 n m Range, Mach 0.85 Speed)

ITEM	KILOGRAM	POUND
Structure	41,538	91,575
Wing	12,381	27,295
Empennage	1,748	3,855
Horizontal Tail	793	1,749
Vertical Tail	955	2,106
Fuselage	17,690	38,998
Landing Gear	7,249	15,982
Nose	942	2,078
Main	6,307	13,904
Nacelle and Pylon	2,470	5,445
Nacelle	943	2,079
Pylon	1,527	3,366
Propulsion System	11,356	25,034
Engines	8,286	18,267
Fuel System	1,167	2,573
Thrust Reversers	751	1,655
Inlet	957	2,110
HH ₂ Tanks	0	0
Miscellaneous	195	429
Systems and Equipment	8,591	18,940
Auxiliary Power System	255	561
Surface Controls	1,765	3,891
Instruments	343	756
Hydraulics and Pneumatics	822	1,813
Electrical	1,231	2,715
Avionics	987	2,175
Furnishings	1,770	3,903
Airconditioning and Al	1,358	2,994
Auxiliary Gear - Equipment	60	132
Weight Empty	61,484	135,549
Operating Equipment	2,224	4,906
Operating Weight	63,708	140,455
Cargo Payload	56,700	125,000
Zero Fuel Weight	120,408	265,455
Fuel	41,083	90,572
Gross Weight	161,491	356,027

TABLE 60. GROUP WEIGHT STATEMENT: LARGE JET A NOSE LOADER

113,400 kg Payload, 10,190 km Range, Mach 0.85 Speed
(250,000 lb Payload, 5500 n m Range, Mach 0.85 Speed)

ITEM	KILOGRAM	POUND
Structure	93,964	207,151
Wing	32,964	72,672
Empennage	4,607	10,156
Horizontal Tail	2,267	4,998
Vertical Tail	2,340	5,158
Fuselage	33,616	74,110
Landing Gear	16,795	37,075
Nose	2,183	4,813
Main	14,612	32,212
Nacelle and Pylon	5,982	13,188
Nacelle	2,284	5,035
Pylon	3,698	8,153
Propulsion System	26,892	59,285
Engine	20,071	44,248
Fuel System	2,220	4,895
Thrust Reversers	1,819	4,009
Inlet	2,818	6,111
Oil Tanks	0	0
Miscellaneous	464	1,022
Systems and Equipment	12,758	28,128
Auxiliary Power System	446	984
Engine Controls	3,687	8,131
Instruments	415	914
Hydraulics and Pneumatics	1,719	3,789
Electrical	1,570	3,461
Avionics	987	2,175
Furnishings	2,136	4,710
Airconditioning and Al	1,650	3,637
Auxiliary Gear - Equipment	148	327
Weight Empty	133,614	294,564
Operating Equipment	5,277	11,624
Operating Weight	138,891	306,188
Carry Payload	113,400	250,000
Zero Fuel Weight	252,291	556,188
Fuel	148,632	327,671
Gross Weight	400,923	883,859

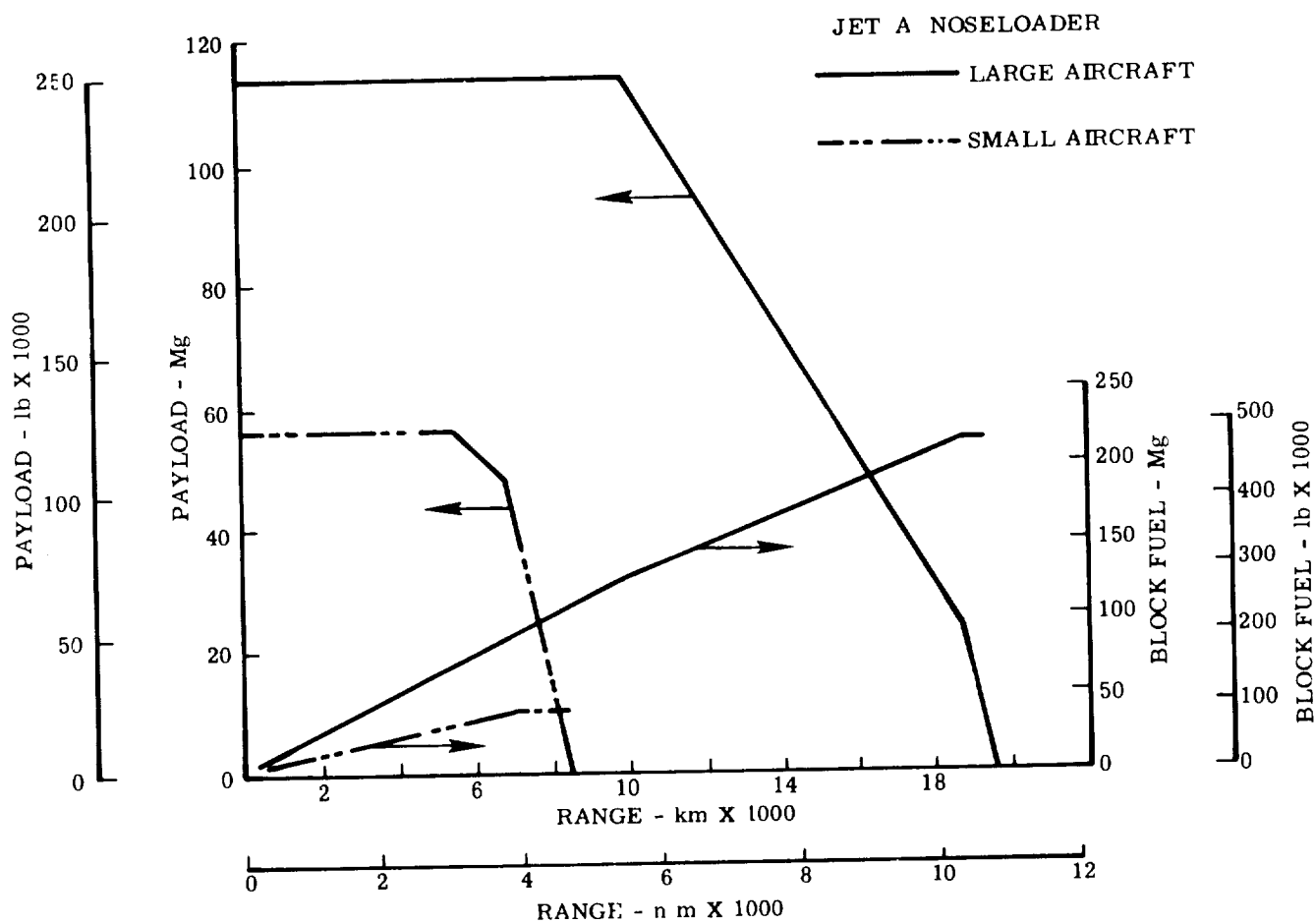


Figure 92. Payload - Range/Block Fuel: Jet A Cargo Aircraft

Aerodynamic characteristics of the Jet A aircraft are given in the following table.

AERODYNAMIC CHARACTERISTICS-JET A NOSELOADER

	SMALL	LARGE
Wing Area - m^2 (ft^2)	263 (2833)	653 (7084)
Wing t/c - Percent	11.11	11.23
Wing Aspect Ratio	10	9
Initial Cruise Wing Loading - kg/m^2 (psf)	597 (122.16)	592 (121.45)
Initial Cruise C_L	.507	.504
Initial Cruise L/D Ratio	17.93	19.49

5.7.4 Aircraft Price and Operating Cost

Unit price for the small aircraft is 18.4 million dollars and for the large aircraft is 38.0 million dollars. Elements of these unit prices are given in Table 61. Direct operating costs for the small and large aircraft are respectively 3.00 and 7.66 $\phi/Per\ km$ (5.04 and 4.47 $\phi/Ton\ n.mi.$) based upon a yearly utilization of 3000 and 4000 hours and stage lengths of 5500 and 10,190 km.

5.8 BENEFITS EVALUATION: LH_2 VS JET A CARGO AIRCRAFT

The potential benefits to be derived by the use of liquid hydrogen as a fuel for cargo aircraft are examined in the following paragraphs by comparing the selected hydrogen nose loader aircraft with the reference Jet A fueled aircraft.

5.8.1 Performance

A summary of performance and characteristic data is given in Tables 62 and 63 for both sizes of hydrogen nose loader and reference Jet A aircraft. Data for aircraft sized to perform each of the design missions are given and compared by

TABLE 61. PRICE SUMMARY - JET A CARGO AIRCRAFT

		COST IN \$10 ⁶	
	RANGE	SMALL	LARGE
<u>Development</u>			
Airframe		\$520.3	\$1,091.7
Engine		418.4	580.0
Avionics		-	-
Total		\$938.7	\$1,671.7
<u>Production</u>			
Airframe Manufacturing Cost		\$ 8.4	\$ 17.7
Other Airframe Cost		4.7	10.0
Sustaining Engineering		0.6	1.3
Tool Maintenance		0.8	1.7
Quality Assurance		0.8	1.8
Miscellaneous		0.2	0.5
Profit		1.7	3.6
Warranty		0.6	1.1
Engine		2.5	5.5
Avionics		0.5	0.5
Subtotal		\$ 16.1	\$ 33.7
*R&D per Aircraft		2.3	4.3
Total Aircraft Price		\$ 18.4	\$ 38.0
*Based on 350 aircraft and 2000 engines			

TABLE C-1. COMPARISON OF TYPICAL PARAMETERS: LH₂ VS. JET A SMALL CARGO AIRCRAFT

[M = 1.67; W, 7,150 kg (15,700 lb); 5000 km (3000 n mi)]

	SI	CUSTOMARY	LH ₂		JET A		FACTOR (JET A/LH ₂)
			SI	CUSTOMARY	SI	CUSTOMARY	
Takeoff Gross Weight	kg	lb	155,760	299,300	161,480	356,000	1.19
Operating Empty Weight	kg	lb	67,640	142,500	63,730	140,500	0.99
Block Fuel Weight	kg	lb	11,560	26,100	33,880	74,700	2.86
Total Fuel Weight	kg	lb	11,470	31,900	41,100	90,600	2.84
Wing Area	m ²	ft ²	240.1	2584	263.2	2833	1.10
Wing Loading, Takeoff	kg/m ²	lb/ft ²	565	115.3	613	125.6	1.08
Landing	kg/m ²	lb/ft ²	536	102.7	536	109.7	1.00
Span	m	ft	40.5	132.5	51.3	168.3	1.10
Fuselage Length	m	ft	57.3	188	56.6	185.6	0.99
Lift/Drag (Cruise)			16.3	16.3	17.9	17.9	1.10
Specific Fuel Consumption (Cruise)	kg/hr	lb/hr	0.213	0.209	0.619	0.608	2.91
Thrust per Engine (SLS)	N	lb	196,310	23,890	112,980	25,400	1.06
Thrust/Weight (SLS)	N/kg	-	0.32	0.32	0.29	0.29	0.91
PAR T.O. Distance	m	ft	4786	5800	2207	7240	1.25
PAR Landing Distance	m	ft	2231	7320	2216	7270	0.99
Approach Speed (PAR)	m/s	knots	69.5	135	69.5	135	1.00
Weight Fractions	percent	percent					
Fuel			11	11	26	26	2.36
Payload			12	12	35	35	0.53
Structure			22	22	25	25	0.86
Propulsion			10	10	7	7	0.7
Equipment and Operating Items			3	3	7	7	0.38
Energy Utilization	kg/km	Stn/ton n mi	4502	7181	4596	7339	1.02

TABLE 63. COMPARISON OF FUEL DESIGNS: LH₂ VS. JET A LARGE CARGO AIRCRAFT

[M = 1.65; 117,000 lb (53,000 kg); 10,190 km (5500 n mi)]

	SI	CUSTOMARY	LH ₂		JET A		FACTOR (JET A/LH ₂)
			SI	CUSTOMARY	SI	CUSTOMARY	
Takeoff Gross Weight	kg	lb	370,060	811,500	400,890	883,800	1.34
Operating Empty Weight	kg	lb	114,670	253,700	133,850	296,100	1.00
Block Fuel Weight	kg	lb	41,300	91,100	139,200	285,000	3.13
Total Fuel Weight	kg	lb	47,920	105,800	148,650	327,700	3.10
Wing Area	m ²	ft ²	453.4	5203	658.1	7084	1.36
Wing Loading, Takeoff	kg/m ²	lb/ft ²	620.5	127.1	609.3	124.8	0.98
Wing Loading, Landing	kg/m ²	lb/ft ²	535.6	109.7	412.5	84.5	0.77
Span	m	ft	55	216.4	77	252.5	1.17
Fuselage Length	m	ft	83.2	275.4	81.7	268.1	0.97
Lift/Drag (Cruise)			13.0	13.0	19.5	19.5	1.08
Specific Fuel Consumption (Cruise)	kg/dwt	lb/gal	0.213	0.209	0.619	0.608	2.91
Thrust per Engine (SLS)	N	lb	212,170	47,700	258,430	58,100	1.22
Thrust/Weight (SLS)	N/kg	-	0.29	0.29	0.26	0.26	0.90
FAR T.O. Distance	m	ft	2185	7170	2438	8000	1.12
FAR Landing Distance	m	ft	2304	7560	2143	7030	0.93
Approach Speed (2AS)	m/s	knots	69.5	135	61.2	119	0.88
Weight Fractions	percent	percent					
Fuel			16	16	37	37	2.31
Payload			38	38	28	28	0.74
Structure			31	31	23	23	0.74
Propulsion			10	10	7	7	0.70
Equipment and Operating Items			5	5	5	5	1.00
Energy Utilization	kJ/kg en	Btu/lb en	4986	6535	4782	7627	1.12

use of the ratio (Jet A/LH₂) for each parameter. The following trends and conclusions are established from these data.

Aircraft size comparisons for both mission capabilities favor the hydrogen fueled aircraft. Area required at the terminal gate is less for both the small and large LH₂ aircraft.

Gross weights of the small and large Jet A fueled aircraft are higher by 19 and 36 percent compared to the respective LH₂ counterpart aircraft. These differences are primarily the result of the high-energy content per unit weight of liquid hydrogen as indicated by block fuel weights of the Jet A aircraft which are approximately 2.86 and 3.13 times greater than those of the hydrogen aircraft.

Comparing lift-to-drag (L/D) ratios, it can be seen that the Jet A aircraft achieve a higher L/D than the corresponding hydrogen aircraft. It is also shown that the large aircraft, both hydrogen and Jet A, configured to perform the 113,600 kg payload mission, achieve a higher L/D than the small aircraft configured to meet the 56,700 kg payload mission.

Each of the four aircraft, as shown in Table 6h, have approximately the same drag coefficient level for the wing, empennage and propulsion package. Since the

TABLE 6h. AERODYNAMIC COEFFICIENT COMPARISONS: LH₂ VS JET A CARGO AIRCRAFT (CRUISE CONDITION)

	SMALL PAYLOAD		LARGE PAYLOAD	
	LH ₂	JET A	LH ₂	JET A
C _D (Wing, Empennage, Inlet & Pylon)	.0104	.0103	.0101	.0102
C _D (Empennage)	.0079	.0068	.0064	.0041
C _D (Including Compressibility)	.0208	.0197	.0188	.0164
C _{D,i} (Induced)	.0084	.0086	.0101	.0095
C _D (Total)	.0292	.0283	.0289	.0259
C _L (Lift)	0.475	0.507	0.522	0.504

hydrogen aircraft require greater fuselage volume than the Jet A aircraft to contain the required large fuel volumes, the fuselage drag coefficient levels of the hydrogen aircraft are higher than the Jet A aircraft fuselage drag coefficient levels. The small aircraft have approximately equal induced drag coefficients. The lift coefficient of the Jet A aircraft does not result in a greater induced drag level due to the Jet A aspect ratio 10 wing as compared to the aspect ratio 9 wing on the hydrogen aircraft.

Although the large aircraft have higher induced drag levels than the small aircraft, they have the best L/D ratios because of their lower fuselage drag level coefficients. These fuselage drag level coefficients are lower for the following reasons:

- Although the fuselages are much larger for the large aircraft, the drag coefficient is referenced to the wing area which is increased much more significantly from the small to the large mission than the fuselage wetted area – this is especially true of the large Jet A aircraft because of the large wing area this aircraft has imposed on it by the takeoff distance constraint.
- The increased length of the large fuselage and the resulting high Reynolds number reduce the skin friction coefficient for the large fuselage.

Airport performance is not a primary input to the sizing routine used to configure the cargo aircraft presented in this study. As previously discussed in Section 5.3.4.3, cruise matched aircraft are defined for a range of wing loadings and aspect ratios and then the various constraints are superimposed. Three of the four aircraft, the two small aircraft shown in Table 62 and the large hydrogen aircraft whose characteristics are listed in Table 63, are constrained by the 69.5 m/s (135 knot) approach condition and, consequently, provide shorter field lengths than the 1940 m (8000 ft) requirement. The fourth aircraft, the large Jet A, is constrained by the specified takeoff field length and as a result, produces approach speeds less than 69.5 m/s (135 knots).

Although identical design point missions were used to establish characteristics of both the Jet A and hydrogen aircraft, it should be noted that the Jet A aircraft offer a greater flexibility for off-design point missions, see Figures 86 and 92. Fuel volume in excess of that required to perform the design point mission is not provided in the hydrogen aircraft. This is necessitated by the low density, high volume characteristics of the hydrogen fuel. The Jet A aircraft can be provided,

at a minimum penalty, with fuel volumes 1.213 and 1.613 times greater, for the small and large aircraft respectively, than is required to perform the design point mission.

This excess fuel volume in the Jet A aircraft provides the ability at a constant gross weight condition to trade payload for additional fuel and hence greater range capability. The hydrogen aircraft however can achieve only a slight increase in range capability beyond the design range by off-loading payload to reduce gross weight.

5.3.2 Unit Price and Operational Cost

Aircraft unit price and direct operating cost (DOC) data are summarized in Table 65. The DOC's were calculated using the baseline price for the two fuels established at the outset of the study. The data in the table shows that at these arbitrary fuel prices the Jet A aircraft have a lower DOC. However, as payload and range are increased, the hydrogen fueled aircraft becomes more competitive with the Jet A fueled aircraft. DOC difference between the two small aircraft is approximately 12.1 percent of the Jet A DOC, whereas for the large aircraft this difference is only 3.7 percent.

5.3.2.1 Cost Sensitivity - Sensitivity analyses are presented which consider parametric variation of three direct operating cost parameters; fuel cost, aircraft utilization rate, and maintenance cost. These parameters were selected for examination because of the significance their values might have on the use of hydrogen fuel. There is a wide variation in fuel cost predictions for the 1990 time frame for both fuels. Aircraft utilization maintenance manhours per flight hour are difficult to

TABLE 65. UNIT PRICE AND OPERATIONAL COST COMPARISON: CARGO AIRCRAFT

	56,700 kg - 5560 km (125,000 lb - 3000 n m)		113,400 kg - 10,190 km (250,000 lb - 5500 n m)	
	LH ₂	JET A	LH ₂	JET A
Price - \$ X 10 ⁶	19.2	18.4	39.12	37.98
*DOC - ¢/Mg km	3.37	3.00	2.89	2.67
*DOC - ¢/ton - n mi	5.67	5.04	4.86	4.47

*Based on fuel price = \$2/1.054 GJ (\$2/10⁶ Btu) for Jet A

= \$3/1.054 GJ (\$3/10⁶ Btu) for LH₂

predict for the hydrogen aircraft until such time that actual experience has been gained on actual flight worthy hardware which is compatible with liquid hydrogen. The aircraft maintenance cost and utilization rates are dependent upon the magnitude of the maintenance manhours required.

Fuel Cost - Hydrogen fuel cost is varied from the base cost of three dollars per 1.054 GJ (10^6 Btu) to a low of one dollar and a high of four dollars. Jet A fuel cost is varied over the same cost range from the base cost of two dollars per 1.054 GJ. The resultant sensitivities of DOC to fuel cost are shown on Figures 93 and 94 for both the small and large aircraft. These sensitivity curves indicate that hydrogen fuel costs can be greater than Jet A fuel costs by 20 and 50 cents per 1.054 GJ (10^6 Btu) for the small and large aircraft respectively, and still achieve DOC equivalency between the hydrogen and Jet A aircraft. See Section 4.8.1 for additional comments regarding recent prices of Jet A fuel and projected costs of LH_2 .

Utilization - The base utilization rate for the small aircraft was 3600 hours per year and 4000 hours per year for the large aircraft. These values were varied over a range from 2500 to 5000 hours per year as shown on Figure 95. The slope of the curves shown is significant and illustrates the effect high utilization has on airline profits. Operational and maintenance procedures for the hydrogen aircraft need to be developed so at least equal utilization, relative to the Jet A aircraft, can be achieved.

Maintenance Cost - Maintenance costs were varied over a range including a 10 percent reduction in costs to a 10 percent increase, as shown in Figure 96. Comparing maintenance cost sensitivities to utilization sensitivities it can be seen that of the two, utilization changes have the greater effect upon DOC. Therefore, reducing maintenance time is of more importance than reducing maintenance costs.

4.8.3 Energy Consumption

Energy consumption comparisons for the four aircraft are shown in Tables 62 and 63. The large and small hydrogen aircraft consume 2.0 and 12 percent less energy in accomplishing a given mission than the respective Jet A reference aircraft. These data indicate that for the hydrogen fueled aircraft the energy consumed per unit work accomplished decreases as payload and range increase, whereas the opposite trend is indicated for the Jet A fueled aircraft. The reasons for

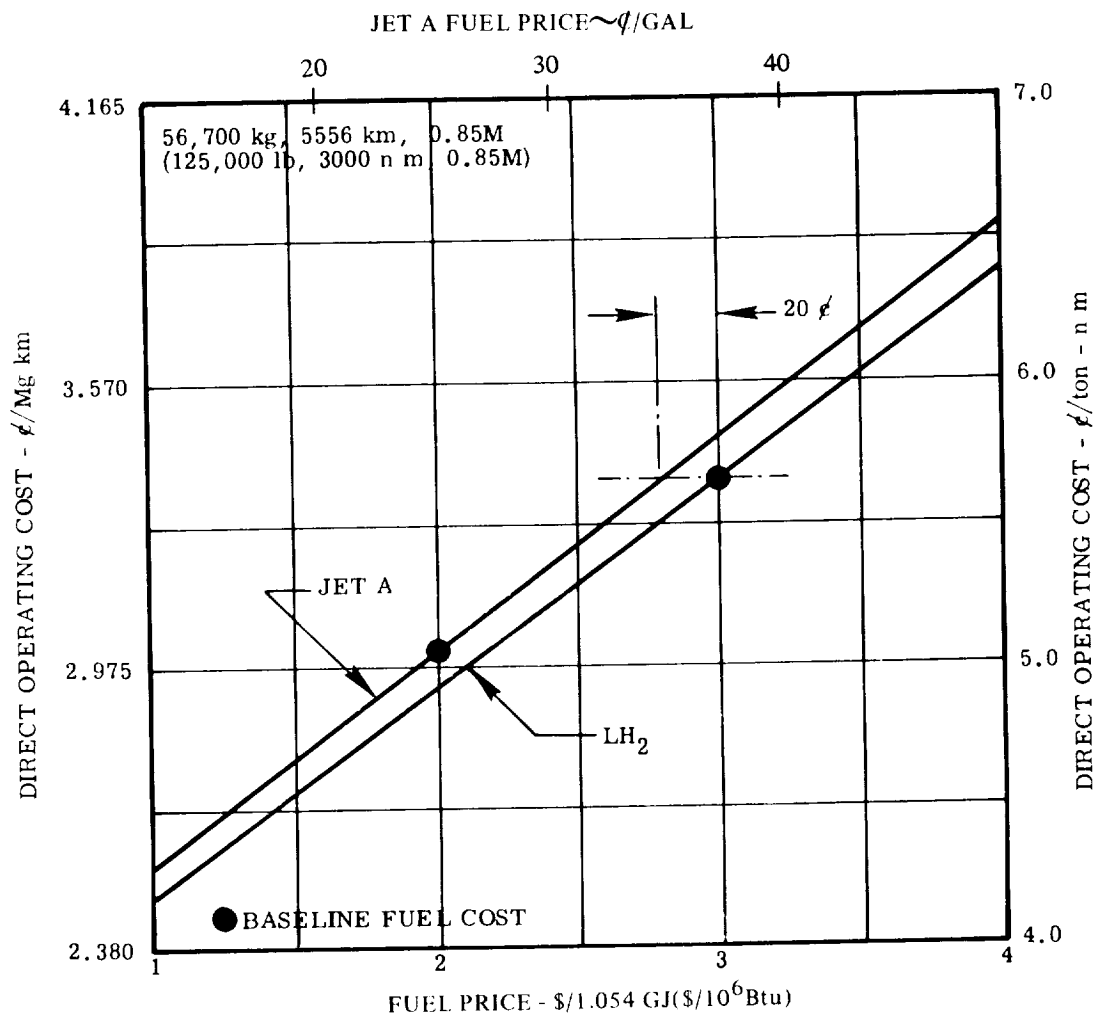


Figure 93. Sensitivity of DOC to Fuel Price (Small Cargo Aircraft)

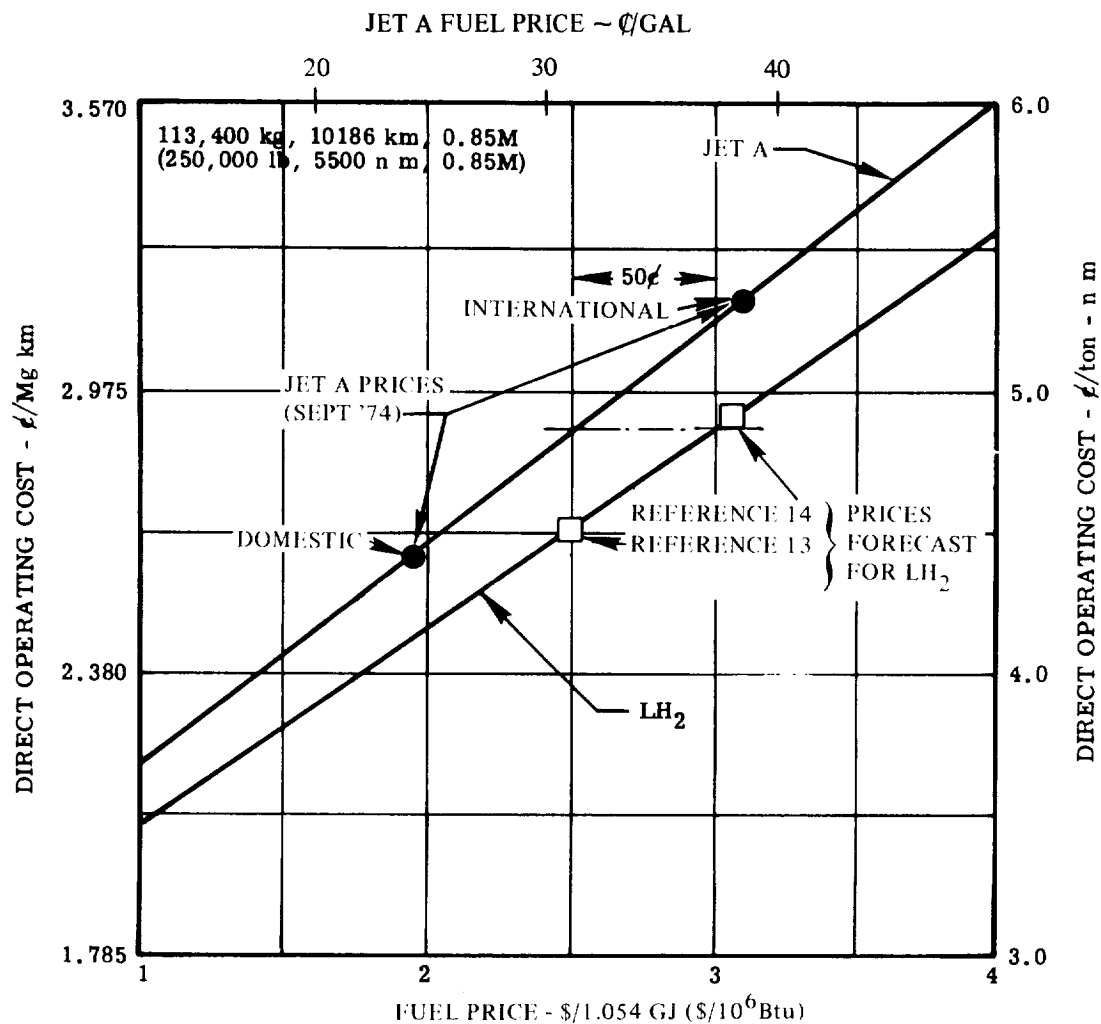


Figure 94. Sensitivity of DOC to Fuel Price (Large Cargo Aircraft)

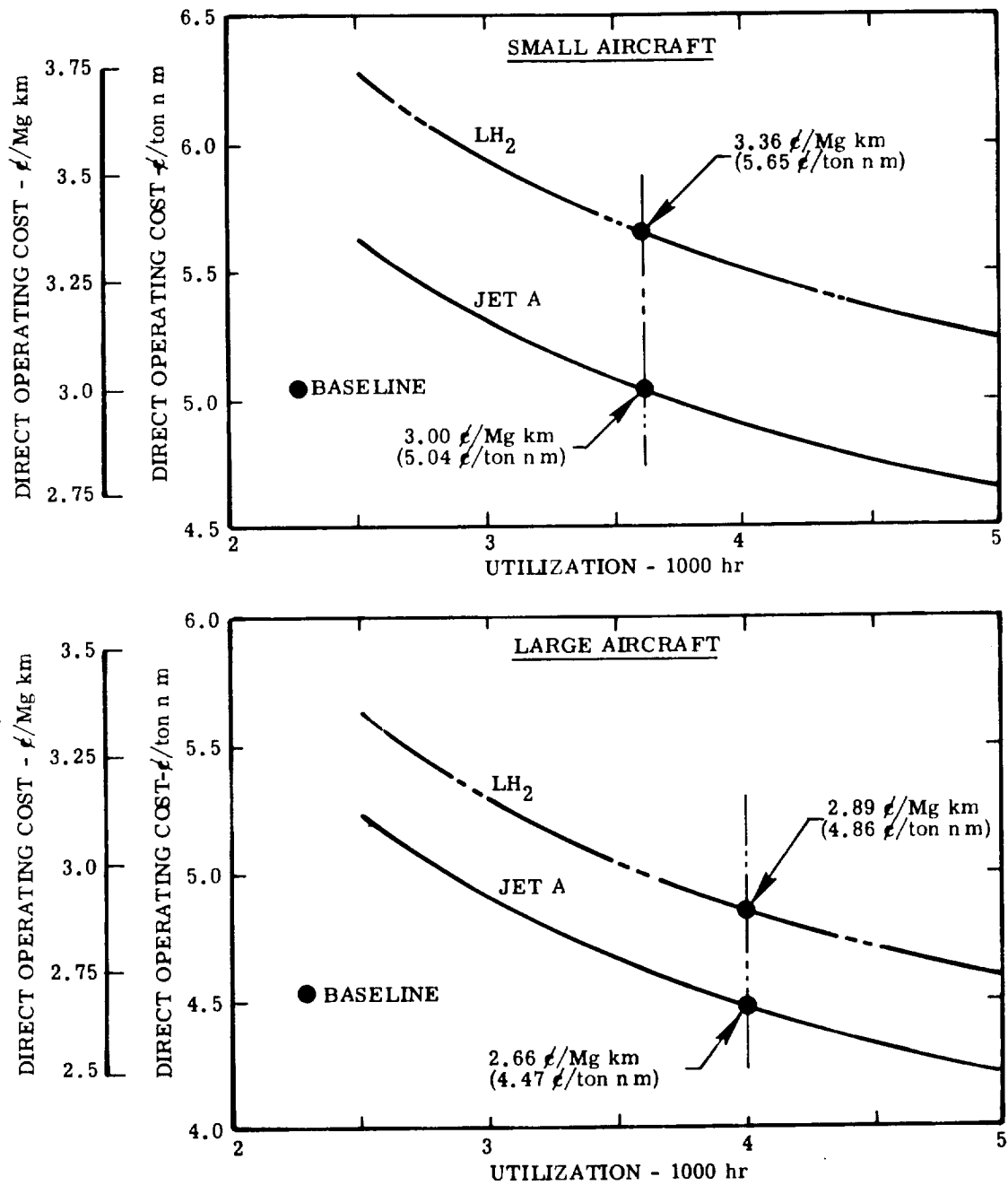


Figure 95. Direct Operating Cost - Utilization Sensitivity

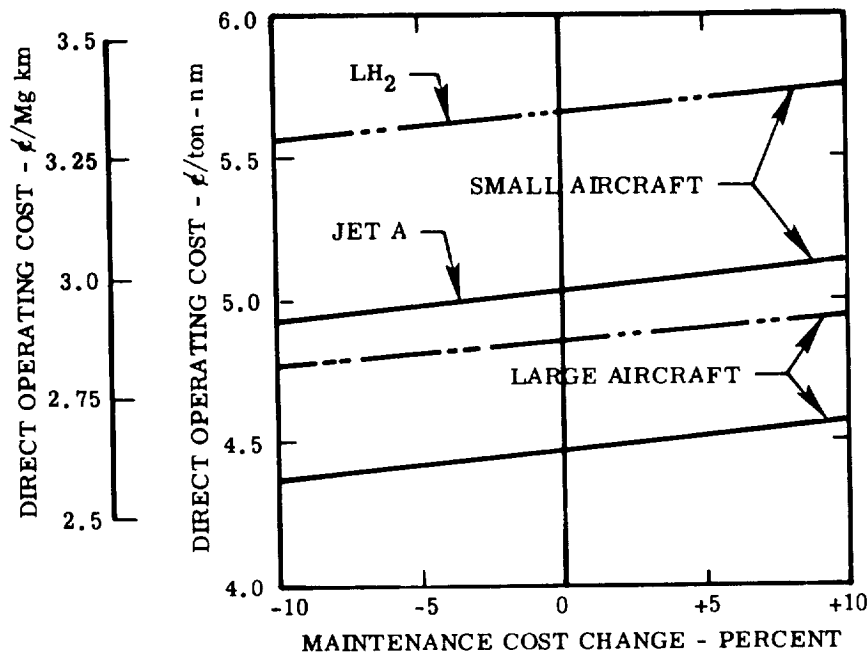


Figure 96. Direct Operating Cost - Maintenance Cost Sensitivity

this seemingly diverse result are obscured because both payload and range were varied in the two example aircraft which were studied for each fuel. Additional studies are required to determine the relative effects of payload and range on energy consumption and to confirm the trends indicated here.

5.3.4 Noise Comparison

Figures 97 and 98 present the takeoff and landing 90 EPNdB footprint areas for the four aircraft. These data are presented for FAR 36 conditions, i.e., sea level, standard day + 10⁰C, and assume full power takeoff; operational techniques such as part power takeoff or power cutback have not been used. The approach glideslope for these aircraft is 0.05 radians (3 degrees).

Footprint areas for takeoff and landing and FAR noise levels for the takeoff flyover, takeoff sideline and approach flyover conditions are given in Table 66. The EPNdB levels given in parentheses are for the FAR 36 noise limit.

Table 66 shows that the takeoff footprints are smaller for the hydrogen than for the Jet A fueled aircraft. In general, takeoff prints are smaller for one

90 EPNdB CONTOUR COMPARISON

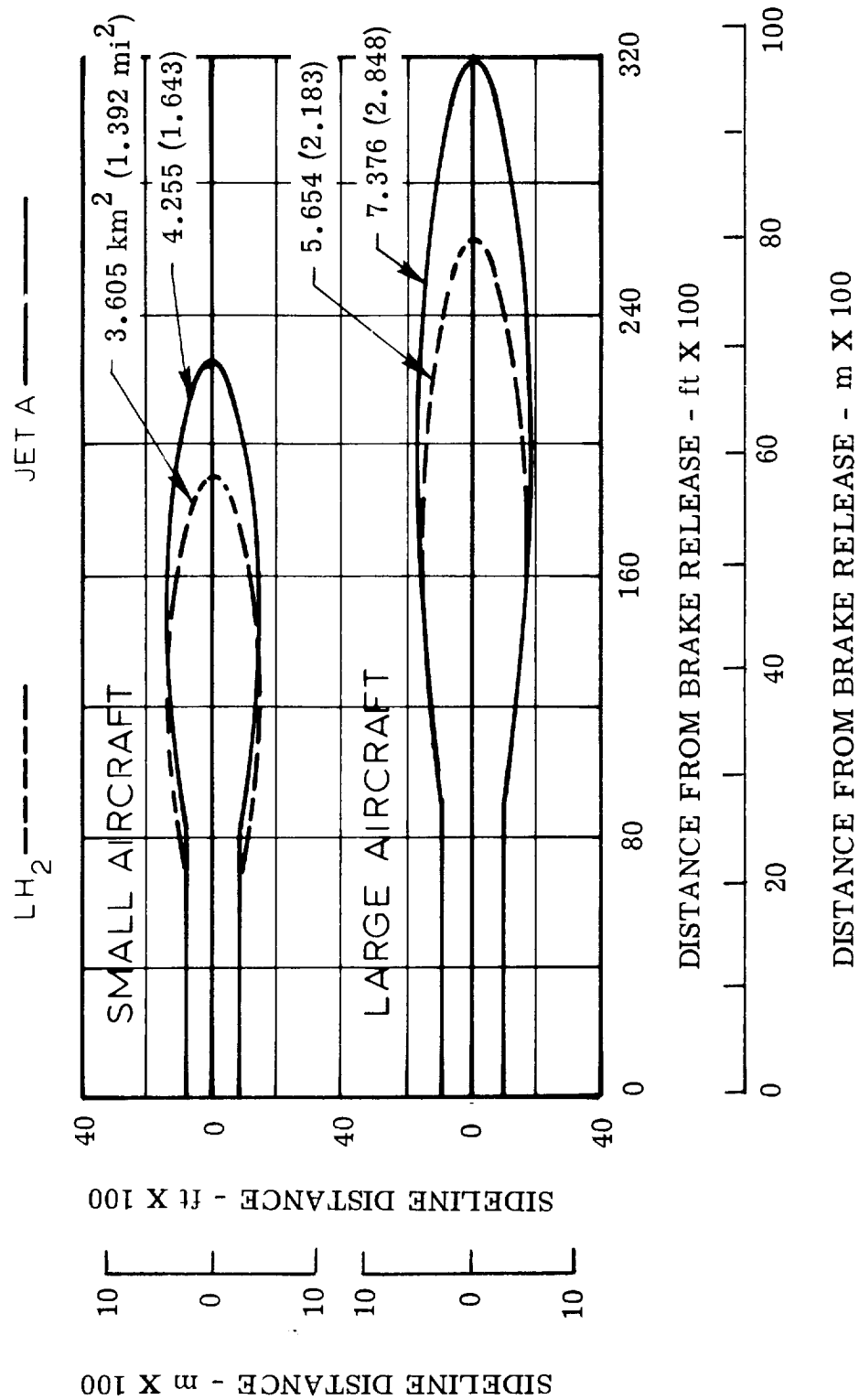


Figure 97. Takeoff Noise Footprint - Cargo Aircraft

90 EPNdB CONTOUR COMPARISON

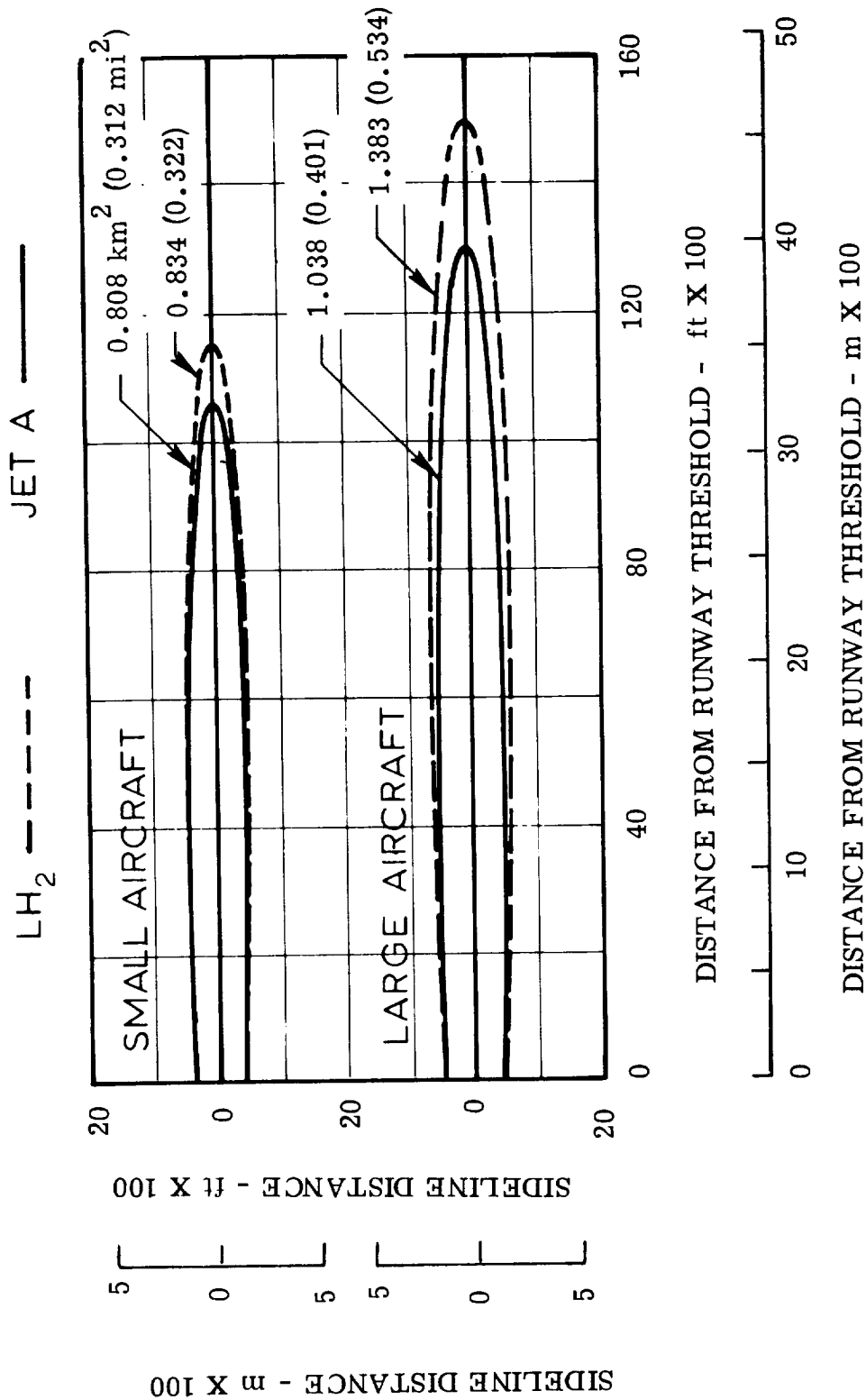


Figure 98. Landing Noise Footprint - Cargo Aircraft

TABLE 66. NOISE COMPARISON - CARGO AIRCRAFT

AIRCRAFT	FAR PART 36 NOISE LEVEL - EPNdB						AREA WITHIN 90 EPNdB CONTOUR km ² (mi. ²)		
	TAKEOFF FLYOVER		TAKEOFF SIDELINE		APPROACH FLYOVER		TAKEOFF	APPROACH	TOTAL
	LIMIT	AIRPLANE	LIMIT	AIRPLANE	LIMIT	AIRPLANE			
<u>Small</u>									
Jet A	104.2	90.7	106.5	86.8	106.5	94.5	4.24 (1.643)	0.80 (0.312)	5.04 (1.955)
LH ₂	102.9	88.7	106.0	86.8	106.0	94.5	3.59 (1.392)	0.83 (0.322)	4.42 (1.714)
<u>Large</u>									
Jet A	108.0	95.1	108.0	88.3	108.0	95.4	7.35 (2.848)	1.03 (0.401)	8.38 (3.249)
LH ₂	108.	92.7	108.0	87.8	108.0	96.4	5.63 (2.183)	1.38 (0.534)	7.01 (2.717)

aircraft, when compared to another, if it has a lower installed thrust and a steeper climb angle. The large aircraft have larger noise footprints simply because their size requires more installed thrust. The hydrogen aircraft, for a given mission, has a smaller footprint than its Jet A counterpart because it has a lower installed thrust combined with a higher thrust-to-weight ratio which gives it better climb out characteristics.

The landing footprints are a function of thrust, power setting, and velocity. The small hydrogen and Jet A aircraft have about the same footprint size because they have essentially the same approach thrust requirements and the same approach speed. The power setting is relatively higher for the hydrogen aircraft because it has a smaller engine and a lower L/D than the Jet A equivalent.

The large Jet A aircraft has a smaller landing footprint than the hydrogen equivalent because it has a considerably lower approach speed and approach power setting even though the actual thrust required for the Jet A aircraft is larger.

The flyover and sideline noise levels of these four aircraft are 11 to 20 EPNdB lower than the limit values defined by FAR 36.

5.8.5 Emissions

See Section 4.8.3 for comparison of emissions from LH₂ and Jet A turbofan engines.

5.8.6 Safety

The comments of Paragraph 4.8.4 pertaining to passenger aircraft safety are equally applicable to cargo aircraft safety.

SECTION 6

RESEARCH AND TECHNOLOGY RECOMMENDATIONS

The results reported in the foregoing sections clearly show that liquid hydrogen is a very attractive fuel for subsonic transport aircraft, including both passenger and cargo types. In this section, research and technology development items are identified which are considered crucial to implementation of hydrogen technology in commercial transport aircraft. The list includes studies, items for experimental development, and demonstration programs involving flight operations.

Following the listing and brief description of the items suggested for technology development, a schedule is presented which shows a proposed sequence and timing of the work. Rough order of magnitude estimates of the level of effort considered reasonable and appropriate for each subject are also shown.

6.1 TECHNOLOGY DEVELOPMENT ITEMS

The following subjects are suggested as items requiring study and development effort before liquid hydrogen can efficiently and successfully be employed as a fuel in commercial transport aircraft. The subjects are presented in three categories: studies, experimental development, and flight operations.

6.1.1 Studies

1. Aircraft Design Studies

Activities:

Study aircraft designs to provide mission capabilities representing the spectrum of commercial user interest for the time period subsequent to 1990. The studies should encompass:

- Passenger aircraft (150 to 800 passengers)
- Cargo aircraft (22,700 to 341,000 kg. [50,000 to 750,000 lbs] payload)

- Ranges from 2780 to 10,190 km (1,500 to 5,500 n.mi.)
- Cruise speeds from Mach 0.7 to 0.85

Objectives:

- A. Determine characteristics of LH_2 fueled aircraft for selected airline requirements.
- B. Establish baseline criteria for selected aircraft and for their major hydrogen-related subsystems:
 - Tank and insulation system
 - Fuel system components
 - Engines
 - Vent system
 - Auxiliary power unit
 - Environmental control system
- C. Establish basis for writing operational and maintenance equipment requirements and procedures.
 - Fueling
 - Routine in-service operations
 - Overnight out-of-service
 - Extended out-of-service
- D. Establish basis for writing requirement for airport facilities.
 - Fuel storage capacity
 - Fuel liquefaction plant capacity
 - Fuel handling equipment
 - Maintenance hangers

2. Tank Design and Insulation Study

Activity:

For a selected commercial transport aircraft design make detail design studies of candidate fuel tanks and insulation systems. Evaluate each fuel containment system in terms of vehicle performance and cost.

Objectives:

- A. Establish detail design characteristics and performance of candidate tank design and insulation systems.
 - Integral tank/foam insulation
 - Non-integral tank/foam insulation
 - Integral tank/vacuum and microsphere insulation system
 - Non-integral tank/vacuum and microsphere insulation system
 - B. Evaluate the candidate designs on basis of vehicle performance and costs (investment, operational, and maintenance).
 - C. Select a preferred design for experimental development (see Item 11).
3. Aircraft Fuel System Design Study

Activity:

For a selected commercial transport aircraft design, make detail design studies of candidate fuel line concepts and determine size, weight, and design requirements of the principle system components.

Objectives:

- A. Establish design characteristics and performance of candidate fuel lines.
 - vacuum-jacketed lines
 - foam insulated lines
- B. Evaluate the candidate fuel line designs on basis of weight, performance, and costs (investment and maintenance).
- C. Select a preferred design of fuel line for experimental development (see Item 11).
- D. Establish size, weight, design characteristics, and approximate cost of principle fuel system components, e.g., low pressure pumps, valves, seals, quantity sensors, etc.

4. Airport Fuel Supply System Design Requirements

Activity:

Study the thermodynamic design requirements of the fuel supply system for a specific airport considering probable fuel volumes required in the 1990-2000 era. Determine design requirements of all significant elements of the fuel supply system from the LH_2 storage vessel to the aircraft tank.

Objectives:

- A. Determine thermodynamically acceptable procedures and pressure schedules for
 - Filling and storing LH_2 in airport reservoir
 - Filling and maintaining pressure in aircraft tanks
 - Starting aircraft engines with "warm" feed lines
- B. Establish feasible procedures for handling gaseous hydrogen from aircraft vent system during filling and extended ground hold.
- C. Determine design requirements of a typical airport/aircraft fueling and defueling system.
- D. Determine design requirements of a practical aircraft vent system and an airport GH_2 recapture system.
- E. Provide input for Item 6.

5. Operations and Maintenance Procedures Study

Activity:

Conduct a study of airline operations and maintenance requirements for a selected design of LH_2 fueled commercial transport aircraft.

Objectives:

- A. Define procedures for routine operations.
 - Fueling into warm tank
 - Fueling into cold tank
 - Defueling
 - Passenger and cargo loading
 - Overnight storage
 - Extended out-of-service storage

- Delay on ground awaiting takeoff
- Etc.

B. Define procedures for fuel system-related maintenance.

- Fuel pump replacement
- Fuel quantity sensor malfunction
- Tank insulation system defect
- Tank structural inspection
- Fuel line inspection
- Vent line valve freeze
- Etc.

C. Provide input for Item 6.

6. Study of Airport/Airplane Interface Facility Requirements

Activity:

Perform an analysis of facilities which will be required at a typical airport in 1990 - 2000 to support LH_2 fueled airline traffic. Layout the facility and design the hydrogen-related elements in sufficient detail to determine realistic cost estimates.

Objectives:

A. Establish requirements for typical airport facilities needed to support airline operations of LH_2 fueled aircraft.

- Fuel storage capacity
- Fuel liquefaction plant capacity
- Fueling system design and capacities
- Defueling system
- Gaseous hydrogen return and disposal system
- Maintenance hanger design requirements
- Airport facility layout

B. Estimate cost of airport facilities for typical installation.

7. Systems Analysis of Ways to Initiate LH₂ Fuel Service in Airline Operations

Activity:

Analyze airline route structures, traffic densities, and aircraft usage throughout the United States as projected for the 1990-2000 time period. In addition, include consideration of connecting international routes, with special attention to routes to those countries most likely to require early relief from use of hydrocarbon fuel.

Objectives:

- A. Determine feasible ways to initiate use of LH₂ fuel in commercial transport aircraft, for example,
 - by airline
 - by city-pair, e.g., L.A. to Washington
 - by region, e.g., West Coast
- B. Project the fuel changeover from U.S. domestic airlines to international carriers.
- C. Establish a feasible schedule for installation of LH₂ facilities at airports and determine costs and fuel requirements vs years.
- D. Define principle problems, costs, and possible methods of funding.

8. Airframe Structural Design Concepts Study

Activity:

For a selected commercial transport aircraft design, make detail studies of candidate fuselage structural concepts for integrating the preferred cryogenic tank and insulation systems.

Objectives:

Determine preferred airframe structural design concept. Include consideration of the following:

- Differential thermal expansion
- Compatibility of materials with hydrogen environment
- Heat leaks to tank structure through attachments
- Necessity of removing tanks for repair and/or replacement.

9. Advanced Engine Design Study

Activity:

Conduct a design study to establish preferred characteristics of a hydrogen-fueled turbofan engine for a specified commercial transport aircraft.

Objectives:

- A. Establish design and performance characteristics of an advanced design, quiet, cleanburning LH_2 fueled engine to match requirements of a selected airplane design. Provide size, weight, cycle characteristics, performance, and cost estimates.
- B. Establish requirements for major components, e.g., high pressure pump, heat exchanger, combustor design, noise suppression devices, engine control system, compressor, fan, turbines, and cooling system.
- C. Provide input for Item 12.

10. Study of Relative Hazards of LH_2 vs Jet A Fuel In Commercial Transport Aircraft

Activity:

Study representative designs of a selected size of commercial transport aircraft; one fueled with LH_2 , the other with conventional Jet A. Analyze the designs for probable failure modes, both in-flight and on the ground. Where appropriate, supplement the study with analysis of accident reports.

Objectives:

- A. By analysis of probabilities of various kinds of accidents, both in-flight and on the ground, estimate probable failure modes and results which can be expected with both fuel systems.
- B. Provide input for Item 15.

6.1.2 Experimental Development

11. Fuel System Technology Development

Activity:

Design, fabricate and test a model of a complete aircraft fuel system including:

- tank
- insulation system
- feed lines and vent systems
- valves
- pumps
- quantity sensor system
- quick disconnect, gaseous hydrogen
- quick disconnect, liquid hydrogen
- leak detection
- fire detection
- fuel dumping system

Objectives:

- A. Determine characteristics of a satisfactory design for the fuel system components.
- B. Establish design specifications for LH_2 fuel systems and components suitable for aircraft service.
- C. Determine procedures for performing inspection and repair of LH_2 system components.
- D. Determine effect of repeated flight cycles on tank structure, insulation system, and fuel feed system.
- E. Begin development of technology with aircraft components related to use of LH_2 , e.g., cryogenic insulation, pumps, valves, seals, which will meet airline standards of long life, reliability, and maintainability.

12. Engine Technology Development

Activity:

Design, fabricate and test components of an advanced design of LH_2 fueled engine including

- High pressure pump
- Heat exchanger
- Combustor
- Cooled turbines and nozzles
- Engine control system

Objectives:

- A. Develop component technology required to build a liquid hydrogen fueled engine incorporating features to capitalize on advantages available with the fuel.
- B. Begin development of technology in engine components such as pumps, valves, bearings, and seals which will meet long-life reliability and maintainability requirements.

13. Materials Development

Activity:

Conduct literature searches, obtain manufacturer's data, and perform laboratory experiments.

Objectives:

- A. Determine materials preferred for use as
 - Cryogenic insulation for fuel tank
 - Impermeable barrier to either GH_2 or air
 - Tank bladder/structural material
 - Structural connection between cryogenic tank and ambient temperature aircraft structure
 - Cryogenic fuel line/bellows/support structure
 - Sealing surfaces for valves

B. Begin determination of effects of long-term exposure to hydrogen of structural and component materials.

14. Hazard Posed by Fire: LH_2 vs Jet A Fuel

Activity:

Expose instrumented fuselage sections of surplus transport aircraft to fire from equal-energy quantities of LH_2 and Jet A fuel.

Objective:

Determine effect of fire from burning fuel adjacent to passenger compartment and compare relative hazards to crew and passengers.

15. Safety in Nonfatal Crashes

Activity:

Simulate nonfatal crashes with surplus aircraft components containing residual fuel in typical tank structures. Duplicate tests for each fuel system (LH_2 and Jet A).

Objective:

Determine effect of simulated crash using each fuel system and compare relative hazard to crew and passengers.

6.1.3 Flight Operations

16. Flight Demonstration Program

Activity:

Convert two subsonic transport aircraft to LH_2 fuel and operate in simulated cargo and/or passenger carrying service for two years.

Objectives:

- A. Learn how to handle LH_2 as an aircraft fuel in an operational manner.
- B. Determine the practicability of the cryogenic fuel system in terms of inspection, maintenance, durability, and performance.

- C. Provide a basis for writing design and operational specifications for hydrogen-related equipment and procedures.
- D. Establish confidence that hydrogen can be used safely in airline-type operations.

17. Airport Fuel-Handling Demonstration Project^{*}

Activity:

Design, fabricate, and operate a complete airport fuel-handling facility using hardware scaled to requirements of Item 16 (above).

Objective:

Determine system and component performance characteristics, operational and maintenance techniques, safety standards, future design criteria, and cost relationships.

6.2 TECHNOLOGY DEVELOPMENT SCHEDULE

Figure 99 presents a schedule for performing the studies, development, and operations described in the preceding section so hydrogen technology can be ready for incorporation in a commercial transport aircraft design on a timely basis.

It is important to keep two things in mind when considering this schedule:

- Development of an industrial capability to produce, transport, and store sufficient quantities of liquid hydrogen to meet America's needs for long-range transport aircraft will probably take at least 15 years, e.g., from 1975 to 1990.
- Development of a LH₂ fueled transport aircraft, ready for first use, will probably take about 10 years after the technology development of

^{*} Suggested in Reference 26, Chapter V-B, Alternate Fuels.

SUBSONIC LH₂ TRANSPORT AIRCRAFT

STUDIES

1. AIRCRAFT DESIGN STUDIES
2. TANK AND INSULATION DESIGN
3. AIRCRAFT FUEL SYSTEM DESIGN
4. AIRPORT FUEL SUPPLY SYSTEM ANALYSIS
5. AIRFRAME STRUCTURAL CONCEPTS STUDY
6. ADVANCED ENGINE DESIGN STUDY
7. OPERATIONS AND MAINTENANCE PROCEDURES ANALYSIS
8. AIRPORT/AIRPLANE FACILITIES REQUIREMENTS
9. LH₂ USE INITIATION STUDY
10. FUEL HAZARDS ANALYSIS

EXPERIMENTAL DEVELOPMENT

11. FUEL SYSTEM TECHNOLOGY DEVELOPMENT
12. ENGINE TECHNOLOGY DEVELOPMENT
13. MATERIALS DEVELOPMENT
14. CRASH SAFETY COMPARISON
15. FIRE HAZARD COMPARISON

FLIGHT OPERATIONS

16. FLIGHT DEMONSTRATION PROGRAM
17. AIRPORT FUEL-HANDLING DEMONSTRATION PROJECT

*REFERENCE 27

**REFERENCE 26

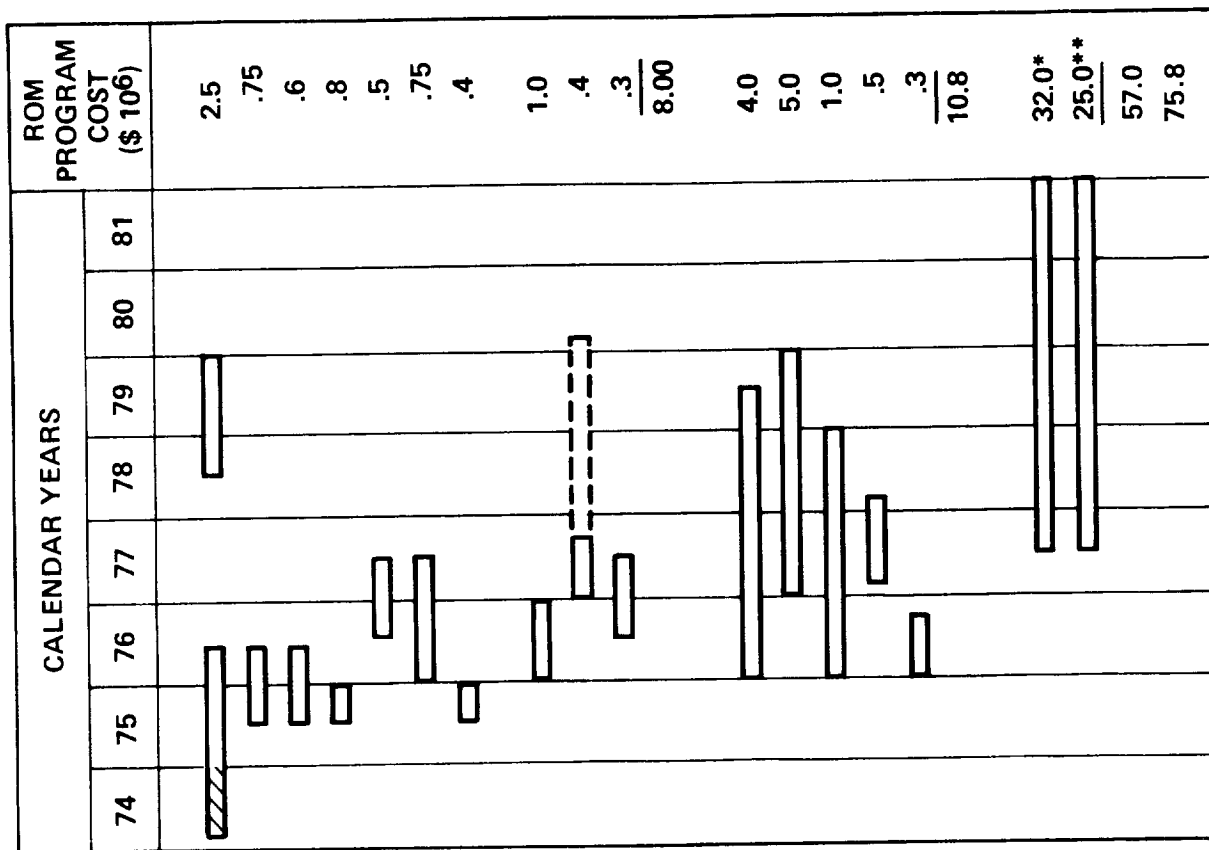


Figure 20. Technology Development Program

Figure 99 has been completed, and after an aircraft design specification has been agreed upon and a decision is made to proceed.

These two factors, together with the Technology Development Program herein proposed, are considered to be the principle requirements which must be met before liquid hydrogen can be successfully employed in commercial transport aircraft. The fundamental pacing item is development of the industrial capability to produce gaseous hydrogen in sufficient quantity, pipeline it to key airports, and there liquefy and store it, all for an economically competitive price. If this capability can be established in 15 years, the program for development of the hydrogen related technology items listed above should begin immediately in order that the aircraft design and development can, in turn, be completed by the time the LH₂ supply is assured.

SECTION 7

CONCLUSIONS

The use of liquid hydrogen as fuel in subsonic transport aircraft results in designs which are lighter, have smaller wings but larger fuselages, require smaller engines, can operate from shorter runways, minimize pollution of the atmosphere, and expend less energy in performing their missions than corresponding designs fueled with conventional hydrocarbon (Jet A). Depending on the payload-range design requirement, the cost of liquid hydrogen can be between 20¢ and 50¢ greater per 1.054GJ (10^6 Btu), relative to Jet A cost, and still provide lower direct operating cost.

To establish a perspective for this DOC comparison, at prices international carriers paid for Jet A in the latest month for which data was available, viz., September 1974, airlines could have realized a reduction in DOC of more than 11 percent, from 0.573 down to 0.508¢/seat km (1.061 down to 0.940¢/seat n. mi.), using the long range passenger aircraft defined in this study as an example, and assuming availability of LH_2 at \$2.50/1.054GJ (10^6 Btu), the price forecast in 1973 by the Linde Division of Union Carbide Corporation (Reference 13).

Transport aircraft designed to use LH_2 probably will not look unconventional. There are sound technical reasons why current subsonic aircraft look the way they do. Although this is not to say that changes will not be made; nevertheless, radical departures from the norm of today's design standards almost invariably involve significant tradeoffs in performance because of either structural weight or aerodynamic penalties. So it is that the preferred design concepts for hydrogen-fueled passenger and cargo transport aircraft evolved in this study have conventional appearance. Unusual configurations which were investigated to see if use of the new fuel would open up design possibilities proved to be flawed. Designs configured to provide specific advantages developed serious problems in other respects such that the net result was unsatisfactory.

The external tank arrangement, investigated in the passenger aircraft part of the study to see if fuel tanks mounted on a short pylon above the wing at about mid-span offered any advantage in passenger safety, operational, or maintenance considerations, proved the point. The configuration was found to offer significant maintenance advantage, but for the size tanks involved on aircraft in this study, to actually be a detriment operationally and to have questionable safety aspects. It was significantly inferior insofar as performance and operational costs were concerned.

Accordingly, the configuration of passenger aircraft which carries the LH_2 fuel within the fuselage in two tanks, one forward and one aft of the double-deck passenger compartment, and which retains conventional design values for relationships like fuselage fineness ratio, wing aspect ratio and sweep, and wing loading, was found to be preferred.

Similarly, the configuration for LH_2 fueled cargo airplanes found to be preferred for the missions of this study has a conventional external appearance, even though a series of preliminary design studies was carried out to investigate unusual approaches which, when originally suggested, appeared to have some special merit. The selected design has a "visor nose" which lifts to permit loading of cargo from the front end. Cargo containers are loaded in two rows side-by-side. LH_2 fuel is contained entirely within the fuselage, mostly in the space above the cargo compartment.

The problems of designing and developing practical, realistic transport aircraft fueled with liquid hydrogen which can meet airline standards for maintenance, operations, and utilization in either passenger or cargo application, are challenging but not insurmountable. Solutions require technology development but are not dependent upon either a breakthrough in capability or invention of new products for success. Development of a production and distribution capability to provide LH_2 in sufficient quantity to meet airline requirements at a reasonable price, is seen as a critical and pacing consideration.

SECTION 3

RECOMMENDATIONS

In view of the many attractive advantages which result from use of liquid hydrogen as fuel for long range subsonic transport aircraft, and because of the recognized problems of maintaining an adequate supply of petroleum-based conventional fuel throughout the world, it is recommended that development of appropriate technology be actively pursued. Section 6, Research and Technology Recommendations, lists 17 items which constitute a recommended program for development of aircraft related technology. A schedule for this program is shown in Figure 99.

Concurrently with this aircraft technology development program, and starting at the conclusion of Item 7 in Figure 99 (indicated by the dashed portion of the bar), advanced econometric and operations analyses with emphasis on societal impact connotations should be conducted to determine an economically feasible and viable plan for converting commercial transport aircraft to hydrogen. Along with that study would come a determination of preferred mission requirements for the initial design of LH_2 fueled transport aircraft. As indicated by the length of the dashed portion of the bar on Item 7, Figure 99, this determination should be made early in 1980 so that a decision can then be made at the end of that same year to proceed with prototype development of the first production aircraft. Allowing ten years from design go-ahead to first delivery for operational use, this would put the first commercial transport airplane designed for LH_2 fuel in service in 1990, about the time airlines would normally be ready to begin replacement of the current wide-bodied transports. Recognizing that several sizes of transport aircraft will ultimately be required to efficiently meet the needs of the air transport industry, both at home and abroad, development and production of a series of aircraft must be planned, in addition to modification and conversion of appropriate existing aircraft.

It is considered technically feasible that hydrogen-fueled transport aircraft can be developed and ready to begin commercial operations in 1990. However, the following significant conditions are recognized as mandatory and supplemental to the aircraft-related technology requirements in order to achieve this goal:

- A national (and international) commitment must be made to develop hydrogen for widespread use, and commercial transport aircraft must be mandated to use it.
- Hydrogen manufacture and distribution systems must be developed and implemented.
- Facilities must be provided on or near airports to liquefy, store, and handle hydrogen.

The critical item which paces the entire operation appears to be development of an industrial capability to produce gaseous hydrogen, pipeline it to areas near key airports, and there liquefy and store it in sufficient quantities and at an economically competitive price that airline needs can be met. Assuming that such an industrial capability can be developed in 15 years, e.g., 1975 to 1990, it is necessary that the aircraft technology development program shown in Figure 99 be started immediately.

REFERENCES

1. Cook, Earl; "The Flow of Energy in an Industrial Society," Scientific American, September 1971, p 135.
2. Transportation Energy Panel, "Research and Development Opportunities for Improved Transportation Energy Usage," Department of Transportation, DOT-TSC-OST-73-14, September 1972.
3. Hord, J., Editor,; "Selected Topics on Hydrogen Fuel", National Bureau of Standards - Cryogenics Division, NBSIR 75-803, January 1975.
4. Anon., NASA Request for Proposal 1-15-4102; "Study of the Application of Hydrogen Fuel to Long Range Subsonic Transport Aircraft," 20 September 1973.
5. McCarty, Robert D. and Weber, Lloyd A.; "Thermophysical Properties of Parahydrogen from the Freezing Liquid Line to 5000 R for Pressures to 10,000 psia," National Bureau of Standards, Technical Note 617, April 1972.
6. Brewer, G. D.; "Advanced Supersonic Technology Concept Study - Hydrogen Fueled Configuration," NASA CR114,718, prepared by the Lockheed California Company under Contract No. NAS 2-7732, January 1974.
7. Keller, C. W.; "Fiberglass Supports for Cryogenic Tanks," NASA CR120937, Lockheed Missiles and Space Co., LMSC-D281476, 10 October 1972.
8. Sens, William H. and Meyer, Robert M.; "New Generation Engines - The Engine Manufacturer's Outlook," SAE Paper No. 680278, 1968.
9. Young, C.; "An Investigation of Annular Aerofoils for Turbofan Engine Aeronautical Research Council, Cowls," Reports and Memoranda No. 3688, Royal Aircraft Establishment, Farnborough, England, 1969.
10. Lange, R. H., et al.; "Study of the Application of Advanced Technologies to Long-Range Transport Aircraft," NASA CR-112088, prepared by the Lockheed-Georgia Company under Contract No. NAS1-10701, May 1972, CONFIDENTIAL
11. Ordin, Paul M.; "Review of Hydrogen Accidents and Incidents in NASA Operations," NASA-Lewis Research Center, NASA TM X-71565, presented at Ninth Intersociety Energy Conversion Engineering Conference, August 26-30, 1974.
12. Bill Herzey's Airline Reports, p 5, October 28, 1974, Wm. V. Herzey and Associates, Washington, D. C.

REFERENCES (Continued)

13. Johnson, J. E., "The Economics of Liquid Hydrogen Supply for Air Transportation," Advances in Cryogenic Engineering, p 12, Vol. 19, Edited by K. D. Timmerhaus, Plenum Press, New York, 1974.
14. Michel, J. W., "Hydrogen and Exotic Fuels," Oak Ridge National Laboratory, ORNL-TM-4461, June 1973.
15. Anon., "Federal Aviation Regulations, Part 36, Noise Standards: Aircraft Type Certification," Dept. of Transportation, FAA, Washington, D. C., November 3, 1969.
16. Anon., "Jet Noise Prediction," Aerospace Information Report AIR 876, Society of Automotive Engineers, New York, 7-10-65.
17. D. G. Dunn, et al., "Aircraft Noise Source and Contour Estimation," CR-114649, NASA, Washington, D. C., July 1973.
18. J. D. Revelle, "The Calculation of Aerodynamic Noise Generated by Large Aircraft at Landing Approach," Paper JJ9, 87th Meeting of Acoustical Society of America, New York, 23-26 April 1974.
19. N. Shapiro, et al., "Commercial Aircraft Noise Definition L-1011 Tristar," FAA-EQ-73-6, Lockheed-California Company for FAA, Washington, D. C., to be published.
20. Brines, G. L., "Studies for Determining the Optimum Propulsion System Characteristics for use in a Long Range Transport Aircraft," NASA CR-120950, 1972.
21. Anon., "Propulsion System Studies for an Advanced High Subsonic Long Range Jet Commercial Transport Aircraft," NASA CR-121016, 1972.
22. Grobman, Jack; Norgren, Carl; and Anderson, David, Turbojet Emissions, Hydrogen Versus JP. NASA TM-X-68258, 1973.
23. Grobman, Jack, and INGEB0, Robert D.: Jet Engine Exhaust Emissions for Future High Altitude Commercial Aircraft. NASA TM-X-71509, 1974.
24. Diehl, Larry A.; and Biaglow, James A.: Measurement of Gaseous Emissions from a Turbofan Engine at Simulated Altitude Conditions. NASA TM-X-3046, 1974.
25. Anon: Weight and Balance Data Reporting Form for Aircraft; Part 1, Group Weight Statement. MIL-STD-254 (ASG), August 26, 1954.
26. Dixy Lee Ray Committee, "Report to the President on Energy Research and Development," Appendix E-2, dated October 27, 1973.

REFERENCES (Continued)

27. "The Energy Dilemma and Its Impact on Air Transportation," NASA/ASEE 1973, NASA-Langley Research Center and Old Dominion University.
28. Anon., Contract NAS1-13233, "Conceptual Design Study of Advanced Acoustic-Composite Nacelles," NASA-Langley Research Center to Lockheed-California Company, May 30, 1974.

APPENDIX A
PHYSICAL PROPERTIES OF HYDROGEN*

LIQUID

Melting point at atmospheric pressure.	$^{\circ}\text{K}$ ($^{\circ}\text{R}$)	13.95	(25.1)
Boiling point at atmospheric pressure.	$^{\circ}\text{K}$ ($^{\circ}\text{R}$)	20.45	(36.8)
Critical temperature	$^{\circ}\text{K}$ ($^{\circ}\text{R}$)	33.17	(59.7)
Critical pressure.	kPa (psia)	1,317	(191)
Specific gravity (liquid water = 1.00)	-	.071	.071
Density (liquid) (at -42°F and 30 in Hg)	kg/m^3 (lb/ft^3)	69.9	(4.42)
Specific heat	kJ/kg (Btu/lb)	1.325	(.57)
Viscosity (at normal b.p.)	Ns/m^2 (poises)	182×10^{-5}	(182×10^{-6})
Heat of fusion	kJ/kg (Btu/lb)	58.6	(25.2)
Inversion point, Joule Thomson	$^{\circ}\text{K}$ ($^{\circ}\text{R}$)	204.1	(367.4)
Heat of vaporization (nearly all pure)	kJ/kg (Btu/lb)	443	(190.5)

GAS

Specific gravity 217.6°K (air = 1.00).	-	.06953	.06953
Density (213.2°K and 762mm Hg)	kg/m^3 (lb/ft^3)	.0853	(.00532)
Specific volume (213.2°K and 762mm Hg)	m^3/kg (ft^3/lb)	11.72	(187.9)
Gross heat of combustion (incl. latent heat energy of steam).	kJ/m^3 (Btu/ ft^3)	26.7×10^3	(325.1)
Gross heat of combustion (incl. latent heat energy of steam).	kJ/kg (Btu/lb)	141.96×10^3	(61,084)**

*From "A Hydrogen Energy Carrier", Vol. II, Systems Analysis, Sept. 1973, a report by the NASA-ASEE Engineering Systems Design Institute (University of Houston, NASA-Johnson Space Center, and Rice University).

**NOTE: The lower heat of combustion = 120,091 kJ/kg (51,590 Btu/lb) was used in the subject study for purposes of thermodynamic calculations.

GAS (CONT)

Energy of gas/air mixture (F/A ratio 0.420 vol.; 0.020 wt.; or 29.6% H ₂ by vol.)	kJ/m^3 (Btu/ft ³)	6.68x10 ³	(81.3)
Vol. of air required per vol. of combustible	-	2.382	2.382
Kg air required per Kg combustible . . .	-	34.226	34.226
Flame temperature (F/A ratio 0.462 vol.; 0.0313 wt.; or 31.6% H ₂ by vol.) . . .	$^{\circ}\text{K}$ ($^{\circ}\text{R}$)	2,311	(4160)
Ignition temperature in air (auto ignition)	$^{\circ}\text{K}$ ($^{\circ}\text{R}$)	847	(1525)
Ignition temperature in oxygen	$^{\circ}\text{K}$ ($^{\circ}\text{R}$)	833	(1500)
Flammability limits, vol. H ₂ in air . .	%	4.1-74.2	-
Flammability limits, vol. H ₂ in oxygen .	%	4.6-93.9	-
Detonation limits, vol. H ₂ in air . . .	%	18.3-59	-
Detonation limits, vol. H ₂ in oxygen . .	%	15-90	-
Nonflammable limits, air-hydrogen- carbon dioxide	-	less than 8%O ₂	-
Nonflammable limits, air-hydrogen- nitrogen	-	less than 6%O ₂	-
Emissivity of flame (blackbody = 1.00)	-	.085	-

CHEMICAL PROPERTIES

Hydrogen in liquid or gaseous form will react violently with strong oxidizers such as oxygen and spontaneously with fluorine and chlorine trifluoride.

Hydrogen gas is colorless, odorless, nontoxic (though asphyxiating), and non-corrosive. When its temperature is that of the ambient air, its density is only about 1/14 of the air density, and the gas is thus strongly buoyant; however, the vapor at the boiling point is as heavy as air at 70°F.

Liquid hydrogen is a transparent, colorless liquid of low viscosity. It does not form solutions with any material except, to a slight extent, with helium. In particular, gases like oxygen and nitrogen condense and freeze to solids in liquid hydrogen without entering into solution. At about 14°K (-435°F) liquid hydrogen freezes to a solid. The temperature and pressure at the triple point (at which solid, liquid and gaseous hydrogen co-exist) are 14.0°K and 0.071 atmospheres for normal hydrogen, and 13.8°K and 0.069 atmospheres for para-hydrogen. Solid hydrogen freezes into a white crystalline or snow-like mass.

Hydrogen diffuses approximately 3.8 times faster than air. A spill of 500 gallons of liquid hydrogen on the ground has diffused to a nonexplosive mixture after about one minute. Air turbulence increases the rate of hydrogen diffusion.

Hydrogen in both the liquid and gaseous states is particularly subject to leakage because of its low viscosity and low molecular weight. Leakage rate is inversely proportional to viscosity. Because of its low viscosity alone, the leakage of liquid hydrogen will be roughly 100 times that of JP-4 fuel, 50 times that of water, and 10 times that of liquid nitrogen. Likewise, the leakage of gaseous hydrogen will be greater than that of air.

Reference: Cloyd, D. R. and N. J. Murphy; Handling Hazardous Materials, Chapter 1, Liquid Hydrogen, NASA SP-5032, September, 1965.

APPENDIX B

EXAMPLE ASSET AUTOPILOT DATA PRESENTATIONS

<u>FIGURE</u>	<u>TITLE</u>
B-1	Takeoff Gross Weight
B-2	Flyaway Cost
B-3	Direct Operating Cost
B-4	Direct Operating Cost

CONSTRAINT LEGEND

<u>LINE</u>	<u>TITLE</u>			
1	Maximum Ceiling	m (ft)	10363	(34000)
2	Maximum Ceiling	m (ft)	10973	(36000)
3	Maximum Ceiling	m (ft)	11582	(38000)
4	Conventional Takeoff Distance	m (ft)	2438	(8000)
5	Engine Out Takeoff Distance	m (ft)	2438	(8000)
6	2nd Segment Climb Gradient		.03	(.03)
7	Approach Speed	m/s (KEAS)	61.7	(120)
8	Approach Speed	m/s (KEAS)	69.4	(135)
9	Approach Speed	m/s (KEAS)	77.2	(150)
10	Conventional Landing Distances	m (ft)	2438	(8000)
11	Approach Speed With + 9072 Kg	m/s (KEAS)	69.4	(135)
12	Landing Distance With + 9072 Kg	m (ft)	2438	(8000)
13	Approach Speed With 95% TOGW	m/s (KEAS)	77.2	(150)
14	Landing Distance With 95% TOGW	m (ft)	2438	(8000)

SUBSONIC JP A/C, 400 PASSENGER, CL 1317-3-1
 RANGE=5500 NMI, MACH=.85 SWEEP(C/4)=30. DEG
 AR= 8.0, T/C=11.00, CT/CR=0.30, ENGINE 83000

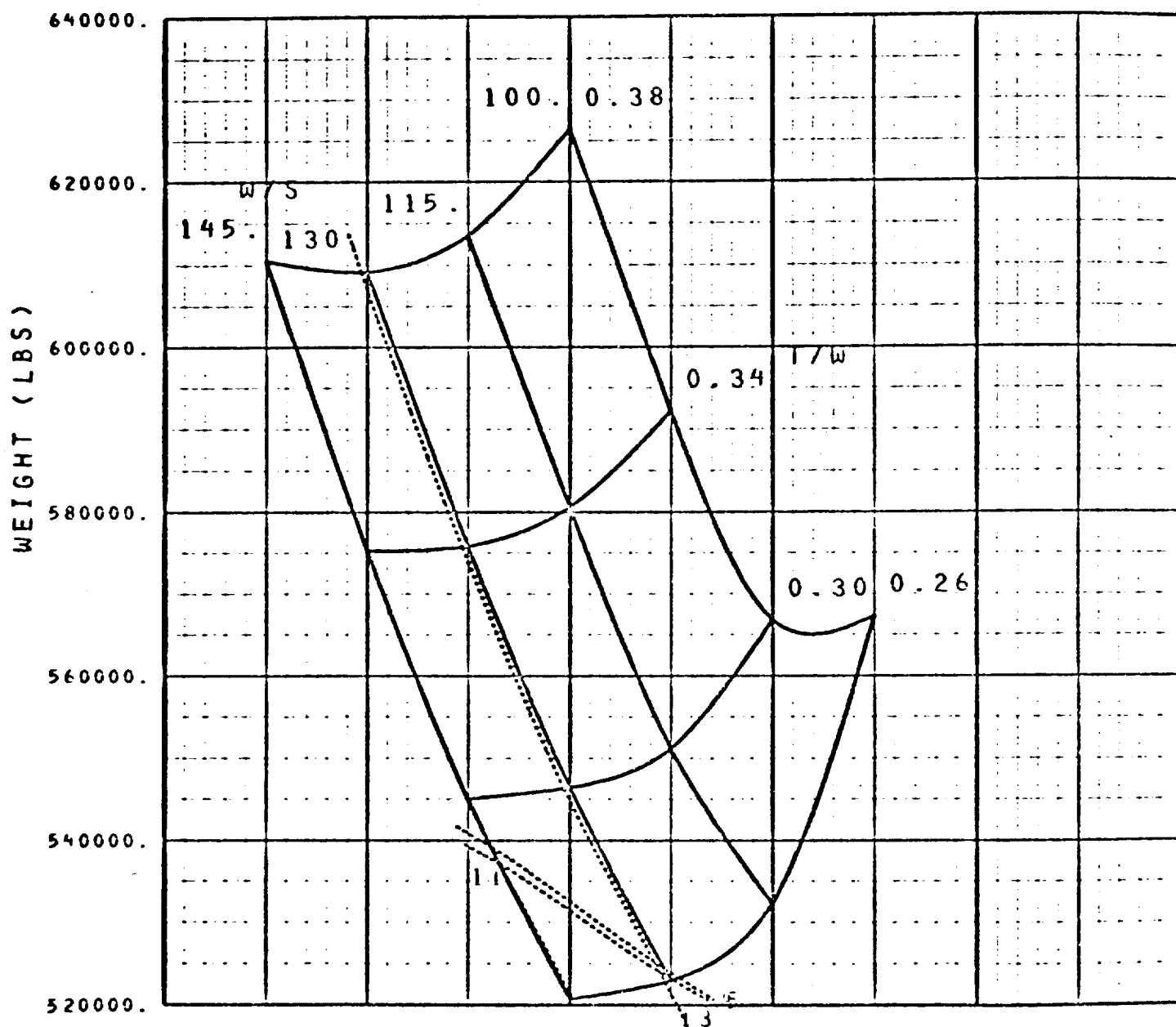


Figure B-1. Takeoff Gross Weight

SUBSONIC JP A/C, 400 PASSENGER, CL 1317-3-1
 RANGE=5500 NMI, MACH=.85 SWEEP(C/4)=30. DEG
 AR= 8.0, T/C=11.00, CT/CR=0.30, ENGINE 83000

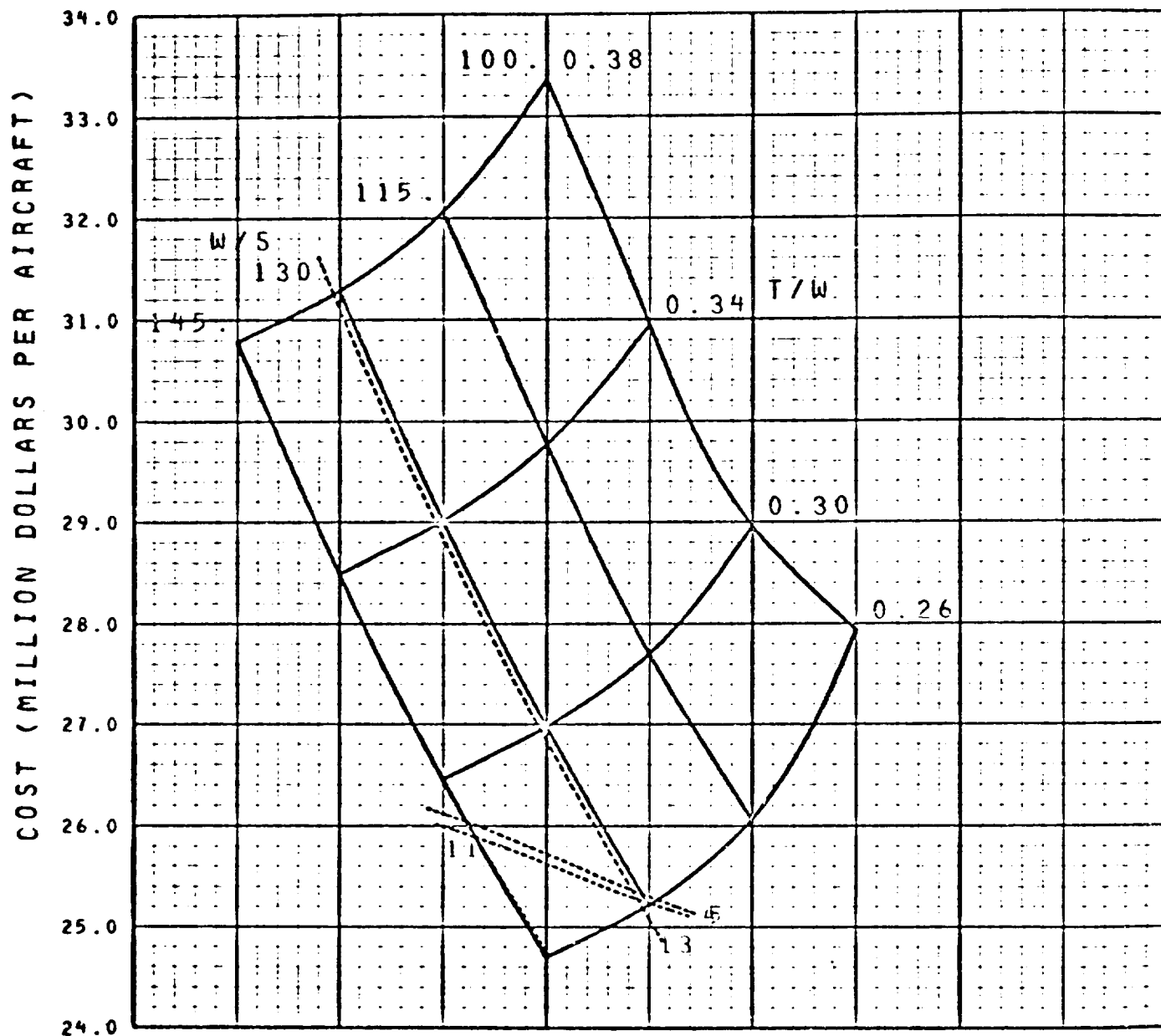
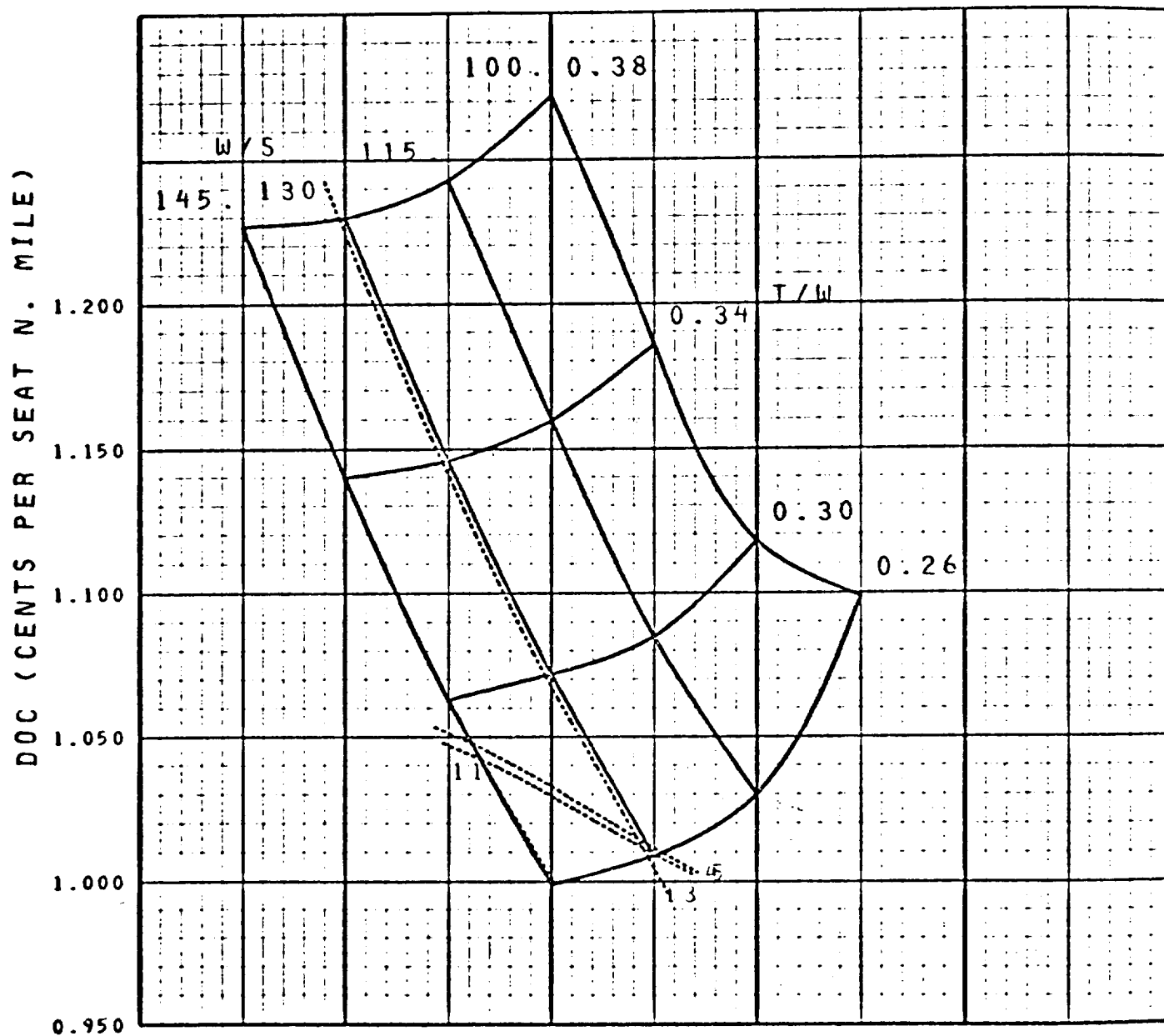


Figure B-2. Flyaway Cost

SUBSONIC JP A/C, 400 PASSENGER, CL 1317-3-1
 RANGE=5500 NMI, MACH=.85 SWEEP(C/4)=30. DEG
 AR= 8.0, T/C=11.00, CT/CR=0.30, ENGINE 83000



SUBSONIC JP A/C, 400 PASSENGER, CL 1317-3-1
 RANGE=5500 NMI, MACH=.85 SWEEP(C/4)=30. DEG
 AR= 8.0, T/C=11.00, CT/CR=0.30, ENGINE 83000

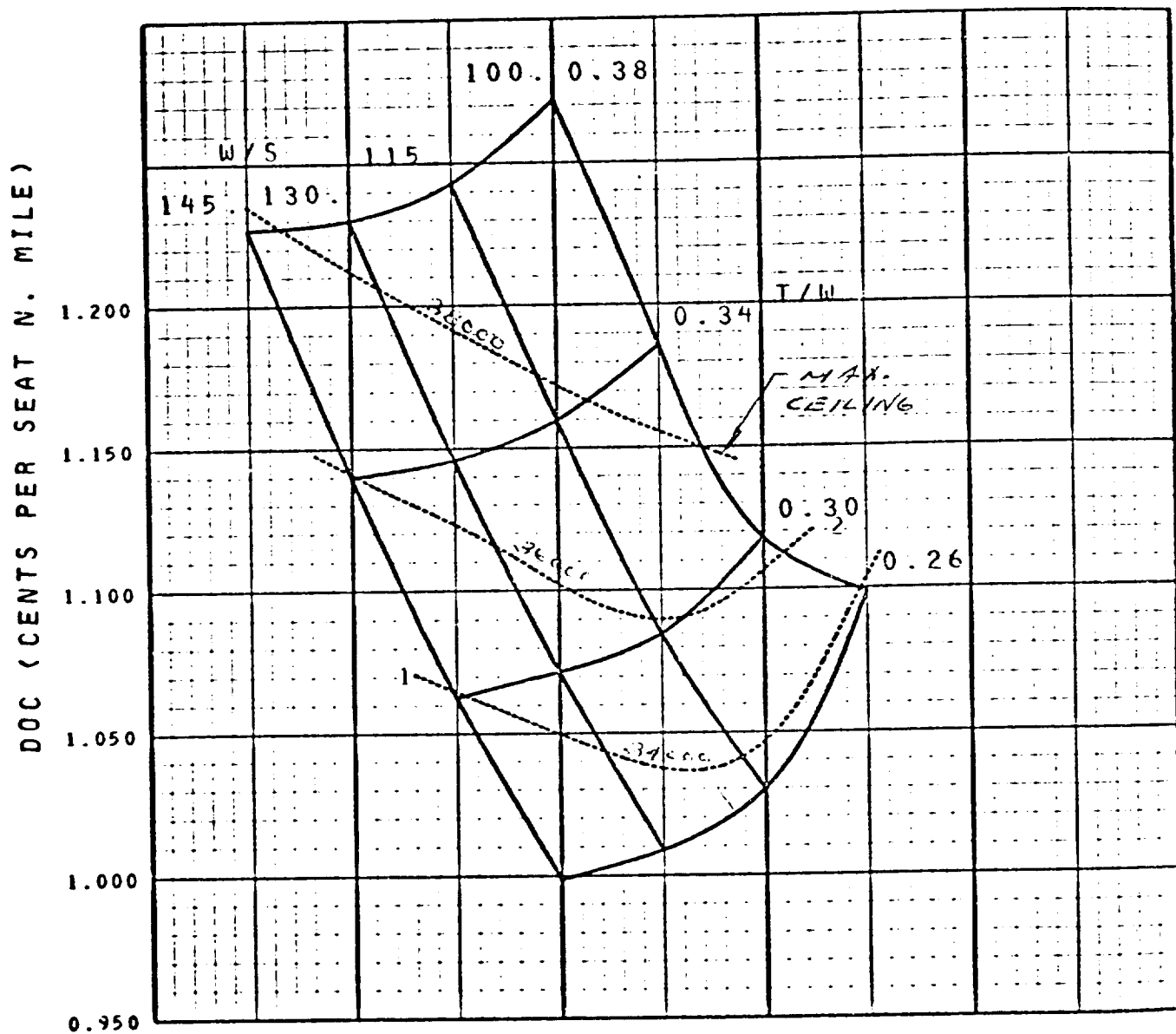


Figure B-4. Direct Operating Cost

APPENDIX C

EXTERNAL LOADS CRITERIA AND LOADS

The purpose of this appendix is to present the structural design criteria, and the preliminary loads resulting from application of these criteria to the configurations discussed in the body of the report. The depth and scope of the loads analysis is sufficient to support the selection of a preferred structural concept, the prediction of structural weight, and the cost.

Criteria and Basis Data

- Airplane Weight

The loads shown in this section are based on the estimated airplane weight buildup shown in Table C-1.

- Design Speeds

The design speed altitude variation used is the same as the L-1011. The significant speeds in this analysis are $V_c/M_c = 354 \text{ KEAS}/.90$ at 26,000 feet and $V_D/M_D = 361/.95$ at 21,700 feet.

- Design Load Factor

Flight maneuver load envelope for the liquid hydrogen transport is based on the same criteria as the L-1011. The limits are:

$$-1.0 < n_z < 2.5 \text{ at } V < V_c/M_c$$

$$0 < n_z < 2.5 \text{ at } V_c/M_c < V < V_D/M_D$$

Gust load factors are based on the same gust velocity variation as the L-1011 at the critical cruise condition $V_{de} = 45 \text{ fps}$ at 26,000 feet.

- Aerodynamic Data

Aerodynamic stability data used in this analysis are based on the L-1011 and have been modified as appropriate to reflect the configuration differences. It is assumed that the vanes on the wing tanks operate in an active mode such that total airplane stability is not affected by the tanks.

TABLE C-1. DESIGN WEIGHT SUMMARY

	FUSELAGE TANK CONFIGURATION	WING TANK CONFIGURATION
Maximum Take-off Gross Weight	400,000	400,000
Landing Gross Weight	380,000	380,000
Operating Weight Empty	238,000	246,000
Structural Reserve Fuel	5,000	6,000
Max. Wt. with Structural Reserve Fuel	370,000	373,000
Minimum Flying Weight	243,000	252,000

- Inertia Data

The inertia distribution data used has been estimated based on the basic geometry and the weights of Table C-1. Forward c.g. for the fuselage tank configuration is assumed to be at 20% MAC and for the external tank configuration at 27% MAC. Structural Reserve Fuel is based on the L-1011 value of 7% total fuel.

Design Loads

- Forebody

Forebody loads for each configuration are given in Figure C-1 for the critical discrete gust conditions. Relieving airloads and pitching accelerations are conservatively ignored. The L-1011 forebody, over most of its length, was critical for dynamic landing followed by dynamic gust. It is not known how a detailed dynamic landing analysis would compare with these loads. It is estimated that such loads might be 10% higher than those shown.

- Afterbody

Three conditions were considered on the afterbody:

- (1) A down horizontal tail load of 100,000 pounds combined with 2.5 g's to simulate a PLA condition.

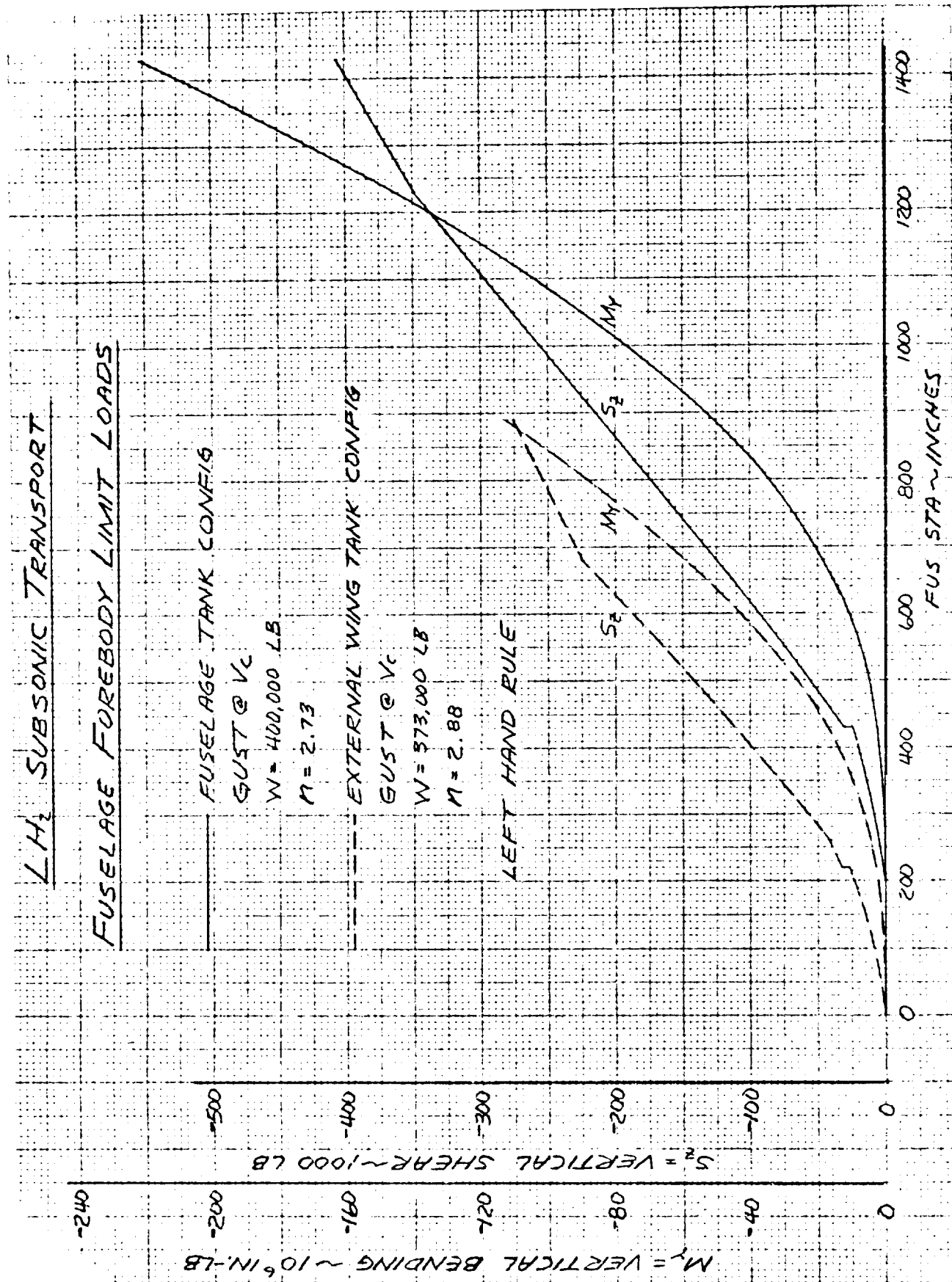


Figure C-1.1. LH₂ Subsonic Transport Fuselage Forebody Limit Loads

(2) A down horizontal tail load of 130,000 pounds combined with 1.0 g to simulate an abrupt pitching maneuver.

(3) A vertical gust at V_c .

Resulting loads for these conditions are shown in Figures C-2 and C-3.

- Wing

Wing additional and basic airloads are taken from L-1011 data. For the external wing tank configuration, a vertical airload of 20,000 pounds is also applied to the tank at its cg. The load axis chosen for each wing is the same as that of the L-1011. When either wing is superimposed on that of the L-1011, such that the 25% chordline and airplane center line coincide, the wing load axes also coincide. The load axis for each wing is defined in terms of its own geometry in Figures C-4, C-5 and C-6.

Wing loads were critical for gust at V_c . The fuselage tank configuration was critical at maximum gross weight and the results are shown in Figure C-4. In the external wing tank configuration, two conditions were critical. The inner wing was critical for gust with maximum cargo and structural reserve fuel. This condition is shown in Figure C-4. The outer wing was critical for maximum gross weight. This condition is shown in Figure C-6.

External Wing Tank

Tank attachment loads are given for two conditions, landing and taxi. Landing loads are based on a tank weight of 55,000 pounds. Taxi loads are based on a full tank weight of 61,700 pounds. These loads are referenced to the tank cg and all combinations are to be considered for criticality.

	<u>LANDING</u>	<u>TAXI</u>
Sz lb.	-165,000	-200,000
Sx lb.	±55,000	0
Sy lb.	±55,000	±40,000
My in. -lb.	±34,000,000	±17,000,000
Mz in. lb.	±17,000,000	±17,000,000

NOTE: All loads in this Appendix are on a LIMIT basis.

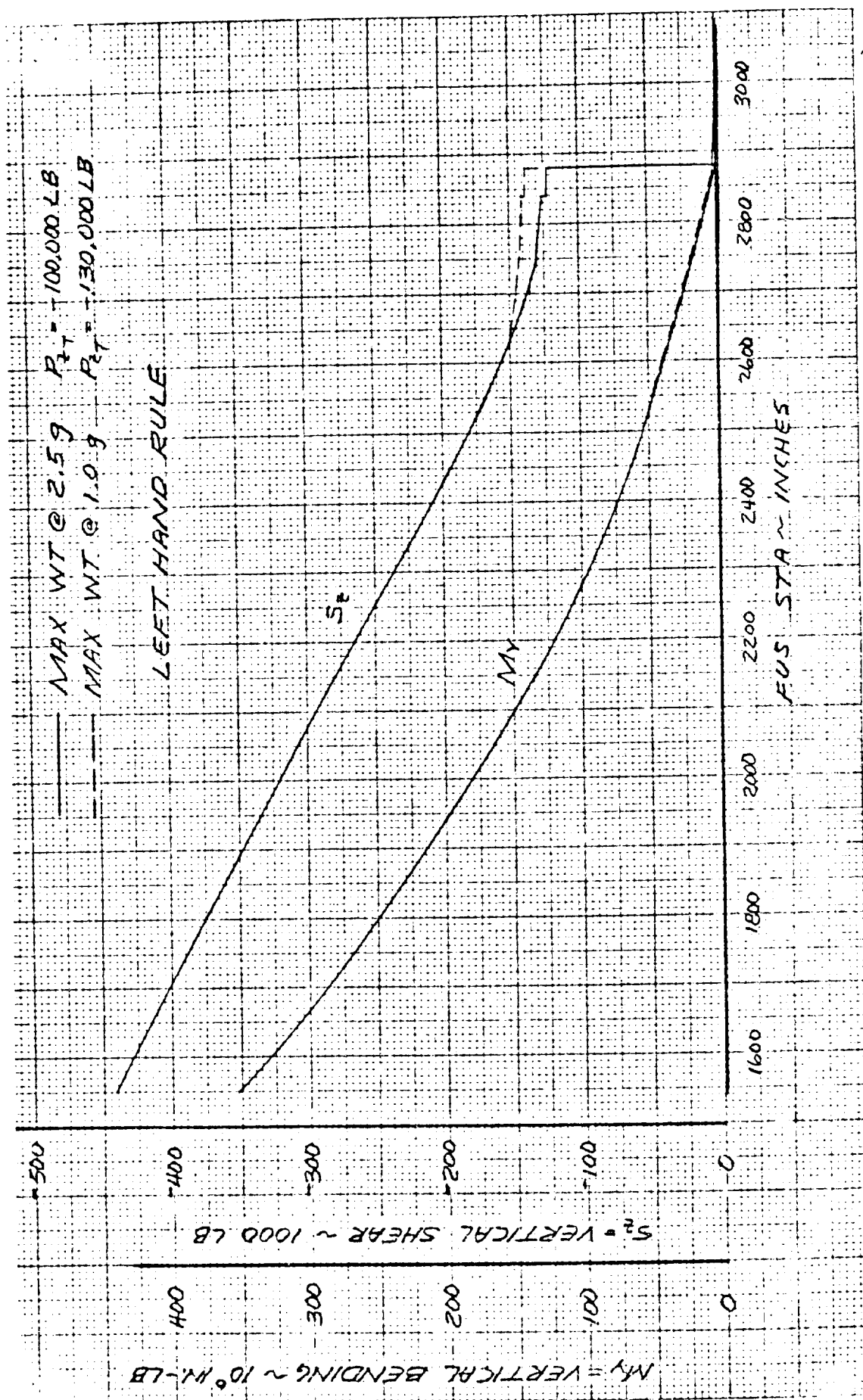


Figure C-2. LH₂ Subsonic Transport Fuselage Aftbody Limit Loads (Fuselage Tank Config.)

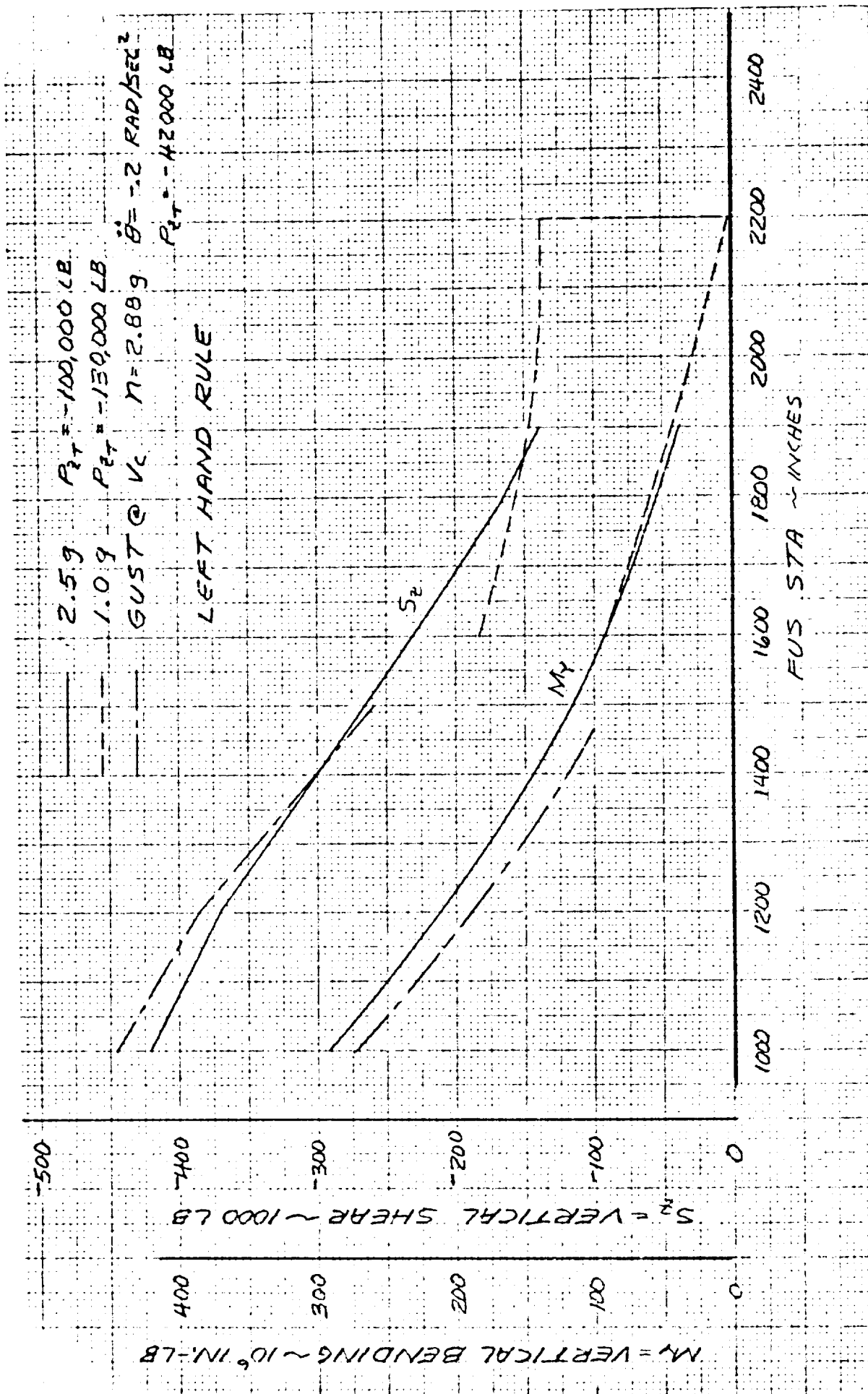


Figure C-3. LH₂ Subsonic Transport Fuselage Aftbody Limit Loads (External Wing Tank Config.)

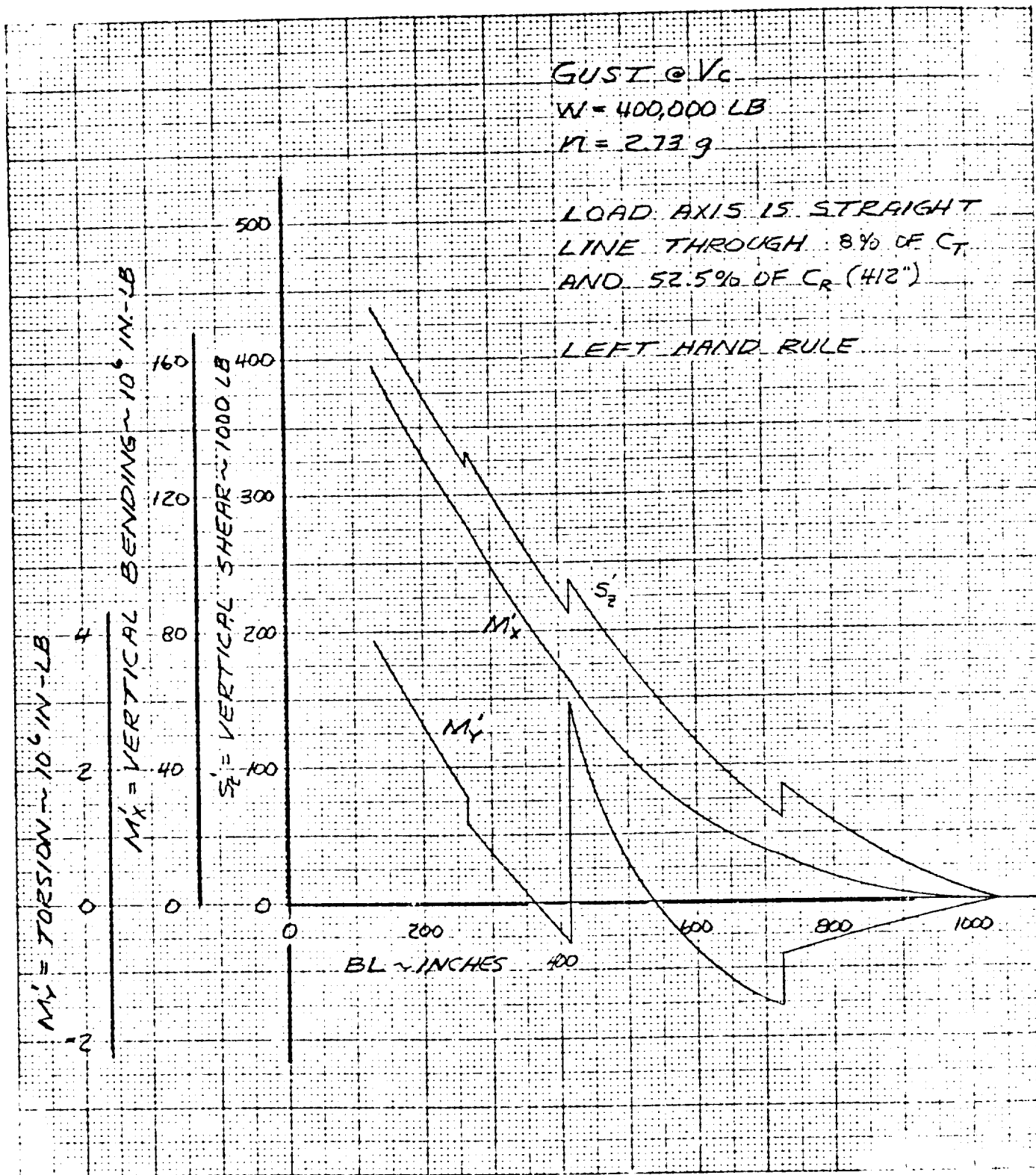


Figure C-4. LH_2 Subsonic Transport Wing Limit Loads (Fuselage Tank Config.)

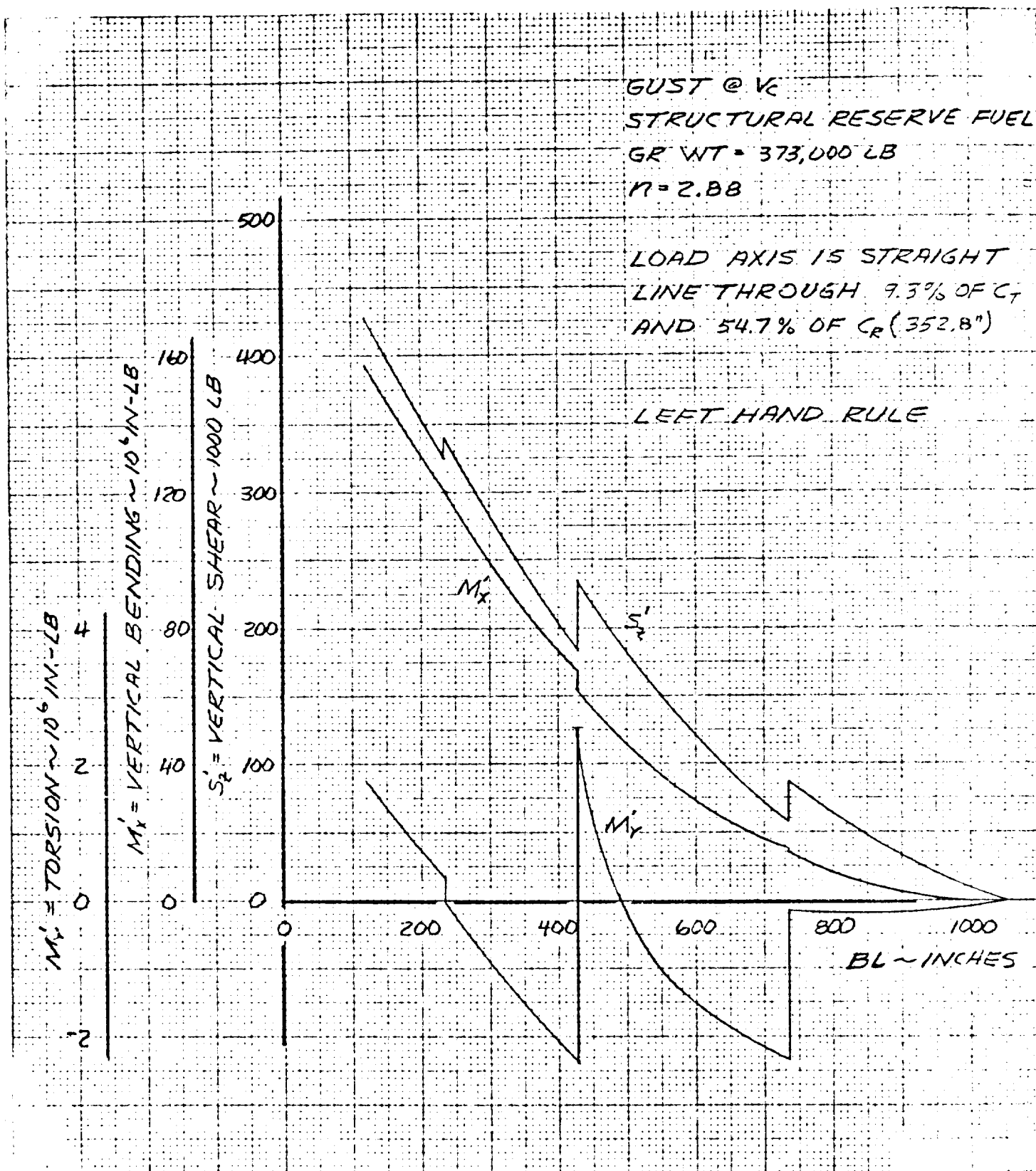


Figure C-5. LH₂ Subsonic Transport Wing Limit Loads
 (External Wing Tank Config.) Cond. 1

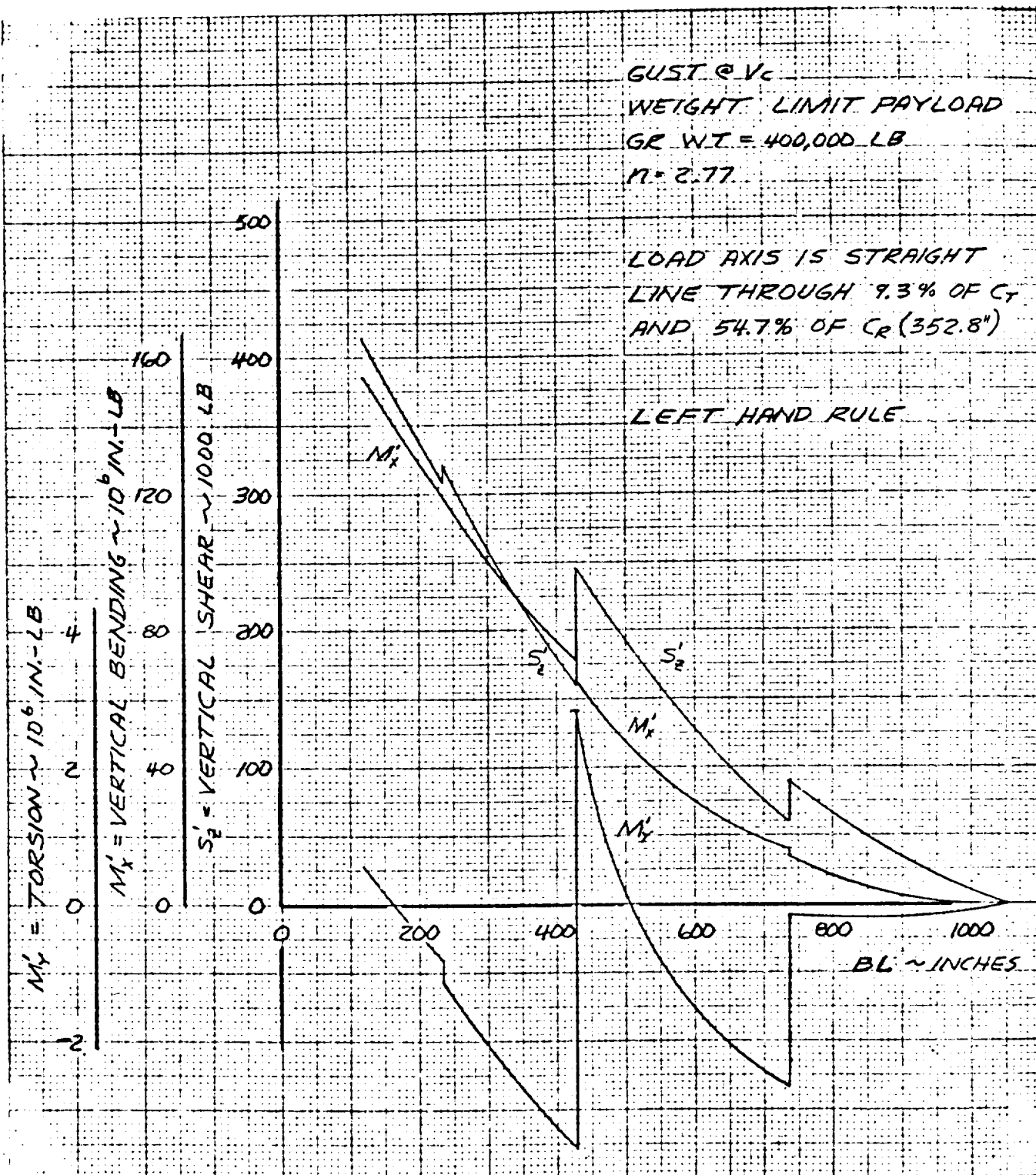


Figure C-6. LH_2 Subsonic Transport Wing Limit Loads
 (External Wing Tank Config.)

APPENDIX D

SELECTED ASSET COMPUTER PRINTOUT PAGES

FINAL POINT - DESIGN AIRCRAFT:

1. LH₂, 400 PAX, 3,000 n mi.
2. LH₂, 400 PAX, 5,500 n mi.
3. Jet A, 400 Pax, 3,000 n mi.
4. Jet A, 400 Pax, 5,500 n mi.

EXTERNAL TANK LH₂ DESIGNS (FROM TASK 3):

5. LH₂, 400 PAX, 3,000 n mi.
6. LH₂, 400 PAX, 5,500 n mi.

LIQUID HYDROGEN-----BASIC DESIGN MISSION/400 PASSES/ 5500 N MI MISS

T/W T/S AS L/W N/S T/N
10.00 0.30 0.00 50.00 116.5 0.203

POUNDS C/O

POUNDS C/O

DESIGN GROSS WEIGHT
FUEL ZERO FUEL WEIGHT
PAYLOAD OPERATING WEIGHT FORTY
OPERATIONAL ITEMS
STORAGE ITEMS
(EMPTY WEIGHT-WEIGHT)

WING

TAIL

FUSELAGE

LANDING GEAR

FLIGHT CONTROLS

NOSE

EXHAUSTION SYSTEM

ENGINE

AIR INTAKE

EXHAUST

EXHAUST

EXHAUST

OIL SYSTEM (LESS OIL)

ENGINE CONTROLS

ENGINE STARTING

TANKS

INSULATION

FUEL-PLUMBING

INSTRUMENTS

HYDRAULICS

ELECTRICAL

ELECTRICAL

ENGINEING AND EQUIP.

AIR CONDITIONING

AUXILIARY POWER UNIT

RELIEF VALVE

NO. OF PASSENGERS

NO. OF CREW

STRUCTURAL W/C

UNFUEL WING FUEL TANK VOLUME CU. FT.

D-2

FINAL DESIGN

LH₂, MACH 0.85

400 PASSENGER

10,190 km (5500 n.mi)

201740. 100.00
61430. 15.72
80000. 22.46
15420. 2.84
5110. 1.30
28400. 8.43
3720. 0.95
50073. 12.78
21006. 5.41
4002. 1.27
4500. 1.68
44195. 12.30

230108.

242100. 61.80

221578.

1196. 0.21
2644. 0.76
6524. 1.42
2252. 0.56
27400. 7.25
6012. 1.66
300. 0.08
1116. 0.28
0. 0.0

400.
11.
11.27
0.

22141.
2550.
2006.
11.
124.
382.
12006.
4567.
2402.

MISSION SUMMARY

LIQUID HYDROGEN---BASIC DESIGN MISSION/400 PASS/ 5500 NM MISS

SEQUENT	INIT ALTITUDE (FT)	INIT MACH NO	INIT WEIGHT (LB)	SEGT FUEL (LB)	TOTAL FUEL (LB)	SEGT DIST (N MI)	TOTAL DIST (N MI)	SEGT TIME (MIN)	TOTAL TIME (MIN)	EXTERN STOPS TAB ID	ENGINE THRUST TAB ID	EXTERN F TANK TAB ID	AVG L/O RATIO	AVG SFC (FF/T)
TAKEOFF														
POWER 1	0	0.0	301740.	156.	156.	0.	0.	14.0	14.0	0.	-83101.	0.	0.0	0.117
POWER 2	0	0.0	301584.	180.	236.	0.	0.	1.0	15.0	0.	83401.	0.	0.0	0.094
CLIMB	0	0.370	301404.	594.	920.	16.	16.	3.5	18.5	0.	83101.	0.	18.44	0.152
ACCLFL	10000.	0.456	300821.	210.	1130.	8.	24.	1.4	19.9	0.	83101.	0.	16.01	0.173
CLIMB	10000.	0.623	300610.	4786.	5916.	364.	388.	44.6	64.5	0.	83101.	0.	14.45	0.200
CRUISE	30000.	0.850	300824.	45723.	51649.	4962.	5350.	610.5	674.9	0.	-83101.	0.	16.07	0.199
DESCENT	35000.	0.850	340001.	155.	51804.	56.	5406.	7.1	682.1	0.	83301.	0.	12.50	-1.654
DECEL	10000.	0.620	320026.	47.	51852.	0.	5415.	1.6	683.7	0.	83301.	0.	15.24	44.724
DESCENT	10000.	0.456	320088.	202.	52143.	37.	5452.	9.3	692.0	0.	83301.	0.	17.78	0.799
CRUISE	30000.	0.650	320507.	414.	52557.	40.	5500.	5.9	697.9	0.	-83101.	0.	16.01	0.199
LOITER	15000.	0.222	320183.	205.	52851.	0.	5500.	6.0	703.9	0.	-83101.	0.	18.29	0.159
RESET	0	0.0	330869.	0.	52851.	0.	5500.	0.0	703.9	0.	0.	0.	0.0	0.0
RESET	0	0.0	330880.	0.	52851.	-5500.	0.	-703.9	0.0	0.	0.	0.	0.0	0.0
CRUISE	20000.	0.650	330808.	4809.	57740.	0.	0.	70.0	70.0	0.	-83101.	0.	15.95	0.199
RESET	0	0.0	333001.	0.	57740.	0.	0.	0.0	70.0	0.	0.	0.	0.0	0.0
CLIMB	0	0.270	333001.	474.	52223.	13.	13.	2.8	72.8	0.	93101.	0.	17.60	0.152
ACCLFL	10000.	0.456	333517.	74.	52297.	2.	15.	0.5	73.3	0.	93101.	0.	16.24	0.165
CLIMB	10000.	0.547	333443.	1223.	54520.	68.	83.	10.1	83.4	0.	83101.	0.	15.20	0.182
CRUISE	30000.	0.605	332220.	150.	59670.	17.	100.	2.5	85.9	0.	-83101.	0.	16.90	0.185
DESCENT	30000.	0.700	332070.	184.	59853.	54.	154.	8.2	94.1	0.	83301.	0.	15.02	-4.983
DECEL	10000.	0.547	331886.	26.	59870.	5.	150.	0.9	95.0	0.	83301.	0.	16.30	1.609
DESCENT	10000.	0.456	331360.	235.	60114.	21.	190.	6.9	101.9	0.	83301.	0.	17.61	0.825
CRUISE	30000.	0.605	331626.	56.	60200.	10.	200.	1.4	103.3	0.	-83101.	0.	16.97	0.185
LOITER	15000.	0.210	331840.	1400.	61639.	0.	200.	30.0	133.3	0.	-83101.	0.	18.27	0.159

TOCRAFT 301740.0 FUEL 45 61632.4 FUEL 85 61638.0

JP FUEL REFERENCE BASELINE DESIGN / 400 PASS / 3000 N MI

MISS

T/C T/R AR LAM W/S T/W
10.00 0.40 9.00 30.00 125.0 0.255

DESIGN GROSS WEIGHT
FUEL ZERO FUEL WEIGHT
PAYLOAD OPERATING WEIGHT EMPTY
OPERATIONAL ITEMS
STANDARD ITEMS
EMPTY WEIGHT-MFG.

WING
TAIL
BODY
LANDING GEAR
FLIGHT CONTROLS
FUELLES
PROPULSION SYSTEM
ENGINE
AIR INTAKE
EXHAUST
COOLING
OIL SYSTEM (LESS OIL)
ENGINE CONTROLS
ENGINE STARTING
TANKS
INSULATION
FUEL-PLUMBING
INSTRUMENTS
HYDRAULICS
ELECTRICAL
FURNISHINGS AND EQUIP.
AIR CONDITIONING
ANTI-ICING
AUXILIARY POWER UNIT
DESIGN RESERVE

19742.
2221.
1739.
0.
11.
111.
341.
574.
0.
1061.

POUNDS O/O POUNDS G/O

404370. 100.00
105756. 26.15
38000. 21.76
15400. 3.61
3730. 0.92
39034. 9.65
3561. 0.88
44219. 10.94
19516. 4.53
5130. 1.27
5384. 1.46
25909. 6.41

D-3

FINAL DESIGN

JET A, MACH 0.85

400 PASSENGER

5560 km (3000 n.mi)

NO. OF PASSENGERS
NO. OF CREW
STRUCTURAL T/C
UNUSED WING FUEL TANK VOLUME CU. FT.

400.
11.
11.27
140.

1205.
3030.
5412.
2211.
29400.
6513.
323.
1116.
0.
0.30
0.75
1.34
0.55
7.02
1.61
0.03
0.23
0.0

MISSION SUMMARY

JP FUEL REFERENCE BASELINE DESIGN / 400 PASS / 3000 N MI MISS

SEGMENT	INIT ALTITUDE (FT)	INIT MACH NO	INIT WEIGHT (LB)	SEGMT FUEL (LB)	TOTAL FUEL (LB)	SEGMT DIST (N MI)	TOTAL DIST (N MI)	SEGMT TIME (MIN)	TOTAL TIME (MIN)	EXTERN STAGE TAB ID	ENGINE THRUST TAB ID	EXTERN F TANK TAB ID	AVG L/D RATIO	AVG SFC (FF/I)
TAKEOFF POWER 1	0.	0.0	404370.	527.	527.	0.	0.	14.0	14.0	0.	-E1101.	0.	0.0	0.436
POWER 2	0.	0.0	402843.	403.	1011.	0.	0.	1.0	15.0	0.	E1401.	0.	0.0	0.261
CLIMB	0.	0.378	403359.	1887.	2897.	19.	19.	4.2	19.2	0.	E1101.	0.	10.35	0.455
ACCEL	10000.	0.456	401473.	661.	3559.	0.	29.	1.6	20.8	0.	E1101.	0.	17.43	0.514
CLIMB	10000.	0.638	400811.	11250.	14808.	290.	319.	35.7	56.5	0.	E1101.	0.	15.24	0.586
CRUISE	34000.	0.850	389561.	62071.	76880.	2431.	2750.	297.8	354.2	0.	-E1101.	0.	16.66	0.582
DESCENT	35000.	0.850	327490.	417.	77296.	60.	2310.	7.6	361.8	0.	E1501.	0.	13.50	-4.641
DECEL	10000.	0.638	327073.	126.	77422.	10.	2819.	1.7	363.5	0.	E1301.	0.	16.12	126.094
ASCENT	10000.	0.456	326947.	768.	78190.	39.	2858.	8.7	372.2	0.	E1501.	0.	18.65	2.240
CRUISE	37000.	0.850	326179.	3310.	81509.	142.	3000.	17.5	389.7	0.	-E1101.	0.	16.51	0.580
LOITER	1500.	0.325	322861.	826.	82335.	0.	3000.	6.0	395.7	0.	-E1101.	0.	19.03	0.488
RESET	0.	0.0	322034.	0.	82335.	0.	2000.	0.0	395.7	0.	0.	0.	0.0	0.0
RESET	0.	0.0	322034.	0.	82335.	-3000.	0.	-395.7	0.0	0.	0.	0.	0.0	0.0
CRUISE	37000.	0.850	322034.	12881.	95216.	0.	0.	70.0	70.0	0.	-E1101.	0.	16.59	0.581
RESET	0.	0.0	309153.	0.	95216.	0.	0.	0.0	70.0	0.	0.	0.	0.0	0.0
CLIMB	0.	0.378	309153.	1311.	96527.	13.	13.	2.9	72.9	0.	E1101.	0.	18.20	0.455
ACCEL	10000.	0.456	307842.	199.	96727.	3.	16.	0.5	73.4	0.	E1101.	0.	14.78	0.487
CLIMB	10000.	0.547	307643.	3239.	99965.	66.	82.	9.9	83.3	0.	E1101.	0.	15.66	0.537
CRUISE	30000.	0.700	304404.	414.	100379.	18.	100.	2.6	85.9	0.	-E1101.	0.	17.40	0.544
DESCENT	30000.	0.700	303990.	476.	100855.	56.	156.	8.4	94.3	0.	E1301.	0.	15.44	-13.5968
DECEL	10000.	0.547	303514.	67.	100922.	5.	160.	0.9	95.2	0.	E1301.	0.	16.76	4.511
DESCENT	10000.	0.456	303447.	609.	101531.	32.	193.	7.1	102.4	0.	E1301.	0.	15.13	2.314
CRUISE	30000.	0.700	302658.	164.	101696.	7.	200.	1.0	103.4	0.	-E1101.	0.	17.36	0.545
LOITER	1500.	0.314	302673.	3882.	105578.	0.	200.	30.0	133.4	0.	-E1101.	0.	18.96	0.490

D-11

TOTAL FUEL = 404370.0 FUEL A = 102756.4 FUEL R = 105577.7

COST SUMMARY

WING 2690694.00
 TAIL 273634.98
 FLY 3712152.00
 LANDING GEAR 462735.63
 FLIGHT CONTROLS 343057.56
 FACILITIES 629455.44

PERCUSSION 25549.84
 ENGINE 184731.06
 AIR INTRODUCTION 288666.63
 FUEL SYSTEM 5220.05
 START SYSTEM 2073.72
 ENGINE CONTROLS 2276.37
 FRI/TREUST REV. 2097.46
 LUBE SYSTEM

TOTAL PERCUSSION

510642.44
 176584.88
 282542.50
 448761.56
 133566.19
 613312.38
 515709.56
 25981.65
 116931.35
 251120.56

TOTAL EMPTY MFG. COST

111111605.00

SUSTAINING ENGINEER 760494.19
 TECHNICAL DATA 0.0
 TOOLING MAINT. 1001435.50
 PASC. 278214.75
 ENG. CHANGE ORDER 6.2
 QUALITY ASSURANCE 1044895.64
 AIRFRAME WARRANTY

705832.06
 2735970.00
 142808.19
 355476.56

AIRFRAME COST
 ENGINE WARRANTY
 ENGINE FEE
 FLIGHT COST
 AVIONICS COST
 RESEARCH AND DEVELOPMENT

TOTAL FLY AWAY COST

22618592.00

DIRECT OPERATING COST-DOLLARS/M. MILE 0.4401
 CREW 12.37
 AIRFRAME LABOR AND BURDEN MAINT. 7.74
 ENGINE LABOR AND BURDEN MAINT. 5.05
 AIRFRAME MATERIAL MAINT. 3.53
 FUELING MATERIAL MAINT. 4.95
 FUEL AND OIL 29.98
 REPAIRS 1.0313
 DEPRECIATION (INCLUDING SPARES) 1.0533
 TOTAL DTC \$/M. MILE 3.5562 100.00

WEIGHT
 CEILING

304370.0 363218.7 36207.4 240014.1 310764.9 298613.6
 32279.0 33395.4 34335.6 35444.5 36704.8 38070.9

R AND D
 DEVELOPMENT TECHNICAL DATA 114460703.
 DESIGN ENGINEERING 24237872.
 DEVELOPMENT TOOLING 159750720.
 DEVELOPMENT TEST ARTICLE 56371696.
 FLIGHT TEST 35420224.
 SPECIAL SUPPORT EQUIPMENT 3050054.
 DEVELOPMENT SPARES 47701536.
 ENGINE DEVELOPMENT 0.
 AVIONICS DEVELOPMENT 0.
 TOTAL R AND D 566062592.

1611. 1045. 2405. 2653. 3000.
 1263. 1045. 2405. 2653. 3000.
 916. 1263. 1045. 2405. 2653. 3000.
 1.0902 1.0162 0.9650 0.9256 0.8873 0.8495
 2.3095 3.0495 3.7595 4.4674 5.1764 5.8854
 4027. 5125. 6243. 7351. 8459. 9567. 10675.

SUMMARY ID NO. 267
OCTOBER 15 1974

AVING QUARTER CHORD SWEEP = 30.00 DEG
AVING TAPER RATIO = 0.400

AIRCRAFT MODEL --CL1317-3-1
I.G.C. DATE --1990
DESIGN SPEED --SUBSONIC

ENGINE 1.0. -- 31000
SLS SCALE 1.0 = 35000
NUMBER OF ENGINES = 4.

[illegible]

JP FUEL REFERENCE BASELINE DESIGN / 400 PASS / 5500 N MI MISS

T/C T/R AR LAR W/S T/R
10.00 0.40 9.00 30.00 125.0 0.250

DESIGN GROSS WEIGHT

FUEL

ZERO FUEL WEIGHT

PAYLOAD

OPERATING WEIGHT EMPTY

OPERATIONAL ITEMS

STANDARD ITEMS

EMPTY WEIGHT-MFG.

WING

TAIL

BODY

LANDING GEAR

FLIGHT CONTROLS

WHEELS

PROPULSION SYSTEM

ENGINE

AIR INTAKE

EXHAUST

COOLING

OIL SYSTEM (LESS OIL)

ENGINE CONTROLS

ENGINE STARTING

TANKS

INSULATION

FUEL-PUMPING

INSTRUMENTS

HYDRAULICS

ELECTRICAL

ELECTRONICS

FUEL SYSTEMS AND EQUIP.

AIR CONDITIONING

ANTI-ICING

AUXILIARY POWER UNIT

COLLECTION RESERVE

25463-

2942-

2507-

0-

11-

143-

439-

924-

0-

1268-

1285-

3438-

5542-

2749-

28400-

6513-

402-

1116-

0-

0.0

POUNDS O/O

523193-

190786-

36.47

16.42

7.95

0.75

9.88

1.06

8.74

4.83

1.22

1.45

6.40

POUNDS

332407-

244407-

46.71

225053-

D-4

FINAL DESIGN

JET A, MACH 0.85

400 PASSENGER

10,190 km (5500 n.mi)

D-14

NO. OF PASSENGERS

NO. OF CREW

STRUCTURAL T/C

UNISED WING FUEL TANK VOLUME CU. FT.

400-

11-

11.27

6-

MISSION SUMMARY

JP FUEL REFERENCE BASELINE DESIGN / 400 PASS / 5500 N MI MISS

SEGMENT	INIT ALTITUDE (FT)	INIT MACH NO	INIT WEIGHT (LB)	SEGMT FUEL (LB)	TOTAL FUEL (LB)	SEGMT DIST (N MI)	TOTAL DIST (N MI)	SEGMT TIME (MIN)	TOTAL TIME (MIN)	EXTERN STORE TAB ID	ENGINE THRUST TAB ID	EXTERN F TANK TAB ID	AVG L/D RATIO	AVG SFC (#F/T)
TAKEOFF POWER 1	0.	0.0	523193.	669.	669.	0.	0.	14.0	14.0	0.	-81101.	0.	0.0	0.438
POWER 2	0.	0.0	522524.	613.	1282.	0.	0.	1.0	15.0	0.	81401.	0.	0.0	0.261
CLIMB	0.	0.378	521911.	2408.	3699.	19.	19.	4.2	19.2	0.	81101.	0.	20.26	0.455
ACCEL	10000.	0.456	519504.	825.	4515.	9.	28.	1.6	20.8	0.	81101.	0.	18.51	0.513
CLIMB	10000.	0.638	518679.	12970.	17485.	269.	297.	33.1	53.9	0.	81101.	0.	16.42	0.588
CRUISE	35000.	0.850	505708.	144466.	161051.	5053.	5350.	621.4	675.3	0.	-81101.	0.	17.91	0.581
DESCENT	35000.	0.850	361243.	503.	162454.	57.	5407.	7.2	682.5	0.	81301.	0.	12.74	-4.631
DECEL	10000.	0.656	360739.	156.	162609.	9.	5416.	1.6	684.2	0.	81301.	0.	15.68	123.604
DESCENT	10000.	0.456	360584.	993.	163602.	40.	5456.	8.0	693.1	0.	81301.	0.	18.55	2.238
CRUISE	41000.	0.850	359591.	1081.	164683.	44.	5500.	5.4	698.5	0.	-81101.	0.	17.54	0.583
LITTER	1500.	0.306	358518.	908.	165591.	0.	5500.	6.0	704.5	0.	-81101.	0.	19.60	0.502
RESET	0.	0.0	357602.	0.	165591.	0.	5500.	0.0	704.5	0.	0.	0.	0.0	0.0
RESET	0.	0.0	357602.	0.	165591.	-5500.	0.	-704.5	0.0	0.	0.	0.	0.0	0.0
CRUISE	41000.	0.850	357602.	13535.	179126.	0.	0.	70.0	70.0	0.	-81101.	0.	17.63	0.583
RESET	0.	0.0	344067.	0.	179126.	0.	0.	0.0	70.0	0.	0.	0.	0.0	0.0
CLIMB	0.	0.378	344067.	1395.	180521.	11.	11.	2.4	72.4	0.	81101.	0.	18.04	0.455
ACCEL	10000.	0.456	342672.	210.	180731.	2.	13.	0.4	72.8	0.	81101.	0.	16.43	0.487
CLIMB	10000.	0.547	342462.	3230.	183960.	52.	65.	7.7	80.6	0.	81101.	0.	15.23	0.536
CRUISE	30000.	0.665	339232.	908.	184869.	35.	100.	5.3	85.9	0.	-81101.	0.	17.82	0.544
DESCENT	30000.	0.700	338324.	585.	185453.	54.	154.	8.2	94.0	0.	81301.	0.	15.00	-13.928
DECEL	10000.	0.547	337739.	84.	185537.	5.	159.	0.9	94.9	0.	81301.	0.	16.41	4.499
DESCENT	10000.	0.456	337655.	723.	186320.	33.	191.	7.2	102.1	0.	81301.	0.	17.98	2.312
CRUISE	30000.	0.665	336372.	219.	186539.	9.	200.	1.3	103.4	0.	-81101.	0.	17.89	0.542
LITTER	1500.	0.296	336693.	4293.	190922.	0.	200.	30.0	133.4	0.	-81101.	0.	18.74	0.506

W H

TIME 41= 523193.2 FUEL A= 196785.9 FUEL R= 190322.2

C O S T S U M M A R Y

WING 3234436.00
TAIL 422293.44
BODY 3813644.00
LANDING GEAR 507860.06
FLIGHT CONTROLS 426161.63
ROCKETLES 825350.63

PROPULSION 32641.36
ENGINE 236408.13
AIR INTRODUCTION 385255.63
FUEL SYSTEM 6706.29
START SYSTEM 2664.15
ENGINE CONTROLS 2400.82
EX-THROST REV. 2074.43
FUEL SYSTEM

TOTAL PROPULSION

668638.69

INSTRUMENTS 189355.56
HYDRAULICS 259154.13
ELECTRICAL 456256.94
ELECTRONIC RACKS 124952.04
FUELING 610593.13
AIR CONDITIONING 512796.19
ANTI ICING 31661.34
AFU 118562.75
SYS. INTEGRATION 242406.28

TOTAL EMPTY MFG. COST

12869732.00

SUSTAINING ENGINEER 882721.31
TECHNICAL DATA 0.0
PROD. TOOLING MAINT. 1162266.00
MISC. 322929.83
LOG. CHANGE ORDER 0.0
QUALITY ASSURANCE 1212831.00
AIRFRAME WARRANTY
AIRFRAME FEE
AIRFRAME COST
ENGINE WARRANTY
ENGINE FEE
ENGINE COST
AVIATION COST
RESEARCH AND DEVELOPMENT
TOTAL FLY AWAY COST

822829.88
2590967.00
175050.56
441127.19

19864080.00
4117189.00
500000.00
1978927.00

26460160.00

DIRECT OPERATING COST-DOLLARS/YR. MILE 0/0
Crew 0.4401 11.82
AIRFRAME LABOR AND BURDEN MAINT. 0.2735 7.35
ENGINE LABOR AND BURDEN MAINT. 0.1903 5.11
AIRFRAME MATERIAL MAINT. 0.1263 3.41
ENGINE MATERIAL MAINT. 0.1996 5.36
FUEL AND OIL 1.1312 30.38
INCIDENT 0.7924 7.59
DEPRECIATION (INCLUDING SPARES) 1.0795 28.99
TOTAL DDC \$/YR. FILE 3.7236 100.00

WEIGHT
Crewing

523193.7 435036.0 446978.9 400721.7 370566.5 332607.4
12631.4 34269.1 35770.3 37920.3 34496.8 41056.9

R AND D
DEVELOPMENT TECHNICAL DATA
DESIGN ENGINEERING
DEVELOPMENT TOOLING
DEVELOPMENT TEST ARTICLE
FLIGHT TEST
SPECIAL SUPPORT EQUIPMENT
DEVELOPMENT SPARES
ENGINE DEVELOPMENT
AVIATICS DEVELOPMENT
TOTAL R AND D

14103469.
313421568.
118346569.
65269120.
47225828.
3761058.
50370144.
0.
0.
642617216.

2612. 3534. 4056.
1891. 1169. 1169.
0.0942 0.0942 0.0919
1.0436 1.0436 0.0919
2.8035 5.8228 7.3025
16410. 12927. 8.7821
17967. 15445. 11.7414
20410.

1.

LIQUID HYDROGEN---BASIC DEFLECTION RESISTANCE/400-1000

[illegible]

EXTERNAL TANK

MISS

5500 LBS

LIQUID FUEL ENGINE--BASIC DESIGN MISSION/400 PASSES/ 5500 LBS

T/C 10.00 T/R 0.40 A/E 0.00 L/W 30.00 W/S 120.0 T/W 0.325

POUNDS C/O

DESIGN GROSS WEIGHT
FUEL

ZERO FUEL WEIGHT

PAYLOAD OPERATING WEIGHT EMPTY

OPERATIONAL ITEMS

STANDARD ITEMS

EMPTY WEIGHT-MFG.

WING

TAIL

BODY

LANDING GEAR

FLIGHT CONTROLS

NACELLES

PROPULSION SYSTEM

ENGINE

AIR INTAKE

EXHAUST

COOLING

OIL SYSTEM (LESS OIL)

ENGINE CONTROLS

ENGINE STARTING

TANKS

INSULATING

FUEL-PLUMBING

INSTRUMENTS

HYDRAULICS

ELECTRICAL

ELECTRONICS

FURNISHINGS AND EQUIP.

AIR CONDITIONING

ANTI-ICING

AUXILIARY POWER UNIT

DESIGN RESERVE

D-6

LH₂ EXTERNAL TANK

MACH 0.85

400 PASSENGER

10,190 km (5500 n.mi)

NO. OF PASSENGERS

NO. OF CREW

STRUCTURAL I/C

UNUSED WING FUEL TANK VOLUME CO. FT.

MISSION SUMMARY

LIQUID HYDROGEN--BASIC DESIGN MISSION/400 PASS/ 5500 NM) MISS

SEGMENT	INIT ALTITUDE (FT)	INIT WGT (LB)	INIT FUEL (LB)	SEGMENT FUEL (LB)	TOTAL FUEL (LB)	SEGMENT DIST (NM)	TOTAL DIST (NM)	SEGMENT TIME (MIN)	TOTAL TIME (MIN)	EXTERIOR STORE TAB ID	ENGINE THROUST TAB ID	EXTERIOR F TANK TAB ID	AVG L/D RATIO	AVG SFC (FF/T)
TAKOFF POWER 1	0.	0.0	436751.	211.	211.	0.	0.	14.0	14.0	0.	-83101.	0.	0.0	0.117
POWER 2	0.	0.0	440540.	243.	454.	0.	0.	1.0	15.0	0.	13401.	0.	0.0	0.094
CLIMB	0.	0.378	436297.	652.	1106.	13.	13.	2.9	17.9	0.	83101.	0.	15.09	0.152
ACCEL	10000.	0.456	435645.	239.	1345.	7.	20.	1.1	19.0	0.	83101.	0.	12.94	0.173
CLIMB	10000.	0.538	435406.	5345.	6690.	298.	317.	36.5	55.5	0.	83101.	0.	11.80	0.200
CRUISE	35000.	0.850	430061.	61270.	67460.	5033.	5350.	619.3	674.7	0.	-83101.	0.	13.38	0.199
DESCENT	35000.	0.850	368790.	166.	68126.	44.	5364.	5.7	680.4	0.	83301.	0.	9.93	-1.646
DECEL	10000.	0.638	366624.	51.	68177.	7.	5402.	1.3	681.6	0.	83301.	0.	12.11	44.307
DESCENT	10000.	0.420	368573.	316.	68495.	36.	5432.	6.7	688.4	0.	83301.	0.	14.33	0.799
CRUISE	38000.	0.850	368256.	781.	69276.	65.	5500.	8.4	690.8	0.	-83101.	0.	13.14	0.199
LOITER	1500.	0.311	367474.	384.	69660.	0.	5500.	6.0	702.8	0.	-83101.	0.	15.05	0.157
RESET	0.	0.0	367090.	0.	69660.	0.	5500.	0.0	702.8	0.	0.	0.	0.0	0.0
RESET	0.	0.0	367090.	0.	69660.	-5500.	0.	-702.8	0.0	0.	0.	0.	0.0	0.0
CRUISE	38000.	0.850	367090.	6349.	76009.	0.	0.	70.0	70.0	0.	-83101.	0.	13.31	0.199
RESET	0.	0.0	360741.	0.	76009.	0.	0.	0.0	70.0	0.	0.	0.	0.0	0.0
CLIMB	0.	0.374	360741.	510.	76519.	10.	10.	2.2	72.2	0.	83101.	0.	14.10	0.152
ACCEL	10000.	0.456	360250.	80.	76599.	2.	12.	0.4	72.6	0.	83101.	0.	12.91	0.165
CLIMB	10000.	0.547	360150.	1451.	77050.	54.	67.	6.1	80.8	0.	83101.	0.	12.07	0.162
CRUISE	30000.	0.680	358819.	390.	76520.	33.	100.	5.0	85.7	0.	-83101.	0.	13.96	0.163
DESCENT	30000.	0.700	358430.	147.	76516.	43.	143.	6.5	92.2	0.	83501.	0.	11.91	-4.975
DECEL	10000.	0.547	358233.	28.	76544.	4.	147.	0.7	92.9	0.	83301.	0.	12.96	1.607
DESCENT	10000.	0.456	358205.	255.	76799.	25.	172.	5.5	98.5	0.	83301.	0.	14.15	0.825
CRUISE	30000.	0.680	357951.	329.	79125.	28.	200.	4.2	102.7	0.	-83101.	0.	13.95	0.183
LOITER	1500.	0.307	357622.	1870.	80087.	0.	200.	30.0	132.7	0.	-83101.	0.	15.03	0.158

P
NO

TOGRWT= 436750.6 FUEL A= 80987.2 FUEL R= 80997.3

COST SUMMARY

WING 2605816.00
 TAIL 340755.94
 BODY 3713114.00
 LANDING GEAR 4476344.13
 FLIGHT CONTROLS 344480.14
 NACELLES 942749.78

PROPULSION 36945.67
 ENGINE 282331.84
 AIR INTRODUCTION 2630880.00
 FUEL SYSTEM 8026.56
 START SYSTEM 3188.77
 ENGINE CONTROLS 3470.58
 EXHAUST/THRUST REV. 2667.16
 LUBE SYSTEM

TOTAL PROPULSION 2568508.00

INSTRUMENTS 180512.44
 HYDRAULICS 215402.06
 ELECTRICAL 444821.75
 ELECTRONIC RACKS 132164.56
 FURNISHING 608776.88
 AIR CONDITIONING 52115.06
 ANTI ICING 27343.04
 APU 110364.31
 SYS. INTEGRATION 318790.00

TOTAL LFTY MFG. COST 14007532.00

TOTAL LFTY MFG. COST

SUSTAINING ENGINEER 980460.13
 TECHNICAL DATA 0.0
 PROD. TOOLING MAINT. 1201117.00
 MISC. 558685.06
 ENG. CHANCE ORDER 0.0
 QUALITY ASSURANCE 1347140.00
 AIRFRAME WARRANTY
 AIRFRAME FEE
 AIRFRAME COST
 AIRFRAME WARRANTY
 ENGINE FEE
 ENGINE COST
 AVIONICS COST
 RESEARCH AND DEVELOPMENT
 TOTAL FLY AWAY COST

855250.31
 2522037.00
 242978.56
 612305.69

21716180.00
 5714556.00
 506000.00
 2362341.00

30234064.00

DIRECT OPERATING COST-DOLLARS/Hr. MILE C/O
 CREW 8.41
 AIRFRAME LABOR AND BURDEN MAINT. 4.96
 ENGINE LABOR AND BURDEN MAINT. 2.75
 AIRFRAME MATERIAL MAINT. 2.71
 ENGINE MATERIAL MAINT. 2.71
 FUEL AND OIL 3.00
 INSURANCE 4.00
 DEPRECIATION (INCLUDING SPARES) 4.00
 TOTAL DOC 1/1. MILE 34.10

4781. 5500.
 1.2873 1.2774
 10.2367 11.7131
 24618. 26102.

R AND D
 DEVELOPMENT TECHNICAL DATA
 DESIGN ENGINEERING
 DEVELOPMENT TOOLING
 DEVELOPMENT TEST ARTICLE
 FLIGHT TEST
 SPECIAL SUPPORT EQUIPMENT
 DEVELOPMENT SPARES
 ENGINE DEVELOPMENT
 AVIONICS DEVELOPMENT
 TOTAL R AND D

18889664.
 419770624.
 187472080.
 72168400.
 42019328.
 5037246.
 59642992.
 0.
 0.
 605819136.

WING 436750.00
 TAIL 347007.1
 BODY 440552.1
 LANDING GEAR 26936.0
 FLIGHT CONTROLS 440552.1
 NACELLES 26936.0
 PROPULSION 440552.1
 ENGINE 26936.0
 AIR INTRODUCTION 440552.1
 FUEL SYSTEM 26936.0
 START SYSTEM 440552.1
 ENGINE CONTROLS 26936.0
 EXHAUST/THRUST REV. 440552.1
 LUBE SYSTEM 26936.0
 INSTRUMENTS 440552.1
 HYDRAULICS 26936.0
 ELECTRICAL 440552.1
 ELECTRONIC RACKS 26936.0
 FURNISHING 440552.1
 AIR CONDITIONING 26936.0
 ANTI ICING 440552.1
 APU 26936.0
 SYS. INTEGRATION 440552.1
 TOTAL LFTY MFG. COST 14007532.00
 SUSTAINING ENGINEER 980460.13
 TECHNICAL DATA 0.0
 PROD. TOOLING MAINT. 1201117.00
 MISC. 558685.06
 ENG. CHANCE ORDER 0.0
 QUALITY ASSURANCE 1347140.00
 AIRFRAME WARRANTY
 AIRFRAME FEE
 AIRFRAME COST
 AIRFRAME WARRANTY
 ENGINE FEE
 ENGINE COST
 AVIONICS COST
 RESEARCH AND DEVELOPMENT
 TOTAL FLY AWAY COST

SUMMARY ID NO. 400

WING QUARTER CHORD SWEEP = 30.00 DEG

ENGINE 1.0. -- 43006

AVC004ET M0001 --C11317-5-1

1	M/S	116.0	111.0	126.0	124.0	116.0	118.0	120.0	n.n	0.0	0.0	0.0	0.0	0.0	0.0	0.0
2	T/W	0.35	0.35	0.35	0.35	0.35	0.35	0.35	0.0	0.0	0.0	0.0	0.0	0.0	0.0	0.0
3	AR	8.00	8.00	8.00	8.00	8.00	8.00	8.00	0.0	0.0	0.0	0.0	0.0	0.0	0.0	0.0
4	T/C	10.00	10.00	10.00	10.00	10.00	10.00	10.00	0.0	0.0	0.0	0.0	0.0	0.0	0.0	0.0
5	RADIUS N. MI	5500	5500	5500	5500	5500	5500	5500	0	0	0	0	0	0	0	0
6	GROSS WEIGHT	44189	440416	430446	436583	435379	438014	436750	0	0	0	0	0	0	0	0
7	FUEL WEIGHT	82070	82785	82352	82112	81420	81192	80987	0	0	0	0	0	0	0	0
8	O.P. WT. EMPTY	276519	285631	285514	286470	285949	287821	287763	0	0	0	0	0	0	0	0
9	ZERO FUEL WT.	358818	365631	355214	354470	357949	356821	355763	0	0	0	0	0	0	0	0
10	THRUST/ENGINE	38665	37556	38410	38201	38594	38875	38761	0.0	0.0	0.0	0.0	0.0	0.0	0.0	0.0
11	ENGINE SCALE	1.2105	1.2101	1.2088	1.2091	1.2114	1.2111	1.2107	0.0	0.0	0.0	0.0	0.0	0.0	0.0	0.0
12	WING AREA	3809.	3732.	3684.	3621.	3703.	3712.	3650.	0.0	0.0	0.0	0.0	0.0	0.0	0.0	0.0
13	WING SPAN	174.6	172.8	171.1	167.8	174.1	172.5	170.6	0.0	0.0	0.0	0.0	0.0	0.0	0.0	0.0
14	H. TAIL AREA	776.	752.	726.	687.	769.	745.	723.	0.0	0.0	0.0	0.0	0.0	0.0	0.0	0.0
15	V. TAIL AREA	415.	402.	380.	368.	412.	399.	387.	0.0	0.0	0.0	0.0	0.0	0.0	0.0	0.0
16	BODY LENGTH	197.0	197.0	197.0	197.0	197.0	197.0	197.0	0.0	0.0	0.0	0.0	0.0	0.0	0.0	0.0
COST DATA--FILLION DOLLARS/AIRCRAFT																
17	FLYWAY COST	30.541	30.400	30.215	30.075	30.477	30.231	30.254	0.0	0.0	0.0	0.0	0.0	0.0	0.0	0.0
18	FRAME COST	24.901	24.770	24.664	24.452	24.775	24.629	24.549	0.0	0.0	0.0	0.0	0.0	0.0	0.0	0.0
19	ENGINE COST	5.703	5.630	5.671	5.644	5.744	5.729	5.715	0.0	0.0	0.0	0.0	0.0	0.0	0.0	0.0
20	AVIATICS COST	0.500	0.500	0.500	0.500	0.500	0.500	0.500	0.0	0.0	0.0	0.0	0.0	0.0	0.0	0.0
COST DATA--DIRECT OPERATIONS COST																
21	\$ PER MILE	5.164	5.165	5.165	5.164	5.161	5.125	5.109	0.0	0.0	0.0	0.0	0.0	0.0	0.0	0.0
22	CENIS/A 5 MILE	1.296	1.291	1.267	1.274	1.285	1.281	1.277	0.0	0.0	0.0	0.0	0.0	0.0	0.0	0.0
FLIGHT PATH MISSION CHARACTERISTICS																
23	MISSION SYM(1)	35000	35000	35000	35000	35000	35000	35000	0	0	0	0	0	0	0	0
24	MISSION SYM(2)	71046	71259	71060	70931	70059	69646	69660	0	0	0	0	0	0	0	0
CONSTRAINT OUTPUT																
25	CEILING PWR(1)	34950	34754	34454	35210	35110	35000	35000	0	0	0	0	0	0	0	0
26	TAKEOFF DST(1)	5174	5260	5359	5544	5106	5196	5237	0	0	0	0	0	0	0	0
27	CLIMB GRAD(1)	0.1651	0.1654	0.1654	0.1654	0.1654	0.1654	0.1654	0.0	0.0	0.0	0.0	0.0	0.0	0.0	0.0
28	TAKEOFF DST(2)	5150	5251	5352	5556	5089	5165	5267	0	0	0	0	0	0	0	0
29	CLIMB GRAD(2)	0.0874	0.0867	0.0860	0.0846	0.0803	0.0768	0.0738	0.0	0.0	0.0	0.0	0.0	0.0	0.0	0.0
30	AP SPEED-KT(1)	132.7	135.3	134.4	137.2	132.1	134.0	135.1	0.0	0.0	0.0	0.0	0.0	0.0	0.0	0.0
31	CTOL LNOG D(1)	5666	5752	5764	5821	5679	5749	5811	0	0	0	0	0	0	0	0
32	AP SPEED-KT(2)	136.2	137.4	136.5	140.9	136.4	137.6	138.7	0.0	0.0	0.0	0.0	0.0	0.0	0.0	0.0
33	CTOL LNOG D(2)	5671	5691	6031	6153	5855	5855	6025	0	0	0	0	0	0	0	0
34	AP SPEED-KT(3)	141.2	142.4	143.6	146.0	141.2	143.0	143.6	0.0	0.0	0.0	0.0	0.0	0.0	0.0	0.0
35	CTOL LNOG D(3)	6173	6247	6322	6470	6174	6270	6323	0	0	0	0	0	0	0	0
36	SEPT 1) - FPS	2	2	2	2	2	2	3	0	0	0	0	0	0	0	0

APPENDIX E
EVALUATION OF AIR CUSHION LANDING SYSTEM
AS APPLIED TO
LIQUID HYDROGEN FUELED CARGO TRANSPORT

Introduction

This conceptual study is conducted to determine the advantages and disadvantages of substituting as Air Cushion Landing System (ACLS) for the conventional landing gear on the large liquid hydrogen cargo transport. The payload and mission fuel are held constant for the performance analysis, thus changes in aircraft weight and drag affect only the design mission range. Specifically, the following items are assessed:

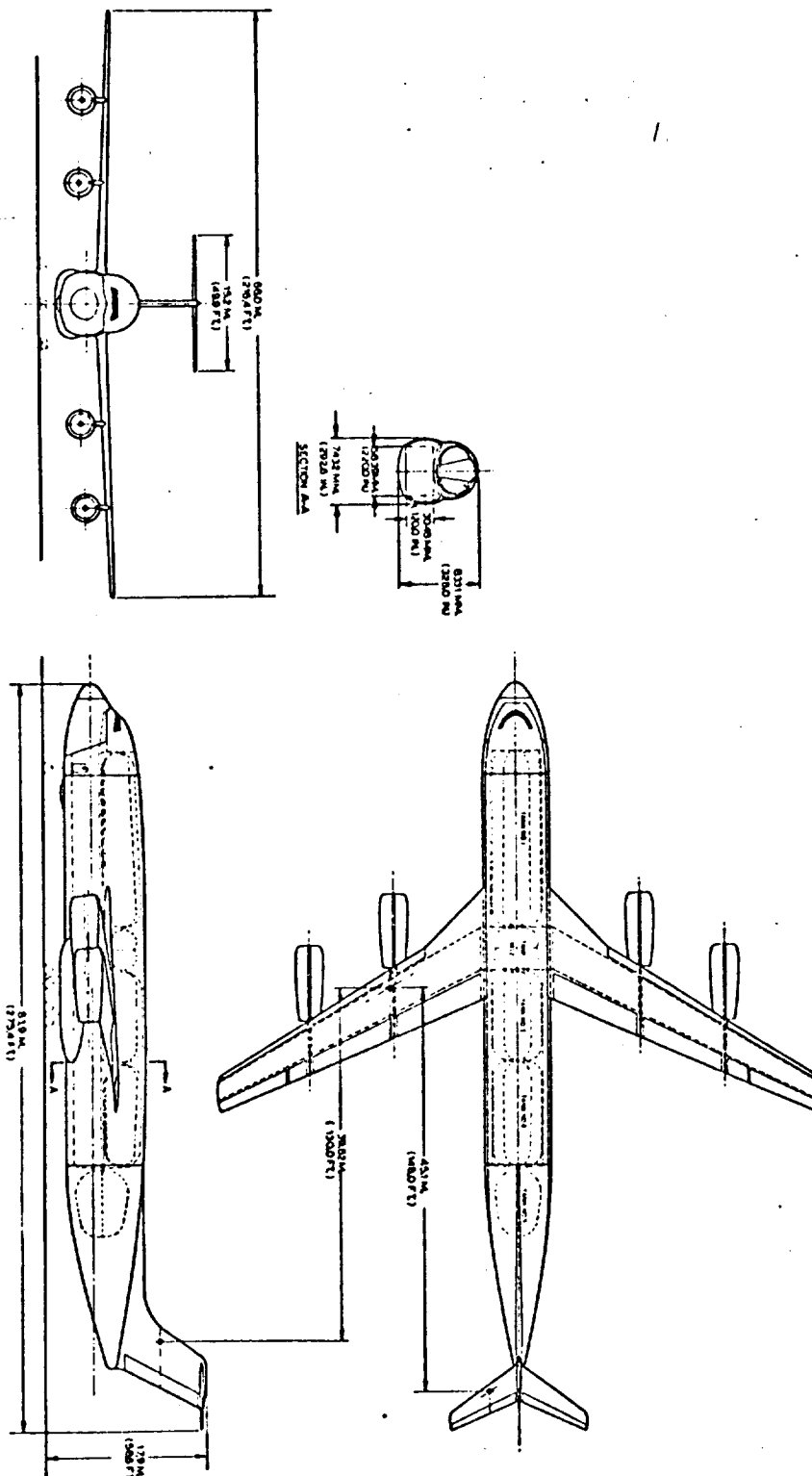
- Weight
- Drag
- Performance
- Cost (Engineering Estimates Only)

The weight and cost data for the ACLS System were based upon previous C-130 ACLS studies performed by the Bell Aerospace Division Testron and the Lockheed-Georgia Company.

The baseline aircraft is shown in Figure E-1 and the ACLS aircraft in Figure E-2. The study results are summarized on Figure E-3.

System Description

The air Cushion Landing System (ACLS) is based upon the "Ground Effect" principle. The conventional undercarriage landing gear, which consists of multiple wheel bogies and shock struts, is replaced by an inflatable pneumatic bag or trunk mounted beneath and surrounding the aircraft fuselage. A continuous air feed maintains the trunk inflation, and escaping jet air creates a low ground-over pressure when the trunk is close to the surface. This air, sealed around the periphery by the trunk, is called the air cushion and supports the weight of the aircraft. The continued flow of air at low pressure provides a film of air that enables the aircraft to operate over the commercial airport surfaced runways and improved surfaces of low bearing strength. The trunk is retracted to reduce excessive drag at flight cruise speeds.



AIRCRAFT DATA
 TYPE: L-1049-1A
 WEIGHT: 11,000 kg (24,250 lb)
 MAXIMUM TAKEOFF WEIGHT: 17,000 kg (37,470 lb)
 MAXIMUM LANDING WEIGHT: 11,000 kg (24,250 lb)
 MAXIMUM GROSS WEIGHT: 17,000 kg (37,470 lb)
 MAXIMUM PASSENGER CAPACITY: 62
 MAXIMUM CARGO CAPACITY: 1,000 kg (2,200 lb)
 MAXIMUM FUEL CAPACITY: 11,000 kg (24,250 lb)
 MAXIMUM RANGE: 3,000 km (1,750 mi)
 MAXIMUM CRUISE SPEED: 480 km/h (285 mph)
 MAXIMUM CLIMB RATE: 10,000 ft/min
 MAXIMUM ALTITUDE: 10,000 ft
 MAXIMUM GROSS WEIGHT: 17,000 kg (37,470 lb)
 MAXIMUM PASSENGER CAPACITY: 62
 MAXIMUM CARGO CAPACITY: 1,000 kg (2,200 lb)
 MAXIMUM FUEL CAPACITY: 11,000 kg (24,250 lb)
 MAXIMUM RANGE: 3,000 km (1,750 mi)
 MAXIMUM CRUISE SPEED: 480 km/h (285 mph)
 MAXIMUM CLIMB RATE: 10,000 ft/min
 MAXIMUM ALTITUDE: 10,000 ft

ENGINE DATA
 TYPE: Pratt & Whitney R-2800-18
 POWER: 2,000 hp (1,491 kW)
 WEIGHT: 1,000 kg (2,200 lb)
 LENGTH: 1.5 m (4 ft 11 in)
 DIAMETER: 0.76 m (2 ft 6 in)
 WEIGHT: 1,000 kg (2,200 lb)
 LENGTH: 1.5 m (4 ft 11 in)
 DIAMETER: 0.76 m (2 ft 6 in)
 WEIGHT: 1,000 kg (2,200 lb)

Figure E-1. L-1049 Super Constellation - Conventional Gear

E-3

E-3

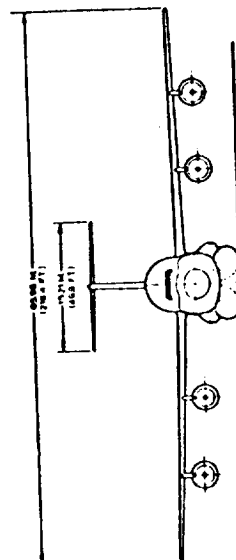
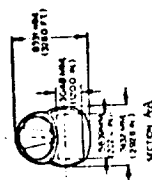
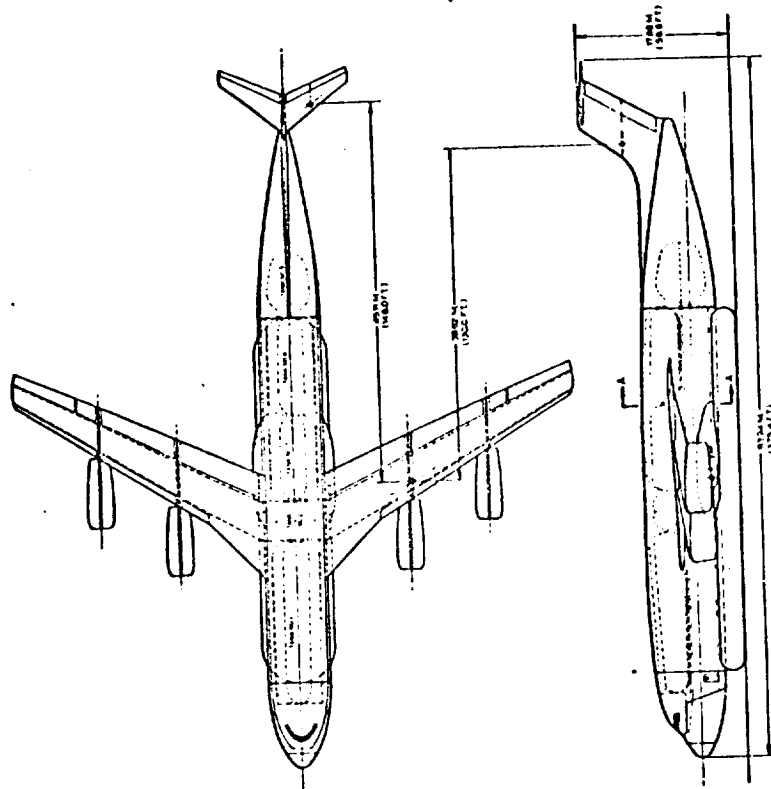


Figure 5-2. LH_2 Fueled Cargo Transport - ACLS

ITEM	CONVENTIONAL GEAR		ACLS	
Operating weight - kg (lb)	138,670	(305,710)	136,842	(301,680)
Payload - kg (lb)	113,400	(250,000)	113,400	(250,000)
Mission fuel - kg (lb)	48,004	(105,830)	48,004	(105,830)
Gross weight - kg (lb)	300,075	(661,540)	298,246	(657,510)
DRAG				
Counts of drag	289		291	
PERFORMANCE				
Range - km (n m)	10,186	(5,500)	10,149	(5,480)
T.O. distance - m (ft)	2,185	(7,170)	2,423	(7,950)
Landing distance - m (ft)	2,304	(7,560)	2,301	(7,550)
COST				
Aircraft cost (\$ X 10 ⁶)	39.12		40.94	
Landing system cost (\$ X 10 ⁶)	1.07		2.89	
DOC - ¢/Mg km	2.89		2.95	
DOC - ¢/ton n m	4.86		4.95	

Figure E-3. Summary of Study Results

Braking capability is provided by addition of brake pillows to the aft portion, and on both sides of the trunk. Braking is provided through controlled inflation of these pillows, which locally deforms the trunk causing brake treads to contact the runway. While steering may be accomplished by aerodynamic and/or propulsion forces, steering by differential braking or lower taxi or maneuver speeds is provided. Parking is accomplished by inflating bladder cells inside the trunk prior to engine shutdown.

ACLS Operation

The aircraft will be parked during the cargo loading, and trunk air pressure maintained by the parking system. The auxiliary ACLS engines and air cushion system will be used to move away from the loading area, either towed or taxied, to the

runway for takeoff. The takeoff run will impose no particular problems other than yawing at low speeds due to possible crosswinds. The lift-off will be accomplished by rotating the aircraft approximately 0.07 radians (4 degrees) once the appropriate takeoff speed has been achieved. The ACLS trunk will be retracted against the fuselage once the aircraft becomes airborne, and the auxiliary engines will be shut down.

The landing sequence involves starting up both ACLS engines and inflating the trunk. Upon touchdown the brake pillows will be inflated to decelerate the aircraft landing speed. Taxiing to the unloading zone will be accomplished on the air cushion. Due to the relatively low ACLS bearing pressures, the pilot may use alternate smooth surfaces denied to conventional gear aircraft due to inherent surface strength. These alternate paths may be asphalt or smooth soil surfaces.

During the unloading process, trunk pressure will be maintained by the parking system in the period is too lengthy. For short-term duration unloading, the ACLS engines will be left running.

Detail Description

Trunk Configuration And Air Supply - The trunk concept representative of present conventional designs is an elongated torus attached to the lower portion of the fuselage. The trunk extends the full length of the cargo compartment or 43.9 meters (144 feet), has a width of 8.2 meters (27 feet), provides a cushion area of 208.8 square meters (2248 square feet), and a perimeter of 82.9 meters (272 feet), Figure E-4. To support the gross weight of the aircraft would require a cushion pressure of 14.0 kPa (2.03 psig); however, the trunk pressure should be twice the cushion pressure or 28.0 kPa (4.06 psig).

Two General Electric TF-34 engines will be used to supply the required pressure for ACLS operation. The engines will be converted to use liquid hydrogen fuel supplied from tanks 2 and 5 (Figure E-2) and are mounted in pods on left and right side of the aircraft centered approximately about the aircraft center of gravity. Each has an air inlet and engine core exhaust exit centered approximately 4.27 meters (14 feet) above the runway to minimize the ingestion of foreign material and minimize the effect of the hot exhaust gases to either personnel or equipment which may be in the local area. Each engine is capable of supplying 184.1 cubic meters (6500 cubic feet) of fan by-pass air per second at static ($M=0$) condition. Engine exhaust air is separately ducted through the exhaust exit location in each pod. During braking, compressor bleed air will be directed to the brake pillows.

The by-pass air from each engine is directed to the trunk. The trunk is also provided with lubrication holes in its surface adjacent to the ground which direct sufficient air to the central cavity to support the aircraft at a predetermined height above the runway. The air escapes around the tangential line between the trunk and the runway providing an air bearing for the aircraft to move upon.

The trunk is made from an elastic composite so that when deflated, it shrinks and retracts upward and against the bottom of the fuselage to make a relatively smooth aerodynamic surface except for the brake treads described later. More specifically, the trunk is made up of several plies of two-way stretch material consisting of arrays of stretch cords placed at right angles in a rubber matrix. The two-way stretch permits clean retraction against the bottom of the fuselage.

Brake System - The brake system consists of a series of six brake pillows, and treads are located on the aft portion of the trunk and on either side as shown in Figure E-4. A replaceable tread, consisting of many brake skid blocks, is attached to the outside of the trunk directly adjacent to the brake pillows. When the trunk is deflated, the treads fold up in accordion fashion and extend 101.6 to 127.0mm (4 to 5 inches) below the lower fuselage skin. Aerodynamic moldings are provided for and aft of the treads to improve the aerodynamic flow. The pillows are rapidly inflated by diverted compressor bleed air from the core engines. This will press the brake skids against the runway or landing surface. Due to this inflation and braking action, the trunk is locally deformed, allowing the cushion air to bleed off, reducing the cushion pressure, and results in the major portion of the aircraft weight being applied to the brake treads. The brakes can be differentially applied through the pilot's and copilot's brake pedals to achieve low speed maneuver and taxi control.

Parking System - The parking system consists of bladder cells fastened beneath the fuselage inside the trunk. These cells are inflated by the engine compressor bleed air. The bladders are located ahead of and behind the series of brake pillows. The parking bladders are inflated prior to shut-down of the ACLS engines, in going from the air cushion mode to the park mode. After the trunk has deflated, the aircraft is supported by the inflated parking bladders which are sealed off by closure of their inflation valves. To go from the parking mode to the air cushion operation, the sequence is reversed. The bladders are made of multi-ply elastic construction, similar to the trunk, and are self-stowing when deflated.

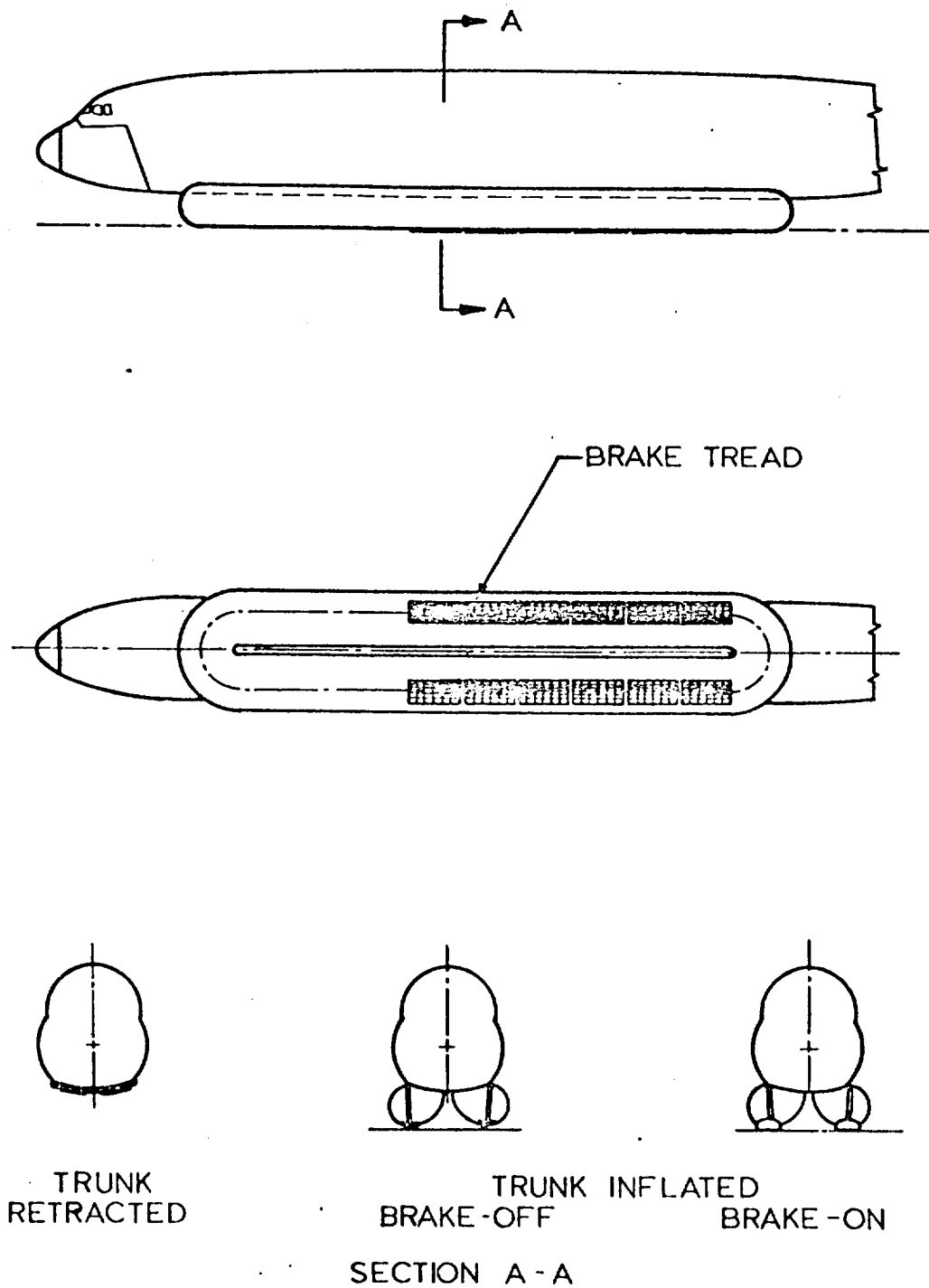


Figure E-4. Pillow Brake System

Control System - The balance of the ACLS System consists mainly of the valves and sensors necessary for control of the inflation and deflation of the trunk, braking, and parking subsystems. A heat exchanger is also included to reduce engine air temperature to a level satisfactory for temperature tolerance of the materials that make up the brake pillows and parking bladders.

Study Results

Weight - The weights for the ACLS are summarized and compared to the weight allocated for conventional landing gear on the selected large noselander liquid hydrogen cargo transport on Figure E-5. The main landing gear pod and actuation accessories were assumed to be equivalent to the pod required to house the ACLS engines and their control, fuel, and LH₂ conversion systems.

The net weight saving attributed to the ACLS gear is 1,828 kilograms (4,030 pounds), which is reflected in the reduction of the baseline aircraft operating weight from 138,670 to 136,842 kilograms (305,710 to 301,680 pounds) for the ACLS aircraft. The trunk weight 4,790 kilograms (10,560 pounds) is compatible with a safety factor of 10. Further analysis of the system could conceivably reduce this factor. The trunk weight for a safety factor of 4 is approximately 1,996 kilograms (4,400 pounds) which could increase the total weight saving to 4,622 kilograms (10,190 pounds).

Drag - A conventional gear contributed to the total aircraft drag by parasite drag and rolling friction. The ACLS also has two drag components, parasite drag and momentum drag. The parasite drag of the two gears is considered approximately equal except for the added wetted area of the retracted trunk and the slightly protruding brake skids. For this difference, two counts of drag were added to the total aircraft drag.

Performance - Both aircraft are configured to the same ground rules which retained the maximum payload of 113,400 kilograms (250,000 pounds) and the mission fuel limit of 48,005 kilograms (105,830 pounds). The substitution of ACLS for the conventional gear results in a drag increase and an operating weight decrease, which when combined, reduce the design mission of the aircraft from 10,186 to 10,148 kilometers (5,500 n m to 5,480 n m). In computing the landing and takeoff performance, it was assumed that the rolling friction of the conventional gear and the momentum drag of the ACLS were equal.

	<u>WEIGHT</u>	
	<u>lb</u>	<u>kg</u>
<u>ACLS</u>		
Trunk	10,560	4,790
Trunk Attachment	4,300	1,951
Parking Bladder	1,140	517
Engines and Fan Assemblies	2,854	1,295
Engine Mountings	1,550	703
Liquid Hydrogen Fuel System	759	344
Brakes	4,557	2,067
Subsystems	600	272
Ducting	951	431
Total Weight	27,271	12,370
<u>Conventional Landing Gear</u>		
Nose Landing Gear	4,069	1,846
Main Landing Gear (4)	27,232	12,352
Total Weight	31,301	14,198

Figure E-5. Weight Comparison

The FAA takeoff distance of the ACLS aircraft is 2,423 meters (7,950 feet). This represents an increase of 11 percent over the conventional gear aircraft and is attributed to limiting the rotational angle of the aircraft to 0.07 radians (4 degrees). This was selected in lieu of the normal 0.14 - 0.21 radians (8 - 12 degrees) due to the long ACLS trunk, 43.9 meters (144 feet), and the desire to maintain a reasonable air cushion until the aircraft becomes airborne. The landing distances are essentially equal, 2,332 vs 2,301 meters (7,560 vs 7,550 feet). A more detailed study could reduce the ACLS landing distance even further, due to higher braking friction of the skids, if the surface area allocated for braking proves conservative.

Cost - The cost of both the conventional landing gear (CLG) and ACLS is based upon production quantities required to produce 350 aircraft.

		<u>\$ X 10⁶</u>
	<u>CLG</u>	<u>ACLS</u>
Non Recurring	108.3	42.9
Unit Price	0.76	2.77
Unit Price Including Non-Recurring Cost	1.07	2.89

The higher cost of the ACLS system increases the price of the baseline aircraft from \$39,120,000 to \$40,940,000. The direct operating cost also increases from 2.89 to 2.95 cents per available megagram - kilometer (4.86 to 4.95 cents per available ton nautical mile). The cost of operating the aircraft at full payload for 10,186 kilometers (5,500 nautical miles) increases from \$33,400 to \$34,000 per trip.

Conclusions

Although the ACLS compared to a conventional landing gear reduces the operating weight of the aircraft slightly, the increase in drag and price result in a reduction in aircraft performance and an increase in direct operating cost, respectively. Both landing systems were evaluated with respect to smooth improved airport runways. The chief attraction for ACLS up to this time has been the ability to operate, within reason, from all types of surfaces or terrain. The ACLS has other potential advantages which did not enter into this evaluation:

- Improved Safety During Takeoff and Landing
- Improved Aircraft Reliability
- Low Cost Airfields
- Improved Runway Maintenance

Future Research And Development Studies

The analysis reported herein assumed state-of-the-art, elastic construction of the ACLS trunk, which utilizes its elastic properties for retraction. Elastic construction may not be the optimum solution. Due to various factors, such as design complexity and care required in manufacture, the elastic trunk is the most expensive component of the ACLS system. Significant savings are potentially realizable with an inelastic trunk.